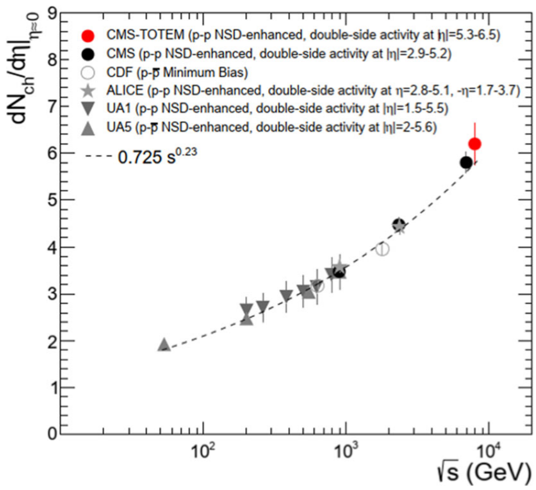

Fig. 342 Value of $dN_{ch}/d\eta$ at $\eta \approx 0$ as a function of the center-of-mass energy for pp and $\bar{p}p$ collisions. Shown are measurements performed with different event selections from a number of experiments listed in the figure. The dashed line is a power-law fit to the data. Figure taken from Ref. [4026]

tion between diffractive and non-diffractive events is somewhat easier, at least for what concerns high mass diffraction.

The richness of the data at the LHC also implies that there are a number of aspects that we have not been able to treat in this short overview. For instance, the interesting topic of particle correlations has not been discussed and neither has multiple parton interactions been considered (For those topics and also for other topics that have not been discussed here, see e.g. PDG [616]).

In the 1970s and 1980s the interest moved from Regge theory and low p_T physics to high p_T reactions and perturbative QCD. The "old" physics lost considerable interest. However it turns out that the tools of the "old" physics work remarkably well also today. The current theoretical efforts try to bridge this gap between "old" physics and "new" and produce convincing descriptions of soft processes in terms of QCD. A lot of theoretical efforts have occurred over the years trying to make the transition from Regge poles and Regge Field Theory to QCD. Some attempts in this direction have been mentioned in this overview, but far from all.

With the abundant data from LHC available today the study of soft interactions has become a more vigorous field again. The hope is that "old" and "new" physics will meet and that a proper calculational framework based upon QCD will be developed in the close future leading to a better understanding of soft processes. A lot of progress have been made until today but the challenge is still there to incorporate a full understanding of soft processes in QCD.

13 Weak decays and quark mixing

Conveners:

Andrzej J. Buras and Eberhard Klempt

One of the main frontiers in the elementary particle physics is the search for new particles and new forces beyond those present in the Standard Model (SM) of particle physics. As the direct searches at Large Hadron Collider (LHC) at CERN, even 10 years after the Higgs discovery, did not provide any clue what these new particles and forces could be, the indirect searches for new physics (NP) through very rare processes caused by virtual exchanges of heavy particles gained in importance. They allow in fact to see footprints of new particles and forces acting at much shorter distance scales than it is possible to explore at the LHC and presently planned high energy colliders. While the LHC can explore distance scales as short as 10^{-19}m, the indirect search with the help of suitably chosen processes can offer us the information about scales as short as 10^{-21} m which cannot be probed even by the planned 100 TeV collider at CERN. Also shorter scales can be explored in this manner.

In fact rare processes like $K_L \to \mu^+\mu^-$ known since the early 1970s implied the existence of the charm quark prior to its discovery in 1974 as only then its branching ratio could be suppressed in the SM with the help of the Glashow–Iliopoulos–Maiani (GIM) mechanism [80], to agree with experiment. Moreover, it was possible to predict successfully its mass with the help of the $K_L - K_S$ mass difference ΔM_K in the $K^0 - \bar{K}^0$ mixing prior to its discovery [4027]. Similary the size of the $B_d^0 - \bar{B}_d^0$ mixing,[116] discovered in the late 1980s, implied a heavy top quark that has been confirmed only in 1995. It is then natural to expect that this indirect search for NP will also be successful at much shorter distance scales.

In this context, rare weak decays of mesons play a prominent role besides the transitions between particles and antiparticles in which flavors of quarks are changed. In particular $K^+ \to \pi^+\nu\bar{\nu}$, $K_L \to \pi^0\nu\bar{\nu}$, $K_S \to \mu^+\mu^-$, $B_s^0 \to \mu^+\mu^-$, $B_d^0 \to \mu^+\mu^-$ and $B_d^0 \to K(K^*)\nu\bar{\nu}$ but also $B_s^0 - \bar{B}_s^0$, $B_d^0 - \bar{B}_d^0$, $K^0 - \bar{K}^0$ mixings and CP-violation in $K \to \pi\pi$, $B_d \to \pi K$ decays among others provide important constraints on NP. Most of these transitions are very strongly loop-suppressed within the SM due to the GIM mechanism and also due to small elements V_{cb}, V_{ub}, V_{td} and V_{ts} of the CKM matrix [86,4028]. The predicted branching ratios for some of them are as low as 10^{-11}. But as the GIM mechanism is generally violated by NP contributions these branching ratios could in fact be much larger.

The first step in this indirect strategy is to search for the departures of the measurements of the branching ratios of the decays in question from SM predictions and similar for mass

[116] The $B_d^0 = (d\bar{b})$ is listed as B^0 in the Review of Particle Physics.

differences like ΔM_K, and analogous mass differences ΔM_s and ΔM_d in $B_s^0-\bar{B}_s^0$ and $B_d^0-\bar{B}_d^0$ mixings, respectively. But while these processes are governed by quark interactions at the fundamental level, the decaying objects are mesons, the bound states of quarks and antiquarks. In particular in the case of non-leptonic transitions like $B_s^0-\bar{B}_s^0$, $B_d^0-\bar{B}_d^0$, $K^0-\bar{K}^0$ mixings and CP-violation in $K\to\pi\pi$ and $B\to\pi K$ decays, QCD plays an important role. It enters at short distance scales, where due to the asymptotic freedom in QCD perturbative calculations can be performed, and at long distance scales where non-perturbative methods are required. QCD has also an impact on semi-leptonic decays like $K^+\to\pi^+\nu\bar{\nu}$, $K_L\to\pi^0\nu\bar{\nu}$, $B\to K(K^*)\nu\bar{\nu}$ and even on leptonic ones like $K_S\to\mu^+\mu^-$, $B_s^0\to\mu^+\mu^-$, and $B_d^0-\bar{B}_d^0\to\mu^+\mu^-$. In order to be able to identify the departures of various experimental results from the SM predictions that would signal NP at work, the latter predictions must be accurate, and this means the effects of QCD have to be brought under control. But this is not the whole story. To make predictions for rare processes in the SM one has to determine the four parameters of the unitary CKM matrix

$$V_{us},\quad V_{cb},\quad V_{ub},\quad \gamma \tag{13.1}$$

with γ being the sole phase in this matrix.

This section is divided into five parts. We present first the effective weak Hamiltonians both in the SM and beyond. We summarize briefly the history of the efforts to construct them and present their status. Here, renormalization-group (RG) methods – used to calculate QCD impact on the Wilson coefficients (WC) of local operators – are essential but also the non-perturbative evaluation of their hadronic matrix elements. This will be followed by the discussion of the present status of the CKM matrix (see Sect. 13.2) which will demonstrate the role of QCD in the determination of its elements. Subsequently, in Sect. 13.3, we will first summarize briefly the impact of QCD effects on rare leptonic and semileptonic decays. Here, these effects are mostly moderate, with the exception of radiative B decays like the one into final states with open strangeness, $B\to X_s\gamma$, and $B\to K^*\gamma$. The efforts to calculate QCD corrections to $B\to X_s\gamma$ will be briefly described. Subsequently, two examples will be discussed where the control over non-perturbative contributions is mandatory to find out whether the SM is able to describe the experimental data or not: the $\Delta I=1/2$ rule in $K\to\pi\pi$ decays and the ratio ε'/ε related to the direct CP violation in $K_L\to\pi\pi$ decays. The last two presentations deal with the role of QCD in the context of the presently most pronounced anomalies in flavor physics: the violation of lepton flavor universality in tree-level B-meson decays (Sect. 13.4) and the departure of data from the SM predictions for $(g-2)_{e,\mu}$ (Sect. 13.5).

13.1 Effective Hamiltonians in the standard model and beyond

Andrzej J. Buras

The basis for any serious phenomenology of weak decays of hadrons is the *Operator Product Expansion* (OPE) [30, 4029], which allows us to write down the effective weak Hamiltonian in full generality simply as follows

$$\mathcal{H}_{\rm eff}=\sum_i C_i\mathcal{O}_i^{\rm SM}+\sum_j C_j^{\rm NP}\mathcal{O}_j^{\rm NP},$$
$$C_i=C_i^{\rm SM}+\Delta_i^{\rm NP}. \tag{13.2}$$

Here

- $\mathcal{O}_i^{\rm SM}$ are local operators present in the SM and $\mathcal{O}_j^{\rm NP}$ are new local operators having typically new Dirac structures, in particular scalar-scalar and tensor-tensor ones.
- C_i and $C_j^{\rm NP}$ are the Wilson coefficients (WCs) of these operators. NP effects modify not only the WCs of the SM operators but also generate new operators with non-vanishing $C_j^{\rm NP}$.

Examples of operators contributing to $K^0-\bar{K}^0$ mixing observables in the SM and in any of its extensions are given as follows

$$\mathcal{O}_1^{\rm VLL}=(\bar{s}\gamma_\mu P_L d)(\bar{s}\gamma^\mu P_L d), \tag{13.3a}$$
$$\mathcal{O}_1^{\rm VRR}=(\bar{s}\gamma_\mu P_R d)(\bar{s}\gamma^\mu P_R d), \tag{13.3b}$$
$$\mathcal{O}_1^{\rm LR}=(\bar{s}\gamma_\mu P_L d)(\bar{s}\gamma^\mu P_R d), \tag{13.3c}$$
$$\mathcal{O}_2^{\rm LR}=(\bar{s}P_L d)(\bar{s}P_R d), \tag{13.3d}$$

$$\mathcal{O}_1^{\rm SLL}=(\bar{s}P_L d)(\bar{s}P_L d), \tag{13.4a}$$
$$\mathcal{O}_1^{\rm SRR}=(\bar{s}P_R d)(\bar{s}P_R d), \tag{13.4b}$$
$$\mathcal{O}_2^{\rm SLL}=(\bar{s}\sigma_{\mu\nu}P_L d)(\bar{s}\sigma^{\mu\nu}P_L d), \tag{13.4c}$$
$$\mathcal{O}_2^{\rm SRR}=(\bar{s}\sigma_{\mu\nu}P_R d)(\bar{s}\sigma^{\mu\nu}P_R d), \tag{13.4d}$$

where

$$P_{R,L}=\frac{1}{2}(1\pm\gamma_5),\qquad \sigma_{\mu\nu}=i\frac{1}{2}[\gamma_\mu,\gamma_\nu], \tag{13.5}$$

and we suppressed color indices as they are summed up in each factor. For instance $\bar{s}\gamma_\mu P_L d$ stands for $\bar{s}_\alpha\gamma_\mu P_L d_\alpha$ and similarly for other factors. Only $\mathcal{O}_1^{\rm VLL}$ is present in the SM. For meson decays the number of operators in the SM is larger. This is also the case for the number of NP operators. We will encounter some of them in Sect. 13.3.

The amplitude for a decay of a given meson $M = K, B, \ldots$ into a final state $F=\mu^+\mu^-,\ \pi\nu\bar{\nu},\ \pi\pi,\ DK$ is then simply given by

$$A(M\to F)=\langle F|\mathcal{H}_{\rm eff}|M\rangle=\textstyle\sum_i C_i(\mu)\langle F|\mathcal{O}_i^{\rm SM}(\mu)|M\rangle$$

$$+\sum_j C_j^{\rm NP}(\mu)\langle F|\mathcal{O}_j^{\rm NP}(\mu)|M\rangle \qquad (13.6)$$

where $\langle F|\mathcal{O}_i(\mu)|M\rangle$ are the matrix elements of $\mathcal{O}_i$ between M and F, evaluated at the renormalization scale μ. The WCs $C_i(\mu)$ describe the strength with which a given operator enters the Hamiltonian. They can be considered as scale dependent "couplings" related to "vertices" $\mathcal{O}_i$ and can be calculated using perturbative methods as long as the scale μ is not too small. In the case of $K^0-\bar{K}^0$ mixing, matrix elements $\langle\bar{K}^0|\mathcal{O}_i(\mu)|K^0\rangle$ are present. Other particle-antiparticle mixings have similar matrix elements.

The essential virtue of the OPE is this one. It allows us to separate the problem of calculating the amplitude $A(M\to F)$ into two distinct parts: the *short distance* (perturbative) calculation of the coefficients $C_i(\mu)$ and the *long-distance* (generally non-perturbative) calculation of the matrix elements $\langle\mathcal{O}_i(\mu)\rangle$. The scale μ separates, roughly speaking, the physics contributions into short distance contributions contained in $C_i(\mu)$ and the long distance contributions contained in $\langle\mathcal{O}_i(\mu)\rangle$.

It should be stressed that this separation of short and long distance contribution is only useful due to the asymptotic freedom in QCD [53,54] that allows us to calculate the WCs by means of ordinary or RG-improved perturbation theory. On the other hand, the matrix elements $\langle\mathcal{O}_i(\mu)\rangle$ can only be calculated by non-perturbative methods like numerical Lattice QCD computations and analytic methods like Dual QCD (DQCD) [4030,4031] and Chiral Perturbation Theory (ChPT) [69,1610].

Now, the coefficients C_i include, in addition to tree-level contributions from the W-exchange, virtual top quark contributions and contributions from other heavy particles such as W, Z bosons, charged Higgs particles, supersymmetric particles and other heavy objects in numerous extensions of this model. Consequently, $C_i(\mu)$ generally depend on m_t and also on the masses of new particles if extensions of the SM are considered. This dependence can be found by evaluating one-loop diagrams, so-called *box* and *penguin* diagrams with full W, Z, top quark and new particles exchanges and *properly* including short distance QCD effects. The latter govern the μ-dependence of $C_i(\mu)$. In models in which the GIM mechanism [80] is absent, also *tree* diagrams can contribute to flavor changing neutral current (FCNC) processes. The point is that a given C_i generally receives contributions from all these three classes of diagrams (Fig. 343).

The value of μ can be chosen arbitrarily but the final result must be μ-independent. Therefore the μ-dependence of $C_i(\mu)$ has to cancel the μ-dependence of $\langle Q_i(\mu)\rangle$. In other words as far as heavy-mass-independent terms are concerned, it is a matter of choice what exactly belongs to $C_i(\mu)$ and what to $\langle Q_i(\mu)\rangle$. This cancellation of the μ-dependence involves generally several terms in the expansion in Eq. (13.6). $C_i(\mu)$ depend also on the renormalization scheme used in the calculation of QCD effects. This scheme-dependence must also be canceled by the one of $\langle Q_i(\mu)\rangle$ so that the physical amplitudes are renormalization-scheme independent. Again, as in the case of the μ-dependence, the cancellation of the renormalization-scheme-dependence involves generally several terms in the expansion in Eq. (13.6). One of the types of scheme-dependence is the manner in which γ_5 is defined in $D=4-2\varepsilon$ dimensions implying various renormalization schemes as analyzed first in the context of weak decays in [4033]. A pedagogical presentation of these issues can be found in [4034].

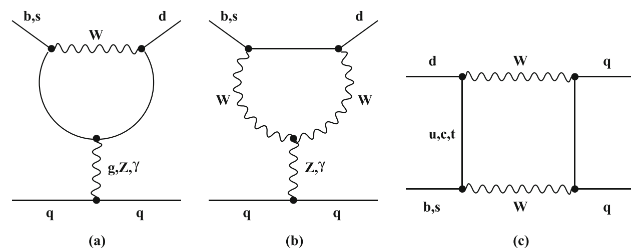

Fig. 343 Penguin and Box Diagrams. From [4032]

13.1.1 *Renormalization group improved perturbation theory*

Generally in weak decays several vastly different scales are involved. These are the hadronic scales of a few GeV, scales like M_W or m_t and – in extensions of the SM – not only of a few TeV but even 100 TeV. Already within the SM, but in particular in its NP extensions, the ordinary perturbation theory in α_s is spoiled by the appearance of large logarithms of the ratios of two very different scales that multiply α_s. Such logarithms have to be summed to all orders of perturbation theory which can be efficiently done by means of renormalization-group methods. Denoting the lower scale simply by μ and the high scale by Λ the general expression for $C_i(\mu)$ is given by:

$$\vec{C}(\mu)=\hat{U}(\mu,\Lambda)\vec{C}(\Lambda), \qquad (13.7)$$

where $\vec{C}$ is a column vector built out of C_i. $\vec{C}(\Lambda)$ are the initial conditions for the RG evolution down to low energy scale μ. They depend on the short distance physics at high energy scales. In particular they depend on m_t and the masses and couplings of new heavy particles.

The evolution matrix $\hat{U}(\mu,\Lambda)$ sums large logarithms $\log\Lambda/\mu$ which appear for $\mu\ll\Lambda$. In the so-called leading logarithmic approximation (LO) terms $(g_s^2\log\Lambda/\mu)^n$ are summed. The next-to-leading logarithmic correction (NLO) to this result involves summation of terms $(g_s^2)^n(\log\Lambda/\mu)^{n-1}$ and so on. This hierarchical structure gives the RG-improved perturbation theory.

As an example let us consider only a single operator so that Eq. (13.7) reduces to

$$C(\mu) = U(\mu, \Lambda) C(\Lambda) \tag{13.8}$$

with $C(\mu)$ denoting the coefficient of the operator in question.

Keeping the first two terms in the expansions of the anomalous dimension of this operator $\gamma(g_s)$ and in $\beta(g_s)$, that governs the evolution of α_s, in powers of α_s and g_s,

$$\gamma(g_s) = \gamma^{(0)} \frac{\alpha_s}{4\pi} + \gamma^{(1)} \left(\frac{\alpha_s}{4\pi}\right)^2, \tag{13.9}$$

$$\beta(g_s) = -\beta_0 \frac{g_s^3}{16\pi^2} - \beta_1 \frac{g_s^5}{(16\pi^2)^2} \tag{13.10}$$

gives:

$$U(\mu, \Lambda) = \left[1 + \frac{\alpha_s(\mu)}{4\pi} J_1\right] \left[\frac{\alpha_s(\Lambda)}{\alpha_s(\mu)}\right]^P \left[1 - \frac{\alpha_s(\Lambda)}{4\pi} J_1\right] \tag{13.11}$$

where

$$P = \frac{\gamma^{(0)}}{2\beta_0}, \qquad J_1 = \frac{P}{\beta_0}\beta_1 - \frac{\gamma^{(1)}}{2\beta_0}. \tag{13.12}$$

General formulae for the evolution matrix $\hat{U}(\mu, \Lambda)$ in the case of operator mixing and valid also for electroweak effects at the NLO level can be found in [4035]. The corresponding NNLO formulae are rather complicated and were given for the first time in [4036].

While by now NLO and NNLO QCD contributions to almost all weak decays are known within the SM, the pioneering LO calculations for current–current operators [1209,1210], penguin operators [4037,4038], $\Delta S = 2$ operators [4039] and rare K decays [4040] should not be forgotten. The first review of NLO QCD calculations can be found in [4035] and more recently including NNLO corrections in [4034,4041].

It should be stressed that at the NLO level not only two-loop anomalous dimensions of operators have to be known but also QCD corrections to the WCs at $\mu = \Lambda$. Only then renormalization-scheme independent results can be obtained. They are known for most processes of interest and this technology is explained in details in [4032,4034]

On the whole, the status of present short distance (SD) contributions within the SM is satisfactory. Let us then see what is the status of these calculations beyond the SM.

13.1.2 QCD effects beyond the SM

As already stated at the beginning, NP contributions can affect the WCs of the SM operators. This modification takes place at the NP scale Λ so that after the RG evolution, the $C_i(\mu)$ in Eq. (13.6) are modified. But in addition new operators with different Dirac structure, with examples given in Eqs. (13.3) and (13.4), can contribute if their coefficients $C_j^{\mathrm{NP}}(\Lambda)$ are non-vanishing or if they are generated by mixing of different operators in the process of the RG evolution. The inclusion of these contributions in the RG analysis requires at the NLO level the calculations of their one-loop and two-loop anomalous dimensions. While the one-loop anomalous dimensions of such operators have been calculated in [717], the first two-loop calculations have been presented in [4042,4043]. Recently, these NLO calculations have been generalized for both $\Delta F = 1$ and $\Delta F = 2$ transitions in the so-called Weak Effective Theory (WET) [4044,4045] and also for the Standard Model Effective Field Theory (SMEFT) [4046]. It turns out that the anomalous dimensions of operators involving both left-handed and right-handed currents, the so-called left-right operators, are much larger than those of most operators within the SM except for QCD-penguin operators. Thus even if their WCs could be small at the scale Λ they can be enhanced at scales of the order of a few GeV. The same applies also to scalar operators.

13.1.3 Hadronic matrix elements

The WCs, that include in the SM the CKM factors, are not the whole story. To obtain the results for the decay amplitudes and the quark mixing observables, also hadronic matrix elements of local operators, like the ones in Eqs. (13.3) and (13.4), have to be calculated. The present status can be summarized as follows.

– For leptonic decays like $B_{s,d} \to \mu^+\mu^-$ and $K_{L,S} \to \mu^+\mu^-$ only the weak decay constants f_{B_s}, f_{B_d} and f_K are required. They are defined e.g. by

$$\langle 0|(\bar{s}\gamma^\mu(1-\gamma_5)u)|K^+\rangle = i f_K p_K^\mu, \tag{13.13}$$

where p_K^μ is the four-momentum of the decaying K^+ mesons. Similar for f_{B_s} and f_{B_d}.
They are known from LQCD calculations already with an impressive precision [68,722,4047]

$$f_{B_s} = 230.3(1.3)\,\mathrm{MeV},\ f_{B_d} = 190.0(1.3)\,\mathrm{MeV},$$
$$f_K = 155.7(3)\,\mathrm{MeV}, \tag{13.14}$$

although in the case of $K_{L,S} \to \mu^+\mu^-$ also genuine long distance QCD contributions enter. They cannot be described by matrix elements of local operators and one has to develop some strategies to isolate the contribution described by the effective Hamiltonian discussed by us. In $B_{s,d}$ and $B^\pm$ decays such effects are much smaller. However, they are significant in charm meson decays.

- In semileptonic decays like $K^+ \to \pi^+ \nu\bar{\nu}$, $K_L \to \pi^0 \nu\bar{\nu}$, $K_L \to \pi^0 \ell^+\ell^-$, $B \to K(K^*)\ell^+\ell^-$, $B \to D(D^*)\,\ell^+\ell^-$ and $B \to K(K^*)\nu\bar{\nu}$ the formfactors for the transitions $K \to \pi$, $B \to K(K^*)$, $B \to D(D^*)$ enter. For K decays these form factors can even be extracted from data on leading decays with the help of ChPT and isospin symmetry [4048–4050]. Those that enter B decays they are usually calculated using lightcone sum rules for low momentum transfer squared q^2 [4051] and LQCD for large q^2 [4052,4053]. Significant progress has been made here by now with most recent analyses in [740,4054–4056] where more information can be found.
- Moreover Heavy Quark Effective Theory (HQET) and Heavy Quark Expansions (HQE) play an important roles here. HQET represents a static approximation for the heavy quark, covariantly formulated in the language of an effective field theory. It allows us to extract the dependence of hadronic matrix elements on the heavy quark mass and to exploit the simplifications that arise in QCD in the static limit. The most important application of HQET has been to the analysis of exclusive semileptonic transitions involving heavy quarks, where this formalism allows us to exploit the consequences of heavy quark symmetry to relate form factors and provides a basis for systematic corrections to the $m \to \infty$ limit. There are several excellent reviews on this subject [711,1429,4057,4058].
- For the calculation of the width differences in $B^0_{s,d} - \bar{B}^0_{s,d}$ mixing $\Delta\Gamma_{s,d}$, lifetimes and totally inclusive decay rates of heavy hadrons, the so-called heavy quark expansion (HQE) has been developed by several authors. It relies on the smallness of the parameter $\Lambda_{\rm QCD}/m_b$, where $\Lambda_{\rm QCD}$ is a hadronic scale. The coefficients in this expansion can be calculated by LQCD. Nice reviews with some details are the ones in [711,1223,1237,4059] and a nice summary of the present situation including historical development can be found in [4060].
- For $\Delta M_{s,d}$ significant progress has been made by LQCD in the recent years. Here the relevant hadronic matrix elements are parametrized by $f_{B_s}\sqrt{\hat{B}_s}$ and $f_{B_d}\sqrt{\hat{B}_d}$ with $\hat{B}_s$ and $\hat{B}_d$ close to unity. Presently the most accurate results are those from HPQCD collaboration [722]

$$f_{B_s}\sqrt{\hat{B}_s} = 256.1(5.7)\,\text{MeV},$$
$$f_{B_d}\sqrt{\hat{B}_d} = 210.6(5.5)\,\text{MeV} \tag{13.15}$$

that in addition to light quarks includes charm quarks. Also corresponding matrix elements for BSM operators are already known but their precision should be still improved. Similarly, the relevant hadronic matrix elements for the parameter ε_K describing the indirect CP-violation in $K_L \to \pi\pi$ decay are already known with respectable precision from LQCD both in the SM and beyond [721,4061,4062]. Some physics insight into the numerical LQCD results has also been gained with the help of the DQCD approach [4063].
- The calculations of hadronic matrix elements for non-leptonic decays like $K \to \pi\pi$, $B \to \pi K$ etc. are much more involved. For $K \to \pi\pi$ the only approaches providing matrix elements that can be consistently combined (matched) with the WCs are LQCD, led by the RBC-UKQCD collaboration and the DQCD approach. But while from LQCD only the matrix elements of SM operators are known, all matrix elements of BSM operators have been calculated using the DQCD approach [4064]. Yet, the accuracy of the latter calculations have to be improved, and one should hope that also LQCD collaborations will calculate these matrix elements one day. However, based on the time required to compute the matrix elements of SM operators using LQCD, it could take even a decade to obtain satisfactory results on these matrix elements from LQCD. This is important in view of the present status of the direct CP violation in $K_L \to \pi\pi$ decay represented by the ratio ε'/ε. We will return to this issue in Sect. 13.3.
- For non-leptonic exclusive B decays LQCD cannot provide the hadronic matrix elements directly but can help in calculating non-perturbative parameters in the context of the so-called *QCD factorization* (QCDF) [4065,4066]. This approach can be applied to $B \to \pi\pi$, but also to rare and radiative decays, such as $B \to K^*\gamma$ or $B \to K^* l^+ l^-$. In the heavy-quark limit, that is up to relative corrections of order $\Lambda_{\rm QCD}/m_b$, the problem of computing exclusive hadronic decay amplitudes simplifies considerably. A nice review by Buchalla can be found in Section 7.4 of [4034], and also the one by Beneke [4067] can be strongly recommended. There, also the so-called soft-collinear effective theory (SCET) [1802,1804] is briefly discussed.
- Last but certainly not least one should mention numerous strategies for the study of the QCD dynamics in non-leptonic B decays like $B \to \pi\pi$, $B \to \pi K$ and $B \to KK$ that utilize $SU(3)$ flavor symmetry. They play a role also in the extraction of the angles of the unitarity triangle, in particular of the angle γ. They are reviewed in Chapter 8 of [4034]. A good example here is the paper [4068] and numerous papers of Fleischer and collaborators. These studies are also useful for the search for new physics.

13.2 The quark mixing matrix

Paolo Gambino

The rich flavor structure of the Standard Model (SM) and its CP violation both follow from the matrices of Yukawa couplings between the fermions (down and up quarks and charged leptons) and the Higgs boson. The diagonalisation of these matrices determines the fermion masses and brings us to the flavor basis, where the charged weak current is no longer diagonal: as first understood in the hadronic sector by Cabibbo [4028] and extended to three generations by Kobayashi and Maskawa [86], charged currents mix the quarks of different generations in a way parameterized by the Cabibbo–Kobayashi–Maskawa (CKM) quark mixing matrix. Interestingly, its elements display a remarkable hierarchy, possibly indicative of the unknown mechanism of flavor breaking [4069]:

$$\hat{V}_{\rm CKM} = \begin{pmatrix} V_{ud} & V_{us} & V_{ub} \\ V_{cd} & V_{cs} & V_{cb} \\ V_{td} & V_{ts} & V_{tb} \end{pmatrix} = \begin{pmatrix} 1-\lambda^2/2 & \lambda & A\lambda^3(\rho - i\eta) \\ -\lambda & 1-\lambda^2/2 & A\lambda^2 \\ A\lambda^3(1-\rho-i\eta) & -A\lambda^2 & 1 \end{pmatrix} + O(\lambda^4) \tag{13.16}$$

where $\lambda = \sin\theta_c \simeq 0.22$ is a small expansion parameter and $A \simeq 0.8$, $\rho \simeq 0.16$, $\eta \simeq 0.36$. As a unitary matrix, $\hat{V}_{\rm CKM}$ has in principle nine free parameters but some of them can be absorbed by phase redefinitions. In the end, $\hat{V}_{\rm CKM}$ has only four independent real parameters: three Euler angles and a phase, or equivalently λ, A, ρ and η. The presence of a nonvanishing phase, i.e. of an imaginary part, implies CP violation. Since unitarity is specific to the three generations of the SM and to the absence of additional flavor violation, testing $\hat{V}^\dagger_{\rm CKM}\hat{V}_{\rm CKM} = 1$ is an important step in the verification of the SM and represents the modern equivalent of the tests of the universality of the charged currents. Any of the off-diagonal relations can be represented by a triangle in the complex plane whose area is a measure of CP violation. In particular, the triangle

$$1 + \frac{V_{ud}V^*_{ub}}{V_{cd}V^*_{cb}} + \frac{V_{td}V^*_{tb}}{V_{cd}V^*_{cb}} = 0 \tag{13.17}$$

is frequently considered because it has sides of comparable length, see Fig. 344, and its parameters can all be well determined in B decays. Fixing the unphysical phases as in the second line of (13.16), the angles β and γ at the basis of this triangle correspond to the phases of the elements V_{ub} and V_{td}: $V_{ub} = |V_{ub}|e^{-i\gamma}$, $V_{td} = |V_{td}|e^{-i\beta}$. Various observables constrain the apex of this triangle. The results of a global fit are shown in Fig. 344, where one can see that different constraints agree well, verifying unitarity and determining the apex of the triangle with high accuracy. As we will see below, there are tests of the unitarity of $\hat{V}_{\rm CKM}$ that cannot be represented in this plot.

The role of QCD in the determination of the CKM elements and in testing the CKM mechanism is crucial, with important perturbative and nonperturbative aspects depending on the observable; some of the nonperturbative methods have already been discussed in Sects. 4.7 and 5.7.

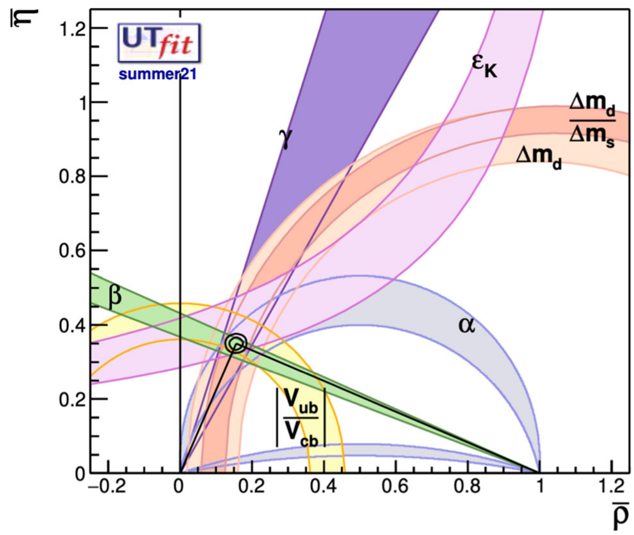

Fig. 344 Constraints on the apex of the Unitarity Triangle of (13.17) and their combination according to the UTFit collaboration. Figure taken from Ref. [4070]. $\bar{\rho} = \rho(1-\lambda^2/2)$, $\bar{\eta} = \eta(1-\lambda^2/2)$

The experimental and theoretical progress made in the last 30 years is enormous and was mostly driven by lattice QCD; it allows for very precise tests of the CKM mechanism, as is apparent from Fig. 344. Further improvements will be possible with LHCb and Belle II data, but will generally require an effective synergy of theory and experiment. In this section I will focus on measurements where QCD effects are most relevant and where tensions have appeared with the SM.

13.2.1 The Cabibbo angle and the first row unitarity

The parameter λ in Eq. (13.16) corresponds to the sine of the Cabibbo angle and is determined, up to very small higher orders in λ, by $|V_{us}|$ or $|V_{cd}|$. The high precision with which $|V_{ud}|$ is known also allows for a competitive λ determination. The unitarity of the CKM matrix implies for the first row the relation

$$\Sigma_1 = |V_{ud}|^2 + |V_{us}|^2 + |V_{ub}|^2 = 1, \tag{13.18}$$

but since $|V_{ub}| \approx 0.004$ only the first two terms are relevant. Precise measurements of $|V_{us}|$ and $|V_{ud}|$ therefore lead to a first important check of the CKM mechanism.

The most precise determination of $|V_{ud}|$ comes from superallowed Fermi transitions (SFT), i.e. $0^+ \to 0^+$ nuclear β decays. At the tree level, these decays are mediated by the vector current, whose conservation allows for a particularly clean theoretical description. Among recent refinements, hadronic effects in the radiative corrections, in particular in the γW box, have been studied with dispersive methods [4071,4072], and the effect of nuclear polarizability, which depends on nuclear structure (NS), has been exposed [4073]. Considering 15 different superallowed transitions gives a consistent result and the error of the final value [4074],

$$|V_{ud}| = 0.97367(32) \qquad (0^+ \to 0^+) \tag{13.19}$$

is dominated by the NS effects. Neutron β decay depends on the nucleon isovector axial charge g_A/g_V and has recently become competitive, $|V_{ud}| = 0.97413(43)$, if one includes only the current best experiments [4075]. Theoretically the cleanest channel is $\pi^+ \to \pi^0 e\nu$, which is however limited by a very small $O(10^{-8})$ BR. The present uncertainty based on PIBETA results [4076], $\delta V_{ud} \sim 0.003$, is still far from being competitive, but there are plans to improve drastically on that [4077].

$|V_{us}|$ can be directly accessed from kaon, hyperon, and tau semileptonic decays. The kaon decays, $K \to \pi\ell\nu$ or $K_{\ell 3}$ are measured in five channels ($K_{L,S}$, K^+ with electron and muons) affected by different systematics, with $K \to \pi$ form factors computed on the lattice, as discussed in Sect. 4.7. Combining experimental data and the average of several $N_f = 2+1+1$ lattice results one obtains [513]

$$|V_{us}| = 0.2231(4)_{exp}(4)_{lat} \qquad (K_{\ell 3}), \tag{13.20}$$

see also [4075]. At this level of precision, however, a consistent treatment of QED effects in the lattice calculation becomes mandatory [68]. Hyperon decays give a consistent $|V_{us}|$ but are presently not competitive with the above result. The ratio of inclusive tau decays into strange and non-strange hadrons can also be used to extract $|V_{us}|/|V_{ud}|$, employing experimental data and Finite Energy Sum Rules, without lattice input. Recent results tend to be over 2σ lower than Eq. (13.20) and are subject to debate [4078,4079], but a combination of experimental and lattice data on the hadronic vacuum polarization functions gives $|V_{us}| = 0.2245(11)_{exp}(13)_{th}$ [4080], in agreement with Eq. (13.20). Exclusive tau decay channels or ratio such as $\mathcal{B}(\tau \to K\nu)/\mathcal{B}(\tau \to \pi\nu)$ can also be used together with $f_{K,\pi}$ computed on the lattice, see Sect. 4.7, to obtain $|V_{us}| = 0.2229(19)$ [4081], again consistent with Eq. (13.20).

A very precise determination of the ratio $|V_{us}|/|V_{ud}|$ can be obtained from the ratio of $K \to \mu\nu(\gamma)$ to $\pi \to \mu\nu(\gamma)$ decays [693]. Here nonperturbative QCD sits almost completely in the ratio of f_K and f_π, which is known with a 0.2% uncertainty in 2+1+1 lattice QCD [68]. It then follows [4075]

$$\left|\frac{V_{us}}{V_{ud}}\right| = 0.2311(5) \qquad (K_{\mu 2}) \tag{13.21}$$

with the uncertainty dominated by lattice QCD. Using unitarity this is equivalent to $|V_{us}| = 0.2245(5)$ and in some tension with Eq. (13.20).

The most precise constraints can be combined in the $(|V_{ud}|, |V_{us}|)$ plane, see Fig. 345. We observe a clear tension

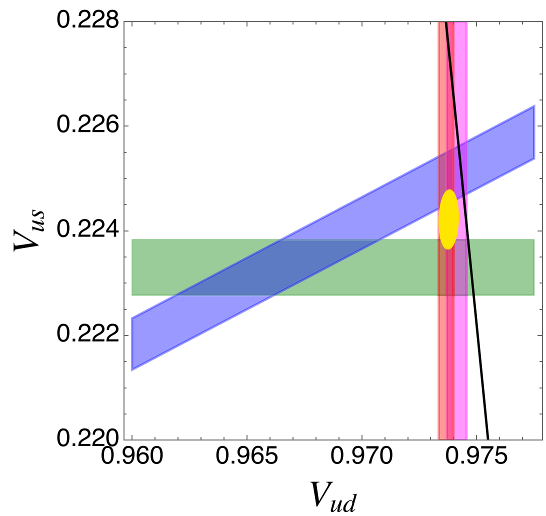

Fig. 345 1σ constraints in the $(|V_{ud}|, |V_{us}|)$ plane from superallowed Fermi transitions (red), from neutron decay (violet), $K_{\ell 3}$ (green), $K_{\mu 2}$ (blue) and the 68% CL contour of the combined fit (yellow). The black line marks the unitarity relation between $|V_{ud}|$ and $|V_{us}|$. Figure taken from [4075]

between the best fit and unitarity, mostly driven by the kaon determinations, which cross far from the unitarity line, and by the superallowed Fermi transitions, which under unitarity imply a very high $|V_{us}|$. On the other hand, $|V_{us}|$ from $K_{\ell 2}$ and the neutron $|V_{ud}|$ are compatible with unitarity. Taking the average of the determinations from Fermi and n decay, $|V_{ud}| = 0.97384(26)$, the actual deviation of Σ_1 from 1 varies between about 1.5σ using Eq. (13.21) and $\sim 3\sigma$ using Eq. (13.20) and it is sometimes referred to as the *Cabibbo anomaly*. It could be due to underestimated uncertainties in the NS correction, in the lattice calculations, in the experimental results, or due to New Physics [4082,4083], and a renewed campaign of $K_{\mu 3}$ and $K_{\mu 2}$ measurements will be crucial to clarify the situation [4075].

As mentioned above, λ can also be determined from $D_{(s)} \to \ell\nu$ and $D \to \pi(K)\ell\nu$. Concerning the former, as lattice calculations for f_D have become very precise, the uncertainties in $|V_{cs}| = 0.982(10)_{exp}(2)_{lat}$ and $|V_{cd}| = 0.2181(49)_{exp}(7)_{lat}$ [4081] are dominated by experiment. These results are consistent with Eqs. (13.19, 13.20). FLAG has performed a combined fit to lattice and experimental data for the two D semileptonic decays that yields $|V_{cs}| = 0.971(7)$ and $|V_{cd}| = 0.234(7)$ [68], but $|V_{cd}|$ is about 2σ above its $D \to \mu\nu$ value. Averaging all these results, one can check the unitarity of the second row of the CKM matrix [68],

$$\Sigma_2 = |V_{cd}|^2 + |V_{cs}|^2 + |V_{cb}|^2 = 1 + 0.001(11), \tag{13.22}$$

where again the last term in the sum is negligible at the present accuracy. Neutrino Deep Inelastic Scattering is also used to extract a consistent but less precise value of $|V_{cd}|$. The second row of $\hat{V}_{CKM}$ appears to be consistent with unitarity, but the accuracy is much lower than for the first row.

13.2.2 Determination of V_{cb} and V_{ub}

The magnitudes of two of the elements of the CKM matrix, $|V_{ub}|$ and $|V_{cb}|$, can be directly extracted from semileptonic b-hadron (mostly B meson) decays. In exclusive decays one looks at specific hadronic final states, while inclusive decays sum over all decays channels to a certain flavor (i.e. $b \to c$). Inclusive and exclusive semileptonic decays are subject to very different theoretical and experimental systematics, see Refs. [4084,4085] for recent reviews.

The results of the B factories, analysed in the light of the most recent theoretical calculations, are puzzling, because – especially for $|V_{cb}|$ – the determinations from exclusive and inclusive decays are in strong tension, and despite recent new experimental and theoretical results the situation remains unclear. While in principle New Physics may explain the tensions, it is significantly constrained by the measured differential distributions in $B \to D^{(*)}\ell\nu$ [4086] and, in the context of the SM Effective Theory or SMEFT, by LEP data [4087]. This tension is all the more relevant as measurements in the semitauonic channels at Belle, BaBar, and LHCb show discrepancies with the SM predictions, pointing to a possible violation of lepton-flavor universality. This V_{cb} puzzle casts a shadow on our understanding of semitauonic decay as well. The inability to determine precisely V_{cb} also hampers significantly NP searches in Flavor Changing Neutral Currents processes: the uncertainty on the value of V_{cb} dominates the theoretical uncertainty in the SM predictions for several observables, from ε_K to the branching fraction of $B_s \to \mu^+\mu^-$.

Our understanding of inclusive semileptonic B decays, see also Sect. 5.7, is based on a simple idea: since inclusive decays sum over all possible hadronic final states, the quark in the final state hadronizes with unit probability and the transition amplitude is sensitive only to the long-distance dynamics of the initial B meson. Thanks to the large hierarchy between the typical energy release, of $O(m_b)$, and the hadronic scale $\Lambda_{\rm QCD}$, and to asymptotic freedom, any residual sensitivity to non-perturbative effects is suppressed by powers of $\Lambda_{\rm QCD}/m_b$. From a phenomenological point of view, it is remarkable that the linear preasymptotic correction is actually absent and that the leading nonperturbative corrections are $O(\Lambda_{\rm QCD}^2/m_b^2)$. This is due to the Operator Product Expansion (OPE) that allows us to express the nonperturbative physics in terms of B meson matrix elements of local operators of dimension $d \geq 5$, while the Wilson coefficients can be expressed as a perturbative series in α_s [1253–1255,4088,4089]. The OPE disentangles the physics associated with *soft* scales of order $\Lambda_{\rm QCD}$ (parameterized by the matrix elements of the local operators) from that associated with *hard* scales $\sim m_b$, which determine the Wilson coefficients. Inclusive observables such as the total semileptonic width and the moments of the kinematic distributions are therefore double expansions in α_s and $\Lambda_{\rm QCD}/m_b$, with a leading term that is given by the free b quark decay. As already noted, the power corrections start at $O(\Lambda_{\rm QCD}^2/m_b^2)$ and are comparatively suppressed. At higher orders in the OPE, terms suppressed by powers of m_c also appear, starting with $O(\Lambda_{\rm QCD}^3/m_b^3 \times \Lambda_{\rm QCD}^2/m_c^2)$ [4090]. The expansion for the total semileptonic width is

$$\Gamma_{sl} = \Gamma_0\Big[1 + a^{(1)}\frac{\alpha_s(m_b)}{\pi} + a^{(2)}\Big(\frac{\alpha_s}{\pi}\Big)^2 + a^{(3)}\Big(\frac{\alpha_s}{\pi}\Big)^3 + \left(-\frac{1}{2} + p^{(1)}\frac{\alpha_s}{\pi}\right)\frac{\mu_\pi^2}{m_b^2} + \left(g^{(0)} + g^{(1)}\frac{\alpha_s}{\pi}\right)\frac{\mu_G^2(m_b)}{m_b^2} + d^{(0)}\frac{\rho_D^3}{m_b^3} - g^{(0)}\frac{\rho_{LS}^3}{m_b^3} + \text{higher orders}\Big], \tag{13.23}$$

where Γ_0 is the tree-level free-quark decay width, and μ_π^2, μ_G^2, ρ_D^3 and ρ_{LS}^3 are hadronic parameters that have to be determined from experimental data, i.e. from the moments of differential distributions, which can be expanded in the same way as the total width. The perturbative corrections are known up to $O(\alpha_s^3)$ and $O(\alpha_s/m_b^3)$ for the total width [1239,4091] and up to $O(\alpha_s^2)$ and $O(\alpha_s/m_b^2)$ for the moments [4092–4095]. In line with the discussion of Sect. 5.7, it is important that m_b and the other Heavy-Quark Expansion (HQE) parameters are free from renormalon ambiguities. The kinetic scheme [4096,4097], for instance, employs a Wilsonian cutoff $\mu \sim 1\,\text{GeV}$. Higher power corrections have been considered in [4098–4100] and appear to have a negligible impact on $|V_{cb}|$. Although the moments are rather sensitive to the difference $m_b - m_c$, a more precise determination of $|V_{cb}|$ can be obtained taking advantage of the precise lattice determinations of the charm and bottom masses, see [513] for a review. The most recent global analysis in the kinetic scheme [4101] gives

$$|V_{cb}| = 42.16(51) \times 10^{-3}, \qquad (B \to X_c\ell\nu) \tag{13.24}$$

where the uncertainty follows from the combination of theoretical and experimental uncertainties. A consistent but less precise result has been recently obtained from an analysis of the new Belle and Belle II measurements of the q^2 moments [4102]. While the estimate in Eq. (13.24) appears solid, new measurements at Belle II will provide welcome checks and may reduce the experimental uncertainty. There are also a few more higher order effects worth computing, and QED effects should be understood better. Most importantly, however, lattice calculations of inclusive quantities are now possible and may soon complement the OPE approach [750,4103].

The inclusive determination of $|V_{ub}|$ from $B \to X_u\ell\nu$ decays differs from that of $|V_{cb}|$ mostly because of the experimental cuts necessary to suppress the large $b \to c\ell\nu$

background: the local OPE does not converge well in the restricted phase space. The modern description of these inclusive decays is therefore based on a non-local OPE [1257,1258], where nonperturbative shape functions (SFs) play the role of parton distribution functions of the b quark inside the B meson. While the first few moments of the SFs are expressed in terms of the same HQE parameters extracted in $B \to X_c \ell\nu$, direct experimental information on the SFs is limited to the $B \to X_s\gamma$ photon spectrum, to which they are only related in the $m_b \to \infty$ limit. There are a few frameworks that incorporate the above picture with a range of additional assumptions: BLNP [4104] and GGOU [4105] use a large set of models for the SFs, while DGE [4106] computes the leading SF in resummed perturbative QCD. Another potential source of theoretical uncertainty in all approaches is represented by the so called Weak Annihilation contributions, namely nonperturbative contributions at high q^2 arising from $b\bar{q}$ weak annihilations (WA) in the B meson, where the $\bar{q}$ is not necessarily the light valence quark [4107]. Charm decays, and particularly moments of the inclusive leptonic spectrum, constrain them effectively, and one can conclude that the WA correction to the total rate of $B \to X_u\ell\nu$ must be smaller than about 2% [4108,4109]. Its localisation at high q^2 and the sensitivity of the q^2 tail to higher power corrections suggest that an upper cut on q^2 would be useful in future analyses.

A few experimental analyses extend the measurement into the phase space region dominated by $b \to c$ transitions, which are then modelled, trading part of the theory uncertainty for a larger systematic experimental uncertainty (in particular, D^{**} and multihadron final states are not known very well): agreement among the various analyses should then increase our confidence in the result, but one should be aware that the reconstruction efficiencies depend on the modelling of the signal, i.e. again on the SFs. The latest Heavy flavor Averaging Group (HFLAV) $|V_{ub}|$ world averages in the three above frameworks [4081] are based on a number of different experimental results with different kinematic cuts and read

$$\begin{aligned} |V_{ub}|^{\rm BLNP} &= 4.28(13)^{+20}_{-21} \times 10^{-3}, \\ |V_{ub}|^{\rm GGOU} &= 4.19(12)^{+11}_{-12} \times 10^{-3}, \\ |V_{ub}|^{\rm DGE} &= 3.93(10)^{+9}_{-10} \times 10^{-3}, \end{aligned} \tag{13.25}$$

where the first uncertainty is experimental and the second comes from theory. Unfortunately, they do not agree well with each other. Moreover, the values obtained from different experimental analyses are not always compatible within their stated theoretical and experimental uncertainties. The latest electron endpoint analysis by BaBar [4110], in particular, shows a dependence on the model used to simulate the signal and leads to sharply different results in BLNP and GGOU. This is the most precise analysis to date; in GGOU it favours a lower $|V_{ub}| = 3.96(10)(17) \times 10^{-3}$ while in BLNP the result is $|V_{ub}| = 4.41(12)(27) \times 10^{-3}$. While it is possible that modelling the signal has biased previous endpoint results, we stress that analyses involving a larger fraction of the phase space are generally less sensitive to SFs and other theoretical systematics, which are inherently difficult to estimate. In this respect, applying a cut on the hadronic invariant mass $M_X < 1.7$ GeV seems to be the safest approach, as it depends little on the reconstruction of the $b \to c$ background, captures almost 60% of the phase space, and strikes a balance between experimental and theoretical uncertainties. In the recent Babar analysis [4111], where machine learning techniques and hadronic tagging were used to reduce backgrounds, the result in GGOU (very much consistent with BLNP and DGE) is

$$|V_{ub}| = 3.97(18)(17) \times 10^{-3}, \qquad (B \to X_u\ell\nu) \tag{13.26}$$

which in my opinion represents the current state of the art. Improvements will certainly come from the higher statistics available at Belle II and from the implementation of higher order calculations such as [4112]. For instance, the complete $O(\alpha_s^2)$ perturbative contributions to the triple differential rate is still missing, despite numerical results for the moments [4113]. A precise study of the differential spectra, recently measured at Belle for the first time [4114], will validate the theoretical frameworks and help constrain the SFs. The SIMBA [1840] and NNVub [4115] methods are well posed to analyse the Belle II data in a model independent and efficient way. In the longer run, lattice studies like those mentioned for inclusive $b \to c$ transitions should also become possible.

The exclusive $B \to D\ell\nu$ and $B \to D^*\ell\nu$ channels are also used to extract $|V_{cb}|$. These decays are described by nonperturbative form factors which are computed in lattice QCD (as discussed in Sect. 4.7) as well as with approximate methods like Light Cone Sum Rules (LCSR), see Sect. 5.7. Typically, the lattice calculations are better under control at large or maximal q^2, corresponding to small or vanishing recoil, while LCSR calculations prefer the small q^2 range and are less precise. Moreover, heavy quark symmetry guarantees that the form factors at zero recoil are absolutely normalized in the heavy quark limit. As the rates vanish at zero recoil in both cases, see Eq. (4.188), the experimental data are much less precise at low recoil and one needs to parameterize the form factors in a model independent way in order to describe the form factors in the whole kinematic range and to interpolate between the small and large recoil regions. Model independent parametrizations based on a dispersive approach have been developed in the 1990s and the two most relevant ones are known as BGL and BCL [4116,4117]; the form factors are expressed, up to known prefactors, as series in the

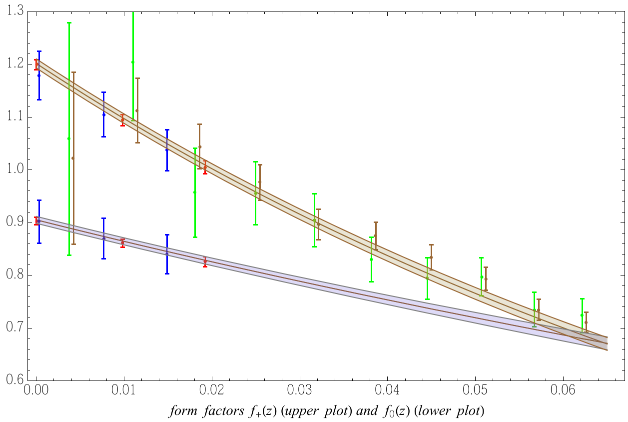

Fig. 346 Form factors $f_{+,0}(z)$ for the $B \to D$ transitions computed by FNAL/MILC [4126] (red) and HPQCD [4127] (blue) and experimental data from Belle (brown) and BaBar (green) normalized by the fitted value of $|V_{cb}|$. The bands show the results of the global fit. Figure from Ref. [4128]

variable

$$z = \frac{\sqrt{w+1} - \sqrt{2}}{\sqrt{w+1} + \sqrt{2}}, \tag{13.27}$$

where $w = (m_B^2 + M_{D^{(*)}} - q^2)/(2m_B m_{D^{(*)}})$. In the physical range z is small, < 0.07, and unitarity puts constraints on the size of the series coefficients. A variant, proposed in [4118] and known as CLN, additionally employs Next to Leading Order Heavy Quark Effective Theory relations and QCD sum rules to reduce the number of relevant parameters to two. These additional inputs imply an uncertainty that can no longer be neglected, see [4119–4122] for updates and improvements on the CLN approach. It is then unfortunate that prior to 2016 the experimental results were generally given in terms of fits to the CLN parametrization, without accounting for this uncertainty. More recent measurements [4123–4125] provide the differential q^2 and angular (for $B \to D^*\ell\nu$) unfolded distributions or the necessary ingredients (efficiencies and response functions) to *fold* theoretical predictions and get the yields in each bin.

In the $B \to D\ell\nu$ case precise lattice calculations at small but non-zero recoil are available since several years [4127, 4129] and have been combined with the experimental results of Refs. [4123,4130] to get [4128]

$$|V_{cb}| = 40.5(1.0)10^{-3} \qquad (B \to D\ell\nu). \tag{13.28}$$

A similar value is found in [68]. Indeed, the lattice and experimental form factor shapes are in good agreement, satisfy the unitarity constraints, and the overall fit is good and stable, see Fig. 346. The BGL and BCL parametrizations give identical results and the fit also provides a SM prediction for the Lepton Flavor Universality ratio $R(D) = \Gamma(B \to D\tau\nu)/\Gamma(B \to D\mu\nu) = 0.299(3)$ [4128], in reasonable agreement with the experimental world average $R(D)_{exp} = 0.339(30)$ [4081].

In the $B \to D^*\ell\nu$ channel the situation is more complicated. From the experimental point of view this channel allows for a more precise determination of $|V_{cb}|$ than the $B \to D$ channel and angular distributions can be studied in addition to the q^2 distribution. On the other hand, the D^* meson decays strongly to $D\pi$ (it cannot be considered stable) and three (four) different form factors contribute for a massless (massive) lepton. The only lattice calculation of these form factors away from the zero-recoil point has been published so far by the Fermilab-MILC Collaboration [745], although JLQCD and HPQCD calculations are in their final stage [747,4131]. Restricting to experimental analyses that provide data in a model independent way, Belle has presented a tagged [4124] and an untagged analysis [4125]. The dataset of [4124] showed for the first time that the extraction of $|V_{cb}|$ could strongly depend on the parametrization employed: BGL and CLN both gave reasonable fits with $|V_{cb}|$ values differing by about 6% [4132,4133]. It has recently been replaced by a new untagged analysis [4134] that does not present this problem, but the point remains valid: parametrizations matter and the related uncertainties have to be carefully considered. The more precise dataset of the untagged analysis [4125], despite a few problems [4135], did not show any parametrization dependence. A global fit based on [4136] that includes the Fermilab calculation [745], unitarity constraints, and the Belle untagged data only, while adjusting for the D'Agostini bias [4137], leads to

$$|V_{cb}| = 39.3(9)10^{-3} \qquad (B \to D^*\ell\nu), \tag{13.29}$$

but the agreement between the Fermilab form factor shape and the experimental distributions is not good and the total χ^2 is large.[117] An additional uncertainty of $\sim 0.5\%$ for missing QED corrections should be added to Eq. (13.29), as well as to Eqs. (13.24) and (13.28). There is also a troubling tension between the Fermilab results and the ratio of form factors computed in NLO HQET. Preliminary results for the $B \to D^*$ form factors have also been disclosed by the JLQCD collaboration [4138] and in this case the agreement with Belle data is much better, with a final $|V_{cb}| = 40.7(^{+1.0}_{-0.9})10^{-3}$. One can also add LCSR constraints on the form factors [4055], with minimal change in $|V_{cb}|$. Despite these latest developments, HFLAV also quotes an average of experimental results in the CLN parametrization based on the form factor at zero recoil only, $|V_{cb}| = 38.46(68)\ 10^{-3}$, but this result is subject to uncontrolled uncertainties related to the way the CLN parametrization has been used. The two Belle datasets have also been analysed in the Dispersive Matrix approach [4139],

[117] The result in (13.29) differs from that reported in [745] and adopted in [513], $|V_{cb}| = 38.4(7)10^{-3}$, mostly because of the D'Agostini bias (not considered in [745]), of the way unitarity constraints are implemented, and of the QED Coulomb factor that is included in [745], neglecting however other QED corrections.

where the form factors are constrained by the Fermilab lattice data and unitarity only; tensions with the experimental data are observed here as well. The fit that originates Eq. (13.29) gives also $R(D^*) = \Gamma(B \to D^*\tau\nu)/\Gamma(B \to D^*\mu\nu) = 0.249(1)$, confirming the tension with the experimental world average $R(D^*)_{exp} = 0.295(14)$ [4081].

LHCb has recently performed the first determination of $|V_{cb}|$ using B_s^0 decays [4140]. Using both $B_s^0 \to D_s^{(*)-}\mu^+\nu$ and the lattice results from Refs. [746,4141], they obtain $|V_{cb}| = 41.7(0.8)(0.9)(1.1)10^{-3}$. On the other hand, BaBar using a simplified BGL parametrization finds $|V_{cb}| = 38.4(9)10^{-3}$ [4142]. In summary, the situation for the exclusive determination of $|V_{cb}|$ is still unsettled, but a tension with the inclusive determination of Eq. (13.24) is undisputable. New lattice calculations performed with relativistic heavy quarks such as [747] will extend their q^2 range, making it possible to extract $|V_{cb}|$ at large recoil, where experimental data are more accurate. New experimental analyses of Belle and Belle II data are also expected soon. As this is paralleled by a renewed experimental and theoretical activity on the inclusive front, we can hope that the V_{cb} puzzle will find its resolution.

Moving to the exclusive determination of $|V_{ub}|$, it proceeds through the $B \to \pi$ channel. In analogy to the $B \to D$ case, only one form factor is relevant for massless leptons and it is standard practice to perform a BCL fit to lattice [741,748,4143] and LCSR calculations and to experimental data from several experiments, see [4081]. HFLAV employs the Fermilab and RBC/UKQCD form factors and the LCSR calculation of [4144] to find $|V_{ub}| = 3.67(15)10^{-3}$. An updated LCSR result is presented in [4145] and leads to

$$|V_{ub}| = 3.77(15)10^{-3} \qquad (B \to \pi\ell\nu). \tag{13.30}$$

The recent JLQCD form factor $f_+(q^2)$ [748] is slightly lower than the Fermilab and RBC/UKQCD and also implies a higher $|V_{ub}|$. The fits in [4081,4145] are both consistent, but there are two outliers which drive the value of $|V_{ub}|$ down. Removing the outliers the result increases $|V_{ub}|$ by about one sigma [4146]. We can conclude that the agreement between inclusive and exclusive determinations of $|V_{ub}|$ has become acceptable, but more stringent tests will be possible in the next few years. With the large statistics that will be available at Belle II the channel $B \to \tau\nu$ will become competitive with $B \to \pi\ell\nu$ for the extraction of $|V_{ub}|$. To this end, neglecting QED effects, the only QCD input is the decay constant f_B, which is already known to better than 1%, see Sect. 4.7.

Finally, two recent semileptonic measurements at LHCb place constraints on $|V_{ub}/V_{cb}|$. The first concerns the ratio of $\Lambda_b \to p\mu\nu$ to $\Lambda_b \to \Lambda_c\mu\nu$ decays [752] and makes use of a pioneering lattice calculation of baryonic form factors [751]; the result is [4081]

$$\frac{|V_{ub}|}{|V_{cb}|} = 0.079(4)(4) \qquad (\Lambda_b \to p\mu\nu) \tag{13.31}$$

where the uncertainties are experimental and from the form factors. The second is the first measurement of $B_s \to K\mu\nu$; the decay is normalized to $B_s \to D_s\mu\nu$ in two bins of q^2 [4147]. Using lattice results from the FNAL/MILC Collaboration [4148] for the high q^2 bin and LCSR [4149] for the low q^2 bin, one obtains values of $|V_{ub}/V_{cb}|$ in sharp disagreement with each other, which requires further scrutiny. Averaging Ref. [4148] with older results in the high q^2 bin of Ref. [4147], FLAG finds $|V_{ub}/V_{cb}| = 0.086(5)$ [68]. We can compare this and Eq. (13.31) with the ratio of Eqs. (13.26, 13.24) or of Eq. (13.30) and the average of Eqs. (13.28, 13.29): from inclusive decays we get $|V_{ub}/V_{cb}| = 0.094(6)$, from exclusive decays $|V_{ub}/V_{cb}| = 0.094(4)$, and in both cases the tension with Eq. (13.31) is over 2σ. The agreement improves for lower $|V_{ub}|$ or higher $|V_{cb}|$. This is another puzzling issue: hopefully, future measurements and lattice calculations of baryonic and mesonic form factors will clarify the situation.

As mentioned above, semileptonic b decays are not the only observables sensitive to $|V_{cb}|$ and $|V_{ub}|$. Assuming the validity of the SM and therefore the unitarity of the CKM matrix, one can also extract V_{cb} from loop induced observables like ε_K and $B_{(s)} - \bar{B}_{(s)}$ mixing, as well as from rare kaon and B decays [4070,4150–4154], and the precision starts to be competitive. For instance, the $B_{(s)}$ meson mass differences are proportional to $|V_{cb}|^2$: $\Delta M_{(d,s)} \propto |V_{td,ts}|^2$ and $|V_{ts}|^2 \approx |V_{cb}|^2$, $|V_{td}|^2 = \lambda^2 \sin^2\gamma |V_{cb}|^2$. ε_K is even more sensitive, $\varepsilon_K \propto |V_{cb}|^{3.4}$, and the branching fraction for $K_L \to \pi^0\nu\bar{\nu}$ is proportional to $|V_{cb}|^4$. Deviations from the direct (semileptonic) determinations would signal New Physics. The present situation is illustrated in Fig. 347, where the constraints from some of these observables in the $(\gamma, |V_{cb}|)$ plane are shown, with a clear preference for a high $|V_{cb}|$. As far as $|V_{ub}|$ is concerned, global fits performed without its direct determination tend to return values close to Eq. (13.30).

13.2.3 Meson mixing and CP asymmetries

So far we have discussed the elements of the first two rows of $\hat{V}_{CKM}$: their magnitudes determine precisely λ and A in Eq. (13.16), and the ratio $|V_{ub}/V_{cb}|$ constrains the apex of the unitarity triangle, as shown in Fig. 344. In order to determine completely the remaining parameters ρ and η, however, one needs additional information. As the elements of the third row cannot yet be measured precisely, we now turn to loop mediated $B_{(s)}$ mixing and rare decays, and CP asymmetries, focussing only on the most constraining observables.

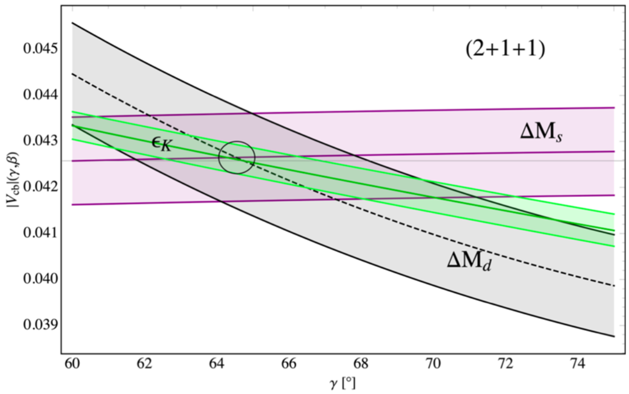

Fig. 347 Present constraints from ε_K, ΔM_d, and ΔM_s in the $(\gamma, |V_{cb}|)$ plane, see Ref. [4152] for details

In the SM the mass difference $\Delta M_{d,s}$ between the two mass eigenstates of the B^0 and B_s^0 systems is proportional to $|V_{td}|^2$ and $|V_{ts}|^2$, respectively, and the relevant nonperturbative QCD physics is all contained in the product $f_{B_q}^2 \hat{B}_{B_q}$ of decay constants and bag parameters, see Eq. (4.186). The ratio $\Delta M_s/\Delta M_d$ is particularly interesting because some uncertainty cancels out: the latest $N_f = 2+1+1$ value [722] for $\xi = f_{B_s}/f_{B_d}\sqrt{B_{B_s}/B_{B_d}}$ is $\xi = 1.216(16)$, which together with accurate measurements [4081] allows for the very strong constraint shown in red in Fig. 344. Individually, $\Delta M_{d,s}$ are slightly less precise but have a very different sensitivity to $|V_{cb}|$, see Fig. 347. In the kaon sector one looks at CP-violation in mixing, quantified by ε_K, see Sect. 13.3.3, which is sensitive to a combination of CKM elements. The bulk of ε_K is due to its *short-distance* component, whose uncertainty is dominated by the bag parameter $\hat{B}_K$, see e.g. [4034]. The recent average of lattice calculations reported in Sect. 4.7, $\hat{B}_K = 0.7625(97)$, leads to the constraints shown in Figs. 344 and 347.

Finally, different CP asymmetries allow for a direct extraction of the phase of some CKM element, with minimal or no QCD input, see [4155–4158] for good reviews. Limiting to the most precise results, the measurement of the time-dependent CP asymmetry in $B \to J/\psi K_S$ gives $\sin 2\beta = 0.699(17)$ (green band in Fig. 344) neglecting small contributions from penguin amplitudes with a different weak phase, but data-driven methods based on flavor symmetries have been devised to account for them [4159–4161], and indicate an additional 0.01 uncertainty; the study of the interference between the tree-level decays $B^- \to D^0 K^-$ and $B^- \to \bar{D}^0 K^-$ gives $\gamma = 66.1(3.5)°$ [4081] (blue band in Fig. 344); an isospin analysis [4162] of the time-dependent asymmetries in $B \to \pi\pi, \rho\rho$ leads to $\alpha = 85.4(4.6)°$ (gray bands in Fig. 344).

The global picture that emerges from all these and additional less important inputs is summarized by the global fit that gives the apex of the unitarity triangle in Fig. 344: $\bar{\rho} = 0.156(12)$ and $\bar{\eta} = 0.350(10)$ [4070]. The consistency between the various constraints is impressive and in the last 18 years the overall precision has improved by a factor 4(3) for $\bar{\rho}(\bar{\eta})$. One can compare some of the above inputs with the values obtained from a global fit performed without them: the results are $\sin 2\beta = 0.750(27)$, $\gamma = 66.1(2.1)°$, $\alpha = 90.5(2.1)°$ [4070]. Very similar results are also obtained by the CKMFitter Collaboration [4154], which reports $\bar{\rho} = 0.157(^{+8}_{-5})$ and $\bar{\eta} = 0.348(^{+12}_{-5})$.

In summary, the CKM mechanism describes successfully a host of data, in many cases with crucial QCD input. As discussed in Sects. 13.2.1 and 13.2.2, there are potential problems that require further scrutiny, and more serious anomalies will be discussed in Sect. 13.4, but it is premature to attribute them to New Physics. On the contrary, present data place very strong constraints on a variety of New Physics scenarios, in particular on those that modify the CKM mechanism more radically, see e.g. [4034,4163]. From an effective field theory point of view, the measurements we have considered in this section imply that the scale Λ of New Physics with a generic flavor structure must be well beyond the TeV range.

13.3 The important role of QCD in flavor physics

Andrzej J. Buras

The importance of QCD effects depends on processes considered. While their inclusion in processes like $K^+ \to \pi^+\nu\bar{\nu}$, $K_L \to \pi^0\nu\bar{\nu}$, $B_{s,d}^0 \to \mu^+\mu^-$ is important in order to increase the precision of SM predictions, neglecting them would result in uncertainties in the ballpark of at most 30%, significant but not crucial if one wants to get a rough idea what are the SM predictions for such decays. There are extensive reviews on them and most of these decays are discussed in [4034]. Here we want to confine our presentation to cases in which QCD plays an essential role and neglecting QCD effects one would fail the description of the data not by 30%, but by factors of at least two and sometimes even by an order of magnitude.

13.3.1 $B \to X_s\gamma$ decay

The calculations of NLO and NNLO QCD corrections to $B \to X_s\gamma$ decay are probably the best known to the physics community among all QCD calculations in the field of weak decays. One of the reasons is the fact that the $b \to s\gamma$ transition was the first penguin-mediated transition in B physics to be discovered in 1993 in the exclusive decay channel $B \to K^*\gamma$ measured in the CLEO experiment [4164]. The inclusive branching ratio $B \to X_s\gamma$ has been measured in 1994 by the same group [4165]. The other reason is the particular structure of the QCD corrections to this decay that requires a two-loop calculation in order to obtain the anomalous dimension matrix in the LO approximation. Because of this it took 6 years after the first QCD calculations in ordinary perturbation theory to obtain the correct result for the QCD corrections to $B \to X_s\gamma$ in the RG-improved perturbation theory at LO. It involved 5 groups and 16 physicists. It is not then surprising that the corresponding NLO calculations took 9 years. In 2022 this decay is known including NNLO corrections. A detailed historical account of NLO calculations can be found in [4041] and an introduction to technical details in [4034]. Most extensive NNLO calculations have been reported first in [4166], and after a number of updates the last one has been presented in [4167]

$$\mathcal{B}(B \to X_s\gamma)_{\rm SM} = (3.36 \pm 0.23) \times 10^{-4}, \tag{13.32}$$

for $E_\gamma \geq 1.6$ GeV. It agrees very well with experiment which reached the accuracy of 4.5% [4168]

$$\mathcal{B}(B \to X_s\gamma)_{\rm exp} = (3.32 \pm 0.15) \times 10^{-4}, \tag{13.33}$$

where again $E_\gamma \geq 1.6$ GeV has been imposed. One expects that in this decade the Belle II experiment will reach the accuracy of 3% so that very precise tests of the SM will be possible. Already now this decay provides an important constraint on new physics.

In order to appreciate these results let us briefly describe why these very difficult calculations were crucial. Indeed in 1987 two groups [4169,4170] calculated $\mathcal{O}(\alpha_s)$ QCD corrections to the $B \to X_s\gamma$ rate finding a huge enhancement of this rate relative to the partonic result without QCD corrections. In 1987, when $m_t \leq M_W$ was still considered, this enhancement was almost by an order of magnitude. With the increased value of m_t in the 1990s also the partonic rate increased, and in 2022 the dominant additive QCD corrections, although still very important, amount roughly to a factor of 2.5.

The additive QCD corrections in question originate in the mixing of the leading current–current operator Q_2 like the one in Eq. (13.36) with the magnetic-photon penguin operator $Q_{7\gamma}$ that is directly responsible for the decay $b \to s\gamma$. The calculation of the relevant anomalous dimensions at LO is a two-loop affair and consequently it took some time before the correct result had been obtained. An important role in resolving these inconsistencies present in the literature was played by the analyses in [4171,4172]. But the final LO result has been provided by the Rome group [4173,4174].

Once this issue had been solved it was possible to outline an NLO calculation in [4175]. Such a calculation was motivated by the finding in [4176] that the LO rate for $B \to X_s\gamma$ exhibited a very large renormalization-scale dependence. Changing the scale μ_b in the Wilson coefficient from $m_b/2$ to $2m_b$ changed the rate of $B \to X_s\gamma$ by roughly 60% making a detailed comparison of theory with experiment impossible.

A large number of authors contributed to the calculation of NLO corrections, with their names and references listed in Table 5 of the review in [4041]. See also the 2002 summary of NLO calculation in [4177].

Yet already in 2001 a motivation for a NNLO calculation was born. While the NLO calculations decreased the μ_b-dependence present in the LO expressions significantly, a new uncertainty had been pointed out by Paolo Gambino and Mikolaj Misiak in 2001 [4178]. It turns out that the $B \to X_s\gamma$ rate suffers at the NLO from a significant, ±6%, uncertainty due to the choice of the charm quark mass in the two-loop matrix elements of the four quark operators, in particular in $\langle s\gamma|Q_2|B\rangle$. In the following years, considerable progress in the NNLO program of $B \to X_s\gamma$ was made. It was an effort of 17 theorists [4166] and led eventually to the result in Eq. (13.32) summarized in [4167].

13.3.2 QCD dynamics and the $\Delta I = 1/2$ rule

One of the puzzles of the 1950s was a large disparity between the measured values of the real parts of the isospin amplitudes A_0 and A_2 in $K \to \pi\pi$ decays, which on the basis of usual isospin considerations were expected to be of the same order. Experimentally, the $\pi\pi$ system in $K \to \pi\pi$ decays was often found to have isospin $I = 0$ and rarely $I = 2$, an effect which is called $\Delta I = 1/2$ rule; $\Delta I = 1/2$ decays are enhanced over the $\Delta I = 3/2$ ones by a factor of 22.4. Altarelli and Maiani [1210] and Gaillard and Lee [1209] made a first unsuccessful attempt to explain this huge enhancement through short distance QCD effects. The precision of the calculation of the WCs increased considerably in the last 50 years since this first pioneering calculation. The basic QCD dynamics behind this rule – contained in the hadronic matrix elements of current–current operators – has been identified analytically first in 1986 in the framework of the Dual QCD in [4030] with some improvements in 2014 [4031]. This has been confirmed more than 30 years later by the RBC-UKQCD collaboration [729] although the modest accuracy of both approaches still allows for some NP contributions. See [4179] for the most recent summary. Despite this summary it is appropriate to describe in this book the present situation of this important rule that is governed by QCD in more details.

In 2022 we knew the experimental values of the real parts of these amplitudes very precisely [4180]

$$\begin{aligned}\mathrm{Re}A_0 &= 27.04(1) \times 10^{-8}\ \mathrm{GeV},\\ \mathrm{Re}A_2 &= 1.210(2) \times 10^{-8}\ \mathrm{GeV}.\end{aligned} \tag{13.34}$$

As $\mathrm{Re}A_2$ is dominated by $\Delta I = 3/2$ transitions but $\mathrm{Re}A_0$ receives contributions also from $\Delta I = 1/2$ transitions, the latter transitions dominate $\mathrm{Re}A_0$ which expresses the so-called $\Delta I = 1/2$ rule [4181,4182]

$$R = \frac{\mathrm{Re}A_0}{\mathrm{Re}A_2} = 22.35. \tag{13.35}$$

In the 1950s QCD and the Operator Product Expansion did not exist and clearly one did not know that $W^{\pm}$ bosons exist in nature, but using the ideas of Fermi [4183], Feynman and Gell-Mann [4184] and Marshak and Sudarshan [4185] one could still evaluate the amplitudes $\mathrm{Re}A_0$ and $\mathrm{Re}A_2$ to find out that such a high value of R is a real puzzle.

In modern times we can reconstruct this puzzle by evaluating the simple $W^{\pm}$ boson exchange between the relevant quarks which after integrating out $W^{\pm}$ generates the current–current operator Q_2:

$$Q_2 = (\bar{s}\gamma_\mu(1-\gamma_5)u)\ (\bar{u}\gamma^\mu(1-\gamma_5)d). \tag{13.36}$$

With only Q_2 contributing we have

$$\mathrm{Re}A_{0,2} = \frac{G_F}{\sqrt{2}} V_{ud} V_{us}^* \langle Q_2\rangle_{0,2}. \tag{13.37}$$

Calculating the matrix elements $\langle Q_2\rangle_{0,2}$ in the strict large N limit, which corresponds to factorization of matrix elements of Q_2 into the product of matrix elements of currents, we find

$$\langle Q_2\rangle_0 = \sqrt{2}\langle Q_2\rangle_2 = \frac{2}{3} f_\pi (m_K^2 - m_\pi^2), \tag{13.38}$$

and consequently

$$\begin{aligned} &\mathrm{Re}A_0 = 3.59\times 10^{-8}\,\mathrm{GeV},\\ &\mathrm{Re}A_2 = 2.54\times 10^{-8}\,\mathrm{GeV},\ R=\sqrt{2}, \end{aligned} \tag{13.39}$$

in plain disagreement with the data in Eqs. (13.34) and (13.35). It should be emphasized that the explanation of the missing enhancement factor of 15.8 in R through some dynamics must simultaneously give the correct values for $\mathrm{Re}A_0$ and $\mathrm{Re}A_2$. This means that this dynamics should suppress $\mathrm{Re}A_2$ by a factor of 2.1, not more, and enhance $\mathrm{Re}A_0$ by a factor of 7.5. This tells us that while the suppression of $\mathrm{Re}A_2$ is an important ingredient in the $\Delta I = 1/2$ rule, it is not the main origin of this rule. It is the enhancement of $\mathrm{Re}A_0$ as already emphasized in [1207]. However, in contrast to this paper, the current–current operators, like Q_2, are responsible dominantly for this rule and not QCD penguins. This was pointed out first in 1986 [4030] and demonstrated in the context of the Dual QCD approach. An update and improvements over the 1986 analysis appeared in 2014 [4031] with the result

$$R \approx 16.0 \pm 1.5, \qquad \mathrm{DQCD}\ \ (1986, 2014), \tag{13.40}$$

that is one order of magnitude enhancement over the result in Eq. (13.39) without QCD up to confinement of quarks in mesons. The missing piece could come from final state interactions as pointed out first by nuclear physicists [4186] and stressed much later by ChPT experts [4187]. Also $1/N^2$ corrections could also change this result but are unknown.

Meanwhile the RBC-UKQCD LQCD collaboration confirmed in 2012 the 1986 DQCD finding that current–current operators dominate the $\Delta I = 1/2$ rule. But the results from the series of their three papers show how difficult these calculations on the lattice are: $R = 12 \pm 1.7$ [4188], $R = 31.0 \pm 11.1$ [728] and finally [4189]

$$\frac{\mathrm{Re}A_0}{\mathrm{Re}A_2} = 19.9(2.3)(4.4), \qquad \mathrm{RBC-UKQCD}\ \ (2020) \tag{13.41}$$

that is consistent with the DQCD value and in agreement with the experimental value 22.4.

While the RBC-UKQCD result is closer to the data than the DQCD one, the dynamics behind this rule, except for the statement that it is QCD, has not been provided by these authors. To this end it is necessary to switch off QCD interactions which can be done in the large N limit in DQCD but it seems to be impossible or very difficult on the lattice.

The anatomy of QCD dynamics as seen within the DQCD approach has been presented in [4030,4031] and in particular in Section 7.2.3 of [4034]. Here we just present an express view of this dynamics.

Starting with the values in Eq. (13.39), the first step is to include the short-distance RG-evolution of WCs from scales $\mathcal{O}(M_W)$ down to scales in the ballpark of 1 GeV. This is the step made already in the pioneering 1974 calculations in [1209,1210] except that they were done at LO in the RG-improved perturbation theory and now can be done at the NLO level. These 1974 papers have shown that the short distance QCD effects enhance $\mathrm{Re}A_0$ and suppress $\mathrm{Re}A_2$. However, the inclusion of NLO QCD corrections to WCs of Q_2 and Q_1 operators [4033,4190] made it clear, as stressed in particular in [4033], that the $K \to \pi\pi$ amplitudes without the proper calculation of hadronic matrix elements of Q_i are both scale and renormalization-scheme dependent. Moreover, further enhancement of $\mathrm{Re}A_0$ and further suppression of $\mathrm{Re}A_2$ are needed in order to be able to understand the $\Delta I = 1/2$ rule.

This brings us to the second step first performed in 1986 in [4030] within the DQCD approach. Namely, the RG-evolution down to the scales $\mathcal{O}(1\,\mathrm{GeV})$ is continued as a short but fast *meson evolution* down to zero momentum scales at which the factorization of hadronic matrix elements is at work and one can in no time calculate the hadronic matrix elements in terms of meson masses and weak decay constants as seen in (13.38). Equivalently, starting with factorizable hadronic matrix elements of current–current operators at $\mu \approx 0$ and evolving them to $\mu = \mathcal{O}(1\,\mathrm{GeV})$ at which the WCs are evaluated one is able to calculate the matrix elements of these operators at $\mu = \mathcal{O}(1\,\mathrm{GeV})$ and properly combine them with their WCs evaluated at this scale. The final step is the inclusion of QCD penguin operators that provide an additional enhancement of A_0 by roughly 10% without changing A_2.

In [4030] only the pseudoscalar meson contributions to meson evolution have been included and the *quark evolution*, RG evolution above $\mu = \mathcal{O}(1\,\text{GeV})$, has been performed at LO. The improvements in 2014 [4031] were the inclusion of vector meson contributions to the meson evolution and the NLO corrections to quark evolution. These improvements practically removed scale and renormalization-scheme dependences and brought the theory closer to data.

Based on DQCD and RBC-UKQCD results we conclude that the QCD dynamics is dominantly responsible for the $\Delta I = 1/2$ rule. However, in view of large uncertainties in both DQCD and RBC-UKQCD results, NP contributions at the level of 15% could still be present. See [4191] to find out what this NP could be.

Finally other authors suggested different explanations of the $\Delta I = 1/2$ rule within QCD that were published dominantly in the 1990s and their list can be found in [4034]. But in my view the DQCD picture of what is going on is more beautiful and transparent as asymptotic freedom and related non-factorizable QCD interactions are primarily responsible for this rule. It is simply the *quark evolution* from M_W down to scale $\mathcal{O}(1\,\text{GeV})$ as analysed first by Altarelli and Maiani [1210] and Gaillard and Lee [1209], followed by the *meson evolution* [4030,4031] down to very low scales at which QCD becomes a theory of weakly interacting mesons and a free theory of mesons in the strict large N limit, a point made by 't Hooft and Witten in 1970s.

13.3.3 QCD dynamics and the ratio ε'/ε

While the parameter $\varepsilon \equiv \varepsilon_K$ measures the indirect CP-violation in $K_L \to \pi\pi$ decays, that is originating in $K^0-\bar{K}^0$ mixing, the parameter ε' describes the direct CP violation, that is in the decay itself.

Experimentally ε and ε' can be found by measuring the ratios

$$\eta_{00} = \frac{A(K_\mathrm{L} \to \pi^0\pi^0)}{A(K_\mathrm{S} \to \pi^0\pi^0)}, \qquad \eta_{+-} = \frac{A(K_\mathrm{L} \to \pi^+\pi^-)}{A(K_\mathrm{S} \to \pi^+\pi^-)}. \tag{13.42}$$

Assuming ε and ε' to be small numbers one finds

$$\eta_{00} = \varepsilon - \frac{2\varepsilon'}{1-\sqrt{2}\omega}, \quad \eta_{+-} = \varepsilon + \frac{\varepsilon'}{1+\omega/\sqrt{2}}, \tag{13.43}$$

where $\omega = \mathrm{Re}A_2/\mathrm{Re}A_0 = 0.045$. In the absence of direct CP violation $\eta_{00} = \eta_{+-}$. The ratio ε'/ε can then be measured through

$$\mathrm{Re}(\varepsilon'/\varepsilon) = \frac{1}{6(1+\omega/\sqrt{2})}\left(1 - \left|\frac{\eta_{00}}{\eta_{+-}}\right|^2\right). \tag{13.44}$$

The story of ε'/ε both in the theory and experiment has been described in detail in [4192]. On the experimental side the chapter on ε'/ε seems to be closed for the near future. After heroic efforts, lasting 15 years, the experimental world average of ε'/ε from NA48 [4193] and KTeV [4194,4195] collaborations reads

$$(\varepsilon'/\varepsilon)_\mathrm{exp} = (16.6 \pm 2.3) \times 10^{-4}. \tag{13.45}$$

On the theoretical side the first calculation of ε'/ε that included RG QCD effects to QCD penguin (QCDP) contributions is due to Gilman and Wise [4196] who – following Shifman, Vainshtein and Zakharov [1207] – assumed that the $\Delta I = 1/2$ rule is explained by QCDP. Using the required values of the QCDP matrix elements for the explanation of this rule, they predicted ε'/ε to be in the ballpark of 5×10^{-2}. During the 1980s this value decreased by roughly a factor of 50 dominantly due to three effects:

- The first calculation of hadronic matrix elements of QCDP operators in QCD – carried out in the framework of the DQCD [4030,4197,4198] in the strict large N limit of colors – proved that QCDPs are not responsible for the $\Delta I = 1/2$ rule and their hadronic matrix elements are much smaller.
- The QCDP contribution to ε'/ε through isospin breaking in the quark masses [4199,4200] is suppressed.
- The suppression of ε'/ε by electroweak penguin (EWP) contributions is increased by the large top quark mass [4201,4202].

In the 1990s these calculations have been refined through NLO QCD calculations to both QCDP and EWP contributions by the Munich and Rome teams [4203–4206] and [4207,4208], respectively. In [4209] the NNLO QCD effects on EWP contributions have been calculated. The NNLO QCD effects on QCDP contributions are expected to be known in 2024.

These NLO and NNLO QCD contributions decreased various scale and renormalization-scheme uncertainties and suppressed ε'/ε within the SM further so that already in 2000 we knew that this ratio should be of the order of 1.0×10^{-3}. Unfortunately even today the theorists do not agree on whether the SM agrees with the experimental value in (13.45) or not. The reason are different estimates of non-perturbative hadronic QCD effects. This has been summarized recently in [4179]. We recall only the main points below.

ε' is governed by the real and imaginary parts of the isospin amplitudes A_0 and A_2 so that ε'/ε is given by [4210]

$$\frac{\varepsilon'}{\varepsilon} = -\frac{\omega_+}{\sqrt{2}\,|\varepsilon|}\left[\frac{\mathrm{Im}A_0}{\mathrm{Re}A_0}(1-\hat{\Omega}_\mathrm{eff}) - \frac{1}{a}\frac{\mathrm{Im}A_2}{\mathrm{Re}A_2}\right], \tag{13.46}$$

with (ω_+, a) and $\hat{\Omega}_{\rm eff}$ given in 2022 as follows

$$\omega_+ = a\,\frac{{\rm Re}A_2}{{\rm Re}A_0} = (4.53 \pm 0.02) \times 10^{-2} \tag{13.47}$$

with $a = 1.017$ and

$$\hat{\Omega}_{\rm eff} = (29 \pm 7) \times 10^{-2}. \tag{13.48}$$

Here a and $\hat{\Omega}_{\rm eff}$ summarize isospin breaking corrections and include strong isospin violation $(m_u \neq m_d)$, the correction to the isospin limit coming from $\Delta I = 5/2$ transitions and electromagnetic corrections [4211–4213]. The most recent value for $\hat{\Omega}_{\rm eff}$ given above includes the nonet of pseudoscalar mesons and $\eta - \eta'$ mixing [4214]. If only the octet of pseudoscalar mesons is included so that $\eta - \eta'$ mixing does not enter, as presently done in ChPT, one finds $\hat{\Omega}_{\rm eff} = (17 \pm 9)\, 10^{-2}$ [4215], a value called $\hat{\Omega}^{(8)}_{\rm eff}$ here. The inclusion of $\eta - \eta'$ mixing yields $\hat{\Omega}^{(9)}_{\rm eff}$ in (13.48). This contribution is important, a fact known already for 35 years [4199,4200].

ImA_0 receives dominantly contributions from QCDP but also from EWP. ImA_2 receives contributions exclusively from EWP. Keeping this in mind it is useful to write [4216]

$$\left(\frac{\varepsilon'}{\varepsilon}\right)_{\rm SM} = \left(\frac{\varepsilon'}{\varepsilon}\right)_{\rm QCDP} - \left(\frac{\varepsilon'}{\varepsilon}\right)_{\rm EWP} \tag{13.49}$$

with

$$\left(\frac{\varepsilon'}{\varepsilon}\right)_{\rm QCDP} = {\rm Im}\lambda_{\rm t} \cdot \left(1 - \hat{\Omega}_{\rm eff}\right)\left[15.4\, B_6^{(1/2)}(\mu^*) - 2.9\right], \tag{13.50}$$

$$\left(\frac{\varepsilon'}{\varepsilon}\right)_{\rm EWP} = {\rm Im}\lambda_{\rm t} \cdot \left[8.0\, B_8^{(3/2)}(\mu^*) - 2.0\right]. \tag{13.51}$$

This formula includes NLO QCD corrections to the QCDP contributions and NNLO contributions to EWP ones mentioned previously. The coefficients in this formula and the parameters $B_6^{(1/2)}$ and $B_8^{(3/2)}$, conventionally normalized to unity at the factorization scale, are scale dependent. Here we will set $\mu^* = 1$ GeV because at this scale it is most convenient to compare the values for $B_6^{(1/2)}$ and $B_8^{(3/2)}$ obtained in the three non-perturbative approaches LQCD, ChPT and DQCD that we already encountered in the context of the $\Delta I = 1/2$ rule.

The $B_6^{(1/2)}$ and $B_8^{(3/2)}$ represent the relevant hadronic matrix elements of the dominant QCDP and EWP operators, respectively:

$$Q_6 = (\bar{s}_\alpha d_\beta)_{V-A} \sum_{q=u,d,s,c,b} (\bar{q}_\beta q_\alpha)_{V+A}, \tag{13.52}$$

$$Q_8 = \frac{3}{2}\,(\bar{s}_\alpha d_\beta)_{V-A} \sum_{q=u,d,s,c,b} e_q\,(\bar{q}_\beta q_\alpha)_{V+A}, \tag{13.53}$$

with $V - A = \gamma_\mu(1 - \gamma_5)$ and $V + A = \gamma_\mu(1 + \gamma_5)$. They are then left-right operators with large hadronic matrix elements which assures their dominance over left-left operators. The remaining QCDP and EWP operators, represented here by -2.9 and -2.0, respectively, play subleading roles. Current–current operators $Q_{1,2}$ that played crucial role in the case of the $\Delta I = 1/2$ rule do not contribute to ε'/ε because their WCs are real. In obtaining the formulae in Eqs. (13.50) and (13.51) it is common to use the experimental values for the real parts of $A_{0,2}$ in Eq. (13.34). Finally, ${\rm Im}\lambda_{\rm t} = {\rm Im}(V_{ts}^* V_{td}) \approx 1.4 \times 10^{-4}$.

There are two main reasons why Q_8 can compete with Q_6 here despite the smallness of the electroweak couplings in the WC of Q_8 relative to the QCD one in the WC of Q_6. In the basic formula (13.46) for ε'/ε its contribution is enhanced relative to the one of Q_6 by the factor ${\rm Re}A_0/{\rm Re}A_2 = 22.4$. In addition its WC is enhanced for the large top-quark mass which is not the case for Q_6 [4201,4202].

In the three non-perturbative approaches the values of $B_6^{(1/2)}$ and $B_8^{(3/2)}$ were found at $\mu = 1\,$GeV to be:

$$\begin{aligned}
&B_6^{(1/2)}(1\,{\rm GeV}) = 1.49 \pm 0.25, \quad ({\rm RBC\text{-}UKQCD} - 2020)\\
&B_8^{(3/2)}(1\,{\rm GeV}) = 0.85 \pm 0.05.\\
&B_6^{(1/2)}(1\,{\rm GeV}) = 1.35 \pm 0.20, \quad ({\rm ChPT} - 2019)\\
&B_8^{(3/2)}(1\,{\rm GeV}) = 0.55 \pm 0.20.\\
&B_6^{(1/2)}(1\,{\rm GeV}) \leq 0.6, \quad ({\rm DQCD} - 2015)\\
&B_8^{(3/2)}(1\,{\rm GeV}) = 0.80 \pm 0.10.
\end{aligned} \tag{13.54}$$

While the large $B_6^{(1/2)}$ and $B_8^{(3/2)} < 1.0$ from LQCD has until now no physical interpretation, the pattern found in ChPT results apparently from final state interactions (FSI) that enhance $B_6^{(1/2)}$ above unity and suppress $B_8^{(3/2)}$ below it [4217–4220]. The suppression of $B_6^{(1/2)}$ and $B_8^{(3/2)}$ below unity in the DQCD approach comes from the meson evolution [4221] which is required to have a proper matching with the WCs of QCDP and EWP operators. The meson evolution is absent in present ChPT calculations and it is argued in [4222] that including it in ChPT calculations will lower $B_6^{(1/2)}$ below unity. On the other hand adding non-leading FSI in the DQCD approach would raise $B_6^{(1/2)}$ above 0.6. Nevertheless $B_6^{(1/2)} \leq 1.0$ is expected to be satisfied even after the inclusion of FSI in DQCD.

Moreover, while ChPT and DQCD use $\hat{\Omega}^{(8)}_{\rm eff} = (17 \pm 9)\, 10^{-2}$ and $\hat{\Omega}^{(9)}_{\rm eff} = (29 \pm 7)\, 10^{-2}$, respectively, as already stated above, RBC-UKQCD still uses $\hat{\Omega}_{\rm eff} = 0$.

These differences in the values of $B_6^{(1/2)}$, $B_8^{(3/2)}$ and $\hat{\Omega}_{\rm eff}$ imply significant differences in ε'/ε presented by these three groups:

$$(\varepsilon'/\varepsilon)_{\rm SM} = (21.7 \pm 8.4) \times 10^{-4} \tag{13.55}$$

from the RBC-UKQCD collaboration [729] which uses $\hat{\Omega}_{\rm eff} = 0$. Here statistical, parametric and systematic uncertainties have been added in quadrature. Next

$$(\varepsilon'/\varepsilon)_{\rm SM} = (14 \pm 5) \times 10^{-4} \tag{13.56}$$

from ChPT [4215]. The large error is related to the problematic matching of LD and SD contributions in this approach which can be traced back to the absence of meson evolution in this approach. Finally

$$(\varepsilon'/\varepsilon)_{\rm SM} = (5 \pm 2) \times 10^{-4}, \tag{13.57}$$

from DQCD [4192,4221,4222], where $B_6^{(1/2)} \leq 1.0$ has been used.

While the results in Eqs. (13.55) and (13.56) are fully consistent with the data shown in Eq. (13.45), the DQCD result in Eq. (13.57) implies a significant anomaly and NP at work. Clearly, the confirmation of the DQCD result is highly important.

Let us end this presentation with good news. There is a very good agreement between LQCD and DQCD as far as EWP contribution to ε'/ε is concerned. This implies that this contribution to ε'/ε, that is unaffected by leading isospin breaking corrections, is already known within the SM with acceptable accuracy:

$$(\varepsilon'/\varepsilon)^{\rm EWP}_{\rm SM} = -(7 \pm 1) \times 10^{-4}, \quad \text{(LQCD and DQCD)}. \tag{13.58}$$

Because both LQCD and DQCD can perform much better in the case of EWP than in the case of QCDP I expect that this result will remain with us for the coming years. On the other hand, the value from ChPT of $B_8^{(3/2)} \approx 0.55$ [4215] implies using Eq. (13.51) that the EWP contribution is roughly by a factor of 2 below the result in Eq. (13.58).

Let us hope that at the 60th birthday of QCD we will know which prediction is right. Further summaries can be found in [4034,4179,4192] and details in original references.

13.4 The role of QCD in B physics anomalies

Danny van Dyk and Javier Virto

The so-called $b \to s\ell^+\ell^-$ anomalies present one of the few current tensions between theory predictions within the SM and experimental measurements. They represent long-standing tensions that first presented themselves in a 2013 publication by the LHCb collaboration [4223]. Here, we discuss how QCD plays a central role at every stage of the interpretation of these anomalies.

QCD and hadronic physics enter the theory predictions, both in the SM and beyond, in one of three ways:

– First, they enter the Weak Effective field Theory (WET) description of neutral-current processes, such as $b \to s\ell^+\ell^-$. The effective Hamiltonian at the leading-mass dimension six reads

$$\mathcal{H}_{\rm WET} = \frac{4G_F}{\sqrt{2}} V_{tb} V_{ts}^* \sum_i \mathcal{C}_i \mathcal{Q}_i, \tag{13.59}$$

with local operators $\mathcal{Q}_i$ and Wilson coefficients $\mathcal{C}_i$. It includes semileptonic operators,

$$\mathcal{Q}_{9(10)} = \frac{e^2}{16\pi^2} \left[\bar{s}\gamma^\mu P_L b\right] \left[\bar{\mu}\gamma_\mu(\gamma_5)\mu\right], \tag{13.60}$$

electromagnetic dipole operators,

$$\mathcal{Q}_7 = \frac{e}{16\pi^2} \left[\bar{s}\sigma_{\mu\nu} P_R b\right] F^{\mu\nu}, \tag{13.61}$$

and four-quark operators

$$\mathcal{Q}_{1q(2q)} = \left[\bar{q}\gamma^\mu P_L b\right] \left[\bar{s}\gamma_\mu P_L q\right]. \tag{13.62}$$

QCD has a substantial effect on the matching of the WET to the SM [4224–4226]. For instance, at the low scale $\mu_b \simeq 5$ GeV, about half of the value of $\mathcal{C}_9$ is generated by QCD effects due to operator running and mixing of the four-quark operators into $\mathcal{Q}_9$ [4224].
Here we discuss only the numerically leading operators needed for a description within the SM. BSM effects are encoded in the values of the Wilson coefficients or through additional operators with a different spin structure.

– Second, they enter the hadronic matrix elements of local $\bar{s}b$ operators, c.f. Eq. (13.66). These matrix elements are then expressed in terms of scalar-valued form factors, which are functions of the momentum transfer (typically: q^2). The $\bar{s}b$ form factors are very similar to the form factors arising in the description of exclusive charged-current semileptonic processes such as $b \to c\mu^-\bar{\nu}$.

– Third, they enter the hadronic form factors of non-local $\bar{s}b$ operators, c.f. Eq. (13.68). These operators arise in the time-ordered product of the four-quark operators and the electromagnetic current. They have no correspondence in charged-current semileptonic decays and currently present the biggest obstacle to accurate and precise theoretical predictions of exclusive $b \to s\mu^+\mu^-$ decays.

In the following, we do not further discuss the effective field theory description, which is well established. The matching coefficients to NNLO in QCD can be found in Refs. [4224–4226]. Instead, we focus on the second and third type of QCD effects in exclusive $b \to s\ell^+\ell^-$ processes.

13.4.1 Anatomy of exclusive $b \to s\ell^+\ell^-$ processes

$\bar{B}_s \to \mu^+\mu^-$

Amongst the exclusive $b \to s\ell^+\ell^-$ decays, the cleanest ones from a theory perspective are the purely leptonic decays $\bar{B}_s \to \ell^+\ell^-$. Up to QED corrections [4227], all QCD effects are contained in a single local hadronic matrix element. This matrix element is commonly parametrized in terms of the B_q-meson decay constant f_{B_q} [301]

$$\langle 0|\bar{q}\gamma^\mu\gamma_5 b|\bar{B}_q(p)\rangle = i f_{B_q} p^\mu. \tag{13.63}$$

It has been calculated ab-initio from lattice QCD simulations. Several analyses with $N_f = 2+1+1$ light quark flavors have become available [692,709,710,1472,4228]. Their world average [301]

$$f_{B_s} = 230.3 \pm 1.3\,\text{MeV}, \tag{13.64}$$

is dominated by a single analysis published by the Fermilab/MILC collaboration [692].

This constant has been computed using a variety of lattice QCD techniques, which have presently reached a precision of 0.5%. The current theoretical uncertainty on the muonic branching ratio is no longer governed by hadronic physics. Instead, it is dominated by CKM matrix elements. The theory predictions have reached the level of 5% [4227], which is much smaller than the uncertainty of the average of the results by the LHC experiments of $\sim$ 13% [4229]. While $\bar{B}_s \to \mu^+\mu^-$ is not sensitive to the Wilson coefficient $\mathcal{C}_9$ (to leading order in QED [4227]), it does constrain very strongly the scalar and pseudoscalar operators, and indirectly also $\mathcal{C}_{10}$, which has an impact on the global interpretations of the $b \to s\mu^+\mu^-$ anomalies.

$\bar{B} \to M\mu^+\mu^-$

Amongst the exclusive semileptonic $b \to s\ell^+\ell^-$ decays, B-meson decays to either a pseudoscalar (P) or a vector (V) meson are presently the best understood. Compared to the purely leptonic decay $\bar{B}_s \to \mu^+\mu^-$, the additional meson in the final state provides the opportunity to test the SM through a larger number of observables that arise in the differential decay rates. The downside for this is – generally – an increased sensitivity to QCD effects in their theoretical description, which leads to larger theoretical uncertainties.

To leading order in QED, the matrix elements of the semileptonic and radiative operators $\mathcal{Q}_{7,9,10}$ factorise. A useful schematic decomposition of the amplitude is given by [4230]

$$A(\bar{B} \to M\ell^+\ell^-) \sim G_F\, V_{tb}V_{ts}^* \Bigg[(\mathcal{C}_9\, L_V^\mu + \mathcal{C}_{10}\, L_A^\mu)\, \mathcal{F}^\mu - \frac{L_V^\mu}{q^2} 2 i m_b \mathcal{C}_7\, \mathcal{F}^{T,\mu} + 16\pi^2 \mathcal{H}^\mu\Bigg]. \tag{13.65}$$

Here $L^\mu_{V(A)} = [\bar{\ell}\gamma^\mu(\gamma_5)\ell]$ are leptonic currents, and a generalization to operators beyond the SM can be found in Ref. [4231]. In the above, we use the hadronic matrix elements

$$\mathcal{F}^\mu_{B\to M}(k,q) \equiv \langle M(k)|\bar{s}\gamma_\mu P_L\, b|\bar{B}(p)\rangle, \tag{13.66}$$

$$\mathcal{F}^{T,\mu}_{B\to M}(k,q) \equiv \langle M(k)|\bar{s}\sigma_{\mu\nu}q^\nu P_R\, b|\bar{B}(p)\rangle, \tag{13.67}$$

$$\mathcal{H}^\mu_{B\to M}(k,q) \equiv i\int d^4x\, e^{iq\cdot x}\langle M(k)|T\Big\{j_\mu^{\text{em}}(x), \sum_i \mathcal{C}_i\, Q_i(0)\Big\}|\bar{B}(p)\rangle \tag{13.68}$$

with $i = 1q, 2q, \ldots,$ which arise from the semileptonic, radiative, and four-quark operators in that order

The first two matrix elements are classified as local matrix elements, and the last one as a non-local matrix element. Both types of matrix elements are needed for reliable and accurate predictions of the amplitudes and therefore of the observables in semileptonic decays. For phenomenological discussions, one commonly encounters projections of the hadronic amplitudes onto some basis of scalar form factors, either the helicity basis [4232] or more commonly the transversity basis [4233–4235]. The number of independent amplitudes depends on the angular momentum of the initial and final state hadrons. The form factors are functions of the momentum transfer from the hadronic system to the leptons. This functional dependence is commonly expressed in terms of q^2, the squared mass of the lepton pair.

The process $B \to K\ell^+\ell^-$ is the most reliably understood one amongst the exclusive semileptonic $b \to s\ell^+\ell^-$ decays. Both the B and K meson are stable in the absence of weak interactions, which facilitates the determination of their hadronic form factors. Conservation of angular momentum limits this process to two amplitudes: the dominant longitudinally polarized amplitude and the lepton-mass suppressed time-like amplitude [4236]. As a consequence, the process provides only a few independent observables.

The processes $B \to K^*\ell^+\ell^-$ and $B_s \to \phi\ell^+\ell^-$ both feature a vector meson in the final state. Compared to $B \to K\ell^+\ell^-$, two further transversely-polarized amplitudes can contribute. This more complex structure leads to numerous independent observables arising from the differential decay rate [4233–4235,4237]. However, this enriched phenomenological reach comes at the expense of somewhat larger uncertainties in the individual hadronic form factors. Since both the K^* and ϕ are not stable in the absence of weak interactions, their description as a “quasi stable” state incurs additional theoretical uncertainty [4238]. Here, the K^* is substantially more affected than the ϕ, due to the hierarchy of their hadronic decay widths.

13.4.2 Hadronic matrix elements

Local form factors

Local form factors for $B \to K$, $B \to K^*$ and $B_s \to \phi$ transitions are accessible at low values of $q^2 \lesssim 10\,\text{GeV}^2$ [1229] with two different continuum QCD methods.

First, QCD factorisation (QCDF) provides a means to relate the various form factors to each other. This relation emerged from a symmetry amongst currents involving one collinear and one heavy quark field [4239]. The breaking of this symmetry occurs due to two effects: (a) contributions beyond leading order in the strong coupling constant, which involves interactions between the quarks inherent to the transition with the spectator quark [4240]; and (b) contributions beyond leading power in the double expansion in the b-quark mass and the energy E of the final-state hadron within the B-meson rest frame. Early predictions for exclusive $b \to s\ell^+\ell^-$ decays relied heavily on the QCDF relations, to construct so-called "clean" observables; i.e., observables in which local hadronic form factors cancel approximately [4241–4243]. Most famously, the P_i' basis of observables in the $\bar{B} \to K^*\ell^+\ell^-$ angular distribution [4243] makes use of this cancellation. The P_5' observable [4244] is commonly used to illustrate the tensions between SM predictions and measurements.

Second, light-cone QCD sum rules (LCSR) are used to predict the full set of local form factors in $B \to K$, $B \to K^*$ and $B_s \to \phi$ transitions. Two different versions of LCSRs can be employed [1228,4245], which differ in the choice of the interpolating current. The LCSRs with B-meson interpolation involve hadronic matrix elements for the final-state hadron, i.e., the K, K^* and ϕ. These sum rules are presently better understood than their competitors, leading to overall smaller *parametric* uncertainties. However, the sum rules with vector-meson final states suffer from hard-to-quantify systematic uncertainties due to the unstable nature of these states. The competing LCSRs with interpolation of the final-state hadrons K, K^*, and ϕ have not yet reached the same level of sophistication [4055].

It remains to be emphasized that both types of LCSRs suffer from systematic uncertainties that are difficult to assess. It is commonly understood that the LCSR results serve as a stop gap, to be replaced by results from more systematic approaches to QCD.

Lattice QCD provides such a systematic approach to the local form factors. Typically, limitations of computational power require a restriction to the phase space $q^2 \gtrsim 12\,\text{GeV}^2$ [4052,4246,4247]. Lattice QCD results for the decays $B \to K^*\ell^+\ell^-$ and $B_s \to \phi\ell^+\ell^-$, which are of great phenomenological interest, are restricted to this range. But this is not an inherent limitation of the method: A very recent study of the $B \to K$ form factors [4056] for the first time accesses

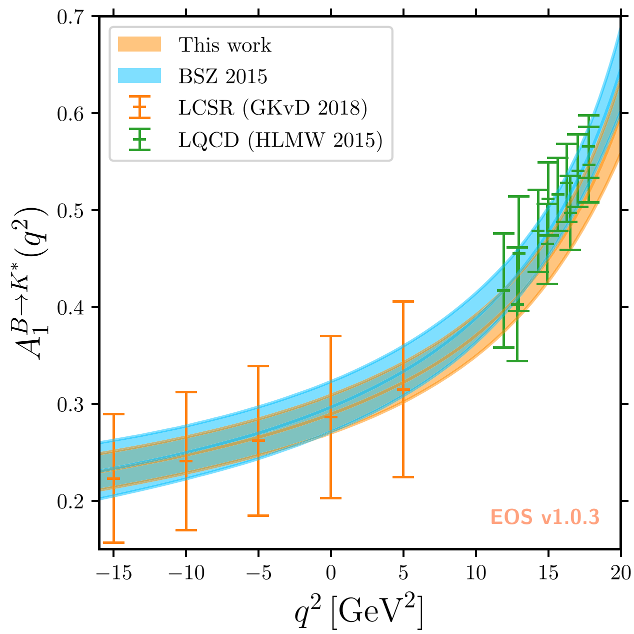

Fig. 348 Simultaneous fit to lattice QCD and LCSR results for the local $B \to K^*$ form factor $A_1 \propto \mathcal{F}_\parallel$, taken from Ref. [4248]

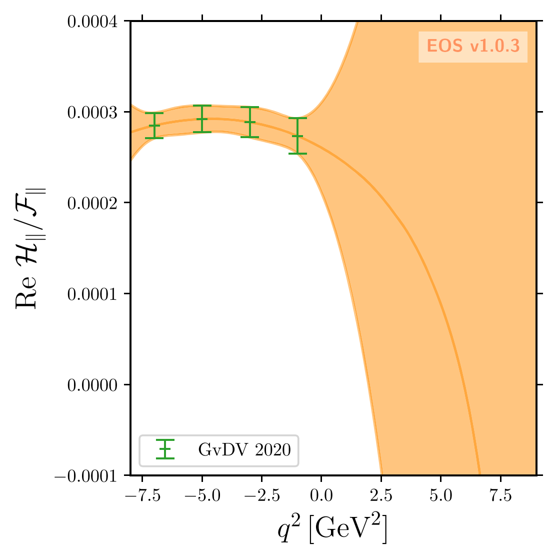

Fig. 349 Fit to the non-local $B \to K^*$ form factor $\mathcal{H}_\parallel$, produced from Ref. [4248]

the full q^2 range available to the semileptonic decay. Their results are in good agreement with previous LCSR estimates, with smaller uncertainties.

Having constraints on the form factors at opposite ends of the semileptonic phase space it is natural to ask if these constraints are mutually compatible. This poses an interpolation problem. For B-meson decays, this problem is usually addressed using the so-called z-expansion [4249]. Using

$$q^2 \mapsto z(q^2; t_0, t_+) \equiv \frac{\sqrt{t_+ - q^2} - \sqrt{t_+ - t_0}}{\sqrt{t_+ - q^2} + \sqrt{t_+ - t_0}} \tag{13.69}$$

the first Riemann sheet of the complex q^2 plane is mapped onto the unit disk in z. A Taylor expansion of the form-factors in z, after removal of any physical poles, converges quickly and provides some control of the interpolation error. Studies of the $B \to V$ form factors find reasonable to good agreement between the available LCSR and lattice QCD results [4055,4245,4248], which is not surprising given the large uncertainties attached to the former. An example of such a fit from Ref. [4248] is displayed in Fig. 348, showcasing the agreement between lattice QCD and LCSR results.

Future prospects on the theoretical precision for local form factors rely dominantly on the expected improvements from the Lattice QCD side. These include enlarging the accessible q^2 range (as recently achieved for the $B \to K$ form factors) and accounting for the non-zero width of the vector final states [543]. The effect due to a non-zero ρ and K^* width on the $B \to \pi\pi$ and $B \to K\pi$ form factors was recently critically discussed within the setup of LCSRs with final-state interpolation, estimating corrections to the zero-width limit of up to 10% in the case of the K^* [4238,4250,4251].

Non-local Hadronic Matrix Elements

Non-local form factors are significantly more difficult to approach theoretically [4252–4255]. The reason is the large number of virtual and on-shell intermediate states that contribute to the time-ordered product in Eq. (13.68). This non-local operator is commonly separated by the electric charge of the quark flavor to which the electro-magnetic current couples:

$$T\left\{ j_\mu^{\text{em}}(x), \sum_{i=1q,2q,\ldots} \mathcal{C}_i Q_i(0) \right\} \equiv \mathcal{K}(x)$$
$$\equiv Q_c \mathcal{K}_c(x) + Q_{bs} \mathcal{K}_{bs}(x) + \ldots . \quad (13.70)$$

In the above, the dots indicate contributions due to up and down quarks, which are suppressed by CKM matrix element or the small Wilson coefficients of QCD-penguin four-quark operators. The terms proportional to bottom and strange-quark charges are only gauge invariant when considered in sum, leading to the joint description with label bs. Our labelling of the non-local form factors follows from the above, i.e., $\mathcal{H}_{\lambda,c}$ arises from the hadronic matrix element of the operator $\mathcal{K}_c$.

The first systematic approach to the non-local form factors has been provided in Refs. [4252,4256], which is expected to work for small values of q^2 sufficiently far below the open charm threshold. This approach was subsequently developed into a light-cone Operator Product Expansion (OPE) of the non-local operator Eq. (13.70) [4252,4253]. This expansion is shown to break down as q^2 approaches the partonic open charm threshold from below. The hadronic matrix elements of the next-to-leading operator in this light-cone OPE have been calculated within a LCSR approach [4253,4257]. The most recent calculation indicated that the term at next-to-leading power is negligible in comparison to the leading-power term.

At $q^2 = \mathcal{O}(m_b^2) \gtrsim 4m_c^2$, an OPE in term of local operators applies [4254,4255]. The simple structure of the OPE leads to phenomenologically powerful theory predictions [4242,4258,4259]. However, the fact that this region of phase space lays on the open-charm branch cut leads to considerable complications in the interpretation of experimental measurements. Chiefly, one cannot expect that the OPE result agrees with nature *locally*, i.e., in every q^2 point [4255]. Instead of such local duality, *semi-local* quark–hadron duality is assumed, i.e., the OPE prediction integrated over a sufficiently large q^2 range is expected to correspond to the q^2 integrated observables [4255]. Nevertheless, this approach gives rise to large unquantifiable systematic uncertainties in the theory predictions [4260,4261]. Due to these limitations, commonly a single bin covering the whole low-q^2 region is used in the BSM analyses. However, the q^2 spectrum can be used to test the level of "duality violation", i.e., the disagreement between the perturbative partonic prediction and the hadronic spectrum. In this way, reliable estimates of these intrinsically non-perturbative effects are obtained. Ref. [4261] uses all currently available data on $B \to K^*\mu\mu$ at low recoil and finds agreement between data and the OPE prediction within $\sim 20\%$ in all the bins.

The first parametrizations of the q^2 dependence of the non-local form factors $\mathcal{H}_{\lambda,c}$ are based on a dispersion relation [4253] or an expansion in powers of q^2 [4232]. A subsequent publication proposes to apply a conformal mapping similar to Eq. (13.69) [4262], very similar to what is done for the local form factors. The dispersive and z-expansion approaches are consistent with analyticity and therefore permit using additional data, such as measurements of the branching ratios and angular distributions of $B \to \psi M$ processes, where $\psi = \{J/\psi, \psi(2S)\}$. In Ref. [4262] it is shown quantitatively how this information can be used *a priori* to produce data-assisted theory predictions for the non-local effect independent of NP, or a posteriori to fit all the $B \to \psi K^*$ and $B \to K^*\mu^+\mu^-$ spectra up to $q^2 = m^2_{\psi(2S)}$ simultaneously to the hadronic parameters and NP. In this last approach, short- and long-distance effects are disentangled by the experimental input from $B \to \psi K^*$, the fixed q^2 dependence of the NP contribution, and by the theory constraints at negative q^2. A notable byproduct is the fact that experimental data *between* the two narrow charmonia can be used in the analyses. An application of the z-expansion, including newly derived dispersive bounds on the expansion coefficients [4257], has been used in Ref. [4248] to challenge the experimental measurements of various exclusive semileptonic $b \to s\ell^+\ell^-$ decays. This parametrization yields results that are compatible with analyses based on a perturbative treatment, albeit with somewhat larger uncertainties. A representative exam-

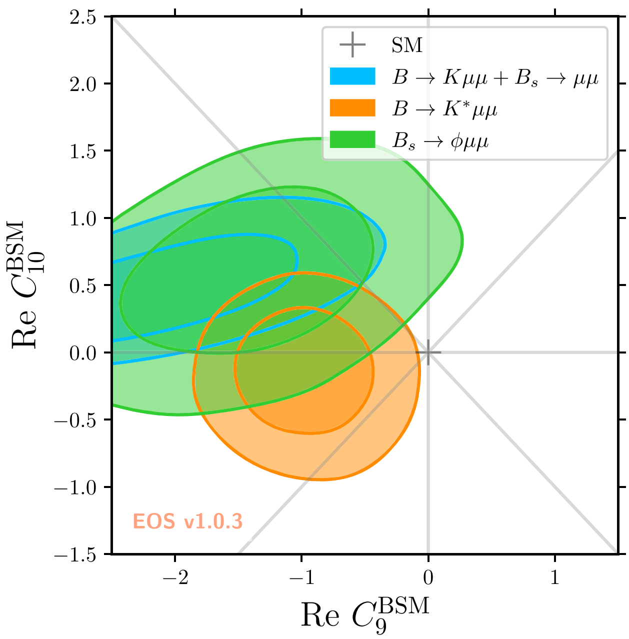

Fig. 350 Overview of the tensions between NP parameters and the SM expectations for three representative processes. Taken from Ref. [4248], which takes into account a parametrization of the non-local effects in the fits

ple of the non-local form factors obtained in this way is shown in Fig. 349. The impact of these improved determinations of non-local form factors on the global fits to separate exclusive $b \to s\mu\mu$ modes has been studied in Ref. [4248] and it is shown in Fig. 350. The overall picture of significant tensions between data and the SM expectations seen in the literature [4263–4267] are confirmed.

The prospects for this data-driven approach with the future data from LHCb, including the prospects of doing without theory input altogether, have been studied in [4268]. The conclusion is that unbinned analyses can infer knowledge about both QCD and potential BSM effects in these decays *simultaneously*. The high statistics studies of $b \to s\mu\mu$ exclusive transitions at the LHC, either with fine q^2 binning or unbinned, will therefore not only probe for BSM effects but also further our understanding of the non-local form factors. While current global fits to different q^2 bins show consistency with the current treatment of non-local effects [4269], future LHC data will require, and provide, a higher level of control over them.

Data-driven and joint theoretical and data-driven methods have been proposed in an effort to control the uncertainties [4257,4262,4270–4272]. Some of these methods will be possible and improve significantly with the high statistics collected at LHCb after the upgrade. They are all based on precise measurements of the q^2 spectra, together with a theoretically motivated parametrization of the q^2 dependence of the amplitudes and a theory benchmark that allows to separate short- from long-distance contributions.

Finally, various hadronic models have been proposed to analyse parts or the entire q^2 phase space. Some of these analyses are carried out within the "Krüger-Sehgal" (naive factorization) approach [4273], which allows to use data on the $R(s)$ ratio in e^+e^- annihilation [4255,4260,4261]. These models have recently been refined to account also for light-meson intermediate states [4274]. Notably, future precision data from the LHC with the expected fine binning will be essential in refining these data-driven methods and disentangling potential BSM contributions, with the prospects of confirming or refuting a BSM origin to the $b \to s\mu\mu$ anomalies.

13.5 QCD and $(g-2)$ of the muon

Achim Denig and Harvey Meyer

The anomalous magnetic moment of the muon, as one of the most precisely measured quantities in fundamental physics, has been at the forefront of testing the Standard Model (SM) of particle physics for decades [4275]. The proportionality factor $g \cdot e/(2m)$ between the spin and the magnetic moment of an elementary particle is predicted in Dirac's theory of the electron to satisfy $g = 2$. Already the deviation of the electron's g factor from this prediction played a central role in testing Quantum Electrodynamics at one loop [4276]. It was understood early on [4277,4278] that the contribution of virtual particles much heavier than the lepton l would be suppressed as $(m_l/m_{\rm heavy})^2$. Hence the strong interest in the analogous property of the muon, denoted $a_\mu = (g-2)_\mu/2$, given that the 207 times larger mass of the muon strongly enhances the virtual contributions from particles upward from the mass scale of a few MeV$/c^2$, and thus provides access to potential new-physics contributions. Since the very first measurement of 1960 [4279], experiments have refined their sensitivity to a_μ, thereby successively testing contributions from all sectors of the SM, and making this observable the paradigmatic example of searching for new physics at the precision frontier.

The experimental measurements of a_μ [4280] rely on the muon spin precessing relative to the direction of the muon momentum under the influence of a static magnetic field: the precession frequency is directly proportional to a_μ. The observation that the (undesirable) impact of an electric field on the muon spin precession is suppressed at a special muon momentum of 3.1 GeV/c [4281] eventually led to the third muon storage ring experiment at CERN [4282], which for the first time probed hadronic effects, among which the hadronic vacuum polarization (HVP) provides the leading contribution. Progress in the experimental techniques culminated in the Brookhaven E821 experiment [4283], which achieved a precision of 0.54 ppm on a_μ.

Meanwhile, the SM prediction for a_μ had been worked out to a very similar degree of precision, as described in the

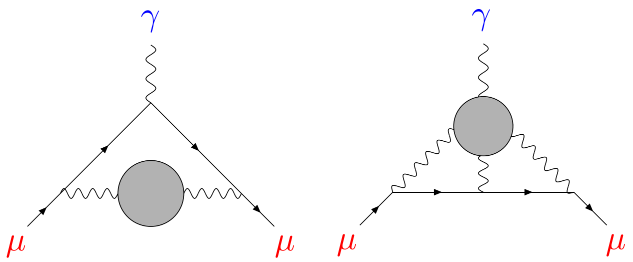

Fig. 351 Feynman diagrams representing the two contributions that currently saturate the uncertainty of the SM prediction for the muon $(g-2)$: the hadronic vacuum polarization (left), $a_\mu^{\mathrm{HVP,LO}}$, and the hadronic light-by-light contributions (right), a_μ^{HLbL}. Solid lines represent muon propagators and wavy lines photon propagators. The external photon line represents the magnetic field of the experiment, which probes the magnetic moment of the muon

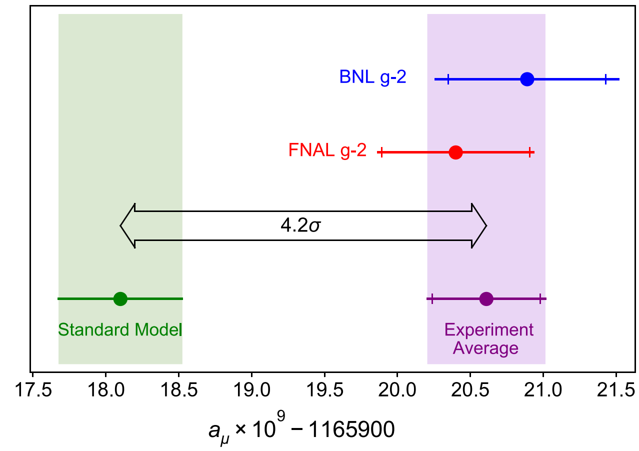

Fig. 352 Status of a_μ after the 2021 FNAL measurement. The tension between the experimental average of the FNAL and the 2001 BNL measurements with the Standard Model prediction provided by the Theory White Paper amounts to 4.2 standard deviations. Figure from [4287]

2009 review [4284]. The QED contribution, by far dominant, and the weak contribution having been calculated to sufficiently high order, the uncertainty of the SM prediction has been entirely dominated by the hadronic contributions, specifically by the HVP and by the hadronic light-by-light (HLbL) contributions, which are both illustrated in Fig. 351. A tension at the level of 3.2 standard deviations was found between the experimental and the theoretical value of a_μ [4284].

In the past decade, a new experimental effort was undertaken in an attempt to clarify the situation. The Fermilab experiment E989 [4285] was designed with the goal of reaching a precision of 0.14 ppm on a_μ. In order to arrive at an up-to-date prediction before the announcement of the first results by the Fermilab experiment, the $(g-2)$ Theory Initiative was launched in 2017, which led to the 2020 Theory White Paper [4286]. The theory precision had by then improved to the level of 0.37 ppm, and the tension with the world experimental average (dominated by the Brookhaven measurement) was found to be at the $3.7\,\sigma$ level.

The Fermilab $(g-2)$ experiment announced its first result on April 7, 2021. Its measurement of a_μ [4287] at the 0.46 ppm level slightly surpassed the precision of the Brookhaven measurement [4283] and led to the situation illustrated in Fig. 352. The new measurement agrees well with the older Brookhaven one, and the tension with the SM prediction (from the 2020 White Paper [4286]) has increased to the level of $4.2\,\sigma$, or

$$a_\mu(\mathrm{Exp}) - a_\mu(\mathrm{WP\,2020}) = (25.1 \pm 5.9) \times 10^{-10} \quad (13.71)$$

in absolute size. From here, it might seem like the next experimental update by the Fermilab experiment could finally raise the tension above the conventional 'discovery' level of five standard deviations.

However, on the same day as the announcement of the experimental result from Fermilab, a lattice QCD calculation of the HVP contribution with a competitive precision was published [4288], which, taken at face value, would increase the SM prediction for a_μ and bring it into better agreement (at the $1.5\,\sigma$ level) with the experimental world average. The tension between this lattice QCD calculation and the dispersive, data-driven evaluation underlying the White Paper prediction of a_μ amounts to $2.1\,\sigma$ (see Eq. (13.77) below). Thus it is the intricacies of hadron–photon interactions that are currently limiting the resolving power of the muon $(g-2)$ to probe new physics. In Sect. 13.5.1, we describe how the evidence for a genuine difference between lattice calculations of the HVP and its dispersive evaluation has strengthened significantly in the past eighteen months. Obviously, finding the origin of this difference is of utmost importance in the ongoing saga of the muon $(g-2)$.

We begin by reviewing the status of the HVP contribution to a_μ in Sect. 13.5.1, whereafter we describe the progress made in the HLbL contribution in Sect. 13.5.2. We close with some concluding remarks and an outlook on the near future of the subject.

13.5.1 The hadronic vacuum polarization contribution

The leading contribution to a_μ is given by Schwinger's result $\alpha/(2\pi) \simeq 0.00116$ [4276]. In contrast, the HVP contribution to a_μ only amounts to about 700×10^{-10}, but given the precision expected from the ongoing Fermilab experiment and the upcoming J-PARC [4289] experiment, the target for the HVP contribution $a_\mu^{\mathrm{HVP,LO}}$ is a precision of 1.5×10^{-10}, or 0.2%. This represents a major challenge for a strong-interaction effect, which has been addressed by the long-established data-driven dispersive method and by ab initio lattice QCD methods.

Dispersive determination

The dispersive approach to computing $a_\mu^{\text{HVP,LO}}$ is based on the expression

$$a_\mu^{\text{HVP,LO}} = \left(\frac{\alpha m_\mu}{3\pi}\right)^2 \int_{m_{\pi_0}^2}^{\infty} \frac{ds}{s^2}\, \widehat{K}(s/m_\mu^2)\, R(s), \tag{13.72}$$

$$R(s) = \frac{\sigma(e^+e^- \to \text{hadrons})}{4\pi\alpha(s)^2/(3s)}. \tag{13.73}$$

The dimensionless function $\widehat{K}$ is a smooth function that increases monotonically from the value 0.63 at the $4m_\pi^2$ threshold to unity in the limit $s \to \infty$. The determination of $R(s)$ requires measurements of the hadronic cross section in e^+e^- collisions, $\sigma(e^+e^- \to \text{hadrons})$. Given the $1/s^2$ dependence in the dispersion integrand, low-energy contributions of the hadronic cross section have a very strong weight and therefore have to be known to high accuracy. The most relevant channels are the exclusive reactions $e^+e^- \to \pi^+\pi^-, 3\pi, 4\pi$, and $K\bar{K}$, for all of which the cross section is peaked at $\sqrt{s}$ <2 GeV.

The channel $e^+e^- \to \pi^+\pi^-$ is dominated by the $\rho(770)$ intermediate state and contributes to more than 70% to the dispersion integral. Figure 353 shows various recent measurements of the two-pion cross section in the ρ peak region between 600 and 900 MeV. Two classes of measurements are shown in Fig. 353. These are energy scan measurements (CMD-2 [4290–4293], SND [4294]), in which the center-of-mass energy of the collider (in this case the VEPP-2M collider in Novosibirsk) is systematically varied to cover the energy range under study. A second class of measurements (KLOE [4295], Babar [4296,4297], BESIII [4298]) is carried out with the colliders running at a fixed center-of-mass energy and by exploiting events in which the initial beam electrons or positrons have radiated a highly energetic photon, lowering in such a way the available hadronic mass in the final state. This method is called initial-state radiation (ISR) or radiative return and has been applied most successfully at modern particle factories [4299]. In the past, also spectral functions from hadronic τ decays have been used [4300] in the phenomenological determination of HVP, since these can be related to $R(s)$ via the *Conserved Vector Current* theorem. However, since the phenomenological estimates of the isospin corrections are not well understood, the recent determinations of HVP were obtained without the use of hadronic τ data.

Figure 353 demonstrates the very high precision of the data. However, sizeable discrepancies have been observed for the cross-section integral contributing to Eq. (13.72). This is demonstrated in Fig. 354, where the two-pion contribution to HVP, $a_\mu^{\pi\pi,\text{LO}}$, in the ρ peak region between 600 and 900 MeV is shown for the individual experiments as well as for two combinations of the data sets (KNT 19 [4303] and DHMZ 19 [4304]). Especially the two most precise determinations of

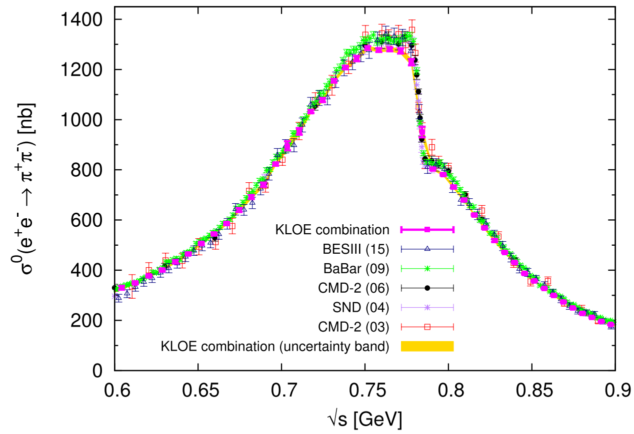

Fig. 353 Recent experimental data on the cross section $\sigma(e^+e^- \to \pi^+\pi^-)$ in the energy range between 600 and 900 MeV. The interference of the ρ decay with the two-pion decay of the $\omega(780)$ is well visible as a structure around the ω mass. Figure taken from [4295]; a new SND analysis [4301] from the VEPP-2000 collider and an ISR analysis from CLEO [4302] are not yet shown

the two-pion cross section from the KLOE [4295] and Babar [4296,4297] collaborations happen to exhibit a significant deviation, which currently limits the overall precision of the dispersive determination of HVP. Furthermore, given the tensions in the experimental data sets, systematic effects have to be considered in the averaging procedures. In Ref. [4286] a conservative merging procedure was applied to reflect the differences between the evaluations in Refs. [4303] and [4304]. The Theory White Paper [4286] estimate for the LO HVP contribution is solely based on the dispersive approach [4303–4308] and reads $a_\mu^{\text{HVP,LO}} = (693.1 \pm 4.0) \times 10^{-10}$.

Fortunately, new experimental measurements of the two-pion channel are expected in the near future by CMD-3, SND, Babar, BESIII, and Belle-II. It remains to be seen whether the currently existing discrepancy between Babar and KLOE can be resolved. Provided the upcoming data sets reach the precision level of 0.5% and agree with each other, the total uncertainty of the HVP contribution obtained via the dispersive approach would decrease from currently 0.6% to 0.3% or better.

Lattice QCD calculation

Since the HVP contribution to the muon $(g-2)$ involves only spacelike photons, it is a natural quantity to be calculated in lattice QCD [4312], which is formulated in Euclidean space. Although initially expressed in momentum space, the master formula now used almost exclusively is in the 'time-momentum representation' [4313],

$$a_\mu^{\text{HVP,LO}} = \left(\frac{\alpha}{\pi m_\mu}\right)^2 \int_0^\infty dt\; G(t)\, \mathcal{K}(m_\mu t), \tag{13.74}$$

$$G(t) = \frac{1}{3}\sum_{k=1}^{3} \int d^3x\; \langle j_k^{\text{em}}(t,\vec{x})\; j_k^{\text{em}\dagger}(0)\rangle, \tag{13.75}$$

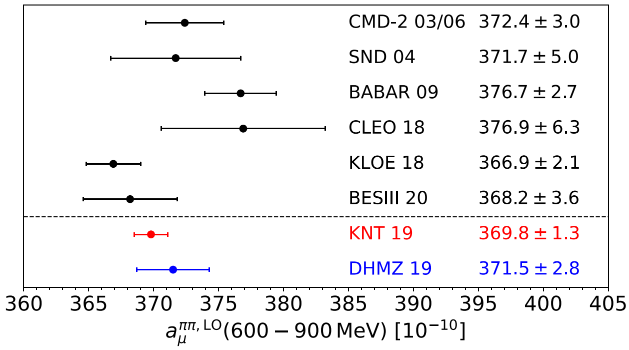

Fig. 354 Comparison of $a_\mu^{\pi\pi,\mathrm{LO}}$ in the energy range between 600 and 900 MeV. The upper part of the plot shows the values of recent experimental measurements in this energy range [4290,4293–4298,4302], while the lower two values in red and blue are the estimates of the KNT [4286,4303] and DHMZ [4286,4304] groups, which carry out a merging procedure of the available data. In the case of DHMZ an additional systematic uncertainty has been included to account for the KLOE/Babar tension. Please note that the KLOE value is the combination of the three analyses published in Refs. [4309–4311]

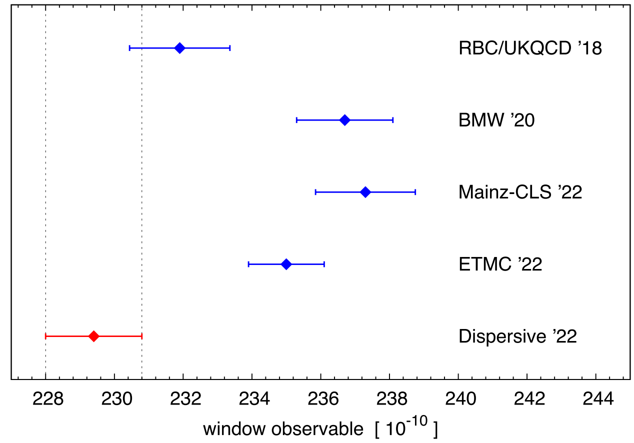

Fig. 355 The partial contribution to $a_\mu^{\mathrm{HVP,LO}}$ called 'window quantity', as computed by four lattice collaborations [4288,4317,4324,4326], compared to its dispersive determination [4327]. Further recent lattice results, particularly for the (dominant) 'light-quark connected contribution', can be found in [4328–4330] as well as in the update [4325] of the RBC/UKQCD '18 result

where $j_k^{\mathrm{em}} = \frac{2}{3}\bar{u}\gamma_k u - \frac{1}{3}\bar{d}\gamma_k d - \frac{1}{3}\bar{s}\gamma_k s + \ldots$ is a spatial component of the electromagnetic current carried by the quarks, and the dimensionless weight function $\mathcal{K}(\hat{t})$ is known analytically in terms of Meijer's function [4314]. It is proportional to $\hat{t}^4$ for arguments well below unity, and to $\hat{t}^2$ for arguments well above unity, thus strongly enhancing the long-distance contribution. The spectral representation [4313]

$$G(t) = \int_0^\infty ds\ \frac{s\,R(s)}{12\pi^2}\ \frac{e^{-\sqrt{s}t}}{2\sqrt{s}} \tag{13.76}$$

between the Euclidean correlator and the R ratio allows for detailed comparisons between the dispersive and the lattice approach.

The recipe for computing $a_\mu^{\mathrm{HVP,LO}}$ on the lattice thus appears remarkably simple. However, many effects must be controlled to reach the subpercent level of precision, including discretization and finite-size effects, as well as the leading effects of the unequal up and down quark masses and of the electromagnetic interactions among quarks. The state-of-the-art lattice calculations available at the time of the 2020 White Paper had uncertainties of two percent and larger [4315–4323]. While they had a tendency to lie above the dispersive estimates, they were broadly consistent with them. The BMW collaboration achieved a reduction of the uncertainty of its lattice calculation down to the 0.8% level and published its result in 2021 [4288]. The difference with the White Paper result amounts to

$$a_\mu^{\mathrm{HVP,LO}}(\mathrm{BMW'21}) - a_\mu^{\mathrm{HVP,LO}}(\mathrm{WP'20}) = (14.4 \pm 6.8) \times 10^{-10}. \tag{13.77}$$

At this point, an independent lattice calculation at the same level of precision would be extremely desirable to help clarify the situation.

Both the very short and the very long distances pose distinct challenges to a lattice calculation [4313]. Given the difficulties associated with controlling the statistical and systematic errors of the tail of the correlator $G(t)$, the lattice community has adopted the strategy of partitioning the Euclidean-time axis into intervals, whose contributions to $a_\mu^{\mathrm{HVP,LO}}$ are individually more tractable. This strategy was first applied in Ref. [4317]. In particular, an intermediate interval from 0.4 to 1.0 fm (with smooth edges of width 0.15 fm) was chosen, thus defining the 'window quantity', which represents about one third of the total $a_\mu^{\mathrm{HVP,LO}}$. This quantity has received a lot of attention, especially since the BMW collaboration found a discrepancy of 3.7 standard deviations with the dispersive estimate [4288]. Since then, the Mainz/CLS [4324] and the ETM collaboration have computed the window quantity on the lattice. The results are summarized in Fig. 355. The RBC/UKQCD collaboration has recently presented an update [4325] based on a blinded analysis, indicating an upward shift in the (dominant) light-quark connected contribution from $(202.9 \pm 1.4) \times 10^{-10}$ to $(206.5 \pm 0.7) \times 10^{-10}$ (where we have added their errors in quadrature) and bringing their result into good agreement with the other lattice calculations displayed in Fig. 355.

Discussion HVP

Beyond the 2.1 σ tension of Eq. (13.77) between the data-driven evaluation of $a_\mu^{\mathrm{HVP,LO}}$ [4286] and the lattice QCD based BMW calculation [4288], a statistically more significant tension between lattice QCD and dispersion theory has arisen in the partial contribution known as the 'window quantity'. The latter has been computed independently by several lattice collaborations, whose results are in good mutual agreement but disagree with the R-ratio based evaluation of [4327], at the level of 3.1, 3.7 and 3.8 σ respectively for Refs. [4288,4324,4326].

If one assumes that the tension is due to an erroneous cross section measurement in a certain interval of $\sqrt{s}$, it is important to clarify which interval and which hadronic channel it might be. In this regard, we note that the window quantity receives a contribution of about 55% from the $\sqrt{s}$ interval between 0.6 and 0.9 GeV, while about 40% comes from higher center-of-mass energies [4324]. Its relative sensitivity to the (ρ, ω)-meson region is thus similar to the full $a_\mu^{\text{HVP,LO}}$. If one therefore assumes the 2π channel to be responsible for the tension, this would require shifts of the 2π cross section which exceed by far the claimed systematic errors of the experiments as well as the observed discrepancies between the various experiments.

On the other hand, one might ask what could go wrong in the lattice calculations of the window quantity. Perhaps the most critical common source of systematic error among lattice calculations is the one associated with taking the continuum limit. After all, the ranges of lattice spacing used by the different collaborations as well as their fit ansätze in the lattice spacing are fairly similar. Thus, new cross-section measurements as well as additional lattice calculations of the full $a_\mu^{\text{HVP,LO}}$ will give important indications as to the origin of the current tension.

In case of an eventual consolidation of the isospin breaking corrections, e.g. by means of auxiliary lattice QCD calculations [4331], the use of hadronic τ decays in the HVP dispersion integral might be reconsidered for the future. New and high–statistics measurements of spectral functions of hadronic τ decays are indeed expected from Belle-II in the upcoming years. It is going to be exciting to see whether such a τ-based dispersive analysis of HVP will be in agreement with the current e^+e^--based methodology.

13.5.2 Hadronic light-by-light scattering in the muon (g-2)

The HLbL contribution a_μ^{HLbL} is of order α^3, and thus of one order higher than $a_\mu^{\text{HVP,LO}}$ in the expansion of a_μ in the fine-structure constant. The absolute precision target is to reach a level under 1×10^{-10}, which given the contribution's approximate size, $a_\mu^{\text{HLbL}} \simeq 10 \times 10^{-10}$, amounts to a result with a precision under 10%. While this requirement is much less stringent than for $a_\mu^{\text{HVP,LO}}$, the physics and kinematics involved in a_μ^{HLbL} are also much more complex. We first review the model and dispersive calculations before describing the status of the lattice QCD approach.

Data-driven determination

The hadronic blob on the right-hand side diagram of Fig. 351 can be decomposed into subgraphs with intermediate pseudoscalar meson exchanges (π^0,η, η') as well as exchanges of heavier scalar, axial-vector, or tensor mesons. Furthermore, intermediate pion, kaon, and even quark loop exchanges need to be considered. In the past, many of these individual contributions were estimated using hadronic models [4284,4332–4335], for which an estimate of the model uncertainty is notoriously difficult and for which possible double counting issues have been discussed as an additional source of uncertainty. A consensus exists among all the various estimates that the exchange of pseudoscalar mesons, particularly the π^0, is the dominant contribution to HLbL. For years, the so called Glasgow consensus value [4336] of $a_\mu^{\text{HLbL}} = (10.5 \pm 2.6) \cdot 10^{-10}$ was considered as a benchmark estimate and was found to be in good agreement with other estimates (see e.g. [4337]), although the individual subgraphs were partly in conflict with each other.

Developing a predictive dispersive representation for the LbL scattering amplitude with three spacelike photons represents a much more complex theoretical task than in the case of the HVP (see Eq. 13.72). The recent developments of dispersion relations for the pseudoscalar and the pion-loop subgraphs within the Refs. [4338,4339] can therefore be considered as a major breakthrough in the analytical treatment of HLbL (see also Ref. [4340] for an alternative representation). Indeed, for the first time an unambiguous definition of individual contributions became possible together with an exact relation to experimental data to be used as input, namely a relation to meson transition form factors (TFFs), which encode the coupling of two virtual photons to mesons. Besides the TFFs, which depend on the two photon virtualities, also meson decays, certain e^+e^- annihilation reactions and Primakoff measurements have been found to be highly relevant. As pointed out in Ref. [4341], the most relevant photon virtualities for a_μ^{HLbL} are on the GeV scale and below, an observation that calls for a dedicated campaign of experimental measurements in this energy range. The BESIII collaboration has recently presented a new high-quality measurement [4342] of the singly-virtual TFF of the π^0, which is shown in Fig. 356, where it is compared with older data [4343,4344] as well as a calculation of this form factor in lattice QCD [4345], a phenomenological estimate based on Canterbury approximants [4346], and with a dispersive treatment of the TFF [4347]. The agreement between data and theory is very good. Unfortunately, at low energies experiments have not been able yet to provide data with two photon virtualities, as needed for the new dispersive treatment of the pseudoscalar and pion loop contributions. Dispersive evaluations of the TFFs [4348] and lattice QCD calculations [4345] have been used instead. The good agreement shown in Fig. 356 and the overall consistency found elsewhere indicate the robustness

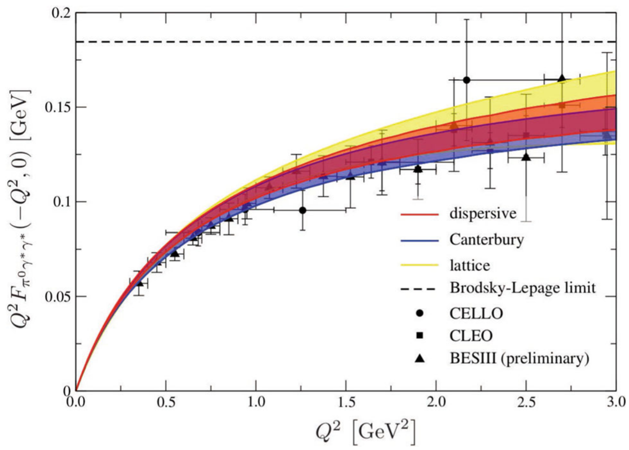

Fig. 356 The single-virtual pion form factor $F_{\pi^0\gamma^*\gamma^*(-Q^2,0)}$ as a function of Q^2 measured by the CELLO [4344], CLEO [4343], and BESIII [4342] experiments as well as phenomenological predictions using a dispersive analysis [4347] and Canterbury approximants [4346]; shown is furthermore an ab-initio calculation within Lattice QCD [4345]

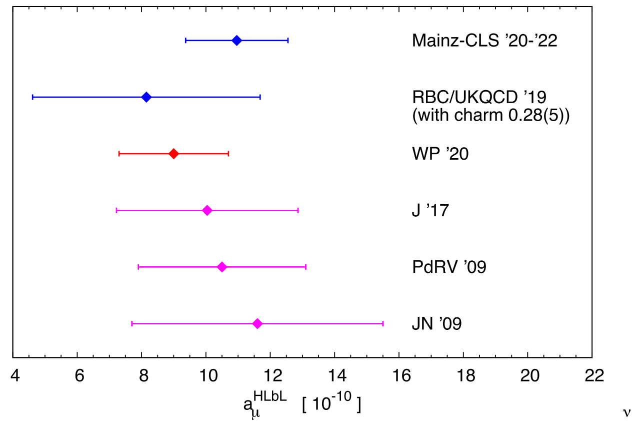

Fig. 357 Overview of results obtained for the hadronic light-by-light contribution to the muon $(g-2)$: the Mainz-CLS [4369,4370] and RBC/UKQCD lattice results [4363], the Theory White Paper 2020 average [4286], and previous model estimates by Jegerlehner [4275], Prades–de Rafael–Vainshtein [4336] (the 'Glasgow consensus') and Jegerlehner–Nyffeler [4284,4371]. We have supplemented the RBC/UKQCD result with the charm contribution computed in [4370]. The WP average is based on the dispersive [4275,4345–4347,4349–4357] and the RBC/UKQCD [4363] lattice result

of the theoretical descriptions of the TFFs. For the future, the first double-virtual TFF measurements are expected from Belle-II and BESIII.

Currently, in the Theory White Paper, the new dispersive treatments have led to a major reduction of the uncertainties of the pseudoscalar exchanges and pion and kaon loop subgraphs. For the remaining scalar, axial vector, and tensor exchange graphs as well as the short-distance contributions, a conservative error estimate has been applied and future research in experiment and theory will eventually lead to a further reduction of the uncertainty of those contributions. The dispersive result arrived at in Ref. [4286] amounts to $a_\mu^{\rm HLbL} = (9.2 \pm 1.9) \times 10^{-10}$ [4275,4345–4347,4349–4357] and is found to be in good agreement with the Glasgow consensus value with a slightly reduced uncertainty, but with a significant reduction of the model dependence compared to this older value.

Lattice QCD calculation

The first proposal for computing the hadronic light-by-light contribution in lattice QCD dates back to 2005 [4358]. The subject lay dormant for some years until 2013 [4359], the new effort leading to first results for the quark-connected contribution at a pion mass of 330 MeV/c^2 [4360]. Important technical improvements to the original methods were made in [4361]. The leading disconnected contribution was calculated for the first time in [4362], along with the connected part, at the physical pion mass. Finally, this multi-year effort culminated into a full calculation [4363] in the (u, d, s) quark sector. This result, displayed in Fig. 357 as RBC/UKQCD '18, contributed to the White Paper 2020 theory average, together with the dispersive estimate quoted above.

The treatment of massless internal photons is an important technical issue in lattice QCD. In the publications cited in the previous paragraph, the photons were treated on the same lattice as the QCD degrees of freedom. In [4364–4366], a position-space method allowing for the photons to be treated in infinite volume was proposed and worked out. Meanwhile, similar methods were also developed by members of the RBC/UKQCD collaboration [4367]. Altogether, the development of optimized position-space methods led to the calculations of [4368–4370] by the Mainz-CLS group. The result, displayed in Fig. 357, has an uncertainty very similar to the dispersive result.

Discussion HLbL

Figure 357 illustrates the good consistency among the data-driven, lattice and earlier hadronic model determinations. This is a good sign, since the dominant sources of uncertainty are very different in the different determinations: for instance, the RBC/UKQCD calculation involves a fairly long extrapolation to infinite volume, while the Mainz-CLS determination results from an extrapolation over a sizeable interval of pion masses. Updates of the lattice calculations are planned in the near future.

In the dispersive data-driven approach, further progress can be achieved by improved TFF measurements and calculations for the η and η' mesons. Most important, however, is a future experimental program of measurements of the two-photon couplings of mesons in the (1–2) GeV/c^2 range, where especially axial vector mesons play an important role and for which the current data base is limited. New results are expected in the future by the BESIII collaboration in a range of momentum transfer similar to the one shown in Fig. 356. Moreover, also Babar and Belle-II will be able to provide new measurements at a higher momentum transfer. New TFF data will also be crucial for a matching of individual hadronic channels to the short-distance behaviour of HLbL.

Given the ongoing program of various groups in experiment, hadron phenomenology and lattice QCD, we expect an improvement of the HLbL error from currently 20% to 10% or lower. An agreement between an ab-initio lattice QCD calculation with a data-driven estimate on such a level will represent a non-trivial cross-check between two completely independent methods.

13.5.3 Conclusions and outlook

Many theoretical and experimental developments have taken place in the past 5 years on the anomalous magnetic moment of the muon a_μ. The direct measurement of a_μ [4283] has been confirmed and improved [4287], while the $(g-2)$ Theory Initiative has helped coordinate many activities to improve the Standard Model prediction for a_μ [4286]. Hadronic effects limit the precision of this prediction, especially the hadronic vacuum polarization (HVP) and the hadronic light-by-light (HLbL) contributions reviewed above.

In the immediate future, the top priority is to clarify the tensions that have emerged in partial and full HVP determinations. Additional lattice QCD calculations of the full $a_\mu^{\mathrm{HVP,LO}}$ contribution are eagerly awaited, in conjunction with a strategy to identify the origin of the existing strong tension with the dispersive approach for the 'intermediate window' subcontribution. On the data-driven side, the accuracy of the dispersive approach for obtaining $a_\mu^{\mathrm{HVP,LO}}$ is currently hampered by inconsistencies in the experimental data bases. The most problematic issues arise from the tension in the determination of the $e^+e^- \to \pi^+\pi^-$ cross section (KLOE/BABAR puzzle), but also in other exclusive channels, e.g. in the process $e^+e^- \to K^+K^-$, inconsistencies have been observed. The clarification of these issues is one of the most important challenges for an improved determination of the SM prediction of $(g-2)_\mu$ and will be addressed by several existing and upcoming e^+e^- experiments in future.[118] In that respect, since the cross section measurements heavily rely on high-precision Monte-Carlo generators [4373], it is of utmost importance to maintain and to refine the PHOKHARA [4374–4391] generator as well as other Monte Carlo programs [4392–4397] for future applications.

As an alternative to the program of hadronic cross section measurements at e^+e^- colliders, it has been proposed [4398] to carry out a spacelike measurement of the effective electromagnetic coupling via a scattering experiment providing thereby input to a dispersion integral for HVP. The MUonE collaboration is currently preparing the design of a detector [4399] at the muon beam of SPS/CERN towards the final approval of the project. Provided that the differential cross section of the μe scattering process can be measured to the desired accuracy, this will allow for an entirely new determination of HVP.

In summary, controlling hadronic effects in the muon $(g-2)$ to match the absolute experimental precision represents a major challenge. Overcoming this challenge will demonstrate that strong-interaction contributions to precision observables can be controlled with the required level of accuracy and consistency between data-driven and lattice QCD approaches. This ability will be crucial to maximize the science output of a future high-energy lepton collider [4400], since non-perturbative QCD effects also dominate the uncertainty of $\alpha(M_Z)$.

14 The future

Conveners:

Eberhard Klempt and Franz Gross

Higher energy, higher intensity, higher precision. These are the frontiers at which experimental tests of new physics beyond the Standard Model is expected. This last section of this volume describes the status and the prospects at new multi-GeV facilities which recently came into operation or which are presently under construction. The large number of facilities necessarily requires a selection. A list of past and present accelerators can be found elsewhere.[119] This section does not attempt to address possible theoretical developments of the future.

The 12 GeV project at JLab, presented by Patrizia Rossi, is dedicated to a study of the structure of nucleons and nuclei, to an intense search for gluonic degrees of freedom in meson and baryon spectroscopy, to a search for new physics in parity violating processes, and to a search for dark matter. The electron-ion collider (EIC) will provide electron–proton and electron–nuclei collisions at CM energies $\sqrt{s}=20$–100 GeV, later possibly up to 140 GeV. Global properties and

[118] Recently the CMD-3 collaboration has announced a new energy scan measurement of the process $e^+e^- \to \pi^+\pi^-$ with a systematic uncertainty of 0.7% in the central ρ peak region [4372]. Surprisingly, the central value of $a_\mu^{\pi\pi,\mathrm{LO}}$, when using the CMD3 measurement only, turns out to be significantly higher than all previous experiments and is found to lead to good agreement with the BMW Lattice QCD determination of HVP. No reasons have been found so far why the new cross section measurement turns out to be significantly higher than all previous experiments. The new CMD-3 measurement is not yet published.

[119] https://en.wikipedia.org/wiki/List_of_accelerators_in_particle_physics.

the partonic structure of hadrons and nuclei will be studied (Christian Weiss).

The study of in-medium properties of hadrons and the nuclear matter Equation of State (EoS) and a search for possible signals of a deconfinement and a chiral-symmetry-restoration phase transitions are at the heart of the NICA (Nuclotron-based Ion Collider fAcility) program at the Joint Institute for Nuclear Research in Dubna and of the J-PARC hadron facility at Tokai. At J-PARC, strange nuclear matter, hypernuclei and the study of hyperons are a focus of research (Shinzo Kumano). NICA provides beams of nuclei with 4.5 GeV per nucleon and protons up to 12.6 GeV. Using polarized beams, the internal structure of the proton and deuteron will also be studied (Alexey Guskov).

The new international Facility for Antiproton and Ion Research (FAIR), presently under construction at Darmstadt, is presented by Johan Messchendorp, Frank Nerling and Joachim Stroth. Its program encompasses hadron physics using anti-proton annihilation, heavy-ion reactions at relativistic energies, and nuclear structure physics at the limit of stability using rare isotope beams.

The e^+e^- colliders in Beijing and Tsukuba have delivered a large number of unexpected results. BES III will increase further the statistics of J/ψ from now 10^{10} and $\psi(2S)$ (2.7×10^9) decays and extend its program to cover the full range up to 5.6 GeV in mass. Meson and baryon spectroscopy form the core of the program with extensions to mesonic and baryonic form factors and to τ decays (Hai-Bo Li, Ryan Edward Mitchell and Xiaorong Zhou). The BELLE II program, presented by Toru Iijima, has a strong part in spectroscopy as well. The experiment operates at an asymmetric e^+e^- collider mostly at the $\Upsilon(4S)$ mass. In addition to the spectroscopy program, BELLE III will search for non-SM contributions in hadronic, semileptonic and leptonic b-quark decays, determine quark mixing parameters, determine parameters in τ physics to precisions and perform searches for dark-sector particles.

The High-Luminosity Large Hadron Collider (HL-LHC) will have a five time larger luminosity than LHC. Major goals are improved tests of the Standard Model, searches for beyond the Standard Model (BSM) physics, studies of the properties of the Higgs boson, flavor physics of heavy quarks and leptons, and studies of QCD matter at high density and temperature. Project and prospects of HL-LHC are summarized by Tim Gershon, Massimiliana Grazzini and Gudrun Heinrich.

These major facilities represent a substantial investment in the experimental study of QCD, and show that the field has matured. It will be exciting to see what new results and deeper understandings emerge in the future.

14.1 JLab: the 12 GeV project and beyond

Patrizia Rossi

14.1.1 Jefferson Lab and CEBAF

Jefferson Lab (JLab), is a US National Lab located in Newport News – Virginia. It is a world-leading research laboratory for exploring the nature of matter in depth, providing unprecedented insight into the details of the particles and forces that build our visible universe inside the nucleus of the atom. Its scientific program spans the study of hadronic physics, the physics of complex nuclei, the hadronization of colored constituents, and precision tests of the Standard Model of particle physics. Figure 358 shows an areal view of the laboratory with the accelerator complex in the foreground. The core of Jefferson Lab is the Continuous Electron Beam Accelerator Facility (CEBAF). It operates as a pair of superconducting radio frequency linear accelerators (linacs) in a "racetrack" configuration and is designed to circulate a near continuous-wave electron beam through one to five passes recirculating arcs (see Fig. 359).

Jefferson Lab started physics operations in 1995, providing up to 6 GeV electron beams to three experimental halls, Halls A, B and C, simultaneously. In May 2012, the 6 GeV beam operations were stopped, with Jefferson Lab upgrading its facility to expand opportunity for discovery. In addition to the accelerator scope of doubling the energy, from 6 GeV to 12 GeV, the upgrade included the addition of a new fourth experimental hall, Hall D, and the construction of upgraded/new detectors hardware in the other halls. In two of the existing halls new spectrometers were added, the large acceptance device CLAS12 in Hall B [4401] and the precision magnetic spectrometer Super High Momentum Spectrometer, or SHMS, in Hall C. The new experimental Hall D makes use of a tagged bremsstrahlung photon beam and solenoidal detector to house the GlueX experiment.The initial energy upgraded program in Hall A made use of both the existing High Resolution Spectrometers.

The equipment in the four halls is well matched to the demands of the broad 12 GeV scientific program [3185] with complementary capabilities of acceptance, precision and required luminosity: high luminosity in Halls A and C and large acceptance detectors in Halls B and D. The upgraded CEBAF accelerator, which can deliver a maximum energy of 12 GeV to Hall D and 11 GeV to Halls A, B, C, delivered the first beam to Halls A and D in the spring of 2014. The full project was completed in spring 2017 with the commissioning of the two remaining halls.

In the meantime, Jefferson Lab has been continuing actively to invest in facilities that make optimum use of CEBAF's capabilities and the existing equipment, to produce science with high impact in Nuclear Physics as well

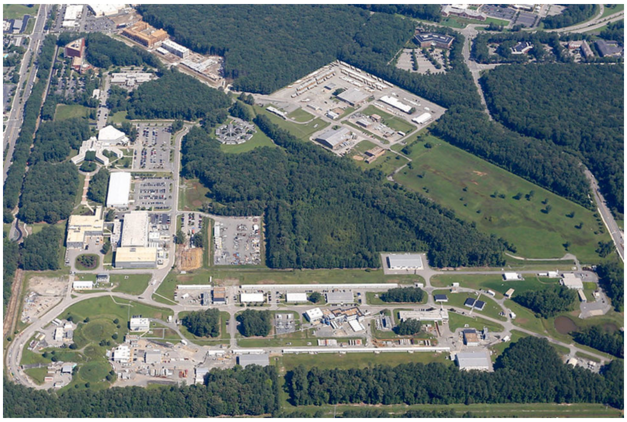

Fig. 358 Areal view of Jefferson Lab with the accelerator complex in the foreground

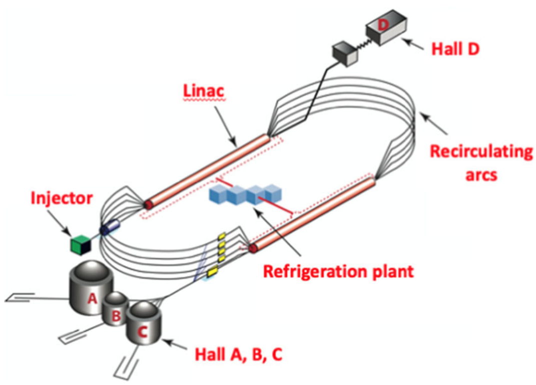

Fig. 359 CEBAF accelerator concept

as High Energy Physics and Astrophysics. In Hall A the Super Big Bite spectrometer (SBS) was installed in 2021, while the Measurement Of Lepton-Lepton Elastic Reaction (MOLLER) equipment is under construction with completion date foreseen for late 2026. On a longer term, Hall A plans to host the SOLenoidal Large Intensity Device (SoLID). Future additions include also: new large angle tagging detectors (TDIS in Hall A and ALERT in Hall B); the neutral particle spectrometer (NPS) and the compact photon source (CPS) in Hall C; and an intense K_L beamline that would serve new experiments in the GlueX spectrometer in Hall D.

14.1.2 The 12 GeV Physics program

CEBAF has been delivering the world's highest intensity and highest precision CW multi-GeV electron beams for more than 25 years. The capabilities of the upgraded CEBAF represent a significant leap over previous technology, with an unmatched combination of beam energy, quality and intensity. At Jefferson Lab experiments can run at luminosity up to 10^{38} cm^{-2} s^{-1} using a highly polarized electron beam (up to 90%), high power cryogenic targets, and several polarized targets using NH_3, ND_3, and ^3He to support a broad range of polarization measurements. This combination of beam, targets and large acceptance and high precision detectors, offers a powerful set of experimental tools that enables unprecedented studies of the inner structure of nucleons and nuclei and allows to push the limits of our understanding of the Standard Model.

The facility serves an international scientific user community of $\sim$ 1700 scientists which, in collaboration with the laboratory and with the guidance of the Jefferson Lab Program Advisory Committee (PAC), develops the scientific program. Following the last PAC meeting in 2022, there are a total of 90 approved experiments in the 12 GeV program,[120] of which more than 1/3 have received the highest scientific rating of A. There are 61 approved experiments still waiting to run, representing at least a decade of running in the future. Furthermore, PAC meetings are expected to continue each summer, with a call for new proposals for beam time. Clearly, CEBAF is a facility in high demand.

The JLab physics program falls into four main categories:

- the study of the transverse, longitudinal and 3-dimensional structure of the nucleon through the measurements of the elastic and transition form factors (FFs), the (un)polarized parton distribution functions (PDFs), and the Transverse Momentum Dependent (TMDs) and Generalized Parton Distributions functions (GPDs), respectively.
- The study of hadron spectroscopy and the search for exotic mesons to explore the nature of confinement.
- The study of the QCD structure in nuclei; its connection with the nucleon–nucleon interactions, including the modification of the valence quark PDFs in a dense nuclear medium, and the investigation of the quark hadronization properties. The neutron distribution radius in medium heavy nuclei, is also part of the program.
- The search of physics beyond the Standard Model in high-precision parity-violating processes and in the search for signals of dark matter.

Due to the limited space, only few selected highlights of the scientific agenda and present results of the JLab 12 GeV rich program are presented in this review. Some key results of the earlier JLab 6 GeV program are also reported for completeness when needed. The part related to the search of physics beyond the Standard Model, instead, are not discussed since it is somewhat beyond the scope of this volume. A more complete summary of the ongoing scientific program of the 12 GeV CEBAF and an outlook into future opportunities can be found in Ref. [4402].

[120] A list of approved experiments is available on the JLab website.

14.1.3 The structure of the nucleon

For the theoretical formalism and a general overview of the structure of the nucleon, the reader should refer to Sect. 10 of this volume.

Elastic Form Factors at high and ultra low Q^2
Since Hofstadter's pioneering experiment in the 1950s, the measurements of the electromagnetic space-like nucleon FFs have been a crucial source of information for our understanding of the internal structure of the nucleons. In 2000 Jefferson Lab rewrote the textbook of the proton and neutron form factors when precise data for the proton's electric to magnetic form factor ratio, G_E^p/G_M^p from double polarization experiments at Q^2 up to 5.6 GeV^2 [2973], didn't show the scaling behavior observed using the Rosenbluth separation method and subsequently confirmed by experiments with improved precision [2971,4403]. According to the pQCD predictions the ratio $Q^2\frac{F_{2p}}{F_{1p}}$, where F_{1p} and F_{2p} are the Dirac and Pauli form factors, respectively, would reach a constant value at high enough Q^2. The data clearly indicate that this asymptotic regime has not been reached yet [2974]. These observations suggest the presence of orbital angular momentum in the leading 3-quark component of the nucleon wave function in QCD Ref. [3040]. Another explanation of this discrepancy has been attributed to "two-photon" exchange (TPE) or higher order corrections to the cross sections. Jefferson Lab is tackling these questions and in the coming years will offer unprecedented opportunities to extend the current proton and neutron FF's measurements to higher momentum transfer Q^2 and to improve statistical and uncertainties at very low Q^2, where the nucleon size can be accurately investigated. The measurements at high Q^2 will also contribute to constraint two of the nucleon Generalized Parton Distributions, and in general will test the validity of quite a few fundamental nucleon models in a region of transition between perturbative and non-perturbative regimes.

One of the first completed experiments in Hall A with the upgraded CEBAF accelerator was a precision measurement of the proton magnetic form factor up to Q^2 = 16 GeV^2[2961]. This experiment nearly doubled the Q^2 range over which direct Rosenbluth separations of G_E and G_M can be performed. It confirmed the discrepancy with polarization measurements to larger Q^2 values and attributed it to hard TPE. These new, high-precision cross section measurement provides also an important baseline for the nucleon form factors program.

A series of experiments [4404–4409] for the measurements of the proton and neutron magnetic and electric form factors, has started at the end of 2021 using the Super Bigbite Spectrometer (SBS) and the upgraded BigBite Spectrometer in Hall A. This facility provides large acceptance at high luminosity so that small cross sections can be measured with high precision allowing a determination of the flavor separated form factors to Q^2 = 10–12 GeV^2. A complementary measurement of the neutron magnetic form factor will be performed with CLAS12 in Hall B [4410]. The SBS form factor experiments will push into a Q^2 regions in which theory expects new degrees of freedom to emerge in our understanding of QCD non-perturbative phenomena in nucleon structure as predicted in Ref. [3040].

From the perspective of QCD in exclusive processes, another important measurement is accessing the structure of the pion and kaon. The E12-06-101 experiment [4411] in Hall C will extract the pion form factor through $p(e,e'\pi^+)n$ and $d(e,e'\pi^-)pp$ with Q^2 extending to 6 GeV^2 from 2 GeV^2 and $-t_{\min} \sim 0.005 \sim 0.2\,\text{GeV}^2$. The proposed separation of longitudinal and transverse structure functions is a critical check of the reaction dynamics. The charged pion electric form factor is a topic of fundamental importance to our understanding of hadronic structure. There is a robust pQCD prediction in the asymptotic limit where $Q^2 \to \infty$: $Q^2 F_\pi(Q^2) \to 16\pi\,\alpha_s(Q^2) f_\pi^2$. Therefore it is an interesting question at what Q^2 this pQCD result will become dominant. The available data indicate that the form factor at $Q^2 = 2\,\text{GeV}$ is at least a factor of 3–4 larger. The new data will provide improved understanding of the non-perturbative contribution to this important property of the pion as well as mapping out the transition to the perturbative regime.

A high precision measurement of the elastic cross section on the proton at ultra low Q^2, the $PRad$ experiment, was performed in 2016 with the aim to solve the proton charge radius puzzle triggered by the muonic hydrogen spectroscopic measurements. To improve the precision of the measurement, the experiment utilized a new type of windowless target system flowing the hydrogen gas directly into the stream of CEBAF's 1.1 and 2.2 GeV electrons, and a calorimeter to detect the scattered electrons, rather than the traditionally used magnetic spectrometer. Moreover, the experiment was able to measure the scattered electron at very low (Q^2), facilitating a highly accurate extrapolation to $Q^2 = 0$ and extraction of the proton charge radius. The new value obtained for the proton radius is 0.831 fm [2958], which is smaller than the previous electron-scattering values and is, within its experimental uncertainty, in agreement with recent muonic atomic spectroscopy results.

To reach the ultimate precision offered by this new method, an enhanced version of $PRad$, the $PRad-II$ experiment [4412] has been approved. It will deliver the most precise measurement of G_E^p reaching the lowest ever Q^2 value ($10^{-5}\,GeV^2$) in lepton scattering experiments, critical for the model independent extraction of r_p. The projected r_p from *PRad-II* is shown in Fig. 360 along with the $PRad$ result, recent electron scattering extractions, atomic physics measurements on ordinary hydrogen and muonic hydrogen,

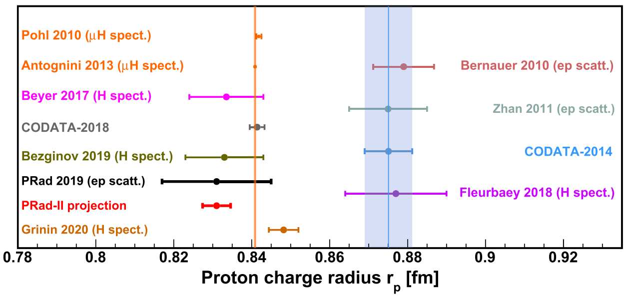

Fig. 360 The projected r_p result from PRad-II, shown along with the result from PRad and other measurements (see text)

and the CODATA values (see [2958] for references of these measurements).

Quark parton distributions at high x

The quark and gluon structure of the proton has been under intense experimental and theoretical investigation for more than five decades. Nevertheless, even for the distributions of the well-studied valence quarks, challenges such as the value of the down quark to up quark ratio at high fractional momenta x ($x \geq 0.5$), where a single parton carries most of the nucleon's momentum, remain. Recently, three JLab unpolarized DIS experiments, MARATHON [4413] in Hall A, BoNUS12 [4414] in Hall B, and F_{2d}/F_{2p} [4415] in Hall-C completed data taking. These experiments aim to provide data to constrain PDFs in the high-x region, especially the d/u PDF ratio.

The experiments in Hall A and Hall B used two different approaches to minimizing nuclear effects in extracting the neutron information: MARATHON measured the ratio of ^3H to ^3He structure functions, while BONUS12 tagged slow recoiling protons in the deuteron. The Hall-C experiment measured H(e, e') and D(e, e') inclusive cross sections in the resonance region and beyond. While there will be nuclear effects in the deuterium data, the experiment provides a significant large x range and reduced uncertainty to be combined with the large global data set of inclusive cross sections for PDF extraction. Figure 361 shows the MARATHON F_2^d/F_2^p results [4413], along with data from the JLab BoNUS experiment [3109] for $W \geq 1.84\,GeV$, evolved to the Q^2 of MARATHON, and results from early SLAC measurements with $W \geq 1.84$ GeV [4416] presented as a band. The results, which cover the Bjorken scaling variable range $0.19 < x < 0.83$, represent a significant improvement compared to previous measurements for the ratio. The results are expected to improve our knowledge of the nucleon PDFs, and to be used in algorithms which fit hadronic data to properly determine the essentially unknown $(u + \bar{u})/(d + \bar{d})$ ratio at large x. A planned experiment using Parity Violation in Deep Inelastic Scattering (PVDIS) [4417] on the proton, with the proposed SoLID [4418] spectrometer, will provide input on the d/u ratio at high x without contamination from nuclear

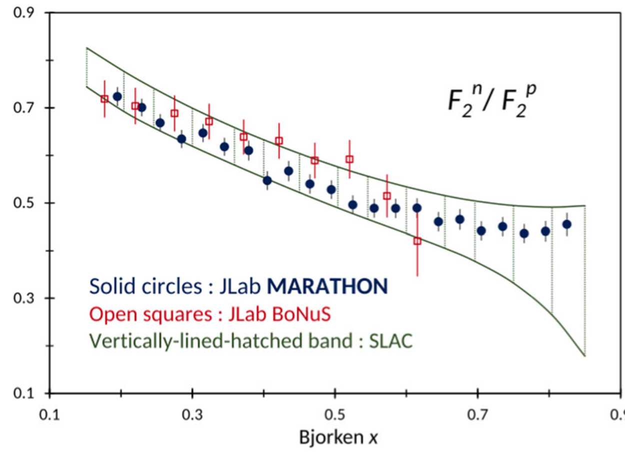

Fig. 361 The F_2^d/F_2^p ratio versus Bjorken x from the JLab MARATHON experiment [4413], together with data from BoNUS [3109] and a band based on the fit of the SLAC data as provided in Ref. [4416], for the MARATHON kinematics $Q^2 = 14x$ (GeV)^2 . All three experimental data-sets include statistical, point to point systematic, and normalization uncertainties

corrections by measuring the ratio of γZ interference to total structure functions.

An extensive experimental program on spin physics at low and moderate Q^2, has been pursued by JLab during the 6 GeV era. The main focus of the DIS experiments has been the $x-$dependence of virtal photon asymmetry $A_1 = g_1/F_1$, to determine the contributions of quark spins to the spin of nucleon. In addition, the high statistical precision data and kinematic coverage allowed an accurate study of sum rules in the parton to hadron transition region as well as higher twist contributions (see Ref. [4419] for a review). A spin physics program has been approved to run with the upgrade CEBAF which extends the kinematical coverage to higher x and can, among other things, answer the key question on what happens when a single quark carries nearly all (more than 80%) of the momentum of the nucleon. This region is well suited to test various theoretical predictions including those from the relativistic constituent quark model and perturbative QCD. The A_1^n high-impact experiment in Hall C [4420] completed data taking in 2020. The experiment ran at a luminosity of $2x10^{36} cm^{-2}s^{-1}$ thanks to the upgraded polarized ^3He target [4421]. The new precision measurement will expand knowledge of the extracted g_1^n structure function to $x = 0.75$. Combined with the currently running experiments to measure the proton and deuteron asymmetries A_1^p and A_1^d with CLAS12 [4411], new global analyses will be able to extract the Δu and Δd quark helicity distributions in the high-x region with much improved precision.

Nuclear femtography: TMDs and GPDs

Pioneering measurements to access Generalized Parton Distributions (GPDs) and Transverse Momentum Distributions (TMDs) were provided by the HERMES, COMPASS, and the JLab 6 GeV program, among others. For recent reviews see Refs. [4422,4423]. The upgraded detectors and CEBAF beam energy and intensity, promise to provide a more detailed three-dimensional (3D) mapping of the nucleon over wider ranges of the relevant kinematic variables. Indeed, this is a major thrust of the 12 GeV program accounting, so far, for almost $\sim 1/3$ of the whole approved experimental program.

Experimentally GPDs are accessible through deep exclusive processes, the most prominent ones being Deeply Virtual Compton Scattering (DVCS), and Deeply Virtual Meson Production (DVMP). TMDs, at JLab, are accessed through Semi-Inclusive Deep Inelastic Scattering (SIDIS), in which the nucleon is no longer intact and one or two of the outgoing hadrons are detected in coincidence with the scattered lepton. GPDs and TMDs are not measured directly. They are extracted through global fits to experimental data of Compton Form Factors (CFFs) for GPDs and Structure Functions for TMDs, and model dependent techniques with various assumptions involved. Therefore, accessing them demands not only a structured connection between theory, experiment and phenomenology, but availability of high precision data in a wide kinematical range and from different targets and several target/beam polarization combinations. A 3D description of the nucleon internal structure comes at the price of an unprecedented complexity. Therefore, for a correct interpretation of the data and a detailed comparison between results and theoretical models, a full differential analysis, using multi-dimensional information is crucial. The high-intensity, high-polarization electron beam provided by CEBAF with the complementary equipment of halls, A, B, C, makes JLab an ideal place for these studies.

SIDIS experiments provide access to the nucleon spin–orbit correlations. Observables are spin azimuthal asymmetries, and in particular single spin azimuthal asymmetries (SSAs), of the detected hadron. SSAs are due to the correlation between the quark transverse momentum and the spin of the quark/nucleon and early measurements indicated that they become larger with increasing x, i.e in the region where valence quarks have visible presence. Measurements of SSAs at JLab with the 6 GeV beam, performed with longitudinally polarized NH_3 [4424], and transversely polarized ^3He [3298,3299,4425,4426] indicate that spin orbit correlations may be significant for certain combinations of spins of quarks and nucleons and transverse momentum of scattered quarks.

Large spin-azimuthal asymmetries have been observed at JLab also for a longitudinally polarized beam [4427] and a transversely polarized ^3He target [4428], which have been interpreted in terms of higher-twist contributions related to quark–gluon correlations and novel aspects of emergent hadron mass. At JLab with upgraded energy, three experimental halls, A, B, and C are involved in TMDs studies. The measurements aim to access leading and higher twists TMDs

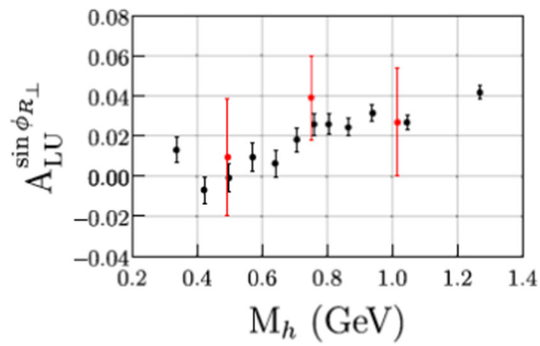

Fig. 362 The new CLAS12 results on beam helicity asymmetry in two-pion semi-inclusive deep inelastic electroproduction [4442] as a function of the invariant mass of pion pairs. The red points are from CLAS6 measurements [4444]

and their flavor and spin dependence, in multi-dimensional binning of x, Q^2, z, P_T. The joint efforts of the three halls, where the high-precision, high-statistics measurements in Hall A and C will be combined with the wide kinematics ones performed in Hall B, by using different targets and several target/beam polarization combinations, will allow a thorough exploration of the 3D structure of the nucleon in momentum space. The program includes the BigBite spectrometer and SBS [4429], as well as, the SoLID detector at Hall A [4430–4432], CLAS12 at Hall B [4433–4437], and High Momentum Spectrometer (HMS) and Super HMS at Hall C [4438–4440].

The first SIDIS publications of the 12 GeV era were reported by the CLAS12 collaboration on measurements of beam SSA for single pion [4441], two-pion [4442] and back-to-back dihadron [4443] productions off an unpolarized proton target using 10.6 and 10.2 GeV longitudinally spin-polarized electron beams. The single π^+ production was measured over a wide range of kinematics in a fully multi-dimensional study. The comparison with calculations shows the promise of high-precision data to enable differentiation between competing reaction models and effects.

The first significant beam spin asymmetries observed in two-pion production provide the first opportunity to extract the higher-twist parton distribution function $e(x)$, interpreted in terms of the average transverse forces acting on a quark after it absorbs the virtual photon. Moreover, this measurement constitutes the first ever signal sensitive to the helicity-dependent two-pion fragmentation function $G_1^\perp$. The comparison of the 6 GeV and 12 GeV measurements shown in Fig. 362) demonstrates the impact of the beam energy on the phase space for production of multiple hadrons in the final state and the huge reduction in the corresponding error bars. Finally, the measured beam-spin asymmetries in back-to-back dihadron electroproduction, $ep \to' p\pi^+X$, with the first hadron produced in the current-fragmentation region and the second in the target-fragmentation region, provide a first access in dihadron production to a previously unobserved leading-twist spin- and transverse-momentum-dependent fracture functions [4445].

A comprehensive program is carried out at JLab in deeply virtual exclusive scattering processes (DVCS and DVMP) with the goal to create the transverse spacial images of quarks and gluons as a function of their longitudinal momentum fraction in the proton, neutron and nuclei through the study of the GPDs. The physical content of the GPDs is quite rich. Among other features, they give access to the contribution of the orbital momentum of the quarks and gluons to the nucleon, and the D-term, a poorly known element of GPD parametrizations, which gives valuable insights to the mechanical properties of the nucleon [2879,4446–4448]. The study of the deeply exclusive processes and the GPDs extraction started, at JLab, in the 6 GeV era. After the first publication by CLAS in 2001 [4449], a series of high-statistics DVCS-dedicated experiments in Hall A and B followed at moderate Q^2 (1–3) GeV^2 and in a x_B range centered around $x_B \sim 0.3$ (for a recent review see [4450]).

The polarized and unpolarized cross sections measured at in Hall A at 6 GeV [4451,4452] indicate, via a Q^2-scaling test, that the factorization and the hypothesis of leading-twist dominance are valid already at relatively low Q^2 ($\sim$ 1–2) GeV^2 and thus the applicability of the GPD-based description. Covering a range in x_B from 0.1 to 0.7 and in Q^2 from 1 to 10 GeV^2, the upgraded JLab is very well matched to study GPDs in the valence regime. The program is executed in the three experimental halls, A, B, C, and aims to measure accurately fully differential beam-polarized cross section differences and unpolarized cross sections, longitudinally polarized target-spin asymmetries along with double polarization observables.

The first result of the 12 GeV era was reported by Hall A on the DVCS cross section measurement at high Bjorken x_B off an unpolarized proton target [4453]. The work presents the first experimental extraction of the four helicity-conserving nucleon Compton Form Factors (CFFs) as a function of x_B. A similar experiment, which will complement the kinematic coverage of the Hall A, is planned to run in Hall C with the HMS and NPS in 2024 [4454]. In Hall B two experiments measuring DVCS off an unpolarized proton target at 11 GeV [4455] and 6.6 and 8.8 GeV [4456] will allow a larger kinematical coverage, while the measurement of the beam-spin asymmetry off a deuteron target, with detected neutron, will allow to constrain the poorly known GPD E, related to the quark orbital angular momentum through the Ji's sum rule, and to perform the GPDs quark-flavor separation. These experiments will release their results soon. Finally, an experiment using longitudinally polarized NH_3 and ND_3 target [4411] is currently running in Hall B and one has been proposed to use a transversely polarized proton [4457]. The precision and kinematical coverage of these asymmetries

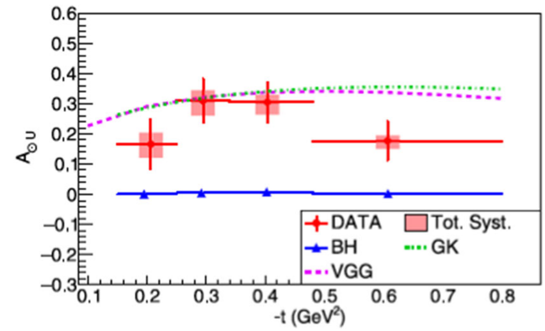

Fig. 363 Photon polarization asymmetry as a function of −t. The dashed and dashed-dotted lines are the predictions of GPDs based models, respectively, the VGG [4464] and the GK [4465] models, evaluated at the average kinematics. For detailed explanation see [2881]

obtained with different combination of targets and polarization will bring stringent constraints to GPD parametrizations.

Meson production at JLab at 6 GeV has not yet shown parton dominance of scattering. Experimental data from 11 GeV beam will provide important test of the deep-exclusive meson production mechanism. Hall A recently published deep exclusive electroproduction of π^0 at high Q^2 [4458] using the 11 GeV beam off an unpolarized proton target. The results suggest the amplitude for transversely polarized virtual photons continues to dominate the cross section throughout this kinematic range. Experiments have also been approved in Hall B for π^0, η [4459] and ϕ production [4460], the latter with the hope to determine the t-slope of the gluon GPDs. In Hall C, it is important to mention the precise measurement of the L/T separation on kaon and pion electroproduction [4461,4462] and the neutral pion cross-section measurements [4454].

Finally, DVCS and DVMP will be measured on the ^4He nucleus (with emphasis on ϕ production) [4463], with the aim of comparing a) the quark and gluon radii of the helium nucleus, b) GPDs of the bound proton and neutron with the free proton and quasi-free neutron.

While the most attention so far is on studies of GPD using spin (beam/target) observables and cross-sections in DVCS, also the Time-like Compton Scattering (TCS), the time-reversal symmetric process of DVCS where the incoming photon is real and the outgoing photon has large time-like virtuality, has much to offer. The first ever measurement of TCS on the proton $\gamma p \to p'\gamma^*(\gamma^* \to e^+e^-)$ has been obtained with CLAS12 [2881]. Both the photon circular polarization and forward/backward asymmetries were measured. The comparison of the measured polarization asymmetries with model predictions points toward the interpretation of GPDs as universal functions. Figure 363 shows the photon polarization asymmetry $A_{\odot U}$ as a function of $-t$ at the averaged kinematic point $E_\gamma = 7.29 \pm 1.55$ GeV; $M = 1.80 \pm 0.26$ GeV, compared with GPDs based models.

14.1.4 Hadron spectroscopy

For the theoretical formalism and a general overview of hadron spectroscopy, the reader should refer to Sect. 8 of this volume.

This is an exciting period in hadron spectroscopy. The last two decades witnessed the discovery of many states that challenged the basic model of hadron physics according to which particles are made of $3q$ (baryons) or a $q\bar{q}$ (mesons), and pointed to states with multi-quark content, or with explicit gluonic components (glueballs and hybrids). Mapping states with explicit gluonic degrees of freedom in the light sector is a challenge.

One example is the π_1 state which has led to controversies. Experiments have reported two different hybrid candidates with spin-exotic signature, which couple separately to $\eta\pi$ and $\eta'\pi$, $\pi_1(1400)$ and $\pi_1(1600)$ (for a review see Ref. [2414]). This picture is not compatible with recent Lattice QCD estimates for hybrid states, nor with most phenomenological models. A recent work by the JPAC [4466] provides a robust extraction of a single exotic π_1 resonant pole, but no evidence for a second exotic state (see Grube's contribution, Sect. 8.3). The main goal of the GlueX experiment [4467,4468] in Hall D is to search for exotic mesons, and together with CLAS12 MesonEx experiment [4469] in Hall B, to provide a unique contribution to the landscape of experimental meson spectroscopy through the novel photoproduction mechanism previously relatively unexplored. Utilizing a real, linearly-polarized photon beam in GlueX and quasi-real, low-Q^2 photons in CLAS12, this program covers a wide range of beam energies from E_γ = 3-12 GeV.

GlueX has already collected high-statistics, high-quality photoproduction data and published various results on photoproduction cross sections for several single pseudoscalar mesons including the $\pi^0, \pi^-, K^+, \eta, \eta'$ over a broad range of momentum transfer [4470–4473], focused on a quantitative understanding of the meson photoproduction mechanism. Polarization observables, such as spin-density matrix elements, provide also valuable input for the theoretical description of the production mechanism, which is essential for the interpretation of possible exotic meson signals. Moreover, these studies require a complete understanding of the detector acceptance and efficiencies in fits to multi-dimensional data and therefore are essential for assessing the Partial Wave Analysis (PWA) machinery.

GlueX published the first measurement of spin density matrix elements of the $\Lambda(1520)$ in the energy range E_γ = 8.2–8.8 GeV [4474] and released preliminary results on spin-density matrix elements of the vector mesons $\rho(770)$, $\phi(1020)$ and $\omega(782)$ [4475]. The statistical precision of the final analysis with the full data set will surpass previous measurements by orders of magnitude. The search for hybrid mesons has started in GlueX by studying $\eta^{(\prime)}\pi$ final-states to eventually confirm the π_1 pole position extracted by JPAC. With a large acceptance to both charged and neutral particles, GlueX has access to both neutral $\gamma p \to \eta^{(\prime)}\pi^0 p$ and charged $\gamma p \to \eta^{(\prime)}\pi^-\Delta^{++}p$ exchanges. Figure 364) shows preliminary results for the measured intensity of the dominant waves in the $\gamma p \to \eta^{(\prime)}\pi^0 p$ channel.

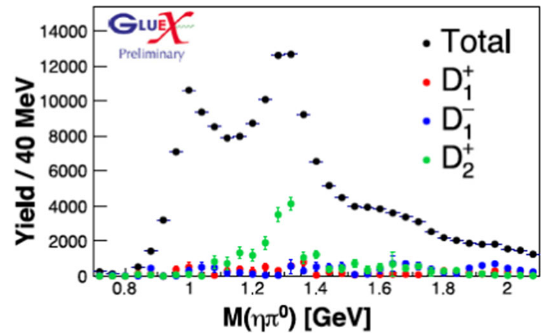

Fig. 364 Preliminary mass spectra and amplitude analysis results from GlueX for the reactions $\gamma p \to \eta^{(\prime)}\pi^0 p$, with $0.1 < -t < 0.3\,\mathrm{GeV}^2$ and $8.2 < E_\gamma < 8.8$ GeV

JLab at 12 GeV will continue the program to study the spectrum and structure of excited nucleon states, which in the last 15 years have provided critical input to global analyses to elucidate the N^* spectrum (see Refs. [2876,4476] for recent reviews). Detailed electrocouplings measurements through exclusive electroproduction study of both strange and non-strange final states, will be extended with the new CLAS12 detector and the upgraded energy beam which will significantly extend the kinematic range to $Q^2 > 5\,\mathrm{GeV}^2$ [4477,4478]. The program comprises also the search of hybrid baryons with constituent gluonic excitations, for which a rich spectrum is predicted by Lattice QCD. Finally, many hyperon spectroscopy measurements are expected from the GlueX and CLAS12 measurements, including the Ξ and Ω [4479,4480]. This program will be expanded by proposal to perform hyperon spectroscopy with the K_L neutral kaon beam in Hall D, which was recently approved by the PAC [4481].

Over the past several years there has been a renewed interest in studying near-threshold J/ψ photoproduction as a tool to experimentally probe important properties of the nucleon target related to its mass and gluon content. Moreover, in the beam energy region of E_γ = 9.4-10.1 GeV, the $\gamma p \to J/\psi p$ process can be used to search, directly in a simple $2 \to 2$ body kinematics [4482–4485] for the pentaquark candidates, $P_c^+(4312)$, $P_c^+(4440)$, and $P_c^+(4457)$, reported by the LHCb experiment but still under debate [2885,2886]. JLab has an active J/ψ physics program. There are either published, ongoing, or planned future J/ψ experiments in each experimental hall. The first measurement was performed by GlueX [4486] and is shown in Fig. 365 , with curves depicting the strength of hypothetical P_c signals. No

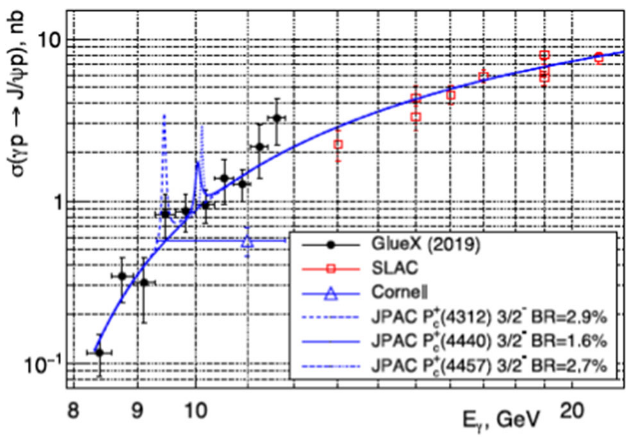

Fig. 365 GlueX results for the J/ψ total cross section vs beam energy, compared to the JPAC model with hypothetical branching ratios provided in the legend for P_c^+ with $J^P = 3/2^-$ as described in Ref. [4486]

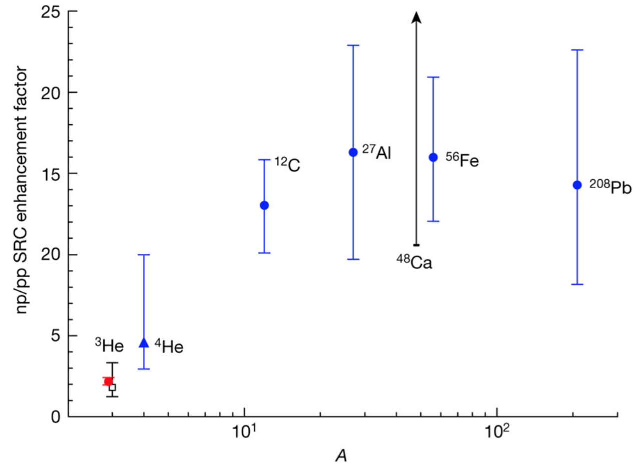

Fig. 366 Ratio of np-SRCs to pp-SRCs relative to the total number of np and pp pairs, for the new inclusive data (red circle), compared with previous measurements [4503].

structures are observed in the measured cross section, however model-dependent upper limits are set on the branching ratio of the possible $P_C \to J/\psi p$ decays. Preliminary results from the $J\psi - 007$ experiment in Hall C also observe no P_c signal and will set more restrictive limits on the branching ratio [4487]. In Hall B analysis of data are ongoing [4488] and in Hall A an experiment has been approved to run with SoLID [4489].

14.1.5 QCD and nuclei

Nuclear interactions are described using effective models that are well constrained at typical internucleon distances in nuclei but not at shorter distances. The strong component of the nucleon–nucleon potential associated with hard, intermediate short-distance interactions between pairs of nucleons, called Short-Range Correlated (SRC) pairs, is a poorly understood parts of nuclear structure and generates a high-momentum tail to the nucleon momentum distribution. The existence and characteristics of SRC pairs are related to outstanding issues in particle, nuclear, and astrophysics, among which are the modification of the internal structure of nucleons bound in atomic nuclei (the EMC effect) [4490] and the nuclear symmetry energy governing neutron star properties [4491].

The studies of SRCs are a sizeable part of the JLab program that started already in the 6 GeV era. After the initial observation of identical structure in the high-momentum components of nuclei at SLAC [4492], electron-scattering measurements at JLab have identified the kinematic region where SRCs dominate [4493,4494] and mapped out the contribution of SRCs in various light and heavy nuclei relative to the deuteron [1362,4495]. Data demonstrated also that the contribution is sensitive to details of the nuclear structure [4496,4497] rather than the previously assumed average nuclear density [4498]. In addition, they showed a clear correlation between the contribution of SRCs [1362] and the size of the EMC effect [4496]. To study the isospin dependence of the SRCs, measurements of two-nucleon knock-out were carried out. These experiments showed dominance of np-SRC pairs over pp and nn-SRC pairs by a factor of about 20 [1363,4499,4500]. The result was confirmed in measurements of quasi-elastic knock-out of protons and neutrons from medium and heavy nuclei [4501], and later through inclusive measurements of the $^{48}Ca/^{40}Ca$ cross section ratio [4502] taking advantage of the target isospin structure.

The first measurement using a novel technique to extract the np/pp ratio of SRCs taking advantage of the isospin structure of the mirror nuclei ^3H and ^3He was carried out in the 12 GeV era [4503]. The np/pp SRC ratio obtained is an order of magnitude more precise than previous experiments, and shows a dramatic deviation from the near-total np dominance observed in heavy nuclei (see Fig. 366). This result implies an unexpected structure in the high-momentum wave-function for ^3He and ^3H. Finally, measurements at $x > 2$ carried out with the 6 GeV beam, tried to establish the presence of three-nucleon SRCs [1362,4504], but didn't come to a definitive conclusion. Experiment [4505] with the 11 GeV beam will provide the first significant test by taking high-statistics $A/^3He$ ratio data at $x > 2$ and $Q^2 = 3\,\mathrm{GeV}^2$.

Determining the origin of the EMC effect, i.e. the modification of nuclear PDFs relative to the sum of the individual nucleon PDFs, is one of the major unsolved problems in the field of nuclear physics and is still a puzzle after 40 years. Measurement at Jlab at 6 GeV in light nuclei demonstrated the correlation between the size of the EMC effect and the contribution of SRCs [1362]. The JLab12 program addresses the three open questions of the EMC effect: (i) the isospin dependence; (ii) the spin dependence; (iii) the configuration/distance dependence. The isospin dependence has been investigated with the already mentioned experiment using mirror nuclei [4503]. Polarization measurements can also help to understand the origin of the EMC effect [4506,4507]. An 11 GeV experiment will measure the EMC effect in polarized ^{7}Li [4508] with the goal to distinguish between mean-field models with explanations based on SRCs. Tagging of recoil nuclei in deep inelastic reactions will be used in [4509] to address point (iii). This is a powerful technique to provide unique information about the nature of medium modifications, through the measurement of the EMC ratio and its dependence on the nucleon off-shellness.

There are several ways to study QCD in nuclei. One is through the hadronization process, a mechanism by which quarks struck in hard processes form the hadrons observed in the final state. This is a poorly known mechanism and more insight can be obtained by systematically studying production of different baryon and meson types using large and small nuclear systems, and observing the multi-variable dependence of observables, such as multiplicity ratios and transverse momentum broadening. These studies started with CLAS at 6 GeV [4510] and will continue with CLAS12 [4508].

Hadron propagation in the medium can also be studied by searching for color transparency, where the final (and/or initial) state interactions of hadrons with the nuclear medium must vanish for exclusive processes at high momentum transfers. Color transparency for pions [4511] and ρ mesons [4512] was observed at 6 GeV while the 11 GeV experiment [1331] ruled out color transparency in quasielastic $^{12}C(e, e'p)$ up to Q^2 of 14.2 GeV^2. These results impose strict constraints on models of color transparency for protons.

Measurements on nuclei which are directly relevant for understanding aspects of astrophysics and neutrino physics are also part of the JLab program. One of the early experiments of the 12 GeV era was the measurements of inclusive quasi-elastic scattering and single proton knockout on ^{40}Ar [4513,4514]. These data will allow for tests of $\nu -^{40} Ar$ scattering simulations needed for the DUNE experiment. Another experiment [4515] measured electron scattering from a variety of targets and different beam energies in CLAS12 in order to test neutrino event selection and energy reconstruction techniques and to benchmark neutrino event generators.

Thanks to the intense and highly polarized CEBAF electron beams, measurements of the parity-violating electron scattering asymmetry from ^{208}Pb and ^{48}Ca have demonstrated a new opportunity to measure the weak charge distribution and hence pin down the neutron radius in nuclei in a relatively clean and model-independent way. A precise measurement of the neutron radius, and hence of the neutron

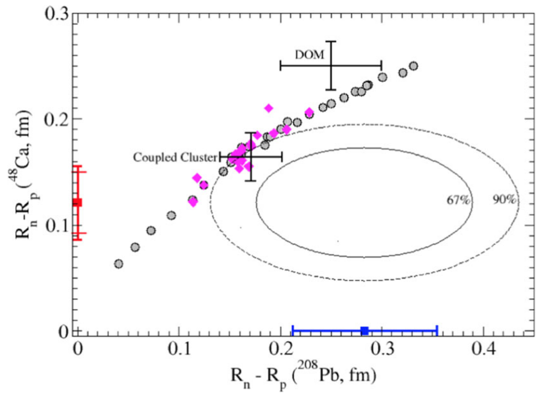

Fig. 367 ^{48}Ca neutron minus proton radius (red square) versus that for ^{208}Pb (blue square). The ellipses are joint PREX-II and CREX 67% and 90% probability contours.The gray circles (magenta diamonds) show a variety of relativistic (non-relativistic) density functionals (see Ref. [4517])

skin thickness, helps to constrain the density dependence of the symmetry energy of neutron rich nuclear matter, which has implications on neutron stars and supernova. The PREX-II experiment [4516] measured the "neutron skin thickness" of ^{208}Pb while CREX[4517] measured that of ^{48}Ca. For CREX, the extracted neutron skin can be directly compared to microscopic calculations [4518] providing a bridge between medium nuclei ab initio calculations and heavy nuclei Density Functional Theory calculations. The extremely precise CREX measurement indicates a thin neutron skin around its nucleus, in contrast with the PREX measurement which revealed a thicker skin (see Fig. 367). This discrepancy is exciting and presents the opportunity for further exploration to determine why there's such a big difference between the medium-density calcium nucleus and the high-density lead nucleus.

14.1.6 Future opportunities

With a fixed target program at the "luminosity frontier," up to 10^{39} cm^{-2} s^{-1}, and large acceptance detection systems, CEBAF will continue to offer unique opportunities to illuminate the nature of QCD and the origin of confinement for decades to come. In fact, CEBAF operates with several orders of magnitude higher in luminosity than the Electron-Ion Collider (EIC) and exciting scientific opportunities using CEBAF beyond the currently planned decade of experiments can provide very complementary capabilities, even in the era of EIC operations. A discovery science program utilizing CEBAF in the EIC era has been developing jointly between JLab and its user community towards exploring both the science and technical case for moving beyond 12 GeV. A series of upgrades to increase luminosity, enable positron beams, and double the energy of CEBAF is envisioned [4402].

- An increase in luminosity with modest detector upgrades will facilitate double DVCS (DDVCS) studies in experimental Halls A and B. DDVCS can bring significant additional information to the three dimensional imaging of the quark structure. This is a process with interaction rates a factor of 100 lower than DVCS. Therefore it is not viable at EIC and must be studied using CEBAF.
- Positron beams, both polarized and unpolarized, are identified as an essential ingredient for the hadronic physics program at JLab, and they are important tools for a precise understanding of the electromagnetic structure of the nucleon, in both the elastic and the deep-inelastic regimes. For instance by comparing the $e^+ - p$ and $e^- - p$ elastic scattering it would be possible to test the validity of the 1γ exchange approximation of the electromagnetic interaction. Proof of principle of a new concept for creating polarized positron beams at CEBAF has been demonstrated and a scientific program has been developed [4519].
- Encouraged by recent success of CBETA at Cornell, a proposal was formulated to increase the CEBAF energy from the present 12 GeV to 20–24 GeV by replacing the highest-energy arcs with Fixed Field Alternating Gradient (FFA) arcs but using the existing CEBAF SRF cavity system. The new pair of arcs would support simultaneous transport of 6 passes with energies spanning a factor of two. This exciting new technology, implemented with permanent magnets, would be a cost-effective method to double the energy of CEBAF, enabling new scientific opportunities in meson spectroscopy and extending the kinematic range of nucleon imaging studies. For instance, with an energy upgrade, JLab will be capable of providing unique and complementary information that could be decisive in understanding the nature of a subset of the XYZ states. Moreover, JLab will be able to do unique precise measurements of the photoproduction cross section of J/ψ and higher mass charmonium states, χ_c and $\psi(2S)$, near threshold. Combined with an increase of the polarization figure-of-merit by an order of magnitude, GlueX will be the only experiment to be able to measure the polarization observables that are critical to disentangle the reaction mechanism and draw conclusions about the mass properties of the proton.Technical studies of the implementation of FFA technology at CEBAF are in progress.

14.1.7 Conclusions

Jefferson Lab is a world-leading research laboratory for exploring the nature of matter in depth. Its powerful experimental program at 12 GeV will advance our understanding of the quark/gluon structure of hadronic matter, the nature of Quantum Chromodynamics, and the properties of a new extended standard model of particle interactions. CEBAF at Jefferson Lab is a facility in high demand due to its unique capability to operate with a fixed target program at the "luminosity frontier" up to 10^{39} cm $^{-2}$ s^{-1}, with exciting scientific opportunities beyond the currently planned decade of experiments. Potential upgrades of CEBAF and their impact on scientific reach are being discussed, such as higher luminosity, the addition of polarized and unpolarized positron beams, and doubling the beam energy. They will keep CEBAF uniquely capable of a large number of important measurements in nuclear and hadronic physics.

14.2 The EIC program

Christian Weiss

The Electron-Ion Collider (EIC) at Brookhaven National Lab (BNL) is planned as a next-generation facility for high-energy ep/eA scattering experiments supporting basic research in hadronic/nuclear physics and QCD. The design combines the RHIC superconducting proton/ion accelerator ring with an electron storage ring in the same tunnel and an injector for on-energy injection of polarized bunches and enables collisions at one (possibly two) interaction points (see Fig. 368) [4520]. It provides ep collisions at CM energies $\sqrt{s} = 20$–100 GeV, upgradable to 140 GeV, using various combinations of beam energies; for eA collisions with the same setup the CM energy per nucleon is lower by a factor $\sqrt{Z/A}$. It is projected to achieve peak luminosities in the range $\sim 10^{33}$–10^{34} cm^{-2} s^{-1} and deliver an integrated lifetime luminosity ∼10–100 fb^{-1}. It accelerates ion species including the proton (p), light ions (D, ^{3}He, others), and heavy ions (Au, U, others). Polarization is available for the electron and the light ion beams (p and ^{3}He) with an average ion polarization ∼70%. The EIC will be the first colliding beam facility delivering electron collisions with ion beams ($A > 1$), and with polarized proton/ion beams. Its luminosity will exceed that of the HERA ep collider by 100–1000. As such it will provide qualitatively new capabilities for physics research [3163].

The concept of a polarized electron-ion collider was inspired by the results of the fixed-target spin physics experiments (CERN, SLAC, DESY), the DESY HERA ep collider, and the BNL RHIC polarized pp and AA collider, and motivated by advances in theoretical concepts for hadron structure and high-energy QCD. The developments began with planning exercises in the 1990s and advanced through extensive community efforts (science studies, program development) [1293,3186] and technical design work (accelerator, facility) at BNL, JLab, and other laboratories in the 2000s and 2010s. Important milestones were the recommendation in 2015 Nuclear Science Advisory Committee Long-Range Plan [4521] and the endorsement by a study of the U.S. National Academy of Sciences 2018 [4522]. The

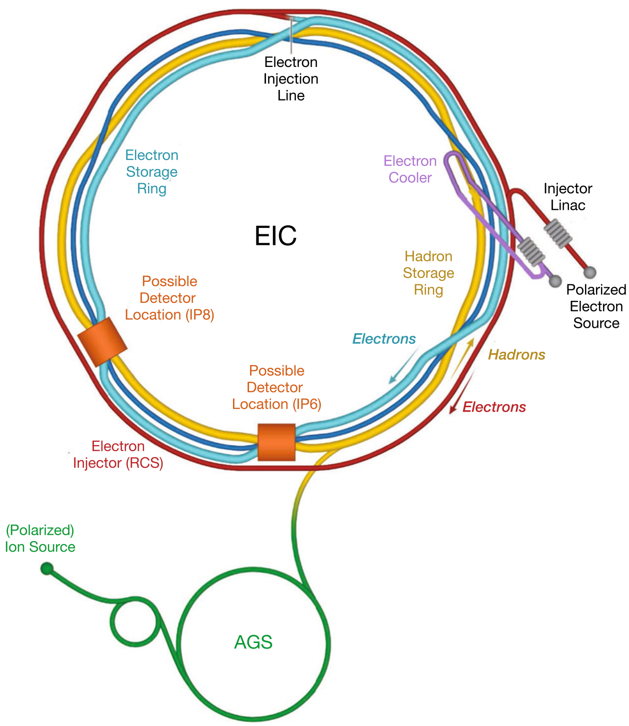

Fig. 368 Schematic of the EIC accelerator complex [3163,4520]

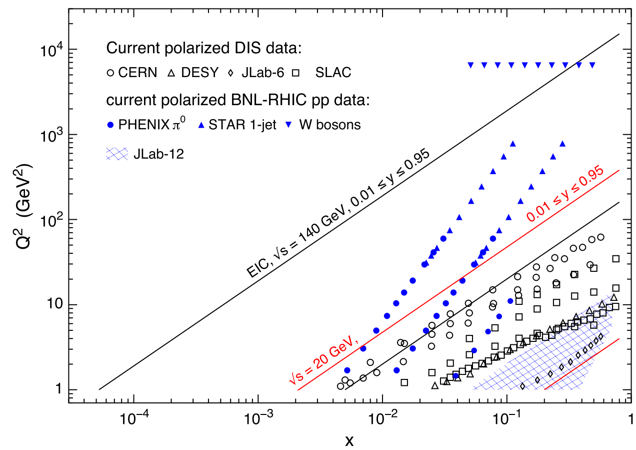

Fig. 369 Kinematic coverage in x and Q^2 in DIS experiments with the EIC at CM energies of 20 GeV and 140 GeV [3163]

EIC was granted Critical Decision Zero (CD-0) by the U.S. Department of Energy in December 2019 and is now an official project of the U.S. Government. It is executed according to project management principles and passed CD-1 in 2021. Completion of construction and begin of operations are expected around 2034.

The EIC will enable a comprehensive science program aimed at understanding hadrons and nuclei as emergent phenomena of QCD. Scattering experiments will be performed at momentum transfers $Q^2 \sim 10^1$–$10^2\,\mathrm{GeV}^2$, corresponding resolution scales where the quark and gluon degrees of freedom are manifest and methods of QCD factorization can be applied (see Fig. 369). The partonic content will be sampled at momentum fractions down to $x \sim 10^{-3}$–10^{-4}, where gluons and sea quarks are abundant and dominate hadron structure. The wide kinematic coverage will enable study of scale dependence and radiation processes building up the parton densities, which provide essential insight into the dynamics. The luminosity and detection systems will permit measurements of the final states of deep-inelastic processes in unprecedented detail (exclusive processes, semi-inclusive production, jets, nuclear breakup, diffraction, etc.) and enable analysis using modern theoretical concepts (GPDs, TMDs, jets).

The EIC science program is organized in four broad themes, defined by basic physics questions and concepts that are explored using various measurements:

- Global properties and partonic structure of hadrons
- Multi-dimensional imaging of hadrons and nuclei
- Nuclear high-energy scattering in QCD
- Emergence of hadrons from QCD

The boundaries between them are not strict, as some measurements serve to answer questions in more than one area. In the following we briefly summarize the objectives and main measurements in each of the themes; further information can be found in Refs. [1293,3163,3186].[121] The program and its organization are still evolving; new topics are being discussed and proposed in response to developments in theory and detector design.

14.2.1 Global properties and partonic structure

One basic objective is to understand how the global properties of hadrons such as spin, mass, charges, and other characteristics emerge from the quark/gluon fields of QCD and their interactions (see Sect. 10.3). The quantities are expressed as matrix elements of QCD composite operators between hadronic states, $\langle h|\mathcal{O}_{\mathrm{QCD}}|h\rangle$, some of which can be measured in deep-inelastic processes. For some quantities the operators have a partonic interpretation, and the matrix elements and can be expressed as integrals of the PDFs/GPDs (sum rules). For other quantities the operators involve interactions (higher twist), and the interpretation is more indirect. The EIC will advance this program through several measurements:

[121] The literature supporting the concepts and measurements of the EIC physics program is very extensive. In this summary we refer to the other sections of the review article for concepts and previous results whenever possible; we refer directly to the literature for simulation and impact studies for the EIC, and for topics not covered elsewhere in the review.

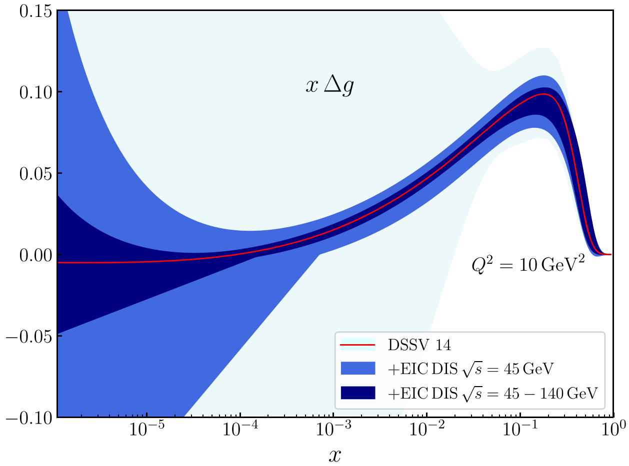

Fig. 370 Gluon spin PDF extracted from polarized inclusive DIS pseudodata at EIC [3131,3163]. Similar results are obtained in studies using other PDF parametrizations [3163]

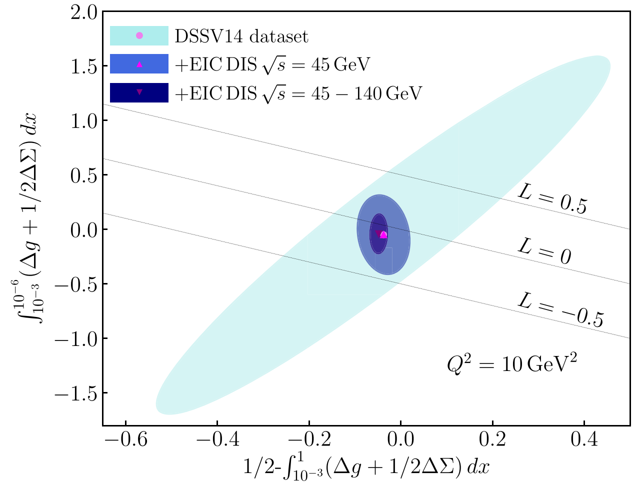

Fig. 371 Room left for potential orbital angular momentum contributions to the proton spin after determining the quark and gluon spin contributions at EIC [3131,3163]

Gluon polarization and nucleon spin
The quark and gluon contributions to the nucleon spin are expressed as the integrals of the quark and gluon spin PDFs, which are measured in various polarized scattering experiments (see Sect. 10.3). Despite much effort, the contributions to the spin sum rule are still poorly known. While fixed-target DIS measurements have determined the quark spin densities, and the RHIC spin program has provided evidence of nonzero gluon spin, the distributions are known with good precision only at $x \gtrsim 0.01$, so that the integrals suffer from large uncertainties (see Sect. 10.2). At EIC, measurements of inclusive polarized *ep* DIS will accurately determine the quark and gluon spin densities down to $x \gtrsim 10^{-4}$. The wide kinematic coverage will make it possible to determine the gluon spin density indirectly through DGLAP evolution (see Fig. 370) [3131,3163,3165]. Complementary information will come from direct measurements of the gluon spin density using dijets or heavy flavor production [4523]. The gluon and quark spin PDFs extracted in this way will permit accurate evaluation of quark and gluon spin contributions to the spin sum rule. The results will also constrain the possible contribution of quark/gluon orbital angular momentum to the nucleon spin (see Fig. 371).

Sea quark spin and flavor distributions
Equally important are the spin distributions of the sea quarks in the nucleon, which exhibit flavor dependence ($\Delta\bar{u} \neq \Delta\bar{d} \neq \Delta\bar{s}$, $\Delta s \neq \Delta\bar{s}$) and attest to flavor-dependent non-perturbative interactions with the valence quarks in the nucleon. Present results on the flavor dependence from fixed-target semi-inclusive DIS and the RHIC $W^{\pm}$ production data show large uncertainties (see Sect. 10.2). EIC will determine the polarized sea quark distributions and their flavor dependence through polarized *ep* semi-inclusive DIS, taking advantage of large phase space for fragmentation (see Fig. 372) [3131,3163]. Complementary information will come from DIS on the neutron measured with polarized ^{3}He beams. The determination of the flavor structure of the polarized sea will also indirectly improve the extraction of the gluon spin distribution and the spin sum rule (separation of flavor singlet and non-singlet distributions). EIC will also enable novel studies of the flavor structure of the unpolarized sea using charged-current DIS.

Orbital angular momentum
The total angular momentum of quarks and gluons in the nucleon can be expressed through integrals of the GPDs (see Sect. 10.3). This representation provides alternative insight into the role of orbital angular momentum in the nucleon spin decomposition. The GPDs appear in the amplitudes of hard exclusive processes (deeply virtual Compton scattering or DVCS, meson production) and can be accessed experimentally in this way; see Refs. [3243–3245,4524] for a review. While the hard exclusive processes sample the GPDs in a restricted domain of variables that is not sufficient for evaluating the angular momentum sum rule, it is possible to establish a connection in the context of dynamical models of the GPDs, or a global analysis recruiting other data. EIC will advance this program through measurements of DVCS and meson production over a wide kinematic range; the same data will be used for the 3D spatial imaging (see below).

Energy–momentum tensor
Other global properties follow from the nucleon matrix elements of the QCD energy–momentum tensor and can be studied by using the connection with scattering processes. The D-term of the energy–momentum tensor, which expresses certain mechanical properties of the nucleon, appears as a subtraction constant in the dispersion relations for the DVCS amplitude and can be extracted from fits to DVCS data with

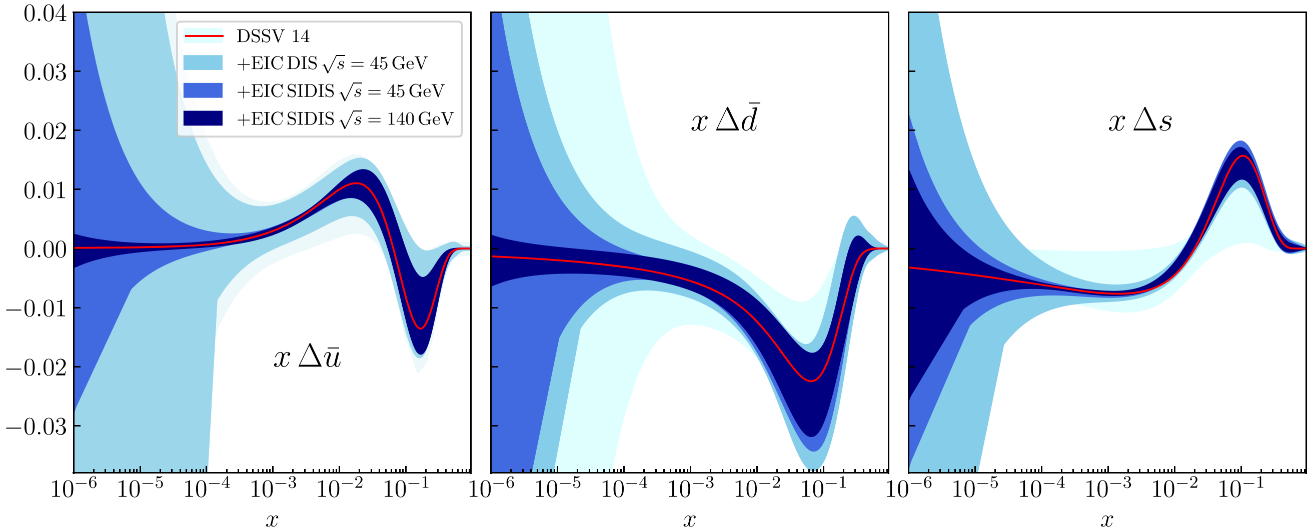

Fig. 372 Flavor decomposition of the polarized sea quark distributions in the proton with projected EIC SIDIS data [3131,3163]. Similar results are obtained in studies using other PDF parametrizations [3163]

minimal model dependence; see Refs. [2882,4525] for a review. EIC measurements will allow one to precisely determine the D-term, taking advantage of the wide energy coverage of the data in evaluating the dispersion integral.

The trace of the QCD energy–momentum tensor contains important information on the emergence of the nucleon mass from QCD; see Refs. [4526–4528] for recent discussion and review. The breaking of scale invariance through the UV divergences of QCD implies that the trace is proportional to the twist-4 gluonic operator $G^2_{\mu\nu}$ (trace anomaly). An interesting question is how much this effect contributes to nucleon mass. It has been suggested that the twist-4 gluonic operator could be accessed in exclusive photo/electroproduction of heavy quarkonia at near-threshold energies [4529–4531]; however, this connection relies on the questionable assumption of vector meson dominance [4532], and the mechanism of heavy quarkonium production near threshold is a matter of current research and discussion; see e.g. Refs. [4533–4536]. EIC will contribute to this program by measuring exclusive Υ production near threshold (measuring J/ψ production near threshold is very challenging with the high-energy collider) [3163,4537]. With a future theoretical framework, these data will constrain the gluonic structure of the nucleon at the higher-twist level and contribute to the understanding of the origin of its mass.

Pion and kaon structure

The spontaneous breaking of chiral symmetry in QCD generates most of the light hadron masses and governs the effective dynamics of strong interactions at low energies (see Sects. 6.2 and 6.3). The pion and kaon are the Goldstone bosons of chiral symmetry, and their quark/gluon structure provides insight into the microscopic mechanism of symmetry breaking. The EIC will pursue a program of pion and kaon structure studies using exclusive scattering to measure the pion/kaon form factor, and peripheral deep-inelastic ep scattering to probe the pion/kaon partonic structure [3163,4538]. The extraction of pion/kaon structure from ep/eA scattering data requires theoretical methods that can be tested with the EIC data.

14.2.2 Multidimensional imaging of hadrons and nuclei

Another basic objective is to understand and visualize hadrons as extended systems in space. This can be accomplished using the concepts of GPDs (transverse coordinate space imaging) and TMDs (momentum space imaging), which provide a spatial representation consistent with the relativistic and quantum nature of the dynamics (see Sect. 10.4). Measurements at EIC will allow one to employ these concepts in regions where they are practically applicable and realize their full potential.

Transverse quark/gluon imaging of the nucleon

The transverse spatial distributions of quarks/gluons and their dependence on x represent the size and shape of the nucleon in QCD (see Sect. 10.4 and Refs. [3244,3245] for a review) and contain rich information about dynamics (parton diffusion, chiral dynamics). Exclusive J/ψ electro- and photoproduction at EIC provides a clean probe of the gluon GPD and will determine transverse spatial distribution of gluons from the t-slope of the differential cross section (see Fig. 373) [1293,3163,3186]. DVCS offers direct access to the quark GPDs and their spin dependence, and provides indirect information on the gluon GPD through NLO effects and Q^2 evolution [3163,4539]. The combination of both will allow for an

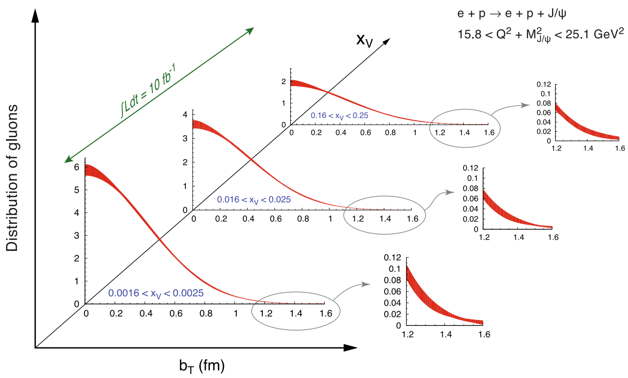

Fig. 373 Transverse spatial distribution of gluons in the nucleon determined from projected EIC exclusive J/ψ electroproduction data [1293,3163]

accurate determination of the quark and gluon GPDs, including validation of the factorized approximation and tests of the universality of the extracted structures. Essential capabilities for this program are the kinematic coverage (probing quarks/gluons down to $x \sim 10^{-3}$, Q^2 dependence in electroproduction), luminosity (differential measurements, e.g. t-dependence at fixed x and Q^2), far-forward proton detection (recoil, exclusivity), and beam polarization (polarization observables). The results can be synthesized in comprehensive transverse images of nucleon structure (see Sect. 10.4).

Transverse quark/gluon imaging of nuclei

The same concepts and measurements can be used to create images of nuclei ($A > 1$) in terms of quark/gluon degrees of freedom. Such studies provide new insight into nuclear structure (comparison of $q - \bar{q}$, $q + \bar{q}$, and g spatial distributions in the nucleus) and a new avenue for studying nuclear modifications of partonic structure (comparison of nucleus with non-interacting ensemble of nucleons) [4540–4546]. EIC measurements of coherent J/ψ [4547] and γ production on nuclei probe the nuclear GPDs, $\langle A'|\mathcal{O}_{\text{partonic}}|A\rangle$, and can be analyzed in the same way as measurements on the proton. The identification of coherent nuclear scattering events places strong demands on the far-forward detection system and is a matter of on-going development (active detection of recoiling nucleus for light nuclei; veto detection of breakup for heavy nuclei) [4548]. A new aspect of light nuclei is that they cover a variety of spins (Spin-1 D, Spin-1/2 ^{3}He, Spin-0 4He) and express it in the GPD structure and the transverse images.

Evolution of TMD distributions

The theoretical formulation of the transverse momentum dependence of partons has made substantial progress in the last decade (see Sect. 10.4). Factorization and renormalization predict a distinctive scale and rapidity dependence of the TMD distributions, generated by gluon radiation with Sudakov suppression, and described by the CSS evolution

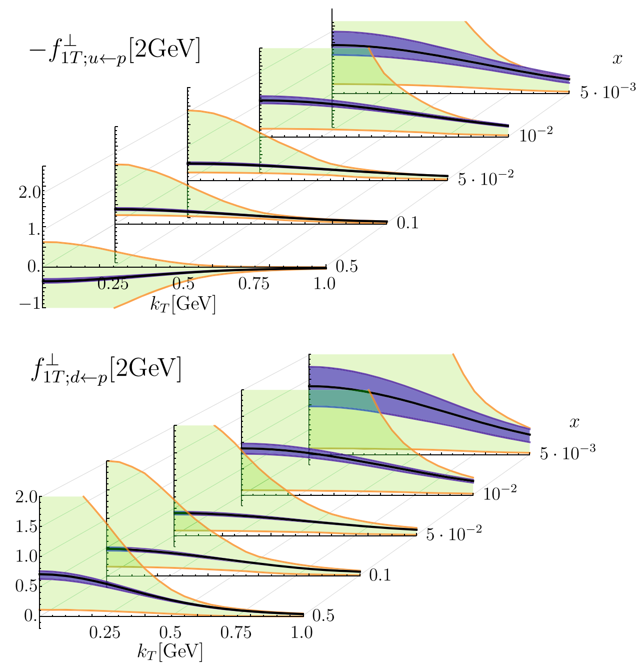

Fig. 374 Expected impact of EIC pseudodata on the determination of the u and d quark Sivers distribution [3163]. Green bands: Present uncertainties [3302]. Blue: Uncertainties when including EIC pseudodata [3163]

equations. The EIC will allow one to test these predictions in measurements of semi-inclusive hadron production $\gamma^* + N \to h + X, h = \pi, K, \ldots$ The wide kinematic range accessible with EIC is essential for observing the logarithmic dependencies implied by the evolution equation and separating perturbative and nonperturbative dynamics (see Fig. 369). The results will provide crucial insight into the theory of CSS-type radiation and its applicability to DIS-type processes.

Spin–orbit correlations in TMD distributions

An interesting feature of the transverse momentum dependence of partons is that it is correlated with the nucleon and parton spin, giving rise to observable spin–orbit effects that provide insights into nucleon structure and color field dynamics (see Sect. 10.4). At EIC these effects can be studied in measurements of hadron production (semi-inclusive DIS, jets) with polarized electron and proton beams. Measurement of the Sivers and Collins asymmetries are possible with the transverse proton beam polarization readily available at collider (see Fig. 374) [3163]. The results will provide extensive information on orbital angular momentum, final state interactions, and the quark transversity distributions in nucleon.

14.2.3 Nuclear high-energy scattering in QCD

High-energy scattering on nuclei ($A > 1$) provides a wealth of information on the effective dynamics emerging from

QCD at various energy and distance scales. Depending on the kinematic regime, such processes reveal the QCD substructure of individual nucleon interactions (intermediate/large x) or coherent QCD phenomena involving the entire nucleus (small x). The EIC will realize the first electron–nucleus collisions in colliding beam experiments, combining the kinematic reach of colliding beams with the precision and control of electromagnetic scattering, and thus transform this field of study.

Nuclear quark/gluon densities

The nuclear PDFs describe the basic particle content of the nucleus in QCD degrees of freedom [4549–4552]. Comparison with the PDFs of an ensemble of non-interacting nucleons provides insight into nucleon interactions and coherent phenomena. Many aspects of the nuclear PDFs are still poorly known, esp. the nuclear gluons and the charge and flavor dependence of the nuclear quarks at $x \lesssim 0.1$. The EIC will determine the nuclear PDFs using inclusive DIS on a broad range of nuclei [3163,4553]. The nuclear gluon PDF will be determined indirectly through the Q^2 dependence of the nuclear DIS cross section (DGLAP evolution), using the wide kinematic coverage available with the collider. It will also be determined directly through measurements of heavy flavor production in nuclear DIS, taking advantage of the high production rates and next-generation reconstruction capabilities provided by the EIC. The results will establish whether the nuclear gluons are suppressed at $x > 0.3$ like the valence quarks (EMC effect), and whether they are enhanced at $x \sim 0.1$ (antishadowing) as suggested by theoretical arguments; both phenomena reveal aspects of the QCD substructure of nucleon interactions.

Shadowing and saturation

In high-energy scattering at $x \ll 0.1$ the coherence length of the process becomes larger than the size of the nucleus, and the high-energy probe interacts with all nucleons along its path. In this regime the gluons "seen" by the probe can no longer be attached to individual nucleons but represent a property of the whole nucleus, giving rise to striking new phenomena. Shadowing is the reduction of the leading-twist nuclear gluon density resulting from destructive interference of amplitudes with gluons attached to different nucleons; see Ref. [4556] for a review. Saturation is the appearance of a new dynamical scale in the form of the transverse density of gluons per area. It emerges from nonlinear QCD evolution equations including gluon recombination [4557–4562] and can be used as the basis of an effective field theory description of strong interactions at small x – the Color Glass Condensate [3334], leading to many interesting predictions; see Refs. [4563–4565] for reviews. Both phenomena are connected, as shadowing reduces the gluon density and modifies the expected $Q^2_{\text{sat}} \sim A^{1/3}$ scaling of the saturation scale. Exploring these phenomena will be a prime task of the EIC.

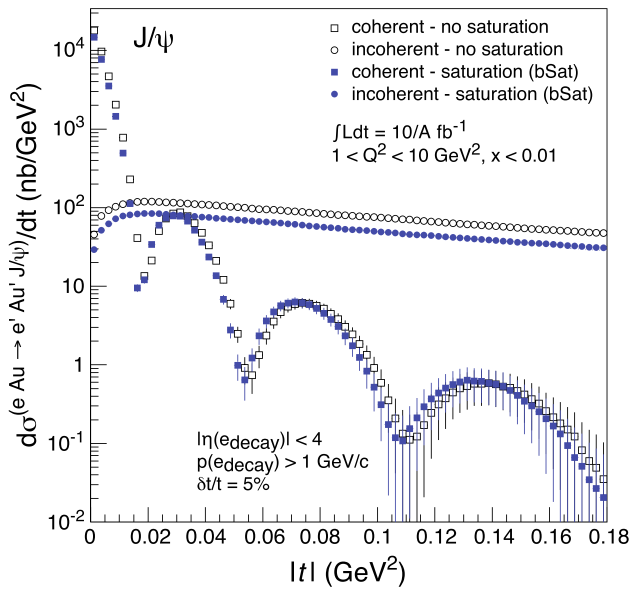

Fig. 375 Differential cross section of coherent and incoherent J/ψ production on a Au nucleus, as a function of the momentum transfer t [3163,4554,4555]. The diffraction pattern in coherent scattering is sensitive to the impact parameter dependence of shadowing and saturation effects in the nuclear gluon density

Basic information will come from the behavior of the nuclear gluon PDF at $x \ll 0.1$ [3163]. More detailed tests of the small-x gluon dynamics will be possible with dijet and dihadron production [3339,4566,4567]. Further insight can be gained from studies of diffractive scattering on nuclei. Measurements of coherent heavy vector meson production on nuclei probe the impact parameter dependence of the shadowing and/or saturation effects through the diffraction pattern in the momentum transfer $|t|$ (see Fig. 375) [3163,4554,4555]. Similar studies can be performed in measurements of coherent inclusive diffraction on nuclei [4568]. The EIC provides the necessary energy for diffractive scattering, and the ability to identify coherent processes through forward detection.

Nuclear breakup and spectator tagging

In high-energy scattering on light ions, detection of the nuclear breakup state provides information on the nuclear configuration present during the high-energy process [4570]. In the case of the deuteron, detection of the "spectator" proton identifies events with scattering on the neutron and fixes the relative momentum of the proton–neutron configuration. This can be used to select scattering in large-size nuclear configurations, where interactions are absent and the neutron is free [4571,4572], or small-size configurations, where the pn system strongly interacts and the partonic structure is modified (short-range nucleon–nucleon correlations) [4573]. The EIC will enable a program of high-energy scattering on the deuteron with proton or neutron spectator tagging. In the

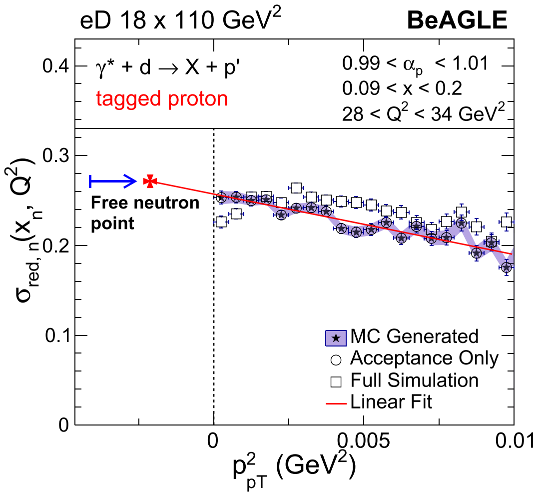

Fig. 376 Simulation of free neutron structure extraction through DIS on the deuteron with proton spectator tagging at EIC [4569]. The neutron reduced cross section is measured as a function of the spectator proton transverse momentum p^2_{pT} and extrapolated to the "free neutron point" at $p^2_{pT} < 0$, corresponding to pn configurations of infinite size

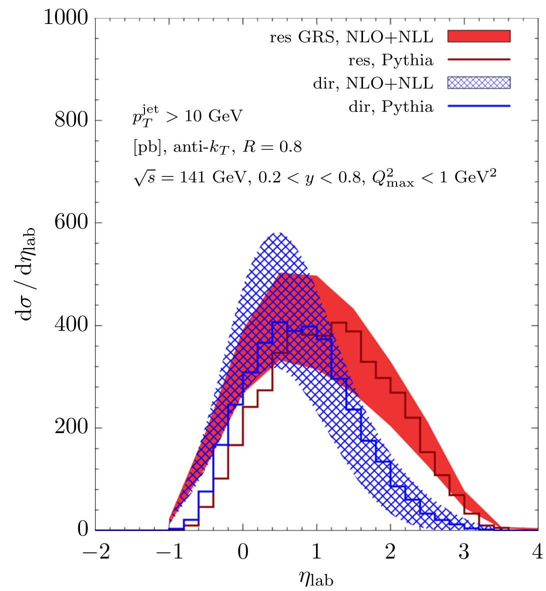

Fig. 377 Inclusive production cross section of jets in photoproduction at EIC, as a function of the pseudorapidity η in the laboratory frame (see Fig. 379) [3163,4583]

collider kinematics the spectator nucleon appears in the forward ion direction and is detected with far-forward detectors (magnetic spectrometer for protons, zero-degree calorimeter for neutrons) [3163]. The setup can be used to extract free neutron structure functions (see Fig. 376) [4569], study the configuration dependence of EMC effect, or explore short-range nucleon–nucleon correlations in deuteron breakup in diffractive scattering [4574].

14.2.4 Emergence of hadrons from QCD

Understanding hadronization – the emergence of hadrons from the energetic quarks/gluons produced in deep-inelastic processes – remains a major challenge of strong interaction physics. The hadronization process is "reciprocal" to the partonic structure of hadrons but much less understood theoretically, because it involves timelike momentum transfers and propagation over large distances, and methods based on imaginary-time (Euclidean) quantum field theory such as Lattice QCD are generally not applicable (see Sect. 4). Basic open questions are the time/distance scales of parton fragmentation and hadron formation; the role of non-perturbative dynamics (chiral symmetry breaking, vacuum fields; see Sect. 5.11), and the effects of the nuclear medium on the hadronization process. In addition to the scientific interest, these topics are of eminent practical importance for the development of event generators describing strong interaction dynamics in high-energy collisions (see Sect. 11.4).

Fragmentation functions
Basic information on the hadronization process is summarized in the quark/gluon fragmentation functions, describing the probability for single-inclusive hadron production by an energetic color charge; see Ref. [4575] for a review. While much information on the fragmentation functions has been extracted from e^+e^- annihilation, pp collisions, and fixed-target semi-inclusive DIS experiments, several features remain poorly known, such as the quark charge dependence (so-called unfavored vs. favored fragmentation), strangeness fragmentation and kaon production, and gluon fragmentation [3123,4576–4578]. The EIC will determine the fragmentation functions from semi-inclusive DIS in ep and en scattering over a broad kinematic range [3163]. These measurements will be able to separate the quark charges in the initial state, extract the gluon through NLO effects, and study the Q^2 evolution of the fragmentation functions. The spin dependence of quark fragmentation will be investigated through measurements of Λ fragmentation [4579]. Precise knowledge of the fragmentation functions will in turn improve the extraction of the flavor dependence of the quark/antiquark spin PDFs from polarized semi-inclusive DIS data.

Dihadron correlations
More detailed information on the fragmentation process comes from measurements of hadron correlations, described by the theoretical framework of dihadron fragmentation functions [4580–4582]. The EIC will measure dihadron fragmentation functions in DIS and allow for the new theoretical concepts to be applied and tested. The kinematic coverage provided by the EIC will ensure that the picture of independent fragmentation remains applicable even in multi-hadron measurements.

Jets and heavy flavors
An alternative view of the hadronization process is obtained by applying the concepts of jet physics, where one defines a system of collinear partons according to quantitative observable criteria without reference to nonperturbative fragmentation functions (see Sects. 6.4, 11.5 and 12). These concepts and methods have been developed for $pp/p\bar{p}$ scattering at hadron colliders (LHC, Tevatron) but can be extended to ep scattering at EIC at lower energies. This extension opens up several new directions for studying the internal properties of jets and using them as a probe of partonic structure. In ep collisions where the scattered electron is detected, it defines the jet energy and scale, and the concepts for leading jets can be applied to the DIS current jet with known initial conditions, providing new possibilities to test the dynamics [4584–4586]. In addition, jet substructure can be investigated [4583]. Jets can also be studied in ep collisions where the scattered electron is not detected, or in γp collisions, where the jet transverse momentum serves as the hard scale (see Fig. 377 as an example). Particularly interesting are jets induced by heavy quarks, which remain stable under strong interactions and create distinct signals in the detector (D, B meson decays). The EIC will support this program through a comprehensive set of measurements of leading jets, jet substructure, heavy flavor jets, and studies of partonic structure and TMD distributions using jets [3163]. This is a rapidly evolving field, where new theoretical methods will become available until the EIC experiments are performed.

Target fragmentation
Equally interesting is the hadronization of the target remnant in DIS processes (target fragmentation). It can be regarded as the materialization of a nucleon with a "hole" in its color wave function (created by the removed parton) and provides information on baryon number transport, multiparton correlations [4587], hadronization dynamics, and spin–orbit effects. A framework for QCD analysis of target fragmentation is provided by the generalized factorization theorems [4022,4588]. The EIC will enable a comprehensive program of nucleon target fragmentation studies, using the detectors in forward pseudorapidity region [3163]. Spin effects in target fragmentation can be studied using polarized proton beams and/or fragmentation into Λ baryons [4589]. Important advantages of the collider compared to fixed-target experiments are that there is no material surrounding the target, and that the fragments move forward with a finite fraction of the proton beam momentum.

Hadronization in medium
The hadronization studies described above can be extended from ep to eA scattering, to investigate the influence of the nuclear medium on the hadronization process. The medium effects depend essentially on the energy E_h of the produced hadron in the nuclear rest frame, usually expressed as a fraction $z = E_h/\nu$ of the virtual photon energy ν. The wide range of scattering energies available at EIC will allow one to move the fragmentation process "in" and "out" of the nucleus, enabling controlled and detailed studies of the medium effects. This will make it possible to test various hadronization models and determine the time/distance scale parameters. The study of nuclear final-state interactions will also improve the modeling of nuclear breakup in DIS processes, which in turn will help with the analysis of coherent nuclear scattering and spectator tagging. Particularly useful for the study of medium effects are heavy-quark probes (see Fig. 378 for an example) [4590,4591].

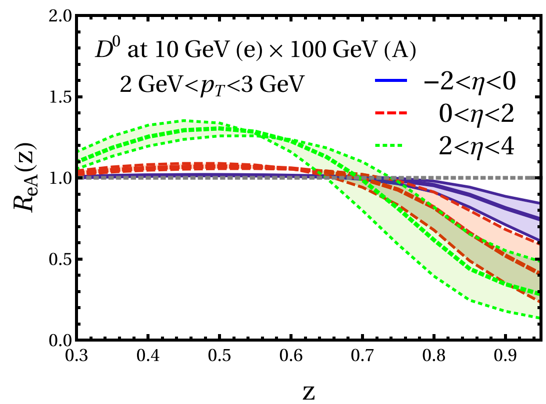

Fig. 378 Medium modification of the D^0 production cross section expected at EIC, as a function of z, in different regions of pseudorapidity η [3163,4590]

Hadron spectroscopy
Hadron production in high-energy ep/eA scattering at EIC can also be used for spectroscopy, complementing experiments using pp and e^+e^- scattering. Exotic heavy quarkonium states (XYZ states, see Sects. 8.5 and 8.6) can be produced in exclusive photo/electroproduction processes $\gamma^* + p \rightarrow M + N$. The production rates and reconstruction efficiency with the EIC detector are presently under study [3163,4592,4593]. At EIC, new possibilities arise from measurements of the spin density matrix elements of heavy vector states, target polarization observables, and the Q^2 dependence in electroproduction. These unique capabilities of the EIC could be used as the focus shifts from spectroscopy to investigations of the structure of exotic states.

14.2.5 Detectors and collaboration

The EIC science program requires a general-purpose detector with large acceptance and high resolution to reconstruct the scattered electron and the multiple different hadronic final states over a wide range of rapidities and energies/momenta. The physics requirements and detector concept are described

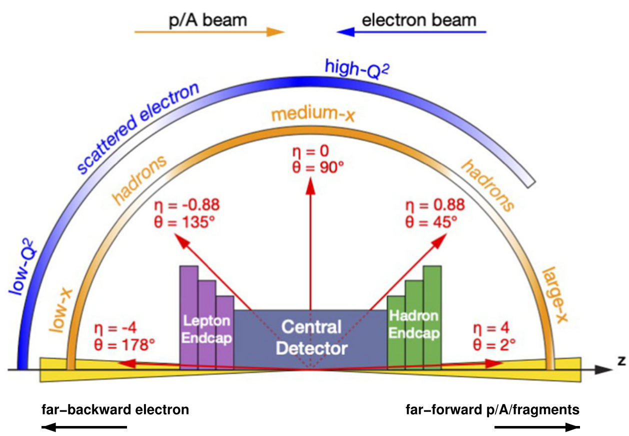

Fig. 379 Schematic of the EIC detector concept

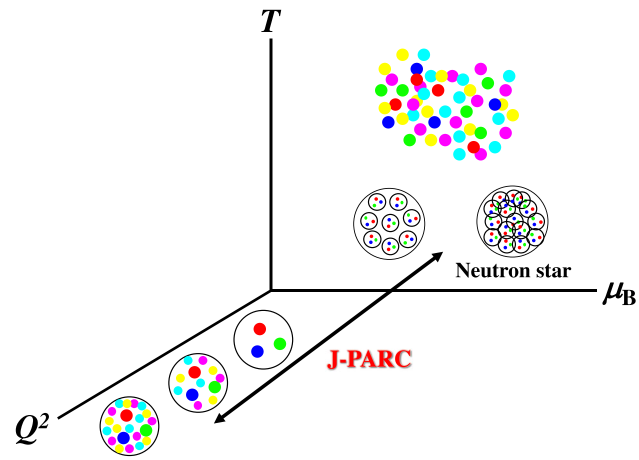

Fig. 380 QCD phase diagram and J-PARC hadron projects

in detail in the EIC Yellow Report [3163]. A schematic is shown in Fig. 379. The pseudorapidity region $-1 \lesssim \eta \lesssim 1$ is covered by the central "barrel" detector with a solenoidal magnetic field; the regions $-4 \lesssim \eta \lesssim -1$ and $1 \lesssim \eta \lesssim 4$ are covered by the "lepton endcap" and "hadron endcap" detectors; the detectors provide capabilities for tracking and vertex detection, electromagnetic and hadronic calorimetry, and particle identification. These systems capture the scattered electron and the final state produced by the struck parton in typical DIS events. The far-backward region (outgoing electron beam direction) is instrumented with a low-Q^2 electron tagger for photoproduction. The far-forward region (outgoing proton/ion beam direction) is equipped with an elaborate detection system for charged and neutral beam fragments, integrated in the interaction region, involving a magnetic dipole spectrometer with tracking detector for charged particles and a zero-degree calorimeter for neutral particles. This system provides essential capabilities for detecting far-forward protons and neutrons in exclusive/diffractive processes on the proton, spectator nucleons or nuclear fragments in scattering on nuclei, and coherent nuclear recoil. It presents a major challenge for design, integration, and engineering, and is critical for large part of the physics program. Further information on the EIC detector requirements and conceptual design can be found in Ref. [3163]. The technical design and formation of a detector collaboration are in progress. The addition of a second detector with complementary capabilities is planned as a future upgrade.

The EIC User Group is an international affiliation of scientists promoting scientific, technological, and educational efforts in the development of the EIC facility and science program. It presently has more than 1200 members from more than 250 institutions (laboratories, universities) worldwide. Resources and information about activities and events can be found on the webpages [4594].

14.3 J-PARC hadron physics

Shunzo Kumano

Hadron physics is the field to understand our visible universe, namely hadronic many-body systems from low to high densities, from low to high temperatures, and from low to high energies, in terms of fundamental particles of quarks and gluons and their interactions. With the significant developments of perturbative QCD during 50 years of QCD, asymptotic freedom and scaling violation are now basically understood. On the other hand, the nonperturbative region is still under investigations by phenomenological models and lattice QCD. One may note that at present lattice QCD cannot be applied to finite density systems, which makes it difficult to predict precisely hadronic and nuclear phenomena at low energies.

Although QCD is known as the correct theory of strong interactions, there are unexpected experimental discoveries of new hadronic and nuclear forms which were not predicted by theorists. Therefore, experimental projects are essential for a deeper understanding and for further developments of QCD beyond the 50-years history. The Japan Proton Accelerator Research Complex (J-PARC) as one of the flagship facilities in hadron physics should play a key role in hadron physics from the low to the medium-energy region, by supplying precise experimental information on new forms of matters, as illustrated in Fig. 380.

The J-PARC is located at Tokai in Japan. It is operated by both the High Energy Accelerator Research Organization (KEK) and the Japan Atomic Energy Agency (JAEA). J-PARC is responsible to coordinate the efforts of KEK and JAEA. KEK is in charge of nuclear and particle-physics projects by using the 30-GeV proton accelerator. J-PARC is a multi-purpose facility to investigate a wide range of scientific topics from life sciences to condensed-matter, nuclear, and particle physics [4595].

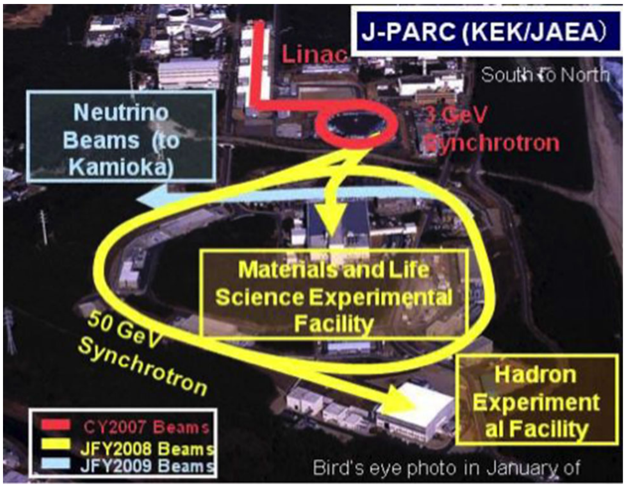

Fig. 381 Aerial view of J-PARC [4595]

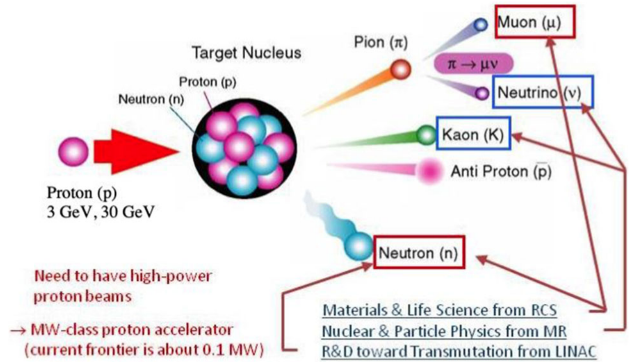

Fig. 382 Secondary beams at J-PARC [4595]

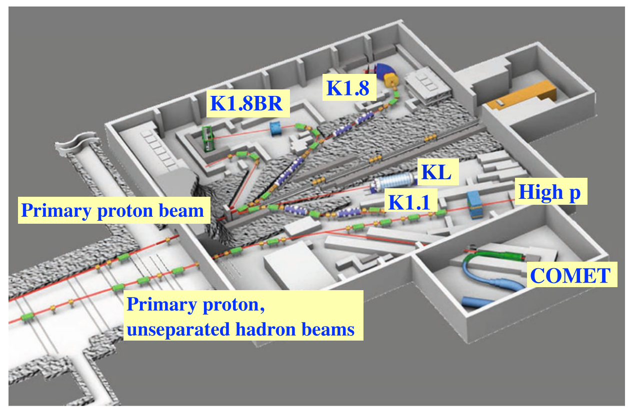

Fig. 383 J-PARC hadron hall

The J-PARC accelerator consists of a 400-MeV linac as an injector, a 3-GeV rapid-cycling synchrotron (RCS), and the 30 GeV main-ring synchrotron. The RCS accelerates the protons up to 3 GeV as shown in Fig. 381. Its beam pulses are delivered mostly to the materials and life-science experimental facility, and a small portion is injected to the main ring. The protons are accelerated to 30 GeV in the main ring, and they are delivered to the neutrino experimental facility and the hadron experimental facility. The beam reached an energy of 30 GeV in 2008, its power was increased towards the design intensity of 0.75 MW. In the near future, we expect to have about 1 MW for the neutrino facility and about 100 kW for the hadron one [4595].

The J-PARC is the most intense accelerator above the multi-GeV energy region. Its aim is to investigate a wide range of nuclear and particle physics by using secondary beams of kaons, pions, antiprotons, neutrinos, and muons as well as the primary proton beam as shown in Fig. 382. There are particle physics experiments on neutrino oscillations, lepton-flavor violation, $g-2$, rare kaon decays, and the neutron electric-dipole moment to search for physics beyond the Standard Model. Since the purpose of this report is to discuss QCD-related topics, only the hadron-physics projects are explained.

14.3.1 J-PARC hadron facility

The layout of the J-PARC hadron facility is shown in Fig. 383 with the hall size of 60 m width and 56 m length. Nuclear and particle physics experiments are done by using the primary proton beam and secondary beams of pions, kaons, antiprotons, and muons. Unique points of this proton accelerator facility are (1) high intensity and (2) intermediate energy. The first point indicates the decisive advantage when secondary beams or the primary proton beam are used for precision experiments. Intermediate energies are important since low-energy hadron projects can bridge the transition region from hadrons to quarks and gluons by variation of the momentum transfer in the QCD phase diagram, as illustrated in Fig. 380. The facility should be able to contribute to the development of QCD from the nonperturbative region to the transition region, then to the perturbative one.

Particle-physics experiments in the hadron hall are lepton-flavor violation (COMET) and rare kaon decays (KL). The COMET experiment uses muons from the decays of pions produced by 8 GeV proton collisions on a production target. COMET will search for the lepton-flavor violation process, the conversion of muons into electrons in the field of a nucleus, $\mu^- + A \to e^- + A$. The KOTO experiment uses the neutral-kaon beamline KL for measuring the frequency of the CP-violating decay $K_L^0 \to \pi^0 \nu \bar{\nu}$. These projects are intended to find a signature beyond the Standard Model in particle physics.

Hadron-physics experiments are done at the beamlines K1.8, K1.8BR, K1.1, and High p, see Fig. 383 [4596]. The K1.1 beamline is yet to be constructed. The K1.8 beamline supplies kaons with the momentum of about 1.8 GeV and is used to study hypernuclei, e.g. Ξ hypernuclei, by (K^-, K^+) reactions. One may note that the cross section of $p(K^-, K^+)\Xi$ reaches a maximum at a momentum of 1.8 GeV. The K1.8BR is a branch line of K1.8 to supply kaons with low momenta of 0.7–1.1 GeV. The cross section of the quasi-elastic reaction $K^- N \to \bar{K} N$ maximizes at 1 GeV momentum, so that this beamline is intended to study $\bar{K} N$ interactions and kaonic nuclei by (K^-, N) reactions with light nuclei.

The K1.1 beamline supplies kaons with momentum around 1.1 GeV for measurements of Λ hypernuclei. Because of the space interference between the K1.1 and high-p beamlines, K1.1 experiments will be done after the first stage of the high-p experiment. These strange nuclear physics projects are explained in Sect. 14.3.3.

The high-momentum beamline provides 30 GeV protons and unseparated hadrons up to 20 GeV. The beam of unseparated hadrons, to be prepared in the near future, consists mainly of pions. The first experiment in this beamline will measure hadron mass modifications in a nuclear medium to study chiral-symmetry breaking and hadron-mass generation (see Sect. 14.3.4).

Then, charmed baryon spectroscopy will be investigated by (π^-, D^{*-}) reactions. This experiment intends to find diquark degrees of freedom, which are not easily found in hadrons consisting of light quarks only, as explained below in Sect. 14.3.5. The hadron tomography project will be performed together with this spectroscopy experiment by studying generalized parton distributions (GPDs) as discussed in Sect. 14.3.6. This experiment is set up to find the origin of hadron masses and spins by the tomography technique. In future, separated hadron beams could become possible; an extension plan of this hadron hall is discussed in the next subsection 14.3.2.

More details of each hadron project are explained in the following sections. The first major experiment will study the role of strangeness in nuclear physics. The next experiment is devoted to hadron mass modifications in the nuclear medium, and then the charmed-baryon project will start. The GPD tomography experiment is expected to join this baryon-spectroscopy project. The scope of the hadron physics projects at J-PARC is thus expanding in the near future.

Furthermore, there is a significant interest to build a new heavy-ion facility at J-PARC to investigate the phase diagram in the low-temperature and high-density region in contrast to the kinematical region of RHIC and LHC. There are interesting topics in cold and dense matters, such as the end point of the phase transition and color superconductor, as explained in Sect. 14.3.7.

When the hadron program will be completed, the heavy-ion facility will be built. This is expected in the 2030s. J-PARC will then become a leading hadron accelerator facility. It will investigate QCD in a wide kinematical region and for a wide range of topics, from strangeness in nuclear physics, charmed-baryon spectroscopy, nucleon structure at intermediate energies, and quark–hadron matter.

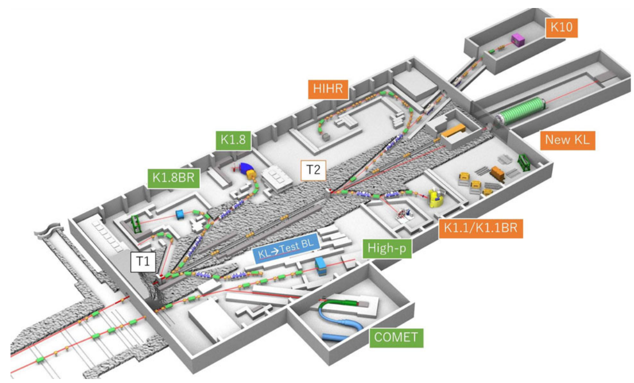

Fig. 384 Extension plan of the J-PARC hadron hall [4597]

14.3.2 Hadron-hall extension

The current hadron hall cannot accommodate enough projects in nuclear and particle physics. The experimental hall size and beamlines are much smaller than, for example, the BNL-AGS facility. The efficient way for utilizing the full ability of the J-PARC is to expand its space and to build additional beamlines.

This extension project, as shown in Fig. 384, was proposed together with the current hall [4597]. The area of the hall becomes twice larger to accommodate new experiments. A new production target T2 will be prepared. The beamlines with orange color are new ones in the extended hall. They are designed for the following topics.

1. HIHR
   This HIHR (High Intensity High Resolution) beamline is intended for precision spectroscopy of Λ hypernuclei through $(\pi^\pm, K^+)$ reactions by using high-intensity and high-resolution charged pions up to 2 GeV momentum with an excellent momentum resolution of 10^{-4} and a missing-mass resolution of a few hundred keV.
2. K10
   This beamline will be used to investigate $S = -3$ strangeness physics and charm physics by using separated secondary hadron beams of high-momentum (2–10 GeV) charged kaons and anti-protons.
3. K1.1
   This beamline will be prepared for physics with strangeness $S = -1$ using charged kaons with momenta of less than 1.2 GeV. The branch beamline K1.1BR is for the stopped kaon experiments.
4. KL2
   The frequency of the kaon rare decay $K_L^0 \to \pi^0 \nu \bar{\nu}$ will be measured. It may provide a hint for New Physics beyond the Standard Model by using this high-intensity neutral kaon beamline.

This extension project was selected as one of top priority projects of KEK in 2022. After the financial approval, it will take 6 years for its construction. When it is realized, it will provide excellent opportunities for nuclear and particle physicists to create innovative fields with unprecedented precision. The following major physics purposes are presently considered for this extension project: (1) precise spectroscopy of hypernuclei to understand neutron stars, (2) novel aspects of charmed baryons, and (3) New Physics beyond the Standard Model. The details of the topics (1) and (2) are discussed in Sects. 14.3.3 and 14.3.5, respectively, along with past J-PARC experiments on hypernuclei.

Because the J-PARC is an intermediate-energy facility, the current scope of physics could be extended in future, for example, by including projects of high-energy QCD such as on nucleon structure, exotic hadrons by the constituent counting rule, and color transparency [4598]. Furthermore, if the heavy-ion accelerator will be built [4599], the unexplored cold and dense region of the QCD phase diagram will be investigated.

Here, we briefly summarize the major purposes related to the hadron-hall extension including possible future topics.

Establishing the role of strangeness in nuclear physics
The nuclear physics without strangeness has been established by precise information on the fundamental NN potentials from abundant experimental measurements on NN scatterings and deuteron properties, whereas the YN scattering information is in a poor situation. The J-PARC will supply precise data on the fundamental YN interactions and also properties of hypernuclei. We expect that spectroscopy of hypernuclei could become a precision field by the J-PARC experiments.

Applications to neutron stars
The existence of strangeness inside neutron stars would make their equations of state much softer. This is in conflict with astrophysical observations of neutron-star masses. By establishing strangeness nuclear physics, we expect that this issue will be solved.

Creation of a di-fermion field in hadron physics
The di-fermion physics has been investigated in quantum many-body systems, especially condensed-matter physics. In hadron physics, the color superconductor, for example, is investigated in such a context. The J-PARC intends to create a new di-fermion field by the spectroscopy of the charmed baryons.

Emergence of hadron masses and spins
Hadron masses and spins are fundamental physics quantities to constitute our visible universe. However, their origins are not understood easily from quark and gluon degrees of freedom. They should originate as emergent phenomena of non-trivial quark–gluon dynamics within hadrons. These should be clarified by the J-PARC projects on hadron-mass modifications in nuclear medium and by hadron tomography via GPDs.

Understanding cold and dense QCD matters
From the RHIC and LHC, the high-temparature region of the QCD phase diagram has been investigated and evidence for quark–gluon-plasma formation was found. J-PARC will clarify the cold and dense region, where interesting phase properties, such as the end point of the phase transition and color superconductor, are theoretically expected.

14.3.3 Strangeness nuclear physics

Major properties of stable nuclei are now relatively well understood, whereas unstable nuclei are still under investigations especially in connection with the nucleosynthesis in astrophysics. One of the major purposes of the J-PARC hadron program is to investigate nuclei by including new flavor degrees of freedom, strangeness and charm [4596,4597].

Under the flavor SU(3) symmetry, nucleons and a part of hyperons constitute a flavor octet. Two-baryon interactions are decomposed into symmetric (under the exchange of baryons) states $\mathbf{27}\oplus\mathbf{8}\oplus\mathbf{1}$ and antisymmetric ones $\mathbf{10}\oplus\mathbf{10}^*\oplus\mathbf{8}$ as

$$\mathbf{8}\otimes\mathbf{8} = \mathbf{27_S}\oplus\mathbf{10_A}\oplus\mathbf{10^*_A}\oplus\mathbf{8_S}\oplus\mathbf{8_A}\oplus\mathbf{1_S}. \tag{14.1}$$

Nucleon–nucleon (NN) interactions provide information only on the $\mathbf{27_S}$ and $\mathbf{10^*_A}$ states. Therefore, hyperon interactions need to be investigated to understand the other terms and to find possible new hadronic many-body systems. These new interactions are relevant in neutron stars. This nuclear-physics project with strangeness has the following advantages [4600].

1. SU(3) flavor symmetry and new interactions
   The new interaction terms $\mathbf{10_A}$, $\mathbf{8_S}$, $\mathbf{8_A}$, and $\mathbf{1_S}$ can be investigated by the hyperon (Y) interactions. In general, YN interactions are expected to be weaker than the NN ones, so that new forms of baryonic many-body systems should be created.
2. Probe of short-range interactions
   Since the pion isospin is 1 and the Λ isospin is 0, the $\pi\Lambda\Lambda$ coupling constant vanishes. Because of its low mass, the pion contributes to the long-range part of the baryon interactions. Without the pion contribution, medium- and short-range baryon interactions should become more apparent when compared to the NN case.
3. Probe of QCD dynamics
   The quark masses and the QCD scale parameter Λ are shown in Fig. 385. We notice that the strange-quark mass is of the order of the scale parameter. This fact suggests an

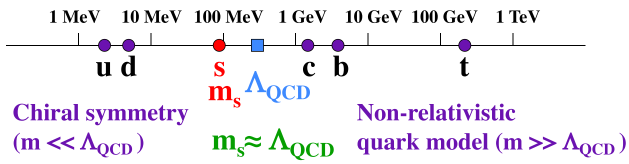

Fig. 385 Strangeness as a probe of QCD dynamics

advantage that the strange quark could be a good probe of QCD dynamics. However, it may also indicate difficulties for describing hadrons with strangeness.

4. New forms of hadronic matters
   Ordinary nuclei consist mainly of up and down quarks. The interactions of hyperons or cascade particles with nucleons are still unexplored. With strangeness, new forms of nuclei should be created such as $\bar{K}NN$, and so on. Another important topic is the possible existence of a H dibaryon with isospin 0, spin 0, and strangeness −2. It corresponds to the term $\mathbf{1_S}$ in Eq. (14.1).
5. Probe of deep regions in nuclei
   The Pauli exclusion plays an important role in nuclear physics. Although nuclei are strongly-interacting systems with nucleons close together, they are often described by a non-interacting Fermi gas model or an independent particle model. It is justified by solving the Bethe–Goldstone equation. Hyperons do not suffer from such an exclusion effect, which indicates the advantage of probing deep regions of nuclei, as the shell structure should become obvious as visualized in Fig. 386 [4597,4601].
6. Equation of state for neutron stars
   Neutron-star physics has significantly developed recently due to new astrophysical experiments and observations of gravitational waves. In the inner high-density region of the neutron stars, the reactions $p + e^- \rightarrow \Lambda + \nu_e$ and $n + e^- \rightarrow \Sigma^- + \nu_e$ could occur because the changes of the Fermi energies of neutrons, protons, and electrons exceed the mass gap of the reactions. The equation of state of neutron stars should be significantly softened by the possible existence of hyperons, which contradicts the neutron-star observations. The appearance of hyperons in the neutron stars is affected by the details of hyperon interactions, which are investigated at J-PARC.

We introduce some of the major experimental results on strangeness in nuclear physics from J-PARC.

Charge symmetry breaking
Charge symmetry is taken as granted as a good symmetry for ordinary nuclei as typically shown in mirror nuclei with exchange of a proton and a neutron. For example, the binding energy difference between ^{3}He and ^{3}H is merely 0.07 MeV after removing QED effects. However, a significant breaking was found by the E13 experiment at J-

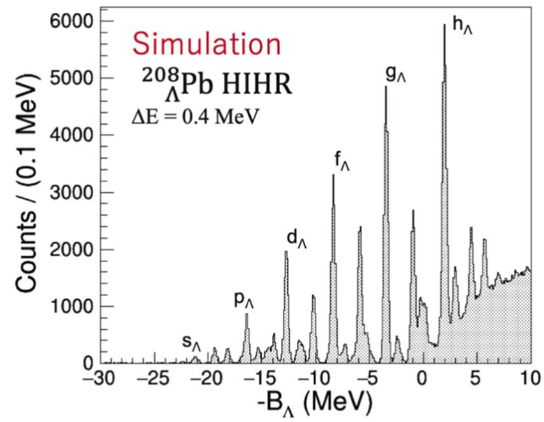

Fig. 386 Simulation for the Λ binding energy spectra of $^{208}_{\Lambda}$Pb for the hadron-extension program [4601]

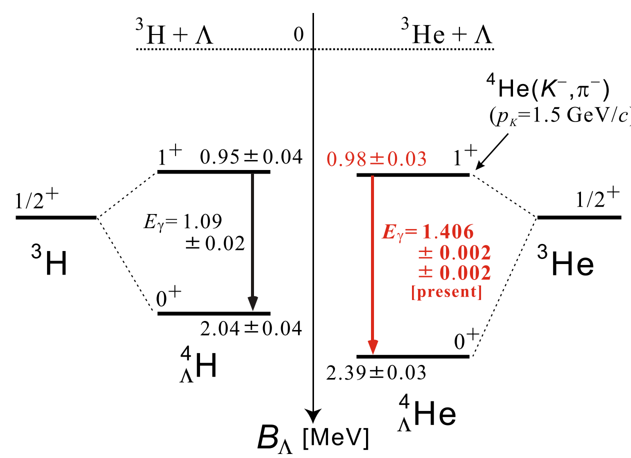

Fig. 387 $^4_\Lambda$He and $^4_\Lambda$H spectra [4602]. (Used with the copyright permission of American Physical Society)

PARC. The 1^+ excited state of $^4_\Lambda$He was produced in the ^{4}He $(K^-, \pi^-)^4_\Lambda$He reaction with a 1.5 GeV K^- beam. Then, by a measurement of the γ rays for the $1^+ \rightarrow 0^+$ transition, a (1.406±0.002±0.002) MeV energy spacing was found. With other measurements, the spectra of $^4_\Lambda$He and $^4_\Lambda$H are compared in Fig. 387 [4602]. The binding energy difference between $^4_\Lambda$He and $^4_\Lambda$H was (0.35±0.05) MeV, which indicates a significant charge-symmetry breaking in hypernuclei. It provided a valuable information on the nature of ΛN interactions which are different from the NN ones. Theoretically, the breaking is considered to come from $\Lambda - \Sigma^0$ mixing.

Double Λ hypernuclei
One of the major purposes of J-PARC program on hypernuclei is to investigate strangeness −2 systems. The J-PARC-E07 experiment was done at the K1.8 beamline with the K^- beam of 1.8 GeV. By using nuclear emulsions tagged by the (K^-, K^+) reaction, the double-Λ hypernucleus $_{\Lambda\Lambda}$Be was found [4603]. It is produced

as ${}^{10}_{\Lambda\Lambda}$Be by $\Xi^- + {}^{16}\mathrm{O} \rightarrow {}^{10}_{\Lambda\Lambda}\mathrm{Be} + {}^{4}\mathrm{He} + t$,
as ${}^{11}_{\Lambda\Lambda}$Be by $\Xi^- + {}^{16}\mathrm{O} \rightarrow {}^{11}_{\Lambda\Lambda}\mathrm{Be} + {}^{4}\mathrm{He} + d$, or
as ${}^{12}_{\Lambda\Lambda}$Be* by $\Xi^- + {}^{16}\mathrm{O} \rightarrow {}^{12}_{\Lambda\Lambda}\mathrm{Be}^* + {}^{4}\mathrm{He} + p$,

and the binding energy of two Λ hyperons is (15.05±0.11) MeV, (19.07±0.11) MeV, or (13.68±0.11) MeV, respectively. This result improves our understanding of the $\Lambda\Lambda$ interaction and double-strange hypernulcei.

Ξ hypernuclei
The J-PARC-E07 collaboration used the 1.81 GeV K^- beam for observing the reaction $\Xi^- + {}^{14}\mathrm{N} \rightarrow {}^{10}_{\Lambda}\mathrm{Be} + {}^{5}_{\Lambda}\mathrm{He}$. From the measurements, the Ξ^- binding energy in the Ξ^--^{14}N system was determined to (1.27±0.21) MeV [4604]. From the experimental data and theoretical calculations, the energy level of the Ξ^- is interpreted as $1p$ state; the ΞN-$\Lambda\Lambda$ coupling must be weak.

Next, Ξ^- capture was studied in the Ξ^--^{14}N system. Two events were found by analyzing KEK-E373 and J-PARC-E07 data signaling deep Ξ^- bound states [4605]. One event from the reaction

$$\Xi^- + {}^{14}\mathrm{N} \rightarrow {}^{5}_{\Lambda}\mathrm{He} + {}^{5}_{\Lambda}\mathrm{He} + {}^{4}\mathrm{He} + \mathrm{n}$$

yields a binding energy in the ^{14}N nucleus of B_{Ξ^-} = (6.27±0.27) MeV. The other event in

$$\Xi^- + {}^{14}\mathrm{N} \rightarrow {}^{9}_{\Lambda}\mathrm{Be} + {}^{5}_{\Lambda}\mathrm{He} + \mathrm{n}$$

yields B_{Ξ^-} given by either (8.00 ± 0.77) MeV or by (4.96±0.77) MeV, depending on the final-state ${}^{9}_{\Lambda}$Be nucleus which can be in the ground or an excited state. These binding energies are larger than the preceding value 1.27 MeV; likely, these events come from the $1s$ state of the Ξ hypernucleus ${}^{15}_{\Xi}$C.

Kaonic nuclei
Kaonic nuclei are new forms of hadronic many-body systems with strangeness. Since $\Lambda(1405)$ can be considered as a $\bar{K}N$ molecule state, a few nucleon systems with a kaon should exist as bound states. The J-PARC-E15 collaboration used the K1.8BR beamline for measuring the reaction $K^- + {}^{3}\mathrm{He} \rightarrow \Lambda + p + n$ with a kaon momentum of 1 GeV. In the Λp invariant mass spectrum, a clear peak was observed. It indicates a kaonic $\bar{K}NN$ nucleus with a binding energy $B_K = (42 \pm 3(\mathrm{stat.})^{+3}_{-4}(\mathrm{syst.}))$ MeV and the decay width $\Gamma_K = (100 \pm 7(\mathrm{stat.})^{+10}_{-9}(\mathrm{syst.}))$ MeV [4606]. The current situation is shown in Fig. 388 for energies and widths of possible K^-pp bound states. The experimental data are shown with the collaboration names, and the other points are theoretical calculations. As it is obvious, the world data do not agree with each other and they are also different from the theoretical results, so that further J-PARC experiments are needed for clarifying the situation.

The J-PARC-E62 collaboration used the K^- beam with 900 MeV momentum at the K1.8BR beamline. The negative kaons were stopped in a liquid-helium target [4607]. They obtained the energies and widths of the $3d \rightarrow 2p$ transition X-rays of kaonic ^{3}He and ^{4}He atoms with 10 times higher accuracy than previous data. On the other hand, using the K^- beam with the momentum 1.8 GeV at the K1.8 beamline, the J-PARC-E05 collaboration measured the missing-mass spectrum of ${}^{12}\mathrm{C}(K^-, p)$ and observed a quasi-elastic peak from $K^-p \rightarrow K^-p$ [4608]. Then, they extracted differential cross sections of the K^-p elastic scattering. These experimental measurements impose a constraint on theoretical models of kaonic nuclei.

$\Sigma^{\pm}p$ scattering cross sections
Good data were not available for hyperon-nucleon and hyperon-hyperon scattering. So far, these interactions had been investigated mainly within hypernuclear models. This approach makes it difficult to establish hypernuclear physics as a precision field on the same level as the NN-interaction and ordinary nuclear physics. Furthermore, hyperon interactions are also essential for applications to neutron stars. Now, the situation is changing due to new results on Σp scattering data from J-PARC.

First, Σ^-p elastic scattering data were reported for a Σ^- momentum range from 470 to 850 MeV by the J-PARC-E40 collaboration [4609]. A π^- beam in the K.18 beamline with a momentum of 1.33 GeV impinged on liquid hydrogen target, where Σ^- particles were produced in the reaction $\pi^-p \rightarrow K^+\Sigma^-$. 4500 events were identified and differential cross sections for Σ^-p elastic scattering were determined. Second, this collaboration reported differential cross sections of $\Sigma^-p \rightarrow \Lambda n$ in the Σ^- momentum range from 470 to 650 MeV [4610]. About 100 events were identified and angular distributions were obtained for the first time. Third, differential cross sections were measured for the Σ^+p elastic scattering in the momentum range from 0.44 to 0.80 GeV [4611]. The π^+ beam with the momentum 1.41 GeV was used to produce Σ^+ in the reaction $\pi^+p \rightarrow K^+\Sigma^+$. About 2400 Σ^+p elastic scattering events were identified, and the ${}^{3}S_1$ and ${}^{1}P_1$ phase shifts were obtained from the precise data for the first time.

These data are valuable for building the full baryon-baryon interactions of the SU(3) multiplets, see Eq. (14.1). With such experimental information, the Nijmegen-type baryon models should become much accurate and lead to a better understanding of hadronic and nuclear many-body systems and neutron stars.

14.3.4 Hadrons in nuclear medium

Hadron masses in nuclear medium will be measured by using the primary protons of 30 GeV at the high-momentum beamline as the J-PARC-E16 experiment [4612]. This project is intended to investigate the role of chiral symmetry in hadron

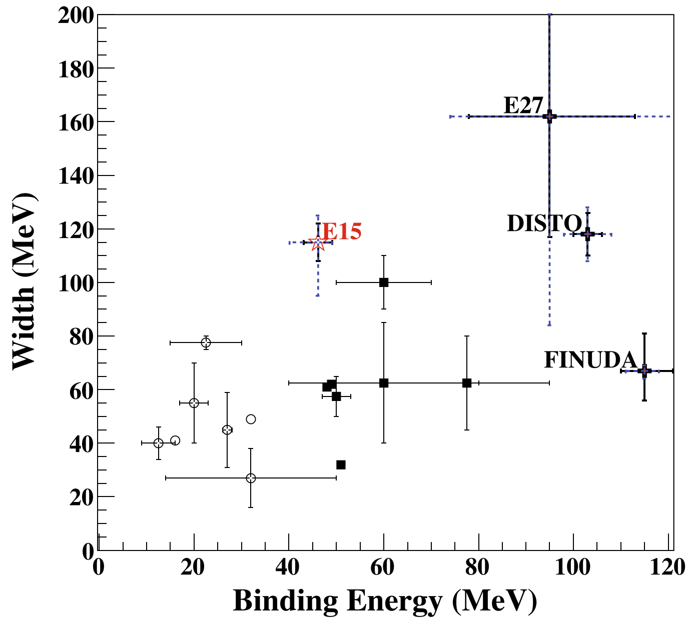

Fig. 388 Situation for the K^-pp-bound state. [4596]. (Used with the permission of the Elsevier Science.)

properties. The study is thus related to a clarification of the origin of hadron masses. The discovery of the Higgs particle clarified the origin of the masses of quarks and leptons. However, this does not imply that masses of our nature, for example, the nucleon mass, are understood. The "god" particle cannot create the hadron masses.

Since the nucleon mass is defined by the matrix element of $\int d^3x T^{00}(x)$, where $T^{\mu\nu}$ is the energy–momentum tensor, it is decomposed into four terms [4613]:

$$M = \text{quark energy} + \text{gluon energy} + \text{quark mass} + \text{trace anomaly}. \quad (14.2)$$

Current masses of up- and down-quarks are very small, so their simple summation is much smaller than the nucleon mass. To understand the origin of hadron masses, it is necessary to clarify the complicated emergence of mass from confined quarks and gluons. The clarification of this mass emergence is one of top priority projects for building electron-ion colliders for physics in 2030s [3163,4614]. In the mass decomposition of Eq. (14.2), the trace anomaly term and the gluon condensate could play an important role in hadron masses. These will be investigated by the J/ψ production process at charged-lepton accelerator facilities, such as the JLab, CERN-AMBER, and EICs. On the other hand, this topic has already been investigated by spacelike GPDs at JLab and CERN-COMPASS and also by timelike GPDs at KEKB. In fact, gravitational form factors of a hadron were already extracted from actual experimental data [4615]. This E16 experiment is intimately related to these world projects.

The original idea for generating the hadron masses is to use chiral-symmetry breaking. It gives rise to a nonvanishing $\langle \bar{q}q \rangle$ condensate [4616,4617], which is called scalar quark condensate. It plays a role of an order parameter for the chiral phase transition. It cannot be directly measured in experiments, so that we have to rely on actual observables. One of such quantities are vector-meson masses in a nuclear medium, they will be measured by the E16 experiment. There are theoretical estimates on their mass modifications from the partial restoration of chiral symmetry inside the nuclear medium [4616,4617].

As for the experimental side, there were already measurements on the masses of vector mesons. For example, the KEK-PS with the primary 12-GeV proton beam provided data on the processes $p + A \to V + X$ $(V = \rho,\ \omega,\ \phi\ \to e^+e^-)$ [4618,4619]. They indicated 9% mass shifts for ω (ρ) and 3% for ϕ-mesons, respectively. From a comparison of theoretical models with the mass-modification data, one can find that the quark condensate provides an important clue for mass generation.

Precise measurements are expected for these mass modifications from the E16 experiment at J-PARC. The first physics run will be taken with C and Cu targets with limited detector acceptance, and then more measurements will be done with the H and Pb targets and full detector acceptance. The expected outcome for the ϕ meson spectrum from the reaction $p + A \to \phi + X$ for the first run with a copper target and 30 GeV protons was simulated using GEANT4, see Fig. 389 [4620]. The momentum distribution of the ϕ meson was evaluated by using the code JAM (Jet AA Microscopic transport model) [4621], and the mass-modification parameter deduced by KEK-E325 [4619] was used. The figure is shown for slowly moving ϕ mesons ($\beta\gamma < 1.25$), the mass resolution is expected as 5.8 MeV. In this slow-ϕ case, nuclear medium effects are large and the spectrum is modified significantly as shown in Fig. 389. The difference between the sim-

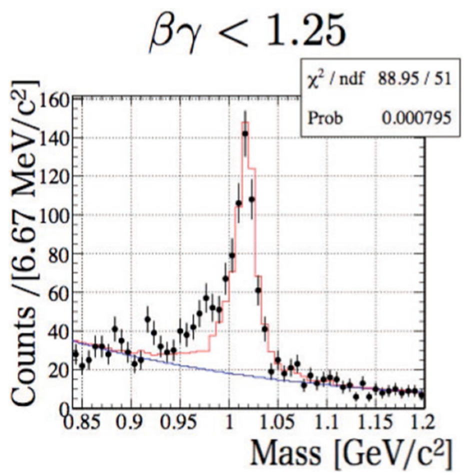

Fig. 389 Expected ϕ meson spectrum with the copper target by the J-PARC-E16 experiment [4620]

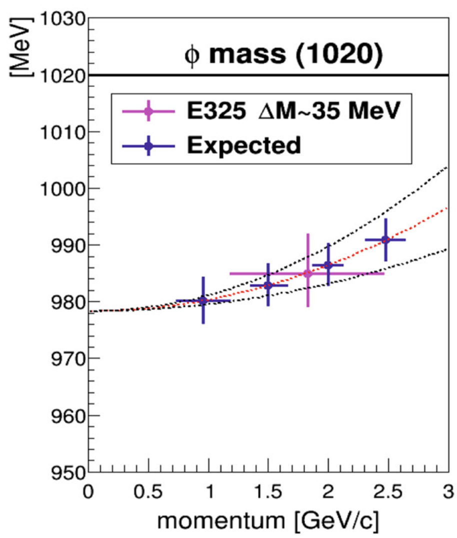

Fig. 390 Expected ϕ-mass data by the J-PARC-E16 and the KEK-E325 one [4620]

ulated data and the red spectrum should come from nuclear medium effects. As the ϕ velocity becomes larger, the spectrum modification becomes smaller. From these simulated data, the mass of ϕ-meson at rest in a nuclear medium can be deduced. In Fig. 390, the mass is extracted by using a theoretical dispersion relation. The KEK-E325 data is shown for comparison. The KEK data was taken at only one point and the errors are large. We notice that the J-PARC data are much more accurate even at the first stage and that four data points will enable us to extrapolate the momentum dependence for determining the ϕ mass at zero momentum.

To relate the actual experimental data of E16 to the quark condensate, it is important to understand hadron interactions in nuclear medium because the ϕ meson is produced with the momentum 1–2.5 GeV/c and it decays into e^+e^- outside or

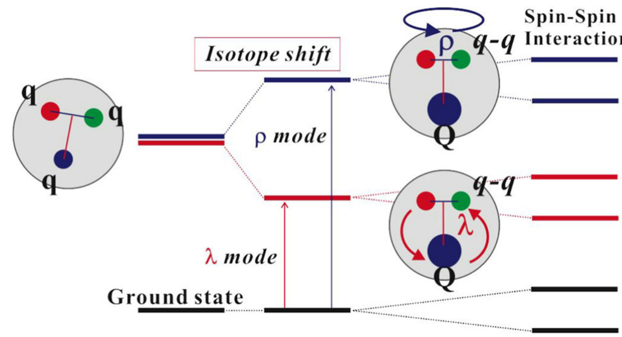

Fig. 391 Expected excitations of $N^*(qqq)$ and $Y_c^*(qqQ)$ [4623]

inside of the nucleus. Such an effort to describe the momentum dependence is in progress by transport simulations by using the Hadron-String Dynamics model [4622], where ϕ-meson spectral function and their density dependence can be specified. Therefore, new J-PARC data should provide a clue in understanding the role of chiral symmetry breaking for the hadron masses.

14.3.5 Hadron spectroscopy

Hadron spectroscopy entered into the new era in the last decade in the sense that there have been many reports on exotic hadron candidates. Exotic hadrons were expected already when the quark model was proposed in 1964. The status of exotic mesons with quantum numbers not accessible within the quark model is reported in Sect. 8.3. In heavy-quark spectroscopy, a large number of states, both mesons (see Sects. 8.5, 8.6) and baryons (see Sect. 9.4) have been found with unusual properties. However, it is often not easy to distinguish so-called cryptoexotic hadrons, i.e. hadrons with quantum numbers compatible with regular hadrons, from ordinary ones because they may have similar masses. Examples are $f_0(980)$, $a_0(980)$ and $\Lambda(1405)$ in the 1 GeV mass region. It took rather a long time to accumulate signatures from various observables for their tetra- or penta-quark-like (or hadron molecular) nature .

In these days, exotic-hadron studies tend to focus on the heavy-quark sector due to KEKB and LHCb discoveries on exotic hadron candidates with charm and bottom quarks (see Sect. 9.4). Since charmed baryons will be copiously produced at J-PARC, it is a good opportunity to investigate details of charmed baryon spectroscopy including exotic candidates. At J-PARC, charmed baryons consist of two light quarks and one heavy quark. These will be investigated by the E50 collaboration. Due to the existence of a heavy quark within a baryon, there are specific interactions and internal configurations, which do not exist in baryons with only light quarks. In the extended hadron hall, Ξ and Ω excitation spectra will be

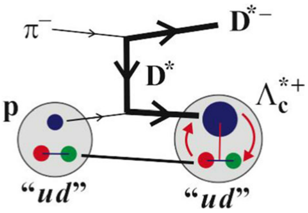

Fig. 392 Schematic picture of $\pi^- p \to D^{*-} \Lambda_c^{*+}$ [4623]

also investigated. Physics motivations of this project include the following.

1. Di-quark correlations in hadrons
The color magnetic interaction between quarks with indices i and j is given by $V_{\text{mag}} \sim \alpha_s(\lambda_i \cdot \lambda_j)(\vec{\sigma}_i \cdot \vec{\sigma}_j)/(m_i m_j)$ where λ is the color SU(3) Gell-Mann matrix, $\vec{\sigma}$ is the Pauli spin matrix, and m is the quark mass. Because it is proportional to $1/(m_i m_j)$, the interaction becomes weak for a heavy quark. Let us denote q and Q for light and heavy quarks, respectively. For a qqQ-type baryon, the qq interaction should be much stronger than the qQ one. It means that a strong qq diquark correlation could appear in such a baryon. Its expected spectrum for qqQ-type baryon in comparison with the qqq-type baryon is shown in Fig. 391 [4623], where ρ and λ are the Jacobi coordinates. The ρ is defined as coordinate between the two quarks qq, and the λ is between qq and Q. The spectrum splits into ρ- and λ-mode excitations, called isotope shift. The ρ mode corresponds to a rotation of the diquark qq, and the λ mode to an orbital excitation between qq and Q. These levels are further split by spin–spin interactions. These studies will lead to new dynamical aspects in hadron physics and, more in general, to di-fermion physics in quantum-many-body systems.
2. Ξ and Ω baryon spectra and their properties
The details of the Ξ and Ω spectroscopy will be investigated. In addition, the Ω electric quadrupole moment is highly interesting. Observations of quadrupole moments provide us information on the nature of interactions among constituents and on system deformations. A finite quadrupole moment suggests that a non-central force should exist. Indeed, the tensor force in the one-gluon-exchange potential leads to the expectation that hadrons should be deformed. The Ω quadruple moment could be measured at J-PARC due to its "stable" nature. The quadrupole moment has never been measured for any hadrons including Δ [4624], it is an ambitious project.

The charmed-baryon-spectroscopy experiment will start in the hadron hall at the high-momentum beamline by using a beam of unseparated hadrons, essentially pions, with momenta up to 20 GeV . The reaction $\pi^- + p \to D^{*-} + \Lambda_c^{*+}$ is used, as illustrated in Fig. 392, for measuring the Λ_c^{*+} spectrum by the $p(\pi^-, D^{*-})$ missing mass. The simulation is shown for the Λ_c^{*+} spectrum in Fig. 393 by considering the pion momentum of 20 GeV and 100-day beam time. A new field of di-quark physics should be developed by this project.

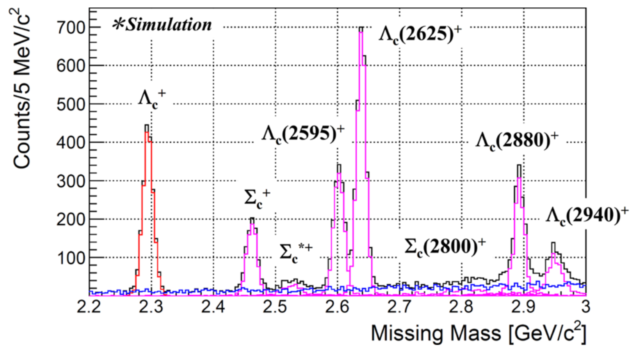

Fig. 393 Simulation for the Λ_c^{*+} spectrum by the K10 beamline experiment at the extended hadron hall [4597]

14.3.6 Hadron structure functions

The J-PARC proton-beam energy of 30 GeV covers the intermediate region from hadron degrees of freedom (d.o.f.) to quark d.o.f. described by perturbative QCD. In addition to hypernuclear and charmed-baryon physics at low energies, the higher-energy region should therefore also be investigated, as illustrated in Fig. 380. The situation is similar to JLab projects, and J-PARC is complementary to JLab in the sense that different observables are available in hadron reactions.

The first experiment on hadron structure functions will be on the GPDs for the proton [4625]. A proposal is being prepared [4598] to study exclusive Drell–Yan processes. The GPDs are observables to probe the three-dimensional structure, namely the transverse structure, in addition to the longitudinal parton distribution functions, and the nucleon spin and mass compositions. This project should be able to contribute to the clarification of the hadron spin and mass in terms of quarks and gluons.

At the J-PARC high-momentum beamline, the exclusive Drell–Yan process $\pi^- p \to \mu^+\mu^- B$ is considered as shown in Fig. 394. The "pion" beam momentum is up to about 20 GeV. If the baryon B is a neutron, the nucleonic GPDs will be measured, and transition GPDs will be investigated if B is different from the neutron. This process is complementary to the pion-production experiment $\gamma^* + p \to \pi + N$ at JLab with spacelike virtual photon, whereas the J-PARC process is with the timelike one.

At the high-momentum beamline, there is an approved experiment E50 for investigating charmed baryons [4626]. The GPD experiment will be proposed as a collaboration

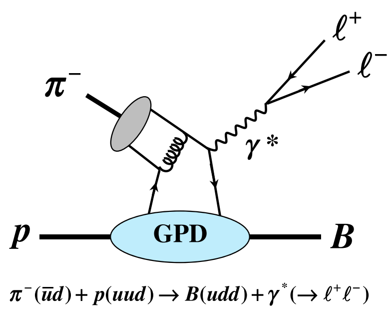

Fig. 394 Exclusive Drell–Yan process for measuring GPDs

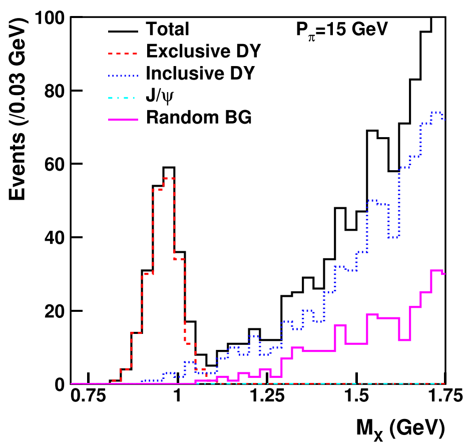

Fig. 395 Simulation for the missing-mass spectra [4625]. (Used with the copyright permission of American Physical Society)

project with this E50 experiment by supplying a dimuon detector. The dimuons could come from various sources; however, the exclusive Drell–Yan process should be identified by the missing-mass (M_X) spectra as shown in Fig. 395. Here, the Monte-Carlo simulation is given for the pion momentum $p_\pi = 15$ GeV. The exclusive peak is obvious just below 1 GeV, and it should be separated from other processes like inclusive Drell–Yan, J/ψ production, or random backgrounds. In this experiment, the GPDs will be measured for $0.1 < x < 0.3$ and timelike photons in contrast to the JLab experiment on the pion production for larger x and spacelike photons.

In future, there are further possibilities to extend this project on GPD-related studies and, more generally, on high-energy hadron physics [4627–4629]. We explain some examples.

1. Pion–nucleon transition distribution amplitudes
   By backward charmonium production in pion–nucleon collisions, pion-to-nucleon transition-distribution amplitudes can be investigated.
2. GPDs in the ERBL region
   The primary proton beam can be used to measure GPDs by using the $2 \to 3$ process $p+p \to p+\pi+B$. If the final pion and proton have nearly opposite and large transverse momenta with a large invariant energy, the cross section is sensitive to the GPDs in the special kinematical region of ERBL (Efremov–Radyushkin–Brodsky–Lepage).
3. Exotic hadrons by constituent counting rule
   The determination of exotic hadrons is not easy in low-energy global observables, and a much clearer determination could be done by using the constituent counting rule in perturbative QCD. Actually, the structure of the exotic-hadron candidate $\Lambda(1405)$ could be determined by the exclusive process $\pi^- + p \to K^0 + \Lambda(1405)$ at J-PARC.
4. Color transparency
   The color transparency indicates that a hadron passes freely through the nuclear medium at large momentum transfer. It is a unique feature of QCD. There was a mysterious BNL-EVA measurement that the transparency drops at a proton momentum $p > 10$ GeV. The J-PARC should be able to clarify this issue.

In future, we expect that a separated high-momentum kaon beam will become available as the hadron-hall extension program in addition to the protons and pions, so that a variety of these type experiments should become possible.

14.3.7 Heavy-ion physics

The purpose of the J-PARC hadron physics is to contribute to our understanding of quantum many-body systems in a wide kinematical range of the phase diagram by precision measurements of new observables as explained in the beginning of this section. Presently, the physics of dense QCD matters is an important missing program in the current J-PARC experiments.

Dense hadronic systems have been investigated by heavy-ion collisions at RHIC and LHC in the high-temperature and low-density region as shown in Fig. 396 [2259,4599]. The creation of a quark–gluon plasma (QGP) was established in the RHIC project by observables such as the collective flow of hadrons and medium modifications of jets. It was surprising to find a small viscosity for the QGP, which initiated interdisciplinary studies with the string theory through the AdS/CFT correspondence (see Sect. 5.4). Higher-energy collisions are now under investigations at LHC. In addition, the signature of the color-glass condensate has been investigated at these facilities.

At zero baryon density, lattice QCD suggests that the phase transition is a crossover, whereas theoretical models indicate that at high densities the phase transition should be a first-order transition [2275]. This implies that an endpoint of the first-order transition should exist as shown in Fig. 396. There are also interesting topics on color superconductivity in the cold and dense matter region. After the QGP discovery and studies of its properties, the frontier of heavy-ion physics

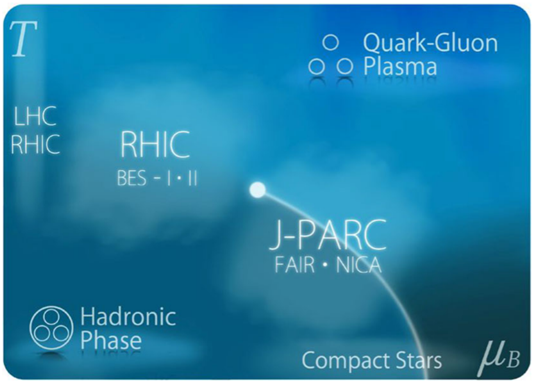

Fig. 396 QCD phase diagram with heavy-ion facilities [4599]

should be this unexplored region. In fact, there are projects at FAIR and NICA to investigate this region in the near future.

In order to realize such experiments at J-PARC, an additional facility is needed to accelerate heavy ions. The possibility of the heavy-ion experiment was studied in a letter of intent in 2016 [4630]; the proposal was submitted to the J-PARC PAC in 2021 [4599,4631]. For this project, it is necessary to construct a new linac and a new booster synchrotron. With this injector consisting of the linac and the synchrotron together with the rapid-cycling and the main-ring synchrotrons (see Fig. 381), high-intensity heavy-ion beams with 2–12 A GeV will be obtained. The J-PARC heavy-ion project has a staging plan for its timeline [4632]. In the sixth year after the financial approval, the phase-1 experiment is expected to start with the LINAC, the reuse of the KEK-PS booster, and upgrades of the existing spectrometer. Therefore, if the project is approved immediately, the phase-1 experiment could start in the end of 2020s. Then, the phase-II experiment could start in the ninth year with the new booster and new spectrometer as the final configuration. The energies of the heavy-ion facilities for the cold and dense experiments are shown in Fig. 397 The J-PARC-HI (heavy ion) project is a unique position as the highest-intensity facility in the several GeV region.

The first purpose of this new facility is to find the phase transition to deconfined quarks and gluons at high densities, by measuring di-electrons, which originate from the virtual photon emission in the hot medium. The advantage of the di-electron measurement is that the virtual photon does not suffer from strong final-state interactions in the medium, so that it directly reflects the information on the QCD matter.

Two simulation studies are shown in Fig. 398 for the di-electron spectrum [4599]. The left-hand side presents the case of no phase transition at $T = 150\,\mathrm{MeV}$, and the right-hand side the case for a first-order phase transition at $T = 120\,\mathrm{MeV}$. The di-electron invariant mass spectrum was taken as $(M_{ee}T)^{3/2}\ \exp(-M_{ee}/T)$. These results were obtained for the mid-rapidity region ($1 \le y_{\mathrm{lab}} \le 2$) with 100-day

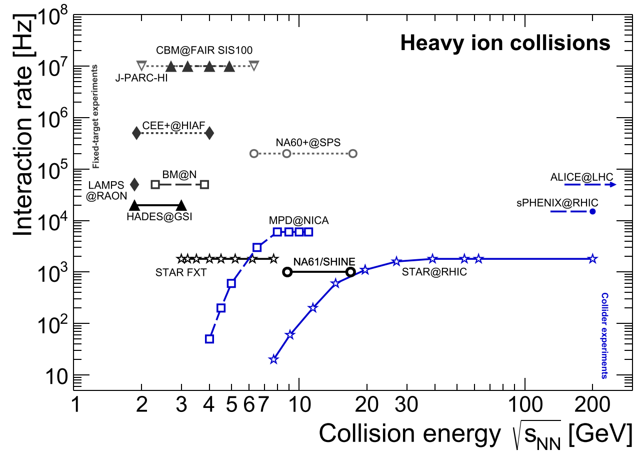

Fig. 397 Maximum instantaneous interaction rates recorded by various existing (full lines), under construction (dashed) and proposed fixed-target (black) and collider (blue) experiments addressing the high-μ_B region of the QCD phase diagram (from [4633], consistently updated based on [4634])

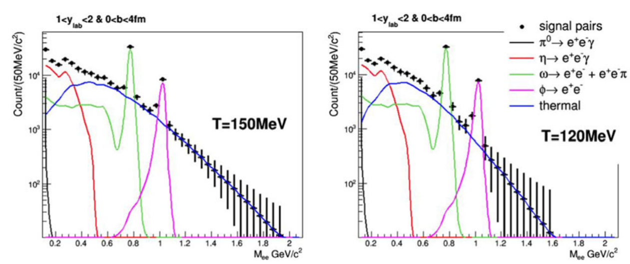

Fig. 398 Simulations for the di-electron mass spectra [4599]

beam time. From such measurements, a determination of the temperature should be possible with the 10% accuracy by the spectrum slope at the mass range $M_{ee} > 1.1\,\mathrm{GeV}$ for the left-side case of Fig. 398. In the right-hand side, 10% accuracy is possible if $M_{ee} > 0.7\,\mathrm{GeV}$ data are selected. This ambitious J-PARC project makes it possible to find new phenomena of cold and dense matter.

14.4 The NICA program

Alexey Guskov

The Nuclotron-based Ion Collider fAcility (NICA) is a new research complex for studying the fundamental properties of the strong interaction under development as a flagship project at the Joint Institute for Nuclear Research [4635–4637]. The heart of NICA is the Nuclotron – a superconducting ion synchrotron put in operation in 1993. It will be equipped with two injection chains: for heavy (including a booster – a small superconducting synchrotron) and light ions, and a storage ring where particle collisions are planned. The storage ring of racetrack shape has a maximum magnetic rigidity of 45 T×m and a circumference of 503 m. The maximum field of superconducting dipole magnets is 1.8 T. NICA will pro-

Fig. 399 View of the NICA site

vide a variety of heavy-ion beams up to Au^{79+} with a kinetic energy up to 4.5 GeV/u. Collisions of high-intensity proton beams with a high degree of longitudinal or transverse polarization and with total energy up to 13.5 GeV will also be available [4638]. Major accelerator challenges include strong intra-beam scattering and space-charge effects which will be partially compensated by extensive use of electron and stochastic cooling systems.

Two experimental setups with different physics programs will run at two interaction points located in the opposite straight sections of the racetrack ring. The MultiPurpose Detector (MPD) placed at the first interaction point will study hot and dense baryonic matter in heavy-ion collisions with luminosity up to 10^{27} cm^{-2} s^{-1}. The Spin Physics Detector (SPD) in the second interaction point is dedicated to the study of the spin structure of the proton and deuteron and other spin-related phenomena in p-p and d-d collisions with luminosity up to 10^{32} cm^{-2} s^{-1}. In addition, the heavy-ion beams can be extracted to the fixed-target experimental setup BM@N (Baryonic Matter at Nuclotron) whose main goals are investigations of strange/multi-strange hyperons, hypernuclei production, and short-range correlations. Extracted beams will also be used for applied research. A view of the NICA site is shown in Fig. 399 while Fig. 400 represents the schematic layout of the accelerator complex.

The implementation of the physic program of the NICA complex is envisioned in three main stages: (i) heavy-ion physics with a fixed target (BM@N), (ii) heavy-ion physics in the colliding mode (MPD), and (iii) spin physics (SPD). The possibility of using NICA in the electron-ion collider mode in the future is under discussion.

14.4.1 The study of dense and hot strongly interacting matter at NICA

Asymptotic freedom has a very deep importance for hadronic matter under extreme conditions. At sufficiently high nuclear density or temperature, average inter-parton distances become small and their interaction strength weakens. Above a critical energy density of about 0.3 GeV/fm^3, a gas of hadrons passes through a deconfinement transition and becomes a system of unbounded quarks and gluons called quark–gluon plasma (QGP). An evidence of this transition has been obtained from lattice simulations of QCD, in the form of a rapid increase of the entropy density around the critical energy density. The deconfinement of quarks and gluons is accompanied by a restoration of chiral symmetry, spontaneously broken in the QCD vacuum.

The phase diagram (see Fig. 159) translates the properties of strong interactions and their underlying QCD theory into a visible pattern. Recent lattice calculations have shown that for vanishing baryon chemical potential, μ_B, and at a pseudocritical temperature 156.5 ± 1.5 MeV, a crossover transition happens from the phase with a broken chiral symmetry to the restored chiral symmetry phase [484,4639]. Different effective models conclude that at higher μ_B, the transition from the ordinary hadron-matter phase to a phase, where chiral symmetry is restored, is of first order. The corresponding critical endpoint is an object of desire of experimenters and theorists, however, its existence is not established yet.

The major goal of MPD and BM@N experiments at NICA is to explore the QCD phase diagram by the study of in-medium properties of hadrons and the nuclear matter Equation of State (EoS), including a search for possible signals of deconfinement and/or chiral symmetry restoration phase transitions, and the QCD critical endpoint. The range of energies and interaction rates covered in different heavy-ion collision experiments including MPD and BM@N experiments at NICA is presented in Fig. 397.

The BM@N experiment
BM@N is a fixed-target experimental setup operating with extracted ion beams from the upgraded Nuclotron. The main final goal of the BM@N experiment is the comprehensive study of the early phase of nuclear interaction at high densities of nuclear matter (3–4n_0) via registration of strange and multi-strange particles (kaons, Λ, Ξ and Ω hyperons, double hypernuclei, etc.) production with enormous statistical precision. Investigation of the reaction dynamics and nuclear equation of state, as well as the study of the in-medium properties of hadrons, are also planned. In order to provide normalization for the measured A+A spectra, a study of elementary reactions (p+p, p+n(d)) will be performed.

The layout of the expected full configuration of the BM@N setup is shown in Fig. 401. The tracking system consists of the silicon strip sensors, and gaseous detectors and is partially placed inside the analyzing magnet with a field up to 1.2 T. Particle identification is provided by the multi-gap Resistive Plate Chamber-based Time-of-Flight system. A Zero Degree Calorimeter is foreseen for the

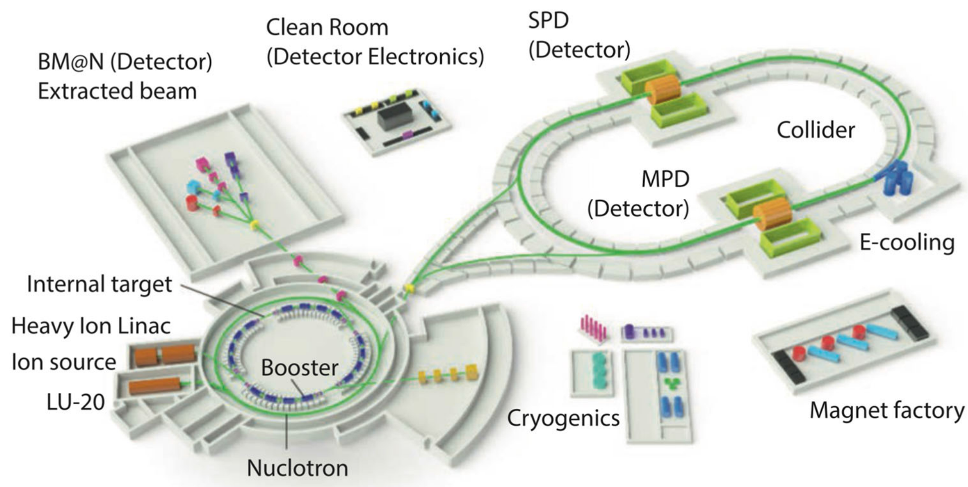

Fig. 400 The NICA accelerator complex at JINR

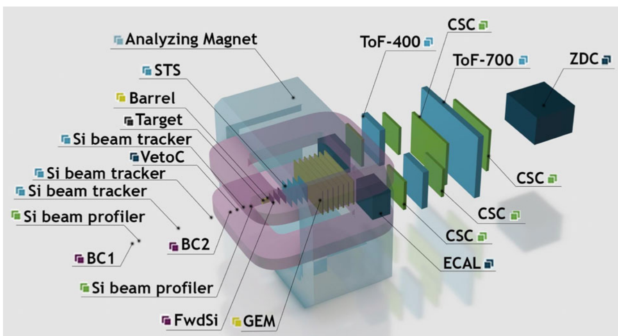

Fig. 401 Layout of the BM@N detector [4640]

extraction of the collision impact parameter and centrality determination. The BM@N setup currently operates in test mode.

The relevant degrees of freedom at the Nuclotron energies are first of all nucleons and their excited states followed by light and strange mesons [4641]. The focus of experimental studies at BM@N will be on hadrons with strangeness, which are early produced in the collision and not present in the initial state of two colliding nuclei. The measured production yields of light and strange mesons, as well as of hyperons and anti-hyperons are shown in Fig. 402 as a function of the nucleon–nucleon collision energy. The Nuclotron heavy-ion beam-energy range corresponds to $\sqrt{s_{NN}}$ = 2.3–3.5 GeV. It is well suited for studies of strange mesons and multi-strange hyperons which are produced in nucleus–nucleus collisions close to the kinematic threshold. Heavy-ion collisions are a rich source of strangeness, and capturing Λ-hyperons by nucleons can produce a variety of light hyper-nuclei [4642,4643]. In heavy-ion collisions, light hypernuclei are expected to be abundantly produced at low energies due to the high baryon density. However, the production mechanisms of hypernuclei in heavy-ion collisions are not well understood, due to the scarcity of data. The study of hyper-nuclei production is expected to provide new insights into the properties of the hyperon-nucleon and hyperon-hyperon interactions. Figure 403 presents the yields of hyper-nuclei as a function of the nucleon–nucleon collision energy in the center-of-mass system in Au+Au collisions, predicted by a thermal model [4644]. The maximum in the hyper-nuclei production rate is predicted at $\sqrt{s_{NN}}$ = 4-5 GeV, which is close to the Nuclotron energy range.

Short-range correlations in nuclei (SRC) are an additional topic for study at BM@N. In an attempt to simplify the description of the nuclei as complex strongly interacting systems, we tend to separate their short- and long-range structure. Effective field theories describe the long-range structure using a mean-field approximation. The short-range structure of nuclei can be described in terms of nucleon–nucleon short-range correlations. SRC are brief fluctuations of two nucleons with high and opposite momenta, where each of them is higher than the Fermi momentum for the given nucleus.

Hard knock-out reactions where the beam probe interacts with a single nucleon are the standard way to study the properties of SRC pairs. In the pilot studies at BM@N the new approach with the inverted kinematics was used [4645]: a carbon beam with the momentum of 4 GeV/c per nucleon scatter off a liquid hydrogen target. A proton with momentum from the SRC pair is scattered off a target proton. Two protons from the (p,2p) reaction were detected by a two-arm spectrometer while a $A-2$ nuclear fragment was identified via p/Z ratio. The events with ^{10}B and ^{10}Be fragments corresponded to p-n and p-p SRC pairs, respectively. The direct experimental evidence for the separation of the pair wave-function from that of the residual many-body nuclear system was obtained. All measured reactions are well described by theoretical calculations that include no distortions from the initial- and final-state interactions (Fig. 404). The obtained results illustrate the ability to study the short-distance structure of short-lived radioactive nuclei at the forthcoming FAIR and FRIB facilities.

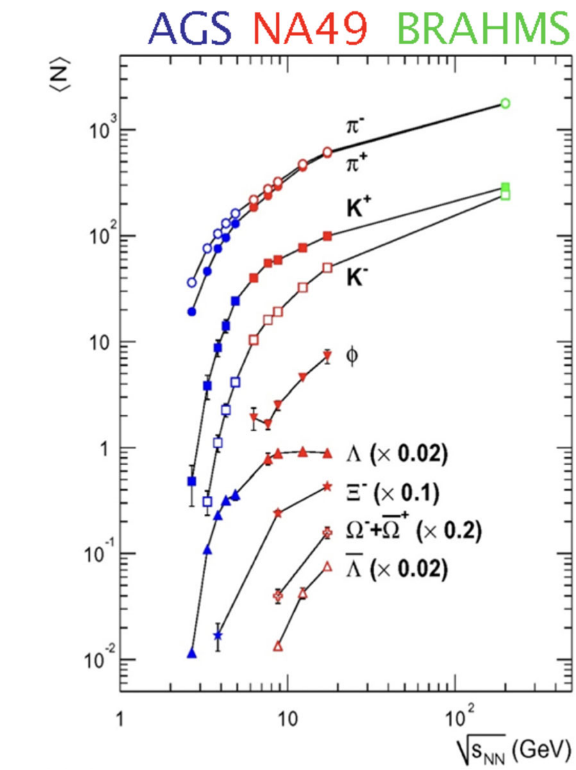

Fig. 402 Yields of mesons and (anti-)hyperons measured in different experiments as a function of the collision energy $\sqrt{s_{NN}}$ for Au+Au and Pb+Pb collisions [4646]

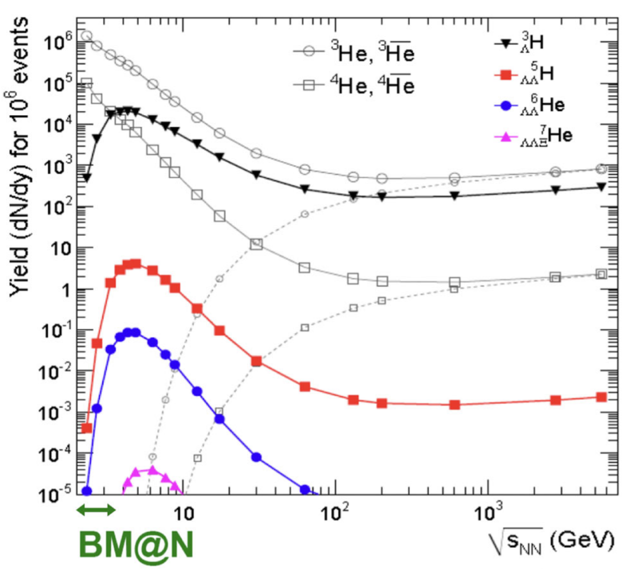

Fig. 403 Yields of hyper-nuclei predicted by the thermal model in Ref. [4644] as a function of the $\sqrt{s_{NN}}$ for Au+Au collisions. Predictions for the yields of ^{3}He and ^{4}He nuclei are presented for comparison

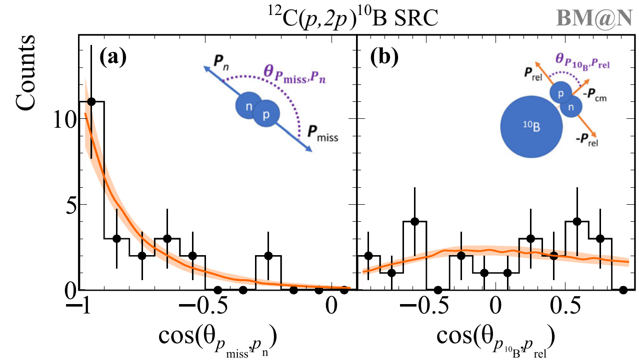

Fig. 404 Opening angle in SRC p–n pair (left) and the angle between the ^{10}B fragment and pair relative momentum (right). The model calculations are shown in orange [4645]

The MPD experiment

MPD is a collider experiment designed to perform a comprehensive scan of the QCD phase diagram with beam species from protons to gold by varying the center-of-mass collision energy from 4 to 11 GeV per nucleon which is complementary to the RHIC beam energy scan towards lower energies. The unique feature of MPD as a collider experiment is the invariant acceptance at different beam energies as compared to fixed-target experiments [4647].

To reach this goal, the experimental program includes the simultaneous measurement of the observables which are sensitive to high density effects and phase transitions. The observables measured on event-by-event basis are particle yields and ratios, correlations and fluctuations. Different species probe different stages of the nucleus–nucleus interaction due to their differences in mass, energy and interaction cross-sections. The hadrons containing heavy strange quarks are especially interesting. These strange heavy hadrons are created in the early high-temperature and high-density stage but may quickly decouple due to their low interaction cross section with the surrounding matter. Among various characteristics, the elliptic flow deserves special attention because this collective motion is formed mainly in the early stage of the collision. The spatio-temporal information on the particle freeze-out source, which depends on the preceding evolution of the system, is provided by the measurement of identical particles interference. The direct information on hot and dense transient matter is provided by penetrating probes, photons and leptons. In this respect, vector mesons which contain information on chiral symmetry restoration are very attractive. Measurement of the positive/negative pion asymmetry with respect to the reaction plane as a function of centrality of heavy-ion collisions opens a possibility to touch such fundamental problem as spontaneous violation of CP parity in strong interactions.

The physics program of the first stage of the MPD experiment includes the following items [4648]:

– multiplicity and spectral characteristics of the identified hadrons including strange particles, multi-strange

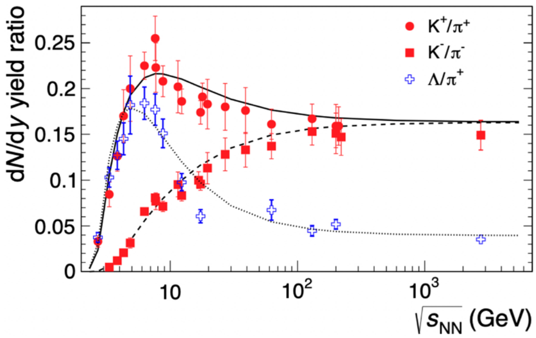

Fig. 405 K^+/π^+, K^-/π^- and Λ/π^+ ratios as a function of $\sqrt{s_{NN}}$ [2203]

baryons and antibaryons characterizing entropy production and system temperature at freeze-out;
- event-by-event fluctuations in multiplicity, charges, transverse momenta and K/π ratios as a generic property of critical phenomena;
- collective flow effects (directed, elliptic and higher ones) for hadrons including strange particles;
- femtoscopy with identified particles and particle correlations.

In the second stage, the physics with electromagnetic probes (photons and dileptons) will be accessed.

The behaviour of hadron abundances along the hydrodynamic trajectories of heavy-ion experiments is closely related with the properties of the strongly interacting matter near the phase transition. For example, a promising observable to study the onset of deconfinement is the pion-to-kaon ratio. The K^+ yield is proportional to the overall strangeness production and pions can be associated with the total entropy produced in the reaction. Thus, the K^+/π^+ production ratio can be a good measure of strangeness-to-entropy ratio, which is different in the confined phase and the QGP. The experimental results for K^+/π^+, K^-/π^- and Λ/π^+ ratios as a function of collision energies in the wide energy range are shown in Fig. 405. The experimental points in the most interesting region around $\sqrt{s_{NN}} = 10$ GeV have large uncertainties that could be significantly reduced by the measurements at MPD.

Measurements of event-by-event fluctuations have been performed by the numerous fixed-target and collider experiments. Recent STAR measurements from the RHIC-BES program [2224] indicate a non-monotonic behaviour of the excitation function for the net-proton moments in central Au+Au collisions in the region below $\sqrt{s_{NN}} = 20$ GeV, which can be a hint for the critical point in the range of finite baryon number density. At MPD the region below 11 GeV will be scanned with much higher precision.

The main task of femtoscopy, the technique of two-particle correlations in momentum space, is to measure the space-

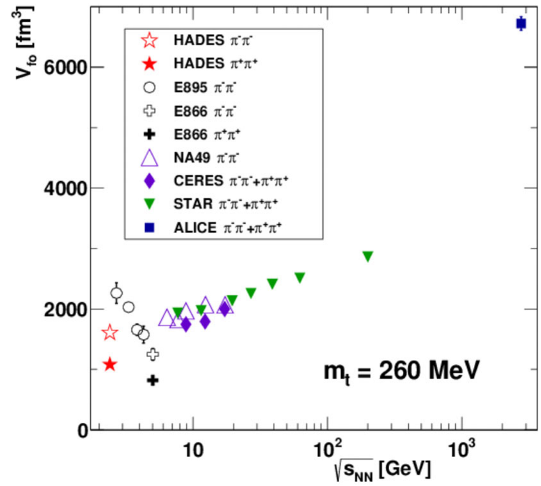

Fig. 406 Freeze-out volume for pions as a function of the collision energy [4649]

time evolution of the system created in particle collisions. The two-pion correlation functions are excellent candidates for first-day physics measurements at MPD. Femtoscopy measurements for pions have been performed in several previous experiments. Figure 406 presents the energy dependence of the freeze-out volume, obtained from two-pion interferometry. A non-monotonic behavior of this volume in the NICA energy range raises interest in such measurements at MPD.

The anisotropic collective flow is also one of the promising observables sensitive to the transport properties of the strongly interacting matter, in particular, the speed of sound, and the specific shear and viscosities. It can be quantified by the Fourier coefficients v_n in the expansion of the particles azimuthal distribution. Relativistic viscous hydrodynamic models have been successful in describing the observed anisotropy v_n for the produced particles in the collisions of heavy ions at RHIC and the LHC [2190,4650,4651]. The directed flow v_1 can probe the very early stages of the collision as it is generated during the passage time of the two colliding nuclei. The results of a model-to-data comparison for the elliptic flow v_2 at $\sqrt{s_{NN}} = 7.7$ GeV and 4.5 GeV may indicate that at NICA energies a transition occurs from partonic to hadronic matter. The high-statistics differential measurements of v_n, that are anticipated from the MPD experiment at NICA, are expected to provide valuable information about this parton–hadron transient energy domain [4652,4653].

The layout of the MPD setup is shown in Fig. 407 [4653]. The components of the MPD barrel part have an approximate cylindrical symmetry. The beam line is surrounded by the large gaseous Time Projection Chamber (TPC) which is enclosed by the TOF barrel. The TPC is the main tracker, and in conjunction with the TOF they will provide precise momentum measurements and particle identification. It is

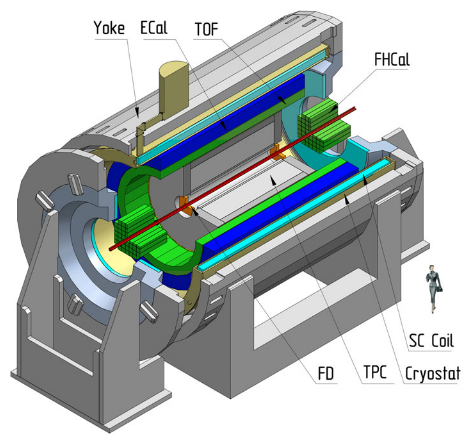

Fig. 407 Layout of the MPD experimental setup [4653]

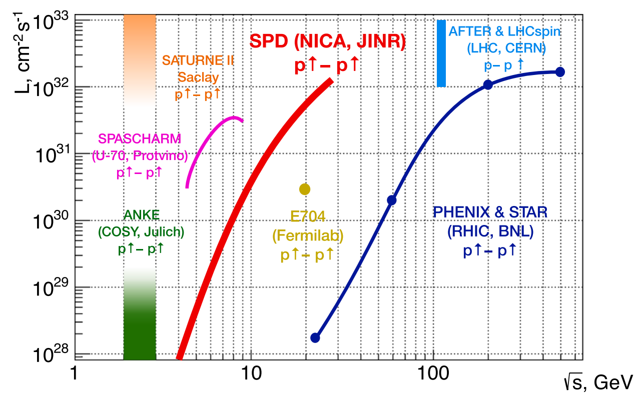

Fig. 408 NICA SPD and the other past, present, and future experiments with polarized protons

placed in a highly homogeneous magnetic field of up to 0.57 T. The Electromagnetic Calorimeter (ECal) is placed in between the TOF and the MPD Magnet. It will be used for detection of electromagnetic showers, and will play the central role in photon and electron measurements. In the forward direction, the Fast Forward Detector (FFD) is located still within the TPC barrel. It will play the role of a wake-up trigger. The Forward Hadronic Calorimeter (FHCal) for determination of the collision centrality and the orientation of the reaction plane is located near the Magnet end-caps. At the moment, this detector configuration is at the assembling stage.

Additional detectors like the silicon-based Inner Tracker System for precision secondary vertex reconstruction, the miniBeBe detector for triggering and start time determination, and the cosmic ray detector on the outside of the magnet yoke are proposed for the later stages.

14.4.2 The spin structure of proton and deuteron in the SPD experiment

While the main goal of the BM@N and MPD experiments is to study deconfinement, the third experiment, SPD, aims to study the internal structure of the proton and deuteron using polarized beams. In the polarized proton–proton collisions, the SPD experiment [4654] will cover the kinematic gap between the low-energy measurements at ANKE-COSY and SATURNE and the high-energy measurements at the Relativistic Heavy Ion Collider, as well as the planned fixed-target experiments at the LHC (see Fig. 408). The possibility for NICA to operate with polarized deuteron beams at such energies is unique. SPD is planned to be operated as a universal facility for comprehensive tests of the basics of the QCD. The main efforts, however, will be devoted to the study of the unpolarized and polarized gluon content of the proton at large Bjorken-x, using different complementary probes [4655].

Quantum chromodynamics has remarkable success in describing the high-energy and large-momentum transfer processes, where quarks and gluons that are the fundamental constituents of hadrons, behave, to some extent, as free particles and, therefore, the perturbative QCD approach can be used. The cross-section of a process in QCD is factorized into two parts: the process-dependent perturbatively-calculable short-distance partonic cross-section (the hard part) and universal long-distance functions, PDFs, and FFs (the soft part), see Sect. 11. The parton distributions could be applied also to describe the spin structure of the nucleon that is built up from the intrinsic spin of the valence and sea quarks (spin-1/2), gluons (spin-1), and their orbital angular momenta.

In recent years, the three-dimensional partonic structure of the nucleon became a subject of careful studies. Precise mapping of the three-dimensional structure of the nucleon is crucial for our understanding of QCD. One of the ways to go beyond the usual collinear approximation is to describe the nucleon content in the momentum space by employing the so-called Transverse-Momentum-Dependent Parton Distribution Functions (TMD PDFs) [1284,3247,3248,4656–4658].

Considerable progress has been achieved during the last decades in the understanding of the quark contribution to the nucleon spin, yet the gluon sector is much less developed. One of the difficulties is the lack of direct probes to access the gluon content in high-energy processes.

The final goal of the SPD experiment is to provide access to the gluon TMD PDFs (see Table 50) in the proton and deuteron via the measurement of specific single and double spin asymmetries in the production of charmonia, open charm, and high-p_T prompt photons. The kinematic region to be covered by SPD for these processes (Fig. 409) is unique and has never been accessed purposefully in polarized hadronic collisions. Quark TMD PDFs, as well as spin-dependent fragmentation functions, could also be studied. The results expected to be obtained by SPD will play an important role in the general understanding of the nucleon gluon content and will serve as a complementary input to the ongoing and planned studies at RHIC, and future measurements at the EIC (BNL) and fixed-target facilities at the LHC (CERN). Simultaneous measurement of the same quantities using different processes at the same experimental setup is of key importance for the minimization of possible systematic effects.

The naive model describes the deuteron as a weakly-bound state of a proton and a neutron mainly in S-state with a small admixture of the D-state. However, such a simplified picture failed to describe the HERMES experimental results on the b_1 tensor structure function [1386]. A unique possibility to operate with polarized deuteron beams brings us to the world of the tensor structure of the deuteron (tensor PDFs). A possible non-baryonic content in the deuteron could be accessed via the measurement of the gluon transversity distribution and the comparison of the unpolarized gluon PDFs in the nucleon and deuteron at high values of x.

Nevertheless, the largest fraction of hadronic interactions involves low-momentum transfer processes in which the effective strong coupling constant is large and the description within a perturbative approach is not adequate. A number of (semi-)phenomenological approaches have been developed through the years to describe strong interaction in the non-perturbative domain starting from the very basic principles. They successfully describe such crucial phenomena as the nuclear properties and interactions, hadronic spectra, deconfinement, various polarized and unpolarized effects in hadronic interaction, etc. The transition between the perturbative and non-perturbative QCD is also a subject of special attention. In spite of a large set of experimental data and huge experience in a few-GeV region with fixed-target experiments worldwide, this energy range still attracts both experimentalists and theoreticians.

SPD has an extensive physics program for the first stage of the NICA collider operation with reduced luminosity and collision energy of the proton and ion beams, devoted to comprehensive tests of the various phenomenological models in the non-perturbative and transitional kinematic domain. It includes such topics as the spin effects in elastic scattering, in exclusive reactions as well as in hyperons production, multiquark correlations and dibaryon resonances, charmonia and open charm production, physics of light and intermediate nuclei collision, hypernuclei, etc. [4659]. The proposed program covers up to 5 years of the NICA collider running.

The SPD experimental setup, shown in Fig. 410, is designed as a universal 4π detector with advanced tracking and particle identification capabilities based on modern technologies, consisting of the barrel part and two end-caps. The silicon vertex detector will provide a reconstruction of secondary vertices of D-meson decays. The straw-tube-based tracking system placed within a solenoidal magnetic field of up to 1 T should provide tracking capability. The time-of-flight system will provide π/K and K/p separation together with an aerogel-based Cherenkov detector in the end-caps. Detection of photons will be provided by the sampling electromagnetic calorimeter. To minimize multiple scattering and photon conversion effects for photons, the detector material will be kept to a minimum throughout the internal part of the detector. The muon (range) system is planned for muon identification. It can also act as a rough hadron calorimeter. The pair of beam-beam counters and zero-degree calorimeters will be responsible for the local polarimetry and luminosity control. To minimize possible systematic effects, SPD will be equipped with a free-running (triggerless) DAQ system. The SPD experimental setup is currently in the phase of the technical project preparation.

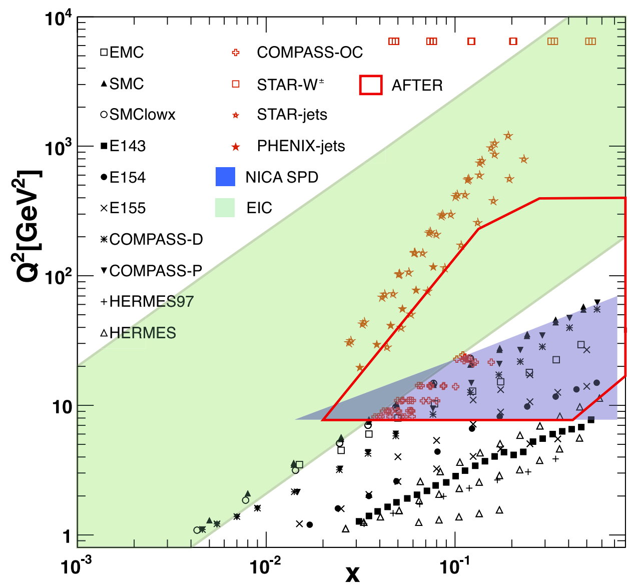

Fig. 409 Kinematic coverage of SPD in the charmonia, open charm, and prompt photon production processes

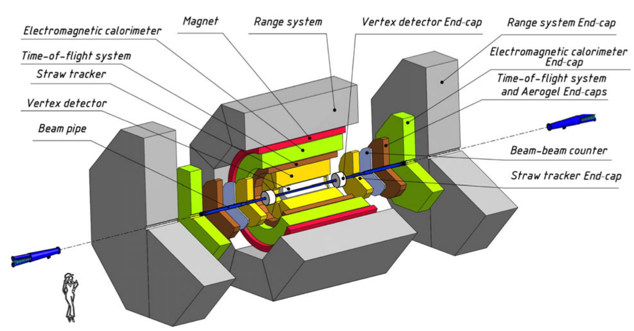

Fig. 410 Layout of the SPD experimental setup

Table 50 Gluon TMD PDFs at twist-2. The columns represent gluon polarization, while the rows represent hadron polarization

	Unpolarized	Circular	Linear
Unpolarized	g(x) density		$h_1^{\perp g}(x, k_T)$ Boer–Mulders function
Longitudinal		$\Delta g(x)$ helicity	Kotzinian–Mulders function
Transverse	$\Delta_N^g(x, k_T)$ Sivers function	Worm-gear function	$\Delta_T g(x)$ transversity, pretzelosity

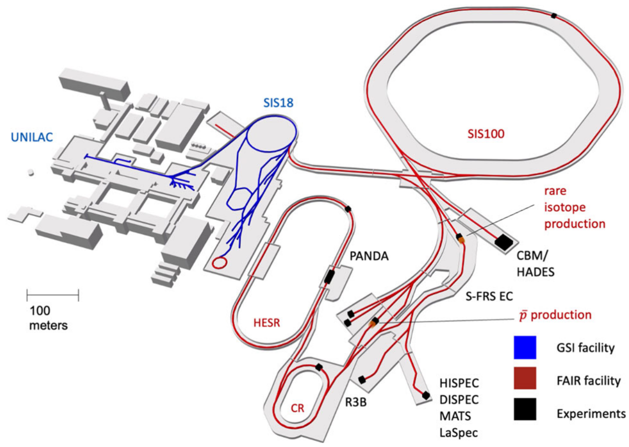

Fig. 411 Layout of the FAIR accelerator complex. See text for the meaning of the various acronyms

14.5 QCD at FAIR

Johan Messchendorp, Frank Nerling, and Joachim Stroth

14.5.1 The FAIR facility

The international Facility for Antiproton and Ion Research FAIR (Fig. 411) is an accelerator complex currently constructed at the site of the national GSI Helmholtz Center for Heavy-ion Research, Germany. It is composed of a rapid cycling synchrotron with maximum rigidity 100 Tm providing beams directly to experimental halls and to production targets for secondary ion and anti-proton beams [4660]. A high-energy storage ring (HESR) enables experiments with antiproton and rare radioactive isotope beams. The latter are selected out of either nuclear fragments or fission products, emerging from reactions of e.g. relativistic uranium beams, by the Super Fragment Separator (S-FRS), providing high transmission for reaction products and high selectivity and purity for selected rare isotopes [4661].

The scientific goals encompass many open questions connected with the formation of matter and the role of the strong force herein. The respective activities are organized in three pillars, hadron physics using anti-proton annihilation (PANDA), heavy-ion reactions at relativistic energies (CBM), and nuclear structure physics at the limit of stability using relativistic, stored or decelerated rare isotope beams (NUSTAR). For the latter, not discussed in the remainder of this section, FAIR will pursue a unique approach enabling nuclear structure studies of e.g. the r-process isotopes relevant for the third r-process abundance peak. Acceleration of 28+ uranium ions in the SIS100 will push the space charge limit and yet provide beam energies around 1 *A* GeV [4662]. SIS100 is particularly designed to accelerate medium charge state ions with a fast cycling rate of 1 Hz. This is achieved ramping the superconducting dipole magnets with 4 T/s to a maximum field of 1.9 T [4663]. Combined with the large acceptance and transmission of the Super-FRS, separated fission fragments will provide fully stripped isotope beams up to the neutron drip line. Such beams can be transferred to a storage ring for precision mass measurements (ILIMA), directed to a secondary target in the high-energy experiment hall for reaction experiments (R3B), or to experiments utilizing γ-spectroscopy in flight (HISPEC) or with stopped beams (DISPEC). Complementary experiments can also be performed at the Super-FRS operating the second half of the separator as high-resolution forward spectrometer and using a secondary target in the middle section of the separator (Super-FRS EC). Last not least isotope beams can also be decelerated and trapped (MATS) or investigated using laser spectroscopy (LaSpec). FAIR will also give home to many other experimental collaborations working in fields of atomic physics, radio biology, plasma physics and material science (APPA).

Civil construction of the accelerator complex has been started in 2017 focusing on the north area of the complex. As of 2022, the shell construction of the ring tunnel, the transfer buildings, the reaction experiment cave and the Super-FRS is mostly finished and the technical building installation has been started. The facility will be completed in a staged approach aligned with the funding profile and first beam from SIS100 to the CBM cave is anticipated for 2028. A FAIR early science program will be started as soon as the Super-FRS is installed providing uranium beam from SIS18 directly to the separator. Already now, a rich research program is ongoing at GSI and various other international facilities employing instrumentation developed for FAIR (FAIR Phase-0).

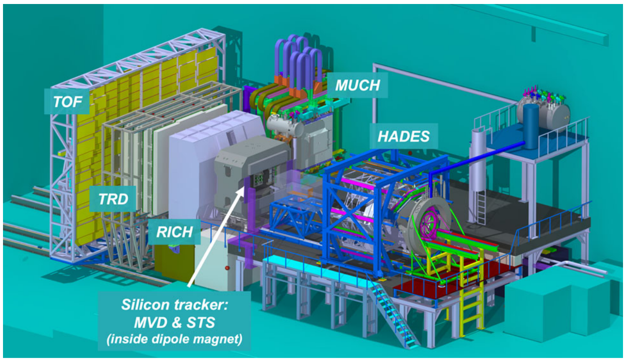

Fig. 412 Computer rendering of the two experiments CBM and HADES installed in the FAIR fixed-target experimental hall. In case CBM is operated, the beam pipe is continuing through the center of the HADES experiment up to the CBM dipole (target vacuum chamber and beam pipe are not drawn). In case HADES is taking beam, a beam stop is placed between the two experiments (half transparent cube shown on a stand). The HADES setup is shown with blue support structure

14.5.2 CBM – QCD studies at high baryon densities

The research pillar *Compressed Baryonic Matter* (CBM) is addressing the physics of QCD matter under extreme conditions of baryon density and temperature. In a dedicated experiment hall, ion beams extracted from SIS100 will be directed onto stationary targets to form transients states of QCD matter in central collisions. The formation process is expected to reach maximum baryon densities of around five times the nuclear ground-state density at temperatures of up to 100 MeV. Model calculations suggest that e.g. in a Au+Au collision at a few A Gev, the incoming nucleons are stopped to a large extent in the collision zone and that the nuclear matter is compressed to densities of $\rho_{\max} \simeq 1\ \mathrm{fm}^{-3}$ [4664]. It is expected that the formed hadronic system is approaching local equilibrium before it freezes out chemically at densities around $\rho_{\mathrm{ch}} \simeq 0.05\ \mathrm{fm}^{-3}$ (see Sect. 7.1). At such initial densities, the system can no longer be understood as resonance gas, but rather as an entangled meson cloud surrounding the baryonic cores (see Sect. 7.2).

Figure 397 demonstrates the world-wide efforts that explore the high-μ_B-region (high net-baryon density) obtained at lower beam energy (c.f. Sect. 7.1) of the QCD phase diagram by means of heavy-ion collisions. Please note that by today no experiment has crossed the 50 kHz line.

The CBM collaboration has designed an experiment to investigate heavy-ion collisions with emphasis on the detection of rare and penetrating probes. Figure 412 shows the configuration of the Compressed Baryonic Matter experiment, together with the already existing HADES experiment placed at the same beam line delivering slow-extracted beam from the heavy-ion synchrotron SIS-100. The unique features of this fixed-target experiment are the rate capability reaching 10 MHz of inspected reactions and a modular composition of detectors for particle identification. The high-rate capability is achieved by performing tracking of charged particles in a compact configuration of 12 planes of silicon detectors placed in a 1 Tm dipole field. The planes are arranged over 1 m downstream the target. The first four planes are composed of monolithic pixel sensors, manufactured in a 180 nm CMOS process, and provide a total of 140 M-Pixels right behind the target and placed inside the beam vacuum (MVD). Behind, and outside the vacuum region, eight planes of silicon strip sensors constitute the core tracking system (STS). This tracking system is contained in a magnetic dipole field providing a maximum bending power of 1 Tm. Behind the tracking station different detector systems can be placed, depending on the observables to be addressed. In the standard configuration, a ring-imaging Cherenkov detector (RICH) provides superb electron/positron identification up to momenta of around 4 GeV. Behind, four stations of transition radiation detector enable intermediate tracking, energy loss measurement and additional electron/positron identification for high momentum tracks (TRD). The last detector is a wall of multichannel resistive-plate counters (TOF) covering about 20 m^2 in the transverse plane. It provides a high-precision time signal to enable particle identification by velocity vs momentum of charged particles. The CBM detector uses a trigger-less data acquisition system where every individual detector cell is digitized and where signals passing their thresholds receive a timestamp. Data streams of up to a TeraByte per second are transferred to the online compute cluster where real-time event building and feature extraction is performed. By selecting events with signatures of interest, the data stream is reduced to a level that allows storage on disks. Up to 40,000 compute nodes will be needed to accomplish this task in the case of operating at the highest interaction rate. The compute cluster will be installed in the FAIR Green Cube. The online event selection and rejection requires a high level of understanding and monitoring of the detector performance at the time of the data taking. To gain experiences and to prepare all software and firmware for fast calibration and event reconstruction, the CBM collaboration has installed a small version of the CBM detector at SIS18 beam line of GSI. This mini-CBM setup is composed out of prototypes or first-of-a-series modules of each detector system of CBM. The detectors are arranged as a single arm telescope and are operated without magnetic field. The performance of the online event selection is benchmarked by investigating the production of hyperons. Their particular decay topology is used as identification.

The prime goal of the CBM program at FAIR is to search for signatures of a first-order phase transition, separating the hadron resonance gas region from a likely novel state of matter (cf. Sect. 7.2). The established strategy for this is to search for non-monotonic behavior of the excitation function of various observables, or more general for trends signaling

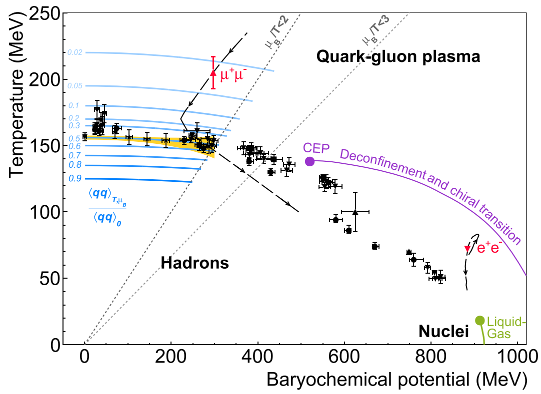

Fig. 413 The QCD phase diagram as function of temperature and baryo-chemical potential. Freeze-out configurations extracted from particle yields assuming sudden freeze-out of a hadron resonance gas are shown as green circles (*cf* 159). Expectation values of the chiral condensate deduced from lattice calculations as sky-blue lines. Measurements of the mean fireball temperature based on the dilepton continuum radiation are shown as red squares together with the expected trajectory of the expanding and radiating system

a change in the number of degrees of freedom of the transient system like the (dis)appearance of a certain scaling behavior. An example is the excitation function of the multiplicity of multi-strange hyperons. The high-rate capability of CBM will enable such measurements well below the proton–proton production threshold.[122]

Indeed, the region in the QCD phase diagram at high baryo-chemical potential is predominantly *terra incognita*. Figure 413 depicts the QCD phase diagram with experimental landmarks and predictions by lattice QCD. The landmarks include, first, chemical-freezeout points that characterize the temperature and the baryochemical potential below which the system can be understood as an expanding hadron gas in which inelastic collisions no longer occur. Two additional points are shown which depict an average temperature of the dense and hot system prior to freeze out. This very promising observable, so far not addressed in excitation functions with the needed precision, is the spectral distribution and yield of dileptons emitted from the dense and hot stage of the collision. Such dileptons couple via virtual intermediary photons directly to the in-medium hadronic current–current correlator and thus probe the microscopic structure of the medium they are expelled from [4665,4666]. In the so-called low-mass region (LMR), i.e. for dilepton invariant masses around the vector-meson pole masses ρ, ω and ϕ and below, the spectral distribution encodes the "melting" of the vector mesons embedded in a hot and dense hadronic environment, while the dilepton spectrum from a purely partonic medium would not feature any particular structure. Moreover, the integral yield of continuum dileptons in the LMR dominantly depends on the size, the lifetime and the temperatures of the emitting source. It has been demonstrated using a hydro model that the fireball ball evolution can significantly change if during the evolution the system experiences a phase transition from a QGP-like to a hadronic equation-of-state. The study observed an increase of the yield by roughly a factor of two in the case of a first-order phase transition [4667]. Dilepton continuum radiation also provides a model independent measurement of the average temperature of the emitting source. This is possible if the imaginary part of the in-medium current–current correlator is sufficiently featureless and approaching a dependence $\propto T^2/M^2$. In that case, the spectral distribution is defined essentially by the thermal Bose factor and the invariant-mass distribution takes the form of black-body radiation, i.e. $\propto (MT)^{3/2}\,\exp{(-M/T)}$ [4668]. A fit of a Planck distribution function to the spectral distribution in the respective invariant mass reveals an invariant measurement of that average temperature, unaffected by any blue shift due to rapid expansion of the emitting source. The two measurements of the average temperature shown in Fig. 413 were obtained by the NA60 collaboration in the dimuon channel [4669] and by the HADES collaboration in the dielectron channel [4670]. The "trajectories" indicated as dashed-dotted lines depict the evolution of the fireball used to integrate the emissivity over the four-volume characterizing the evolution of the collision zone. For details see [4670].

In order to obtain the continuum radiation, contributions to the dilepton invariant-mass distribution from the early pre-equilibrium stage and from late decays of long-lived hadronic states have to be determined and subtracted [4671]. An important part of the CBM program are therefore reference measurements of elementary collision systems or the production of dileptons in collisions of protons on nuclei. For this, the HADES detector will be moved to the SIS100 experimental hall where it will be installed in front of the CBM detector. HADES, with its large polar acceptance, is well suited to study in particular the production and propagation of vector mesons in cold nuclear matter. The feasibility of reconstructing the dilepton continuum radiation in heavy-ion collisions at energies SIS18 energies has been demonstrated for the system Au+Au at $\sqrt{s_{\mathrm{NN}}} = 2.42\,\mathrm{GeV}$. Figure 414 depicts the respective invariant-mass distribution together with various model calculations. It is important to note that at this collision energy, the ρ meson is substantially broadened due to the high baryon density, thus satisfying the criteria for temperature measurement outlined above also in the LMR.

[122] The threshold is here defined as the energy needed to produce a given hyperon in an elementary proton–proton collision and the beam energy is referred to as $\sqrt{s_{\mathrm{NN}}}$.

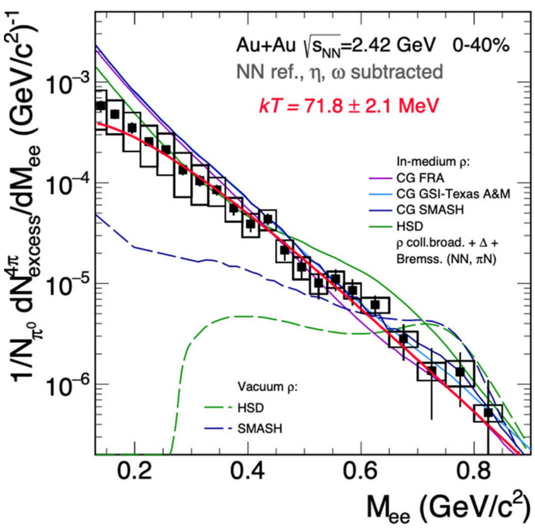

Fig. 414 Di-electron excess radiation measured by HADES for the collision system Au+Au at $\sqrt{s_{\rm NN}} = 2.42$ GeV (black squares). Systematic uncertainties are depicted as open boxes while the statistical errors are shown as vertical lines. Various model calculations are shown as colored lines (see inserts for explanation). Lines labeled CG refer to calculations using coarse grained microscopic transport calculations for the fireball evolution folded with thermal emissivities derived from many-body theory. The line labeled HSD is the result of a full microscopic transport simulation treating the dilepton emission perturbatively, i.e. after the full hadron cascade has been processed. Also shown as dashed lines are the descriptions of dilepton emission from ρ-meson decay used in the full microscopic (shining) approach. The spectrum has been obtained by subtracting from the total yield in the centrality class 0–40% the contributions from late hadron neutron meson decays (cocktail) and from first-chance collisions

14.5.3 PANDA – hadron structure and spectroscopy studies using antiprotons

Physics with antiprotons and PANDA

The ambition of PANDA is to exploit the annihilation of antiprotons with protons and nuclei to study the properties of hadrons and their interactions with unprecedented precision and coverage in parity, spin, and gluon and quark flavor contents. Partly as the successor of the successful LEAR facility at CERN, PANDA will combine a high-resolution and intense antiproton beam with a state-of-art detector system. The experiment is designed to produce hadrons with masses of up to about 5.5 GeV and to unambiguously detect a large variety of final-state particles with excellent momentum resolution, particle identification capabilities, and exclusivity.

PANDA will be an internal-target experiment installed at the High Energy Storage Ring (HESR). The antiproton beam from HESR has several key advantages, namely (i) the production cross sections of hadrons are generally large, resulting in large data samples; (ii) meson-like states of any quark–antiquark spin-parity combination can be produced in formation with a superb mass resolution; (iii) baryon-antibaryon pairs, including multi-strange and charm, can be produced in two-body reactions, which provide clean conditions for baryon studies; (iv) proton–antiproton annihilations constitute a gluon-rich environment.

In the initial phase, HESR will be able to store 10^{10} antiprotons with momenta p from 1.5 GeV up to 15 GeV. By making use of the stochastic cooling technique, the relative beam-momentum spread ($\Delta p/p$) will be $< 5\times10^{-5}$. The antiprotons will interact with a cluster jet target or pellet target, which results in a luminosity during the first phase (Phase One) of data taking of about 10^{31} s^{-1} cm^{-2}. The final goal is a luminosity of up to 2×10^{32} s^{-1} cm^{-2}, referred to as Phase Three.

The PANDA detector is designed to measure momenta of charged and neutral final-state particles with 1–2% resolution and with excellent particle identification, vertex reconstruction, and count-rate capabilities. The nearly 4π acceptance allows to study exclusive reactions covering a large part of their phase spaces, thereby enabling a conclusive partial-wave analysis. The detector consists of a Target Spectrometer (TS) and a Forward Spectrometer (FS). The TS provides precise vertex tracking by the micro vertex detector, surrounded by straw tube trackers and gas electron multiplier detectors in the forward direction. The trajectories of charged particles in the TS are bent by the field of a solenoid magnet providing a field of 2 T, with muon detectors within the segmented yoke. For particle identification, the TS will consist of time-of-flight and Cherenkov detectors and an electromagnetic calorimeter composed of $PbWO_2$ crystals. With the electromagnetic calorimeter, nearly covering the full phase space using a barrel and two endcaps, the measurement of energies and scattering angles of photons, electrons, and positrons will become possible.

The FS consists of straw tube stations for tracking, a dipole magnet, a ring imaging Cherenkov detector, a forward time-of-flight system and a Shashlyk electromagnetic calorimeter, followed by a muon range system. The luminosity at PANDA will be determined by using elastic antiproton–proton scattering as the reference channel registered by a dedicated luminosity detector.

The combination of the intense, high resolution antiproton beam with the nearly 4π PANDA detector, opens up unprecedented possibilities with a very rich physics program, particularly suited to provide a deeper understanding of QCD in the non-perturbative regime. In the following, we discuss some of the QCD-driven highlights from the various pillars of the physics program of PANDA. We note that PANDA has a more extensive physics program that includes various nuclear physics aspects as well, such as the foreseen hypernuclei and hyperatom topics. We limit ourselves here to those topics in which the quarks, gluon, and their interactions are expected to be the most important degrees of freedom. For a more detailed description of the complete physics program at the first phase of the experiment, we refer to [2635].

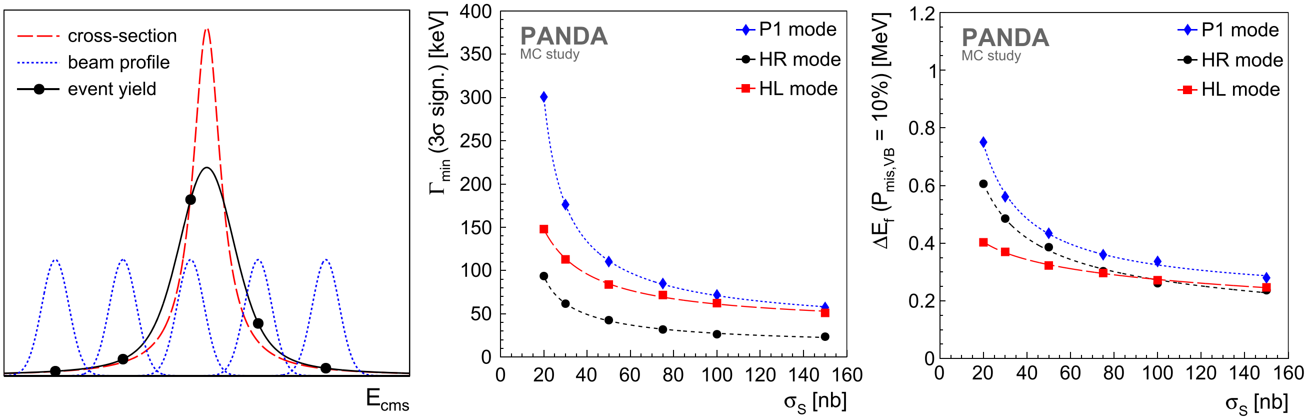

Fig. 415 Illustration and summary of a comprehensive Monte Carlo simulated scan experiment study for PANDA [4672]. Schematic of the resonance energy scan principle (left). Summary of the sensitivity study for an absolute (Breit–Wigner) decay width measurement in terms of the minimum decay width $\Gamma_{\min}$ that can be measured with an relative precision of 33% as a function of the assumed input σ_S (center). Summary of the sensitivity study for line-shape measurements via the E_f parameter (Molecule case) to distinguish between a bound and a virtual state scenario in terms of the probability to mis-identify a virtual as a bound state (right)

Hidden charm and exotics

PANDA will be devoted to provide precision data for hadron spectroscopy with light to charm constituent quarks, and gluons. Given the anti-proton beam momentum range of up to 15 GeV, the accessible invariant-mass range in direct formation is about 2–5.5 GeV, and the PANDA experiment is thus designed and optimized to cover the charmonium mass region. In addition, the light quark sector can be explored via the production with recoil particles.

The cross sections associated with antiproton–proton annihilations are generally several orders of magnitude larger than those of experiments using electromagnetic probes, allowing for excellent statistical precision already at moderate luminosities available in the initial Phase One ($\sim 10^{31}$ cm$^{-2}s^{-1}$).

In the charmonium mass region, different unexpected charmonium-like states have been discovered since the beginning of the millenium. Some of these so-called XYZ states are electrically charged and in combination with the mass those are manifestly exotic states. They have unambiguously a minimum quark content of four quarks (e.g. $c\bar{c}d\bar{u}$) and are, among others, discussed to be tetraquark or molecular states in form of a loosely bound di-meson system. PANDA will contribute to solve the puzzle of the nature of these unexpected charmonium-like XYZ states. Moreover, there is a number of pentaquark states and other exotic candidates reported by LHCb recently that will be accessible with PANDA.

In order to understand the nature of the XYZ states, e.g. which of the different four-quark configurations are realized by nature, and to confirm further candidates reported, PANDA will play an unique role. The different multiplets need to be completed, especially the corresponding high-spin states. Those can uniquely be addressed by PANDA, since there is no restriction in produced J^{PC} quantum numbers in $\bar{p}p$ annihilation and thanks to the mostly 4π acceptance of the detector. Given the excellent electromagnetic calorimetry in the barrel as well as in the forward part of the detector, PANDA will have full acceptance not only for charged but also for neutral final-state particles.

Another crucial and unique tool are precision line-shape measurements. The energy-dependent resonance cross sections of these states are strongly connected with the inner structure of such states – theoretical interpretations come along with predictions for absolute decay widths and line shapes. The narrow and famous $X(3872)$, meanwhile renamed by the PDG to $\chi_{c1}(3872)$, was the first of these XYZ states discovered in 2003 [2514]. Its nature is still not understood.

As shown by a comprehensive Monte Carlo based feasibility study [4672], the line shape of narrow states, particularly the $X(3872)$, can be measured precisely and directly by PANDA with sub-MeV resolution, Fig. 415, allowing for sorting out models, Fig. 415, right. Thanks to the unprecedented beam momentum and energy resolution of the HESR of up to $\Delta p/p = 2 \times 10^{-5}$ and $\Delta E_{\text{cms}}/E_{\text{cms}} = 34$ keV, even very similar line-shape models can be discriminated by employing the technique of a resonance energy scan [4672].

At LHCb, it was not possible to distinguish between a Breit–Wigner and a Flatté-like line-shape for the $X(3872)$ even though huge statistics has been accumulated [2554]. This state cannot be produced in direct formation at LHCb, and the energy-scan technique cannot be employed. Consequently, the resolution of the measurement is dominated by the detector resolution (order of a few MeV) and the LHCb

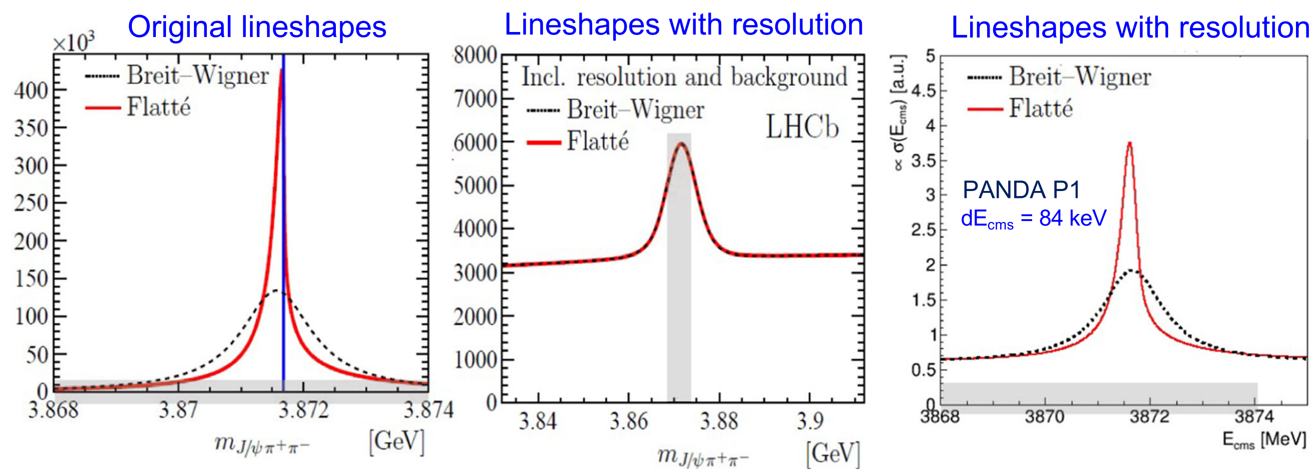

Fig. 416 Comparison of the Breit–Wigner and Flatté-like line shapes without and with the LHCb and PANDA resolutions convolved. Left: The two line shapes (Breit–Wigner vs. Flatté-like) obtained from the fit to the LHCb data [2554]. Center: The same two line shapes when including backgrounds and resolution, i.e. convolved with the detector resolution. Due to the resolution, the two line shapes are just indistinguishable based on the LHCb data [2554]. Right: The same two line shapes (Breit–Wigner vs. Flatté-like) convolved with the foreseen beam-energy resolution expected for the initial phase of the experiment. Thanks to the excellent beam energy resolution, they are well distinguishable with PANDA at HESR [4673]

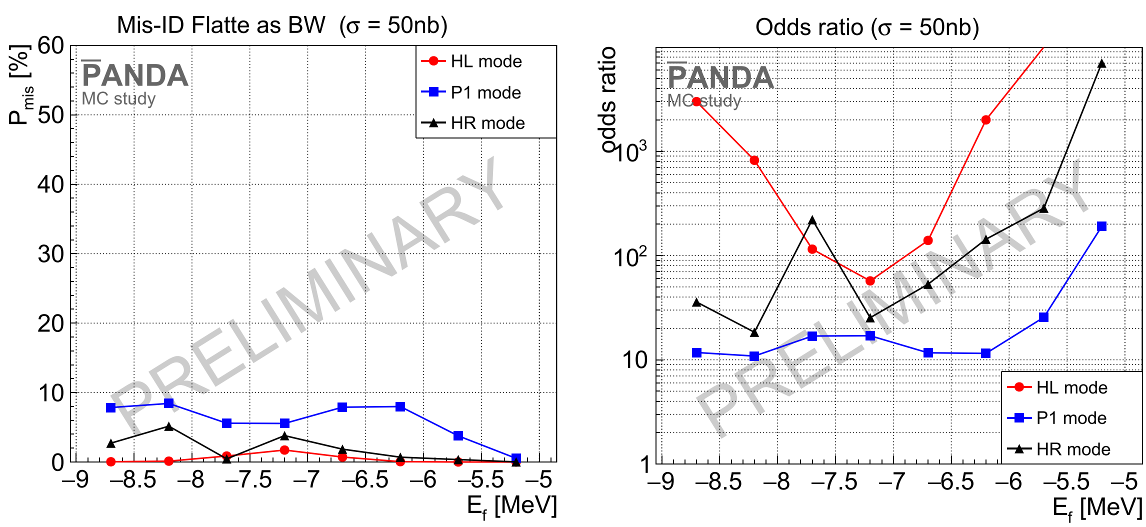

Fig. 417 Performances to distinguish between a Breit–Wigner and a Flatté-like line shape with PANDA/HESR at FAIR. Left: Sensitivity in terms of the mis-identification probability P_{mis} to wrongly assign the Breit–Wigner line shape instead of the correct Flatté-like line shape as a function of the Flatté energy parameter E_{f}, whereas $P_{\text{mis}} = 50\,\%$ corresponds to "indistinguishable". Right: The correspondingly computed so-called "odds", i.e. the number of correct assignments per wrong one, defined as $odds{:=}(1 - P_{\text{mis}})/P_{\text{mis}}$. Using this measure, the expected performance is at least ten times better than "indistinguishable", i.e. as it is achieved based on the LHCb data [2554], see also [4673]

data are equally well described using both line-shape models (Fig. 416).

As an addendum to the published sensitivity study [4672], the expected PANDA performance in distinguishing these two different line-shape models has been investigated and quantified [4673]. The achievable performance has been evaluated in terms of the mis-identification probability P_{mis} to assign the wrong line-shape model, namely the Breit–Wigner line shape for Monte Carlo data generated using a Flatté line shape, and vice versa. The outcome is summarized in Fig. 417, where the resultant sensitivities in assigning the correct line shape (shown here for the Flatté-like line shape) are better than 90% and 98%, depending on the given accelerator operation mode (Fig. 417, left). For this figure of merit, a mis-identification probability of $P_{\text{mis}} = 50\%$ corresponds to "indistinguishable". To answer the question, how much better the expected PANDA performance is as compared to "indistinguishable", one may consider the so-called "odds" defined as the number of correct assignments per wrong one: $odds := (1 - P_{\mathrm{mis}})/P_{\mathrm{mis}}$. The corresponding results are shown in Fig. 417 (right). Using this measure, PANDA is expected to be at least a factor of 10 better than "indistinguishable", a feature that is only possible due to the excellent beam-momentum resolution expected for PANDA and the direct formation of the X(3872) state in antiproton-proton annihilations.

Energy-dependent line shape measurements for $J^{PC} = 1^{--}$ states are also possible at BESIII. The beam energy resolution of about 1–2 MeV is due to initial state radiation, however, significantly worse as compared to PANDA ($\sim$50 keV). For non-vector states, such energy scans are possible in e^+e^- annihilation via two-photon fusion. The production cross section is, however, highly suppressed due to the two virtual photons to be produced.

Concerning the light-quark and gluon sector, PANDA will search for exotic forms of matter such as hybrid mesons and glueballs. In the mass range accessible at FAIR, a large number of glueballs is expected and some of them might be narrow. Their SU(3) structure can be determined from an analysis of their decay modes.

For light hybrid mesons, such as the $\pi_1(1400)$ and $\pi_1(1600)$, the most conclusive results so far have been provided by the COMPASS experiment at CERN/SPS, employing a 190 GeV pion beam, see e.g. [2324,2457,4674]. The GlueX photoproduction experiment has been under construction and is dedicated to map the full spectrum of hybrid mesons with masses of up to about 2.5 GeV. The findings by both of these experiments and others on hybrids as well as on non-exotic new light meson states, such as the [4675], will complementary be addressed in $\bar{p}p$ annihilation processes at PANDA. These kind of investigations will moreover be extended to the charmonium region, for which several glueball and hybrid states are predicted, e.g. a spin-exotic state at about 4.2 GeV [4676].

Presently, there is no experiment dedicated to glueballs. In comparison to glueball searches in J/ψ decays e.g. at BESIII, they are expected to be produced with orders of magnitude higher production rate in $\bar{p}p$ annihilation [4677]. In particular in the charm region, glueball candidates with masses above 4 GeV are predicted, some of which might be narrow and could thus be found. An analysis of their decay fraction could be used to decide if the state has a large glueball component.

Strangeness physics

With antiproton–proton annihilations and baryon number conservation, the final state has zero total baryon number. This feature has the advantage that relatively clean two-body final-state topologies may emerge involving exclusively a baryon together with its antibaryon. The maximum center-of-mass foreseen with PANDA amounts to 5.5 GeV which provides access to produce pairs of various hadrons including strange and charm quarks such as $\bar{p}p \to \Lambda\bar{\Lambda}$, $\Sigma\bar{\Sigma}$, $\Xi\bar{\Xi}$, $\Omega\bar{\Omega}$, $\Lambda_c\bar{\Lambda}_c$, $\Sigma_c\bar{\Sigma}_c$, $\Xi_c\bar{\Xi}_c$, $\Omega_c\bar{\Omega}_c$, together with various excited states of these hadrons. The production of these pairs has various benefits, namely (i) close to the appropriate production threshold, the identification and analysis of these reactions are fairly simple, since one may apply tagging methods, deal with limited number of partial waves, and with a good signal-to-background level; (ii) combined with the excellent momentum resolution of the initial antiproton beam, a near-threshold scan allows to determine basic properties, such as mass and width, of these states, and their excitations very accurately [4678]; (iii) the self-analyzing feature of the weak decays of these (anti)baryons can be exploited to study spin degrees-of-freedom of their production process. The latter feature is a powerful tool that can be used for various physics aspects ranging from particle physics (test CP conservation in the hyperon sector), spectroscopy studies (baryon resonances with strangeness), and spin physics (detailed study of hyperon production and interactions). In the following, we highlight two aspects that will be foreseen with PANDA, namely the spin-physics and hyperon-spectroscopy programs.

The spin-physics program of PANDA aims to measure accurately differential cross sections and spin observables such as polarization and spin correlations. These observables provide a deeper understanding of the spin production mechanisms or, more generally, of the dynamics that lead to the production of hyperons in antiproton proton collisions. Which effective degrees of freedom are adequate to describe the hadronic reaction dynamics: quarks and gluons or mesons and baryons? And how does this picture change with center-of-mass energy? The high production rates of hyperon and antihyperon pairs in combination with the excellent signal to background yield give perfect conditions to perform these measurements. Already with moderate initial luminosities, a spectacular production rate of hyperon and antihyperon pairs are to be expected. The reaction $\bar{p}p \to \Lambda\bar{\Lambda}$, with $\Lambda \to p\pi^-$ and $\bar{\Lambda} \to \bar{p}\pi^+$, was studied in detailed Monte Carlo simulations. At a luminosity of 10^{31} cm^{-2} s^{-1} and at an antiproton beam momentum of 1.64 GeV we expect 3.8×10^6 of fully reconstructed $\Lambda\bar{\Lambda}$ pairs per day. For strangeness $|S| = 2$ baryon pairs via $\bar{p}p \to \bar{\Xi}^+\Xi^-$ at a beam momentum of 4.6 GeV, the expected rate is about 2.6×10^4/day exclusively reconstructed pairs in the $\Xi^- \to \Lambda\pi^-$ and $\bar{\Xi}^+ \to \bar{\Lambda}\pi^+$ decay modes. Moreover, the signal-to-background ratio is estimated to be better than 100 (250) for the $\bar{\Lambda}\Lambda$ ($\bar{\Xi}^+\Xi^-$) channel. With the perspectives of PANDA to reach the high luminosity conditions at HESR at Phase Three, precision studies of hyperons with charm contents will become feasible and CP violation tests will become competitive [4679].

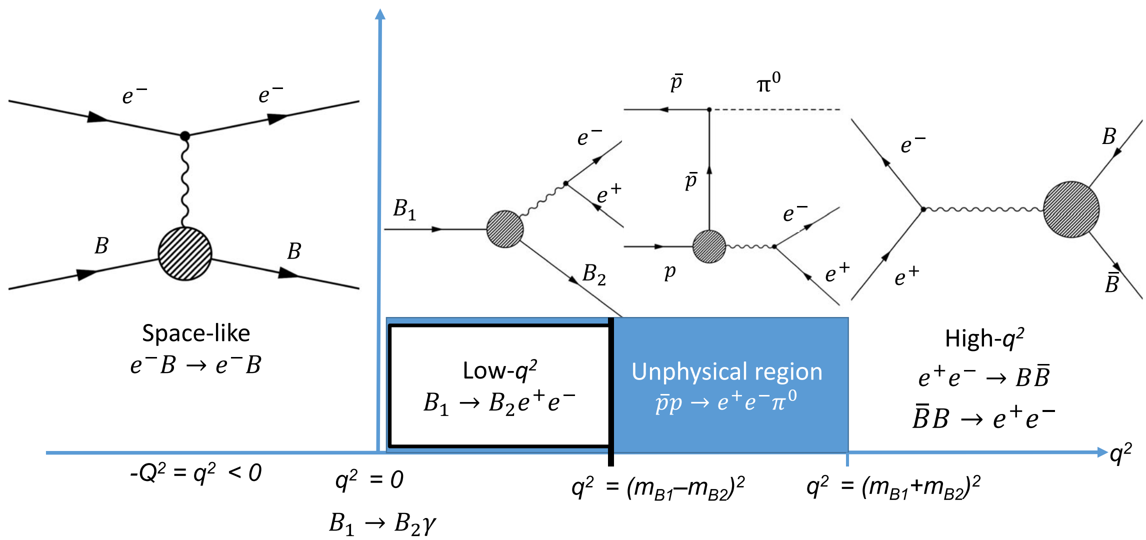

Fig. 418 The various processes that are used to extract information about the EMFF in the space-like ($q^2 < 0$) and time-like ($q^2 > 0$) regions. The time-like region $0 < q^2 < (M_{B1} - M_{B2})^2$) is studied by Dalitz decays. The so-called unphysical region ($4m_e^2 < q^2 < (M_{B1} + M_{B2})^2$) by $\bar{p}p \to \ell^+\ell^-\pi^0$ and the high-q^2 region ($q^2 > (M_{B1} + M_{B2})^2$) by $B\bar{B} \leftrightarrow e^+e^-$. Figure is taken from [2635]

PANDA's environment to produce abundantly pairs of hyperons and antihyperon is also the ideal setting to carry out detailed spectroscopy studies of these baryons. The underlying physics motivation is to understand the internal structure of baryons. For this purposes, baryon spectroscopy has demonstrated to be a very powerful tool. In the case of PANDA, the conceptual idea is to replace light valence quarks of the (anti)proton with heavier strange and charm ones via the processes sketches above, measure the excitation spectrum of excited hyperon states, determine their properties such as mass, width, spin, parity, and decay modes, and compare such observations between the various baryonic systems including those of the light-quark sector, i.e. N^* and Δ resonance levels. With these measurements some of the open questions will be addressed, such as (i) Which baryonic excitations are efficiently and well described in a three-quark picture and which are generated by coupled-channel effects of hadronic interactions? (ii) To which extent do the excitation spectra of baryons consisting of *u, d, s* obey SU(3) flavor symmetry? (iii) Are there exotic baryon states, e.g. pentaquarks or dibaryons? (iv) What is the role of diquark correlations inside baryons? (v) Can we understand the missing resonance phenomena and the observed level ordering in the light-quark baryon sector? PANDA has the potential to be the key player in providing conclusive data for the strangeness $|S| = 2, 3$ (anti)baryons thereby complementary to the future activities planned at J-PARC [4597] and the wealth of baryon spectroscopy data that have been obtained with photo- and pion-induced reactions at JLab, ELSA, MAMI, GRAAL, Spring-8, HADES, etc. As an illustration of the capabilities of PANDA to determine spin-parity assignment of excited Ξ^* states, we refer to the results of a preliminary feasible study described in [4680].

Nucleon structure

In the past 60 years, the structure of the proton has been extensively studied with great success exploiting lepton–hadron scattering (see Sect. 10). With the annihilation of antiproton with protons, it will be possible to extract electromagnetic form factors (EMFF) and structure functions of the (anti)proton in a region of phase space not accessible using electromagnetic probes.

EMFFs quantify the hadron structure as a function of the four-momentum transfer squared q^2 and are defined on the complex q^2 plane. Space-like EMFFs ($q^2 < 0$) are real functions of q^2 and have been studied extensively using elastic electron–hadron scattering. Time-like EMFFs are complex and will be studied at PANDA using different processes in various q^2 regions. Figure 418 sketches the various processes that can be exploited to study EMFFs for various q^2 regions. Here, B, B_1 and B_2 denote various baryons. With antiproton–proton annihilations, EMFFs of the (anti)proton will be probed for the q^2 range starting from the unphysical region, using the reaction $\bar{p}p \to e^+e^-\pi^0$, to high-q^2 via $\bar{p}p \to \ell^+\ell^-$ whereby ℓ refers to both electrons and muons. Detailed Monte Carlo simulations demonstrated that both G_E and G_M can be measured with a precision of about 3% in the e^+e^- final state at q^2 around 5 GeV and with a total integrated luminosity of 0.1 fb^{-1}, which is well suitable for the first years of data taking. Figure 419 depicts the present state-of-the-art of the $R = |G_E|/|G_M|$ measurements as a function of q^2 together with the precision perspectives of PANDA for the early phases of the experiment (green band) and for the high luminosity mode (purple band). PANDA will be able to harvest more precise form factor data compared to today's measurement and extend the measurements towards higher values of q^2 including, for the first time, both the di-electron and di-muon as probes. Being analytic functions of q^2, space-like and time-like form factors are related by dispersion theory. With the future data taken at PANDA and the various other complementary facilities, it will become feasibly to rigorously test the analyticity and universality of the measured EMFFs. Besides measuring the EMFFs of the (anti)proton, also transition form factors ($B_1 \neq B_2$) are accessible. With the copious production of hyperons and antihyperons in antiproton–proton collisions, PANDA will provide unique data to extract transition form factors of various hyperons and their corresponding antihyperons.

With PANDA operating at the highest beam energies, the partonic degrees of freedom at distances much smaller than the size of the proton can be studied via measurements of various structure functions. A key in such studies is the factorization theorem stating that the interaction can be factorized into a hard, reaction-specific but perturbative and hence calculable part and a soft, reaction-universal and measurable part. In the space-like region, probed by deep inelastic lepton–hadron scattering, the structure is described by parton distribution functions (PDFs), generalized parton distributions (GPDs), transverse-momentum-dependent parton distribution functions (TMDs), and transition distribution amplitudes (TDAs). These observables extend the information provided by EMFFs and give further insight in the spatial and momentum distributions of the constituent partons and the spin structure. With PANDA, the time-like counterpart becomes experimentally accessible via hard proton–antiproton annihilations. Detailed studies to access πN TDAs at PANDA in the reactions $\bar{p}p \rightarrow \gamma\pi^0 \rightarrow e^+e^-\pi^0$ and $\bar{p}p \rightarrow J/\Psi\pi^0 \rightarrow e^+e^-\pi^0$ can be found in [4681,4682]. For these measurements, as well as for the TMD studies, the designed high luminosity of PANDA is needed to accumulate reasonable statistics. The counterparts of the GPDs in the annihilation processes are the generalized distribution amplitudes (GDAs). They can be measured in the hard exclusive processes $\bar{p}p \rightarrow \gamma\gamma$ [4683] and $\bar{p}p \rightarrow \gamma M$ [4684,4685], where M could be a pseudo-scalar or vector meson (e.g. π^0, η, ρ^0, ϕ). Differential cross section measurements become already feasible to study with the Phase One luminosity of PANDA during the first years of data taking.

14.6 BESIII

Hai-Bo Li, Ryan Edward Mitchell, and Xiaorong Zhou

14.6.1 Introduction to the BESIII experiment

The BESIII collaboration, which operates the BESIII spectrometer (Fig. 420) at the Beijing Electron Positron Collider (BEPCII), uses e^+e^- collisions with center-of-mass (CM) energies ranging from 2.0 to 5.0 GeV to study the

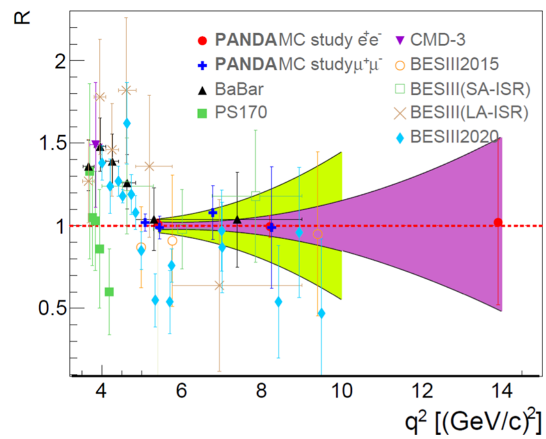

Fig. 419 The form factor ratio $R = |G_E|/|G_M|$ of the proton as function of the square of the four momentum, q^2. The data are from PS170 [4686], BaBar [4687,4688], BESIII [4689–4692], CMD-3 [4693]. The expected precisions of PANDA for the e^+e^- final state are indicated as shaded areas for Phase One corresponding to an integrated luminosity of 0.1 fb^{-1} (green band) and for Phase Three with an integrated luminosity of 2 fb^{-1} (purple band and red filled circles). Also shown are the expected performances for the di-muon channel for Phase Three (dark blue crosses)

broad spectrum of physics accessible in the tau-charm energy region. Since the start of operations in 2009, BESIII has collected more than 40 fb^{-1} of data, comprising several world-leading data samples, including:

- 10 billion J/ψ decays, giving unprecedented access to the light hadron spectrum;
- 2.7 billion $\psi(2S)$ decays, allowing precision studies of charmonium and its transitions;
- targeted data samples above 4 GeV, providing unique access to exotic XYZ hadrons;
- 8.6 fb^{-1} of data at the $\psi(3770)$ mass, providing a large sample of D decays and quantum-correlated $D^0\bar{D}^0$ pairs, crucial for global flavor physics efforts;
- 3 fb^{-1} at 4.18 GeV, near the peak of the $D_s^{\pm}D_s^{*\mp}$ cross section, for D_s studies;
- more than 3 fb^{-1} above $\Lambda_c\bar{\Lambda}_c$ threshold for precision Λ_c studies; and
- fine-scan samples for measurements of R, the mass of the τ, and electromagnetic form factors.

The program will continue for at least the next 5–10 years, building on the data sets already collected, and ensuring the BESIII collaboration will remain a key player in future global efforts in hadron spectroscopy, flavor physics, and searches for new physics. The maximum energy of BEPCII will soon be upgraded to 5.6 GeV, and there are plans to more than double the BEPCII luminosity at high CM energies by increasing the maximum achievable beam currents. Below we briefly outline a few highlights from BESIII, how these achieve-

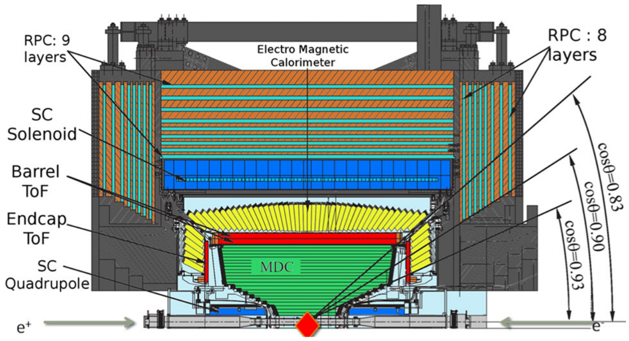

Fig. 420 Schematic view of the BESIII detector, covering 93% of the 4π solid angle. It consists of a Helium-gas based drift chamber, a Time-of-Flight system, a CsI(Tl) crystal calorimeter and a 9-layer RPC-based muon chamber. Figure taken from the official BESIII website

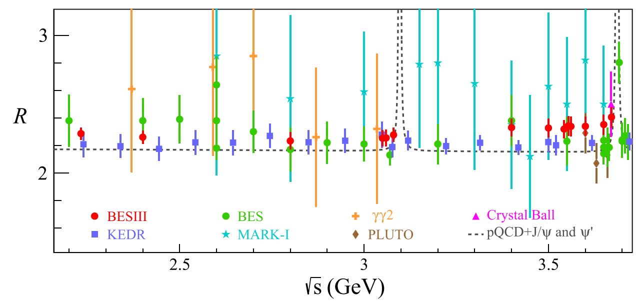

Fig. 421 Comparison of R values in the CM energy from 2.2 to 3.7 GeV. Figure taken from Ref. [4695]

ments have contributed to global physics efforts, and how the next era at BESIII will build on this momentum. More details and references can be found in a recent white paper describing the future physics program at BESIII [2634] and in a recent contribution to the 2021 Snowmass process [4694].

14.6.2 The BEPCII-U upgrade

BEPCII delivered its first physics data in 2009 on the $\psi(2S)$ resonance. Since then, BESIII has collected more than 40 fb^{-1} of integrated luminosity at different CM energies from 2.0 to 4.95 GeV. In order to extend the physics potential of BESIII, two upgrade plans for BEPCII were proposed and approved in 2020. The first upgrade will increase the maximum beam energy to 2.8 GeV (corresponding to a CM energy of 5.6 GeV), which will expand the energy reach of the collider into new territory. The second upgrade will increase the peak luminosity by a factor of 3 for beam energies from 2.0 to 2.8 GeV (CM energies from 4.0 to 5.6 GeV).

To perform these upgrades, BEPCII will increase the beam current and suppress bunch lengthening, which will require higher RF voltage. The RF, cryogenic, and feedback systems will be upgraded accordingly. Nearly all of the photon absorbers along the ring and some vacuum chambers will also be replaced in order to protect the machine from the heat of synchrotron radiation. The budget is estimated to be about 200 million CNY and it will take about 3 years to prepare the upgraded components and half a year for installation and commissioning, which will start in June 2024 and finish in December 2024. With these upgrades, BESIII will enhance its capabilities to explore XYZ physics and will have the unique ability to perform precision measurements of the production and decays of charmed mesons and baryons at threshold.

14.6.3 Hadronic production: via direct e^+e^- annihilation

Precision measurements of hadron production help make QCD-related models more reliable and help test SM parameters with an unprecedented sensitivity. BESIII has advanced our knowledge of hadron production using both inclusive and exclusive approaches, mainly via direct production in e^+e^- collisions.

R value measurement
The R ratio, defined as the lowest-order cross section for inclusive hadron production, $e^+e^- \to hadrons$, normalized by the lowest-order cross section for the QED process $e^+e^- \to \mu^+\mu^-$, is a central quantity in particle physics. Precision measurements of the R ratio below 5 GeV contribute to the SM prediction of the muon anomalous magnetic moment. The R ratio also contributes in the determination of the QED running coupling constant evaluated at the Z pole. In a first measurement at BESIII [4695], 14 data points with CM energies from 2.2324 to 3.6710 GeV are used for the inclusive R value measurement. An accuracy of better than 2.6% below 3.1 GeV and 3.0% above is achieved in the R ratios, as shown in Fig. 421. Previous results had uncertainties at the level of 3–6%. The average R value in the CM range from 3.4 to 3.6 GeV obtained by BESIII is larger than the corresponding KEDR result and the theoretical expectation by 1.9 and 2.7 standard deviations, respectively.

The complete data set for the R value measurement at BESIII consists in a total of 130 energy points with an integrated luminosity of about 1300 pb^{-1}, corresponding to more than 10^5 hadronic events at each of the points between 2 and 4.6 GeV. Thus, the final result is expected to be dominated by a systematic uncertainty of less than 3%.

Fragmentation functions
Fragmentation functions describe the probability of finding a given hadron within the fragmentation of a quark, and carrying a given fraction of the quark momentum. Precise knowledge of fragmentation functions are essential ingredients for studies of the internal structure of the nucleon as carried out by semi-inclusive deep inelastic scattering (SIDIS) exper-

iments (e.g. at a future Electron-Ion Collider). At BESIII, using data collected in the continuum energy region, unpolarized fragmentation functions are extracted from inclusive hadron production processes $e^+e^- \rightarrow h + X$, where h denotes π^0, η, K_S, or charged hadrons. Polarized fragmentation functions, i.e. the Collins effects, have been obtained by BESIII using pairs of pions produced at $\sqrt{s} = 3.65\,\mathrm{GeV}$ [4696]. In the future, the Collins effect for strange quarks could be studied in $e^+e^- \rightarrow \pi K + X$ and $e^+e^- \rightarrow KK + X$. It is also interesting to study the Collins effect in neutral hadrons like $e^+e^- \rightarrow PP' + X$ with $P/P' = \pi^0/\eta$.

Exclusive cross section measurements using initial state radiation

The dispersive integral formalism used to determine the HVP contribution to a_μ relies heavily on the hadronic e^+e^- cross sections at CM energies $\sqrt{s} \leq 2\,\mathrm{GeV}$. At BESIII, these energies are only accessible by exploiting the initial state radiation (ISR) method. With an initial data set of $2.83\,\mathrm{fb}^{-1}$ at $\sqrt{s} = 3.773\,\mathrm{GeV}$, this technique already produces results competitive with the B-factories for hadronic masses above approximately 1.3 GeV.

In a first measurement by BESIII, the largest hadronic cross section, for $e^+e^- \rightarrow \pi^+\pi^-$, was measured in the mass region from 600 to 900 MeV by reconstructing the ISR photon at large angles only [4298]. With $20\,\mathrm{fb}^{-1}$ of data at $\sqrt{s} = 3.773\,\mathrm{GeV}$ expected soon, a new measurement of the $\pi^+\pi^-$ cross section will use the improved statistical accuracy to implement an alternative normalization scheme relative to the muon yield. With this approach, the largest uncertainties will cancel, bringing the expected final uncertainty down to 0.5%, as illustrated in Fig. 422. Additionally, the multi-meson cross sections for $e^+e^- \rightarrow \pi^+\pi^-\pi^0$ as well as $e^+e^- \rightarrow \pi^+\pi^-\pi^0\pi^0$ have been measured using the same analysis strategy. Uncertainties of approximately 3% were achieved. These cross sections can be used to study resonances in the final state as well as in the intermediate states. Further improvements are expected with additional data at $\sqrt{s} = 3.773\,\mathrm{GeV}$.

Meson transition form factors

Transition form factors (TFF) of mesons M describe the effects of the strong interaction on the $\gamma^*\gamma^*M$ vertex. At BESIII, TFFs are studied in the region of time-like virtualities through meson Dalitz decays and radiative meson production in e^+e^- annihilations. Space-like virtualities are studied in two-photon fusion reactions, which in principle give access to TFFs over a wide range of virtualities by measuring the momentum transfer of the scattered electrons. Due to the rapid drop of the cross section with $Q_i^2 = -q_i^2$, BESIII currently uses single-tagged measurements, where the TFF is only studied depending on one of the virtualities.

A first measurement of the π^0 TFF based on $2.83\,\mathrm{fb}^{-1}$ of data at $\sqrt{s} = 3.773\,\mathrm{GeV}$ covers virtualities from $0.3\,\mathrm{GeV}^2$ to $3.1\,\mathrm{Gev}^2$. The results confirm the recent calculations in dispersion theory and on the lattice. Analogous studies are performed for η and η' mesons, and also for multi-meson systems. The production of charged and neutral two-pion systems in two-photon fusion gives access to pion masses from threshold to 2 GeV and virtualities from $0.2\,\mathrm{GeV}^2$ to $3\,\mathrm{GeV}^2$ at a full coverage of the pion helicity angle. The results will be complementary to all previous measurements, which have mostly been performed with quasi-real photons. The production of higher meson multiplicities in two-photon fusion allows access to scalar, tensor and axial resonances. The single-tagged strategy allows for the production of axial mesons due to the presence of a highly virtual photon. A first measurement of the $f_1(1285)$ will be performed using the $\pi^+\pi^-\eta$ final state for reconstruction. With the upcoming data set of $20\,\mathrm{fb}^{-1}$ at $\sqrt{s} = 3.773\,\mathrm{GeV}$ all two-photon fusion analysis will benefit from higher statistics, which will be sensitive to higher virtualities.

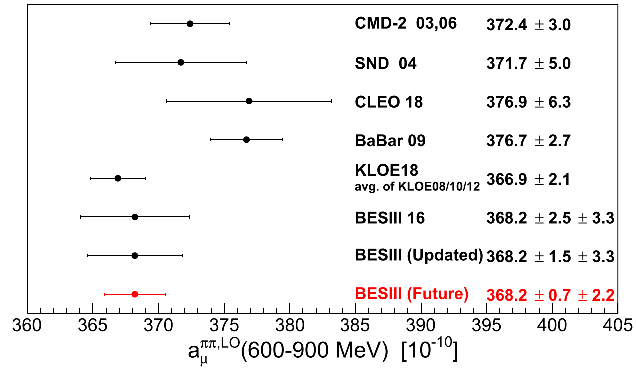

Fig. 422 Comparison of the leading-order hadronic vacuum polarization contribution to $(g-2)_\mu$ due to $\pi^+\pi^-$ in the energy range 600–900 MeV from various experiments and the prospect result with $20\,\mathrm{fb}^{-1}$ of data at $\sqrt{s} = 3.773\,\mathrm{GeV}$ at BESIII. Figure modified according to Ref. [4298]

Time-like baryon electromagnetic form factors

At BESIII, the $|G_E/G_M|$ of the proton in the time-like region is determined over a large q^2 from threshold to $9.5\,\mathrm{GeV}^2$ with the best precision reaching 3.7% [4690]. With more data samples collected, the form factor ratio of proton will be obtained in a wide q^2 region from 10 to $20\,\mathrm{GeV}^2$, similar to the q^2 region from the PANDA expectation. The cross section of $e^+e^- \rightarrow n\bar{n}$ [4697] is found to be smaller than that of $e^+e^- \rightarrow p\bar{p}$. The effective FFs of the neutron show a periodic behavior, similar to earlier observations of proton FFs reported by BaBar. The energy region of BESIII covers the production threshold of all SU(3) octet hyperons and several charmed baryons. At BESIII, the Born cross sections of electron–positron annihilation to various baryon pairs are measured from threshold [4698], including $\Lambda\bar{\Lambda}$, $\Sigma\bar{\Sigma}$, $\Xi\bar{\Xi}$ and $\Lambda_c\bar{\Lambda}_c^+$. Obvious threshold effects are observed. The $|G_E/G_M|$ of the Λ, Σ^+, and Λ_c are obtained from angular analyses while effective FFs are extracted for other baryons. More precise data or finer scans are necessary for deeper insight into these results. The hyperon EMFFs and the cross section line shapes can also be studied with improved precision via ISR approaches with a 20 fb^{-1} data set collected at $\sqrt{s} = 3.773$ GeV.

The EMFFs in the time-like region are complex and the relative phase between G_E and G_M will lead to the transverse polarization of the final baryons. At BESIII, the relative phase of the Λ is determined at $\sqrt{s} = 2.396$ GeV with a joint angular distribution analysis, to be $\Delta\Phi = 37° \pm 12° \pm 6°$ [4699]. Combining with the obtained $|G_E/G_M|$ at the same CM energy, the complete EMFFs are determined for the first time. Similarly, the relative phase of the Λ_c is determined at $\sqrt{s} = 4.60$ GeV [4700]. The currently available data set from $\sqrt{s} = 4.6$ to 4.95 GeV will help complete determinations of Λ_c EMFFs in a wide q^2 range. As the energy dependence of the relative phase is essential for distinguishing various theoretical predictions, a complete determination of EMFFs for SU(3) octet hyperons are necessary in the future.

Precision measurement of the τ mass
The τ lepton is one of three charged elementary leptons in nature, and its mass is an important parameter of the Standard Model. The τ mass can and should be provided by experiment precisely. Precision τ mass measurements probe lepton universality, which is a basic ingredient in the Standard Model.

To aid in the τ mass measurement, a high-accuracy beam energy measurement system (BEMS), located at the north crossing point of BEPCII, was designed, constructed, and finally commissioned at the end of 2010. By comparing a $\psi(2S)$ scan result with the PDG value of the $\psi(2S)$ mass, the relative accuracy of the BEMS was determined to be at the level of 2×10^{-5} [4701]. The BESIII collaboration performed a fine mass scan experiment in the spring of 2018. The τ mass scan data were collected at five scan points near the τ pair production threshold with total luminosity of 137 pb^{-1}. The analysis is in progress. The uncertainty, including statistical and systematic error, will be less than 0.1 MeV.

14.6.4 Hadron spectroscopy: from light to heavy

Light hadron physics
QCD allows for a richer meson spectrum than the conventional quark model predicts, including tetraquark states, mesonic molecules, hybrid mesons and glueballs.

Lattice QCD predicts the lightest glueballs to be scalar, tensor and pseudo-scalar, allowing mixing with the conventional mesons of the same quantum numbers. Generally, glueballs are expected to be produced in gluon-rich processes such as radiative J/ψ decays, so that the high-statistics J/ψ sample puts BESIII in a unique position to study glueball candidates. Partial wave analyses (PWA) of the radiative decays $J/\psi \to \gamma\pi^0\pi^0, \gamma K_S^0 K_S^0$ and $\gamma\eta\eta$ reveal a strong production of the $f_0(1710)$ and $f_0(2100)$ [4702]. One might speculate that these resonances have a large gluonic component. Similarly, the tensor meson $f_2(2340)$ is strongly produced in the radiative decays $J/\psi \to \gamma\eta\eta$ and $\gamma\phi\phi$ [4702], rendering it a good candidate for a tensor glueball. Two recent coupled channel analyses [2493,2494] of BESIII data on radiative J/ψ decays came to different conclusions concerning the number of contributing resonances and the identification of a glueball candidate, so that additional studies using the full 10 billion J/ψ data sample will be of high importance in the future.

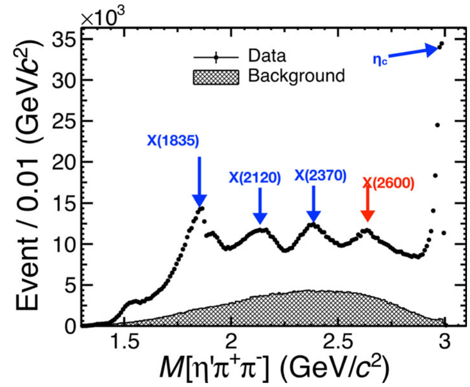

Fig. 423 The invariant mass spectrum of the final state $\pi^+\pi^-\eta'$ for $J/\psi \to \gamma\pi^+\pi^-\eta'$ candidates. A series of new particles are observed including $X(1835)$, $X(2100)$, $X(2370)$ and $X(2600)$. Figure taken from Ref. [4704]

Based on 10 billion J/ψ events, the decay $J/\psi \to \gamma f_0(1500) \to \gamma\eta\eta'$ has been observed with a significance over 30σ while $J/\psi \to \gamma f_0(1710) \to \gamma\eta\eta'$ is found to be insignificant [2461,2462]. The suppressed decay rate of the $f_0(1710)$ into $\eta\eta'$ lends further support to the hypothesis that $f_0(1710)$ has a large overlap with the ground state scalar glueball [4703].

In the search for the pseudo-scalar glueball, the decay $J/\psi \to \gamma\eta'\pi^+\pi^-$ has proven to be particularly interesting [4702]. Here, the $X(1835)$ can be observed with a lineshape that appears to be distorted at the proton anti-proton threshold, indicating a potential $p\bar{p}$ bound-state or resonance. In addition, the higher mass structures $X(2120)$, $X(2370)$ and $X(2600)$ are observed, as shown in Fig. 423, although their spin-parity remains to be determined, a task that will be possible using the new, high precision J/ψ data.

Motivated by multiple studies of the hybrid meson candidate $\pi_1(1600)$, a recent search for the isoscalar partner states η_1 and η_1' in the radiative decays $J/\psi \to \gamma\eta\eta'$ revealed a significant contribution from a new structure $\eta_1(1855)$ with exotic quantum numbers $J^{PC} = 1^{-+}$ [2461,2462]. While it is too early to say whether the $\eta_1(1855)$ is indeed an isoscalar hybrid meson, future studies of alternative decay modes will help reveal its nature.

The light scalar mesons $f_0(980)$ and $a_0(980)$ are frequently discussed as potential multiquark candidates, either as $K\bar{K}$ molecules or as compact tetraquark states. One possible way to probe their structure is the study of $f_0(980)$–$a_0(980)$ mixing first observed by BESIII in the isospin-violating processes $J/\psi \to \phi a_0^0(980)$ and $\chi_{c1} \to \pi^0 f_0(980)$ [4702]. These results provide constraints in the development of theoretical models concerning the $f_0(980)$ and $a_0(980)$.

With 10 billion J/ψ decays and the newly acquired 2.7 billion $\psi(2S)$, precision studies of conventional and exotic mesons, including multiquark states, glueballs and hybrid mesons, in radiative and hadronic J/ψ, $\psi(2S)$ and χ_{cJ} decays will be key tasks in the coming years.

Light baryon spectroscopy

The high production rate of baryons in charmonium decays, combined with the large data samples of J/ψ and $\psi(2S)$ decays produced from e^+e^- annihilations, provides excellent opportunities for studying excited baryons. Therefore, the BES experiment launched a program to study the excited baryon spectrum. At present, the search for hyperon resonances remains an important challenge. Some of the lowest excitation resonances have not yet been experimentally resolved, which are necessary to establish the spectral pattern of hyperon resonances. The large data samples of J/ψ and $\psi(2S)$ decays accumulated by the BESIII experiment enable us to complete the hyperon (e.g., Λ^*, Σ^* and Ξ^*) spectrum and examine various pictures for their internal structures. Such pictures include a simple $3q$ quark structure or a more complicated structure with pentaquark components dominating. In particular, $\psi(2S)$ decays, because of the larger mass of the $\psi(2S)$, have great potential to uncover new higher excitations of hyperons.

At BESIII, 10^{10} J/ψ and 2.7×10^9 $\psi(2S)$ decays are now available, which offer great additional opportunities for investigating baryon spectroscopy. Together with other high-precision experiments, such as GlueX and JPARC, these very abundant and clean event samples will bring the study of baryon spectroscopy into a new era, and will make significant contributions to our understanding of hadron physics in the non-perturbative regime.

Charmonium physics

Below the open-charm threshold, the spin-triplet charmonium states are produced copiously in e^+e^- annihilation and in B decays so they are understood much better than the spin-singlet charmonium states, including the lowest lying S-wave state η_c, its radial excited partner $\eta_c(2S)$, and the P-wave spin-singlet state h_c. The 2.7 billion $\psi(2S)$ decays at BESIII make it possible to study the properties of these states with improved precision. In addition, the unexpectedly large production cross section for $e^+e^- \to \pi^+\pi^- h_c$ in the BESIII high-energy region provides a new mechanism for studying the h_c and η_c (from $h_c \to \gamma\eta_c$).

The coupling of vector charmonium states to the open-charm meson pairs will provide crucial information in identifying the states in this region. The hadronic and radiative transitions between the (excited) charmonium states can be investigated to study the transition rates and decay dynamics. The cross section of $e^+e^- \to \eta J/\psi$ [4705] shows an enhancement around the $\psi(4040)$ mass, while the cross sections of $e^+e^- \to \pi^+\pi^-\psi(3770)$ [4706] and $e^+e^- \to \pi^+\pi^-\psi_2(3823)$ [4707] show an enhancement around the $\psi(4415)$ mass. The process $e^+e^- \to \gamma\chi_{cJ}$ is studied to search for radiative transitions between the excited vector charmonium states and the χ_{cJ} [4708]. Whether they are produced via hadronic transitions from the excited vector charmonium states or via vector charmonium-like states is not yet clear and can be addressed using improved luminosity and more decay channels.

Using the $e^+e^- \to \pi^+\pi^-\psi_2(3823)$ process, the most precise mass of the $\psi_2(3823)$ has been determined [4707] and new decay modes of the $\psi_2(3823)$ have been searched for [4709]. These recent measurements at BESIII are examples that the transitions between charmonium states can also serve as production sources of non-vector charmonium states, and can be used to study the properties (mass, width and decay modes) of non-vector charmonium states. They will also be important study topics in the future at BESIII.

With a dedicated data sample taken in the χ_{c1} mass region, the direct production of the C-even resonance, χ_{c1}, in e^+e^- annihilation is observed for the first time with a statistical significance larger than 5σ [4710]. A typical interference pattern around the χ_{c1} mass is observed as shown in Fig. 424. The electronic width of the χ_{c1} has been determined for the first time from a common fit to the four scan samples to be $\Gamma_{ee} = (0.12^{+0.13}_{-0.08})$ eV, in contrast of a few keV for vector states, which is 4 orders of magnitude smaller. This observation proves that the direct production of C-even resonances through two virtual photons is accessible and measurable at the current generation of electron–positron colliders.

XYZ physics

The discovery of the XYZ states has revolutionized traditional studies of the charmonium spectrum [4711]. These exotic states cannot be embedded in the conventional charm-anticharm potential model framework, but instead point towards novel quark configurations, such as tetraquarks, hybrids, or hadronic molecules. Studying them opens a new window into nonperturbative QCD, which underlies the formation of hadrons via the strong interaction. The existence of the XYZ states poses several problems, which are addressed as the “Y problem”, “Z problem”, and “X problem” below.

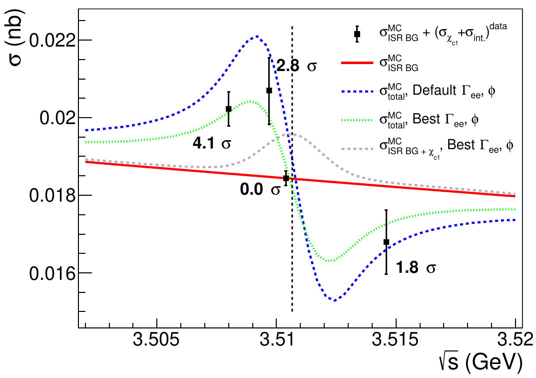

Fig. 424 The energy-dependent cross sections of $e^+e^- \to \gamma J/\psi \to \gamma\mu^+\mu^-$ including (blue and green curves) and not including (red curve) the signal process $e^+e^- \to \chi_{c1}(1P)$. The gray curve denotes the signal strength in the hypothetical case of no interference. The black dots with error bars are measured results from data. Figure taken from Ref. [4710]

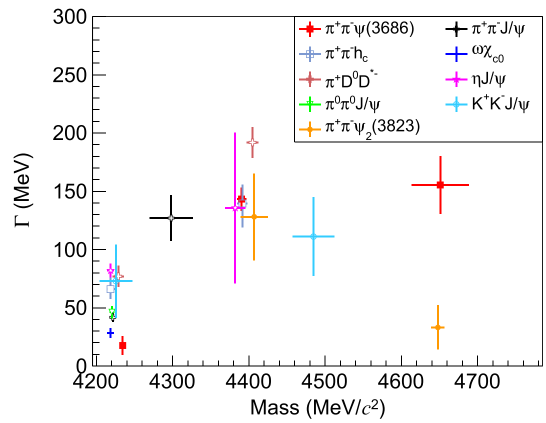

Fig. 425 Masses versus widths of the Y states obtained from different processes at BESIII. Figure modified according to Ref. [4712]

The Y problem

BESIII has systematically measured the cross sections of various exclusive e^+e^- annihilations with hidden charm, open charm, and light hadronic final states [4711], and has shown that the lineshapes are complicated as a function of CM energy. The masses and widths of various structures appearing in these cross sections are shown in Fig. 425. However, the extracted parameters of these Y states are not consistent with each other in different channels. Furthermore, they deviate from the resonances observed in inclusive channels, such as the $\psi(4040)$, $\psi(4160)$, and $\psi(4415)$, that are believed to be conventional charmonia. This leads to the Y problem. What are the exact lineshapes of these cross sections? Are these observed structures new resonances or just results of some subtle kinematic effects? To address these issues, a detailed scan between 4.0 and 4.6 GeV is proposed [2634], with 500 pb^{-1} per point, for points spaced at 10 MeV intervals. This target has been partially achieved with about 22 fb^{-1} integrated luminosity, and will be updated with larger maximum energy (5.6 GeV) after the upgrade of the BEPCII.

The Z problem

The $Z_c(3900)$ [4711] was discovered at BESIII in the process $e^+e^- \to \pi^\mp Z_c^\pm$ with $Z_c^\pm \to \pi^\pm J/\psi$, and the $Z_c(4020)$ was discovered in the process $e^+e^- \to \pi^\mp Z_c^\pm$ with $Z_c^\pm \to \pi^\pm h_c$. The $Z_c(3900)$ has also been observed in the open-charm channel $(D\bar{D}^* + c.c.)^\pm$, similarly the $Z_c(4020)$ was seen via the open-charm channel $(D^*\bar{D}^*)^\pm$. Furthermore, neutral partners of these charged Z_c states have been observed at BESIII via processes $e^+e^- \to \pi^0\pi^0 J/\psi$ and $e^+e^- \to \pi^0\pi^0 h_c$. BESIII has also determined the quantum numbers of the $Z_c(3900)$ to be $J^P = 1^+$. Recently, BESIII has observed a new near-threshold structure in the K^+ recoil-mass spectra in $e^+e^- \to K^+(D_s^- D^{*0} + D_s^{*-} D^0)$ [2568]. This structure, named $Z_{cs}(3985)$, is a good candidate for a charged hidden-charm tetraquark with strangeness. Besides, the evidence for its neutral partner, $Z_{cs}(3985)^0$ is observed via $e^+e^- \to K_S(D_s^+ D^{*-} + D_s^{*+} D^-)$ [4713].

However, at the energy region higher than 4.3 GeV the data have revealed more complex structure in the Daliz plots of $e^+e^- \to \pi^+\pi^- J/\psi$. A similar situation is found in the $e^+e^- \to \pi^+\pi^-\psi(2S)$ [4714]. This is the Z problem. Are the properties of these Z_c states constant (corresponding to real resonant states) or energy dependent (corresponding to kinematic effects such as cusps or singularities)? What are the exact lineshapes of them? Can we find more decay patterns for them, especially for the newly discovered Z_{cs} states? Are there spin multiplets of these Z_c states? To answer these questions, BESIII may take advantage of the fine scan data mentioned before, but at a few points, a set of samples with very high statistics will be very helpful. BESIII currently has 1 fb^{-1} of data for e^+e^- cms energy at 4.23 and 4.42 GeV. Additional data including three or four points with an order of 5 fb^{-1} or more per point is proposed to guarantee adequate statistics for amplitude analyses [2634]. After the upgrade of BEPCII with triple the luminosity, this goal will be achieved more easily.

The X problem

For the $X(3872)$, BESIII has discovered the process $e^+e^- \to \gamma X(3872)$, studied the open-charm decay and radiative transitions of the $X(3872)$, and has observed the hadronic transitions $X(3872) \to \pi^0\chi_{c1}(1P)$ and $X(3872) \to \omega J/\psi$ [4711]. The $X(3872)$, with its quantum numbers $J^{PC} = 1^{++}$, has a mass very close to the predicted $\chi_{c1}(2P)$ state with a very narrow width. Then the X problem is finding a way to separate the $X(3872)$ from the $\chi_{c1}(2P)$. Is the $X(3872)$ really exotic or conventional, or even a mixture state? Can we measure the line shape of the $X(3872)$? Are there other X states (for example close to the $D^*\bar{D}^*$ threshold) that have not been observed yet? The related studies will benefit from the large scan and other data samples mentioned before. The measurement of $X(3872)$ lineshape could be improved by performing the simultaneous fit of the available observed channels at BESIII, i.e. $X(3872) \to \pi^+\pi^- J/\psi$ and $X(3872) \to D^0\bar{D}^0\pi^0$, taking into account the coupled-channel effect. Furthermore, at $E_{cm} > 4.7$ GeV with highly excited ψ or Y states produced, the hadronic transitions, that take larger production rates than the radiative transitions, are accessible. After the upgrade of BEPCII to its maximum CM energy, BESIII will have the ability to search for the J^{++} states via hadronic transitions such as the processes $e^+e^- \to \omega X$ and $e^+e^- \to \phi X$.

Relationships
There are two kinds of relationships that deserve discussion. One is the relationship between XYZ states and conventional charmonia. For example, the $\chi_{c1}(2P)$ has a similar mass and the same J^{PC} as the $X(3872)$. So a detailed understanding of the spectrum of the conventional $2P$ charmonium states, that include the spin triplet $\chi_{cJ}(2P)$ and singlet $h_c(2P)$, is crucial for understanding the nature of the $X(3872)$. This is also true for the other conventional charmonia and XYZ states under similar conditions. The studies of the conventional charmonia and exotic XYZ are complementary to each other. Understanding the relations between the two kinds of states, even the possible mixing between them, will be helpful for understanding the properties of the XYZ states. The other relationship is among the XYZ states. The analyses of processes $e^+e^- \to \gamma X(3872)$ and $e^+e^- \to \pi^0\pi^0 J/\psi$ have already shown that there is evidence for the radiative transition $Y(4230) \to \gamma X(3872)$ and the hadronic transition [4711]

$$Y(4230) \to \pi^0 Z_c^0(3900).$$

Searching for new transition modes and confirming these relations may be a unique chance for BESIII to reveal the nature of the internal structure of the XYZ states [4715].

Pentaquark states
The LHCb experiment reported the observation of three pentaquark states with a $c\bar{c}$ component in the $J/\psi p$ system via $\Lambda_b^0 \to J/\psi K^- p$. To confirm these states, further experimental research should be pursued with the current available and the forthcoming experimental data [4716]. BESIII may search for such and similar states with data to be collected at CM energies above 5 GeV in the processes $e^+e^- \to J/\psi p + X$, $\chi_{cJ} p + X$, $J/\psi \Lambda + X$, $\bar{D}^{(*)} p + X$, $D^{(*)} p + X$, and so on. It is clear that a systematic search for baryon-meson resonances should be pursed in various processes, where the baryon could be p, Λ, Σ, Σ_c, ..., and the meson could be η_c, J/ψ, χ_{cJ}, $D^{(*)}$, etc. It is worth pointing out that the tetraquark and pentaquark candidates mentioned above have a pair of charm-anticharm quarks which may annihilate. Observations of states like T_{cc}^+ $(cc\overline{ud})$ or Θ_c^0 $(uudd\bar{c})$ or P_{cc}^0 $(ccdd\bar{u})$ or similar serve as more direct evidence for multiquark states. The BES experiment pioneered a search for the pentaquark candidate $\Theta(1540)$ in $\psi(2S)$ and J/ψ decays to $K_S p K^- \bar{n}$ and $K_S p K^+ n$ [4717]. More attempts will be performed with 10 billion J/ψ and 3 billion $\psi(2S)$ at BESIII.

14.6.5 Hadron decay: from light to heavy

Light meson decays
The η and η' mesons, the neutral members of the ground state pseudoscalar nonet, are important for understanding low energy quantum QCD [4718]. The 10 billion J/ψ events collected at BESIII offer an unique opportunity to investigate all these aspects, as well as the search for rare η and η' decays needed to test fundamental QCD symmetries and probe physics beyond the SM. The decays $J/\psi \to \gamma\eta(\eta')$ and $J/\psi \to \phi\eta(\eta')$ provide clean and efficient sources of η/η' mesons for the decay studies.

The observation of new η' decay modes [4719], including $\eta' \to \rho^{\mp}\pi^{\pm}$, $\eta' \to \gamma e^+e^-$, and $\eta' \to 4\pi$ have been reported for the first time using about 10^9 J/ψ decays. Using the same data set, the branching fractions of the five dominant decay channels of the η' were measured for the first time using events in which the radiative photon converts to e^+e^-.

The double Dalitz decay $\eta' \to e^+e^+e^-e^-$ is of great interest for understanding the pseudoscalar transition form factor and the interaction between pseudoscalar and virtual photons. This process has not been observed to date, while the predicted branching fraction is of the order of 2×10^{-6} [4720,4721]. Another interesting study is the hadronic decay $\eta' \to \pi^0\pi^0\eta$ which is sensitive to the elastic $\pi\pi$ S-wave scattering lengths, and causes a prominent cusp effect in the $\pi^0\pi^0$ invariant mass spectrum at the $\pi^+\pi^-$ mass threshold [4722]. The full J/ψ data set collected by BESIII offers unique opportunities to investigate the cusp effect in this decay for which no evidence has yet been found.

The absolute branching fraction of the decay $J/\psi \to \gamma\eta$ has been measured with high precision using radiative photon conversions [4719], and the four dominant η decays have been measured for the first time. The $\eta/\eta' \to \gamma\pi^+\pi^-$ decay results are related to details of chiral dynamics; $\eta/\eta' \to 3\pi$ decays provide information on the up and down quark masses; and the decay widths of $\eta/\eta' \to \gamma\gamma$ are related to the quark content of the two mesons. Despite the impressive progress in the last years, many η and η' decays are still to be observed and explored. The full J/ψ data set now available at BESIII makes possible more detailed studies with unprecedented precision. It allows, in addition, an intensive investigation of the properties of the pseudoscalar states $\eta(1405)/\eta(1475)$ [4719]; a thorough study of all states observed in the 1.4−1.5 GeV/c^2 mass region; a deep investigation of the $\omega \to \pi^+\pi^-\pi^0$ Dalitz plot; and searches for rare ω decays.

Hyperon decays
Observation of a significant polarization of the Λ and $\bar{\Lambda}$ from $J/\psi \to \Lambda\bar{\Lambda}$ led to the revision of the decay asymmetry parameter α_Λ [4723,4724], and has shown BESIII has the potential to study properties of the ground-state (anti)hyperons. Moreover, the cascade decays of $J/\psi \to \Xi^-\Xi^+$ made it possible to measure the strong and weak phases of the Ξ^- decay [4679]. The branching fractions for J/ψ decays into a hyperon–antihyperon pair are relatively large, $\mathcal{O}(10^{-3})$, and thus the collected 10 billion J/ψ decays can be used for precision studies of hyperon decays and tests of CP symmetry. The hyperon–antihyperon pair is produced in a well-defined spin-entangled state based on the two possible partial waves (parity symmetry in this strong decay allows for an S- and a D-wave). The charge-conjugated decay modes of the hyperon and antihyperon can be measured simultaneously and their properties compared directly. In the first round of analyses both the hyperon and antihyperon decay via the common pionic modes. The full data set will be used to improve the precision of the CP-violation searches within these decays. The next stage will be to use a common decay of one of the (anti)hyperons to study rare decays of the produced partner. For example, the kinematical constraints make it possible to perform complete reconstruction of the semileptonic decays and radiative decays of polarized hyperons.

Leptonic decays of charm mesons
In the SM, the partial widths of the leptonic decay $D^+_{(s)} \to \ell^+\nu_\ell$ can be expressed in terms of the $D^+_{(s)}$ decay constant $f_{D^+_{(s)}}$ and the CKM matrix element $|V_{cd(s)}|$. Using the measured branching fractions of the leptonic $D^+_{(s)}$ decays, the product $f_{D^+_{(s)}}|V_{cs(d)}|$ can be determined. By taking the $f_{D^+_{(s)}}$ calculated by LQCD with a precision of 0.2% [692,695] one can precisely determine the CKM matrix elements $|V_{cs}|$ and $|V_{cd}|$. Conversely, taking the $|V_{cs}|$ and $|V_{cd}|$ from the standard model global fit, one can precisely measure the $D^+_{(s)}$ decay constants, which are crucial to calibrate LQCD for heavy-quark studies. Comparing the obtained branching fractions of $D^+_{(s)} \to \tau^+\nu_\tau$ and $D^+_{(s)} \to \mu^+\nu_\mu$ gives an important comprehensive test of $\tau - \mu$ lepton-flavor universality.

In recent years, BESIII reported the most precise experimental studies of $D^+_{(s)} \to \ell^+\nu_\ell$ by using 2.93, 0.48, and 6.32 fb^{-1} of data taken at $\sqrt{s} = 3.773$, 4.009, and 4.178–4.226 GeV [4725]. However, the statistical uncertainty still dominates studies of $D^+ \to \ell^+\nu_\ell$ decays, whereas the statistical and systematic uncertainties are comparable in measurements of $D^+_s \to \ell^+\nu_\ell$ decays. The full BESIII data samples to be collected in the coming years allow improvements in the precision of these important constants. The current results of f_{D^+} and $|V_{cd}|$ and their expected precision are shown in Fig. 426. Furthermore, the accuracy of the lepton-flavor universality tests in $D^+ \to \ell^+\nu_\ell$ and $D^+_s \to \ell^+\nu_\ell$ decays are

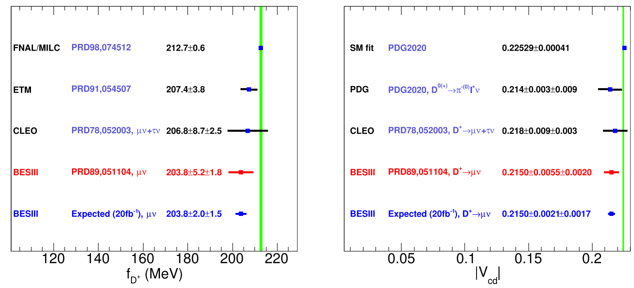

Fig. 426 Comparison of extracted D^+ decay constant and $|V_{cd}|$ from various experiments and the expected precision with 20 fb^{-1} $\psi(3770)$ data at BESIII

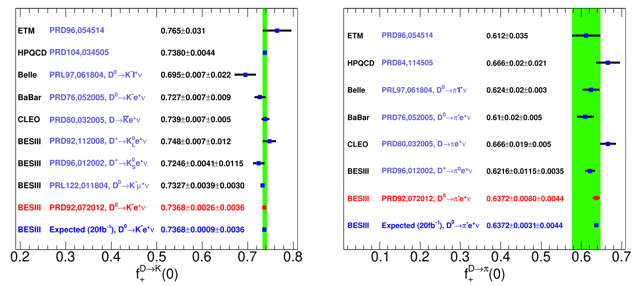

Fig. 427 Comparison of $f^\pi_+(0)$ and $f^K_+(0)$ from various experiments and the expected precision with 20 fb^{-1} $\psi(3770)$ data at BESIII

expected to be reduced from 24.0% and 4.0% to about 10.0% and 3.0%, respectively.

Semileptonic decays of charm mesons
Over the years, BESIII reported experimental studies of the semi-leptonic $D^{0(+)}_{(s)}$ decays into P, V, S, and A [4725], where P denotes pseudoscalar mesons of K, π, η, η'; V denotes vector mesons of K^*, ρ, ω, and ϕ; S denotes scalar mesons of f_0 and a_0; and A denotes axial vector mesons of K_1 and b_1. These measurements were carried out by using 2.93, 0.48, and 6.32 fb^{-1} of data taken at $\sqrt{s} = 3.773$, 4.009, and 4.178–4.226 GeV, respectively.

Except for the $D^{0(+)} \to K$ and $D^{0(+)} \to K^*$ form factors, the precision of all other measurements of the $D^{0(+)}_{(s)} \to P$ and $D^{0(+)}_{(s)} \to V$ form factors are restricted due to the limited size of the data sets. Therefore, with the full BESIII data samples, all the form-factor measurement uncertainties that are limited by the size of the data sample will improve by factors of up to 2.6 for semi-leptonic $D^{0(+)}$ and 1.4 for semi-leptonic D^+_s decays. Complementary studies of the semi-muonic charmed meson decays further improve the form factor knowledge. In addition, we plan to extract the $D \to S$ and $D \to A$ form factors for the first time.

The best precision in the $c \to s$ and $c \to d$ semi-leptonic $D^{0(+)}$ decay form factors will be from the studies of $D^{0(+)} \to \bar{K}\ell^+\nu_\ell$ and $D^{0(+)} \to \pi\ell^+\nu_\ell$. Combining analysis of semi-electronic and semi-muonic D^0, as well as D^+ decays will give more precise results. The experimental uncertainties are expected to be reduced from 0.6% to 0.4% on $c \to s$ decays and from 1.5% to 0.7% on $c \to d$ decays, as indicated in Fig. 427.

For semi-leptonic $D_{(s)}^{0(+)}$ decays, the best test of $\mu - e$ lepton-flavor universality is expected to be from $D \to \bar{K}\ell^+\nu_\ell$ decays, where the test precision can be reduced from 1.3% to the level of 0.8% in the near future. At present, it is not conclusive whether the $\mu - e$ lepton-flavor universality always holds in semi-leptonic $D_{(s)}^{0(+)}$ decays, because there are still many unobserved semi-muonic decays such as

$$
\begin{aligned}
&D^+ \to \eta'\mu^+\nu_\mu,\ D^{0(+)} \to a_0(980)\mu^+\nu_\mu,\\
&D^{0(+)} \to K_1(1270)\mu^+\nu_\mu,\ D^+ \to f_0(500)\mu^+\nu_\mu,\\
&D_s^+ \to K^0\mu^+\nu_\mu,\ D_s^+ \to K^{*0}\mu^+\nu_\mu,\\
&D_s^+ \to f_0(980)\mu^+\nu_\mu,\ D_s^+ \to \eta'\mu^+\nu_\mu.
\end{aligned}
$$

Larger data samples provide improved opportunities to search for these decays, whose observation will help clarify if there is violation of $\mu - e$ lepton-flavor universality in the charm sector.

Moreover, the studies on the intermediate resonances in hadronic final states, e.g., $K_1(1270)$ and $a_0(980)$, in the semi-leptonic $D_{(s)}^{0(+)}$ decays provide a clean environment to explore meson spectroscopy, as no other particles interfere. This corresponds to a much simpler treatment than those studies in charmonium decays or hadronic $D_{(s)}^{0(+)}$ decays.

Hadronic decays of charm mesons

Some experiments, for example LHCb, have the ability to measure a large number of charm and beauty hadron relative branching-fraction ratios due to the high yields given by the large charm and beauty production cross section. The conversion from the branching-fraction ratio to the absolute branching fraction incurs the uncertainty of the branching fraction of the reference mode, such as, $D^0 \to K^-\pi^+$, $D^0 \to K^-\pi^+\pi^+\pi^-$, $D^+ \to K^-\pi^+\pi^+$, $D_s^+ \to K^-K^+\pi^+$, and $\Lambda_c^+ \to pK^-\pi^+$. Improved measurements of these absolute branching fractions at BESIII will be highly beneficial to some key measurements at LHCb. With 20 fb^{-1} data taken around $\sqrt{s} = 3.773$ and 4.18 GeV at BESIII, these decays are expected to be measured with an uncertainty of about 1%.

At present, the sum of the branching fractions for the known exclusive decays of D^0, D^+ and D_s^+ are more than 80%. However, there is still significant room to explore more hadronic decays to increase the known branching fractions for D^0, D^+ and D_s^+. A 20 fb^{-1} dataset will allow the determination of the absolute branching fractions of those missing decays $K\pi\pi\pi$, $KK\pi\pi$, and $KK\pi\pi\pi$ and exploring the sub-structures in these decays using amplitude analyses is also interesting. In addition, precise measurements of the branching fractions for D^0, D_s^+ and D^+ inclusive decays to three charged pions and other neutral particles, and exclusive decays to final states with neutral kaons and pions (e.g. $D_s^+ \to \eta'\pi^+\pi^0$, $D^+ \to \bar{K}^0\pi^+\pi^+\pi^-\pi^0$ and decay modes contributing to $D^{0(+)} \to \eta X$) are also highly desirable to better understand backgrounds in several measurements, particularly $B \to D^*\tau^+\nu_\tau$.

Studies of such multi-body decays benefit from amplitude analyses to understand the intermediate resonances. Even though it is possible to accumulate large samples of singly tagged D mesons, they have very high backgrounds making them unsuitable to perform amplitude analyses. In contrast to this, the doubly tagged $D\bar{D}$ mesons can provide clean D samples with low backgrounds. However, the sample size limits the precision with the current data. Therefore, such measurements will be significantly improved with the full BESIII data sets.

Decays of charmed baryons

The lightest charmed baryon, Λ_c^+, which was observed in 1979, is the cornerstone of the charmed baryon spectra. The improved knowledge of Λ_c^+ decays, especially for the normalization mode $\Lambda_c^+ \to pK^-\pi^+$, is key for the studies of the charmed baryon family. Moreover, the Λ_c^+ decays can also open a window upon a deeper understanding of strong and weak interactions in the charm sector. In addition, these will provide important inputs for the studies of beauty baryons that decay into final states involving Λ_c^+.

Compared to the significant progress in the study of charmed mesons, the advancements in the knowledge of the charmed baryons are relatively slow in the past 40 years. Before 2014, almost all the decays of Λ_c^+ were measured relative to the normalization mode $\Lambda_c^+ \to pK^-\pi^+$, whose branching fraction suffered a large uncertainty of 25%. Moreover, no data sample taken around the $\Lambda_c^+\bar{\Lambda}_c^-$ pair production threshold had been used to study the Λ_c^+ decays.

BESIII have already collected 4.4 fb^{-1} of data above $\Lambda_c\bar{\Lambda}_c$ threshold, which will provide the most precise values of many absolute branching fractions and polarization parameters [2634]. Future running with the upgraded BEPC-II will allow large samples of Σ_c and Ξ_c pairs to be collected, which will lead to many absolute branching fractions of charm baryon decays to be determined for the first time [2634].

The "post-BEPCII era"

The super τ-Charm facility (STCF) [4726] is one of the major options for future accelerator-based high energy projects in China. The proposed STCF is a symmetric double ring electron–positron collider that would operate in the CM region $\sqrt{s} = 2 \sim 7$ GeV with a peaking luminosity of 0.5×10^{35} cm^{-2} s^{-1} or higher. It is expected to deliver more than 1 ab^{-1} of integrated luminosity per year. Huge samples of exotic charmonium-like states (XYZ), J/ψ, D, D_s and Λ_c decays could be used to make precision measurements of the properties of XYZ particles, and map out the spectroscopies of QCD hybrids and glueballs. High statistics data samples could also be used to search for new sources of CP violation in the hyperon and τ-lepton sectors with unprecedented sensitivity and search for anomalous decays of various hadrons with sensitivities extending down to the level of SM-model expectations.

Since 2012, when the STCF was proposed, the Chinese STCF working group, together with international teams, have carried out a series of feasibility studies, completed the preliminary Conceptual Design Report (CDR) and made significant progress. Compared to the BEPCII/BESIII experiments, the substantial improvement in the performance of the STCF will lay the foundation for breakthroughs in the relevant frontiers of research. Meanwhile, it will pose major technical challenges in accelerator and detector development. At present, the STCF project for the research and development of key technologies is actively performed with the support of Anhui Province of China. More efforts are being made to promote the implementation and construction of the STCF project.

14.7 BELLE II

Toru Iijima

The Belle II experiment is a particle-physics experiment operating at the SuperKEKB collider built in the KEK laboratory in Japan (Fig. 428). It is a successor of the Belle experiment at the KEKB collider, which experimentally established the Kobayashi-Maskawa theory of the CP violation, together with the BaBar experiment at the SLAC PEP II collider. Over the next decades, Belle II will record the decay of billions of bottom mesons, charm hadrons, and τ leptons produced in electron–positron collisions at and near the $\Upsilon(4S)$ energy. The ultimate goal is to accumulate 50 ab^{-1} data of e^+e^- collisions, which is about 50 times larger than the data set of the Belle experiment. These data, collected in the low background and kinematically known conditions, will provide a complementary approach to experiments at hadron machines. It will allow us to critically test the standard model (SM) and search for new particles through processes sensitive to virtual heavy particles at mass scale orders of magnitudes higher than direct searches at the energy frontier experiment.

The Belle II physics program includes variety of subjects in the areas of;

– Precision CKM measurements to critically test SM and find or constrain non-SM physics contribution in a model-independent way.
– Search for non-SM CP violation in rare B processes, such as $b \to q\bar{q}s$.
– Search for non-SM physics in semileptonic, radiative and other rare B decays, including precision tests of the lepton-universality in $b \to c\ell\nu$ and $b \to s\ell^+\ell^-$, where ℓ stands for either of e, μ and τ.
– Measurements of many parameters in decays of charm hadrons and the τ leptons with world-leading precisions, including their masses, lifetimes, CP violation parameters, and branching fractions for charged-lepton-flavor-violating decays.
– Unique searches for dark-sector particles with masses in the MeV-GeV range, where some of them are possible dark matter candidates.
– Broad spectroscopy program for both conventional and multi-quark $c\bar{c}$ and $b\bar{b}$ states using different production processes; through B decays, through initial state radiation processes, two-photon collisions and double charmonia productions.
– Provide essential inputs to sharpen the interpretation of results for the anomalous magnetic moment of the muon $(g-2)_\mu$, which indicates 4.2σ deviation from the SM.

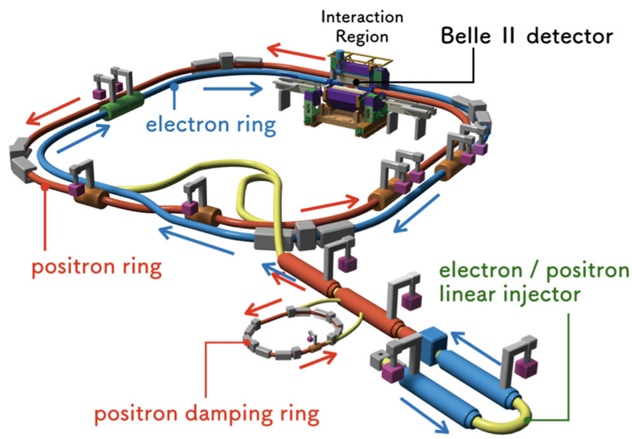

Fig. 428 Layout of the SuperKEKB accelerator

In these physics studies at Belle II, the importance of QCD is two-fold. First, better understandings of non-perturbative QCD properties associated with particle decays are essential ingredients for sharpening the SM predictions as references for non-SM physics searches. Second, a variety of low-energy QCD phenomena, such as the $c\bar{c}$ and $b\bar{b}$ spectroscopy as mentioned above, are the subjects that could be uniquely studied at the Belle II experiment. Also, the e^+e^- collisions to hadron final states offer unique opportunities to study hadronization processes like the Collins effect. The variety of physics studies that can be carried out at Belle II is discussed in detail in Ref. [4158]. In the subsections following Sect. 14.7.2, we describe only a brief summary for subjects that are of primary relevance to QCD, where Belle II will be unique and will be world-leading.

14.7.1 SuperKEKB/Belle II experiment

The SuperKEKB accelerator is an asymmetric energy collider of 4.0 GeV e^+ and 7.0 GeV e^-. The target instantaneous luminosity is $\sim 6 \times 10^{35}$ cm^{-2} s^{-1}, enabling accumulation of 50 ab $^{-1}$ over the next decade. It is the world's leading luminosity machine with an innovative "nano-beam scheme", where the two beams collide with a large horizontal crossing angle and the vertical beam size is squeezed down to a level of 50–60 nm at the interaction point (IP).

The Belle II detector, as shown in Fig. 429, is located at the single collision point (IP) of the SuperKEKB. It is nearly a 4π magnetic spectrometer surrounded by a calorimeter and muon detectors and comprises several subdetectors arranged cylindrically around IP and with a polar structure reflective of the asymmetric distribution of final-state particles resulting from the asymmetric energy collision. From the innermost out, these subdetectors are the vertex detector (VXD), central drift chamber (CDC), electromagnetic calorimeter (ECL), and K-long and muon detector (KLM). In between CDC and ECL, are charged-particle-identification subdetectors: a time-of-propagation Cherenkov counter (TOP) in the barrel, and an aerogel ring-imaging Cherenkov detector (ARICH) in the forward region. Between ECL and KLM, is a solenoid coil that provides a 1.5 T axial magnetic field for measurements of the momenta and electric charge of charged particles. The vertex detector consists of two layers of pixel sensors (PXD) surrounded by four layers of microstrip sensors (SVD) to determine the positions of decaying particles with the typical impact-parameter resolution of $10-15\,\mu m$, resulting in $20-30 \mu m$ typical vertex resolution.[123] The small-cell helium-ethane central drift chamber measures the positions of charged particles at large radii and their energy losses due to ionization. The relative charged-particle transverse momentum resolution is typically 0.4%/pT [GeV]. The observed hadron identification efficiencies are typically 90% at 10% contamination. Typical uncertainties in hadron-identification performance are 1%. The CsI(Tl)-crystal electromagnetic calorimeter measures the energies of electrons and photons with energy-dependent resolutions in the 1.6–4% range. Layers of plastic scintillators and resistive-plate chambers interspersed between the magnetic flux-return yoke's iron plates allow us to identify K_L and muons. Our observed lepton-identification performance shows 0.5% pion contamination at 90% electron efficiency, and 7% kaon contamination at 90% muon efficiency. Typical uncertainties in lepton-identification performance are $1\% - 2\%$.

[123] The second pixel layer is currently incomplete, covering approximately 15% of the azimuthal acceptance. Installation of the pixel detector will be completed in 2023.

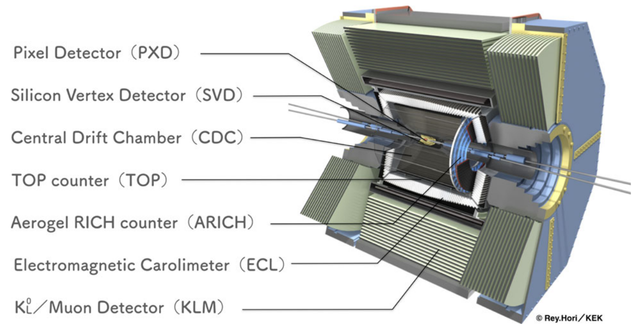

Fig. 429 The Belle II detector which consists of seven subsystems

The Belle II experiment has unique advantages over hadron-collider experiments, such as the LHCb experiment. Despite having comparatively less data and fewer accessible initial states;

- It produces heavy flavor particles in a less background environment, which enables efficient detection of neutral particles, such as γ, π^0, K_S^0, K_L^0.
- It produces quantum correlated B^0-$\bar{B}^0$ pairs, by which we can tag the B meson flavor with high effective efficiency. We can also measure precisely B decay modes with neutrinos in the final state, by fully reconstructing one of the B mesons, referred to as "full reconstruction tagging".
- It provides a large sample of τ leptons obtained, which allows us to study in detail the property of the τ lepton, including Lepton-Flavor-Violating (LFV) decays.

As for the full reconstruction tagging, a new "Full Event Interpretation (FEI)" tool has been developed [4727]. The basic idea of FEI is to reconstruct, in a hierarchical manner, individual particle decay channels that occur in the decay chain of the B meson. For each unique decay channel of a particle, a multivariate classifier (MVC) is trained using simulated events. Both hadronic and semileptonic B decays are used. The typical tag-side efficiency, defined as the number of correctly reconstructed tag-side B mesons divided by the total number of $\Upsilon(4S)$ events, is 0.61% (0.34%) for hadronic B^+ (B^0) decays and 1.45%(1.25%) for semileptonic B^+ (B^0) decays. The full reconstruction tagging provides unique methods to measure B decays with neutrinos in the final states, such as $B \to \pi \ell \nu$, $B \to D^{(*)} \tau \nu$ and $B \to K \nu \bar{\nu}$.

14.7.2 Precision CKM measurements

In the Standard Model (SM), CP violation in the K/B meson decays can occur as the complex phase in the Cabibbo–Kobayashi–Maskawa (CKM) quark mixing matrix [86, 4028]. The high luminosity data at Belle II enable precision

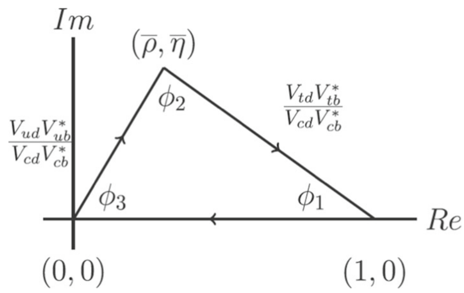

Fig. 430 The unitarity triangle

measurements of the three internal angles, $(\phi_1, \phi_2, \phi_3) \equiv (\alpha, \beta, \gamma)$, and the three sides of the unitarity triangle, which represents the unitarity condition of the CKM matrix elements, $V_{ud}^* V_{ub} + V_{cd}^* V_{cb} + V_{td}^* V_{tb} = 0$, in the complex plane with the three terms divided by $V_{cd} V_{cb}^*$, as shown in Fig. 430.

Measurement of ϕ_1
The internal angle $\phi_1 \equiv \arg(-V_{cd} V_{cb}^* / V_{td} V_{tb}^*)$ is determined from measurements of time-dependent CP asymmetries, which occurs via interference between $B_d - \bar{B}_d$ oscillation and $b \to c\bar{c}s$ decay amplitudes. Most of the hadronic uncertainties cancel out in the CP asymmetry, therefore, these measurements provide very clean and precise determinations of ϕ_1. In the experiment, after the $B^0 - \bar{B}^0$ system is coherently produced from an $\Upsilon(4S)$ decay, one of the B mesons, B_{CP}, decays to a CP eigenstate f_{CP} at $t = t_{CP}$ whereas the other, B_{tag}, may decay to favor specific final state at $t = t_{\text{tag}}$. The distribution of the proper-time difference $\Delta t \equiv t_{CP} - t_{\text{tag}}$ is expressed by

$$\mathcal{P}_{f_{CP}}(\Delta t, q) = \frac{e^{-|\Delta t|/\tau_{B^0}}}{4\tau_{B^0}} \{1 + q[\mathcal{A}_{f_{CP}} \cos(\Delta m_d \Delta t) + \mathcal{S}_{f_{CP}} \sin(\Delta m_d \Delta t)]\}, \quad (14.3)$$

where τ_{B^0} and Δm_d are the average lifetime and mass difference between neutral B physical states, respectively, and $\mathcal{A}_{f_{CP}}$ and $\mathcal{S}_{f_{CP}}$ are the direct and mixing-induced CP-violating asymmetries, respectively. The B meson flavor q takes values $+1(-1)$ when B_{tag} is $B^0(\bar{B}^0)$ and it is statistically determined from the favor tagging algorithm based on final-state information [4728]. The time-difference Δt is approximated by the distance between the two B-meson decay vertices divided by the speed of the $\Upsilon(4S)$ projected onto the boost axis.

The previous experiments Belle, BaBar, and LHCb achieved determination of ϕ_1 at 2.4% precision [4729], using tree dominated $(c\bar{c})K^0$ decays, such as $J/\psi K_S^0$, $\psi(2S)K_S^0$, $\chi_{c1} K_S^0$ and $J/\psi K_L^0$. The error is still dominated by systematic uncertainties, associated with imperfections in vertex reconstruction and flavor tagging. The precision is expected to further improve to below 1% in the next decade, and it will provide a firm basis to search for non-SM contributions.

Measurement of ϕ_2
Studies of $b \to u$ charmless B decays give access to $\phi_2 \equiv \arg[-V_{tb}^* V_{td} / V_{ub}^* V_{ud}]$, the least known angle of the CKM unitarity triangle, and probe non-SM contributions in processes mediated by loop decay-amplitudes. However, clean extraction of $\phi 2$ is not trivial due to hadronic uncertainties, which are hardly tractable in perturbative calculations. Appropriate combinations of measurements from decays related by flavor (isospin) symmetries reduce the impact of such uncertainties [4730]. The most promising determination of ϕ_2 relies on the combined analysis of the decays $B^+ \to \rho^+ \rho^0$, $B^0 \to \rho^+ \rho^-$, $B^0 \to \rho^0 \rho^0$, and corresponding decay into pions. The current global precision of 4 degrees is dominated by $B \to \rho\rho$ data [4729]. Leveraging efficient reconstruction of low-energy π^0, improved measurements in $B^+ \to \rho^+ \rho^0$ and $B^0 \to \rho^+ \rho^-$ decays will be unique to Belle II. The expected experimental accuracy for the ϕ_2 determination is less than 1° at 50ab^{-1}.

Measurement of ϕ_3
The third internal angle $\phi_3 \equiv \arg[-V_{ud} V_{ub}^* / V_{cd} V_{cb}^*]$ is accessible via tree-level decays, such as $B \to DK$, where D represents a generic superposition of D^0 and $\overline{D}^0$. Assuming that non-SM amplitudes do not affect appreciably tree-level processes, precise measurements of ϕ_3 and $|V_{\text{ub}}/V_{\text{cb}}|$ set strong constraints on the SM description of CP violation, to be compared with measurements from higher-order processes potentially sensitive to non-SM amplitudes, such as mixing-induced CP violation through $\sin 2\phi_1$. Extraction of ϕ_3 involves measurement of $B^- \to \overline{D}^0 K^-$ and $B^- \to D^0 K^-$ amplitudes, which are expressed as

$$\frac{\mathcal{A}(B^- \to \overline{D}^0 K^-)}{\mathcal{A}(B^- \to D^0 K^-)} = r_B e^{i(\delta_B - \phi_3)}, \quad (14.4)$$

where $r_B \approx 0.1$ is the ratio of amplitude magnitudes and δ_B is the strong-phase difference. Since the hadronic parameters, r_B and δ_B can be determined from data together with ϕ_3, these measurements are essentially free of theoretical uncertainties [4731]. The precision of ϕ_3 is mostly limited by the small branching fractions of the decays involved (around 10^{-7}). The current world average is $\phi_3 = (66.2^{+3.4}_{-3.6})°$ [4729], whereas the indirect determination is $(63.4 \pm 0.9)°$ [4150]. Various methods with different choices of final states accessible to both D^0 and $\overline{D}^0$ have been proposed to extract ϕ_3. They include CP-eigenstates (GLW method) [4732,4733], Cabibbo-favoured (CF) and doubly-Cabibbo-suppressed (DCS) decays (ADS method) [4734], self-conjugate modes (BPGGSZ method) [4735–4737], and singly Cabibbo-suppressed (SCS) decays (GLS method) [4738].

Currently, precision is dominated by measurements based on $B^- \to D(K^0_S\pi^+\pi^-)K^-$ as well as $B^- \to D(K^0_L\pi^+\pi^-)K^-$ decays [4735–4737]. Belle II will be competitive in this mode and others involving final-state K^0_S, π^0, and γ such as $K^0_S\pi^0$, $K^0_S\pi^+\pi^-\pi^0$ or $B^- \to D^*(D(\gamma,\pi^0))h^-$. Precision will further improve following the expected three-fold improvements on the external charm-strong-phase inputs from BESIII [4158]. In addition, $B^- \to D(K^0_S\pi^+\pi^-\pi^0)K^-$ is promising at Belle II due to its sizable branching fraction and rich resonance substructures, as shown by Belle [4739]. Improved charm-strong-phase inputs, availability of a suitable amplitude model of $D \to K^0_S\pi^+\pi^-\pi^0$ and a larger B decay sample will render $B^- \to D(K^0_S\pi^+\pi^-\pi^0)K^-$ a strong contributor for determination of ϕ_3. The precision of ϕ_3 is expected to be $\mathcal{O}(1°)$ with the full 50 $^{-1}$ data set.

Determination of $|V_{cb}|$ and $|V_{ub}|$

The magnitudes of the CKM matrix elements $|V_{cb}|$ and $|V_{ub}|$ can be deduced from tree $b \to c$ and $b \to u$ processes and provide reliable SM references to test non-SM contributions. The most precise determinations of $|V_{cb}|$ and $|V_{ub}|$ come from measurements of semileptonic transitions $b \to cl\nu$ and $b \to ul\nu$, either in inclusive or exclusive final states, combined with theoretical inputs to characterize the QCD effects associated with B decays. There has been significant disagreement in the results obtained from exclusive and inclusive measurements [4729]. The reason for this discrepancy is unknown and has been a long-standing issue. It can be possibly inconsistent experimental or theory inputs, but also interpretations in terms of non-SM physics cannot be excluded [4084]. The large data set at Belle II will offer more precise and richer experimental information to test theoretical investigations and to clarify the issue.

Exclusive $|V_{ub}|$

Belle-II will provide a variety of ways for exclusive $|V_{\rm ub}|$ determinations. While $\overline{B}^0 \to \pi^+\ell^-\bar{\nu}_\ell$ is currently the most effective in terms of availability of experimental data and theoretical calculations of the form factor, Belle II will also measure other exclusive $b \to u\ell\nu_\ell$ modes with good precision, in particular those involving neutral final-state particles such as

$$B^- \to (\pi^0, \rho^0, \omega, \eta, \eta')\ell^-\nu_\ell$$

and $\overline{B}^0 \to \rho^+\ell^-\nu_\ell$. The excellent resolution in $q^2 \equiv (p_\ell + p_\nu)^2$ also gives access to the decay form factors equally important for determining $|V_{ub}|$. Typically, experimental uncertainties are smallest for low q^2 whereas uncertainties in the form factors from lattice QCD are smallest at high q^2. Improvements in the experimental constraints will be driven mainly by data set sizes. Belle II can also measure the variety of exclusive decays with high purities in analyses, where the (non-signal) partner B-meson is reconstructed [4740]. Belle II will double the global precision in exclusive

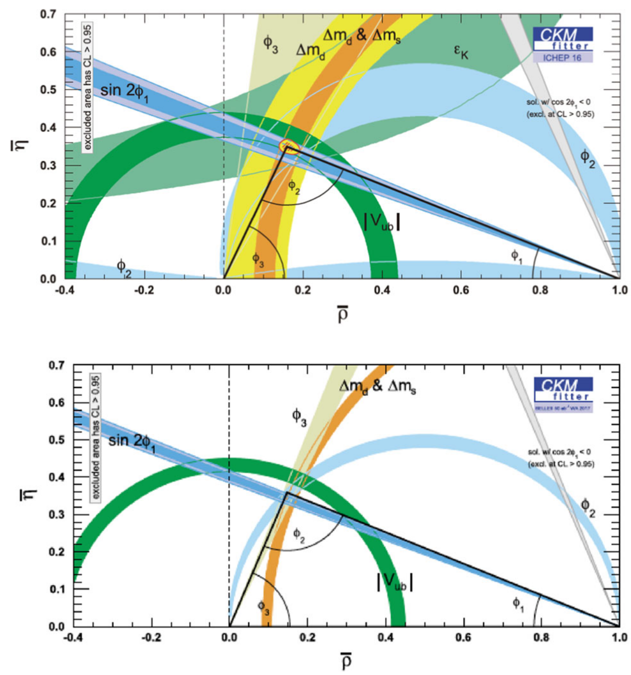

Fig. 431 Current unitarity triangle fit (top) and extrapolated to 50 ab^{-1} (bottom) [4158]

$|V_{ub}|$ results below 3%. Expected progress in lattice QCD [4158] will offer further significant improvement.

Inclusive $|V_{ub}|$:

Belle II will provide a unique opportunity to measure inclusive $B \to X_u\ell\nu$ decays, where X_u is a charmless hadronic system. Taking advantage of the $B\overline{B}$ threshold experiment, after reconstructing a signal lepton and the partner B meson, all remaining tracks and energy clusters can be associated with the X_u candidate. Measurements require accurate modeling of the $b \to u$ signal and the $b \to c$ background as demonstrated in the latest Belle measurement of $B \to X_u\ell\nu$, which indeed reports results closer to exclusive [4111]. With larger sample sizes and continuing developments in reconstruction algorithms (e.g., improved partner B reconstruction), Belle II will accomplish measurements of inclusive $|V_{ub}|$ to $\mathcal{O}(1)$% precision. Belle II can also explore novel ideas of measurements, such as the measurement of differential branching fractions of $B \to X_u\ell\nu$ which enables shape-function model-independent determinations of $|V_{\rm ub}|$ as demonstrated by Refs. [4114,4115,4741].

Determination of $|V_{cb}|$

Belle II will be able to improve also determinations of $|V_{cb}|$ from exclusive $B \to D^{(*)}\ell\nu$ decays and inclusive $B \to X_c\ell\nu$ decays. For exclusive analyses, the key experimental challenges will be to understand better the composition and form factors of $B \to D^{**}\ell\nu$ decays and reduce relevant systematic uncertainties as those associated with lepton identification and low-momentum-pion reconstruction for $B \to D^*\ell\nu$ decays. Belle II will tackle this with a detailed program based on dedicated auxiliary studies of $B \to D^{**}\ell\nu$ decays. The precision of inclusive determinations, which is limited by theory, will benefit from measurements of the kinematic moments of $B \to X_c\ell\nu$ decays that will constrain hadronic matrix elements in the operator-product-expansion based theory. Ultimately Belle II will accomplish measurements of $|V_{cb}|$ to $\mathcal{O}(1)\%$ precision.

Summary of CKM measurements

Figure 431 presents the improvements of the CKM measurements, currently achieved and expected at Belle II. The `CKMFitter` group has performed analyses of non-SM physics in mixing, assuming that tree decays are not affected by non-SM effects. Within this framework, non-SM contributions to the B_d mixing amplitudes can be parametrized as

$$M_{12}^d = (M_{12}^d)_{SM} \times (1 + h_d e^{2i\sigma_d}) \tag{14.5}$$

Here h_d and σ_d stand for the amplitude and phase of the non-SM physics, which are related to the mass-scale parameter Λ via

$$h \simeq \frac{|C_{ij}|^2}{|\lambda_{ij}^t|^2}\left(\frac{4.5\,\text{TeV}}{\Lambda}\right) \tag{14.6}$$

$$\sigma = \arg(C_{ij}\lambda_{ij}^{t*}), \tag{14.7}$$

where $\lambda_{ij}^t = V_{ti}^* V_{tj}$ and V is the CKM matrix. The scales Λ probed in B_d mixing by the end of the Belle II data-taking will be 17 TeV and 1.4 TeV for CKMI-like couplings in a tree and one-loop-level non-SM interactions respectively. For a scenario with no hierarchy, i.e. $|C_{ij}| = 1$, the corresponding scale of operators probed will be 2×10^3 TeV and 2×10^2 TeV in a tree- and one-loop-level non-SM interactions respectively.

14.7.3 Search for non-SM CP violation in rare B processes

In order to search for the non-SM contribution, the most promising channel is $B^0 \to \eta' K_S^0$; it has a sizable decay rate dominated by the $b \to s$ loop amplitude, where non-SM physics can contribute, and its associated hadronic uncertainties is relatively small. The quantity of interest is $\Delta\mathcal{S}_{\eta' K_S^0} \equiv \mathcal{S}_{\eta' K_S^0} - \sin\phi_1$. The SM predictions that include a systematic treatment of low-energy QCD amplitudes assuming factorization yield $0.00 < \Delta\mathcal{S}_{\eta' K_S^0} < 0.03$ [4742]. The current world average of $\Delta\mathcal{S}_{\eta' K_S^0}$ is -0.07 ± 0.06 [4729]. Low backgrounds and a high-resolution electromagnetic calorimeter offer Belle II unique access to this measurement. Similarly promising is the channel $B^0 \to \phi K_S^0$, whose final state makes Belle II strongly competitive despite challenges associated with model-related systematic uncertainties from the Dalitz plot analysis. The expected experimental accuracy at 50ab^{-1} is $\sim 0.01(\sim 0.02)\%$ for $\mathcal{S}_{\eta' K_S^0}(\mathcal{S}_{\phi K_S^0})$. Figure 432 demonstrates the time-dependent CP asymmetry for the final state $\eta' K_S^0$ compared to $J/\psi K_S^0$, using $\mathcal{S}_{\eta' K S^0} = 0.55$ and $\mathcal{S}_{J/\psi K_S^0} = 0.70$ in a Monte Carlo simulation with the integrated luminosity of 50 ab^{-1}, where the two values would be unambiguously distinguishable, signifying the existence of new physics. In addition, the processes $B^0 \to K_S^0\pi^0\gamma$, $B^0 \to K_S^0\pi^+\pi^-\gamma$, and $B^0 \to \rho^0\gamma$ are greatly sensitive to non-SM physics through $b \to s$ and $b \to d$ loops and offer Belle II further exclusive opportunities.

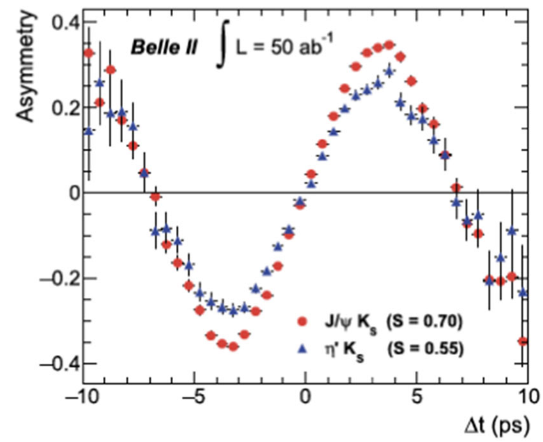

Fig. 432 Time-dependent CP asymmetry for the final state $\eta' K_S^0$ compared to $J/\psi K_S^0$, using $\mathcal{S}_{\eta' K_S^0} = 0.55$ and $\mathcal{S}_{J/\psi K_S^0} = 0.70$ in a Monte Carlo simulation with the integrated luminosity of 50 ab^{-1} [4158]

14.7.4 Search for non-SM physics in semileptonic and radiative B decays

A number of persistent anomalies have been observed in semileptonic B meson decays; deviation from lepton-flavor universality in the decays $B \to D^{(*)}\tau\nu_\tau$ consistently stayed at the 3σ level since these decays were first measured [4729]. Another case of lepton-flavor universality violation has been seen in $B \to K^{(*)}\ell^+\ell^-$. The unique capability of Belle II to reconstruct final states with missing energy and identify efficiently all species of leptons will considerably improve the understanding of these anomalies.

Semitauonic B decays

Decays $B \to D^{(*)}\tau\nu_\tau$ offer precious opportunities for testing lepton-flavor universality at high precision opening a window onto lower-mass (TeV range) non-SM particles. Sensitive observables are the ratio $R(D)$ and $R(D^*)$ of branching fractions of $B \to D^{(*)}\tau\nu_\tau$ to those of $B \to D^{(*)}\ell\nu_\ell$ decays, where $\ell = e$ or μ. There have been numerous SM calculations of $R(D^{(*)})$ and experimentally, the ratio allows for numerous systematic uncertainties to cancel. The SM predictions for the ratios $R(D)$ and $R(D^*)$ are:

$$R(D) = 0.299 \pm 0.011 \tag{14.8}$$

$$R(D^*) = 0.252 \pm 0.003 \tag{14.9}$$

Current best results on $R(D^{(*)})$ are reported by the Belle experiment [4743] and are consistent with previous measurements [4744–4748] in showing a (combined) 3.1σ excess with respect to the SM expectation [4729].

$$R(D) = 0.349 \pm 0.027_{(stat)} \pm 0.015_{(syst)} \tag{14.10}$$

$$R(D^*) = 0.298 \pm 0.011_{(stat)} \pm 0.007_{(syst)} \tag{14.11}$$

This deviation has attracted significant interest in the community as it could be a potential indication of non-SM dynamics.

The main experimental challenge is achieving a detailed understanding of poorly known $B \to D^{**}\ell\nu$ backgrounds, whose feed-down may bias the results. The anticipated data set size will allow for accurate tagged measurements of $B \to D^{**}\ell\nu$ decays for several D^{**} states using samples reconstructing on the signal-side a lepton, a $D^{(*)}$ meson and n pions. If a non-SM source of the anomaly would be established, angle-dependent asymmetries and differences between forward-backward asymmetries observed in muons and electrons, which are ideally suited for Belle II, may offer insight into the properties of the non-SM couplings involved.

Measurements of polarization of the τ lepton $((\Gamma^+ - \Gamma^-)/(\Gamma^+ + \Gamma^-))$ and D^* mesons $(\Gamma_L/(\Gamma_T + \Gamma_L))$ provide supplementary sensitivity to non-SM physics. Here, $\Gamma^+(\Gamma^-)$ is the semitauonic decay rate where the τ has $+\frac{1}{2}$ $(-\frac{1}{2})$ helicity and $\Gamma_L(\Gamma_T)$ is the rate where the D^* has longitudinal (transverse) polarization. Figure 433 shows the expected Belle II constraints on the $R(D) - R(D^*)$ plane (top) and the $R(D^*) - P_\tau(D^*)$ plane (bottom). Furthermore, differential angular distributions in $B \to D^{(*)}\tau\nu$, usually studied as functions of q^2, may also be important to decipher the dynamics and are distinctive to Belle II.

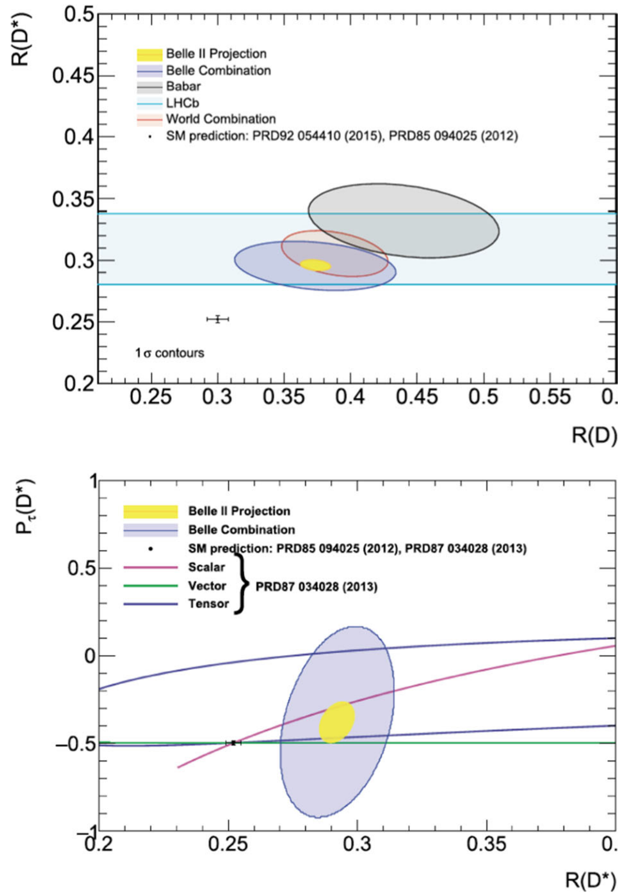

Fig. 433 Expected Belle II constraints on the $R(D) - R(D^*)$ plane (top) and the $R(D^*) - P_\tau(D^*)$ plane (bottom) compared to existing experimental constraints from Belle. The SM predictions are indicated by the black points with theoretical error bars [4158]

$B \to K^*\ell^+\ell^-$ decays

The transitions $b \to s\mu\mu$ and $b \to see$ are under extensive experimental investigation due to several observed anomalies [4749,4749–4753] that prompted interpretations in terms of $\mathcal{O}(10)$ TeV non-SM particles. The unique feature of Belle II is its high efficiency and similar performance for muons and electrons, along with access to absolute branching fractions. Based on a recent Belle II analysis [4754], we expect to provide distinctive information to assess independently the existence of the anomalies (at current central values) with samples of 5 ab^{-1} to 10 ab^{-1} of data. Belle II can provide also results based on inclusive $B \to X_S\ell^+\ell^-$ decays, which do not specify the final strange hadronic states X_S and has fewer theoretical ambiguities.

Belle II can reach also $b \to s\tau\tau$ transitions. These can be enhanced, by up to three orders of magnitude, in several SM extensions that allow for lepton-flavor universality violation in the third generation [4755,4756]. The SM branching fraction for the $B \to K^*\tau\tau$ decay is around 10^{-7} [4757], much smaller than current experimental upper limits, which are at around 2.0×10^{-3} at 90% CL [4755,4758]. The presence of two τ leptons in the final state makes access to these decays ideally suited to Belle II.

Radiative B decays

Radiative $b \to s\gamma$ transitions are dominated by a one-loop amplitude involving a t quark and W boson. Extensions of the SM predict particles that can contribute to the loop, potentially altering various observables from their SM predictions [4759,4760]. Belle II has a unique capability to study these transitions both inclusively and using specific channels.

The availability of precise and reliable SM predictions of inclusive $B \to X_s\gamma$ rates, where X_s identifies a particle with strangeness, make these rates sensitive probes for non-SM physics. In addition, these analyses enable the determination of observables like the b-quark mass and can provide input to inclusive determinations of $|V_{ub}|$ [4158]. Ability to measure precisely the decay properties of the partner B recoiling against the signal B is key for inclusive analyses[4727]. Current best results show 10% fractional precision mostly limited by systematic uncertainties associated with understanding the large backgrounds. The expected relative uncertainties on the branching fractions are $\sim 6\%$ at 5 ab^{-1} and $\sim 2\%$ at 50 ab^{-1} slightly depending on the lower E_γ threshold. The construction of relative quantities like asymmetries will offer a further reduction of systematic uncertainties and enhanced reach. Inclusive analyses of radiative B decays will offer unique windows over non-SM physics throughout the next decade.

14.7.5 Hadron spectroscopy

While many hadron states are categorized into mesons and baryons containing constituent quark–antiquark ($q\bar{q}$) and three quarks (qqq), respectively, there is no proof in QCD to exclude the hadrons having other structures than the ordinary mesons and baryons. The situation has largely changed by the series of discoveries of charmonium-like states, $X(3872)$ [2514], $Y_c(4260)$ [4761], $Z_c^{\pm}(3900)$ [2588], and several others that do not fit the well-established quark model. Analogous discoveries containing bottom quarks (e.g., $\Upsilon(5S)$ decays to $Z_b^{\pm}(10610/50)$ [2598]) indicate a similar unexplored family of particles in the bottomonium sector. The Belle II experiment offers several unique opportunities in this domain. It will exploit 40 times more data than the previous generation B-factories and, compared with hadron-collisions experiments, leverages a greater variety of quarkonium production mechanisms including B meson decays, initial state radiation (ISR), double $c\bar{c}$ processes, two-photon processes, and direct production by changing collider center-of-mass energy [4158]. Belle II is the only experiment with the ability to operate at tuneable center-of-mass energy near the $\Upsilon(4S)$ resonance, providing direct access to multi-quark states containing bottom quarks. In addition, Belle II's good efficiency for reconstructing neutral final-state particles opens the pathway for first observations of the predicted neutral partners of charged tetraquark states.

Belle II has the unique opportunity to explore bottomonium(-like) states by operating at center-of-mass energies around 10 GeV, where only small samples exist worldwide: $\mathcal{O}(10)$ fb^{-1} at $\Upsilon(1S, 2S, 3S, 6S)$, $\mathcal{O}(100)$ fb^{-1} at $\Upsilon(5S)$, and typically less than 1 fb^{-1} at intermediate points. This opens a fruitful program, as demonstrated by previous discoveries at e^+e^- colliders that yielded first observations of predicted bottomonia ($\eta_b(1S, 2S)$, $h_b(1P, 2P)$, and $\Upsilon(1D_2)$) and unexpected four-quark states ($Z_b^{\pm}(10610, 10650)$, $Y_b(10753)$) [4762,4763]. Collisions at energies below the $\Upsilon(4S)$ allow for testing non-SM predictions in Υ decays to invisible or lepton-flavor-violating final states [4764,4765].

14.7.6 Constraining hadronic vacuum-polarization in muon g-2

The anomalous magnetic moment of the muon often parametrized as $a_\mu = (g-2)_\mu/2$, is one of the observables which indicate significant deviation from the SM and has attracted much attention from the community. The current experimental value (combining the BNL E821 result with the first result from the Fermilab $g-2$ experiment) differs from SM predictions based on dispersion relations by 4.2σ, $a_\mu(\text{exp}) - a_\mu(\text{theory}) = (26.0 \pm 7.9) \times 10^{-10}$ [4286,4287]. In order to clarify the deviation, it is important to improve the precision of both experiments and the SM predictions. On the experimental side, the experiment at Fermilab will provide results by further accumulated data and also an experiment with different methods and thus have different systematic errors has been proposed and is being prepared at J-PARC [4766]. The uncertainty in the SM prediction is dominated by the leading-order hadronic contribution (HVP), which can be calculated from the cross-section $\sigma(e^+e^- \to \text{hadrons})$ measured in e^+e^- experiments. The result, HVP=$(693.1 \pm 4.0) \times 10^{-10}$, is dominated by BaBar and KLOE measurements of $\sigma(e^+e^- \to \pi^+\pi^-)$. However, the BaBar and KLOE measurements notably differ. This difference introduces a systematic uncertainty of 2.8×10^{-10} [4304].

Belle II will perform these measurements with larger data sets, and at least comparable systematic uncertainty, to resolve this discrepancy. Furthermore, large statistics data at Belle II will allow us to use new approaches to suppress systematic uncertainties, particularly from particle identification. Although the specific systematic studies still need to be refined, the goal for the final accuracy including both statistical and systematic uncertainties is to be 0.5% or lower [4158]. This will match the expected experimental precision on $g-2$[4158,4286]. Belle II's operation at the highest luminosity $\boldsymbol{e^+e^-}$ collider, as well as its excellent particle-identification capabilities, places it in a unique position to further the studies of the HVP contribution to $(g-2)_\mu$ in the next decade. HVP can be estimated also by τ hadronic spectral functions and CVC, together with isospin-breaking corrections.

14.7.7 Status and outlook

The physics data taking with all the Belle II subdetector components started in March 2019, following the SuperKEKB main ring commissioning run in 2016, and the collision test runs in 2018. At the time when this article is written, the SuperKEKB accelerator has achieved the peak luminosity of 4.7×10^{34} cm^{-2} s^{-1}, more than two times higher than the record of the previous KEKB accelerator. The Belle II experiment has accumulated 428 fb^{-1}, almost similar to the

BaBar and about half of the Belle experiments. Some results are already world-leading thanks to the efficiency and resolution improved significantly compared to the previous experiments. The operation is suspended since June 2022 for the upgrade work on the SuperKEKB and Belle II instrumentations. The operation is planned to resume in autumn 2023. Many world-leading results in heavy flavor decays will be obtained with $\mathcal{O}(1)$ ab^{-1} data in the near future, and then with $O(10)$ ab^{-1} toward the next decade.

14.8 Heavy flavors at the HL-LHC

Tim Gershon

Proton–proton collisions at energies of the LHC collider result in production of vast quantities of beauty and charm quarks. The production cross-sections at centre-of-mass collision energies of 7−14 TeV are around 100 μb for beauty hadrons and an order of magnitude larger for charm hadrons [4767,4768]. Thus, for each fb^{-1} of integrated luminosity, there are around 10^{11} beauty hadrons and around 10^{12} charm hadrons produced. As there are no constraints on the quantum numbers of the particles that emerge from the primary interaction followed by hadronization, essentially all physically possible hadrons are produced in LHC collisions. Since effects of double parton scattering, where multiple heavy quark–antiquark pairs are produced in the same proton–proton interaction, are significant, this includes states with more than one heavy-flavor quark.

The LHC and its high luminosity upgrade therefore provide a unique and unprecedented opportunity to learn about QCD from the production and decays of these hadrons. However, in order for this experimental program to be realized, it is necessary to have dedicated and state-of-the-art detection capability. In particular, focusing on charged particle detection, one needs:

- acceptance, with good reconstruction efficiency, in the kinematic region that the majority of the decay products will travel through (production of beauty and charm hadrons at the LHC predominantly occurs at small angles to the beam axis);
- good momentum resolution, so that narrow signal peaks in invariant mass distributions originating from states close to each other in mass can be resolved
- capability to discriminate between different final-state charged particles, in particular electrons, pions, muons, kaons and protons;
- ability to reject background from random combinations of particles, which must be achieved in real-time (online) in order to avoid the data rate overwhelming the available computing resources.

As regards the last point, the presence of one or more well-identified muons in the decay, above a p_T threshold of typically a few GeV, is a signature which has traditionally been used in triggers for heavy-flavor physics in hadron collider experiments. This signature continues to be exploited at the LHC, and will be throughout the HL-LHC era. However, the fact that the ground-state hadrons with heavy-flavor quantum numbers can only decay by the weak interaction provides an extremely valuable handle, as their non-negligible lifetimes cause a significant – and potentially measurable – displacement between the production and decay vertices. Consider for example a state of mass 5 GeV and lifetime $\tau = 1$ ps. If produced with 50 GeV momentum, corresponding to a Lorentz boost factor of $\beta\gamma = 10$, it will travel a mean distance of $\beta\gamma c\tau \approx 3$ mm before decaying. Therefore if the vertex position can be reconstructed with resolution significantly better than this, the potentially huge background from combinations of the large numbers of tracks produced at the primary proton–proton interaction point can be removed. Indeed, while proton–proton collisions are generally considered a difficult (or "dirty") environment due to the large numbers of particles produced, if one only needs to consider particles originating from displaced secondary vertices the signatures can be extremely clean.

The LHCb detector is designed in order to provide this detection capability. It is the only dedicated heavy-flavor experiment at the LHC, although ALICE, ATLAS and CMS all have some ability to reconstruct heavy-flavor hadrons. The original LHCb detector operated during Runs 1 and 2 of the LHC, 2011–12 and 2015–2018 respectively, enabling the collection of a data sample corresponding to 9 fb^{-1} of proton–proton collisions. This has led to a wealth of publications on a diverse range of topics. An upgraded detector has been installed during the LHC long shutdown 2 (2019–2021) and is designed for the collection of a sample of 50 fb^{-1} during Runs 3 and 4, with significantly improved efficiencies for many channels of interest. In order to exploit fully the flavor-physics potential of the HL-LHC, a second major upgrade of the LHCb detector is now being planned [4769]; this will allow 300 fb^{-1} to be collected in the final operational periods of the HL-LHC. Together with the 3 ab^{-1} anticipated to be collected by ATLAS and CMS, this provides exciting potential in heavy-flavor physics (Fig. 434).

The above discussion focussed on charged particles. For neutral particles it is much harder both to obtain good momentum resolution and to associate them correctly to the vertex they originated from, particularly bearing in mind that they will be reconstructed in the forward kinematic region. Nonetheless, information from calorimeters can be used to broaden the flavor-physics program to include decays with photons in the final state, including those from neutral pion decays and from bremstrahlung emission from electrons. Moreover, timing information can be used to provide

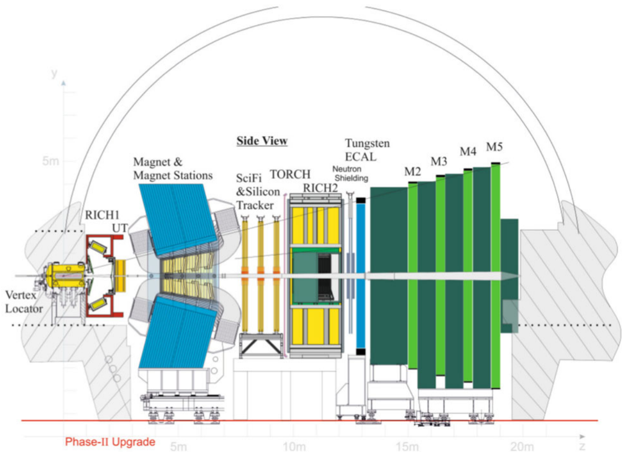

Fig. 434 The proposed LHCb Upgrade II detector [4769]

some capability to associate calorimeter clusters with reconstructed vertices; indeed the addition of timing capability is central to the plans for LHCb Upgrade II, not only for the calorimeter but also for the vertex and charged hadron identification detectors [4769].

The opportunities in flavor physics at the HL-LHC are discussed in Ref. [4770], while the LHCb Upgrade II physics program is described in Ref. [2633]. Here only a brief summary of some aspects that are most interesting with regard to QCD are discussed. The focus is primarily on LHCb, but areas where other LHC experiments can contribute are also mentioned.

CP violation

Violation of symmetry under the combined charge conjugation and parity (CP) operation can occur in the Standard Model as the complex phase in the Cabibbo–Kobayashi–Maskawa (CKM) quark mixing matrix [86,4028] results in the charged-current weak-interaction coupling constants being different for quarks and antiquarks. The uniqueness of the origin of all CP violating effects in the SM – and the knowledge that additional sources must be present in nature in order to explain the baryon asymmetry of the Universe – make experimental probes of CP-violating phenomena a well-motivated way to search for physics beyond the SM.

There are a number of theoretically clean probes of CP violation, where QCD effects that may otherwise render the interpretation of results difficult are either minimal or can be determined directly from data. In particular, the determination of the phase

$$\gamma \equiv \arg\left(-\frac{V_{ud}V_{ub}^*}{V_{cd}V_{cb}^*}\right)$$

from $B \to DK$ and similar processes is essentially unaffected by theoretical uncertainties in the SM [4731]. However, there are many more measurements where uncertainties related to QCD need to be reduced in order to obtain the best sensitivity to physics beyond the SM. An interesting class of such measurements are those where decays can be related by flavor symmetries, as the breaking of this symmetry by QCD can often be calculated theoretically. The fact that both B^0 and B_s^0 mesons can be studied at the LHC opens a number of possibilities involving U-spin symmetry, related to interchange of d and s quarks. For example, the determination of the phase

$$2\beta \equiv 2\arg\left(-\frac{V_{cd}V_{cb}^*}{V_{td}V_{tb}^*}\right)$$

from $B^0 \to J/\psi K_S^0$ decays has a small but hard-to-quantify uncertainty due to subleading amplitudes; the size of this effect can be constrained using the U-spin partner $B_s^0 \to J/\psi K_S^0$ decays [4771,4772]. In a similar way, the $B_s^0 \to K^{*0}\overline{K}^{*0}$ decay is considered a golden channel to probe for CP-violation effects beyond the SM, as theoretical uncertainties can be constrained from the U-spin partner $B^0 \to K^{*0}\overline{K}^{*0}$ decay [4773–4775].

The above examples are special cases where the final state is left unchanged by U-spin. Similar ideas can be also exploited for U-spin pairs where this is not the case, such as $B^0 \to D^+D^- \leftrightarrow B_s^0 \to D_s^+D_s^-$, $B^0 \to \pi^+\pi^- \leftrightarrow B_s^0 \to K^+K^-$ and $B^0 \to K^+\pi^- \leftrightarrow B_s^0 \to K^-\pi^+$ [4776–4781]. In these cases however the U-spin breaking effects can be larger, making it harder to use them for precise tests of the SM. However, with the data samples available at the HL-LHC it will be possible to reverse the argument: assuming the SM, the extent of U-spin breaking in these decays can be precisely measured and compared to theoretical calculations. Moreover, the samples will be large enough that similar exercises can also be done for suppressed partner decays (e.g. $B^0 \to D_s^+D_s^- \leftrightarrow B_s^0 \to D^+D^-$ and $B^0 \to K^+K^- \leftrightarrow B_s^0 \to \pi^+\pi^-$) where effects of subleading amplitudes are enhanced. Studies of U-spin breaking and its influence on CP violation in the charm meson decays $D^0 \to K^+K^-, \pi^+\pi^-, K^-\pi^+$ and $K^+\pi^-$ provide a complementary probe [4782–4785]. These measurements will provide a unique handle on our understanding of flavor symmetry breaking effects in QCD.

A number of null tests of the SM can be made by testing the prediction of small or vanishing CP-violating effects in specific processes. In such cases it is necessary to ensure that theoretical uncertainties in the prediction are well under control. One example is the determination of the phase ϕ_s through $B_s^0 \to J/\psi\phi$ and similar processes, where LHCb, ATLAS and CMS all have potential to reach sufficient precision to observe a non-zero effect at the SM rate [4786–4788]. Another example is the corresponding phase in the neutral charm system, ϕ_D, where recent progress measuring the mixing parameters has set the stage for precise determinations when more data are available [4789,4790]. It remains an open question to what extent QCD effects can enhance SM CP violation in the charm sector [4791], and further progress on this front will be essential.

Data on two-body decays are in general easier to interpret than those in three- or multi-body decays (including quasi-two-body resonant contributions). Nevertheless, the latter remain of great interest as interference effects can provide sensitivity to additional CP-violating observables: the range of effects observed in three-body B meson decays illustrate this clearly [4792–4796]. Overcoming hadronic uncertainties is challenging, but with HL-LHC data ambitious coupled-channel analyses will allow additional constraints. In particular, effects related to $\pi\pi \leftrightarrow KK$ scattering can be fitted for directly in coupled-channel analyses of B^0 and (separately or simultaneously) B^0_s decays to the $J/\psi\pi^+\pi^-$ and $J/\psi K^+K^-$ final states [4797]. Similar analyses can also be carried out in $B^0_{(s)} \to \overline{D}^0\pi^+\pi^-$ and $\overline{D}^0K^+K^-$ decays, and in $B^+ \to K^+\pi^+\pi^-$ and $K^+K^+K^-$ decays. The latter, and also the more suppressed $B^+ \to \pi^+\pi^+\pi^-$ and $\pi^+K^+K^-$ decays, are known to feature regions of phase space with large CP violation, which could be used to test the SM if theoretical uncertainties can be controlled sufficiently.

As mentioned above, the CKM angle γ can be determined with negligible uncertainty using $B \to DK$ and related decays. The reason for this is that by combining results with multiple different D decay modes, all hadronic parameters can be determined from data. Recent examples of such combinations can be found in Refs. [4798,4799]. From the point of view of understanding QCD, this provides an opportunity to compare the values of the hadronic parameters obtained from the combinations to those from theoretical calculations. In the case of multibody decays such as $B \to DK\pi$, the parameters that can be obtained include those related to variation of hadronic phases across the phase-space of the decay [4800,4801]. These can be determined model-independently as a by-product of the measurement of γ, thus providing insight into a poorly understand aspect of QCD.

Semileptonic decays and form factors

As discussed in Sect. 13.2.2, the rates of semileptonic b-hadron decays, $X_b \to X_c\ell^-\overline{\nu}_\ell$ depend on the square of the magnitude of the CKM matrix element V_{cb}. Here, X_b represents a hadron containing a b quark, X_c the corresponding hadron with b replaced by c, ℓ^- a negatively charged lepton and $\overline{\nu}_\ell$ the corresponding antineutrino. Thus, measurements of the rates can allow $|V_{cb}|^2$ to be determined if the form factors, which encode the probability for the X_c hadron to be produced in the final state as a function of the $\ell^-\overline{\nu}_\ell$ invariant mass squared (q^2), are known from theoretical calculations. Likewise, studies of $X_b \to X_u\ell^-\overline{\nu}_\ell$ transitions, with obvious definition of X_u, provide sensitivity to $|V_{ub}|^2$.

The reconstruction of decays involving neutrinos in the final state is challenging in the environment of a hadron collider, as one cannot exploit the kinematic constraints that are available in the $e^+e^- \to \Upsilon(4S) \to B\overline{B}$ system. Nonetheless, exploiting LHCb's capability in reconstruction of vertices and charged hadron identification, it has been possible to study semileptonic Λ^0_b (to $p\mu^-\overline{\nu}_\mu$ and $\Lambda^+_c\mu^-\overline{\nu}_\mu$) and $\overline{B}^0_s$ (to $K^+\mu^-\overline{\nu}_\mu$ and $D^+_s\mu^-\overline{\nu}_\mu$) decays [752,4147]. In each case measuring the ratio allows the cancellation of some potential sources of systematic uncertainty, leading to competitive measurements of $|V_{ub}/V_{cb}|^2$.

With the full HL-LHC statistics it will be possible to extend this program to the full range of b hadrons. This will provide complementary information to the determinations using B mesons alone, and will test QCD by comparison of the form factors in heavy-to-light transitions (such as $B \to \pi$) with those in heavy-to-heavy transitions. A particularly interesting example occurs in B^-_c decays, where study of $B^-_c \to D^0\mu^-\overline{\nu}_\mu$ could potentially allow a theoretically clean determination of $|V_{ub}|^2$. In fact, the large samples of B^-_c mesons that will be available at HL-LHC present a further opportunity, since these particles preferentially decay through transitions of the charm quark. Thus, $B^-_c \to \overline{B}^0_s\mu^-\overline{\nu}_\mu$ and $\overline{B}^0\mu^-\overline{\nu}_\mu$ decays could be used to make novel measurements of the squared magnitudes of V_{cs} and V_{cd}, respectively, thereby allowing a quantitative comparison of the form factors observed in data with those calculated from first principles QCD.

Understanding QCD effects encoded in form factors and, more generally, the effects of hadronization in semileptonic b-hadron decays, will also be crucial for tests of lepton universality at HL-LHC. Within the Standard Model the W and Z couplings to all lepton flavors are identical; any deviation from this prediction would provide a clear signature of non-SM physics contributing to the decay amplitude. Due to the heavier τ mass, compared to the electron and muon, contributions from different form factors have to be understood in order to predict the SM value of the ratio of branching fractions [4120–4122]. Given the indications of potential violation on lepton universality in previous measurements of these processes at the BaBar, Belle and LHCb experiments [4743–4748] there is intense interest in the significantly more precise results that the HL-LHC can potentially provide. The challenge will be to control experimental systematic uncertainties to the required level; this is even harder for ATLAS and CMS than for LHCb, but if the background composition can be understood then all three experiments may be able to test the SM in this sector.

Rare decays

Decays which proceed by flavor-changing neutral currents are highly suppressed in the Standard Model as they involve loop diagrams, typically with additional CKM suppression factors. As physics beyond the SM does not have to have the same structure, the rates and phase space distributions of these channels allow detailed tests for new contributions to the amplitudes.

In order to obtain the best sensitivity from these measurements, it is necessary to have QCD uncertainties, related to the hadrons in initial, intermediate and final states of the decay, under excellent control. Thus, typically the theoretically cleanest probes are decays involving leptons or photons. However, even in these cases there can be residual QCD effects that must be well understood. Recent progress is therefore focussed mainly on theoretically clean channels and data-driven approaches to constrain hadronic parameters.

The purely leptonic $B^0_{(s)}$ meson decays are a good example of channels where theoretically clean predictions are possible. Moreover, the helicity-suppression of these processes that occurs in the SM – resulting in small branching fractions for the dimuon and, especially, dielectron, processes – need not be replicated in beyond SM contributions to the amplitudes, so that large deviations from the SM predictions are possible in principle. The decay rates for these processes depend on the $B^0_{(s)}$ decay constants, which can be (and have been) calculated in lattice QCD to good precision [301]. The experimentally most amenable channel is the dimuon final state; the $B^0_s \to \mu^+\mu^-$ decay has been observed by LHCb, CMS and ATLAS, and the sensitivity to the B^0 decay branching fraction approaches the level required to observe it at the SM expectation [4802–4804]. The limits on decays to dielectron and ditau final states remain considerably above the SM expectations [4805,4806].

Further improvement in the knowledge of the $B^0_{(s)} \to \mu^+\mu^-$ branching fractions and their ratio is well motivated, as the experimental uncertainties remain larger than those for theory. These measurements can be expected as a key component of the HL-LHC era heavy-flavor physics programs of all of the LHCb, CMS and ATLAS experiments: it is anticipated that relative uncertainties on $\mathcal{B}\left(B^0_s \to \mu^+\mu^-\right)$ of 4%, 7% and 12–15% can be achieved by each of the three experiments, respectively [4769,4807,4808]. In addition, the increasingly large sample sizes will make additional probes possible. In particular, the $B^0_s \to \mu^+\mu^-$ effective lifetime can be used as an independent probe for physics beyond the SM [4809], with first measurements already available, albeit with large uncertainties. With the full HL-LHC statistics it will also be possible to measure CP violation parameters in this decay, providing one more independent probe, also with negligible theoretical uncertainty.

The $b \to s\ell^+\ell^-$ and $b \to d\ell^+\ell^-$ processes can also be studied through decays in which the s or d quark is found in the final state. These do not have the helicity suppression of the purely leptonic decays, but as a corollary have sensitivity to additional effective field theory operators. A large range of final states and a large number of observables can be studied. Those related to angular distributions in $B \to V\ell^+\ell^-$ processes are particularly interesting (where V is a vector meson, i.e. decays such as $B^0 \to K^{*0}\ell^+\ell^-$). In these measurements, all relevant operators can be constrained from data. Indeed, as discussed in Sect. 13.4, existing measurements of the rates and of angular observables in $B^0 \to K^{*0}\mu^+\mu^-$ and $B^0_s \to \phi\mu^+\mu^-$ decays constrain possible contributions from physics beyond the SM and, excitingly, hint at these contributions being non-zero [4753,4810–4813]. However, the possibility of these effects being caused by larger than expected non-perturbative QCD corrections is not yet ruled out [4270,4272].

Progress in this area, with the larger data samples available at the HL-LHC, can be expected in two complementary approaches. Firstly, model-dependent fits to the data can be used to attempt to constrain the non-perturbative QCD effects within specific parameterizations [4262,4268,4274,4814]. Secondly, the SM property of lepton universality in these processes can be tested – comparison of equivalent parameters for decays involving $\mu^+\mu^-$ and e^+e^- pairs provide theoretically clean tests of the SM. While the second case can provide an unambiguous signal of physics beyond the SM, this is only possible if the new physics violates lepton universality. Progress on both fronts is therefore essential in order to be able to constrain the full range of potential operators. Early measurements from LHCb of the ratios of decay rates for $B^+ \to K^+\ell^+\ell^-$ and $B^0 \to K^{*0}\ell^+\ell^-$ (with $\ell = e, \mu$) give tantalizing hints of disagreement with SM predictions, but do not reach a level of significance for which strong claims would be justified [4750,4815]. In addition to larger data samples, improved electron reconstruction can help to reduce the uncertainties in future measurements. The range of lepton universality tests can also be expected to be increased in future beyond the rates alone to include also angular observables.

A further way to test the SM is through its prediction that the photon emitted in $b \to s\gamma$ flavor-changing neutral-current transitions should be predominantly left-handed, as a consequence of the V−A structure of the SM weak interaction. This can be tested in a number of ways, including through studies of the decay-time dependence of $B^0 \to K^{*0}\gamma$ and $B^0_s \to \phi\gamma$ decays, and of the angular distributions in $\Lambda^0_b \to \Lambda\gamma$ decays [4816–4819]. The angular distribution of $B^0 \to K^{*0}e^+e^-$ decays at very low e^+e^- invariant mass also probes the same physics [4820]. However, the statistically most powerful approach involves analysis of the phase-space distribution of $B^+ \to K^+\pi^+\pi^-\gamma$ decays, complemented by measurement of the decay-time dependence of the $B^0 \to K^0_S\pi^+\pi^-\gamma$ process [4821–4825]. To realise the full potential of this method will require improved understanding of hadronic effects in the $K\pi\pi$ system. The large data samples available at the HL-LHC will provide a number of ways to acquire such knowledge, including measurement

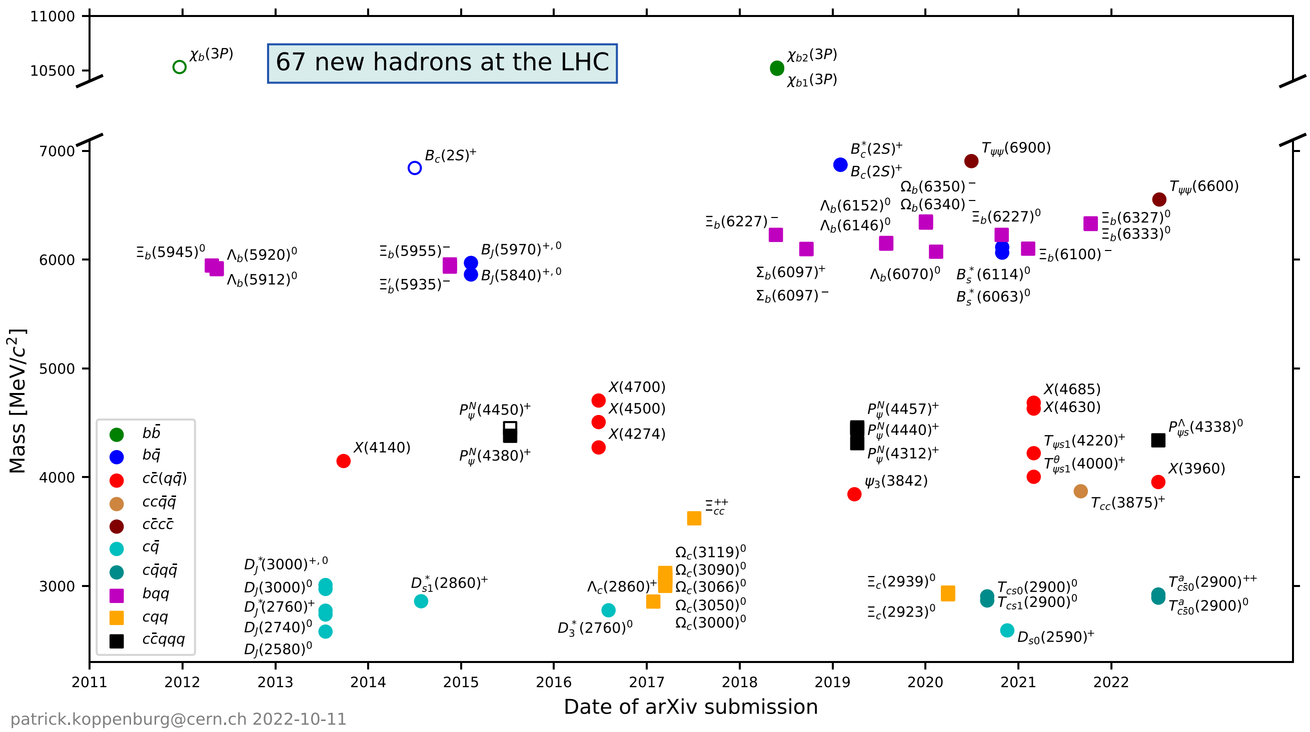

Fig. 435 Discoveries of hadrons at the LHC, by year of arXiv submission [4826]. Only states observed with significance larger than 5σ are included

of the corresponding processes where the final-state photon is replaced by a J/ψ meson.

Hadron spectroscopy

As mentioned previously, the copious production of beauty and charm quarks in LHC collisions provides opportunities for detailed studies of hadron spectroscopy, including discoveries of previously unmeasured states. Various production mechanisms are available, including central exclusive production. However, the two mechanisms for which studies have proved most productive to date are so-called prompt production, where a hadron is produced directly in a proton–proton collision (including via strongly decaying resonances), and production in weak decays of a heavier hadron. Prompt decays tend to have large backgrounds, and are limited to cases with a distinctive signature – but they provide the only possible approach for hadrons too heavy to be produced in weak decays. Weak decays of heavy hadrons can provide an extremely clean environment; moreover this approach makes possible determination of the quantum numbers of intermediate resonances produced in multibody final states.

At the time of writing, 67 hadrons have been observed for the first time at the LHC as illustrated in Fig. 435. As discussed in Sects. 8.5 and 9.4, these include a number of states that do not fit into the conventional scheme of $q\bar{q}$ mesons and $qq'q''$ baryons. One of the most exciting topics, related to furthering knowledge of QCD, is what new hadrons may be discovered at the HL-LHC. This is, of course, impossible to predict with confidence; nonetheless there are certain areas where progress appears likely. In what follows states with four and five quarks are referred to as tetraquarks and pentaquarks respectively, with no prejudice as to their internal binding mechanisms – indeed, addressing the question of how such states are bound is one of the main goals for the HL-LHC in this area – and the naming convention of Ref. [2522] is used.

Perhaps the most striking discovery of exotic hadrons to date is that of the P_ψ states, observed as resonances decaying to $J/\psi p$, and hence with minimal quark content $c\bar{c}uud$ in $\Lambda_b^0 \to J/\psi p K^-$ decays [2885,2886]. The proximity of the P_ψ masses to $\Sigma_c D$ thresholds has led to much speculation on their nature. Further progress requires the determination of the P_ψ spin-parity quantum numbers. Discoveries of other production modes and decays to other final states will also provide insight. The data samples of the HL-LHC should allow LHCb to perform such studies, and also to make detailed studies of lineshapes.

The P_ψ pentaquarks contain a $c\bar{c}$ pair, as do all tetraquarks that had been observed prior to 2020. This fueled theoretical speculation that a $c\bar{c}$ component, or at least the presence of two heavy quarks or antiquarks, was necessary for the formation of exotic hadrons. Such models were, however, ruled out by the observation of T_{cs} tetraquarks decaying to D^+K^-, produced in $B^- \to D^-D^+K^-$ decays [4827,4828]. This observation implies the existence of many more tetraquarks, containing different sets of quark flavors, which may be discoverable with the HL-LHC. As such states are observed and can be arranged in families, it will allow for a new understanding of strong interactions in much the same way as occurred for the "particle zoo" in the 1960s and 70s.

Even if a $c\bar{c}$ component is not required for the formation of exotic hadrons, a J/ψ meson in the final state facilitates the observation of new particles due to the clean signature provided by the J/ψ dimuon decay. This has been exploited in the observations of $T_{\psi\psi}$ states decaying to $J/\psi J/\psi$ [2619,4829,4830]. The discovery of states with minimal quark content of $cc\bar{c}\bar{c}$ motivates searches for partner states, including decays to final states such as $J/\psi \chi_{c1}$, which may cause feed-down into the $J/\psi J/\psi$ spectrum, as well as for tetraquarks with other fully heavy-quark content (e.g. $b\bar{b}c\bar{c}$). Knowledge of bottomonia decays to double charmonia final states will also be necessary for a full understanding in this area.

The first doubly charmed hadron, the Ξ_{cc}^{++} state, was observed by LHCb in 2017 [2615], and precise measurements of its mass and lifetime have followed [2617,2618]. Its flavor partners, the Ξ_{cc}^{+} and Ω_{cc}^{+} baryons have also been searched for, but not yet discovered [2889,4831,4832]. The reason for this may be the shorter lifetimes that are expected for these states, since a short lifetime makes it harder to separate signal from background. The improved vertex resolution of the upgraded LHCb detector, together with larger data samples, will hence provide excellent prospects for discovery. Doubly heavy states containing beauty and charm quarks also appear within reach, while double beauty states appear more challenging.

The discovery of the T_{cc}^{+} tetraquark, seen in prompt production as a narrow structure decaying to $D^0D^0\pi^+$ [1067,2566], complements both the previous observations of the Ξ_{cc}^{++} baryon and of tetraquarks with $c\bar{c}$ content. Its mass is only just above threshold for D^0D^{*+} decays, supporting the hypothesis that ground-state tetraquarks containing beauty and charm or double beauty (T_{bc} or T_{bb}), which are expected to be more tightly bound, may be stable to strong decays. If so, they would decay only via the weak interaction and hence have lifetimes comparable to those of ground state beauty and charm hadrons. As such, they may have displaced vertex signatures that could be exploited in the LHCb experiment to enhance their observability [4833]. It is also possible that P_{cc}, P_{bc} and P_{bb} pentaquarks could be detected, with the appropriate analysis strategy depending on whether or not they are stable against strong decay. Furthermore, it is plausible (albeit speculative) that six quark, dibaryon states containing at least two beauty or charm quarks may be measurable. Studies of hadron spectroscopy with the HL-LHC data sample may therefore provide dramatic breakthroughs in the knowledge of the possible range of states that can be bound together within QCD.

14.9 High-p_{T} physics at HL-LHC

Massimiliano Grazzini and **Gudrun Heinrich**

14.9.1 Introduction

The High-Luminosity LHC (HL-LHC) is scheduled to start operation in 2029. By colliding protons with an instantaneous luminosity that is five times higher than what is achieved at the LHC, the HL-LHC is expected to deliver data corresponding to an integrated luminosity of 3000 fb^{-1} by the end of the 2030s, which is a factor of 20 more than what has been collected so far. Despite the highly challenging experimental environment, such an increased dataset – collected with upgraded detectors – has an immense physics potential: it will give access to the rarest phenomena, and will be critical to reduce systematic uncertainties or bypass their limitations with new analyses, leading to measurements of unprecedented precision. It will allow us to achieve a sensitivity to sectors of Beyond-the-Standard-Model (BSM) phenomena that are beyond the reach of current analyses, and will ultimately help us to get closer to answering fundamental questions of particle physics.

14.9.2 Higgs properties

The study of Higgs boson (H) properties is central in the HL-LHC physics programme. Since its discovery in 2012, analyses related to the Higgs boson have significantly expanded, and have now turned into a vast campaign of precision measurements, with fundamental opportunities to indirectly constrain the Higgs boson width and to access its trilinear coupling. Small deviations from the SM can be described in a consistent framework by using effective field theory (EFT).

The main measurements of Higgs boson properties are based on five production modes (gluon fusion ggF, vector boson fusion VBF, associated production with a W or Z vector boson or with a top-quark pair) and five decay modes: $H \to \gamma\gamma, ZZ, WW, \tau\tau, b\bar{b}$. The $H \to \mu\mu$ and $Z\gamma$ channels should become visible in the future. The rate measurements in the production and decay channels mentioned above yield measurements of the Higgs boson couplings in the so-called "κ-framework" [4834]. The latter introduces a set of scaling factors κ_i that linearly modify the couplings of the Higgs boson to the corresponding SM elementary particles, including the effective couplings to gluons and photons. The projected uncertainties, combining ATLAS and CMS, are summarized in Fig. 436. Note that theory uncertainties are assumed to be halved with respect to their current values.

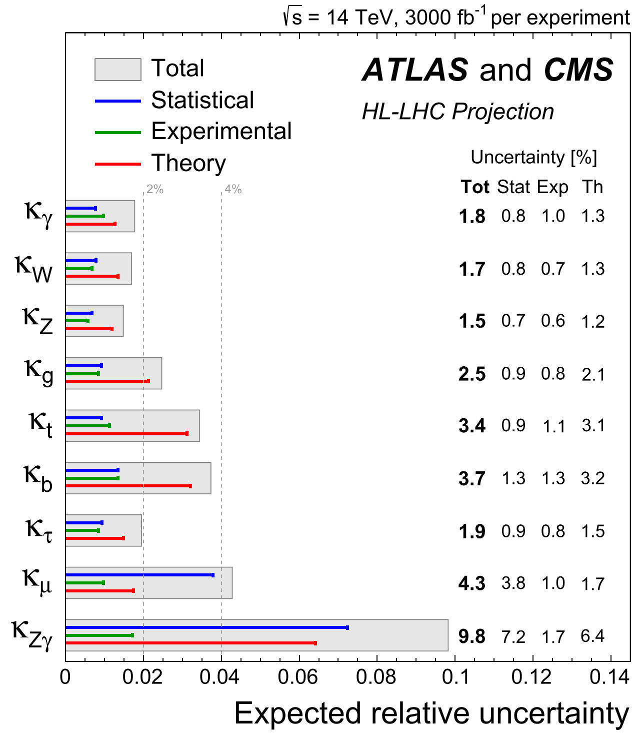

Fig. 436 Projected uncertainties for the scaling parameters κ_i, combining ATLAS and CMS: total (grey box), statistical (blue), experimental (green) and theory (red) uncertainties. From Ref. [4835]

Except for rare decays, the overall uncertainties will be dominated by the theoretical systematics, with a precision close to the percent level. These coupling measurements assume the absence of sizable additional contributions to Γ_H. As observed in Ref. [4836], the signal-background interference in the production of Z-boson pairs is sensitive to Γ_H. Measuring the off-shell four-lepton final states and assuming that the Higgs boson couplings can be extrapolated in the off-shell region from their SM values, the HL-LHC will extract Γ_H using this indirect measurement with a 20% precision at 68% CL [4835].

The production of Higgs boson pairs is a central process to access the Higgs trilinear coupling. The Run 2 experience in searches for Higgs boson pair production led to a reassessment of the HL-LHC sensitivity, including additional channels that were not considered in previous projections. ATLAS and CMS anticipate a sensitivity to the HH signal of approximately 3σ per experiment, leading to a combined observation sensitivity of 4σ. These analyses lead to the combined likelihood profile as a function of κ_λ shown in Fig. 437.

It should be noted that the upper limit on the signal strength for HH production can reach the SM expectation already for Run 3 by combining ATLAS and CMS results if the improvements in the reconstruction and analysis techniques continue at the same pace (see e.g. Elisabeth Brost, talk at Higgs10 meeting, CERN, July 2022).

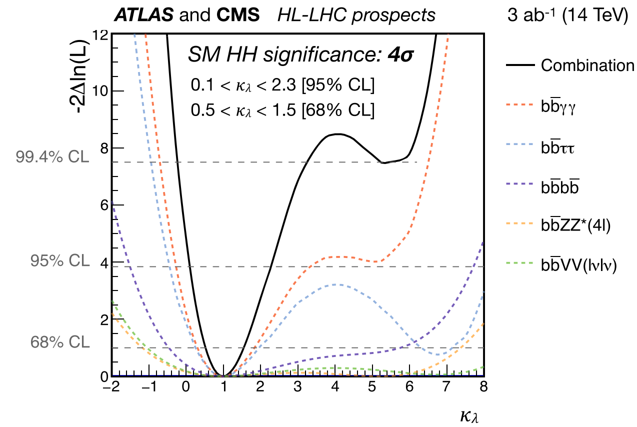

Fig. 437 Projected combined HL-LHC sensitivity to the Higgs boson trilinear coupling expressed in terms of κ_λ, from direct search channels. From Ref. [4835]

14.9.3 Multiple gauge bosons

The study of multiple gauge boson production is of crucial importance to test the EW gauge symmetry, since it can signal the presence of anomalous gauge couplings [4837]. At HL-LHC, evidence for the production of three gauge bosons can be obtained at the 3σ level in the WWZ and WZZ channels and at the 5σ level in the WWW channel considering the fully leptonic decay modes [3940]. Following the first observation of vector-boson scattering (VBS) at the LHC, the HL-LHC is expected to provide a more complete picture of these processes, including the option to measure polarized components, thanks to the higher statistics and improved detectors.

14.9.4 New-physics searches

The HL-LHC will allow us to test BSM phenomena that are beyond the reach of current analyses [1279]. Many BSM models predict the existence of new particles, which can be searched for at HL-LHC, exploiting the much larger statistics and detector upgrades.

In the case of supersymmetry (SUSY), the extension of the kinematic reach is reflected in improved sensitivity to sleptons, gluinos and squarks. In the strong SUSY sector, HL-LHC will probe gluino masses up to 3.2 TeV, in R-parity conserving scenarios and under several possible assumptions on the gluino prompt decay mode. This significantly extends the reach of LHC Run 2. In the context of R-parity conserving models, scenarios in which the mass difference between the produced superpartners and the lightest superpartner (LSP) they decay into is small (usually called *compressed* SUSY) are the most difficult to study experimentally, and have been barely covered at the LHC till now. At the HL-LHC, these scenarios will be studied by using mono-jet and mono-photon signatures as well as VBF production.

An interesting scenario in the search for dark matter is the one containing a dark photon that couples very weakly to charged particles. Prospects for an inclusive search for dark photons decaying into muon or electron pairs indicate that the HL-LHC could cover a large fraction of the theoretically favored parameter space.

The flavor anomalies in B-decays suggest the possible presence of new states, such as Z' or leptoquarks (LQ), coupling to second and/or third generation SM fermions. The HL-LHC will be able to cover a significant portion of the parameter space of these models, with an exclusion reach up to 4 TeV for the Z'. Pair produced scalar LQs coupling to μ (τ) and b-quarks, on the other hand, can be excluded up to masses of 2.5 (1.5) TeV, depending on the assumptions on the couplings.

14.9.5 QCD challenges

Already now the LHC experiments have reached a very high level of sophistication in the reconstruction of collision events, thereby making precise measurements possible despite the complex environment and substantial pileup.

Even though significant progress has been made in QCD and electro-weak (EW) calculations for hard processes in the last few years (see Sect. 11.1), further progress will be needed to avoid theory uncertainties to become the limiting factor in interpreting a wide range of HL-LHC data. For example, in the case of Higgs boson couplings, the projections of Fig. 436 show that theory uncertainties will be a limiting factor even if reduced by a factor of two with respect to their current values. Progress on the theory side is therefore needed and it is indeed expected in the following areas:

1. **Parton distribution functions:** All hard scattering reactions at the LHC are eventually initiated by a partonic collision. The parton scattering rate, which is computed perturbatively, is weighted by the PDFs, whose knowledge is therefore required to extract fundamental couplings from cross section measurements or from kinematic distributions. PDFs are also a fundamental input to predict the tails of the distributions of SM processes at high Q^2 or high p_T, which in turn allow us to probe possible new physics effects. The current knowledge of PDFs will be improved at HL-LHC by accurate measurements of SM processes with jets, vector bosons and top quarks. LHCb data also have the potential to further constrain the PDFs. At scales $Q > 100\,\text{GeV}$ the HL-LHC data can reduce PDF uncertainties by a factor between 2 and 4, depending on the process and on the assumptions on systematic uncertainties [3940].
2. **Benchmark processes at high accuracy:** The experimental precision for many benchmark $2 \to 1$ and $2 \to 2$ processes (the most significant example being Drell–Yan lepton pair production) is likely to approach the 1% level, over a substantial range of phase space. Perturbative QCD predictions at next-to-next-leading order (NNLO) normally do not reach 1% precision, and N^{3}LO accuracy might be needed for a range of $2 \to 1$ and $2 \to 2$ processes. For example, N^{3}LO predictions for Higgs and vector boson production are already available [1949,3461,3462,3468,3469,3552,4838] and are crucial to control perturbative uncertainties. The improved theoretical control of simple processes will in turn improve our knowledge of PDFs, allowing N^{3}LO PDF fits, with impact on the whole range of LHC processes, and will also increase the sensitivity to BSM effects manifesting themselves as small deviations from SM predictions. A first approximate N^{3}LO PDF fit has been recently presented in Ref. [3101].
3. $2 \to 3$ **processes at few-percent accuracy:** There are a number of crucially important signal and background processes that involve a $2 \to 3$ scattering structure at parton level; these are at the current frontier of NNLO calculations.
   While calculations of 3-jet production rates became recently available [3426], processes like $t\bar{t}H$, $t\bar{t}V$, $H +$ 2 jets are only known up to NLO and would benefit from the extension to NNLO.[124] The $t\bar{t}H$ cross section, e.g., is now measured with roughly 15% statistical precision and is expected to be known with a statistical precision of $\sim 2\%$ at the end of the HL-LHC. Without NNLO QCD and NLO EW accurate calculations for signal and backgrounds, this experimental precision cannot be matched on the theory side, thereby limiting the exploitation of the results for physics studies.
   A significant amount of work is currently being devoted to break the $2 \to 3$ barrier for two-loop amplitudes involving massive particles. At the same time, an effort is ongoing to improve available methods to isolate and cancel infrared singularities (see Sect. 11.1 for more details). In the HL-LHC era the complete availability of combined NNLO precision in the strong coupling and NLO precision in the EW coupling would be desirable.
4. **Accuracy at high** p_T: Current measurements have only explored a limited range of the available phase space. NNLO accurate differential cross sections pave the way to more detailed data/theory comparisons in less populated phase-space regions where new physics effects could be hidden.
   An important example is provided by high-p_T Higgs pro-

[124] First NNLO results for inclusive $t\bar{t}H$ production have been recently presented in Ref. [4839].

duction. The ATLAS and CMS collaborations anticipate an $\mathcal{O}(10\%)$ precision in the Higgs boson production rate for $p_T \geq 350\,\text{GeV}$ at the end of the HL phase of the LHC [4835].
The recent computations of $2 \to 2$ amplitudes mediated by massive quarks [3405,4840], combined with NNLO calculations in the heavy-top limit [3457,3458,4841–4843] offer a comparable precision in the SM prediction, and will therefore allow us to disentangle possible new physics effects in this region.
5. **Bottlenecks in NLO multi-particle simulations:** The full deployment of NLO precision through automated MC frameworks in the huge range of HL-LHC analyses raises important technical challenges. Establishing the predictivity of MC tools at precision levels of order 10% – as well as their correct usage within the experiments – will require quantitatively and qualitatively unprecedented validation work. Already now, the accuracy at which event samples for $2 \to 4$ processes can be calculated at NLO is limited by dramatic efficiency bottlenecks related to the poor convergence of the phase-space integration and by various other technical aspects. The HL-LHC era will require efficiency improvements by an order of magnitude. This can only be achieved through a significant step forward in the optimization of event generators and new techniques in the calculation of amplitudes.
6. **Theory systematics:** The appropriate estimate of theory uncertainties in the presence of experimental cuts or in the context of sophisticated multi-variate analyses is a challenging problem. A typical example is provided by $t\bar{t}H$ analyses in the $H \to b\bar{b}$ decay mode. The sensitivity is presently limited by theory uncertainties in the $t\bar{t}b\bar{b}$ QCD background. In this kind of analyses, MC predictions for the large QCD background are constrained by data through a profile likelihood fit of several kinematic distributions in different event categories. In this context, theoretical predictions for the correlations across different categories and kinematic regions play a key role. All related uncertainties, e.g. at the level of NLO matrix elements, parton showers and NLO matching, need to be properly identified and modelled. This task is further complicated by the presence of multiple scales, which may require resummations. This type of problem is characteristic for a broad range of LHC analyses; its solution will require a joint effort between theorists and experimentalists.
7. **Non-perturbative effects:** While the perturbative computations follow a systematic approach based on perturbation theory and factorization, our understanding of non-perturbative effects is still quite rough. With the increasing accuracy of perturbative calculations, which in some cases now reach the N^{3}LO level, non-perturbative effects might become relevant, also in inclusive observables. Moreover, in the case of measurements dealing with hadronic final states, the poor control of the hadronization stage limits the precision that can be attained, thereby potentially affecting the extraction of important parameters, such as the top quark mass.
8. **Resummation and parton showers:** For key observables depending on disparate scales, advances in the all-order resummation of large logarithmic corrections will be crucial. Such advances require to increase the logarithmic accuracy of the resummed calculations, but also the extension to multiple-differential resummations, the inclusion of power suppressed effects, as well as the understanding of sub-leading and super-leading structures (see Sect. 11.2). In parallel, work towards the extension of the logarithmic accuracy of parton showers will be essential (see Sect. 11.3).
9. **BSM effects:**
The great success of the SM in describing all phenomena observed at the LHC suggests that the key to a potential discovery of new physics is precision. Precision measurements indeed provide an important tool to search for BSM physics associated to mass scales beyond direct reach of the LHC. EFT frameworks, where the SM Lagrangian is supplemented with additional operators built from SM fields, consistent with gauge symmetries and based on a well-defined counting scheme, allow us to systematically parameterize BSM effects and their modifications to SM processes. These operators can either modify existing SM couplings, or generate new couplings. In the case of BSM operators that mix with the SM ones, if r is the relative precision on a given physical observable, the new physics mass scale Λ that can be probed with this observable will scale as $1/\sqrt{r}$ in the generic case.

14.9.6 Outlook

While the HL-LHC offers great opportunities due to the enormous reduction of statistical uncertainties compared to previous LHC runs, some measurements remain difficult and will leave questions that could be addressed more straightforwardly with the great precision that future lepton colliders, such as the ILC [4844], CEPC [4845], FCC-ee [4846] or CLIC [4847] could achieve, or with the impressive energy reach and statistics a future hadron collider (FCC-hh [4848]) could provide. For example, the trilinear Higgs boson self-coupling – a parameter which is crucial to probe the mechanism of EW symmetry breaking – is expected to be constrained with an uncertainty of 50% after the HL-LHC runs, as shown in Fig. 437, while a combination of FCC-ee and HL-LHC results could reach a precision of about 30%, and a future hadron collider operating at a center-of-mass energy of 100 TeV could achieve a clear measurement with a precision of about 5% [4849]. Similar arguments hold for other quantities that are important to probe the SM at an unprecedented level of precision, such as the W-boson mass, the couplings of the Higgs boson to light fermions, or the line-shape and therefore the total width of the Higgs boson [4850].

Apart from the potential of future lepton colliders to find hints for new phenomena through a scrutiny of the Higgs sector and other SM particles and interactions, they offer new possibilities to search for physics beyond the SM, including the production of dark matter particles at colliders, taking advantage from the fact that the final state can be fully reconstructed. Direct searches for additional gauge bosons, such as Z', or for heavy neutral leptons, could also shed light on the flavor anomalies, thereby providing complementary information to experiments at lower energies, to give just some examples. Finally, FCC-hh energies would give access to a huge, so far uncharted energy range and parton kinematic region, offering the possibility of a direct production of so far unknown particles.

This review shows how multi-faceted QCD is, as well as its embedding in the SM. The quest to answer fundamental questions about matter, its interactions and, on a large scale, the origin and evolution of the Universe, needs to be addressed by a diverse experimental program, and high-energy colliders are just one part of it. However, they offer the unique possibility to produce particles that are simply inaccessible by other means in a controlled way. Therefore, high energy colliders form an important building block in a coordinated global effort towards a more complete theory of fundamental interactions, where the Standard Model might be embedded as a sub-part, as much as QCD today is embedded in the Standard Model.

Postscript

This volume tries to give a comprehensive and balanced view of the progress in the development of QCD since its inception. To do so presented many challenges: are all important topics adequately covered, are all opposing views represented, and is all important work included? As the volume was being developed, we often added new material that our conveners suggested (see the title page for the names of the conveners). This process was greatly aided by the use of Overleaf, which allowed all of the contributors to follow developments. In a real sense, this volume is the work of many people who often worked together to shape the final result even though they were under the intense pressures of their very busy professional schedules. We thank all of them; this volume is truly a collective effort. Still, we leave it to you to judge if we succeeded.

Another goal was to produce a coherent discussion useful for new Ph.D's and postdocs. Here we know our efforts were only partially successful. There was never enough time to fully coordinate all of the contributions, and we are sure you will find many places where more cross references would have been helpful. Again, it is up to our intended audience to judge the extent to which we were successful.

Finally, as we reflect back on this effort, we realize that the timing of this volume was more urgent that we realized at the start. Fifty years is a long time, and many who have made important contributions to the subject are no longer alive. This was never more apparent than when we learned of Harald Fritzsch's untimely death on August 16, 2022. We were delighted when he accepted our invitation to write his contribution, guided by his early and helpful suggestions, and surprised at how quickly he completed his work. His contribution was among those that were completed very early and could serve as examples for other contributors.

Both of us learned a lot about QCD as we edited the contributions and participated in the discussions. This was a great pleasure, for which we thank all of the contributors.

Acknowledgements The help of many people is acknowledged: Chiara Mariotti thanks A.C. Marini and A. Mecca; Per Grafstrom thanks Peter Jenni, Valery Khoze and Mikhail Ryskin who were kind enough to read his text and given him many useful comments and suggestions to improve his contribution; Andreas Schafer thanks the University of the Basque Country, Bilbao for hospitality; Mikhail Shifman is grateful to Alexander Khodjamirian, Alexander Lenz and Blaženka Melić for very useful discussions and comments; S. Kumano thanks A. Dote, M. Kitazawa, K. Ozawa, S. Sawada, T. Takahashi, M. Takizawa, and S. Yokkaichi for suggestions on the J-PARC experiments; Stanley J. Brodsky, Guy F. de Téramond and Hans Günter Dosch are grateful to Tianbo Liu, Raza Sabbir Sufian and Alexandre Deur, who have greatly contributed to the new applications of the holographic ideas reviewed in this volume. Eberhard Klempt and Ulrike Thoma thank Andrey V. Sarantsev for many years of collaboration on meson and baryon spectroscopy. Peter Braun-Munzinger, Anar Rustamov, and Johanna Stachel acknowledge continued and long-term collaboration with Anton Andronic and Krzysztof Redlich on many of the topics described in their contribution; Daniel Britzger, Klaus Rabbertz and Markus Wobish would like to thank Monica Dunford, Karl Jakobs, and Jürgen Scheins for their careful reading of the manuscript; Kostas Orginos thanks Carl Carlson for many discussions on the charge radius and Anatoly Radyushkin for many discussions on aspects of hadron structure. Volker Burkert expresses his gratitude to Inna Aznauryan for many years of collaboration on the subject of electroproduction of nucleon resonances, which has lead to many of the results discussed in his contribution. He also wishes to acknowledge Victor Mokeev for numerous discussions and collaboration on many aspects of resonance electroproduction. Finally, Volker Burkert thanks Francois-Xavier Girod for contributing Fig. 232 to his section.
The editors wish to thank Brad Sawatzky for setting up the original Overleaf site and for many hours of invaluable technical help, essential to the production of this volume, and Nora Brambilla, Karl Jakobs, and J. Peter LePage for several long discussions at the early stages in the preparation of this volume that influenced its structure and content.
The editors express their gratitude to Dieter Haidt, the Review Editor of the European Physical Journal C, for continuous encouragement and valuable suggestions. The authors received funding from
Australia:
National Computational Infrastructure (NCI) and the Australian Research Council through Grants No. DP190102215 and DP210103706 (*D. Leinweber*).

People's Republic of China:
National Natural Science Foundation of China (NSFC) under Contracts Nos. 11935018, 11875054 (*H-B. Li*).
France
CNRS and ANR (*B. Malaescu*).
Germany:
The Bundesministerium für Bildung und Forschung (BMBF) (*M. Dunford, E. Epelbaum, K. Jakobs, S. Neubert, and K. Rabbertz*);
Gesellschaft für Schwerionenforschung Gmb (GSI), Darmstadt, Germany (*J. Messchendorp*);
The Deutsche Forschungsgemeinschaft (DFG, German Research Foundation) through the funds provided to the Sino-German Collaborative Research Center TRR110 "Symmetries and the Emergence of Structure in QCD" (DFG Project-ID 196253076-TRR 110) (*N. Brambilla, E. Epelbaum, U. Thoma, and A. Vairo*);
The DFG Collaborative Research Centre "SFB 1225 (ISOQUANT)" (*P. Braun-Munzinger, A. Rustamov, and J. Stachel*);
The DFG Collaborative Research Centre 396021762-TRR 257, "Particle Physics Phenomenology after the Higgs Discovery" (*G. Heinrich*);
The DFG Collaborative Research Centre 315477589-TRR 211, "Strong interaction matter under extreme conditions" (*F. Karsch*);
The DFG Emmy-Nöther project NE2185/1-1: "Spektroskopie exotischer Baryonen mit LHCb" (*S. Neubert*)
DFG individual grant, Project Number 455635585
(*A. Denig*);
The Excellence Cluster ORIGINS (http://www.origins-cluster.de), funded by the DFG, German Research Foundation, Excellence Strategy, EXC-2094, 390783311 (*N. Brambilla, A. J. Buras, and A. Vairo*);
The Helmholtz Forschungsakademie Hessen für FAIR (HFHF) (*F. Nerling and J. Stroth*);
The Ministry of Culture and Science of the State of North Rhine-Westphalia (MKW NRW, Germany), project "NRW-FAIR" (*S. Neubert and U. Thoma*);
European Research Council (ERC) under the European Union's Horizon 2020 research and innovation program through grant agreements 885150-NuclearTheory (*E. Epelbaum*); 771971-SIMDAMA (*H. Meyer*); 824093-STRONG2020 (*U. Thoma*).
Italy:
Italian Ministry of Research (MIUR) under grant PRIN 20172LNEEZ (*P. Gambino and S. Marzani*)
Japan:
Japan Society for the Promotion of Science (JSPS) Grants-in-Aid for Scientific Research (KAKENHI):
Grant Number 19K03830 (*S. Kumano*);
Grant Number 18H05226(*T. Iijima*).
Spain
MINECO through the "Ramón y Cajal" program RYC-2017-21870, the "Unit of Excellence María de Maeztu 2020–2023" award to the Institute of Cosmos Sciences (CEX2019-000918-M) and from the grants PID2019-105614GB-C21 and 2017-SGR-929 (*J. Virto*);
The Spanish Ministerio de Ciencia e Innovación grant PID2019-106080GB-C21 and the European Union's Horizon 2020 research and innovation program under grant agreement No 824093 (STRONG2020) (*J. R. Peláez*);
European Research Council project ERC-2018-ADG-835105 YoctoLHC, by Maria de Maetzu excellence program under project CEX-2020-001035-M, by Spanish Research State Agency under project PID2020-119632GB-I00, and by Xunta de Galicia (Centro singular de investigación de Galicia accreditation 2019–2022), by European Union ERDF (*M. Escobedo*);
The Spanish Ministerio de Ciencia e Innovación grant PID2021-122134NB-C21 and by the Generalitat Valenciana under grant CIPROM/2021/073 and by CSIC under grant LINKB20065 (*M. Vos*).
Sweden:
The Swedish Research Council, contract number 2016-05996 (*T. Sjöstrand*).
Switzerland:
The European Research Council (ERC) under the European Union's Horizon 2020 research and innovation programme (Grant agreement No. 948254) and from the Swiss National Science Foundation (SNSF) under Eccellenza grant number PCEFP2-194658 (*S. Schramm*).
UK
Science and Technology Facilities Council (STCF): Ernest Rutherford Fellowship grants
ST/T000945/1 and ST/P000746/1 (*C. Davies*);
ST/P000630/1 (*L. Del Debbio*);
ST/V003941/1 (*D. Van Dyk*);
Royal Society Wolfson fellowship and STFC (*F. Krauss*).
USA:
The US Department of Energy, Office of Science, Office of Nuclear Physics (contract DE-AC05-06 OR23177-under which Jefferson Science Associates operates, LLC, operates Jefferson Lab) (*V. Burkert, J. Dudek, F. Gross, W. Melnitchouk, J. Qiu, and P. Rossi*);
DE-AC02-76SF00515 (*S. J. Brodsky*);
Early Career Award under Grant No. DE-SC0020405 (*M. Constantinou*);
DE-FG02-92ER40735 *V. Crede*);
DE-SC0018416 (*J. Dudek*);
DESC0018223 (*P. Maris and J. Vary*)
DE-SC0023495 (*P. Maris and J. Vary*)
DE-FG02-87ER40315 (*C. Meyer*);
DE-FG02-04ER41302 (*K. Orginos*);
DE-SC0021027 (*S. Pastore*);
DE-SC0021200 (*A. Puckett*);
DE-SC0019647 (*M. Schindler*);
DE-AC02-05CH11231 (*A. Schafer, F. Yuan*);
DE-SC0011842 (*M. Shifman*);
DE-SC0013470 (*M. Strickland*)
DE-SC0011090 and Simons Foundation Investigator grant 327942 (*I. Stewart*);
DE-FG02-87ER40371 (*J. Vary*)
DE-FG02-95ER40896, (*S. L. Wu*);
University of Wisconsin through the Wisconsin Alumni Research Foundation and the Vilas Foundation (*S. L. Wu*);
The National Science Foundation under grants PHY-1915093 and PHY-2210533 (*G. Sterman*);
NSF grant PHY20-13064 (*C. DeTar*).

Data Availability Statement This manuscript has no associated data or the data will not be deposited. [Authors' comment: Data sharing is not applicable to this article as no datasets were generated or analysed for this review.]

References

1. H. Leutwyler, On the history of the strong interaction. Mod. Phys. Lett. A **29**, 1430023 (2014) **(Ed. by Antonino Zichichi)**
2. J. Chadwick, The existence of a neutron. Proc. R. Soc. Lond. A **136**(830), 692–708 (1932)
3. W. Heisenberg, On the structure of atomic nuclei. Z. Phys. **77**, 1–11 (1932)
4. H. Yukawa, On the interaction of elementary particles I. Proc. Phys. Math. Soc. Jpn. **17**, 48–57 (1935)
5. E.C.G. Stueckelberg, Interaction energy in electrodynamics and in the field theory of nuclear forces. Helv. Phys. Acta **11**(225–244), 299–328 (1938)
6. H. Pietschmann, On the early history of current algebra. Eur. Phys. J. H **36**, 75–84 (2011)
7. G. Veneziano, Construction of a crossing-symmetric, Regge behaved amplitude for linearly rising trajectories. Nuovo Cim. A **57**, 190–197 (1968)
8. M. Gell-Mann, Isotopic spin and new unstable particles. Phys. Rev. **92**, 833–834 (1953)
9. T. Nakano, K. Nishijima, Charge independence for V-particles. Prog. Theor. Phys. **10**, 581–582 (1953)
10. M.L. Goldberger, S.B. Treiman, Decay of the π meson. Phys. Rev. **110**, 1178–1184 (1958)
11. Y. Nambu, Axial vector current conservation in weak interactions. Phys. Rev. Lett. **4**, 380–382 (1960) **(Ed. by T. Eguchi)**
12. J. Goldstone, A. Salam, S. Weinberg, Broken symmetries. Phys. Rev. **127**, 965–970 (1962)
13. Y. Ne'eman, Derivation of strong interactions from a gauge invariance. Nucl. Phys. **26**, 222–229 (1961) **(Ed. by R. Ruffini and Y. Verbin)**
14. M. Gell-Mann, Symmetries of baryons and mesons. Phys. Rev. **125**, 1067–1084 (1962)
15. S. Okubo, Note on unitary symmetry in strong interactions. Prog. Theor. Phys. **27**, 949–966 (1962)
16. V.E. Barnes et al., Observation of a hyperon with strangeness minus three. Phys. Rev. Lett. **12**, 204–206 (1964)
17. M. Gell-Mann, A schematic model of baryons and mesons. Phys. Lett. **8**, 214–215 (1964)
18. G. Zweig, An SU(3) model for strong interaction symmetry and its breaking. Version 1, in: *Developments in the Quark Theory of Hadron*, vol. 1, ed. by D.B. Lichtenberg, S.P. Rosen. 1964–1978, pp. 22–101, January 1964, CERN-TH-401, see also: Version 2, CERN-TH-412 and NP-14146, PRINT-64-170
19. M. Gell-Mann, The symmetry group of vector and axial vector currents. Phys. Phys. Fizika **1**, 63–75 (1964)
20. S.L. Adler, Consistency conditions on the strong interactions implied by a partially conserved axial vector current. Phys. Rev. B **137**, 1022 (1965)
21. W.I. Weisberger, Renormalization of the weak axial vector coupling constant. Phys. Rev. Lett. **14**, 1047–1051 (1965)
22. S. Weinberg, Pion scattering lengths. Phys. Rev. Lett. **17**, 616–621 (1966)
23. J.D. Bjorken, Asymptotic sum rules at infinite momentum. Phys. Rev. **179**, 1547–1553 (1969)
24. R.E. Taylor, Deep inelastic scattering: the early years. Rev. Mod. Phys. **63**, 573 (1991)
25. H.W. Kendall, Deep inelastic scattering: experiments on the proton and the observation of scaling. Rev. Mod. Phys. **63**, 597 (1991)
26. J.I. Friedman, Deep inelastic scattering: comparisons with the quark model. Rev. Mod. Phys. **63**, 615 (1991)
27. T. Eichten et al., Measurement of the neutrino-nucleon anti-neutrino-nucleon total cross-sections. Phys. Lett. B **46**, 274–280 (1973)
28. H. Deden et al., Experimental study of structure functions and sum rules in charge changing interactions of neutrinos and anti-neutrinos on nucleons. Nucl. Phys. B **85**, 269–288 (1975)
29. H. Abramowicz et al., Tests of QCD and Nonasymptotically Free Theories of the Strong Interaction by an Analysis of the Nucleon Structure Functions xF_3, F_2, and $\bar{q}$. Z. Phys. C **13**, 199 (1982)
30. K.G. Wilson, Nonlagrangian models of current algebra. Phys. Rev. **179**, 1499–1512 (1969)
31. O.W. Greenberg, Spin and unitary spin independence in a paraquark model of baryons and mesons. Phys. Rev. Lett. **13**, 598–602 (1964)
32. N.N. Bogolyubov, B.V. Struminsky, A.N. Tavkhelidze, On composite models in the theory of elementary particles. In: Preprint JINR D-1968, Dubna (1965)
33. M.Y. Han, Y. Nambu, Three triplet model with double SU(3) symmetry. Phys. Rev. **139**, B1006–B1010 (1965)
34. Y. Miyamoto, Three kinds of triplet mode. In: Prog. Theor. Phys. Suppl., Extra Number, 187 (1965)
35. H. Fritzsch, M. Gell-Mann, Current algebra: quarks and what else? In: *Proceedings of the XIV International Conference on High Energy Physics*, Chicago 1972, vol. 2, pp. 135–165 (1972)
36. M. Gell-Mann, Quarks. Acta Phys. Austriaca Suppl. **9**, 733–761 (1972) **(Ed. by Harald Fritzsch and Murray Gell-Mann)**
37. V. Fock, On the invariant form of the wave equation and the equations of motion for a charged point mass (in German and English). In: Z. Phys. **39** (1926). ed. by J.C. Taylor. [Surveys H.E. Phys. 5, 245 (1986)]. For a discussion of the significance of this paper, see, L.B. Okun, V.A. Fock and gauge symmetry, Phys. Usp. 53 (2010) 835 [Usp. Fiz. Nauk 180 (2010) 871], pp. 226–232
38. Th. Kaluza, Zum Unitätsproblem der Physik. Sitzungsber. Preuss. Akad. Wiss. Berlin (Math. Phys.) **1921**, 966–972 (1921)
39. O. Klein, Quantum theory and five-dimensional theory of relativity (in German and English). Z. Phys. **37**, 895–906 (1926). (**Ed. by J. C. Taylor**)
40. N. Straumann, W. Pauli, Modern physics. Space Sci. Rev. **148**, 25–36 (2009)
41. C.-N. Yang, R.L. Mills, Conservation of isotopic spin and isotopic gauge invariance. Phys. Rev. **96**, 191–195 (1954) **(Ed. by Jong-Ping Hsu and D. Fine)**
42. R. Shaw, The problem of particle types and other contributions to the theory of elementary particles. Cambridge PhD thesis (1955) **(unpublished)**
43. P.W. Higgs, Broken symmetries, massless particles and gauge fields. Phys. Lett. **12**, 132 (1964)
44. F. Englert, R. Brout, Broken symmetry and the mass of gauge vector mesons. Phys. Rev. Lett. **13**, 321–323 (1964) **(Ed. by J. C. Taylor)**
45. G.S. Guralnik, C.R. Hagen, T.W.B. Kibble, Global conservation laws and massless particles. Phys. Rev. Lett. **13**, 585–587 (1964) **(Ed. by J. C. Taylor)**
46. S.L. Glashow, Partial symmetries of weak interactions. Nucl. Phys. **22**, 579–588 (1961)
47. S. Weinberg, A model of leptons. Phys. Rev. Lett. **19**, 1264–1266 (1967)
48. A. Salam, Weak and electromagnetic interactions. Conf. Proc. C **680519**, 367–377 (1968)
49. V.S. Vanyashin, M.V. Terentev, The vacuum polarization of a charged vector field. Zh. Eksp. Teor. Fiz. **48**(2), 565–573 (1965)
50. I.B. Khriplovich, Green's functions in theories with non-abelian gauge group. Sov. J. Nucl. Phys. **10**, 235–242 (1969)
51. G. 't Hooft, Renormalizable Lagrangians for massive Yang–Mills fields. Nucl. Phys. B **35**, 167–188 (1971) **(Ed. by J. C. Taylor)**
52. G. 't Hooft, Renormalization of massless Yang–Mills fields. Nucl. Phys. B **33**, 173–199 (1971)

53. D.J. Gross, F. Wilczek, Ultraviolet behavior of nonabelian gauge theories. Phys. Rev. Lett. **30**, 1343–1346 (1973) **(Ed. by J. C. Taylor)**
54. H. David Politzer, Reliable perturbative results for strong interactions? Phys. Rev. Lett. **30**, 1346–1349 (1973) **(Ed. by J. C. Taylor)**
55. H. Fritzsch, M. Gell-Mann, H. Leutwyler, Advantages of the color octet gluon picture. Phys. Lett. B **47**, 365–368 (1973)
56. J.C. Pati, A. Salam, Unified lepton-hadron symmetry and a gauge theory of the basic interactions. Phys. Rev. D **8**, 1240–1251 (1973)
57. S. Weinberg, Nonabelian gauge theories of the strong interactions. Phys. Rev. Lett. **31**, 494 (1973)
58. H. Leutwyler, Is the quark mass as small as 5 MeV? Phys. Lett. B **48**, 431–434 (1974)
59. Y. Nambu, G. Jona-Lasinio, Dynamical model of elementary particles based on an analogy with superconductivity. 1. Phys. Rev. **122**, 345–358 (1961) **(Ed. by T. Eguchi)**
60. S. Okubo, Asymptotic SU(6)w spectral sum rules. II. Applications and bare quark masses. Phys. Rev. **188**, 2300–2307 (1969)
61. W.N. Cottingham, The neutron proton mass difference and electron scattering experiments. Ann. Phys. **25**, 424–432 (1963)
62. J. Gasser, H. Leutwyler, Implications of scaling for the proton neutron mass-difference. Nucl. Phys. B **94**, 269–310 (1975)
63. R.F. Dashen, Chiral SU(3) $\times$ SU(3) as a symmetry of the strong interactions. Phys. Rev. **183**, 1245–1260 (1969)
64. S. Weinberg, The problem of mass. Trans. N. Y. Acad. Sci. **38**, 185 (1977)
65. G. 't Hooft, Dimensional regularization and the renormalization group. Nucl. Phys. B **61**, 455–468 (1973)
66. S. Weinberg, New approach to the renormalization group. Phys. Rev. D **8**, 3497–3509 (1973)
67. W.A. Bardeen et al., Deep inelastic scattering beyond the leading order in asymptotically free gauge theories. Phys. Rev. D **18**, 3998 (1978)
68. Y. Aoki et al., FLAG Review 2021. Eur. Phys. J. C **82**(10), 869 (2022)
69. J. Gasser, H. Leutwyler, Chiral perturbation theory: expansions in the mass of the strange quark. Nucl. Phys. B **250**, 465–516 (1985)
70. G. Colangelo et al., Dispersive analysis of $\eta \to 3\pi$. Eur. Phys. J. C **78**(11), 947 (2018)
71. B. Ananthanarayan et al., Analytic representations of m_K, F_K, m_η and F_η in two loop $SU(3)$ chiral perturbation theory. Phys. Rev. D **97**, 114004 (2018)
72. S.L. Adler, Axial vector vertex in spinor electrodynamics. Phys. Rev. **177**, 2426–2438 (1969)
73. J.S. Bell, R. Jackiw, A PCAC puzzle: $\pi^0 \to \gamma\gamma$ in the σ model. Nuovo Cim. A **60**, 47–61 (1969)
74. W.A. Bardeen, Anomalous Ward identities in spinor field theories. Phys. Rev. **184**, 1848–1857 (1969)
75. H. Fritzsch, M. Gell-Mann, Light cone current algebra. In: *Proceedings of the International Conference on Duality and Symmetry in Hadron Physics, Tel Aviv 1971* (Weizmann Science Press, 1971), pp. 317–374
76. W. Bardeen, H. Fritzsch, M. Gell-Mann, Light-cone current algebra, π^0 decay and e^+e^- annihilation, in *Scale and Conformal Symmetry in Hadron Physics*. ed. by R. Gatto (Wiley, New York, 1973), pp.139–151
77. A. De Rujula et al., Can one tell QCD from a hole in the ground? A drama in five acts. In: *17th International School of Subnuclear Physics: Pointlike Structures Inside and Outside Hadrons*. Erice, Italy (1979)
78. P.M. Zerwas, H.A. Kastrup (eds.), *QCD 20 Years Later: Proceedings, Workshop, Aachen, Germany, June 9–13, 1992* (World Scientific, New Jersey, 1993)
79. H. Fritzsch, QCD: 20 years later. In: *Workshop on QCD: 20 Years Later*, pp. 827–852 (1992)
80. S.L. Glashow, J. Iliopoulos, L. Maiani, Weak interactions with lepton-hadron symmetry. Phys. Rev. D **2**, 1285–1292 (1970)
81. M.L. Perl et al., Evidence for anomalous lepton production in $e^+ - e^-$ annihilation. Phys. Rev. Lett. **35**, 1489–1492 (1975)
82. K. Kodama et al., Observation of tau neutrino interactions. Phys. Lett. B **504**, 218–224 (2001)
83. S.W. Herb et al., Observation of a dimuon resonance at 9.5-GeV in 400-GeV proton-nucleus collisions. Phys. Rev. Lett. **39**, 252–255 (1977)
84. D. Schaile, P.M. Zerwas, Measuring the weak isospin of B quarks. Phys. Rev. D **45**, 3262–3265 (1992)
85. F. Abe et al., Observation of top quark production in $\bar{p}p$ collisions. Phys. Rev. Lett. **74**, 2626–2631 (1995)
86. M. Kobayashi, T. Maskawa, CP violation in the renormalizable theory of weak interaction. Prog. Theor. Phys. **49**, 652–657 (1973)
87. G. Altarelli, G. Parisi, Asymptotic freedom in parton language. Nucl. Phys. B **126**, 298–318 (1977)
88. J.B. Kogut, D.E. Soper, Quantum electrodynamics in the infinite momentum frame. Phys. Rev. D **1**, 2901–2913 (1970)
89. S.M. Berman, J.D. Bjorken, J.B. Kogut, Inclusive processes at high transverse momentum. Phys. Rev. D **4**, 3388 (1971)
90. T. Appelquist, H.D. Politzer, Heavy quarks and e^+e^- annihilation. Phys. Rev. Lett. **34**, 43–45 (1975)
91. J.E. Augustin et al., Discovery of a narrow resonance in e^+e^- annihilation. Phys. Rev. Lett. **33**, 1406–1408 (1974)
92. J.J. Aubert et al., Experimental observation of a heavy particle. J. Phys. Rev. Lett. **33**, 1404 (1974)
93. G.S. Abrams et al., The discovery of a second narrow resonance in e^+e^- annihilation. Phys. Rev. Lett. **33**, 1453–1455 (1974)
94. S.C.C. Ting, The discovery of the J particle: a personal recollection. Rev. Mod. Phys. **49**, 235–249 (1977)
95. B. Richter, From the psi to charm: the experiments of 1975 and 1976. Rev. Mod. Phys. **49**, 251 (1977)
96. A. Casher, J.B. Kogut, L. Susskind, Vacuum polarization and the quark parton puzzle. Phys. Rev. Lett. **31**, 792–795 (1973)
97. K.G. Wilson, Confinement of quarks. Phys. Rev. D **10**, 2445–2459 (1974) **(Ed. by J. C. Taylor)**
98. J.B. Kogut, L. Susskind, Hamiltonian formulation of Wilson's lattice gauge theories. Phys. Rev. D **11**, 395–408 (1975)
99. E. Eichten et al., The spectrum of charmonium. Phys. Rev. Lett. **34**, 369–372 (1975) [Erratum: Phys. Rev. Lett. 36, 1276 (1976)]
100. T. Appelquist et al., Charmonium spectroscopy. Phys. Rev. Lett. **34**, 365 (1975)
101. S. Williams, The ring on the parking lot. CERN Cour. **43N5**, 16–18 (2003)
102. D. Hitlin, SPEAR MARK-II magnetic detector. SLAC Beam Line **7**(6), S1-s4 (1976)
103. M. Oreglia et al., A study of the reaction $\psi^{'} \to \gamma\gamma J/\psi$. Phys. Rev. D **25**, 2259 (1982)
104. G. Goldhaber et al., Observation in e^+e^- annihilation of a narrow state at $1865 - \mathrm{MeV/c^2}$ Decaying to $K\pi$ and $K\pi\pi\pi$. Phys. Rev. Lett. **37**, 255 (1976)
105. J.B. Kogut, An introduction to lattice gauge theory and spin systems. Rev. Mod. Phys. **51**, 659 (1979)
106. C.W. Bauer et al., Quantum simulation for high energy physics. https://indico.fnal.gov/event/22303/contributions/246478/attachments/157551/206155/Wed-07-20-22.pdf (2022)
107. C.W. Bauer et al., Quantum Simulation of Strong Interactions (QuaSI), Workshop 2 (online): Implementation Strategies for Gauge Theories (2022)
108. B.H. Wiik, First results from PETRA. Conf. Proc. C **7906181**, 113–154 (1979)
109. R. Brandelik et al., Evidence for planar events in e^+e^- annihilation at high-energies. Phys. Lett. B **86**, 243–249 (1979)
110. E.D. Bloom et al., High-energy inelastic e p scattering at 6-degrees and 10-degrees. Phys. Rev. Lett. **23**, 930–934 (1969)

111. H.W. Kendall, Deep inelastic electron scattering in the continuum region. **710823**, 248–261 (1971)
112. J.I. Friedman, H.W. Kendall, Deep inelastic electron scattering. Annu. Rev. Nucl. Part. Sci. **22**, 203–254 (1972)
113. G. Miller et al., Inelastic electron-proton scattering at large momentum transfers. Phys. Rev. D **5**, 528 (1972)
114. E. Eichten, F. Feinberg, J.F. Willemsen, Current and constituent quarks in the light cone quantization. Phys. Rev. D **8**, 1204–1219 (1973)
115. Y. Watanabe et al., Test of scale invariance in ratios of muon scattering cross-sections at 150-GeV and 56-GeV. Phys. Rev. Lett. **35**, 898 (1975)
116. C. Chang et al., Observed deviations from scale invariance in high-energy muon scattering. Phys. Rev. Lett. **35**, 901 (1975)
117. W.B. Atwood et al., Inelastic electron scattering from hydrogen at 50-degrees and 60-degrees. Phys. Lett. B **64**, 479–482 (1976)
118. P.C. Bosetti et al., Analysis of nucleon structure functions in CERN bubble chamber neutrino experiments. Nucl. Phys. B **142**, 1–28 (1978)
119. J.G.H. de Groot et al., QCD analysis of charged current structure functions. Phys. Lett. B **82**, 456–460 (1979)
120. J.G.H. de Groot et al., Inclusive interactions of high-energy neutrinos and anti-neutrinos in iron. Z. Phys. C **1**, 143 (1979)
121. J.R. Ellis, M.K. Gaillard, G.G. Ross, Search for gluons in e^+e^- annihilation. Nucl. Phys. B **111**, 253 (1976) [Erratum: Nucl. Phys. B 130, 516 (1977)]
122. G. Hanson et al., Evidence for jet structure in hadron production by e^+e^- annihilation. Phys. Rev. Lett. **35**, 1609–1612 (1975) **(Ed. by Martha C. Zipf)**
123. S.L. Wu, Discovery of the first Yang-Mills gauge particle–the gluon. Int. J. Mod. Phys. A **30**(34), 1530066 (2015)
124. S.L. Wu, G. Zobernig, A method of three jet analysis in e^+e^- annihilation. Z. Phys. C **2**, 107 (1979)
125. P. Söding, Jet analysis, in *EPS High-Energy Physics Conference*, vol. 1 (CERN, Geneva), pp. 271–281 (1979)
126. D.P. Barber et al., Discovery of three jet events and a test of quantum chromodynamics at PETRA energies. Phys. Rev. Lett. **43**, 830 (1979)
127. C. Berger et al., Evidence for gluon bremsstrahlung in e^+e^- annihilations at high-energies. Phys. Lett. B **86**, 418–425 (1979)
128. W. Bartel et al., Observation of planar three jet events in e^+e^- annihilation and evidence for gluon bremsstrahlung. Phys. Lett. B **91**, 142–147 (1980)
129. P. Söding, On the discovery of the gluon. Eur. Phys. J. H **35**, 3–28 (2010)
130. A. Ali, G. Kramer, Jets and QCD: a historical review of the discovery of the quark and gluon jets and its impact on QCD. Eur. Phys. J. H **36**, 245–326 (2011)
131. G. Arnison et al., Experimental observation of isolated large transverse energy electrons with associated missing energy at $\sqrt{s} = 540$ GeV. Phys. Lett. B **122**, 103–116 (1983)
132. G. Arnison et al., Experimental observation of lepton pairs of invariant mass around 95-GeV/c^2 at the CERN SPS collider. Phys. Lett. B **126**, 398–410 (1983)
133. M. Banner et al., Observation of single isolated electrons of high transverse momentum in events with missing transverse energy at the CERN $\bar{p}p$ collider. Phys. Lett. B **122**, 476–485 (1983)
134. P. Bagnaia et al., Evidence for $Z^0 \to e^+e^-$ at the CERN $\bar{p}p$ collider. Phys. Lett. B **129**, 130–140 (1983)
135. C.N. Yang, *Selected Papers (1945–1980) with Commentary* (World Scientific, 2005)
136. F. Abe et al., Observation of top quark production in p $\bar{p}$ collisions with the collider detector at Fermilab. Phys. Rev. Lett. **74**, 2626 (1995)
137. S. Abachi et al., Observation of the top quark. Phys. Rev. Lett. **74**, 2632 (1995)
138. S.W. Herb, D. Hom, L. Lederman et al., Observation of a dimuon resonance at 9.5 GeV in 400-GeV proton-nucleus collisions. Phys. Rev. Lett. **39**, 252 (1977)
139. G. Aad et al., Observation of a new particle in the search for the Standard Model Higgs boson with the ATLAS detector at the LHC. Phys. Lett. B **716**, 1–29 (2012)
140. S. Chatrchyan et al., Observation of a new boson at a mass of 125 GeV with the CMS experiment at the LHC. Phys. Lett. B **716**, 30–61 (2012)
141. T.T. Wu, S.L. Wu, in *A Festschrift for Yang Centenary: Scientific Papers*. ed. by F.C. Chen et al. (World Scientific Publisher, Singapore, 2022)
142. T.T. Wu, S.L. Wu, Concept of the basic standard model and a relation between the three gauge coupling constants, unpublished note (2022)
143. J.D. Bjorken, E.A. Paschos, Inelastic electron proton and γ-proton scattering, and the structure of the nucleon. Phys. Rev. **185**, 1975–1982 (1969)
144. E.D. Bloom, F.J. Gilman, Scaling, duality, and the behavior of resonances in inelastic electron-proton scattering. Phys. Rev. Lett. **25**, 1140 (1970)
145. M.A. Shifman, A.I. Vainshtein, V.I. Zakharov, QCD and resonance physics. Theoretical foundations. Nucl. Phys. B **147**, 385–447 (1979)
146. E. Braaten, S. Narison, A. Pich, QCD analysis of the tau hadronic width. Nucl. Phys. B **373**, 581–612 (1992)
147. P. Ball, M. Beneke, V.M. Braun, Resummation of $(\beta_0\alpha_s)^n$ corrections in QCD: techniques and applications to the tau hadronic width and the heavy quark pole mass. Nucl. Phys. B **452**, 563–625 (1995)
148. M. Davier, A. Hoecker, Z. Zhang, The physics of hadronic tau decays. Rev. Mod. Phys. **78**, 1043–1109 (2006)
149. S. Bethke, Experimental tests of asymptotic freedom. Prog. Part. Nucl. Phys. **58**, 351–386 (2007)
150. E.M. Levin, L.L. Frankfurt, The quark hypothesis and relations between cross-sections at high-energies. JETP Lett. **2**, 65–70 (1965)
151. M. Gupta, Baryon magnetic moments and the naive quark model. J. Phys. G **16**, L213–L217 (1990)
152. V.A. Matveev, R.M. Muradyan, A.N. Tavkhelidze, Automodelity in strong interactions. Lett. Nuovo Cim. **5S2**, 907–912 (1972)
153. S.J. Brodsky, G.R. Farrar, Scaling laws at large transverse momentum. Phys. Rev. Lett. **31**, 1153–1156 (1973)
154. C. Bochna et al., Measurements of deuteron photodisintegration up to 4.0-GeV. Phys. Rev. Lett. **81**, 4576–4579 (1998)
155. Y.L. Dokshitzer, QCD phenomenology. In: *2002 European School of High-Energy Physics*, pp. 1–33 (2003)
156. F.E. Low, A model of the bare pomeron. Phys. Rev. D **12**, 163–173 (1975)
157. S. Nussinov, Colored quark version of some hadronic puzzles. Phys. Rev. Lett. **34**, 1286–1289 (1975)
158. J.F. Gunion, D.E. Soper, Quark counting and hadron size effects for total cross-sections. Phys. Rev. D **15**, 2617–2621 (1977)
159. V.S. Fadin, E.A. Kuraev, L.N. Lipatov, On the Pomeranchuk singularity in asymptotically free theories. Phys. Lett. B **60**, 50–52 (1975)
160. V.N. Gribov, Interaction of gamma quanta and electrons with nuclei at high-energies. Zh. Eksp. Teor. Fiz. **57**, 1306–1323 (1969)
161. R.P. Feynman, Very high-energy collisions of hadrons. Phys. Rev. Lett. **23**, 1415–1417 (1969) **(Ed. by L. M. Brown)**
162. G. 't Hooft, M.J.G. Veltman, Regularization and renormalization of gauge fields. Nucl. Phys. B **44**, 189–213 (1972)
163. C.G. Bollini, J.J. Giambiagi, Dimensional renormalization: the number of dimensions as a regularizing parameter. Nuovo Cim. B **12**, 20–26 (1972)

164. W. Siegel, Supersymmetric dimensional regularization via dimensional reduction. Phys. Lett. B **84**, 193–196 (1979)
165. G. Grunberg, Renormalization scheme independent QCD and QED: the method of effective charges. Phys. Rev. D **29**, 2315–2338 (1984)
166. A.C. Mattingly, P.M. Stevenson, Optimization of $R_{e^+e^-}$ and 'freezing' of the QCD couplant at low-energies. Phys. Rev. D **49**, 437–450 (1994)
167. J.D. Bjorken, Applications of the chiral $U(6) \times U(6)$ algebra of current densities. Phys. Rev. **148**, 1467–1478 (1966)
168. T. Appelquist, M. Dine, I.J. Muzinich, The static potential in quantum chromodynamics. Phys. Lett. B **69**, 231–236 (1977)
169. A. Czarnecki, K. Melnikov, N. Uraltsev, NonAbelian dipole radiation and the heavy quark expansion. Phys. Rev. Lett. **80**, 3189–3192 (1998)
170. P.A. Baikov, K.G. Chetyrkin, J.H. Kuhn, Adler function, Bjorken sum rule, and the Crewther relation to order α_s^4 in a general gauge theory. Phys. Rev. Lett. **104**, 132004 (2010)
171. S. Catani, B.R. Webber, G. Marchesini, QCD coherent branching and semiinclusive processes at large x. Nucl. Phys. B **349**, 635–654 (1991)
172. Y.L. Dokshitzer, V.A. Khoze, S.I. Troian, Specific features of heavy quark production LPHD approach to heavy particle spectra. Phys. Rev. D **53**, 89–119 (1996)
173. G.P. Korchemsky, Asymptotics of the Altarelli-Parisi-Lipatov evolution kernels of parton distributions. Mod. Phys. Lett. A **4**, 1257–1276 (1989)
174. G.P. Korchemsky, G. Marchesini, Structure function for large x and renormalization of Wilson loop. Nucl. Phys. B **406**, 225–258 (1993)
175. F.E. Low, Bremsstrahlung of very low-energy quanta in elementary particle collisions. Phys. Rev. **110**, 974–977 (1958)
176. D.M. Howe, C.J. Maxwell, All orders infrared freezing of observables in perturbative QCD. Phys. Rev. D **70**, 014002 (2004)
177. S.J. Brodsky, G.F. de Teramond, A. Deur, Non-perturbative QCD coupling and its β-function from light-front holography. Phys. Rev. D **81**, 096010 (2010)
178. G. Parisi, R. Petronzio, Small transverse momentum distributions in hard processes. Nucl. Phys. B **154**, 427–440 (1979)
179. Y.L. Dokshitzer, G. Marchesini, B.R. Webber, Dispersive approach to power behaved contributions in QCD hard processes. Nucl. Phys. B **469**, 93–142 (1996)
180. F. Caola et al., On linear power corrections in certain collider observables. JHEP **01**, 093 (2022)
181. S.D. Drell, D.J. Levy, T.-M. Yan, A theory of deep inelastic lepton-nucleon scattering and lepton pair annihilation processes. 3. Deep inelastic electron-positron annihilation. Phys. Rev. D **1**, 1617–1639 (1970)
182. N. Cabibbo, G. Parisi, M. Testa, Hadron production in e^+e^- collisions. Lett. Nuovo Cim. **4S1**, 35–39 (1970)
183. B.L. Ioffe, Space-time picture of photon and neutrino scattering and electroproduction cross-section asymptotics. Phys. Lett. B **30**, 123–125 (1969)
184. B. Andersson et al., Parton fragmentation and string dynamics. Phys. Rep. **97**, 31–145 (1983)
185. G.F. Sterman, S. Weinberg, Jets from quantum chromodynamics. Phys. Rev. Lett. **39**, 1436 (1977)
186. W. James Stirling, Hard QCD working group: theory summary. J. Phys. G **17**, 1567–1574 (1991)
187. S. Catani et al., New clustering algorithm for multi-jet cross-sections in e^+e^- annihilation. Phys. Lett. B **269**, 432–438 (1991)
188. S. Bethke et al., New jet cluster algorithms: next-to-leading order QCD and hadronization corrections. Nucl. Phys. B **370**, 310–334 (1992) [Erratum: Nucl. Phys. B 523, 681–681 (1998)]
189. Y.L. Dokshitzer et al., Better jet clustering algorithms. JHEP **08**, 001 (1997)
190. M. Wobisch, T. Wengler, Hadronization corrections to jet cross-sections in deep inelastic scattering. In: *Workshop on Monte Carlo Generators for HERA Physics (Plenary Starting Meeting)*, pp. 270–279 (1998)
191. S. Catani et al., Longitudinally invariant K_t clustering algorithms for hadron hadron collisions. Nucl. Phys. B **406**, 187–224 (1993)
192. M. Cacciari, G.P. Salam, Dispelling the N^3 myth for the k_t jet-finder. Phys. Lett. B **641**, 57–61 (2006)
193. M. Cacciari, G.P. Salam, G. Soyez, The anti-k_t jet clustering algorithm. JHEP **04**, 063 (2008)
194. G.P. Salam, Towards jetography. Eur. Phys. J. C **67**, 637–686 (2010)
195. S. Acharya et al., Direct observation of the dead-cone effect in quantum chromodynamics. Nature **605**(7910), 440–446 (2022)
196. G. Altarelli, R. Keith Ellis, G. Martinelli, Large perturbative corrections to the Drell–Yan process in QCD. Nucl. Phys. B **157**, 461–497 (1979)
197. R. Keith Ellis et al., Large corrections to high p(T) hadron–hadron scattering in QCD. Nucl. Phys. B **173**, 397–421 (1980)
198. W.T. Giele, E.W. Nigel Glover, Higher order corrections to jet cross-sections in e^+e^- annihilation. Phys. Rev. D **46**, 1980–2010 (1992)
199. S. Catani, M.H. Seymour, A general algorithm for calculating jet cross-sections in NLO QCD. Nucl. Phys. B **485**, 291–419 (1997) [Erratum: Nucl. Phys. B 510, 503–504 (1998)]
200. from Feynman diagrams to unitarity cuts, R. Keith Ellis et al., One-loop calculations in quantum field theory. Phys. Rep. **518**, 141–250 (2012)
201. R. Keith Ellis, W.T. Giele, G. Zanderighi, The one-loop amplitude for six-gluon scattering. JHEP **05**, 027 (2006)
202. M. Dasgupta et al., Parton showers beyond leading logarithmic accuracy. Phys. Rev. Lett. **125**(5), 052002 (2020)
203. S. Amoroso, et al., Les Houches 2019: Physics at TeV Colliders: Standard Model Working Group Report. In: *11th Les Houches Workshop on Physics at TeV Colliders* (2020)
204. C. Anastasiou et al., Higgs boson gluon-fusion production beyond threshold in N^3LO QCD. JHEP **03**, 091 (2015)
205. A. Banfi et al., Jet-vetoed Higgs cross section in gluon fusion at $N^3LO+NNLL$ with small-R resummation. JHEP **04**, 049 (2016)
206. B. Mistlberger, Higgs boson production at hadron colliders at N^3LO in QCD. JHEP **05**, 028 (2018)
207. S. Camarda, L. Cieri, G. Ferrera, Drell-Yan lepton-pair production: q_T resummation at N^3LL accuracy and fiducial cross sections at N^3LO. Phys. Rev. D **104**(11), L111503 (2021)
208. J. Currie et al., N^3LO corrections to jet production in deep inelastic scattering using the Projection-to-Born method. JHEP **05**, 209 (2018)
209. M. Abele, D. de Florian, W. Vogelsang, Threshold resummation at N^3LL accuracy and approximate N^3LO corrections to semi-inclusive DIS. Phys. Rev. D **106**(1), 014015 (2022)
210. C. Gnendiger et al., To d, or not to d: recent developments and comparisons of regularization schemes. Eur. Phys. J. C **77**(7), 471 (2017)
211. Z. Bern, L.J. Dixon, D.A. Kosower, Progress in one loop QCD computations. Annu. Rev. Nucl. Part. Sci. **46**, 109–148 (1996)
212. I. Bierenbaum et al., A tree-loop duality relation at two loops and beyond. JHEP **10**, 073 (2010)
213. G.F.R. Sborlini et al., Four-dimensional unsubtraction from the loop-tree duality. JHEP **08**, 160 (2016)
214. W.J. Torres Bobadilla et al., May the four be with you: novel IR-subtraction methods to tackle NNLO calculations. Eur. Phys. J. C **81**(3), 250 (2021)
215. G. Travaglini et al., The SAGEX review on scattering amplitudes. J. Phys. A **55**(44), 443001 (2022)

216. S. Catani et al., Diphoton production at hadron colliders: a fully-differential QCD calculation at NNLO. Phys. Rev. Lett. **108**, 072001 (2012) [Erratum: Phys. Rev. Lett. 117, 089901 (2016)]
217. M. Beneke, Renormalons. Phys. Rep. **317**, 1–142 (1999)
218. Y.L. Dokshitzer, D. Diakonov, S.I. Troian, Hard semiinclusive processes in QCD. Phys. Lett. B **78**, 290–294 (1978)
219. Y.L. Dokshitzer, D. Diakonov, S.I. Troian, Hard processes in quantum chromodynamics. Phys. Rep. **58**, 269–395 (1980)
220. V.N. Gribov, Bremsstrahlung of hadrons at high energies. Sov. J. Nucl. Phys. **5**, 280 (1967)
221. R. Kirschner, L.N. Lipatov, Double logarithmic asymptotics and Regge singularities of quark amplitudes with flavor exchange. Nucl. Phys. B **213**, 122–148 (1983)
222. N. Kidonakis, G. Oderda, G.F. Sterman, Evolution of color exchange in QCD hard scattering. Nucl. Phys. B **531**, 365–402 (1998)
223. A. Grozin et al., The three-loop cusp anomalous dimension in QCD and its supersymmetric extensions. JHEP **01**, 140 (2016)
224. Yu.L. Dokshitzer, G. Marchesini, Soft gluons at large angles in hadron collisions. JHEP **01**, 007 (2006)
225. A.V. Efremov, A.V. Radyushkin, Factorization and asymptotical behavior of pion form-factor in QCD. Phys. Lett. B **94**, 245–250 (1980)
226. G. Peter Lepage, S.J. Brodsky, Exclusive processes in perturbative quantum chromodynamics. Phys. Rev. D **22**, 2157 (1980)
227. B.Z. Kopeliovich et al., Decisive test of color transparency in exclusive electroproduction of vector mesons. Phys. Lett. B **324**, 469–476 (1994)
228. S.J. Brodsky et al., Diffractive leptoproduction of vector mesons in QCD. Phys. Rev. D **50**, 3134–3144 (1994)
229. E.M. Aitala et al., Observation of color transparency in diffractive dissociation of pions. Phys. Rev. Lett. **86**, 4773–4777 (2001)
230. V.N. Gribov, L.N. Lipatov, Deep inelastic ep scattering in perturbation theory. Sov. J. Nucl. Phys. **15**, 438–450 (1972)
231. V.N. Gribov, L.N. Lipatov, e^+e^- pair annihilation and deep inelastic ep scattering in perturbation theory. Sov. J. Nucl. Phys. **15**, 675–684 (1972)
232. L.N. Lipatov, The parton model and perturbation theory. Yad. Fiz. **20**, 181–198 (1974)
233. Y.L. Dokshitzer, Calculation of the structure functions for deep inelastic scattering and e^+e^- annihilation by perturbation theory in quantum chromodynamics. Sov. Phys. JETP **46**, 641–653 (1977)
234. S. Moch, J.A.M. Vermaseren, A. Vogt, The three loop splitting functions in QCD: the nonsinglet case. Nucl. Phys. B **688**, 101–134 (2004)
235. A. Vogt, S. Moch, J.A.M. Vermaseren, The three-loop splitting functions in QCD: the singlet case. Nucl. Phys. B **691**, 129–181 (2004)
236. I.I. Balitsky, L.N. Lipatov, The Pomeranchuk singularity in quantum chromodynamics. Sov. J. Nucl. Phys. **28**, 822–829 (1978)
237. A.H. Mueller, A simple derivation of the JIMWLK equation. Phys. Lett. B **523**, 243–248 (2001)
238. G. Camici, M. Ciafaloni, Model (in)dependent features of the hard pomeron. Phys. Lett. B **395**, 118–122 (1997)
239. A.H. Mueller, Limitations on using the operator product expansion at small values of x. Phys. Lett. B **396**, 251–256 (1997)
240. A.H. Mueller, H. Navelet, An inclusive minijet cross-section and the bare pomeron in QCD. Nucl. Phys. B **282**, 727–744 (1987)
241. G. Safronov, Beyond-DGLAP searches with Mueller–Navelet jets, and measurements of low-p_T and forward jets at CMS. PoS DIS2014, p. 094 (2014)
242. J.C. Collins, D.E. Soper, G.F. Sterman, Factorization of hard processes in QCD. Adv. Ser. Direct. High Energy Phys. **5**, 1–91 (1989)
243. A.V. Kotikov, L.N. Lipatov, DGLAP and BFKL equations in the $N = 4$ supersymmetric gauge theory. Nucl. Phys. B **661**, 19–61 (2003) [Erratum: Nucl. Phys. B 685, 405–407 (2004)]
244. M.Z. Akrawy et al., A study of coherence of soft gluons in hadron jets. Phys. Lett. B **247**, 617–628 (1990)
245. K. Charchula, Coherence effects in the current fragmentation region at HERA. J. Phys. G **19**, 1587–1593 (1993)
246. Y.I. Azimov et al., Similarity of parton and hadron spectra in QCD jets. Z. Phys. C **27**, 65–72 (1985)
247. A. Korytov, Inclusive momentum distributions of charged particles in jets at CDF. Nucl. Phys. B Proc. Suppl. **54**, 67–70 (1997) **(Ed. by Z. Ajduk and A. K. Wroblewski)**
248. D. Acosta et al., Momentum distribution of charged particles in jets in dijet events in $p\bar{p}$ collisions at $\sqrt{s} = 1.8$ TeV and comparisons to perturbative QCD predictions. Phys. Rev. D **68**, 012003 (2003)
249. Y.L. Dokshitzer et al., Basics of perturbative QCD. https://www.lpthe.jussieu.fr/yuri/BPQCD/BPQCD-print.pdf (1991)
250. V.A. Khoze, S. Lupia, W. Ochs, Perturbative universality in soft particle production. Eur. Phys. J. C **5**, 77–90 (1998)
251. J. Abdallah et al., Coherent soft particle production in Z decays into three jets. Phys. Lett. B **605**, 37–48 (2005) **(Ed. by D. Bruncko, J. Ferencei, and P. Strizenec)**
252. Y.L. Dokshitzer, V.A. Khoze, S.I. Troian, On the concept of local parton hadron duality. J. Phys. G **17**, 1585–1587 (1991)
253. Y.L. Dokshitzer, D. Diakonov, Angular distribution of energy in jets. Phys. Lett. B **84**, 234–236 (1979)
254. G. Curci, W. Furmanski, R. Petronzio, Evolution of parton densities beyond leading order: the nonsinglet case. Nucl. Phys. B **175**, 27–92 (1980)
255. L. Del Debbio, A. Ramos, Lattice determinations of the strong coupling. Phys. Rep. **920**, 1–71 (2021)
256. Y. Aoki et al., FLAG Review 2021 (2021)
257. M. Luscher, P. Weisz, U. Wolff, A Numerical method to compute the running coupling in asymptotically free theories. Nucl. Phys. B **359**, 221–243 (1991)
258. M. Dalla Brida et al., Non-perturbative renormalization by decoupling. Phys. Lett. B **807**, 135571 (2020)
259. M. Dalla Brida, Past, present, and future of precision determinations of the QCD parameters from lattice QCD. Eur. Phys. J. A **57**(2), 66 (2021)
260. A. Athenodorou et al., How perturbative are heavy sea quarks? Nucl. Phys. B **943**, 114612 (2019)
261. M. Dalla Brida et al., Determination of $\alpha_s(m_Z)$ by the non-perturbative decoupling method (2022)
262. V.N. Gribov, Quantization of nonabelian gauge theories. Nucl. Phys. B **139**, 1 (1978) **(Ed. by J. Nyiri)**
263. N. Vandersickel, D. Zwanziger, The Gribov problem and QCD dynamics. Phys. Rep. **520**, 175–251 (2012)
264. P. Petreczky, J.H. Weber, Strong coupling constant and heavy quark masses in (2+1)-flavor QCD. Phys. Rev. D **100**(3), 034519 (2019)
265. E. Shintani et al., Strong coupling constant from vacuum polarization functions in three-flavor lattice QCD with dynamical overlap fermions. Phys. Rev. D **82**(7), 074505 (2010) [Erratum: Phys. Rev. D 89(9), 099903 (2014)]
266. R.J. Hudspith et al., α_s from the lattice hadronic vacuum polarisation (2018). arXiv:1804.10286
267. K. Nakayama, H. Fukaya, S. Hashimoto, Lattice computation of the Dirac eigenvalue density in the perturbative regime of QCD. Phys. Rev. D **98**(1), 014501 (2018)
268. Z. Fodor et al., Up and down quark masses and corrections to Dashen's theorem from lattice QCD and quenched QED. Phys. Rev. Lett. **117**(8), 082001 (2016)

269. D. Giusti et al., Leading isospin-breaking corrections to pion, kaon and charmed-meson masses with Twisted-Mass fermions. Phys. Rev. D **95**(11), 114504 (2017)
270. M. Bruno et al., Light and strange quark masses from $N_f = 2+1$ simulations with Wilson fermions. PoS LATTICE **2018**, 220 (2019)
271. S. Dürr et al., Lattice QCD at the physical point: light quark masses. Phys. Lett. B **701**, 265–268 (2011)
272. S. Dürr et al., Lattice QCD at the physical point: simulation and analysis details. JHEP **08**, 148 (2011)
273. C. McNeile et al., High-precision c and b masses, and QCD coupling from current-current correlators in lattice and continuum QCD. Phys. Rev. D **82**, 034512 (2010)
274. A.T. Lytle et al., Determination of quark masses from $n_f = 4$ lattice QCD and the RI-SMOM intermediate scheme. Phys. Rev. D **98**(1), 014513 (2018)
275. B. Chakraborty et al., High-precision quark masses and QCD coupling from $n_f = 4$ lattice QCD. Phys. Rev. D **91**(5), 054508 (2015)
276. Y.-B. Yang et al., Charm and strange quark masses and f_{D_s} from overlap fermions. Phys. Rev. D **92**(3), 034517 (2015)
277. K. Nakayama, B. Fahy, S. Hashimoto, Short-distance charmonium correlator on the lattice with Möbius domain-wall fermion and a determination of charm quark mass. Phys. Rev. D **94**(5), 054507 (2016)
278. C. Alexandrou et al., Baryon spectrum with $N_f = 2+1+1$ twisted mass fermions. Phys. Rev. D **90**(7), 074501 (2014)
279. D. Hatton et al., Charmonium properties from lattice QCD+QED?: Hyperfine splitting, J/ψ leptonic width, charm quark mass, and a_π^c. Phys. Rev. D **102**(5), 054511 (2020)
280. D. Hatton et al., Determination of $\bar{m}b/\bar{m}c$ and $\bar{m}b$ from $n_f = 4$ lattice QCD+QED. Phys. Rev. D **103**(11), 114508 (2021)
281. B. Colquhoun et al., Υ and $\Upsilon^{'}$ Leptonic Widths, a_μ^b and m_b from full lattice QCD. Phys. Rev. D **91**(7), 074514 (2015)
282. N. Carrasco et al., Up, down, strange and charm quark masses with $N_f = 2+1+1$ twisted mass lattice QCD. Nucl. Phys. B **887**, 19–68 (2014)
283. A. Bussone et al., Mass of the b quark and B -meson decay constants from $N_f = 2+1+1$ twisted-mass lattice QCD. Phys. Rev. D **93**(11), 114505 (2016)
284. P. Gambino, A. Melis, S. Simula, Extraction of heavy-quark-expansion parameters from unquenched lattice data on pseudoscalar and vector heavy-light meson masses. Phys. Rev. D **96**(1), 014511 (2017)
285. T. Blum et al., Domain wall QCD with physical quark masses. Phys. Rev. D **93**(7), 074505 (2016)
286. A. Bazavov et al., MILC results for light pseudoscalars. PoS **CD09**, 007 (2009)
287. A. Bazavov et al., Up-, down-, strange-, charm-and bottom-quark masses from four-flavor lattice QCD. Phys. Rev. D **98**(5), 054517 (2018)
288. R. Sommer, Introduction to non-perturbative heavy quark effective theory. In: *Les Houches Summer School: Session 93: Modern Perspectives in lattice QCD: Quantum Field Theory and High Performance Computing*, pp. 517–590 (2010)
289. G. Peter Lepage et al., Improved nonrelativistic QCD for heavy quark physics. Phys. Rev. D **46**, 4052–4067 (1992)
290. A. Patella, QED corrections to hadronic observables. PoS LATTICE **2017**, 020 (2016)
291. M. Luscher et al., A precise determination of the running coupling in the SU(3) Yang-Mills theory. Nucl. Phys. B **413**, 481–502 (1994)
292. M. Della Morte et al., Computation of the strong coupling in QCD with two dynamical flavors. Nucl. Phys. B **713**, 378–406 (2005)
293. S. Aoki et al., Precise determination of the strong coupling constant in N(f) = 2+1 lattice QCD with the Schrodinger functional scheme. JHEP **10**, 053 (2009)
294. S. Capitani et al., Non-perturbative quark mass renormalization in quenched lattice QCD. Nucl. Phys. B **544**, 669–698 (1999) [Erratum: Nucl. Phys. B 582, 762–762 (2000)]
295. M. Della Morte et al., Non-perturbative quark mass renormalization in two-flavor QCD. Nucl. Phys. B **729**, 117–134 (2005)
296. I. Campos et al., Non-perturbative quark mass renormalisation and running in $N_f = 3$ QCD. Eur. Phys. J. C **78**(5), 387 (2018)
297. M. Dalla Brida et al., Slow running of the gradient flow coupling from 200 MeV to 4 GeV in $N_{\rm f} = 3$ QCD. Phys. Rev. D **95**(1), 014507 (2017)
298. M. Bruno et al., QCD coupling from a nonperturbative determination of the three-flavor Λ parameter. Phys. Rev. Lett. **119**(10), 102001 (2017)
299. J. Heitger, F. Joswig, S. Kuberski, Determination of the charm quark mass in lattice QCD with 2 + 1 flavours on fine lattices. JHEP **05**, 288 (2021)
300. P.A. Zyla et al., Review of particle physics. PTEP **2020**(8), 083C01 (2020)
301. S. Aoki et al., FLAG Review 2019: Flavour Lattice Averaging Group (FLAG). Eur. Phys. J. C **80**(2), 113 (2020)
302. R. Abbate et al., Thrust at N^3LL with power corrections and a precision global fit for $\alpha_s(mZ)$. Phys. Rev. D **83**, 074021 (2011)
303. A.H. Hoang et al., Precise determination of α_s from the C-parameter distribution. Phys. Rev. D **91**(9), 094018 (2015)
304. D. d'Enterria, et al., The strong coupling constant: state of the art and the decade ahead (2022). Snowmass 2021 White Paper. arXiv:2203.08271
305. G. Luisoni, P. Francesco Monni, G.P. Salam, C-parameter hadronisation in the symmetric 3-jet limit and impact on α_s fits. Eur. Phys. J. C **81**(2), 158 (2021)
306. K.G. Wilson, Quarks and strings on a lattice. In: *13th International School of Subnuclear Physics: New Phenomena in Subnuclear Physics* (1975)
307. B. Sheikholeslami, R. Wohlert, Improved continuum limit lattice action for QCD with Wilson fermions. Nucl. Phys. B **259**, 572 (1985)
308. M. Luscher, P. Weisz, O(a) improvement of the axial current in lattice QCD to one loop order of perturbation theory. Nucl. Phys. B **479**, 429–458 (1996)
309. R. Wohlert, Improved continuum limit lattice action for quarks. In: DESY-87-069 (1987)
310. M. Lüscher et al., Chiral symmetry and O(a) improvement in lattice QCD. Nucl. Phys. B **478**, 365–400 (1996)
311. M. Lüscher et al., Nonperturbative O(a) improvement of lattice QCD. Nucl. Phys. B **491**, 323–343 (1997)
312. K. Symanzik, Cutoff dependence in lattice ϕ^4 in four-dimensions theory. NATO Sci. Ser. B **59**, 313–330 (1980)
313. K. Symanzik, Continuum limit and improved action in lattice theories. 1. Principles and ϕ^4 theory. Nucl. Phys. B **226**, 187–204 (1983)
314. G. Bali et al., Lattice gauge ensembles and data management. PoS LATTICE **2022**, 203 (2022)
315. W.A. Bardeen et al., Light quarks, zero modes, and exceptional configurations. Phys. Rev. D **57**, 1633–1641 (1998)
316. R. Frezzotti et al., Lattice QCD with a chirally twisted mass term. JHEP **08**, 058 (2001)
317. T. Banks, L. Susskind, J.B. Kogut, Strong coupling calculations of lattice gauge theories: (1+1)-dimensional exercises. Phys. Rev. D **13**, 1043 (1976)
318. T. Banks et al., Strong coupling calculations of the hadron spectrum of quantum chromodynamics. Phys. Rev. D **15**, 1111 (1977)
319. L. Susskind, Lattice fermions. Phys. Rev. D **16**, 3031–3039 (1977)

320. T. DeGrand, C.E. DeTar, *Lattice Methods for Quantum Chromodynamics* (World Scientific, Singapore, 2006)
321. J. Smit, *Introduction to Quantum Fields on a Lattice: A Robust Mate*, vol. 15 (Cambridge University Press, Cambridge, 2011)
322. A. Bazavov et al., Nonperturbative QCD simulations with 2+1 flavors of improved staggered quarks. Rev. Mod. Phys. **82**, 1349–1417 (2010)
323. S. Naik, On-shell improved lattice action for QCD with Susskind fermions and asymptotic freedom scale. Nucl. Phys. B **316**, 238–268 (1989)
324. M. Luscher, P. Weisz, On-shell improved lattice gauge theories. Commun. Math. Phys. **97**, 59 (1985)
325. M. Luscher, P. Weisz, Computation of the action for on-shell improved lattice gauge theories at weak coupling. Phys. Lett. B **158**, 250–254 (1985)
326. T. Blum et al., Improving flavor symmetry in the Kogut-Susskind hadron spectrum. Phys. Rev. D **55**, R1133–R1137 (1997)
327. J.F. Lagae, D.K. Sinclair, Improved staggered quark actions with reduced flavor symmetry violations for lattice QCD. Phys. Rev. D **59**, 014511 (1999)
328. P. Lepage, Perturbative improvement for lattice QCD: an update. Nucl. Phys. B Proc. Suppl. **60**, 267–278 (1998) **(Ed. by Y. Iwasaki and A. Ukawa)**
329. K. Orginos, D. Toussaint, Testing improved actions for dynamical Kogut-Susskind quarks. Phys. Rev. D **59**, 014501 (1999)
330. K. Orginos, D. Toussaint, R.L. Sugar, Variants of fattening and flavor symmetry restoration. Phys. Rev. D **60**, 054503 (1999)
331. E. Follana et al., Highly improved staggered quarks on the lattice, with applications to charm physics. Phys. Rev. D **75**, 054502 (2007)
332. A. Bazavov et al., Lattice QCD ensembles with four flavors of highly improved staggered quarks. Phys. Rev. D **87**(5), 054505 (2013)
333. K.C. Bowler et al., Quenched QCD with O(a) improvement. 1. The spectrum of light hadrons. Phys. Rev. D **62**, 054506 (2000)
334. S. Collins et al., Comparing Wilson and Clover quenched SU(3) spectroscopy with an improved gauge action. Nucl. Phys. B Proc. Suppl. **53**, 877–879 (1997) **(Ed. by C. Bernard et al.)**
335. P.H. Ginsparg, K.G. Wilson, A remnant of chiral symmetry on the lattice. Phys. Rev. D **25**, 2649 (1982)
336. R. Narayanan, H. Neuberger, Infinitely many regulator fields for chiral fermions. Phys. Lett. B **302**, 62–69 (1993)
337. R. Narayanan, H. Neuberger, Chiral fermions on the lattice. Phys. Rev. Lett. **71**(20), 3251 (1993)
338. R. Narayanan, H. Neuberger, Chiral determinant as an overlap of two vacua. Nucl. Phys. B **412**, 574–606 (1994)
339. R. Narayanan, H. Neuberger, A construction of lattice chiral gauge theories. Nucl. Phys. B **443**, 305–385 (1995)
340. H. Neuberger, Exactly massless quarks on the lattice. Phys. Lett. B **417**, 141–144 (1998)
341. P. Hasenfratz, V. Laliena, F. Niedermayer, The index theorem in QCD with a finite cutoff. Phys. Lett. B **427**, 125–131 (1998)
342. M. Luscher, Exact chiral symmetry on the lattice and the Ginsparg-Wilson relation. Phys. Lett. B **428**, 342–345 (1998)
343. D.B. Kaplan, A method for simulating chiral fermions on the lattice. Phys. Lett. B **288**, 342–347 (1992)
344. Y. Shamir, Chiral fermions from lattice boundaries. Nucl. Phys. B **406**, 90–106 (1993)
345. Y. Shamir, Constraints on the existence of chiral fermions in interacting lattice theories. Phys. Rev. Lett. **71**, 2691–2694 (1993)
346. V. Furman, Y. Shamir, Axial symmetries in lattice QCD with Kaplan fermions. Nucl. Phys. B **439**, 54–78 (1995)
347. C. Gattringer, C.B. Lang, *Quantum Chromodynamics on the Lattice*, vol. 788 (Springer, Berlin, 2010)
348. M. Creutz, *Quarks* (Cambridge Monographs on Mathematical Physics (Cambridge University Press, Cambridge, Gluons and Lattices, 1985)
349. M. Creutz (ed.), *Quantum Fields on the Computer* (WSP, Singapore, 1992)
350. T.A. DeGrand, D. Toussaint (eds.), From actions to answers. In: *Proceedings, Theoretical Advanced Study Institute in Elementary Particle Physics*, Boulder, June 5–30, 1989 (1990)
351. H.J. Rothe, *Lattice Gauge Theories?: An Introduction*, vol. 43, 4th edn. (World Scientific Publishing Company, Singapore, 2012)
352. I. Montvay, G. Munster, *Quantum Fields on a Lattice* (Cambridge Monographs on Mathematical Physics (Cambridge University Press, Cambridge, 1997)
353. M. Creutz, Monte Carlo study of quantized SU(2) gauge theory. Phys. Rev. D **21**, 2308–2315 (1980)
354. M. Creutz, Asymptotic freedom scales. Phys. Rev. Lett. **45**, 313 (1980) **(Ed. by J. Julve and M. Ramón-Medrano)**
355. R.P. Feynman, A.R. Hibbs, *Quantum Mechanics and Path Integrals* (International Series in Pure and Applied Physics (McGraw-Hill, New York, 1965)
356. M. Byrd, The Geometry of SU(3) (1997). arXiv:physics/9708015
357. W.K. Hastings, Monte Carlo sampling methods using Markov chains and their applications. Biometrika **57**, 97–109 (1970)
358. S. Duane et al., Hybrid Monte Carlo. Phys. Lett. B **195**, 216–222 (1987)
359. S.A. Gottlieb et al., Hybrid molecular dynamics algorithms for the numerical simulation of quantum chromodynamics. Phys. Rev. D **35**, 2531–2542 (1987)
360. T. Misumi, J. Yumoto, Varieties and properties of central-branch Wilson fermions. Phys. Rev. D **102**(3), 034516 (2020)
361. R.C. Brower et al., Multigrid for chiral lattice fermions: domain wall. Phys. Rev. D **102**(9), 094517 (2020)
362. C. Gattringer, S. Solbrig, Remnant index theorem and low-lying eigenmodes for twisted mass fermions. Phys. Lett. B **621**, 195–200 (2005)
363. M.A. Clark, A.D. Kennedy, The RHMC algorithm for two flavors of dynamical staggered fermions. Nucl. Phys. B Proc. Suppl. **129**, 850–852 (2004) **(Ed. by S. Aoki et al.)**
364. E.I. Zolotarev, Application of elliptic functions to the questions of functions deviating least and most from zero. In: *Zap. Imp. Akad. Nauk. St. Petersburg 30 (1877). Reprinted in his Collected works*, vol. 2 (Izdat, Akad. Nauk SSSR, Moscow), pp. 1–59 (1932)
365. M. Hasenbusch, Speeding up the hybrid Monte Carlo algorithm for dynamical fermions. Phys. Lett. B **519**, 177–182 (2001)
366. J. Brannick et al., Adaptive multigrid algorithm for lattice QCD. Phys. Rev. Lett. **100**, 041601 (2008)
367. R. Babich et al., Adaptive multigrid algorithm for the lattice Wilson-Dirac operator. Phys. Rev. Lett. **105**, 201602 (2010)
368. B. Jóo, Personal communication (2019)
369. R.C. Brower et al., Multigrid algorithm for staggered lattice fermions. Phys. Rev. D **97**(11), 114513 (2018)
370. P. Boyle, A. Yamaguchi, Comparison of domain wall fermion multigrid methods (2021). arXiv:2103.05034
371. A.D. Kennedy, B. Pendleton, Cost of the generalized hybrid Monte Carlo algorithm for free field theory. Nucl. Phys. B **607**, 456–510 (2001)
372. T. Nguyen et al., Riemannian manifold hybrid Monte Carlo in lattice QCD. PoS LATTICE **2021**, 582 (2022)
373. H. Nicolai, On a new characterization of scalar supersymmetric theories. Phys. Lett. B **89**, 341 (1980)
374. A. Aurilia, H. Nicolai, P.K. Townsend, Hidden constants: the theta parameter of QCD and the cosmological constant of N=8 supergravity. Nucl. Phys. B **176**, 509–522 (1980)
375. M. Luscher, Trivializing maps, the Wilson flow and the HMC algorithm. Commun. Math. Phys. **293**, 899–919 (2010)

376. R. Abbott,et al., Sampling QCD field configurations with gauge-equivariant flow models. In: *39th International Symposium on Lattice Field Theory* (2022)
377. D.B. Leinweber, E. Puckridge, Structure of the QCD Vacuum—CSSM Visualisations—YouTube. Online link. (2019)
378. M.C. Chu et al., Evidence for the role of instantons in hadron structure from lattice QCD. Nucl. Phys. B Proc. Suppl. **34**, 170–175 (1994)
379. M. Garcia Perez et al., Instantons from over-improved cooling. Nucl. Phys. B **413**, 535–552 (1994)
380. S.O. Bilson-Thompson, D.B. Leinweber, A.G. Williams, Highly improved lattice field strength tensor. Ann. Phys. **304**, 1–21 (2003)
381. S.O. Bilson-Thompson et al., Comparison of $|Q| = 1$ and $|Q| = 2$ gauge-field configurations on the lattice four-torus. Ann. Phys. **311**, 267–287 (2004)
382. P.J. Moran, D.B. Leinweber, Over-improved stout-link smearing. Phys. Rev. D **77**, 094501 (2008)
383. D.B. Leinweber, Visual QCD Archive. http://www.physics.adelaide.edu.au/theory/staff/leinweber/VisualQCD/QCDvacuum/ (2002)
384. D. Leinweber, QCD Lava Lamp. http://www.physics.adelaide.edu.au/theory/staff/leinweber/VisualQCD/QCDvacuum/su3b600s24t36cool30action.gif (2004)
385. F. Wilczek, 2004 Nobel Prize Lecture. https://www.nobelprize.org/prizes/physics/2004/wilczek/lecture/ (2004)
386. D.B. Leinweber, Visualizations of quantum chromodynamics. Online link (2004)
387. F.D.R. Bonnet, D.B. Leinweber, A.G. Williams, General algorithm for improved lattice actions on parallel computing architectures. J. Comput. Phys. **170**, 1–17 (2001)
388. D. Muller, Empty space is NOT empty. https://youtu.be/J3xLuZNKhlY?si=KGkhmv6PZYJxCeiM (2013)
389. D. Muller, Your mass is NOT from the Higgs boson. https://youtu.be/Ztc6QPNUqls?si=K48Zuj5L0EZ4vm7y (2013)
390. J. Biddle et al., Publicizing lattice field theory through visualization. PoS LATTICE **2018**, 325 (2019)
391. D. DeMartini, E. Shuryak, Deconfinement phase transition in the SU(3) instanton-dyon ensemble. Phys. Rev. D **104**(5), 054010 (2021)
392. F.D.R. Bonnet et al., Discretization errors in Landau gauge on the lattice. Austral. J. Phys. **52**, 939–948 (1999)
393. E.M. Ilgenfritz et al., Vacuum structure revealed by over-improved stout-link smearing compared with the overlap analysis for quenched QCD. Phys. Rev. D **77**, 074502 (2008) [Erratum: Phys. Rev. D 77, 099902 (2008)]
394. I. Horvath et al., The negativity of the overlap-based topological charge density correlator in pure-glue QCD and the non-integrable nature of its contact part. Phys. Lett. B **617**, 49–59 (2005)
395. P.J. Moran, D.B. Leinweber, Impact of dynamical fermions on QCD vacuum structure. Phys. Rev. D **78**, 054506 (2008)
396. I. Horvath et al., Low dimensional long range topological charge structure in the QCD vacuum. Phys. Rev. D **68**, 114505 (2003)
397. A. Portelli, Inclusion of isospin breaking effects in lattice simulations. PoS LATTICE **2014**, 013 (2015)
398. N. Tantalo, Matching lattice QC+ED to Nature. PoS LATTICE **2022**, 249 (2023)
399. R. Horsley et al., Isospin splittings of meson and baryon masses from three-flavor lattice QCD + QED. J. Phys. **G43**(10), 10LT02 (2016)
400. R. Horsley et al., QED effects in the pseudoscalar meson sector. JHEP **04**, 093 (2016)
401. C. Gattringer, A. Schmidt, Center clusters in the Yang-Mills vacuum. JHEP **01**, 051 (2011)
402. F.M. Stokes, W. Kamleh, D.B. Leinweber, Visualizations of coherent center domains in local Polyakov loops. Ann. Phys. **348**, 341–361 (2014)
403. C. Morningstar, M.J. Peardon, Analytic smearing of SU(3) link variables in lattice QCD. Phys. Rev. D **69**, 054501 (2004)
404. F. Bissey et al., Gluon flux-tube distribution and linear confinement in baryons. Phys. Rev. D **76**, 114512 (2007)
405. F.M. Stokes, W. Kamleh, D.B. Leinweber, Centre domains in the QCD vacuum-smeared phase. https://youtu.be/KkiOQOOb69k (2014)
406. M. Luscher, K. Symanzik, P. Weisz, Anomalies of the free loop wave equation in the WKB approximation. Nucl. Phys. B **173**, 365 (1980)
407. M. Luscher, G. Munster, P. Weisz, How thick are chromoelectric flux tubes? Nucl. Phys. B **180**, 1–12 (1981)
408. M. Luscher, Symmetry breaking aspects of the roughening transition in gauge theories. Nucl. Phys. B **180**, 317–329 (1981)
409. F. Gliozzi, M. Pepe, U.J. Wiese, The width of the confining string in Yang-Mills theory. Phys. Rev. Lett. **104**, 232001 (2010)
410. C. Michael, Adjoint sources in lattice gauge theory. Nucl. Phys. B **259**, 58–76 (1985)
411. M. Luscher, U. Wolff, How to calculate the elastic scattering matrix in two-dimensional quantum field theories by numerical simulation. Nucl. Phys. B **339**, 222–252 (1990)
412. B. Blossier et al., On the generalized eigenvalue method for energies and matrix elements in lattice field theory. JHEP **04**, 094 (2009)
413. P. de Forcrand, O. Jahn, The baryon static potential from lattice QCD. Nucl. Phys. A **755**, 475–480 (2005) **(Ed. by M. Guidal et al.)**
414. K.J. Juge, J. Kuti, C.J. Morningstar, Ab initio study of hybrid $\bar{b}gb$ mesons. Phys. Rev. Lett. **82**, 4400–4403 (1999)
415. K. Jimmy Juge, J. Kuti, C. Morningstar, Fine structure of the QCD string spectrum. Phys. Rev. Lett. **90**, 161601 (2003)
416. J.M.M. Hall et al., Lattice QCD evidence that the $\Lambda(1405)$ resonance is an antikaon-nucleon molecule. Phys. Rev. Lett. **114**(13), 132002 (2015)
417. J.M.M. Hall et al., Light-quark contributions to the magnetic form factor of the $\Lambda(1405)$. Phys. Rev. D **95**(5), 054510 (2017)
418. G.S. Bali et al., Observation of string breaking in QCD. Phys. Rev. D **71**, 114513 (2005)
419. J. Bulava et al., String breaking by light and strange quarks in QCD. Phys. Lett. B **793**, 493–498 (2019)
420. E. Klempt, A. Zaitsev, Glueballs, hybrids, multi-quarks. experimental facts versus QCD inspired concepts. Phys. Rep. **454**, 1–202 (2007)
421. C.W. Bernard et al., The QCD spectrum with three quark flavors. Phys. Rev. D **64**, 054506 (2001)
422. C. Aubin et al., Light hadrons with improved staggered quarks: approaching the continuum limit. Phys. Rev. D **70**, 094505 (2004)
423. G. 't Hooft, On the phase transition towards permanent quark confinement. Nucl. Phys. B **138**, 1–25 (1978)
424. G. 't Hooft, A property of electric and magnetic flux in nonabelian gauge theories. Nucl. Phys. B **153**, 141–160 (1979)
425. H. Bech Nielsen, P. Olesen, A quantum liquid model for the QCD vacuum: gauge and rotational invariance of domained and quantized homogeneous color fields. Nucl. Phys. B **160**, 380–396 (1979)
426. L. Del Debbio et al., Center dominance and Z(2) vortices in SU(2) lattice gauge theory. Phys. Rev. D **55**, 2298–2306 (1997)
427. M. Faber, J. Greensite, S. Olejnik, Casimir scaling from center vortices: towards an understanding of the adjoint string tension. Phys. Rev. D **57**, 2603–2609 (1998)
428. L. Del Debbio et al., Detection of center vortices in the lattice Yang-Mills vacuum. Phys. Rev. D **58**, 094501 (1998)
429. R. Bertle et al., The Structure of projected center vortices in lattice gauge theory. JHEP **03**, 019 (1999)
430. M. Faber et al., The vortex finding property of maximal center (and other) gauges. JHEP **12**, 012 (1999)

431. M. Engelhardt, H. Reinhardt, Center projection vortices in continuum Yang-Mills theory. Nucl. Phys. B **567**, 249 (2000)
432. J. Greensite, The confinement problem in lattice gauge theory. Prog. Part. Nucl. Phys. **51**, 1 (2003)
433. A. Trewartha, W. Kamleh, D. Leinweber, Evidence that centre vortices underpin dynamical chiral symmetry breaking in SU(3) gauge theory. Phys. Lett. B **747**, 373–377 (2015)
434. A. Trewartha, W. Kamleh, D. Leinweber, Centre vortex removal restores chiral symmetry. J. Phys. **G44**(12), 125002 (2017)
435. A. Virgili, W. Kamleh, D. Leinweber, Impact of centre vortex removal on the Landau-gauge quark propagator in dynamical QCD. PoS LATTICE **2021**, 082 (2021)
436. K. Langfeld, Vortex structures in pure SU(3) lattice gauge theory. Phys. Rev. D **69**, 014503 (2004)
437. P.O. Bowman et al., Role of center vortices in chiral symmetry breaking in SU(3) gauge theory. Phys. Rev. D **84**, 034501 (2011)
438. J.C. Biddle, W. Kamleh, D.B. Leinweber, Static quark potential from center vortices in the presence of dynamical fermions. Phys. Rev. D **106**(5), 054505 (2022)
439. D. Leinweber, J. Biddle, W. Kamleh, Centre vortex structure of QCD-vacuum fields and confinement. SciPost Phys. Proc. **6**, 004 (2022)
440. K. Langfeld, H. Reinhardt, J. Gattnar, Gluon propagators and quark confinement. Nucl. Phys. B **621**, 131–156 (2002)
441. J.C. Biddle, W. Kamleh, D.B. Leinweber, Gluon propagator on a center-vortex background. Phys. Rev. D **98**(9), 094504 (2018)
442. J.C. Biddle, W. Kamleh, D.B. Leinweber, Impact of dynamical fermions on the center vortex gluon propagator. Phys. Rev. D **106**(1), 014506 (2022)
443. A. O'Cais et al., Preconditioning maximal center gauge with stout link smearing in SU(3). Phys. Rev. D **82**, 114512 (2010)
444. A. Trewartha, W. Kamleh, D. Leinweber, Connection between center vortices and instantons through gauge-field smoothing. Phys. Rev. D **92**(7), 074507 (2015)
445. J.C. Biddle, W. Kamleh, D.B. Leinweber, Visualization of center vortex structure. Phys. Rev. D **102**(3), 034504 (2020)
446. E.-A. O'Malley et al., SU(3) centre vortices underpin confinement and dynamical chiral symmetry breaking. Phys. Rev. D **86**, 054503 (2012)
447. J.C. Biddle, W. Kamleh, D.B. Leinweber, Emergent structure in QCD. EPJ Web Conf. **245**, 06009 (2020) **(Ed. by C. Doglioni et al.)**
448. D. Leinweber, J. Biddle, W. Kamleh, Impact of dynamical fermions on centre vortex structure. PoS LATTICE **2021**, 197 (2021)
449. L. Del Debbio et al., Center dominance and Z(2) vortices in SU(2) lattice gauge theory. Phys. Rev. D **55**, 2298–2306 (1997)
450. K. Langfeld, H. Reinhardt, O. Tennert, Confinement and scaling of the vortex vacuum of SU(2) lattice gauge theory. Phys. Lett. B **419**, 317–321 (1998)
451. F. Bruckmann, M. Engelhardt, Writhe of center vortices and topological charge: an explicit example. Phys. Rev. D **68**, 105011 (2003)
452. M. Engelhardt, Center vortex model for the infrared sector of SU(3) Yang-Mills theory: topological susceptibility. Phys. Rev. D **83**, 025015 (2011)
453. M. Engelhardt, Center vortex model for the infrared sector of Yang-Mills theory: topological susceptibility. Nucl. Phys. B **585**, 614 (2000)
454. S. Aoki et al., 2+1 flavor lattice QCD toward the physical point. Phys. Rev. D **79**, 034503 (2009)
455. R. Sommer, A new way to set the energy scale in lattice gauge theories and its applications to the static force and α_s in SU(2) Yang-Mills theory. Nucl. Phys. B **411**, 839–854 (1994)
456. M. D'Elia, M.-P. Lombardo, Finite density QCD via imaginary chemical potential. Phys. Rev. D **67**, 014505 (2003)
457. P. de Forcrand, O. Philipsen, The QCD phase diagram for small densities from imaginary chemical potential. Nucl. Phys. B **642**, 290–306 (2002)
458. R.V. Gavai, S. Gupta, Quark number susceptibilities, strangeness and dynamical confinement. Phys. Rev. D **64**, 074506 (2001)
459. C.R. Allton et al., The QCD thermal phase transition in the presence of a small chemical potential. Phys. Rev. D **66**, 074507 (2002)
460. L.D. McLerran, B. Svetitsky, A Monte Carlo study of SU(2) Yang-Mills theory at finite temperature. Phys. Lett. B **98**, 195–198 (1981)
461. J. Kuti, J. Polonyi, K. Szlachanyi, Monte Carlo study of SU(2) gauge theory at finite temperature. Phys. Lett. B **98**, 199–204 (1981)
462. J.B. Kogut et al., Deconfinement and chiral symmetry restoration at finite temperatures in SU(2) and SU(3) gauge theories. Phys. Rev. Lett. **50**, 393 (1983)
463. J.C. Collins, M.J. Perry, Superdense matter: neutrons or asymptotically free quarks? Phys. Rev. Lett. **34**, 1353 (1975)
464. N. Cabibbo, G. Parisi, Exponential hadronic spectrum and quark liberation. Phys. Lett. B **59**, 67–69 (1975)
465. G. Baym, Confinement of quarks in nuclear matter. Physica A **96**(1–2), 131–135 (1979) **(Ed. by S. Deser)**
466. R.D. Pisarski, F. Wilczek, Remarks on the chiral phase transition in chromodynamics. Phys. Rev. D **29**, 338–341 (1984)
467. E.V. Shuryak, Quark-gluon plasma and hadronic production of leptons, photons and psions. Phys. Lett. B **78**, 150 (1978)
468. K. Kajantie, C. Montonen, E. Pietarinen, Phase transition of SU(3) gauge theory at finite temperature. Z. Phys. C **9**, 253 (1981)
469. L.G. Yaffe, B. Svetitsky, First order phase transition in the SU(3) gauge theory at finite temperature. Phys. Rev. D **26**, 963 (1982)
470. J. Engels et al., High temperature SU(2) gluon matter on the lattice. Phys. Lett. B **101**, 89 (1981) **(Ed. by J. Julve and M. Ramón-Medrano)**
471. J. Engels et al., Gauge field thermodynamics for the SU(2) Yang-Mills system. Nucl. Phys. B **205**, 545–577 (1982)
472. O. Kaczmarek, F. Zantow, Static quark anti-quark interactions in zero and finite temperature QCD. I. Heavy quark free energies, running coupling and quarkonium binding. Phys. Rev. D **71**, 114510 (2005)
473. K. Rajagopal, F. Wilczek, Static and dynamic critical phenomena at a second order QCD phase transition. Nucl. Phys. B **399**, 395–425 (1993)
474. K. Rajagopal, F. Wilczek, The condensed matter physics of QCD, in *At the frontier of particle physics. Handbook of QCD*, vols. 1–3, ed. by M. Shifman, B. Ioffe, pp. 2061–2151 (2000)
475. B. Svetitsky, L.G. Yaffe, Critical behavior at finite temperature confinement transitions. Nucl. Phys. B **210**, 423–447 (1982)
476. F.R. Brown et al., Nature of the deconfining phase transition in SU(3) lattice gauge theory. Phys. Rev. Lett. **61**, 2058 (1988)
477. J. Engels, J. Fingberg, M. Weber, Finite size scaling analysis of SU(2) lattice gauge theory in (3+1)-dimensions. Nucl. Phys. B **332**, 737–759 (1990)
478. H.T. Ding et al., Chiral phase transition temperature in (2+1)-flavor QCD. Phys. Rev. Lett. **123**(6), 062002 (2019)
479. O. Kaczmarek et al., Universal scaling properties of QCD close to the chiral limit. Acta Phys. Polon. Suppl. **14**, 291 (2021)
480. F. Cuteri, O. Philipsen, A. Sciarra, On the order of the QCD chiral phase transition for different numbers of quark flavours. JHEP **11**, 141 (2021)
481. F.R. Brown et al., On the existence of a phase transition for QCD with three light quarks. Phys. Rev. Lett. **65**, 2491–2494 (1990)
482. L. Dini et al., Chiral phase transition in three-flavor QCD from lattice QCD. Phys. Rev. D **105**(3), 034510 (2022)
483. A.Y. Kotov, M. Paola Lombardo, A. Trunin, QCD transition at the physical point, and its scaling window from twisted mass Wilson fermions. Phys. Lett. B **823**, 136749 (2021)

484. A. Bazavov et al., Chiral crossover in QCD at zero and non-zero chemical potentials. Phys. Lett. B **795**, 15–21 (2019)
485. C. Bonati et al., Curvature of the chiral pseudocritical line in QCD: continuum extrapolated results. Phys. Rev. D **92**(5), 054503 (2015)
486. C. Bonati et al., Curvature of the pseudocritical line in QCD: Taylor expansion matches analytic continuation. Phys. Rev. D **98**(5), 054510 (2018)
487. S. Borsanyi et al., QCD crossover at finite chemical potential from lattice simulations. Phys. Rev. Lett. **125**(5), 052001 (2020)
488. R. Guida, J. Zinn-Justin, Critical exponents of the N vector model. J. Phys. A **31**, 8103–8121 (1998)
489. A. Pelissetto, E. Vicari, Relevance of the axial anomaly at the finite-temperature chiral transition in QCD. Phys. Rev. D **88**(10), 105018 (2013)
490. A. Lahiri, Aspects of finite temperature QCD towards the chiral limit. In: *PoS LATTICE2021*, 003 (2022)
491. G. Aarts et al., Hyperons in thermal QCD: a lattice view. Phys. Rev. D **99**(7), 074503 (2019)
492. A. Bazavov et al., Meson screening masses in (2+1)-flavor QCD. Phys. Rev. D **100**(9), 094510 (2019)
493. S. Dentinger, O. Kaczmarek, A. Lahiri, Screening masses towards chiral limit. Acta Phys. Polon. Suppl. **14**, 321 (2021)
494. C.E. Detar, J.B. Kogut, The hadronic spectrum of the quark plasma. Phys. Rev. Lett. **59**, 399 (1987)
495. C.E. Detar, J.B. Kogut, Measuring the hadronic spectrum of the quark plasma. Phys. Rev. D **36**, 2828 (1987)
496. H.T. Ding et al., Correlated Dirac eigenvalues and axial anomaly in chiral symmetric QCD. Phys. Rev. Lett. **126**(8), 082001 (2021)
497. G. Cossu et al., Finite temperature study of the axial U(1) symmetry on the lattice with overlap fermion formulation. Phys. Rev. D **87**(11), 114514 (2013) [Erratum: Phys. Rev. D 88, 019901 (2013)]
498. A. Tomiya et al., Evidence of effective axial U(1) symmetry restoration at high temperature QCD. Phys. Rev. D **96**(3), 034509 (2017) [Addendum: Phys. Rev. D 96, 079902 (2017)]
499. M.I. Buchoff et al., QCD chiral transition, U(1)A symmetry and the Dirac spectrum using domain wall fermions. Phys. Rev. D **89**(5), 054514 (2014)
500. V. Dick et al., Microscopic origin of $U_A(1)$ symmetry violation in the high temperature phase of QCD. Phys. Rev. D **91**(9), 094504 (2015)
501. A. Bazavov et al., Equation of state in (2+1)-flavor QCD. Phys. Rev. D **90**, 094503 (2014)
502. S. Borsanyi et al., Full result for the QCD equation of state with 2+1 flavors. Phys. Lett. B **730**, 99–104 (2014)
503. D. Bollweg et al., Taylor expansions and Padé approximants for cumulants of conserved charge fluctuations at nonvanishing chemical potentials. Phys. Rev. D **105**(7), 074511 (2022)
504. A. Miklos Halasz et al., On the phase diagram of QCD. Phys. Rev. D **58**, 096007 (1998)
505. M. Buballa, S. Carignano, Inhomogeneous chiral phases away from the chiral limit. Phys. Lett. B **791**, 361–366 (2019)
506. C.M. Hung, E.V. Shuryak, Hydrodynamics near the QCD phase transition: looking for the longest lived fireball. Phys. Rev. Lett. **75**, 4003–4006 (1995)
507. S. Borsanyi et al., QCD equation of state at nonzero chemical potential: continuum results with physical quark masses at order μ^2. JHEP **08**, 053 (2012)
508. S. Mukherjee, V. Skokov, Universality driven analytic structure of the QCD crossover: radius of convergence in the baryon chemical potential. Phys. Rev. D **103**(7), L071501 (2021)
509. S. Mondal, S. Mukherjee, P. Hegde, Lattice QCD equation of state for nonvanishing chemical potential by resumming Taylor expansions. Phys. Rev. Lett. **128**(2), 022001 (2022)
510. P. Dimopoulos et al., Contribution to understanding the phase structure of strong interaction matter: Lee-Yang edge singularities from lattice QCD. Phys. Rev. D **105**(3), 034513 (2022)
511. S. Borsanyi et al., Resummed lattice QCD equation of state at finite baryon density: strangeness neutrality and beyond. Phys. Rev. D **105**(11), 114504 (2022)
512. S. Datta, R.V. Gavai, S. Gupta, Quark number susceptibilities and equation of state at finite chemical potential in staggered QCD with Nt = 8. Phys. Rev. D **95**(5), 054512 (2017)
513. R.L. Workman, Review of particle physics. PTEP **2022**, 083C01 (2022)
514. M.R. Shepherd, J.J. Dudek, R.E. Mitchell, Searching for the rules that govern hadron construction. Nature **534**(7608), 487–493 (2016)
515. A.S. Kronfeld, Twenty-first century lattice gauge theory: results from the QCD Lagrangian. Annu. Rev. Nucl. Part. Sci. **62**, 265–284 (2012)
516. S. Aoki et al., 1+1+1 flavor QCD + QED simulation at the physical point. Phys. Rev. D **86**, 034507 (2012)
517. Sz. Borsanyi et al., Isospin splittings in the light baryon octet from lattice QCD and QED. Phys. Rev. Lett. **111**(25), 252001 (2013)
518. Sz. Borsanyi et al., Ab initio calculation of the neutron-proton mass difference. Science **347**, 1452–1455 (2015)
519. R. Horsley et al., Isospin splittings in the decuplet baryon spectrum from dynamical QCD+QED. J. Phys. G **46**, 115004 (2019)
520. M. Peardon et al., A novel quark-field creation operator construction for hadronic physics in lattice QCD. Phys. Rev. D **80**, 054506 (2009)
521. J.J. Dudek et al., Toward the excited isoscalar meson spectrum from lattice QCD. Phys. Rev. D **88**(9), 094505 (2013)
522. C. Morningstar et al., Improved stochastic estimation of quark propagation with Laplacian Heaviside smearing in lattice QCD. Phys. Rev. D **83**, 114505 (2011)
523. J.J. Dudek et al., Highly excited and exotic meson spectrum from dynamical lattice QCD. Phys. Rev. Lett. **103**, 262001 (2009)
524. J.J. Dudek et al., Toward the excited meson spectrum of dynamical QCD. Phys. Rev. D **82**, 034508 (2010)
525. J.J. Dudek et al., Isoscalar meson spectroscopy from lattice QCD. Phys. Rev. D **83**, 111502 (2011)
526. C.E. Thomas, R.G. Edwards, J.J. Dudek, Helicity operators for mesons in flight on the lattice. Phys. Rev. D **85**, 014507 (2012)
527. J.J. Dudek, The lightest hybrid meson supermultiplet in QCD. Phys. Rev. D **84**, 074023 (2011)
528. R.G. Edwards et al., Excited state baryon spectroscopy from lattice QCD. Phys. Rev. D **84**, 074508 (2011)
529. J.J. Dudek, R.G. Edwards, Hybrid baryons in QCD. Phys. Rev. D **85**, 054016 (2012)
530. M. Luscher, Volume dependence of the energy spectrum in massive quantum field theories. 2. Scattering states. Commun. Math. Phys. **105**, 153–188 (1986)
531. M. Luscher, Two particle states on a torus and their relation to the scattering matrix. Nucl. Phys. B **354**, 531–578 (1991)
532. R.A. Briceno, J.J. Dudek, R.D. Young, Scattering processes and resonances from lattice QCD. Rev. Mod. Phys. **90**(2), 025001 (2018)
533. J.J. Dudek, R.G. Edwards, C.E. Thomas, Energy dependence of the ρ resonance in $\pi\pi$ elastic scattering from lattice QCD. Phys. Rev. D **87**(3), 034505 (2013) [Erratum: Phys. Rev. D 90, 099902 (2014)]
534. J.J. Dudek, R.G. Edwards, C.E. Thomas, S and D-wave phase shifts in isospin-2 pi pi scattering from lattice QCD. Phys. Rev. D **86**, 034031 (2012)
535. D.J. Wilson et al., Coupled $\pi\pi$, $K\bar{K}$ scattering in P-wave and the ρ resonance from lattice QCD. Phys. Rev. D **92**(9), 094502 (2015)

536. S. Aoki et al., Lattice QCD calculation of the rho meson decay width. Phys. Rev. D **76**, 094506 (2007)
537. X. Feng, K. Jansen, D.B. Renner, Resonance parameters of the rho-meson from lattice QCD. Phys. Rev. D **83**, 094505 (2011)
538. C.B. Lang et al., Coupled channel analysis of the rho meson decay in lattice QCD. Phys. Rev. D **84**(5), 054503 (2011) [Erratum: Phys. Rev. D 89, 059903 (2014)]
539. S. Aoki et al., ρ meson decay in 2+1 flavor lattice QCD. Phys. Rev. D **84**, 094505 (2011)
540. C. Pelissier, A. Alexandru, Resonance parameters of the rho-meson from asymmetrical lattices. Phys. Rev. D **87**(1), 014503 (2013)
541. G.S. Bali et al., ρ and K^* resonances on the lattice at nearly physical quark masses and $N_f = 2$. Phys. Rev. D **93**(5), 054509 (2016)
542. J. Bulava et al., $I = 1$ and $I = 2\pi - \pi$ scattering phase shifts from $N_{\rm f} = 2+1$ lattice QCD. Nucl. Phys. B **910**, 842–867 (2016)
543. C. Alexandrou et al., P-wave $\pi\pi$ scattering and the ρ resonance from lattice QCD. Phys. Rev. D **96**(3), 034525 (2017)
544. C. Andersen et al., The $I = 1$ pion-pion scattering amplitude and timelike pion form factor from $N_{\rm f} = 2 + 1$ lattice QCD. Nucl. Phys. B **939**, 145–173 (2019)
545. M. Werner et al., Hadron-hadron interactions from $N_f = 2+1+1$ lattice QCD: the ρ-resonance. Eur. Phys. J. A **56**(2), 61 (2020)
546. F. Erben et al., Rho resonance, timelike pion form factor, and implications for lattice studies of the hadronic vacuum polarization. Phys. Rev. D **101**(5), 054504 (2020)
547. M. Fischer et al., The ρ-resonance from $N_f = 2$ lattice QCD including the physical pion mass. Phys. Lett. B **819**, 136449 (2021)
548. C.B. Lang et al., $K\pi$ scattering for isospin 1/2 and 3/2 in lattice QCD. Phys. Rev. D **86**, 054508 (2012)
549. Fu. Ziwen, Fu. Kan, Lattice QCD study on K^* (892) meson decay width. Phys. Rev. D **86**, 094507 (2012)
550. S. Prelovsek et al., K π scattering and the K* decay width from lattice QCD. Phys. Rev. D **88**(5), 054508 (2013)
551. R. Brett et al., Determination of s- and p-wave $I = 1/2 K\pi$ scattering amplitudes in $N_{\rm f} = 2 + 1$ lattice QCD. Nucl. Phys. B **932**, 29–51 (2018)
552. D.J. Wilson et al., The quark-mass dependence of elastic πK scattering from QCD. Phys. Rev. Lett. **123**(4), 042002 (2019)
553. J.J. Dudek et al., Phase shift of isospin-2 $\pi\pi$ scattering from lattice QCD. Phys. Rev. D **83**, 071504 (2011)
554. S.R. Beane et al., The I = 2 pipi S-wave scattering phase shift from lattice QCD. Phys. Rev. D **85**, 034505 (2012)
555. C. Culver et al., Pion scattering in the isospin $I = 2$ channel from elongated lattices. Phys. Rev. D **100**(3), 034509 (2019)
556. M. Fischer et al., Scattering of two and three physical pions at maximal isospin from lattice QCD. Eur. Phys. J. C **81**(5), 436 (2021)
557. T. Blum et al., Lattice determination of I = 0 and $2\pi\pi$ scattering phase shifts with a physical pion mass. Phys. Rev. D **104**(11), 114506 (2021)
558. R.A. Briceno et al., Isoscalar $\pi\pi$ scattering and the σ meson resonance from QCD. Phys. Rev. Lett. **118**(2), 022002 (2017)
559. D. Guo et al., Extraction of isoscalar $\pi\pi$ phase-shifts from lattice QCD. Phys. Rev. D **98**(1), 014507 (2018)
560. R.A. Briceno et al., Isoscalar $\pi\pi$, $K\bar{K}$, $\eta\eta$ scattering and the σ, f_0,f_2 mesons from QCD. Phys. Rev. D **97**(5), 054513 (2018)
561. D. Mohler, S. Prelovsek, R.M. Woloshyn, $D\pi$ scattering and D meson resonances from lattice QCD. Phys. Rev. D **87**(3), 034501 (2013)
562. S. Prelovsek, L. Leskovec, Evidence for X(3872) from DD* scattering on the lattice. Phys. Rev. Lett. **111**, 192001 (2013)
563. C.B. Lang et al., D_s mesons with DK and $D*K$ scattering near threshold. Phys. Rev. D **90**(3), 034510 (2014)
564. C.B. Lang et al., Vector and scalar charmonium resonances with lattice QCD. JHEP **09**, 089 (2015)
565. C.B. Lang, D. Mohler, S. Prelovsek, $B_s\pi^+$ scattering and search for X(5568) with lattice QCD. Phys. Rev. D **94**, 074509 (2016)
566. G. Moir et al., Coupled-channel $D\pi$, $D\eta$ and $D_s\bar{K}$ scattering from lattice QCD. JHEP **10**, 011 (2016)
567. L. Gayer et al., Isospin-1/2 Dπ scattering and the lightest D_0^* resonance from lattice QCD. JHEP **07**, 123 (2021)
568. L. Liu et al., Interactions of charmed mesons with light pseudoscalar mesons from lattice QCD and implications on the nature of the D_{s0}^* (2317). Phys. Rev. D **87**(1), 014508 (2013)
569. D. Mohler et al., D_{s0}^*(2317) meson and D-meson-kaon scattering from lattice QCD. Phys. Rev. Lett. **111**(22), 222001 (2013)
570. G.S. Bali et al., Masses and decay constants of the D_{s0}^*(2317) and D_{s1}(2460) from $N_f = 2$ lattice QCD close to the physical point. Phys. Rev. D **96**(7), 074501 (2017)
571. C. Alexandrou et al., Tetraquark interpolating fields in a lattice QCD investigation of the D_{s0}^*(2317) meson. Phys. Rev. D **101**(3), 034502 (2020)
572. G.K.C. Cheung et al., DK I = 0, $D\bar{K}$I = 0, 1 scattering and the D_{s0}^*(2317) from lattice QCD. JHEP **02**, 100 (2021)
573. N. Lang, D.J. Wilson, Axial-vector D1 hadrons in $D^*\pi$ scattering from QCD. Phys. Rev. Lett. **129**(25), 252001 (2022)
574. C.B. Lang et al., Pion-nucleon scattering in the Roper channel from lattice QCD. Phys. Rev. D **95**(1), 014510 (2017)
575. C. Walther Andersen et al., Elastic $I = 3/2p$-wave nucleon-pion scattering amplitude and the Δ(1232) resonance from $\rm N_f = 2+1$ lattice QCD. Phys. Rev. D **97**(1), 014506 (2018)
576. G. Silvi et al., P-wave nucleon-pion scattering amplitude in the Δ(1232) channel from lattice QCD. Phys. Rev. D **103**(9), 094508 (2021)
577. J.J. Dudek et al., Resonances in coupled $\pi K - \eta K$ scattering from quantum chromodynamics. Phys. Rev. Lett. **113**(18), 182001 (2014)
578. D.J. Wilson et al., Resonances in coupled πK, ηK scattering from lattice QCD. Phys. Rev. D **91**(5), 054008 (2015)
579. J.J. Dudek, R.G. Edwards, D.J. Wilson, An a_0 resonance in strongly coupled $\pi\eta$, $K\bar{K}$ scattering from lattice QCD. Phys. Rev. D **93**(9), 094506 (2016)
580. A. Woss et al., Dynamically-coupled partial-waves in $\rho\pi$ isospin-2 scattering from lattice QCD. JHEP **07**, 043 (2018)
581. A.J. Woss et al., b_1 resonance in coupled $\pi\omega$, $\pi\phi$ scattering from lattice QCD. Phys. Rev. D **100**(5), 054506 (2019)
582. A.J. Woss et al., Decays of an exotic 1^{-+} hybrid meson resonance in QCD. Phys. Rev. D **103**(5), 054502 (2021)
583. C.T. Johnson, J.J. Dudek, Excited J^- meson resonances at the SU(3) flavor point from lattice QCD. Phys. Rev. D **103**(7), 074502 (2021)
584. S. Prelovsek et al., Charmonium-like resonances with $\rm J^{PC} = 0^{++}, 2^{++}$ in coupled $\rm D\bar{D}$, $\rm D_s\bar{D}_s$ scattering on the lattice. JHEP **06**, 035 (2021)
585. R.A. Briceno et al., The resonant $\pi^+\gamma \to \pi^+\pi^0$ amplitude from quantum chromodynamics. Phys. Rev. Lett. **115**, 242001 (2015)
586. R.A. Briceño et al., The $\pi\pi \to \pi\gamma^*$ amplitude and the resonant $\rho \to \pi\gamma^*$ transition from lattice QCD. Phys. Rev. D **93**(11), 114508 (2016)
587. C. Alexandrou et al., $\pi\gamma \to \pi\pi$ transition and the ρ radiative decay width from lattice QCD. Phys. Rev. D **98**(7), 074502 (2018)
588. L. Lellouch, M. Luscher, Weak transition matrix elements from finite volume correlation functions. Commun. Math. Phys. **219**, 31–44 (2001)
589. R.A. Briceño, M.T. Hansen, A. Walker-Loud, Multichannel 1 → 2 transition amplitudes in a finite volume. Phys. Rev. D **91**, 034501 (2015)

590. R.A. Briceño, M.T. Hansen, Multichannel $0 \to 2$ and $1 \to 2$ transition amplitudes for arbitrary spin particles in a finite volume. Phys. Rev. D **92**(7), 074509 (2015)
591. M.T. Hansen et al., Energy-dependent $\pi^+\pi^+\pi^+$ scattering amplitude from QCD. Phys. Rev. Lett. **126**, 012001 (2021)
592. A. Baroni et al., Form factors of two-hadron states from a covariant finite-volume formalism. Phys. Rev. D **100**(3), 034511 (2019)
593. M.T. Hansen, S.R. Sharpe, Lattice QCD and three-particle decays of resonances. Annu. Rev. Nucl. Part. Sci. **69**, 65–107 (2019)
594. B. Hörz, A. Hanlon, Two-and three-pion finite-volume spectra at maximal isospin from lattice QCD. Phys. Rev. Lett. **123**(14), 142002 (2019)
595. T.D. Blanton, F. Romero-López, S.R. Sharpe, $I = 3$ three-pion scattering amplitude from lattice QCD. Phys. Rev. Lett. **124**(3), 032001 (2020)
596. M. Mai et al., Three-body dynamics of the a1(1260) resonance from lattice QCD. Phys. Rev. Lett. **127**(22), 222001 (2021)
597. R. Brett et al., Three-body interactions from the finite-volume QCD spectrum. Phys. Rev. D **104**(1), 014501 (2021)
598. T.D. Blanton et al., Interactions of two and three mesons including higher partial waves from lattice QCD. JHEP **10**, 023 (2021)
599. R. Hofstadter, Electron scattering and nuclear structure. Rev. Mod. Phys. **28**, 214–254 (1956)
600. S. Basak et al., Lattice QCD determination of patterns of excited baryon states. Phys. Rev. D **76**, 074504 (2007)
601. S. Sint, Nonperturbative renormalization in lattice field theory. Nucl. Phys. B Proc. Suppl. **94**, 79–94 (2001) **(Ed. by T. Bhattacharya, R. Gupta, and A. Patel)**
602. M. Constantinou et al., Parton distributions and lattice-QCD calculations: toward 3D structure. Prog. Part. Nucl. Phys. **121**, 103908 (2021)
603. R. Acciarri et al., Long-Baseline Neutrino Facility (LBNF) and Deep Underground Neutrino Experiment (DUNE): Conceptual Design Report, Volume 2: The Physics Program for DUNE at LBNF (2015). arXiv:1512.06148
604. K. Abe et al., Hyper-Kamiokande Design Report (2018). arXiv:1805.04163
605. A.S. Meyer, A. Walker-Loud, C. Wilkinson, Status of lattice QCD determination of nucleon form factors and their relevance for the few-GeV neutrino program (2022). arXiv:2201.01839
606. S. Park et al., Precision nucleon charges and form factors using (2+1)-flavor lattice QCD. Phys. Rev. D **105**(5), 054505 (2022)
607. Y.-C. Jang et al., Nucleon electromagnetic form factors in the continuum limit from $(2 + 1 + 1)$-flavor lattice QCD. Phys. Rev. D **101**(1), 014507 (2020)
608. R.J. Hill, G. Paz, Model independent extraction of the proton charge radius from electron scattering. Phys. Rev. D **82**, 113005 (2010)
609. D. Djukanovic, Recent progress on nucleon form factors. In: PoS LATTICE2021, p. 009 (2022)
610. J.J. Kelly, Simple parametrization of nucleon form factors. Phys. Rev. C **70**, 068202 (2004)
611. D. Djukanovic et al., Isovector electromagnetic form factors of the nucleon from lattice QCD and the proton radius puzzle. Phys. Rev. D **103**(9), 094522 (2021)
612. C. Alexandrou et al., Proton and neutron electromagnetic form factors from lattice QCD. Phys. Rev. D **100**(1), 014509 (2019)
613. E. Shintani et al., Nucleon form factors and root-mean-square radii on a $(10.8\text{fm})^4$ lattice at the physical point. Phys. Rev. D **99**(1), 014510 (2019) [Erratum: Phys. Rev. D 102, 019902 (2020)]
614. C. Alexandrou et al., Model-independent determination of the nucleon charge radius from lattice QCD. Phys. Rev. D **101**(11), 114504 (2020)
615. K.-I. Ishikawa et al., Calculation of the derivative of nucleon form factors in $N_f = 2 + 1$ lattice QCD at $M_\pi = 138$MeV on a (5.5 fm)3 volume. Phys. Rev. D **104**(7), 074514 (2021)
616. R.L. Workman et al., Review of particle physics. PTEP **2022**, 083C01 (2022)
617. H. Atac et al., Measurement of the neutron charge radius and the role of its constituents. Nat. Commun. **12**(1), 1759 (2021)
618. J.C. Bernauer et al., Electric and magnetic form factors of the proton. Phys. Rev. C **90**(1), 015206 (2014)
619. A.S. Meyer et al., Deuterium target data for precision neutrino-nucleus cross sections. Phys. Rev. D **93**(11), 113015 (2016)
620. G.S. Bali et al., Nucleon axial structure from lattice QCD. JHEP **05**, 126 (2020)
621. K.-I. Ishikawa et al., Nucleon form factors on a large volume lattice near the physical point in 2+1 flavor QCD. Phys. Rev. D **98**(7), 074510 (2018)
622. A.S. Meyer et al., Nucleon axial form factor from domain wall on HISQ. PoS LATTICE **2021**, 081 (2022)
623. N. Hasan et al., Computing the nucleon charge and axial radii directly at $Q^2 = 0$ in lattice QCD. Phys. Rev. D **97**(3), 034504 (2018)
624. C. Alexandrou et al., Nucleon axial and pseudoscalar form factors from lattice QCD at the physical point. Phys. Rev. D **103**(3), 034509 (2021)
625. S. Capitani, G. Rossi, Deep inelastic scattering in improved lattice QCD. 1. The first moment of structure functions. Nucl. Phys. B **433**, 351–389 (1995)
626. G. Beccarini et al., Deep inelastic scattering in improved lattice QCD. 2. The second moment of structure functions. Nucl. Phys. B **456**, 271–295 (1995)
627. M. Gockeler et al., Lattice operators for moments of the structure functions and their transformation under the hypercubic group. Phys. Rev. D **54**, 5705–5714 (1996)
628. S. Capitani, Perturbative renormalization of the first two moments of nonsinglet quark distributions with overlap fermions. Nucl. Phys. B **592**, 183–202 (2001)
629. S. Capitani, Perturbative renormalization of moments of quark momentum, helicity and transversity distributions with overlap and Wilson fermions. Nucl. Phys. B **597**, 313–336 (2001)
630. K.-F. Liu, S.-J. Dong, Origin of difference between $\bar{d}$ and $\bar{u}$ partons in the nucleon. Phys. Rev. Lett. **72**, 1790–1793 (1994)
631. K.F. Liu et al., Valence QCD: connecting QCD to the quark model. Phys. Rev. D **59**, 112001 (1999)
632. K.-F. Liu, Parton degrees of freedom from the path integral formalism. Phys. Rev. D **62**, 074501 (2000)
633. C.J. William Detmold, D. Lin, Deep-inelastic scattering and the operator product expansion in lattice QCD. Phys. Rev. D **73**, 014501 (2006)
634. W. Detmold et al., Parton physics from a heavy-quark operator product expansion: formalism and Wilson coefficients. Phys. Rev. D **104**(7), 074511 (2021)
635. V. Braun, D. Müller, Exclusive processes in position space and the pion distribution amplitude. Eur. Phys. J. C **55**, 349–361 (2008)
636. Z. Davoudi, M.J. Savage, Restoration of rotational symmetry in the continuum limit of lattice field theories. Phys. Rev. D **86**, 054505 (2012)
637. X. Ji, Parton physics on a Euclidean lattice. Phys. Rev. Lett. **110**, 262002 (2013)
638. X. Ji, Parton physics from large-momentum effective field theory. Sci. China Phys. Mech. Astron. **57**, 1407–1412 (2014)
639. A. Radyushkin, Nonperturbative evolution of parton quasi-distributions. Phys. Lett. B **767**, 314–320 (2017)
640. Y.-Q. Ma, J.-W. Qiu, Extracting parton distribution functions from lattice QCD calculations. Phys. Rev. D **98**(7), 074021 (2018)
641. Y.-Q. Ma, J.-W. Qiu, QCD factorization and PDFs from lattice QCD calculation. Int. J. Mod. Phys. Conf. Ser. **37**, 1560041 (2015) **(Ed. by Alexei Prokudin, Anatoly Radyushkin, and Leonard Gamberg)**

642. Y.-Q. Ma, J.-W. Qiu, Exploring partonic structure of hadrons using ab initio lattice QCD calculations. Phys. Rev. Lett. **120**(2), 022003 (2018)
643. A.J. Chambers et al., Nucleon structure functions from operator product expansion on the lattice. Phys. Rev. Lett. **118**(24), 242001 (2017)
644. C. Monahan, Recent developments in x-dependent structure calculations. In: *PoS* LATTICE2018, p. 018 (2018)
645. K. Cichy, M. Constantinou, A guide to light-cone PDFs from lattice QCD: an overview of approaches, techniques and results. Adv. High Energy Phys. **2019**, 3036904 (2019)
646. X. Ji et al., Large-momentum effective theory. Rev. Mod. Phys. **93**(3), 035005 (2021)
647. M. Constantinou, The x-dependence of hadronic parton distributions: a review on the progress of lattice QCD. Eur. Phys. J. A **57**(2), 77 (2021)
648. K. Cichy, Progress in x-dependent partonic distributions from lattice QCD. PoS LATTICE2021, p. 017 (2022)
649. C. Alexandrou et al., Light-cone parton distribution functions from lattice QCD. Phys. Rev. Lett. **121**(11), 112001 (2018)
650. C. Alexandrou et al., Systematic uncertainties in parton distribution functions from lattice QCD simulations at the physical point. Phys. Rev. D **99**(11), 114504 (2019)
651. B. Joó et al., Parton distribution functions from Ioffe time pseudodistributions from lattice calculations: approaching the physical point. Phys. Rev. Lett. **125**(23), 232003 (2020)
652. M. Bhat et al., Flavor nonsinglet parton distribution functions from lattice QCD at physical quark masses via the pseudodistribution approach. Phys. Rev. D **103**(3), 034510 (2021)
653. H.-W. Lin et al., Proton isovector helicity distribution on the lattice at physical pion mass. Phys. Rev. Lett. **121**(24), 242003 (2018)
654. C. Alexandrou et al., Transversity parton distribution functions from lattice QCD. Phys. Rev. D **98**(9), 091503 (2018)
655. C. Egerer et al., Transversity parton distribution function of the nucleon using the pseudodistribution approach. Phys. Rev. D **105**(3), 034507 (2022)
656. V. Braun, P. Gornicki, L. Mankiewicz, Ioffe-time distributions instead of parton momentum distributions in description of deep inelastic scattering. Phys. Rev. D **51**, 6036–6051 (1995)
657. V.N. Gribov, B.L. Ioffe, I.Y. Pomeranchuk, On the total annihilation cross-section of electron-positron pairs into hadrons at high-energies. Yad. Fiz. **6**, 587 (1967)
658. V.N. Gribov, B.L. Ioffe, I.Y. Pomeranchuk, What is the range of interactions at high-energies. Yad. Fiz. **2**, 768–776 (1965)
659. T. Khan et al., Unpolarized gluon distribution in the nucleon from lattice quantum chromodynamics. Phys. Rev. D **104**(9), 094516 (2021)
660. Z. Fan, H.-W. Lin, Gluon parton distribution of the pion from lattice QCD. Phys. Lett. B **823**, 136778 (2021)
661. C. Egerer et al., Distillation at high-momentum. Phys. Rev. D **103**(3), 034502 (2021)
662. J. Karpie et al., The continuum and leading twist limits of parton distribution functions in lattice QCD. JHEP **11**, 024 (2021)
663. T.-J. Hou et al., New CTEQ global analysis of quantum chromodynamics with high-precision data from the LHC. Phys. Rev. D **103**(1), 014013 (2021)
664. R.D. Ball et al., Parton distributions from high-precision collider data. Eur. Phys. J. C **77**(10), 663 (2017)
665. E. Moffat et al., Simultaneous Monte Carlo analysis of parton densities and fragmentation functions. Phys. Rev. D **104**(1), 016015 (2021)
666. C. Alexandrou et al., Flavor decomposition for the proton helicity parton distribution functions. Phys. Rev. Lett. **126**(10), 102003 (2021)
667. C. Alexandrou et al., Flavor decomposition of the nucleon unpolarized, helicity, and transversity parton distribution functions from lattice QCD simulations. Phys. Rev. D **104**(5), 054503 (2021)
668. R. Zhang, H.-W. Lin, B. Yoon, Probing nucleon strange and charm distributions with lattice QCD. Phys. Rev. D **104**(9), 094511 (2021)
669. S. Bhattacharya et al., Generalized parton distributions from lattice QCD with asymmetric momentum transfer: unpolarized quarks. Phys. Rev. D **106**(11), 114512 (2022)
670. C. Alexandrou et al., Transversity GPDs of the proton from lattice QCD. Phys. Rev. D **105**(3), 034501 (2022)
671. H.-W. Lin, Nucleon tomography and generalized parton distribution at physical pion mass from lattice QCD. Phys. Rev. Lett. **127**(18), 182001 (2021)
672. P. Shanahan, M. Wagman, Y. Zhao, Collins-Soper kernel for TMD evolution from lattice QCD. Phys. Rev. D **102**(1), 014511 (2020)
673. Q.-A. Zhang et al., Lattice-QCD calculations of TMD soft function through large-momentum effective theory. Phys. Rev. Lett. **125**(19), 192001 (2020)
674. M. Schlemmer et al., Determination of the Collins-Soper kernel from lattice QCD. JHEP **08**, 004 (2021)
675. Y. Li et al., Lattice QCD study of transverse-momentum dependent soft function. Phys. Rev. Lett. **128**(6), 062002 (2022)
676. P. Shanahan, M. Wagman, Y. Zhao, Lattice QCD calculation of the Collins-Soper kernel from quasi-TMDPDFs. Phys. Rev. D **104**(11), 114502 (2021)
677. S. Bhattacharya et al., Insights on proton structure from lattice QCD: the twist-3 parton distribution function $g_T(x)$. Phys. Rev. D **102**(11), 111501 (2020)
678. M.A. Ebert, I.W. Stewart, Y. Zhao, Determining the nonperturbative Collins-Soper kernel from lattice QCD. Phys. Rev. D **99**(3), 034505 (2019)
679. I.I. Balitsky, V.M. Braun, Evolution equations for QCD string operators. Nucl. Phys. B **311**, 541–584 (1989)
680. M. Burkardt, Transverse force on quarks in deep-inelastic scattering. Phys. Rev. D **88**, 114502 (2013)
681. C.-Y. Seng, Relating hadronic CP-violation to higher-twist distributions. Phys. Rev. Lett. **122**(7), 072001 (2019)
682. S. Bhattacharya et al., One-loop matching for the twist-3 parton distribution $g_T(x)$. Phys. Rev. D **102**(3), 034005 (2020)
683. S. Bhattacharya et al., The role of zero-mode contributions in the matching for the twist-3 PDFs $e(x)$ and $h_L(x)$. Phys. Rev. D **102**, 114025 (2020)
684. S. Bhattacharya et al., Parton distribution functions beyond leading twist from lattice QCD: the $h_L(x)$ case. Phys. Rev. D **104**(11), 114510 (2021)
685. S. Wandzura, F. Wilczek, Sum rules for spin dependent electroproduction: test of relativistic constituent quarks. Phys. Lett. **72B**, 195–198 (1977)
686. V.M. Braun, Y. Ji, A. Vladimirov, QCD factorization for twist-three axial-vector parton quasidistributions. JHEP **05**, 086 (2021)
687. V.M. Braun, Y. Ji, A. Vladimirov, QCD factorization for chiral-odd parton quasi-and pseudo-distributions. JHEP **10**, 087 (2021)
688. M. Wingate, Quark flavor physics and lattice QCD. Eur. Phys. J. A **57**, 239 (2021)
689. C. Aubin et al., Light pseudoscalar decay constants, quark masses, and low energy constants from three-flavor lattice QCD. Phys. Rev. D **70**, 114501 (2004)
690. G. Colangelo, S. Durr, C. Haefeli, Finite volume effects for meson masses and decay constants. Nucl. Phys. B **721**, 136–174 (2005)
691. C. McNeile et al., High-precision $f B_s$ and HQET from relativistic lattice QCD. Phys. Rev. D **85**, 031503 (2012)
692. A. Bazavov et al., B and D meson leptonic decay constants from four-flavor lattice QCD. Phys. Rev. D **98**, 074512 (2018)
693. W.J. Marciano, Precise determination of $|V(us)|$ from lattice calculations of pseudoscalar decay constants. Phys. Rev. Lett. **93**, 231803 (2004)

694. R.J. Dowdall et al., V_{us} from pi and K decay constants in full lattice QCD with physical u, d, s and c quarks. Phys. Rev. D **88**, 074504 (2013)
695. N. Carrasco et al., Leptonic decay constants f_K, f_D, and f_{D_s} with $N_f = 2+1+1$ twisted-mass lattice QCD. Phys. Rev. D **91**, 054507 (2015)
696. N. Miller et al., F_K/F_π from Möbius domain-wall fermions solved on gradient-flowed HISQ ensembles. Phys. Rev. D **102**, 034507 (2020)
697. M. Di Carlo et al., Light-meson leptonic decay rates in lattice QCD+QED. Phys. Rev. D **100**, 034514 (2019)
698. C. McNeile et al., Heavy meson masses and decay constants from relativistic heavy quarks in full lattice QCD. Phys. Rev. D **86**, 074503 (2012)
699. V. Lubicz, A. Melis, S. Simula, Masses and decay constants of $D*_{(s)}$ and $B*_{(s)}$ mesons with $N_f = 2+1+1$ twisted mass fermions. Phys. Rev. D **96**, 034524 (2017)
700. B. Colquhoun et al., B-meson decay constants: a more complete picture from full lattice QCD. Phys. Rev. D **91**, 114509 (2015)
701. B. Chakraborty et al., Nonperturbative comparison of clover and highly improved staggered quarks in lattice QCD and the properties of the ϕ meson. Phys. Rev. D **96**, 074502 (2017)
702. D. Hatton et al., Bottomonium precision tests from full lattice QCD: hyperfine splitting, Υ leptonic width, and b quark contribution to $e^+e^- \to$ hadrons. Phys. Rev. D **103**, 054512 (2021)
703. C.T.H. Davies et al., Update: precision D_s decay constant from full lattice QCD using very fine lattices. Phys. Rev. D **82**, 114504 (2010)
704. E. Eichten, B. Russell Hill, An effective field theory for the calculation of matrix elements involving heavy quarks. Phys. Lett. B **234**, 511–516 (1990)
705. A.X. El-Khadra, A.S. Kronfeld, P.B. Mackenzie, Massive fermions in lattice gauge theory. Phys. Rev. D **55**, 3933–3957 (1997)
706. E. Eichten, B. Russell Hill, Renormalization of heavy-light bilinears and F(B) for Wilson fermions. Phys. Lett. B **240**, 193–199 (1990)
707. C.J. Morningstar, J. Shigemitsu, One loop matching of lattice and continuum heavy light axial vector currents using NRQCD. Phys. Rev. D **57**, 6741–6751 (1998)
708. J. Harada et al., Application of heavy quark effective theory to lattice QCD. 2. Radiative corrections to heavy light currents. Phys. Rev. D **65**, 094513 (2002) [Erratum: Phys. Rev. D 71, 019903 (2005)]
709. A. Bussone et al., Mass of the b quark and B -meson decay constants from $N_f = 2+1+1$ twisted-mass lattice QCD. Phys. Rev. D **93**(11), 114505 (2016)
710. R.J. Dowdall et al., B-meson decay constants from improved lattice nonrelativistic QCD with physical u, d, s, and c quarks. Phys. Rev. Lett. **110**, 222003 (2013)
711. A.V. Manohar, M.B. Wise, *Heavy Quark Physics*, vol. 10 (Cambridge University Press, Cambridge, 2000)
712. G.C. Donald et al., Prediction of the D_s^* width from a calculation of its radiative decay in full lattice QCD. Phys. Rev. Lett. **112**, 212002 (2014)
713. C.J. Morningstar, J. Shigemitsu, Perturbative matching of lattice and continuum heavy light currents with NRQCD heavy quarks. Phys. Rev. D **59**, 094504 (1999)
714. G. Martinelli et al., A general method for nonperturbative renormalization of lattice operators. Nucl. Phys. B **445**, 81–108 (1995)
715. C. Sturm et al., Renormalization of quark bilinear operators in a momentum-subtraction scheme with a nonexceptional subtraction point. Phys. Rev. D **80**, 014501 (2009)
716. D. Hatton et al., Renormalizing vector currents in lattice QCD using momentum-subtraction schemes. Phys. Rev. D **100**, 114513 (2019)
717. F. Gabbiani et al., A complete analysis of FCNC and CP constraints in general SUSY extensions of the standard model. Nucl. Phys. B **477**, 321–352 (1996)
718. J. Laiho, R.S. Van de Water, Pseudoscalar decay constants, light-quark masses, and B_K from mixed-action lattice QCD. PoS LATTICE **2011**, 293 (2011) **(Ed. by Pavlos Vranas)**
719. S. Durr et al., Precision computation of the kaon bag parameter. Phys. Lett. B **705**, 477–481 (2011)
720. B.J. Choi et al., Kaon BSM B-parameters using improved staggered fermions from $N_f = 2+1$ unquenched QCD. Phys. Rev. D **93**, 014511 (2016)
721. N. Carrasco et al., $\Delta S = 2$ and $\Delta C = 2$ bag parameters in the standard model and beyond from $N_f = 2+1+1$ twisted-mass lattice QCD. Phys. Rev. D **92**, 034516 (2015)
722. R.J. Dowdall et al., Neutral B-meson mixing from full lattice QCD at the physical point. Phys. Rev. D **100**, 094508 (2019)
723. C. Monahan et al., Matching lattice and continuum four-fermion operators with nonrelativistic QCD and highly improved staggered quarks. Phys. Rev. D **90**, 054015 (2014)
724. E. Gamiz et al., Neutral B meson mixing in unquenched lattice QCD. Phys. Rev. D **80**, 014503 (2009)
725. Y. Aoki et al., Neutral B meson mixings and B meson decay constants with static heavy and domain-wall light quarks. Phys. Rev. D **91**, 114505 (2015)
726. A. Bazavov et al., $B^0_{(s)}$-mixing matrix elements from lattice QCD for the Standard Model and beyond. Phys. Rev. D **93**, 113016 (2016)
727. A. Bazavov et al., Short-distance matrix elements for D^0-meson mixing for $N_f = 2+1$ lattice QCD. Phys. Rev. D **97**, 034513 (2018)
728. T. Blum et al., $K \to \pi\pi \Delta I = 3/2$ decay amplitude in the continuum limit. Phys. Rev. D **91**, 074502 (2015)
729. R. Abbott et al., Direct CP violation and the $\Delta I = 1/2$ rule in $K \to \pi\pi$ decay from the standard model. Phys. Rev. D **102**, 054509 (2020)
730. P.A. Boyle et al., Emerging understanding of the $\Delta I = 1/2$ rule from lattice QCD. Phys. Rev. Lett. **110**, 152001 (2013)
731. Z. Bai et al., $K_L - K_S$ mass difference from lattice QCD. Phys. Rev. Lett. **113**, 112003 (2014)
732. A. Suzuki et al., Four quark operators for kaon bag parameter with gradient flow. Phys. Rev. D **102**, 034508 (2020)
733. H. Na et al., The $D \to K, l\nu$ semileptonic decay scalar form factor and $|V_{cs}|$ from lattice QCD. Phys. Rev. D **82**, 114506 (2010)
734. B. Chakraborty et al., Improved Vcs determination using precise lattice QCD form factors for $D \to K\ell\nu$. Phys. Rev. D **104**, 034505 (2021)
735. C.-Y. Seng et al., Update on -Vus- and -Vus/Vud- from semileptonic kaon and pion decays. Phys. Rev. D **105**, 013005 (2022)
736. N. Carrasco et al., $K \to \pi$ semileptonic form factors with $N_f = 2+1+1$ twisted mass fermions. Phys. Rev. D **93**, 114512 (2016)
737. A. Bazavov et al., $|V_{us}|$ from $K_{\ell 3}$ decay and four-flavor lattice QCD. Phys. Rev. D **99**, 114509 (2019)
738. P.F. Bedaque, Aharonov-Bohm effect and nucleon nucleon phase shifts on the lattice. Phys. Lett. B **593**, 82–88 (2004)
739. L. Riggio, G. Salerno, S. Simula, Extraction of $|V_{cd}|$ and $|V_{cs}|$ from experimental decay rates using lattice QCD $D \to \pi(K)\ell\nu$ form factors. Eur. Phys. J. C **78**, 501 (2018)
740. W.G. Parrott, C. Bouchard, C.T.H. Davies, $B \to K$ and $D \to K$ form factors from fully relativistic lattice QCD (2022)
741. J.M. Flynn et al., $B \to \pi\ell\nu$ and $B_s \to K\ell\nu$ form factors and $|V_{ub}|$ from 2+1-flavor lattice QCD with domain-wall light quarks and relativistic heavy quarks. Phys. Rev. D **91**, 074510 (2015)
742. J.A. Bailey et al., $|V_{ub}|$ from $B \to \pi\ell\nu$ decays and (2+1)-flavor lattice QCD. Phys. Rev. D **92**, 014024 (2015)

743. J.A. Bailey et al., Update of $|V_{cb}|$ from the $B \rightarrow D * \ell\bar{\nu}$ form factor at zero recoil with three-flavor lattice QCD. Phys. Rev. D **89**, 114504 (2014)
744. J. Harrison, C. Davies, M. Wingate, Lattice QCD calculation of the $B_{(s)} \rightarrow D^*_{(s)}\ell\nu$ form factors at zero recoil and implications for $|V_{cb}|$. Phys. Rev. D **97**, 054502 (2018)
745. A. Bazavov et al., Semileptonic form factors for $B \rightarrow D * \ell\nu$ at nonzero recoil from 2 + 1-flavor lattice QCD: Fermilab Lattice and MILC Collaborations. Eur. Phys. J. C **82**, 1141 (2022) [Erratum: Eur. Phys. J. C 83, 21 (2023)]
746. E. McLean et al., $B_s \rightarrow D_s\ell\nu$ Form Factors for the full q^2 range from Lattice QCD with non-perturbatively normalized currents. Phys. Rev. D **101**, 074513 (2020)
747. J. Harrison, C.T.H. Davies, $B_s \rightarrow D^*_s$ form factors for the full q^2 range from lattice QCD. Phys. Rev. D **105**, 094506 (2022)
748. B. Colquhoun et al., Form factors of B $\rightarrow \pi\ell\nu$ and a determination of $|V_{ub}|$ with Möbius domain-wall fermions. Phys. Rev. D **106**, 054502 (2022)
749. A.S. Kronfeld et al., Lattice QCD and particle physics (2022). arXiv:2207.07641
750. P. Gambino et al., Lattice QCD study of inclusive semileptonic decays of heavy mesons. JHEP **07**, 083 (2022)
751. W. Detmold, C. Lehner, S. Meinel, $\Lambda_b \rightarrow p\ell^-\bar{\nu}_\ell$ and $\Lambda_b \rightarrow \Lambda_c\ell^-\bar{\nu}_\ell$ form factors from lattice QCD with relativistic heavy quarks. Phys. Rev. D **92**, 034503 (2015)
752. R. Aaij et al., Determination of the quark coupling strength $|V_{ub}|$ using baryonic decays. Nat. Phys. **11**, 743–747 (2015)
753. G. Zweig, Origins of the quark model. In: *4th International Conference on Baryon Resonances* (1980)
754. R.H. Dalitz, Symmetries and strong interactions. In: *Proceedings of the Thirteenth International Conference on High Energy Physics*, Berkeley (University of California Press, Berkeley, 1967), p. 215
755. C. Becchi, G. Morpurgo, Vanishing of the E2 part of the $N^{33} \rightarrow N + \gamma$ amplitude in the non-relativistic quark model of elementary particles. Phys. Lett. **17**, 352–354 (1965)
756. H.R. Rubinstein, F. Scheck, R.H. Socolow, Electromagnetic properties of hadrons in the quark model. Phys. Rev. **154**, 1608–1616 (1967)
757. H.J. Lipkin, F. Scheck, Quark model for forward scattering amplitudes. Phys. Rev. Lett. **16**, 71–75 (1966)
758. J.J.J. Kokkedee, *The Quark Model* (W.A. Benjamin, New York, 1969)
759. R.H. Dalitz, Quark models for the elementary particles. In: *Summer School of Theoretical Physics: High Energy Physics*, pp. 251–324 (1965)
760. R.G. Moorhouse, Photoproduction of N^* resonances in the quark model. Phys. Rev. Lett. **16**, 772–774 (1966)
761. R. Van Royen, V.F. Weisskopf, Hadron decay processes and the quark model. Nuovo Cim. A **50**, 617–645 (1967) [Erratum: Nuovo Cim. A 51, 583 (1967)]
762. L.A. Copley, G. Karl, E. Obryk, Single pion photoproduction in the quark model. Nucl. Phys. B **13**, 303–319 (1969)
763. A. De Rujula, H. Georgi, S.L. Glashow, Hadron masses in a gauge theory. Phys. Rev. D **12**, 147–162 (1975)
764. N. Isgur, G. Karl, P wave baryons in the quark model. Phys. Rev. D **18**, 4187 (1978)
765. H.J. Schnitzer, Inverted charmed meson multiplets as a test for scalar confinement. Phys. Lett. B **76**, 461–465 (1978)
766. W. Buchmuller, Fine and hyperfine structure of quarkonia. Phys. Lett. B **112**, 479–483 (1982)
767. L. Micu, Decay rates of meson resonances in a quark model. Nucl. Phys. B **10**, 521–526 (1969)
768. H.R. Rubinstein, I. Talmi, Quark model decay rates for spin 2^+ mesons. Phys. Lett. **23**, 693–695 (1966)
769. E. Eichten et al., Charmonium: the model. Phys. Rev. D **17**, 3090 (1978) [Erratum: Phys. Rev. D 21, 313 (1980)]
770. S. Godfrey, N. Isgur, Mesons in a relativized quark model with chromodynamics. Phys. Rev. D **32**, 189–231 (1985)
771. S. Capstick, N. Isgur, Baryons in a relativized quark model with chromodynamics. Phys. Rev. D **34**(9), 2809–2835 (1986)
772. D.P. Stanley, D. Robson, Nonperturbative potential model for light and heavy quark anti-quark systems. Phys. Rev. D **21**, 3180–3196 (1980)
773. A. Chodos et al., A new extended model of hadrons. Phys. Rev. D **9**, 3471–3495 (1974)
774. W.A. Bardeen et al., Heavy quarks and strong binding: a field theory of hadron structure. Phys. Rev. D **11**, 1094 (1975)
775. C.E. DeTar, J.F. Donoghue, Bag models of hadrons. Annu. Rev. Nucl. Part. Sci. **33**, 235–264 (1983)
776. R. Friedberg, T.D. Lee, QCD and the soliton model of hadrons. Phys. Rev. D **18**, 2623 (1978)
777. A. William Thomas, S. Theberge, G.A. Miller, The cloudy bag model of the nucleon. Phys. Rev. D **24**, 216 (1981)
778. A. William Thomas, Chiral symmetry and the bag model: a new starting point for nuclear physics. Adv. Nucl. Phys. **13**, 1–137 (1984)
779. A. Chodos, C.B. Thorn, Chiral hedgehogs in the bag theory. Phys. Rev. D **12**, 2733 (1975)
780. T.A. DeGrand, R.L. Jaffe, Excited states of confined quarks. Ann. Phys. **100**, 425 (1976)
781. P. Hasenfratz et al., The effects of colored glue in the QCD motivated bag of heavy quark-anti-quark systems. Phys. Lett. B **95**, 299–305 (1980)
782. R.L. Jaffe, K. Johnson, Unconventional states of confined quarks and gluons. Phys. Lett. B **60**, 201–204 (1976)
783. T. Barnes, F.E. Close, S. Monaghan, Hyperfine splittings of bag model gluonia. Nucl. Phys. B **198**, 380–406 (1982)
784. T.F.E. Barnes, Quarks, gluons, bags, and hadrons. PhD thesis. Caltech (1977)
785. M.S. Chanowitz, S.R. Sharpe, Hybrids: mixed states of quarks and gluons. Nucl. Phys. B **222**, 211–244 (1983) [Erratum: Nucl. Phys. B 228, 588–588 (1983)]
786. T. Barnes, F.E. Close, F. de Viron, Q anti-Q G hermaphrodite mesons in the MIT bag model. Nucl. Phys. B **224**, 241 (1983)
787. T. Barnes, F.E. Close, A light exotic $q\bar{q}g$ hermaphrodite meson? Phys. Lett. B **116**, 365–368 (1982)
788. R.L. Jaffe, Exotica. Phys. Rep. **409**, 1–45 (2005) **(Ed. by Teiji Kunihiro et al.)**
789. M. Ida, R. Kobayashi, Baryon resonances in a quark model. Prog. Theor. Phys. **36**, 846 (1966)
790. D.B. Lichtenberg, L.J. Tassie, Baryon mass splitting in a boson-fermion model. Phys. Rev. **155**, 1601–1606 (1967)
791. M. Anselmino et al., Diquarks. Rev. Mod. Phys. **65**, 1199–1234 (1993)
792. D.B. Lichtenberg, Baryon supermultiplets of SU(6) x O(3) in a quark-diquark model. Phys. Rev. **178**, 2197–2200 (1969)
793. M.Y. Barabanov et al., Diquark correlations in hadron physics: origin, impact and evidence. Prog. Part. Nucl. Phys. **116**, 103835 (2021)
794. A. Francis et al., Good and bad diquark properties and spatial correlations in lattice QCD. Rev. Mex. Fis. Suppl. **3**(3), 0308082 (2022)
795. L. Maiani et al., Diquark-antidiquark states with hidden or open charm and the nature of X(3872). Phys. Rev. D **71**, 014028 (2005)
796. M.J. Savage, M.B. Wise, Spectrum of baryons with two heavy quarks. Phys. Lett. B **248**, 177–180 (1990)
797. A. Francis et al., Lattice prediction for deeply bound doubly heavy tetraquarks. Phys. Rev. Lett. **118**(14), 142001 (2017)

798. N. Isgur, Nuclear physics from the quark model with chromodynamics. Acta Phys. Austriaca Suppl. **27**, 177–266 (1985) **(Ed. by H. Mitter and Willibald Plessas)**
799. A.P. Szczepaniak, E.S. Swanson, Chiral extrapolation, renormalization, and the viability of the quark model. Phys. Rev. Lett. **87**, 072001 (2001)
800. P. Maris, C.D. Roberts, Dyson-Schwinger equations: a tool for hadron physics. Int. J. Mod. Phys. E **12**, 297–365 (2003)
801. A.P. Szczepaniak, E.S. Swanson, From current to constituent quarks: a renormalization group improved Hamiltonian based description of hadrons. Phys. Rev. D **55**, 1578–1591 (1997)
802. A.P. Szczepaniak, E.S. Swanson, On the Dirac structure of confinement. Phys. Rev. D **55**, 3987–3993 (1997)
803. E. Eichten, F. Feinberg, Spin dependent forces in QCD. Phys. Rev. D **23**, 2724 (1981)
804. Y. Koma, M. Koma, Spin-dependent potentials from lattice QCD. Nucl. Phys. B **769**, 79–107 (2007)
805. O. Lakhina, E.S. Swanson, Dynamic properties of charmonium. Phys. Rev. D **74**, 014012 (2006)
806. K.J. Juge, J. Kuti, C.J. Morningstar, Gluon excitations of the static quark potential and the hybrid quarkonium spectrum. Nucl. Phys. B Proc. Suppl. **63**, 326–331 (1998) **(Ed. by C. T. H. Davies et al.)**
807. N.A. Campbell, I.H. Jorysz, C. Michael, The adjoint source potential in SU(3) lattice gauge theory. Phys. Lett. B **167**, 91–93 (1986)
808. M. Foster, C. Michael, Hadrons with a heavy color adjoint particle. Phys. Rev. D **59**, 094509 (1999)
809. G.S. Bali, A. Pineda, QCD phenomenology of static sources and gluonic excitations at short distances. Phys. Rev. D **69**, 094001 (2004)
810. L. Liu et al., Excited and exotic charmonium spectroscopy from lattice QCD. JHEP **07**, 126 (2012)
811. G.K.C. Cheung et al., Excited and exotic charmonium, D_s and D meson spectra for two light quark masses from lattice QCD. JHEP **12**, 089 (2016)
812. F. Knechtli, Charmonium and exotics from lattice QCD. EPJ Web Conf. **202**, 01006 (2019) **(Ed. by A. Bondar and S. Eidelman)**
813. F.J. Dyson, The S matrix in quantum electrodynamics. Phys. Rev. **75**, 1736–1755 (1949)
814. J.S. Schwinger, On the Green's functions of quantized fields. 1. Proc. Natl. Acad. Sci. **37**, 452–455 (1951)
815. J.S. Schwinger, On the Green's functions of quantized fields. 2. Proc. Natl. Acad. Sci. **37**, 455–459 (1951)
816. E.E. Salpeter, H.A. Bethe, A relativistic equation for bound state problems. Phys. Rev. **84**, 1232–1242 (1951)
817. C.D. Roberts, S.M. Schmidt, Dyson-Schwinger equations: density, temperature and continuum strong QCD. Prog. Part. Nucl. Phys. **45**, S1–S103 (2000)
818. R. Alkofer, L. von Smekal, The infrared behavior of QCD Green's functions: confinement dynamical symmetry breaking, and hadrons as relativistic bound states. Phys. Rep. **353**, 281 (2001)
819. R. Alkofer et al., The quark-gluon vertex in Landau gauge QCD: its role in dynamical chiral symmetry breaking and quark confinement. Ann. Phys. **324**, 106–172 (2009)
820. A. Bashir et al., Collective perspective on advances in Dyson-Schwinger equation QCD. Commun. Theor. Phys. **58**, 79–134 (2012)
821. I.C. Cloet, C.D. Roberts, Explanation and prediction of observables using continuum strong QCD. Prog. Part. Nucl. Phys. **77**, 1–69 (2014)
822. G. Eichmann et al., Baryons as relativistic three-quark bound states. Prog. Part. Nucl. Phys. **91**, 1–100 (2016)
823. C. Itzykson, J.B. Zuber, *Quantum Field Theory* (International Series In Pure and Applied Physics (McGraw-Hill, New York, 1980)
824. F. Gross, *Relativistic Quantum Mechanics and Field Theory* (McGraw-Hill, New York, 1993)
825. G.C. Wick, Properties of Bethe-Salpeter wave functions. Phys. Rev. **96**, 1124–1134 (1954)
826. R.E. Cutkosky, Solutions of a Bethe-Salpeter equations. Phys. Rev. **96**, 1135–1141 (1954)
827. N. Nakanishi, A general survey of the theory of the Bethe-Salpeter equation. Prog. Theor. Phys. Suppl. **43**, 1–81 (1969)
828. K. Kusaka, K.M. Simpson, A.G. Williams, Solving the Bethe-Salpeter equation for bound states of scalar theories in Minkowski space. Phys. Rev. D **56**, 5071–5085 (1997)
829. V. Sauli, Solving the Bethe-Salpeter equation for a pseudoscalar meson in Minkowski space. J. Phys. G **35**, 035005 (2008)
830. J. Carbonell, V.A. Karmanov, Solving Bethe-Salpeter equation for two fermions in Minkowski space. Eur. Phys. J. A **46**, 387–397 (2010)
831. W. de Paula et al., Advances in solving the two-fermion homogeneous Bethe-Salpeter equation in Minkowski space. Phys. Rev. D **94**(7), 071901 (2016)
832. A. Castro et al., The Bethe–Salpeter approach to bound states: from Euclidean to Minkowski space. J. Phys. Conf. Ser. **1291**(1), 012006 (2019) **(Ed. by Valdir Guimaraes et al.)**
833. G. Eichmann, E. Ferreira, A. Stadler, Going to the light front with contour deformations. Phys. Rev. D **105**(3), 034009 (2022)
834. S. Weinberg, Dynamics at infinite momentum. Phys. Rev. **150**, 1313–1318 (1966)
835. L.A. Kondratyuk, M.I. Strikman, Relativistic correction to the deuteron magnetic moment and angular condition. Nucl. Phys. A **426**, 575–598 (1984)
836. L. Chang et al., Imaging dynamical chiral symmetry breaking: pion wave function on the light front. Phys. Rev. Lett. **110**(13), 132001 (2013)
837. C. Chen et al., Valence-quark distribution functions in the kaon and pion. Phys. Rev. D **93**(7), 074021 (2016)
838. C. Shi et al., Spatial and momentum imaging of the pion and kaon. Phys. Rev. D **101**(7), 074014 (2020)
839. F. Gross, Three-dimensional covariant integral equations for low-energy systems. Phys. Rev. **186**, 1448–1462 (1969)
840. Y.A. Simonov, J.A. Tjon, The Feynman-Schwinger representation for the relativistic two particle amplitude in field theory. Ann. Phys. **228**, 1–18 (1993)
841. T. Nieuwenhuis, J.A. Tjon, Nonperturbative study of generalized ladder graphs in a $\phi^2\chi$ theory. Phys. Rev. Lett. **77**, 814–817 (1996)
842. M. Mangin-Brinet, J. Carbonell, Solutions of the Wick-Cutkosky model in the light front dynamics. Phys. Lett. B **474**, 237–244 (2000)
843. V.A. Karmanov, P. Maris, Manifestation of three-body forces in three-body Bethe-Salpeter and light-front equations. Few Body Syst. **46**, 95–113 (2009)
844. P.C. Tiemeijer, J.A. Tjon, Meson mass spectrum from relativistic equations in configuration space. Phys. Rev. C **49**, 494–512 (1994)
845. C. Savkli, F. Gross, J. Tjon, The role of interaction vertices in bound state calculations. Phys. Lett. B **531**, 161–166 (2002)
846. F. Gross, A. Stadler, Covariant spectator theory of np scattering: phase shifts obtained from precision fits to data below 350-MeV. Phys. Rev. C **78**, 014005 (2008)
847. F. Gross, Removal of singularities from the covariant spectator theory. Phys. Rev. D **104**(5), 054020 (2021)
848. F. Gross, Covariant spectator theory of np scattering: deuteron quadrupole moment. Phys. Rev. C **91**(1), 014005 (2015)
849. E.O. Alt, P. Grassberger, W. Sandhas, Reduction of the three-particle collision problem to multichannel two -particle Lippmann-Schwinger equations. Nucl. Phys. B **2**, 167–180 (1967)
850. R.A. Malfliet, J.A. Tjon, Three-nucleon calculations with realistic forces. Ann. Phys. **61**, 425–450 (1970)

851. G. Rupp, J.A. Tjon, Bethe-Salpeter calculation of three nucleon observables with rank one separable potentials. Phys. Rev. C **37**, 1729 (1988)
852. L.E. Marcucci et al., Electromagnetic structure of few-nucleon ground states. J. Phys. G **43**, 023002 (2016)
853. A. Stadler, F. Gross, M. Frank, Covariant equations for the three-body bound state. Phys. Rev. C **56**, 2396 (1997)
854. A. Stadler, F. Gross, Relativistic calculation of the triton binding energy and its implications. Phys. Rev. Lett. **78**, 26–29 (1997)
855. S. Alexandre Pinto, A. Stadler, F. Gross, Covariant spectator theory for the electromagnetic three-nucleon form factors: complete impulse approximation. Phys. Rev. C **79**, 054006 (2009)
856. S. Alexandre Pinto, A. Stadler, F. Gross, First results for electromagnetic three-nucleon form factors from high-precision two-nucleon interactions. Phys. Rev. C **81**, 014007 (2010)
857. F. Gross, J. Milana, Covariant, chirally symmetric, confining model of mesons. Phys. Rev. D **43**, 2401–2417 (1991)
858. C. Savkli, F. Gross, Quark -anti-quark bound states in the relativistic spectator formalism. Phys. Rev. C **63**, 035208 (2001)
859. E.P. Biernat et al., Confinement, quark mass functions, and spontaneous chiral symmetry breaking in Minkowski space. Phys. Rev. D **89**(1), 016005 (2014)
860. S. Leitão et al., Linear confinement in momentum space: singularity-free bound-state equations. Phys. Rev. D **90**(9), 096003 (2014)
861. S. Leitão et al., Covariant spectator theory of quark-antiquark bound states: mass spectra and vertex functions of heavy and heavy-light mesons. Phys. Rev. D **96**(7), 074007 (2017)
862. S. Leitão et al., Comparison of two Minkowski-space approaches to heavy quarkonia. Eur. Phys. J. C **77**(10), 696 (2017)
863. F. Gross, The CST: its achievements and its connection to the light cone. Few Body Syst. **58**(2), 39 (2017)
864. Y. Hatta, B.-W. Xiao, F. Yuan, Semi-inclusive diffractive deep inelastic scattering at small x. Phys. Rev. D **106**(9), 094015 (2022)
865. F. Gross, D.O. Riska, Current conservation and interaction currents in relativistic meson theories. Phys. Rev. C **36**, 1928 (1987)
866. A. Bender, C.D. Roberts, L. Von Smekal, Goldstone theorem and diquark confinement beyond rainbow ladder approximation. Phys. Lett. B **380**, 7–12 (1996)
867. A. Bender et al., Bethe-Salpeter equation and a nonperturbative quark gluon vertex. Phys. Rev. C **65**, 065203 (2002)
868. P. Maris, P.C. Tandy, Bethe-Salpeter study of vector meson masses and decay constants. Phys. Rev. C **60**, 055214 (1999)
869. P. Maris, P.C. Tandy, QCD modeling of hadron physics. Nucl. Phys. B Proc. Suppl. **161**, 136–152 (2006) **(Ed. by D. B. Leinweber, L. von Smekal, and A. G. Williams)**
870. C.S. Fischer, R. Alkofer, Nonperturbative propagators, running coupling and dynamical quark mass of Landau gauge QCD. Phys. Rev. D **67**, 094020 (2003)
871. F.D.R. Bonnet et al., Overlap quark propagator in Landau gauge. Phys. Rev. D **65**, 114503 (2002)
872. P.O. Bowman, U.M. Heller, A.G. Williams, Lattice quark propagator with staggered quarks in Landau and Laplacian gauges. Phys. Rev. D **66**, 014505 (2002)
873. R. Alkofer et al., Analytic properties of the Landau gauge gluon and quark propagators. Phys. Rev. D **70**, 014014 (2004)
874. P. Maris, C.D. Roberts, Pi-and K meson Bethe-Salpeter amplitudes. Phys. Rev. C **56**, 3369–3383 (1997)
875. H. David Politzer, Effective quark masses in the chiral limit. Nucl. Phys. B **117**, 397–406 (1976)
876. D.C. Curtis, M.R. Pennington, Truncating the Schwinger-Dyson equations: how multiplicative renormalizability and the Ward identity restrict the three point vertex in QED. Phys. Rev. D **42**, 4165–4169 (1990)
877. R. Fukuda, T. Kugo, Schwinger-Dyson equation for massless vector theory and absence of fermion pole. Nucl. Phys. B **117**, 250–264 (1976)
878. D. Atkinson, D.W.E. Blatt, Determination of the singularities of the electron propagator. Nucl. Phys. B **151**, 342–352 (1979)
879. P. Maris, Analytic structure of the full fermion propagator in quenched and unquenched QED. Phys. Rev. D **50**, 4189–4193 (1994)
880. S.J. Stainsby, R.T. Cahill, Is space-time Euclidean 'inside' hadrons? Phys. Lett. A **146**, 467–470 (1990)
881. G. Krein, C.D. Roberts, A.G. Williams, On the implications of confinement. Int. J. Mod. Phys. A **7**, 5607–5624 (1992)
882. S. Jia et al., Minkowski-space solutions of the Schwinger-Dyson equation for the fermion propagator with the rainbow-ladder truncation. In: *18th International Conference on Hadron Spectroscopy and Structure*, pp. 560–564 (2020)
883. J.S. Ball, T.-W. Chiu, Analytic properties of the vertex function in gauge theories. 1. Phys. Rev. D **22**, 2542 (1980)
884. P. Maris, C.D. Roberts, P.C. Tandy, Pion mass and decay constant. Phys. Lett. B **420**, 267–273 (1998)
885. J.J. Sakurai, Theory of strong interactions. Ann. Phys. **11**, 1–48 (1960)
886. M.S. Bhagwat, P. Maris, Vector meson form factors and their quark-mass dependence. Phys. Rev. C **77**, 025203 (2008)
887. P. Maris, P.C. Tandy, The π, K^+, and K^0 electromagnetic form-factors. Phys. Rev. C **62**, 055204 (2000)
888. J. Lan et al., Light mesons with one dynamical gluon on the light front. Phys. Lett. B **825**, 136890 (2022)
889. S.R. Amendolia et al., A measurement of the space-like pion electromagnetic form-factor. Nucl. Phys. B **277**, 168 (1986) **(Ed. by S. C. Loken)**
890. G.M. Huber et al., Charged pion form-factor between $Q^2 = 0.60 - \text{GeV}^2$ and $2.45 - \text{GeV}^2$. II. Determination of, and results for, the pion form-factor. Phys. Rev. C **78**, 045203 (2008)
891. P. Maris, P.C. Tandy, Electromagnetic transition form-factors of light mesons. Phys. Rev. C **65**, 045211 (2002)
892. S.R. Cotanch, P. Maris, Ladder Dyson-Schwinger calculation of the anomalous $\gamma - 3\pi$ form-factor. Phys. Rev. D **68**, 036006 (2003)
893. P. Bicudo et al., Chirally symmetric quark description of low-energy $\pi\pi$ scattering. Phys. Rev. D **65**, 076008 (2002)
894. L. Chang, C.D. Roberts, Sketching the Bethe-Salpeter kernel. Phys. Rev. Lett. **103**, 081601 (2009)
895. D. Binosi et al., Symmetry preserving truncations of the gap and Bethe-Salpeter equations. Phys. Rev. D **93**(9), 096010 (2016)
896. R. Williams, C.S. Fischer, W. Heupel, Light mesons in QCD and unquenching effects from the 3PI effective action. Phys. Rev. D **93**(3), 034026 (2016)
897. Á.S. Miramontes, H. Sanchis Alepuz, R. Alkofer, Elucidating the effect of intermediate resonances in the quark interaction kernel on the timelike electromagnetic pion form factor. Phys. Rev. D **103**(11), 116006 (2021)
898. N. Santowsky, C.S. Fischer, Light scalars: four-quark versus two-quark states in the complex energy plane from Bethe-Salpeter equations. Phys. Rev. D **105**(3), 034025 (2022)
899. G. Eichmann, C.S. Fischer, H. Sanchis-Alepuz, Light baryons and their excitations. Phys. Rev. D **94**(9), 094033 (2016)
900. S.J. Brodsky, H.-C. Pauli, S.S. Pinsky, Quantum chromodynamics and other field theories on the light cone. Phys. Rep. **301**, 299–486 (1998)
901. J.R. Hiller, Nonperturbative light-front Hamiltonian methods. Prog. Part. Nucl. Phys. **90**, 75–124 (2016)
902. P.A.M. Dirac, Forms of relativistic dynamics. Rev. Mod. Phys. **21**, 392–399 (1949)
903. D.E. Soper, Infinite-momentum helicity states. Phys. Rev. D **5**, 1956–1962 (1972)

904. Y. Li et al., Introduction to basis light-front quantization approach to QCD bound state problems. In: *International Conference on Nuclear Theory in the Supercomputing Era*, p. 136 (2013)
905. E. Tomboulis, Quantization of the Yang-Mills field in the null-plane frame. Phys. Rev. D **8**, 2736–2740 (1973)
906. A. Casher, Gauge fields on the null plane. Phys. Rev. D **14**, 452 (1976)
907. V.A. Karmanov, J.F. Mathiot, A.V. Smirnov, Systematic renormalization scheme in light-front dynamics with Fock space truncation. Phys. Rev. D **77**, 085028 (2008)
908. S.D. Glazek, K.G. Wilson, Renormalization of Hamiltonians. Phys. Rev. D **48**, 5863–5872 (1993)
909. K.G. Wilson et al., Nonperturbative QCD: a weak coupling treatment on the light front. Phys. Rev. D **49**, 6720–6766 (1994)
910. R.J. Perry, A renormalization group approach to Hamiltonian light front field theory. Ann. Phys. **232**, 116–222 (1994)
911. S.D. Glazek, Perturbative formulae for relativistic interactions of effective particles. Acta Phys. Polon. B **43**, 1843–1862 (2012)
912. S.D. Glazek et al., Renormalized quark-antiquark Hamiltonian induced by a gluon mass ansatz in heavy-flavor QCD. Phys. Lett. B **773**, 172–178 (2017)
913. M. Gómez-Rocha, S.D. Glazek, Asymptotic freedom in the front-form Hamiltonian for quantum chromodynamics of gluons. Phys. Rev. D **92**(6), 065005 (2015)
914. R.J. Perry, A. Harindranath, K.G. Wilson, Light front Tamm-Dancoff field theory. Phys. Rev. Lett. **65**, 2959–2962 (1990)
915. Y. Li et al., Ab initio approach to the non-perturbative scalar Yukawa model. Phys. Lett. B **748**, 278–283 (2015)
916. S.S. Chabysheva, J.R. Hiller, A light-front coupled-cluster method for the nonperturbative solution of quantum field theories. Phys. Lett. B **711**, 417–422 (2012)
917. M. Krautgartner, H.C. Pauli, F. Wolz, Positronium and heavy quarkonia as testing case for discretized light cone quantization. 1. Phys. Rev. D **45**, 3755–3774 (1992)
918. K. Hornbostel, S.J. Brodsky, H. Christian Pauli, Light cone quantized QCD in (1+1)-dimensions. Phys. Rev. D **41**, 3814 (1990)
919. M. Burkardt, S. Dalley, The relativistic bound state problem in QCD: transverse lattice methods. Prog. Part. Nucl. Phys. **48**, 317–362 (2002)
920. D. Chakrabarti, A. Harindranath, J.P. Vary, A study of $q\bar{q}$ states in transverse lattice QCD using alternative fermion formulations. Phys. Rev. D **69**, 034502 (2004)
921. A. Harindranath, R.J. Perry, J. Shigemitsu, Bound state problem in the light front Tamm-Dancoff approximation: numerical study in (1+1)-dimensions. Phys. Rev. D **46**, 4580–4602 (1992)
922. J.P. Vary et al., Hamiltonian light-front field theory in a basis function approach. Phys. Rev. C **81**, 035205 (2010)
923. H. Honkanen et al., Electron in a transverse harmonic cavity. Phys. Rev. Lett. **106**, 061603 (2011)
924. X. Zhao et al., Electron anomalous magnetic moment in basis light-front quantization approach. Few Body Syst. **52**, 339–344 (2012) **(Ed. by S. Dalley)**
925. X. Zhao et al., Electron g-2 in light-front quantization. Phys. Lett. B **737**, 65–69 (2014)
926. D. Chakrabarti et al., Generalized parton distributions in a light-front nonperturbative approach. Phys. Rev. D **89**(11), 116004 (2014)
927. H. Zhi et al., Transverse structure of electron in momentum space in basis light-front quantization. Phys. Rev. D **103**(3), 036005 (2021)
928. P. Wiecki et al., Non-perturbative calculation of the positronium mass spectrum in basis light-front quantization. Few Body Syst. **56**(6–9), 489–494 (2015) **(Ed. by Chueng-Ryong Ji)**
929. H.A. Bethe, E.E. Salpeter, *Quantum Mechanics of One-and Two-Electron Atoms* (1957)
930. Y. Li, P. Maris, J.P. Vary, Quarkonium as a relativistic bound state on the light front. Phys. Rev. D **96**, 016022 (2017)
931. C.S. Fischer, S. Kubrak, R. Williams, Spectra of heavy mesons in the Bethe-Salpeter approach. Eur. Phys. J. A **51**, 10 (2015)
932. P. Wiecki et al., Basis light-front quantization approach to positronium. Phys. Rev. D **91**(10), 105009 (2015)
933. D. Chakrabarti, A. Harindranath, Mesons in light front QCD(2+1): investigation of a Bloch effective Hamiltonian. Phys. Rev. D **64**, 105002 (2001)
934. L. Adhikari et al., Form factors and generalized parton distributions in basis light-front quantization. Phys. Rev. C **93**(5), 055202 (2016)
935. S. Nair et al., Basis light-front quantization approach to photon. Phys. Lett. B **827**, 137005 (2022)
936. Y. Li, M. Li, J.P. Vary, Two-photon transitions of charmonia on the light front. Phys. Rev. D **105**(7), L071901 (2022)
937. J.P. Lees et al., Measurement of the $\gamma\gamma^* \to \eta_c$ transition form factor. Phys. Rev. D **81**, 052010 (2010)
938. M. Li et al., Radiative transitions between 0^{-+} and 1^{-} heavy quarkonia on the light front. Phys. Rev. D **98**(3), 034024 (2018)
939. J. Lan et al., Parton distribution functions of heavy mesons on the light front. Phys. Rev. D **102**(1), 014020 (2020)
940. J. Lan et al., Parton distribution functions from a light front hamiltonian and QCD evolution for light mesons. Phys. Rev. Lett. **122**(17), 172001 (2019)
941. X. Siqi et al., Nucleon structure from basis light-front quantization. Phys. Rev. D **104**(9), 094036 (2021)
942. Y. Li et al., Heavy quarkonium in a holographic basis. Phys. Lett. B **758**, 118–124 (2016)
943. L. Adhikari et al., Form factors and generalized parton distributions of heavy quarkonia in basis light front quantization. Phys. Rev. C **99**(3), 035208 (2019)
944. M. Li et al., Frame dependence of transition form factors in light-front dynamics. Phys. Rev. D **100**(3), 036006 (2019)
945. S. Tang et al., Semileptonic decay of $B_c \to \eta_c$ and J/ψ on the light front. Phys. Rev. D **104**(1), 016002 (2021)
946. S. Tang et al., B_c mesons and their properties on the light front. Phys. Rev. D **98**(11), 114038 (2018)
947. S. Tang et al., Heavy-light mesons on the light front. Eur. Phys. J. C **80**(6), 522 (2020)
948. P. Maris et al., On the light-front wave functions of quarkonia. In: *PoS LC2019*, p. 007 (2020)
949. S. Jia, J.P. Vary, Basis light front quantization for the charged light mesons with color singlet Nambu-Jona-Lasinio interactions. Phys. Rev. C **99**(3), 035206 (2019)
950. W. Qian et al., Light mesons within the basis light-front quantization framework. Phys. Rev. C **102**(5), 055207 (2020)
951. J. Lan et al., Pion and kaon parton distribution functions from basis light front quantization and QCD evolution. Phys. Rev. D **101**(3), 034024 (2020)
952. J. Lan et al., Light meson parton distribution functions from basis light-front quantization and QCD evolution. In: *18th International Conference on Hadron Spectroscopy and Structure*, pp. 581–585 (2020)
953. S. Xu et al., Nucleon spin decomposition with one dynamical gluon (2022). arXiv:2209.08584
954. C. Mondal et al., Proton structure from a light-front Hamiltonian. Phys. Rev. D **102**(1), 016008 (2020)
955. H. Zhi et al., Transverse momentum structure of proton within the basis light-front quantization framework. Phys. Lett. B **833**, 137360 (2022)
956. T. Peng et al., Basis light-front quantization approach to Λ and Λc and their isospin triplet baryons. Phys. Rev. D **106**(11), 114040 (2022)
957. R.J. Hill et al., Nucleon axial radius and muonic hydrogen–a new analysis and review. Rep. Prog. Phys. **81**(9), 096301 (2018)

958. S.D. Drell, T.-M. Yan, Connection of elastic electromagnetic nucleon form-factors at large Q^2 and deep inelastic structure functions near threshold. Phys. Rev. Lett. **24**, 181–185 (1970)
959. G.B. West, Phenomenological model for the electromagnetic structure of the proton. Phys. Rev. Lett. **24**, 1206–1209 (1970)
960. S.J. Brodsky, M. Burkardt, I. Schmidt, Perturbative QCD constraints on the shape of polarized quark and gluon distributions. Nucl. Phys. B **441**, 197–214 (1995)
961. M.G. Alekseev et al., Quark helicity distributions from longitudinal spin asymmetries in muon-proton and muon-deuteron scattering. Phys. Lett. B **693**, 227–235 (2010)
962. R. Dupre, M. Guidal, M. Vanderhaeghen, Tomographic image of the proton. Phys. Rev. D **95**(1), 011501 (2017)
963. Y. Liu et al., Angular momentum and generalized parton distributions for the proton with basis light-front quantization. Phys. Rev. D **105**(9), 094018 (2022)
964. M. Burkardt, Impact parameter dependent parton distributions and off forward parton distributions for $\zeta \to 0$. Phys. Rev. D **62**, 071503 (2000) [Erratum: Phys. Rev. D 66, 119903 (2002)]
965. Z. Kuang et al., All-charm tetraquark in front form dynamics. Phys. Rev. D **105**(9), 094028 (2022)
966. M. Kaluza, H.C. Pauli, Discretized light cone quantization: $e^+e^-(\gamma)$ model for positronium. Phys. Rev. D **45**, 2968–2981 (1992)
967. K. Fu et al., Positronium on the light front. In: *18th International Conference on Hadron Spectroscopy and Structure*, pp. 550–554 (2020)
968. X. Zhao et al., Positronium: an illustration of nonperturbative renormalization in a basis light-front approach. In: *PoS LC2019*, 090 (2020)
969. X. Zhao, F. Kaiyu, J.P. Vary, Bound states in QED from a light-front approach. Rev. Mex. Fis. Suppl. **3**(3), 0308105 (2022)
970. P.C. Barry et al., First Monte Carlo global QCD analysis of pion parton distributions. Phys. Rev. Lett. **121**(15), 152001 (2018)
971. I. Novikov et al., Parton distribution functions of the charged pion within the xFitter framework. Phys. Rev. D **102**, 014040 (2020)
972. D. Abrams et al., Measurement of the nucleon F_2^n/F_2^p structure function ratio by the Jefferson Lab MARATHON tritium/helium-3 deep inelastic scattering experiment. Phys. Rev. Lett. **128**(13), 132003 (2022)
973. L.A. Harland-Lang et al., Parton distributions in the LHC era: MMHT 2014 PDFs. Eur. Phys. J. C **75**(5), 204 (2015)
974. N. Sato et al., Iterative Monte Carlo analysis of spin-dependent parton distributions. Phys. Rev. D **93**(7), 074005 (2016)
975. E.R. Nocera et al., A first unbiased global determination of polarized PDFs and their uncertainties. Nucl. Phys. B **887**, 276–308 (2014)
976. Y. Zhou, N. Sato, W. Melnitchouk, How well do we know the gluon polarization in the proton? Phys. Rev. D **105**(7), 074022 (2022)
977. J.P. Vary et al., Critical coupling for two-dimensional $\phi 4$ theory in discretized light-cone quantization. Phys. Rev. D **105**(1), 016020 (2022)
978. M. Kreshchuk et al., Quantum simulation of quantum field theory in the light-front formulation. Phys. Rev. A **105**(3), 032418 (2022)
979. Y. Li, P. Maris, J.P. Vary, Chiral sum rule on the light front and the 3D image of the pion. Phys. Lett. B **836**, 137598 (2023)
980. S.R. Beane, Broken chiral symmetry on a null plane. Ann. Phys. **337**, 111–142 (2013)
981. Y. Li, J.P. Vary, Light-front holography with chiral symmetry breaking. Phys. Lett. B **825**, 136860 (2022)
982. S.J. Brodsky et al., Essence of the vacuum quark condensate. Phys. Rev. C **82**, 022201 (2010)
983. X. Zhao et al., Scattering in time-dependent basis light-front quantization. Phys. Rev. D **88**, 065014 (2013)
984. D. Weijie et al., Coulomb excitation of the deuteron in peripheral collisions with a heavy ion. Phys. Rev. C **97**(6), 064620 (2018)
985. M. Li et al., Ultrarelativistic quark-nucleus scattering in a light-front Hamiltonian approach. Phys. Rev. D **101**(7), 076016 (2020)
986. S.J. Brodsky, T. Huang, G. Peter Lepage, *The Hadronic Wave Function in Quantum Chromodynamics* (1980)
987. M. Li, T. Lappi, X. Zhao, Scattering and gluon emission in a color field: a light-front Hamiltonian approach. Phys. Rev. D **104**(5), 056014 (2021)
988. Meijian Li, Tuomas Lappi, Xingbo Zhao, Carlos A. Salgado, Momentum broadening of an in-medium jet evolution using a light-front Hamiltonian approach. Phys. Review D **108**, 036016 (2023)
989. X. Zhao et al., Non-perturbative quantum time evolution on the light-front. Phys. Lett. B **726**, 856–860 (2013)
990. H. Bolun, A. Ilderton, X. Zhao, Scattering in strong electromagnetic fields: transverse size effects in time-dependent basis light-front quantization. Phys. Rev. D **102**(1), 016017 (2020)
991. Z. Lei, B. Hu, X. Zhao, Pair production in strong electric fields (2022)
992. G. Chen et al., Particle distribution in intense fields in a light-front Hamiltonian approach. Phys. Rev. D **95**(9), 096012 (2017)
993. J. Martin Maldacena, The large N limit of superconformal field theories and supergravity. Adv. Theor. Math. Phys. **2**, 231–252 (1998)
994. S.S. Gubser, I.R. Klebanov, A.M. Polyakov, Gauge theory correlators from noncritical string theory. Phys. Lett. B **428**, 105–114 (1998)
995. E. Witten, Anti-de Sitter space and holography. Adv. Theor. Math. Phys. **2**, 253–291 (1998)
996. O. Aharony et al., Large N field theories, string theory and gravity. Phys. Rep. **323**, 183–386 (2000)
997. G. Mack, A. Salam, Finite component field representations of the conformal group. Ann. Phys. **53**, 174–202 (1969)
998. J. Polchinski, M.J. Strassler, Hard scattering and gauge/string duality. Phys. Rev. Lett. **88**, 031601 (2002)
999. A. Rebhan, The Witten–Sakai–Sugimoto model: a brief review and some recent results. EPJ Web Conf. **95**, 02005 (2015). (**Ed. by L. Bravina, Y. Foka, and S. Kabana**)
1000. J. Erlich et al., QCD and a holographic model of hadrons. Phys. Rev. Lett. **95**, 261602 (2005)
1001. L. Da Rold, A. Pomarol, Chiral symmetry breaking from five dimensional spaces. Nucl. Phys. B **721**, 79–97 (2005)
1002. A. Karch et al., Linear confinement and AdS/QCD. Phys. Rev. D **74**, 015005 (2006)
1003. S.J. Brodsky et al., Light-front holographic QCD and emerging confinement. Phys. Rep. **584**, 1–105 (2015)
1004. G.F. de Téramond, S.J. Brodsky, Light-front. Holography, a first approximation to QCD. Phys. Rev. Lett. **102**, 081601 (2009)
1005. V.A. Matveev, R.M. Muradian, A.N. Tavkhelidze, Automodellism in the large-angle elastic scattering and structure of hadrons. Lett. Nuovo Cim. **7**, 719–723 (1973)
1006. J. Polchinski, M.J. Strassler, Deep inelastic scattering and gauge/string duality. JHEP **05**, 012 (2003)
1007. S.J. Brodsky, G.F. de Téramond, Hadronic spectra and light-front wave functions in holographic QCD. Phys. Rev. Lett. **96**, 201601 (2006)
1008. S.J. Brodsky, G.F. de Téramond, Light-front dynamics and AdS/QCD correspondence: the pion form factor in the space- and time-like regions. Phys. Rev. D **77**, 056007 (2008)
1009. S.J. Brodsky, G.F. de Téramond, Light-front dynamics and AdS/QCD correspondence: gravitational form factors of composite hadrons. Phys. Rev. D **78**, 025032 (2008)
1010. V. de Alfaro, S. Fubini, G. Furlan, Conformal invariance in quantum mechanics. Nuovo Cim. A **34**, 569 (1976)

1011. S. Fubini, E. Rabinovici, Super conformal quantum mechanics. Nucl. Phys. B **245**, 17 (1984)
1012. V.P. Akulov, A.I. Pashnev, Quantum superconformsl model in (1,2) space. Theor. Math. Phys. **56**, 862–866 (1983)
1013. S.J. Brodsky, G.F. de Téramond, H. Günter Dosch, Threefold complementary approach to holographic QCD. Phys. Lett. B **729**, 3–8 (2014)
1014. G.F. de Téramond, H. Gunter Dosch, S.J. Brodsky, Baryon spectrum from superconformal quantum mechanics and its light-front holographic embedding. Phys. Rev. D **91**(4), 045040 (2015)
1015. H. Gunter Dosch, G.F. de Téramond, S.J. Brodsky, Superconformal baryon-meson symmetry and light-front holographic QCD. Phys. Rev. D **91**(8), 085016 (2015)
1016. H. Miyazawa, Baryon number changing currents. Prog. Theor. Phys. **36**(6), 1266–1276 (1966)
1017. S. Catto, F. Gursey, Algebraic treatment of effective supersymmetry. Nuovo Cim. A **8**, 201 (1985)
1018. D.B. Lichtenberg, Whither hadron supersymmetry? In: *International Conference on Orbis Scientiae 1999: Quantum Gravity, Generalized Theory of Gravitation and Superstring Theory Based Unification (28th Conference on High-Energy Physics and Cosmology Since 1964)*, pp. 203–208 (1999)
1019. G.F. de Teramond et al., Universality of generalized parton distributions in light-front holographic QCD. Phys. Rev. Lett. **120**(18), 182001 (2018)
1020. T. Liu et al., Unified description of polarized and unpolarized quark distributions in the proton. Phys. Rev. Lett. **124**(8), 082003 (2020)
1021. G.F. de Téramond et al., Gluon matter distribution in the proton and pion from extended holographic light-front QCD. Phys. Rev. D **104**(11), 114005 (2021)
1022. L. Zou, H.G. Dosch, *A Very Practical Guide to Light Front Holographic QCD* (2018). arXiv:1801.00607
1023. S.J. Brodsky, Supersymmetric and conformal features of hadron physics. Universe **4**(11), 120 (2018)
1024. S.J. Brodsky, G.F. de Téramond, H.G. Dosch, *Light-Front Holography and Supersymmetric Conformal Algebra: A Novel Approach to Hadron Spectroscopy, Structure, and Dynamics* arXiv:2004.07756 (2020)
1025. U. Gursoy, E. Kiritsis, F. Nitti, Exploring improved holographic theories for QCD: Part II. JHEP **02**, 019 (2008)
1026. Y. Kim, I. Jae Shin, T. Tsukioka, Holographic QCD: past, present, and future. Prog. Part. Nucl. Phys. **68**, 55–112 (2013)
1027. J. Erlich, An introduction to holographic QCD for nonspecialists. Contemp. Phys. **56**(2), 159–171 (2015)
1028. M. Ammon, J. Erdmenger, *Gauge/Gravity Duality: Foundations and Applications* (Cambridge University Press, Cambridge, 2015)
1029. O. Andreev, V.I. Zakharov, Heavy-quark potentials and AdS/QCD. Phys. Rev. D **74**, 025023 (2006)
1030. O. Andreev, $QQqq\bar{q}$ quark system, compact pentaquark, and gauge/string duality. Phys. Rev. D **107**(2), 026023 (2023)
1031. J. Sonnenschein, D. Weissman, Excited mesons, baryons, glueballs and tetraquarks: predictions of the holography inspired stringy hadron model. Eur. Phys. J. C **79**(4), 326 (2019)
1032. G.F. de Teramond, H. Gunter Dosch, S.J. Brodsky, Kinematical and dynamical aspects of higher-spin bound-state equations in holographic QCD. Phys. Rev. D **87**(7), 075005 (2013)
1033. P. Breitenlohner, D.Z. Freedman, Stability in gauged extended supergravity. Ann. Phys. **144**, 249 (1982)
1034. I. Kirsch, Spectroscopy of fermionic operators in AdS/CFT. JHEP **09**, 052 (2006)
1035. Z. Abidin, C.E. Carlson, Nucleon electromagnetic and gravitational form factors from holography. Phys. Rev. D **79**, 115003 (2009)
1036. T. Gutsche et al., Dilaton in a soft-wall holographic approach to mesons and baryons. Phys. Rev. D **85**, 076003 (2012)
1037. G.F. de Téramond, S.J. Brodsky, Hadronic form factor models and spectroscopy within the gauge/gravity correspondence. In: *Ferrara International School Niccoló Cabeo 2011: Hadronic Physics*, pp. 54–109 (2011)
1038. E. Witten, Dynamical breaking of supersymmetry. Nucl. Phys. B **188**, 513 (1981)
1039. H. Gunter Dosch, G.F. de Teramond, S.J. Brodsky, Supersymmetry across the light and heavy-light hadronic spectrum II. Phys. Rev. D **95**(3), 034016 (2017)
1040. S.J. Brodsky et al., Universal effective hadron dynamics from superconformal algebra. Phys. Lett. B **759**, 171–177 (2016)
1041. S.W. MacDowell, Analytic properties of partial amplitudes in meson-nucleon scattering. Phys. Rev. **116**, 774–778 (1959)
1042. E. Klempt, B.C. Metsch, Multiplet classification of light-quark baryons. Eur. Phys. J. A **48**, 127 (2012)
1043. S.J. Brodsky, G.F. de Téramond, AdS/CFT and light-front QCD. Subnucl. Ser. **45**, 139–183 (2009) **(Ed. by Antonino Zichichi)**
1044. H. Gunter Dosch, G.F. de Téramond, S.J. Brodsky, Supersymmetry across the light and heavy-light hadronic spectrum. Phys. Rev. D **92**(7), 074010 (2015)
1045. J.R. Forshaw, R. Sandapen, An AdS/QCD holographic wavefunction for the rho meson and diffractive rho meson electroproduction. Phys. Rev. Lett. **109**, 081601 (2012)
1046. E.V. Shuryak, Hadrons containing a heavy quark and QCD sum rules. Nucl. Phys. B **198**, 83–101 (1982)
1047. N. Isgur, M.B. Wise, Spectroscopy with heavy quark symmetry. Phys. Rev. Lett. **66**, 1130–1133 (1991)
1048. T. Gutsche et al., Chiral symmetry breaking and meson wave functions in soft-wall AdS/QCD. Phys. Rev. D **87**(5), 056001 (2013)
1049. M. Nielsen et al., Supersymmetry in the double-heavy hadronic spectrum. Phys. Rev. D **98**(3), 034002 (2018)
1050. H.G. Dosch et al., Exotic states in a holographic theory. Nucl. Part. Phys. Proc. **312–317**, 135–139 (2021)
1051. A.P. Trawinski et al., Effective confining potentials for QCD. Phys. Rev. D **90**(7), 074017 (2014)
1052. S. Afonin, T. Solomko, Cornell potential in generalized soft wall holographic model. J. Phys. G **49**(10), 105003 (2022)
1053. G. Hooft, A two-dimensional model for mesons. Nucl. Phys. B **75**, 461–470 (1974)
1054. S.S. Chabysheva, J.R. Hiller, Dynamical model for longitudinal wave functions in light-front holographic QCD. Ann. Phys. **337**, 143–152 (2013)
1055. G.F. de Teramond, S.J. Brodsky, Longitudinal dynamics and chiral symmetry breaking in holographic light-front QCD. Phys. Rev. D **104**(11), 116009 (2021)
1056. M. Ahmady et al., Extending light-front holographic QCD using the 't Hooft equation. Phys. Lett. B **823**, 136754 (2021)
1057. M. Ahmady et al., Hadron spectroscopy using the light-front holographic Schrödinger equation and the 't Hooft equation. Phys. Rev. D **104**(7), 074013 (2021)
1058. E. Shuryak, I. Zahed, Hadronic structure on the light front. II. QCD strings, Wilson lines, and potentials. Phys. Rev. D **107**(3), 034024 (2023)
1059. E. Shuryak, I. Zahed, Meson structure on the light-front III : the Hamiltonian, heavy quarkonia, spin and orbit mixing (2021). arXiv:2112.15586
1060. C.M. Weller, G.A. Miller, Confinement in two-dimensional QCD and the infinitely long pion. Phys. Rev. D **105**, 036009 (2022)
1061. Y. Li, J.P. Vary, Longitudinal dynamics for mesons on the light cone. Phys. Rev. D **105**(11), 114006 (2022)
1062. V.E. Lyubovitskij, I. Schmidt, Meson masses and decay constants in holographic QCD consistent with ChPT and HQET. Phys. Rev. D **105**(7), 074009 (2022)

1063. M. Rinaldi, F. Alberto Ceccopieri, V. Vento, The pion in the graviton soft-wall model: phenomenological applications. Eur. Phys. J. C **82**(7), 626 (2022)
1064. M. Ahmady et al., Pion spectroscopy and dynamics using the holographic light-front Schrödinger equation and the 't Hooft equation. Phys. Lett. B **836**, 137628 (2023)
1065. M. Nielsen, S.J. Brodsky, Hadronic superpartners from a superconformal and supersymmetric algebra. Phys. Rev. D **97**(11), 114001 (2018)
1066. M. Karliner, J.L. Rosner, Discovery of doubly-charmed Ξ_{cc} baryon implies a stable $(bb\bar{u}\bar{d})$ tetraquark. Phys. Rev. Lett. **119**(20), 202001 (2017)
1067. R. Aaij et al., Observation of an exotic narrow doubly charmed tetraquark. Nat. Phys. **18**(7), 751–754 (2022)
1068. G.F. Chew, S.C. Frautschi, Regge trajectories and the principle of maximum strength for strong interactions. Phys. Rev. Lett. **8**, 41–44 (1962)
1069. T. Regge, Introduction to complex orbital momenta. Nuovo Cim. **14**, 951 (1959)
1070. R. Dolen, D. Horn, C. Schmid, Finite-energy sum rules and their application to πN charge exchange. Phys. Rev. **166**, 1768–1781 (1968)
1071. M. Bianchi et al., Partonic behavior of string scattering amplitudes from holographic QCD models. JHEP **05**, 058 (2022)
1072. H.R. Grigoryan, A.V. Radyushkin, Structure of vector mesons in holographic model with linear confinement. Phys. Rev. D **76**, 095007 (2007)
1073. R. Sabbir Sufian et al., Analysis of nucleon electromagnetic form factors from light-front holographic QCD: the spacelike region. Phys. Rev. D **95**(1), 014011 (2017)
1074. M. Ademollo, E. Del Giudice, Nonstrong amplitudes in a Veneziano-type model. Nuovo Cim. A **63**, 639–656 (1969)
1075. P.V. Landshoff, J.C. Polkinghorne, The scaling law for deep inelastic scattering in a new Veneziano-like amplitude. Nucl. Phys. B **19**, 432–444 (1970)
1076. Z. Ye et al., Proton and neutron electromagnetic form factors and uncertainties. Phys. Lett. B **777**, 8–15 (2018)
1077. R. Sabbir Sufian et al., Nonperturbative strange-quark sea from lattice QCD, light-front holography, and meson-baryon fluctuation models. Phys. Rev. D **98**(11), 114004 (2018)
1078. S.J. Brodsky, G. Peter Lepage, Exclusive processes and the exclusive inclusive connection in quantum chromodynamics. In: *Workshop on the Baryon Number of the Universe and Unified Theories* (1979)
1079. D. Müller et al., Wave functions, evolution equations and evolution kernels from light ray operators of QCD. Fortsch. Phys. **42**, 101–141 (1994)
1080. A.V. Radyushkin, Scaling limit of deeply virtual Compton scattering. Phys. Lett. B **380**, 417–425 (1996)
1081. X.-D. Ji, Gauge-invariant decomposition of nucleon spin. Phys. Rev. Lett. **78**, 610–613 (1997)
1082. S. Dulat et al., New parton distribution functions from a global analysis of quantum chromodynamics. Phys. Rev. D **93**(3), 033006 (2016)
1083. R.D. Ball et al., Parton distributions for the LHC Run II. JHEP **04**, 040 (2015)
1084. K. Wijesooriya, P.E. Reimer, R.J. Holt, The pion parton distribution function in the valence region. Phys. Rev. C **72**, 065203 (2005)
1085. M. Aicher, A. Schafer, W. Vogelsang, Soft-gluon resummation and the valence parton distribution function of the pion. Phys. Rev. Lett. **105**, 252003 (2010)
1086. J.S. Conway et al., Experimental study of muon pairs produced by 252-GeV pions on tungsten. Phys. Rev. D **39**, 92–122 (1989)
1087. A. Deur, S.J. Brodsky, G.F. de Teramond, On the interface between perturbative and nonperturbative QCD. Phys. Lett. B **757**, 275–281 (2016)
1088. G.R. Farrar, D.R. Jackson, Pion and nucleon structure functions near $x = 1$. Phys. Rev. Lett. **35**, 1416 (1975)
1089. P.C. Barry et al., Global QCD analysis of pion parton distributions with threshold resummation. Phys. Rev. Lett. **127**(23), 232001 (2021)
1090. P.C. Barry et al., Complementarity of experimental and lattice QCD data on pion parton distributions. Phys. Rev. D **105**(11), 114051 (2022)
1091. R. Sabbir Sufian et al., Constraints on charm-anticharm asymmetry in the nucleon from lattice QCD. Phys. Lett. B **808**, 135633 (2020)
1092. S.J. Brodsky, G.F. de Téramond, Onset of color transparency in holographic light-front QCD. MDPIPhysics **4**(2), 633–646 (2022)
1093. D.N. Kim, G.A. Miller, Light-front holography model of the EMC effect. Phys. Rev. C **106**(5), 055202 (2022)
1094. R.C. Brower et al., The Pomeron and gauge/string duality. JHEP **12**, 005 (2007)
1095. L. Cornalba, M.S. Costa, Saturation in deep inelastic scattering from AdS/CFT. Phys. Rev. D **78**, 096010 (2008)
1096. S.K. Domokos, J.A. Harvey, N. Mann, The Pomeron contribution to p p and p anti-p scattering in AdS/QCD. Phys. Rev. D **80**, 126015 (2009)
1097. R.C. Brower et al., String-gauge dual description of deep inelastic scattering at small-x. JHEP **11**, 051 (2010)
1098. M.S. Costa, M. Djuric, Deeply virtual Compton scattering from gauge/gravity duality. Phys. Rev. D **86**, 016009 (2012)
1099. D. Jorrin, M. Schvellinger, Scope and limitations of a string theory dual description of the proton structure. Phys. Rev. D **106**(6), 066024 (2022)
1100. A. Donnachie, P.V. Landshoff, Total cross-sections. Phys. Lett. B **296**, 227–232 (1992)
1101. Z. Abidin, C.E. Carlson, Gravitational form factors of vector mesons in an AdS/ QCD model. Phys. Rev. D **77**, 095007 (2008)
1102. C. Csaki et al., Glueball mass spectrum from supergravity. JHEP **01**, 017 (1999)
1103. H. Boschi-Filho, N.R.F. Braga, H.L. Carrion, Glueball Regge trajectories from gauge/string duality and the Pomeron. Phys. Rev. D **73**, 047901 (2006)
1104. M. Rinaldi, V. Vento, Meson and glueball spectroscopy within the graviton soft wall model. Phys. Rev. D **104**, 034016 (2021)
1105. P.E. Shanahan, W. Detmold, Gluon gravitational form factors of the nucleon and the pion from lattice QCD. Phys. Rev. D **99**(1), 014511 (2019)
1106. D.A. Pefkou, D.C. Hackett, P.E. Shanahan, Gluon gravitational structure of hadrons of different spin. Phys. Rev. D **105**(5), 054509 (2022)
1107. S. Bailey et al., Parton distributions from LHC, HERA, Tevatron and fixed target data: MSHT20 PDFs. Eur. Phys. J. C **81**(4), 341 (2021)
1108. N.Y. Cao et al., Towards the three-dimensional parton structure of the pion: integrating transverse momentum data into global QCD analysis. Phys. Rev. D **103**(11), 114014 (2021)
1109. E.A. Kuraev, L.N. Lipatov, V.S. Fadin, The Pomeranchuk singularity in nonabelian gauge theories. Sov. Phys. JETP **45**, 199–204 (1977) [Zh. Eksp. Teor. Fiz. 72, 377 (1977)]
1110. H. Günter Dosch et al., Towards a single scale-dependent Pomeron in holographic light-front QCD. Phys. Rev. D **105**(3), 034029 (2022)
1111. H.G. Dosch, E. Ferreira, Diffractive electromagnetic processes from a Regge point of view. Phys. Rev. D **92**, 034002 (2015)
1112. R. Aaij et al., Updated measurements of exclusive J/ψ and ψ(2S) production cross-sections in pp collisions at $\sqrt{s} = 7$TeV. J. Phys. G **41**, 055002 (2014)

1113. B. Bezverkhny Abelev et al., Exclusive J/ψ photoproduction off protons in ultra-peripheral p-Pb collisions at $\sqrt{s_{\rm NN}} = 5.02$ TeV. Phys. Rev. Lett. **113**(23), 232504 (2014)
1114. A. Deur et al., Experimental determination of the QCD effective charge $\alpha_{g1}(Q)$. Particles **5**, 171 (2022)
1115. J. Stern, G. Clement, Quarks, gluons, pions and the Gottfried sum rule. Phys. Lett. B **264**, 426–431 (1991)
1116. S.J. Brodsky et al., Angular distributions of massive quarks and leptons close to threshold. Phys. Lett. B **359**, 355–361 (1995)
1117. S. Catani et al., The resummation of soft gluons in hadronic collisions. Nucl. Phys. B **478**, 273–310 (1996)
1118. D. Binosi et al., Bridging a gap between continuum-QCD and ab initio predictions of hadron observables. Phys. Lett. B **742**, 183–188 (2015)
1119. C.D. Roberts et al., Insights into the emergence of mass from studies of pion and kaon structure. Prog. Part. Nucl. Phys. **120**, 103883 (2021)
1120. J.C. Taylor, Ward identities and charge renormalization of the Yang-Mills field. Nucl. Phys. B **33**, 436–444 (1971)
1121. A.A. Slavnov, Ward identities in gauge theories. Theor. Math. Phys. **10**, 99–107 (1972)
1122. J. Clive Ward, An identity in quantum electrodynamics. Phys. Rev. **78**, 182 (1950)
1123. Y. Takahashi, On the generalized Ward identity. Nuovo Cim. **6**, 371 (1957)
1124. F.E. Murray Gell-Mann, Low, quantum electrodynamics at small distances. Phys. Rev. **95**, 1300–1312 (1954)
1125. A. Deur, S.J. Brodsky, G.F. de Teramond, The QCD running coupling. Nucl. Phys. **90**, 1 (2016)
1126. A. Deur, S.J. Brodsky, C.D. Roberts, *QCD Running Couplings and Effective Charges* (2023)
1127. W.E. Caswell, Asymptotic behavior of nonabelian gauge theories to two loop order. Phys. Rev. Lett. **33**, 244 (1974)
1128. A.I. Sanda, A nonperturbative determination of $\alpha(q^2)$ and its experimental implications. Phys. Rev. Lett. **42**, 1658 (1979)
1129. T. Banks, A. Zaks, On the phase structure of vector-like gauge theories with massless fermions. Nucl. Phys. B **196**, 189–204 (1982)
1130. J.M. Cornwall, Dynamical mass generation in continuum QCD. Phys. Rev. D **26**, 1453 (1982)
1131. J.L. Richardson, The heavy quark potential and the Υ, J/ψ systems. Phys. Lett. B **82**, 272–274 (1979)
1132. D.V. Shirkov, I.L. Solovtsov, Analytic model for the QCD running coupling with universal $\bar{\alpha}_s(0)$ value. Phys. Rev. Lett. **79**, 1209–1212 (1997)
1133. P. Boucaud et al., The strong coupling constant at small momentum as an instanton detector. JHEP **04**, 005 (2003)
1134. S.J. Brodsky, G. Peter Lepage, P.B. Mackenzie, On the elimination of scale ambiguities in perturbative quantum chromodynamics. Phys. Rev. D **28**, 228 (1983)
1135. S.J. Brodsky, X.-G. Wu, Scale setting using the extended renormalization group and the principle of maximum conformality: the QCD coupling constant at four loops. Phys. Rev. D **85**, 034038 [Erratum: Phys. Rev. D 86, 079903 (2012)]
1136. L. Di Giustino et al., High precision tests of QCD without scale or scheme ambiguities (2023). arXiv:2307.03951
1137. C. Lerche, L. von Smekal, On the infrared exponent for gluon and ghost propagation in Landau gauge QCD. Phys. Rev. D **65**, 125006 (2002)
1138. W. Celmaster, F.S. Henyey, The quark-anti-quark interaction at all momentum transfers. Phys. Rev. D **18**, 1688 (1978)
1139. R. Levine, Y. Tomozawa, An effective potential for heavy quark-anti-quark bound systems. Phys. Rev. D **19**, 1572 (1979)
1140. W. Buchmuller, G. Grunberg, S.H.H. Tye, The Regge slope and the lambda parameter in QCD: an empirical approach via quarkonia. Phys. Rev. Lett. **45**, 103 (1980) [Erratum: Phys. Rev. Lett. 45, 587 (1980)]
1141. W. Buchmuller, S.H.H. Tye, Quarkonia and quantum chromodynamics. Phys. Rev. D **24**, 132 (1981)
1142. D. Binosi et al., Process-independent strong running coupling. Phys. Rev. D **96**(5), 054026 (2017)
1143. Z.-F. Cui et al., Effective charge from lattice QCD. Chin. Phys. C **44**(8), 083102 (2020)
1144. A. Deur et al., Experimental determination of the effective strong coupling constant. Phys. Lett. B **650**, 244–248 (2007)
1145. A. Deur et al., Determination of the effective strong coupling constant $\alpha s, g1(Q^2)$ from CLAS spin structure function data. Phys. Lett. B **665**, 349–351 (2008)
1146. S.B. Gerasimov, A Sum rule for magnetic moments and the damping of the nucleon magnetic moment in nuclei. Yad. Fiz. **2**, 598–602 (1965)
1147. S.D. Drell, A.C. Hearn, Exact sum rule for nucleon magnetic moments. Phys. Rev. Lett. **16**, 908–911 (1966)
1148. A.W. Peet, J. Polchinski, UV/IR relations in AdS dynamics. Phys. Rev. D **59**, 065011 (1999)
1149. A. Deur, S.J. Brodsky, G.F. de Teramond, Connecting the hadron mass scale to the fundamental mass scale of quantum chromodynamics. Phys. Lett. B **750**, 528–532 (2015)
1150. A. Deur, S.J. Brodsky, G.F. de Teramond, Determination of $\Lambda_{\bar{M}S}$ at five loops from holographic QCD. J. Phys. G **44**(10), 105005 (2017)
1151. K. Raya et al., Structure of the neutral pion and its electromagnetic transition form factor. Phys. Rev. D **93**(7), 074017 (2016)
1152. K. Raya et al., Partonic structure of neutral pseudoscalars via two photon transition form factors. Phys. Rev. D **95**(7), 074014 (2017)
1153. J. Rodríguez-Quintero et al., Process-independent effective coupling. From QCD Green's functions to phenomenology. Few Body Syst. **59**(6), 121 (2018) **(Ed. by R. Gothe et al.)**
1154. C. Shi et al., Kaon and pion parton distribution amplitudes to twist-three. Phys. Rev. D **92**, 014035 (2015)
1155. M. Ding et al., Leading-twist parton distribution amplitudes of S-wave heavy-quarkonia. Phys. Lett. B **753**, 330–335 (2016)
1156. M. Ding et al., Drawing insights from pion parton distributions. Chin. Phys. C **44**(3), 031002 (2020)
1157. M. Ding et al., Symmetry, symmetry breaking, and pion parton distributions. Phys. Rev. D **101**(5), 054014 (2020)
1158. L. Chang, C.D. Roberts, Tracing masses of ground-state light-quark mesons. Phys. Rev. C **85**, 052201 (2012)
1159. S.J. Brodsky, R. Shrock, Maximum wavelength of confined quarks and gluons and properties of quantum chromodynamics. Phys. Lett. B **666**, 95–99 (2008)
1160. D.J. Gross, F. Wilczek, Asymptotically free gauge theories-I. Phys. Rev. D **8**, 3633–3652 (1973)
1161. D.J. Gross, F. Wilczek, Asymptotically free gauge theories-II. Phys. Rev. D **9**, 980–993 (1974)
1162. G. 't Hooft, A planar diagram theory for strong interactions. Nucl. Phys. B **72**, 461 (1974) **(Ed. by J. C. Taylor)**
1163. E. Ellen Jenkins, R.F. Lebed, Baryon mass splittings in the $1/N_c$ expansion. Phys. Rev. D **52**, 282–294 (1995)
1164. R. Kaiser, H. Leutwyler, Large N_c in chiral perturbation theory. Eur. Phys. J. C **17**, 623–649 (2000)
1165. S. Coleman, *Aspects of Symmetry: Selected Erice Lectures* (Cambridge University Press, Cambridge, 1985)
1166. B. Lucini, M. Panero, SU(N) gauge theories at large N. Phys. Rep. **526**, 93–163 (2013)
1167. N. Matagne, F. Stancu, Baryon resonances in large N_cQCD. Rev. Mod. Phys. **87**, 211–245 (2015)
1168. E. Witten, Baryons in the 1/n expansion. Nucl. Phys. B **160**, 57–115 (1979)
1169. T.D. Cohen, Quantum number exotic hybrid mesons and large N_cQCD. Phys. Lett. B **427**, 348–352 (1998)

1170. S. Okubo, Phi meson and unitary symmetry model. Phys. Lett. **5**, 165–168 (1963)
1171. J. Iizuka, Systematics and phenomenology of meson family. Prog. Theor. Phys. Suppl. **37**, 21–34 (1966)
1172. T.D. Cohen, R.F. Lebed, Are there tetraquarks at large N_c in QCD(F)? Phys. Rev. D **90**(1), 016001 (2014)
1173. E. Witten, Current algebra theorems for the U(l) goldstone boson. Nucl. Phys. B **156**, 269–283 (1979)
1174. A.R. Zhitnitsky, On chiral symmetry breaking in QCD in two-dimensions ($N_c \to$ infinity). Phys. Lett. B **165**, 405–409 (1985)
1175. S.R. Coleman, There are no Goldstone bosons in two-dimensions. Commun. Math. Phys. **31**, 259–264 (1973)
1176. E. Witten, C. Symmetry, The 1/n expansion, and the SU(N) Thirring model. Nucl. Phys. B **145**, 110–118 (1978)
1177. V.L. Berezinski, Phys. JETP **32**, 493 (1970)
1178. J.M. Kosterlitz, D.J. Thouless, Ordering, metastability and phase transitions in two-dimensional systems. J. Phys. C **6**, 1181–1203 (1973)
1179. G.S. Adkins, C.R. Nappi, The Skyrme model with pion masses. Nucl. Phys. B **233**, 109–115 (1984)
1180. G.S. Adkins, C.R. Nappi, E. Witten, Static properties of nucleons in the Skyrme model. Nucl. Phys. B **228**, 552 (1983)
1181. I. Zahed, G.E. Brown, The Skyrme model. Phys. Rep. **142**, 1–102 (1986)
1182. G.E. Brown, (ed.) *Selected papers, with commentary, of Tony Hilton Royle Skyrme. World Scientific Series in 20th Century Physics*, vol. 3, p. 456 (1994)
1183. G.S. Adkins, C.R. Nappi, Model independent relations for baryons as solitons in mesonic theories. Nucl. Phys. B **249**, 507–518 (1985)
1184. J.-L. Gervais, B. Sakita, Large N QCD baryon dynamics: exact results from its relation to the static strong coupling theory. Phys. Rev. Lett. **52**, 87 (1984)
1185. R.F. Dashen, A.V. Manohar, Baryonpion couplings from large N_c QCD. Phys. Lett. B **315**, 425–430 (1993)
1186. R.F. Dashen, E. Ellen Jenkins, A.V. Manohar, The $1/N_c$ expansion for baryons. Phys. Rev. D **49**, 4713 (1994) [Erratum: Phys. Rev. D 51, 2489 (1995)]
1187. R.F. Dashen, A.V. Manohar, $1/N_c$ corrections to the baryon axial currents in QCD. Phys. Lett. B **315**, 438–440 (1993)
1188. T.D. Cohen, B.A. Gelman, Nucleon-nucleon scattering observables in large N_c QCD. Phys. Lett. B **540**, 227–232 (2002)
1189. T.D. Cohen, B.A. Gelman, Total nucleon-nucleon cross sections in large N_c QCD. Phys. Rev. C **85**, 024001 (2012)
1190. D.B. Kaplan, M.J. Savage, The spin flavor dependence of nuclear forces from large n QCD. Phys. Lett. B **365**, 244–251 (1996)
1191. D.B. Kaplan, A.V. Manohar, The nucleon-nucleon potential in the $1/N_c$ expansion. Phys. Rev. C **56**, 76–83 (1997)
1192. M.K. Banerjee, T.D. Cohen, B.A. Gelman, The nucleon nucleon interaction and large N_c QCD. Phys. Rev. C **65**, 034011 (2002)
1193. G. Veneziano, Some aspects of a unified approach to gauge, dual and Gribov theories. Nucl. Phys. B **117**, 519–545 (1976)
1194. A. Armoni, M. Shifman, G. Veneziano, SUSY relics in one flavor QCD from a new 1/N expansion. Phys. Rev. Lett. **91**, 191–601 (2003)
1195. A. Armoni, M. Shifman, G. Veneziano, Exact results in non-supersymmetric large N orientifold field theories. Nucl. Phys. B **667**, 170–182 (2003)
1196. A. Armoni, M. Shifman, G. Veneziano, From super Yang–Mills theory to QCD: planar equivalence and its implications, in *From Fields to Strings: Circumnavigating Theoretical Physics. Ian Kogan Memorial Collection (3 volume set)*, ed. by M. Shifman, A. Vainshtein, J. Wheater, pp. 353–444 (2004)
1197. T.D. Cohen, R.F. Lebed, Tetraquarks with exotic flavor quantum numbers at large N_c in QCD_{AS}. Phys. Rev. D **89**(5), 054018 (2014)
1198. T.D. Cohen, D.L. Shafer, R.F. Lebed, Baryons in QCD_{AS} at large N_c: a roundabout approach. Phys. Rev. D **81**, 036006 (2010)
1199. A. Cherman, T.D. Cohen, R.F. Lebed, All you need is N: baryon spectroscopy in two large N limits. Phys. Rev. D **80**, 036002 (2009)
1200. *Proceedings of the 16th International Conference On High-Energy Physics*, ed. by A. Roberts J.D. Jackson. Batavia (1972)
1201. L.D. Faddeev, V.N. Popov, Feynman diagrams for the Yang-Mills field. Phys. Lett. B **25**, 29–30 (1967)
1202. D.J. Gross, Twenty five years of asymptotic freedom. Nucl. Phys. B Proc. Suppl. **74**, 426–446 (1999)
1203. M. Shifman, Historical curiosity: How asymptotic freedom of the Yang–Mills theory could have been discovered three times before Gross, Wilczek, and Politzer, but was not, in *At the Frontier of Particle Physics. Handbook of QCD*. ed. by M. Shifman (World Scientific, Singapore, 2001), pp.126–130
1204. S. Weinberg, The U(l) Problem. Phys. Rev. D **11**, 3583–3593 (1975)
1205. E.B. Bogomolnyi, V.A. Novikov, M.A. Shifman, Behaviour of the physical charge at small distances in nonabelian gauge theories. Sov. J. Nucl. Phys. **20**, 110 (1974)
1206. A.I. Vainshtein, V.I. Zakharov, M.A. Shifman, A possible mechanism for the Delta T = 1/2 rule in nonleptonic decays of strange particles. JETP Lett. **22**, 55–56 (1975)
1207. M.A. Shifman, A.I. Vainshtein, V.I. Zakharov, Light quarks and the origin of the $\Delta I = 1/2$ rule in the nonleptonic decays of strange particles. Nucl. Phys. B **120**, 316 (1977)
1208. A.I. Vainshtein, How penguins started to fly. Int. J. Mod. Phys. A **14**, 4705–4719 (1999)
1209. M.K. Gaillard, B.W. Lee, $\Delta I = 1/2$ rule for nonleptonic decays in asymptotically free field theories. Phys. Rev. Lett. **33**, 108 (1974)
1210. G. Altarelli, L. Maiani, Octet enhancement of nonleptonic weak interactions in asymptotically free gauge theories. Phys. Lett. B **52**, 351–354 (1974)
1211. A.I. Vainshtein, V.I. Zakharov, M.A. Shifman, Gluon condensate and lepton decays of vector mesons (in Russian). JETP Lett. **27**, 55–58 (1978)
1212. V.A. Novikov et al., Wilson's operator expansion: can it fail? Nucl. Phys. B **249**, 445–471 (1985)
1213. M.A. Shifman, Snapshots of hadrons or the story of how the vacuum medium determines the properties of the classical mesons which are produced, live and die in the QCD vacuum. Prog. Theor. Phys. Suppl. **131**, 1–71 (1998)
1214. M. Shifman, Resurgence, operator product expansion, and remarks on renormalons in supersymmetric Yang-Mills theory. J. Exp. Theor. Phys. **120**(3), 386–398 (2015)
1215. N. Seiberg, E. Witten, Electric–magnetic duality, monopole condensation, and confinement in N=2 supersymmetric Yang–Mills theory. Nucl. Phys. B **426**, 19–52 (1994) [Erratum: Nucl. Phys. B 430, 485–486 (1994)]
1216. N. Seiberg, E. Witten, Monopoles, duality and chiral symmetry breaking in N = 2 supersymmetric QCD. Nucl. Phys. B **431**, 484–550 (1994)
1217. M.A. Shifman, A.I. Vainshtein, V.I. Zakharov, QCD and resonance physics: applications. Nucl. Phys. B **147**, 448–518 (1979)
1218. M.A. Shifman, A.I. Vainshtein, V.I. Zakharov, QCD and resonance physics. The $\rho - \omega$ mixing. Nucl. Phys. B **147**, 519–534 (1979)
1219. V.A. Novikov et al., Are all hadrons alike? Nucl. Phys. B **191**, 301–369 (1981)
1220. M. Shifman, New and old about renormalons: in memoriam of Kolya Uraltsev. Int. J. Mod. Phys. A **30**(10), 1543001 (2015)
1221. I.I.Y. Bigi et al., The Pole mass of the heavy quark. Perturbation theory and beyond. Phys. Rev. D **50**, 2234–2246 (1994)

1222. M. Beneke, V.M. Braun, Heavy quark effective theory beyond perturbation theory: renormalons, the pole mass and the residual mass term. Nucl. Phys. B **426**, 301–343 (1994)
1223. I.I.Y. Bigi, M.A. Shifman, N. Uraltsev, Aspects of heavy quark theory. Annu. Rev. Nucl. Part. Sci. **47**, 591–661 (1997)
1224. D. Schubring, C.-H. Sheu, M. Shifman, Treating divergent perturbation theory: lessons from exactly solvable 2D models at large N. Phys. Rev. D **104**(8), 085016 (2021)
1225. M.A. Shifman (ed.), *Vacuum Structure and QCD Sum Rules* (North-Holland, Elsevier Science Publishers, Amsterdam, 1992)
1226. M. Shifman, Vacuum structure and QCD sum rules: introduction. Int. J. Mod. Phys. A **25**, 226–235 (2010)
1227. V.M. Braun, Light cone sum rules, pp. 105–118 (1997)
1228. A. Khodjamirian, T. Mannel, N. Offen, Form-factors from light-cone sum rules with B-meson distribution amplitudes. Phys. Rev. D **75**, 054013 (2007)
1229. P. Colangelo, A. Khodjamirian, QCD sum rules, a modern perspective, pp. 1495–1576 (2000)
1230. W. Braunschweig et al., Radiative decays of the J/ψ and evidence for a new heavy resonance. Phys. Lett. B **67**, 243–248 (1977)
1231. M.A. Shifman et al., η_c puzzle in quantum chromodynamics. Phys. Lett. B **77**, 80–83 (1978)
1232. R. Partridge et al., Observation of an η_c candidate state with mass 2978 MeV $\pm$ 9 MeV. Phys. Rev. Lett. **45**, 1150–1153 (1980)
1233. M.A. Shifman, M.B. Voloshin, Preasymptotic effects in inclusive weak decays of charmed particles. Sov. J. Nucl. Phys. **41**, 120 (1985)
1234. M.A. Shifman, M.B. Voloshin, Hierarchy of lifetimes of charmed and beautiful hadrons. Sov. Phys. JETP **64**, 698 (1986)
1235. N. Uraltsev, Topics in the heavy quark expansion, pp. 1577–1670 (2000)
1236. M.A. Shifman, Recent progress in the heavy quark theory. In: *PASCOS/HOPKINS 1995 (Joint Meeting of the International Symposium on Particles, Strings and Cosmology and the 19th Johns Hopkins Workshop on Current Problems in Particle Theory)*, pp. 006-994 (1995)
1237. A. Lenz, Lifetimes and heavy quark expansion. Int. J. Mod. Phys. A **30**(10), 1543005 (2015)
1238. M. Kirk, A. Lenz, T. Rauh, Dimension-six matrix elements for meson mixing and lifetimes from sum rules. JHEP **12**, 068 (2017) [Erratum: JHEP 06, 162 (2020)]
1239. M. Fael, K. Schonwald, M. Steinhauser, Third order corrections to the semileptonic $b \to c$ and the muon decays. Phys. Rev. D **104**(1), 016003 (2021)
1240. A. Lenz, M. Laura Piscopo, A.V. Rusov, Contribution of the Darwin operator to non-leptonic decays of heavy quarks. JHEP **12**, 199 (2020)
1241. T. Mannel, D. Moreno, A. Pivovarov, Heavy quark expansion for heavy hadron lifetimes: completing the $1/{m_b}^3$, corrections. JHEP **08**, 089 (2020)
1242. D. King et al., Revisiting inclusive decay widths of charmed mesons (2021)
1243. J. Gratrex, B. Melic, I. Nišandžic, Lifetimes of singly charmed hadrons. JHEP **07**, 058 (2022)
1244. R. Aaij et al., Measurement of the ${\Omega_c}^0$ baryon lifetime. Phys. Rev. Lett. **121**(9), 092003 (2018)
1245. R. Aaij et al., Precision measurement of the ${\Lambda_c}^+$, ${\Xi_c}^+$ and ${\Xi_c}^0$ baryon lifetimes. Phys. Rev. D **100**(3), 032001 (2019)
1246. R. Aaij et al., Measurement of the lifetimes of promptly produced ${\Omega_c}^0$ and ${\Xi_c}^0$ baryons. Sci. Bull. **67**(5), 479–487 (2022)
1247. B. Blok, M.A. Shifman, Lifetimes of charmed hadrons revisited. Facts and fancy. In: *3rd Workshop on the Tau-Charm Factory* (1993)
1248. S. Nussinov, W. Wetzel, Comparison of exclusive decay rates for $b \to u$ and $b \to c$ transitions. Phys. Rev. D **36**, 130 (1987)
1249. M.A. Shifman, M.B. Voloshin, On production of D and $D*$ mesons in B-meson decays. Sov. J. Nucl. Phys. **47**, 511 (1988)
1250. N. Isgur, M.B. Wise, Weak decays of heavy mesons in the static quark approximation. Phys. Lett. B **232**, 113–117 (1989)
1251. N. Isgur, M.B. Wise, Weak transition form-factors between heavy mesons. Phys. Lett. B **237**, 527–530 (1990)
1252. H. Georgi, An effective field theory for heavy quarks at low-energies. Phys. Lett. B **240**, 447–450 (1990)
1253. J. Chay, H. Georgi, B. Grinstein, Lepton energy distributions in heavy meson decays from QCD. Phys. Lett. B **247**, 399–405 (1990)
1254. I.I.Y. Bigi, N.G. Uraltsev, A.I. Vainshtein, Nonperturbative corrections to inclusive beauty and charm decays: QCD versus phenomenological models. Phys. Lett. B **293**, 430–436 (1992) [Erratum: Phys. Lett. B 297, 477–477 (1992)]
1255. I.I.Y. Bigi et al., QCD predictions for lepton spectra in inclusive heavy flavor decays. Phys. Rev. Lett. **71**, 496–499 (1993)
1256. R.L. Jaffe, L. Randall, Heavy quark fragmentation into heavy mesons. Nucl. Phys. B **412**, 79–105 (1994)
1257. M. Neubert, QCD based interpretation of the lepton spectrum in inclusive $\bar{B} \to X_u l \bar{\nu}$ decays. Phys. Rev. D **49**, 3392–3398 (1994)
1258. I.I.Y. Bigi et al., On the motion of heavy quarks inside hadrons: universal distributions and inclusive decays. Int. J. Mod. Phys. A **9**, 2467–2504 (1994)
1259. M.B. Voloshin, M.A. Shifman, On the annihilation constants of mesons consisting of a heavy and a light quark, and $B^0 \leftrightarrow \bar{B}^0$ oscillations. Sov. J. Nucl. Phys. **45**, 292 (1987)
1260. H. David Politzer, M.B. Wise, Leading logarithms of heavy quark masses in processes with light and heavy quarks. Phys. Lett. B **206**, 681–684 (1988)
1261. M.A. Shifman, Quark hadron duality. In: *8th International Symposium on Heavy Flavor Physics*, vol. 3 (World Scientific, Singapore, 2000), pp. 1447–1494
1262. M.A. Shifman, QCD sum rules: the second decade. In: *Workshop on QCD: 20 Years Later*, pp. 775–794 (1993)
1263. D. Gaiotto et al., Generalized global symmetries. JHEP **02**, 172 (2015)
1264. D. Gaiotto et al., Theta, time reversal, and temperature. JHEP **05**, 091 (2017)
1265. S.B. Libby, G.F. Sterman, Jet and lepton pair production in high-energy lepton-hadron and hadron-hadron scattering. Phys. Rev. D **18**, 3252 (1978)
1266. S.B. Libby, G.F. Sterman, Mass divergences in two particle inelastic scattering. Phys. Rev. D **18**, 4737 (1978)
1267. J. Collins, *Foundations of Perturbative QCD*, vol. 32 (Cambridge University Press, Cambridge, 2013)
1268. J.-W. Qiu, Twist four contributions to the parton structure functions. Phys. Rev. D **42**, 30–44 (1990)
1269. E. Reya, Perturbative quantum chromodynamics. Phys. Rep. **69**, 195 (1981)
1270. A.H. Mueller, Perturbative QCD at high-energies. Phys. Rep. **73**, 237 (1981)
1271. G. Altarelli, Partons in quantum chromodynamics. Phys. Rep. **81**, 1 (1982)
1272. J.C. Collins, D.E. Soper, Parton distribution, decay functions. Nucl. Phys. B **194**, 445–492 (1982)
1273. R. Brock et al., Handbook of perturbative QCD: version 1.0. Rev. Mod. Phys. **67**, 157–248 (1995)
1274. J.-W. Qiu et al., Factorization of jet cross sections in heavy-ion collisions. Phys. Rev. Lett. **122**(25), 252301 (2019)
1275. G.C. Nayak, J.-W. Qiu, G.F. Sterman, Fragmentation, NRQCD and NNLO factorization analysis in heavy quarkonium production. Phys. Rev. D **72**, 114012 (2005)
1276. E.-C. Aschenauer et al. The RHIC SPIN Program: Achievements and Future Opportunities (2015). arXiv:1501.01220

1277. P. Aurenche et al., Large-pT inclusive π^0 cross-sections and next-to-leading-order QCD predictions. Eur. Phys. J. C **13**, 347–355 (2000)
1278. D. de Florian, W. Vogelsang, Threshold resummation for the inclusive-hadron cross-section in pp collisions. Phys. Rev. D **71**, 114004 (2005)
1279. X. Cid Vidal et al., Report from Working Group 3: Beyond the Standard Model physics at the HL-LHC and HE-LHC. CERN Yellow Rep. Monogr. **7**, 585–865 (2019) **(Ed. by Andrea Dainese et al.)**
1280. J.C. Collins, D.E. Soper, G.F. Sterman, Transverse momentum distribution in Drell-Yan pair and W and Z boson production. Nucl. Phys. B **250**, 199–224 (1985)
1281. D.W. Sivers, Single spin production asymmetries from the hard scattering of point-like constituents. Phys. Rev. D **41**, 83 (1990)
1282. J.C. Collins, Fragmentation of transversely polarized quarks probed in transverse momentum distributions. Nucl. Phys. B **396**, 161–182 (1993)
1283. X. Ji, J. Ma, F. Yuan, QCD factorization for semi-inclusive deep-inelastic scattering at low transverse momentum. Phys. Rev. D **71**, 034005 (2005)
1284. A. Bacchetta et al., Semi-inclusive deep inelastic scattering at small transverse momentum. JHEP **02**, 093 (2007)
1285. M. Diehl, Introduction to GPDs and TMDs. Eur. Phys. J. A **52**(6), 149 (2016)
1286. X.-D. Ji, Deeply virtual Compton scattering. Phys. Rev. D **55**, 7114–7125 (1997)
1287. J.C. Collins, L. Frankfurt, M. Strikman, Proof of factorization for exclusive deep inelastic processes. In: *Madrid Workshop on Low x Physics*, pp. 296–303 (1997)
1288. J.C. Collins, L. Frankfurt, M. Strikman, Factorization for hard exclusive electroproduction of mesons in QCD. Phys. Rev. D **56**, 2982–3006 (1997)
1289. J.C. Collins, A. Freund, Proof of factorization for deeply virtual Compton scattering in QCD. Phys. Rev. D **59**, 074009 (1999)
1290. X.-D. Ji, J. Osborne, One loop corrections and all order factorization in deeply virtual Compton scattering. Phys. Rev. D **58**, 094018 (1998)
1291. J.-W. Qiu, Yu. Zhite, Exclusive production of a pair of high transverse momentum photons in pion-nucleon collisions for extracting generalized parton distributions. JHEP **08**, 103 (2022)
1292. J.-W. Qiu, Z. Yu, Single diffractive hard exclusive processes for the study of generalized parton distributions. Phys. Rev. D **107**(1), 014007 (2023)
1293. A. Accardi et al., Electron ion collider: the next QCD Frontier: understanding the glue that binds us all. Eur. Phys. J. A **52**(9), 268 (2016) **(Ed. by A. Deshpande, Z. E. Meziani, and J. W. Qiu)**
1294. D. de Florian et al., Extraction of spin-dependent parton densities and their uncertainties. Phys. Rev. D **80**, 034030 (2009)
1295. J.J. Ethier, N. Sato, W. Melnitchouk, First simultaneous extraction of spin-dependent parton distributions and fragmentation functions from a global QCD analysis. Phys. Rev. Lett. **119**(13), 132001 (2017)
1296. S.J. Brodsky, D. Sung Hwang, I. Schmidt, Final state interactions and single spin asymmetries in semiinclusive deep inelastic scattering. Phys. Lett. B **530**, 99–107 (2002)
1297. X. Ji, F. Yuan, Parton distributions in light cone gauge: where are the final state interactions? Phys. Lett. B **543**, 66–72 (2002)
1298. J.C. Collins, A. Metz, Universality of soft and collinear factors in hard-scattering factorization. Phys. Rev. Lett. **93**, 252001 (2004)
1299. A. Bacchetta et al., Single spin asymmetries in hadron-hadron collisions. Phys. Rev. D **72**, 034030 (2005)
1300. A.V. Efremov, O.V. Teryaev, QCD asymmetry and polarized hadron structure functions. Phys. Lett. B **150**, 383 (1985)
1301. J. Qiu, G.F. Sterman, Single transverse spin asymmetries. Phys. Rev. Lett. **67**, 2264–2267 (1991)
1302. J. Qiu, G.F. Sterman, Single transverse spin asymmetries in direct photon production. Nucl. Phys. B **378**, 52–78 (1992)
1303. J. Qiu, G.F. Sterman, Single transverse spin asymmetries in hadronic pion production. Phys. Rev. D **59**, 014004 (1999)
1304. C. Kouvaris et al., Single transverse-spin asymmetry in high transverse momentum pion production in pp collisions. Phys. Rev. D **74**, 114013 (2006)
1305. Y. Koike, K. Tanaka, Master formula for twist-3 soft-gluon-pole mechanism to single transverse-spin asymmetry. Phys. Lett. B **646**, 232–241 (2007) [Erratum: Phys. Lett. B 668, 458–459 (2008)]
1306. J.-W. Qiu, W. Vogelsang, F. Yuan, Asymmetric di-jet production in polarized hadronic collisions. Phys. Lett. B **650**, 373–378 (2007)
1307. Z.-B. Kang, J.-W. Qiu, Testing the time-reversal modified universality of the Sivers function. Phys. Rev. Lett. **103**, 172001 (2009)
1308. Z.-B. Kang, F. Yuan, J. Zhou, Twist-three fragmentation function contribution to the single spin asymmetry in pp collisions. Phys. Lett. B **691**, 243–248 (2010)
1309. A.V. Belitsky, X. Ji, F. Yuan, Final state interactions and gauge invariant parton distributions. Nucl. Phys. B **656**, 165–198 (2003)
1310. J.C. Collins, Leading twist single transverse-spin asymmetries: Drell-Yan and deep inelastic scattering. Phys. Lett. B **536**, 43–48 (2002)
1311. J.-W. Qiu, G.F. Sterman, Power corrections to hadronic scattering. 2. Factorization. Nucl. Phys. B **353**, 137–164 (1991)
1312. J.-W. Qiu, G.F. Sterman, Power corrections in hadronic scattering. 1. Leading $1/Q^2$ corrections to the Drell–Yan cross-section. Nucl. Phys. B **353**, 105–136 (1991)
1313. Z.-B. Kang et al., Heavy quarkonium production at collider energies: factorization and evolution. Phys. Rev. D **90**(3), 034006 (2014)
1314. X.-D. Ji, Gluon correlations in the transversely polarized nucleon. Phys. Lett. B **289**, 137–142 (1992)
1315. Y. Koike, K. Tanaka, Universal structure of twist-3 softgluon-pole cross-sections for single transverse-spin asymmetry. Phys. Rev. D **76**, 011502 (2007)
1316. A. Metz, D. Pitonyak, Fragmentation contribution to the transverse single-spin asymmetry in proton-proton collisions. Phys. Lett. B **723**, 365–370 (2013) [Erratum: Phys. Lett. B 762, 549–549 (2016)]
1317. Z.-B. Kang, J.-W. Qiu, Evolution of twist-3 multi-parton correlation functions relevant to single transverse-spin asymmetry. Phys. Rev. D **79**, 016003 (2009)
1318. V.M. Braun, A.N. Manashov, B. Pirnay, Scale dependence of twist-three contributions to single spin asymmetries. Phys. Rev. D **80**, 114002 (2009) [Erratum: Phys. Rev. D 86, 119902 (2012)]
1319. Z.-B. Kang, QCD evolution of naive-time-reversal-odd fragmentation functions. Phys. Rev. D **83**, 036006 (2011)
1320. X. Ji et al., A unified picture for single transverse-spin asymmetries in hard processes. Phys. Rev. Lett. **97**, 082002 (2006)
1321. A. Bacchetta et al., Matches and mismatches in the descriptions of semi-inclusive processes at low and high transverse momentum. JHEP **08**, 023 (2008)
1322. M.L. Perl, *High Energy Hadron Physics* (Wiley, New York, 1974)
1323. T.T. Chou, C.-N. Yang, Model of elastic high-energy scattering. Phys. Rev. **170**, 1591–1596 (1968)
1324. G. Antchev et al., Proton-proton elastic scattering at the LHC energy of $s^{1/2} = 7$ TeV. EPL **95**(4), 41001 (2011)
1325. S.J. Brodsky, G.R. Farrar, Scaling laws for large momentum transfer processes. Phys. Rev. D **11**, 1309 (1975)
1326. G. Sterman, Fixed angle scattering and the transverse structure of hadrons. In: *4th Workshop on Exclusive Reactions at High Momentum Transfer*, pp. 16–25 (2011)
1327. S.J. Brodsky, Exclusive processes and the fundamental structure of hadrons. Int. J. Mod. Phys. A **30**(02), 1530014 (2015)

1328. C. White et al., Comparison of 20 exclusive reactions at large t. Phys. Rev. D **49**, 58–78 (1994)
1329. S. Brodsky, G. de Teramond, M. Karliner, Puzzles in hadronic physics and novel quantum chromodynamics phenomenology. Annu. Rev. Nucl. Part. Sci. **62**, 2082 (2011)
1330. S.J. Brodsky, A.H. Mueller, Using nuclei to probe hadronization in QCD. Phys. Lett. B **206**, 685–690 (1988)
1331. D. Bhetuwal et al., Ruling out color transparency in quasielastic ^{12}C(e,e'p) up to Q^2 of 14.2 (GeV/c)^2. Phys. Rev. Lett. **126**(8), 082301 (2021)
1332. L. Frankfurt, G.A. Miller, M. Strikman, Coherent nuclear diffractive production of mini-jets: illuminating color transparency. Phys. Lett. B **304**, 1–7 (1993)
1333. P. Jain, B. Pire, J.P. Ralston, Quantum color transparency and nuclear filtering. Phys. Rep. **271**, 67–179 (1996)
1334. P.V. Landshoff, Model for elastic scattering at wide angle. Phys. Rev. D **10**, 1024–1030 (1974)
1335. E. Nagy et al., Measurements of elastic proton proton scattering at large momentum transfer at the CERN intersecting storage rings. Nucl. Phys. B **150**, 221–267 (1979)
1336. W. Faissler et al., Large angle proton proton elastic scattering at 201-GeV/c and 400-GeV/c. Phys. Rev. D **23**, 33 (1981)
1337. A. Sen, Asymptotic behavior of the wide angle on-shell quark scattering amplitudes in nonabelian gauge theories. Phys. Rev. D **28**, 860 (1983)
1338. Y. Ma, A forest formula to subtract infrared singularities in amplitudes for wide-angle scattering. JHEP **05**, 012 (2020)
1339. N. Agarwal et al., The infrared structure of perturbative gauge theories (2021)
1340. L.J. Dixon, L. Magnea, G.F. Sterman, Universal structure of subleading infrared poles in gauge theory amplitudes. JHEP **08**, 022 (2008)
1341. R.P. Feynman, Photon-hadron interactions (1973)
1342. V.A. Nesterenko, A.V. Radyushkin, Sum rules and pion form-factor in QCD. Phys. Lett. B **115**, 410 (1982)
1343. A. Duncan, A.H. Mueller, Asymptotic behavior of composite particle form-factors and the renormalization group. Phys. Rev. D **21**, 1636 (1980)
1344. B. Kundu et al., The perturbative proton form-factor reexamined. Eur. Phys. J. C **8**, 637–642 (1999)
1345. S.K. Dagaonkar, P. Jain, J.P. Ralston, Uncovering the scaling laws of hard exclusive hadronic processes in a comprehensive endpoint model. Eur. Phys. J. C **74**(8), 3000 (2014)
1346. J. Botts, G.F. Sterman, Hard elastic scattering in QCD: leading behavior. Nucl. Phys. B **325**, 62–100 (1989)
1347. J.C. Collins, D.E. Soper, Back-to-back jets in QCD. Nucl. Phys. B **193**, 381 (1981) [Erratum: Nucl. Phys. B 213, 545 (1983)]
1348. S.J. Brodsky, B.T. Chertok, The deuteron form-factor and the short distance behavior of the nuclear force. Phys. Rev. Lett. **37**, 269 (1976)
1349. S.J. Brodsky, B.T. Chertok, The asymptotic form-factors of hadrons and nuclei and the continuity of particle and nuclear dynamics. Phys. Rev. D **14**, 3003–3020 (1976)
1350. V.A. Matveev, P. Sorba, Is deuteron a six quark system? Lett. Nuovo Cim. **20**, 435 (1977)
1351. M. Harvey, On the fractional parentage expansions of color singlet six quark states in a cluster model. Nucl. Phys. A **352**, 301 (1981) [Erratum: Nucl. Phys. A 481, 834 (1988)]
1352. M. Harvey, Effective nuclear forces in the quark model with Delta and hidden color channel coupling. Nucl. Phys. A **352**, 326–342 (1981)
1353. M. Harvey, J. Letourneux, B. Lorazo, Nucleon nucleon scattering in the quark cluster model. Nucl. Phys. A **424**, 428–446 (1984)
1354. S.J. Brodsky, C.-R. Ji, Applications of quantum chromodynamics to hadronic and nuclear interactions. Lect. Notes Phys. **248**, 153–245 (1986) **(Ed. by C. A. Engelbrecht)**
1355. S.J. Brodsky, C.-R. Ji, G. Peter Lepage, Quantum chromodynamic predictions for the deuteron form-factor. Phys. Rev. Lett. **51**, 83 (1983)
1356. S.J. Brodsky, C.-R. Ji, Evolution of relativistic multi-quark systems. Phys. Rev. D **33**, 1406 (1986)
1357. C.-R. Ji, S.J. Brodsky, Quantum chromodynamic evolution of six quark states. Phys. Rev. D **34**, 1460 (1986)
1358. B.L.G. Bakker, C.-R. Ji, Nuclear chromodynamics: novel nuclear phenomena predicted by QCD. Prog. Part. Nucl. Phys. **74**, 1–34 (2014)
1359. S.J. Brodsky, J.R. Hiller, Reduced nuclear amplitudes in quantum chromodynamics. Phys. Rev. C **28**, 475 (1983) [Erratum: Phys. Rev. C 30, 412–412 (1984)]
1360. S.J. Brodsky, A. Deur, C.D. Roberts, Artificial dynamical effects in quantum field theory. Nat. Rev. Phys. **4**(7), 489–495 (2022)
1361. G.A. Miller, Pionic and hidden-color, six-quark contributions to the deuteron b1 structure function. Phys. Rev. C **89**(4), 045203 (2014)
1362. N. Fomin et al., New measurements of high-momentum nucleons and short-range structures in nuclei. Phys. Rev. Lett. **108**, 092502 (2012)
1363. R. Subedi et al., Probing cold dense nuclear matter. Science **320**, 1476–1478 (2008)
1364. M. Bashkanov, S.J. Brodsky, H. Clement, Novel six-quark hidden-color dibaryon states in QCD. Phys. Lett. B **727**, 438–442 (2013)
1365. I. Vidaña et al., The $d^*(2380)$ in neutron stars–a new degree of freedom? Phys. Lett. B **781**, 112–116 (2018)
1366. M. Bashkanov et al., Double-pionic fusion of nuclear systems and the ABC effect: approaching a puzzle by exclusive and kinematically complete measurements. Phys. Rev. Lett. **102**, 052301 (2009)
1367. P. Adlarson et al., ABC effect in basic double-pionic fusion-observation of a new resonance? Phys. Rev. Lett. **106**, 242302 (2011)
1368. P. Adlarson et al., Isospin decomposition of the basic double-pionic fusion in the region of the ABC effect. Phys. Lett. B **721**, 229–236 (2013)
1369. P. Adlarson et al., Measurement of the $pn \rightarrow pp\pi^0\pi^-$ in search for the recently observed resonance structure in $d\pi^0\pi^0$ and $d\pi^+\pi^-$ systems. Phys. Rev. C **88**(5), 055208 (2013)
1370. P. Adlarson et al., Evidence for a new resonance from polarized neutron-proton scattering. Phys. Rev. Lett. **112**(20), 202301 (2014)
1371. P. Adlarson et al., Neutron-proton scattering in the context of the $d*$ (2380) resonance. Phys. Rev. C **90**(3), 035204 (2014)
1372. P. Adlarson et al., Measurement of the $\vec{n}p \rightarrow np\pi^0\pi^0$ reaction in search for the recently observed d*(2380) resonance. Phys. Lett. B **743**, 325–332 (2015)
1373. P. Adlarson et al., Measurement of the $\vec{n}p \rightarrow d\pi^0\pi^0$ reaction with polarized beam in the region of the d*(2380) resonance. Eur. Phys. J. A **52**(5), 147 (2016)
1374. M. Bashkanov et al., Signatures of the $d*$ (2380) Hexaquark in $d(\gamma, p\vec{n})$. Phys. Rev. Lett. **124**(13), 132001 (2020)
1375. X.Q. Yuan et al., Deltaron dibaryon structure in chiral SU(3) quark model. Phys. Rev. C **60**, 045203 (1999)
1376. Q.B. Li, P.N. Shen, Possible delta-delta dibaryons in the quark cluster model. J. Phys. G **26**, 1207–1216 (2000)
1377. Q.B. Li et al., Dibaryon systems in chiral SU(3) quark model. Nucl. Phys. A **683**, 487–509 (2001)
1378. F. Huang et al., Is d* a candidate for a hexaquark-dominated exotic state? Chin. Phys. C **39**(7), 071001 (2015)
1379. Y. Dong et al., Theoretical study of the $d*(2380) \rightarrow d\pi\pi$ decay width. Phys. Rev. C **91**(6), 064002 (2015)
1380. Y. Dong et al., Decay width of $d^*(2380) \rightarrow NN\pi\pi$ processes. Phys. Rev. C **94**(1), 014003 (2016)

1381. M. Bashkanov, D.P. Watts, A. Pastore, Electromagnetic properties of the $d^*(2380)$ hexaquark. Phys. Rev. C **100**(1), 012201 (2019)
1382. H. Clement, T. Skorodko, Dibaryons: molecular versus compact hexaquarks. Chin. Phys. C **45**(2), 022001 (2021)
1383. A.J. Krasznahorkay et al., New anomaly observed in He4 supports the existence of the hypothetical X17 particle. Phys. Rev. C **104**(4), 044003 (2021)
1384. J.R. West et al., QCD hidden-color hexadiquark in the core of nuclei. Nucl. Phys. A **1007**, 122134 (2021)
1385. V. Kubarovsky, J. Rittenhouse West, S.J. Brodsky, Quantum chromodynamics resolution of the ATOMKI anomaly in ^{4}He nuclear transitions (2022). arXiv:2206.14441
1386. A. Airapetian et al., First measurement of the tensor structure function b_1 of the deuteron. Phys. Rev. Lett. **95**, 242001 (2005)
1387. G. 't Hooft, Magnetic monopoles in unified gauge theories. Nucl. Phys. B **79**, 276–284 (1974) **(Ed. by J. C. Taylor)**
1388. A.M. Polyakov, Particle spectrum in quantum field theory. JETP Lett. **20**, 194–195 (1974) **(Ed. by J. C. Taylor)**
1389. A.A. Belavin et al., Pseudoparticle solutions of the Yang–Mills equations. Phys. Lett. B **59**, 85–87 (1975) **(Ed. by J. C. Taylor)**
1390. Y. Nambu, Strings, monopoles and gauge fields. Phys. Rev. D **10**, 4262 (1974) **(Ed. by T. Eguchi)**
1391. T.C. Kraan, P. Baal, Monopole constituents inside SU(n) calorons. Phys. Lett. B **435**, 389–395 (1998)
1392. E.V. Shuryak, Theory of hadronic plasma. Sov. Phys. JETP **47**, 212–219 (1978)
1393. S. Mandelstam, Vortices and quark confinement in nonabelian gauge theories. Phys. Rep. **23**, 245–249 (1976)
1394. G. 't Hooft, On the phase transition towards permanent quark confinement. Nucl. Phys. B **138**, 1–25 (1978)
1395. P.A.M. Dirac, Quantised singularities in the electromagnetic field. Proc. R. Soc. Lond. A **133**(821), 60–72 (1931)
1396. Y.M. Shnir, *Magnetic Monopoles, Text and Monographs in Physics* (Springer, Berlin, 2005)
1397. G.S. Bali, The Mechanism of quark confinement. In: *3rd International Conference in Quark Confinement and Hadron Spectrum (Confinement III)*, pp. 17–36 (1998)
1398. A. D'Alessandro, M. D'Elia, E.V. Shuryak, Thermal monopole condensation and confinement in finite temperature Yang-Mills theories. Phys. Rev. D **81**, 094501 (2010)
1399. A. D'Alessandro, M. D'Elia, Magnetic monopoles in the high temperature phase of Yang-Mills theories. Nucl. Phys. B **799**, 241–254 (2008)
1400. J. Liao, E. Shuryak, Magnetic component of quark-gluon plasma is also a liquid! Phys. Rev. Lett. **101**, 162302 (2008)
1401. J. Liao, E. Shuryak, Angular dependence of jet quenching indicates its strong enhancement near the QCD phase transition. Phys. Rev. Lett. **102**, 202302 (2009)
1402. S.-S. Chern, J. Simons, Characteristic forms and geometric invariants. Ann. Math. **99**, 48–69 (1974)
1403. D.M. Ostrovsky, G.W. Carter, E.V. Shuryak, Forced tunneling and turning state explosion in pure Yang-Mills theory. Phys. Rev. D **66**, 036004 (2002)
1404. R.F. Dashen, B. Hasslacher, A. Neveu, Nonperturbative methods and extended hadron models in field theory. 3. Four-dimensional nonabelian models. Phys. Rev. D **10**, 4138 (1974)
1405. F.R. Klinkhamer, N.S. Manton, A saddle point solution in the Weinberg-Salam theory. Phys. Rev. D **30**, 2212 (1984)
1406. E. Shuryak, I. Zahed, How to observe the QCD instanton/sphaleron processes at hadron colliders? (2021). arXiv:2102.00256
1407. E.V. Shuryak, The role of instantons in quantum chromodynamics. 3. Quark-gluon plasma. Nucl. Phys. B **203**, 140–156 (1982)
1408. D.B. Leinweber, Visualizations of the QCD vacuum. In: *Workshop on Light-Cone QCD and Nonperturbative Hadron Physics*, pp. 138–143 (1999)
1409. G. 't Hooft, Computation of the quantum effects due to a four-dimensional pseudoparticle. Phys. Rev. D **14**, 3432–3450 (1976) **(Ed. by Mikhail A. Shifman)** [Erratum: Phys. Rev. D 18, 2199 (1978)]
1410. T. Schäfer, E.V. Shuryak, Instantons in QCD. Rev. Mod. Phys. **70**, 323–426 (1998)
1411. E.V. Shuryak, Correlation functions in the QCD vacuum. Rev. Mod. Phys. **65**, 1–46 (1993)
1412. E.V. Shuryak, J.J.M. Verbaarschot, Quark propagation in the random instanton vacuum. Nucl. Phys. B **410**, 37–54 (1993)
1413. E.V. Shuryak, J.J.M. Verbaarschot, Mesonic correlation functions in the random instanton vacuum. Nucl. Phys. B **410**, 55–89 (1993)
1414. T. Schäfer, E.V. Shuryak, J.J.M. Verbaarschot, Baryonic correlators in the random instanton vacuum. Nucl. Phys. B **412**, 143–168 (1994)
1415. V. Thorsson, I. Zahed, Diquarks in the Nambu-Jona-Lasinio Model. Phys. Rev. D **41**, 3442 (1990)
1416. T. Schäfer, E.V. Shuryak, Phases of QCD at high baryon density. Lect. Notes Phys. **578**, 203–217 (2001) **(Ed. by D. Blaschke, N. K. Glendenning, and A. Sedrakian)**
1417. K.-M. Lee, L. Chang-hai, SU(2) calorons and magnetic monopoles. Phys. Rev. D **58**, 025011 (1998)
1418. K. Langfeld, E.-M. Ilgenfritz, Confinement from semiclassical gluon fields in SU(2) gauge theory. Nucl. Phys. B **848**, 33–61 (2011)
1419. R.N. Larsen, S. Sharma, E. Shuryak, The topological objects near the chiral crossover transition in QCD. Phys. Lett. B **794**, 14–18 (2019)
1420. R.N. Larsen, S. Sharma, E. Shuryak, Towards a semiclassical description of QCD vacuum around T_c. Phys. Rev. D **102**(3), 034501 (2020)
1421. R. Larsen, E. Shuryak, Interacting ensemble of the instantondyons and the deconfinement phase transition in the SU(2) gauge theory. Phys. Rev. D **92**(9), 094022 (2015)
1422. R. Larsen, E. Shuryak, Instanton-dyon ensemble with two dynamical quarks: the chiral symmetry breaking. Phys. Rev. D **93**(5), 054029 (2016)
1423. D. DeMartini, E. Shuryak, Chiral symmetry breaking and confinement from an interacting ensemble of instanton dyons in two-flavor massless QCD. Phys. Rev. D **104**(9), 094031 (2021)
1424. N. Dorey, A. Parnachev, Instantons, compactification and S duality in N = 4 SUSY Yang–Mills theory. 2. JHEP **08**, 059 (2001)
1425. E. Shuryak, *Nonperturbative Topological Phenomena in QCD and Related Theories*, vol. 977. Lecture Notes in Physics (2021)
1426. S. Weinberg, Phenomenological Lagrangians. Physica A **96**(1–2), 327–340 (1979) **(Ed. by S. Deser)**
1427. N. Brambilla et al., The XYZ states: experimental and theoretical status and perspectives. Phys. Rep. **873**, 1–154 (2020)
1428. N. Isgur, M.B. Wise, Weak transition form-factors between heavy mesons. Phys. Lett. B **237**, 527 (1990)
1429. M. Neubert, Heavy quark symmetry. Phys. Rep. **245**, 259 (1994)
1430. W.E. Caswell, G.P. Lepage, Effective Lagrangians for bound state problems in QED, QCD, and other field theories. Phys. Lett. B **167**, 437 (1986)
1431. A. Gunawardana, G. Paz, On HQET and NRQCD operators of dimension 8 and above. JHEP **07**, 137 (2017)
1432. A. Kobach, S. Pal, Hilbert series and operator basis for NRQED and NRQCD/HQET. Phys. Lett. B **772**, 225 (2017)
1433. A.V. Manohar, Heavy quark effective theory and nonrelativistic QCD Lagrangian to order a_s/m^3. Phys. Rev. D **56**, 230 (1997)
1434. A.G. Grozin et al., Three-loop chromomagnetic interaction in HQET. Nucl. Phys. B **789**, 277 (2008)
1435. C. Balzereit, Spectator effects in heavy quark effective theory at $O(1/m_Q^3)$. Phys. Rev. D **59**, 094015 (1999)

1436. D. Moreno, A. Pineda, Chromopolarizabilities of a heavy quark at weak coupling. Phys. Rev. D **97**, 016012 (2018) [Erratum: Phys. Rev. D 98, 059902 (2018)]
1437. M.E. Luke, A.V. Manohar, Reparametrization invariance constraints on heavy particle effective field theories. Phys. Lett. B **286**, 348 (1992)
1438. N. Brambilla, D. Gromes, A. Vairo, Poincaré invariance constraints on NRQCD and potential NRQCD. Phys. Lett. B **576**, 314 (2003)
1439. J. Heinonen, R.J. Hill, M.P. Solon, Lorentz invariance in heavy particle effective theories. Phys. Rev. D **86**, 094020 (2012)
1440. A.F. Falk, M. Neubert, Second-order power corrections in the heavy-quark effective theory. 1. Formalism and meson form factors. Phys. Rev. D **47**, 2965 (1993)
1441. P. Marquard et al., Quark mass relations to four-loop order in perturbative QCD. Phys. Rev. Lett. **114**(14), 142002 (2015)
1442. P. Marquard et al., MS-on-shell quark mass relation up to four loops in QCD and a general SU(N) gauge group. Phys. Rev. D **94**, 074025 (2016)
1443. N. Uraltsev, BLM resummation and OPE in heavy flavor transitions. Nucl. Phys. B **491**, 303 (1997)
1444. M. Beneke, A quark mass definition adequate for threshold problems. Phys. Lett. B **434**, 115 (1998)
1445. A.H. Hoang, $1S$ and $\bar{M}S$ bottom quark masses from Υ sum rules. Phys. Rev. D **61**, 034005 (2000)
1446. A. Pineda, Determination of the bottom quark mass from the $\Upsilon(1S)$ system. JHEP **06**, 022 (2001)
1447. A.H. Hoang et al., Infrared renormalization group flow for heavy quark masses. Phys. Rev. Lett. **101**, 151602 (2008)
1448. N. Brambilla et al., Relations between heavy-light meson and quark masses. Phys. Rev. D **97**, 034503 (2018)
1449. A. Bazavov et al., Up-, down-, strange-, charm-, and bottom-quark masses from four-flavor lattice QCD. Phys. Rev. D **98**, 054517 (2018)
1450. W.A. Bardeen, E.J. Eichten, C.T. Hill, Chiral multiplets of heavy-light mesons. Phys. Rev. D **68**, 054024 (2003)
1451. N. Brambilla, A. Vairo, T. Rosch, Effective field theory Lagrangians for baryons with two and three heavy quarks. Phys. Rev. D **72**, 034021 (2005)
1452. S. Fleming, T. Mehen, Doubly heavy baryons, heavy quarkdiquark symmetry and NRQCD. Phys. Rev. D **73**, 034502 (2006)
1453. T. Mehen, B.C. Tiburzi, Doubly heavy baryons and quarkdiquark symmetry in quenched and partially quenched chiral perturbation theory. Phys. Rev. D **74**, 054505 (2006)
1454. Y.-L. Ma, M. Harada, Degeneracy of doubly heavy baryons from heavy quark symmetry. Phys. Lett. B **754**, 125 (2016)
1455. T. Mehen, Implications of heavy quark-diquark symmetry for excited doubly heavy baryons and tetraquarks. Phys. Rev. D **96**, 094028 (2017)
1456. Y.-L. Ma, M. Harada, Chiral partner structure of doubly heavy baryons with heavy quark spin-flavor symmetry. J. Phys. **G45**, 075006 (2018)
1457. H.-Y. Cheng, Y.-L. Shi, Lifetimes of doubly charmed baryons. Phys. Rev. D **98**, 113005 (2018)
1458. T.C. Mehen, A. Mohapatra, Perturbative corrections to heavy quark-diquark symmetry predictions for doubly heavy baryon hyperfine splittings. Phys. Rev. D **100**(7), 076014 (2019)
1459. J. Soto, J. Tarrús Castellà, Effective field theory for double heavy baryons at strong coupling. Phys. Rev. D **102**(1), 014013 (2020) [Erratum: Phys. Rev. D 104, 059901 (2021)]
1460. E.J. Eichten, C. Quigg, Heavy-quark symmetry implies stable heavy tetraquark mesons $Q_i Q_j \bar{q}_k \bar{q}_\ell$. Phys. Rev. Lett. 119, 202002 (2017)
1461. J. Soto, J.T. Castellà, Nonrelativistic effective field theory for heavy exotic hadrons. Phys. Rev. D **102**(1), 014012 (2020)
1462. N. Brambilla et al., Effective field theories for heavy quarkonium. Rev. Mod. Phys. **77**, 1423 (2005)
1463. N. Brambilla et al., Heavy quarkonium physics. In: *CERN Yellow Reports: Monographs* (2004)
1464. N. Brambilla et al., Heavy quarkonium: progress, puzzles, and opportunities. Eur. Phys. J. C **71**, 1534 (2011)
1465. N. Brambilla et al., QCD and strongly coupled gauge theories: challenges and perspectives. Eur. Phys. J. C **74**, 2981 (2014)
1466. A. Vairo, Non-relativistic bound states: the long way back from the Bethe-Salpeter to the Schrödinger equation (2009). arXiv:0902.3346
1467. T. Kinoshita, M. Nio, Radiative corrections to the muonium hyperfine structure. 1. The $\alpha^2(Z\alpha)$ correction. Phys. Rev. D **53**, 4909–4929 (1996)
1468. P. Labelle, Effective field theories for QED bound states: extending nonrelativistic QED to study retardation effects. Phys. Rev. D **58**, 093013 (1998)
1469. B.A. Thacker, G. Peter Lepage, Heavy quark bound states in lattice QCD. Phys. Rev. D **43**, 196–208 (1991)
1470. C. Hughes et al., Hindered M1 radiative decay of $\Upsilon(2S)$ from lattice NRQCD. Phys. Rev. D **92**, 094501 (2015)
1471. B. Colquhoun et al., Phenomenology with lattice NRQCD b quarks. PoS LATTICE **2015**, 334 (2016)
1472. C. Hughes, C.T.H. Davies, C.J. Monahan, New methods for B meson decay constants and form factors from lattice NRQCD. Phys. Rev. D **97**, 054509 (2018)
1473. A. Lytle et al., B_c spectroscopy using highly improved staggered quarks. In: *36th International Symposium on Lattice Field Theory (Lattice 2018)*, East Lansing, July 22–28 (2018)
1474. S.M. Ryan, D.J. Wilson, Excited and exotic bottomonium spectroscopy from lattice QCD. JHEP **02**, 214 (2021)
1475. G.T. Bodwin, E. Braaten, G. Peter Lepage, Rigorous QCD predictions for decays of P-wave quarkonia. Phys. Rev. D **46**, R1914 (1992)
1476. G.T. Bodwin, E. Braaten, G. Peter Lepage, Rigorous QCD analysis of inclusive annihilation and production of heavy quarkonium. Phys. Rev. D **51**, 1125 (1995) [Erratum: Phys. Rev. D 55, 5853 (1997)]
1477. G.T. Bodwin et al., Quarkonium at the Frontiers of High Energy Physics: A Snowmass White Paper. In: *Community Summer Study 2013: Snowmass on the Mississippi* (2013)
1478. H.S. Chung, Review of quarkonium production: status and prospects. In: *PoS Confinement 2018*, 007 (2018)
1479. J.-P. Lansberg, New observables in inclusive production of quarkonia. Phys. Rep. **889**, 1–106 (2020)
1480. G.C. Nayak, J.-W. Qiu, G.F. Sterman, Fragmentation, factorization and infrared poles in heavy quarkonium production. Phys. Lett. B **613**, 45 (2005)
1481. Y.-Q. Ma et al., Factorized power expansion for high-pT heavy quarkonium production. Phys. Rev. Lett. **113**, 142002 (2014)
1482. Z.-B. Kang et al., Heavy quarkonium production at collider energies: partonic cross section and polarization. Phys. Rev. D **91**, 014030 (2015)
1483. A. Pineda, J. Soto, Matching at one loop for the four quark operators in NRQCD. Phys. Rev. D **58**, 114011 (1998)
1484. A. Vairo, A theoretical review of heavy quarkonium inclusive decays. Mod. Phys. Lett. A **19**, 253 (2004)
1485. N. Brambilla, E. Mereghetti, A. Vairo, Electromagnetic quarkonium decays at order v^7. JHEP **08**, 039 (2006) [Erratum: JHEP 04 (2011) 058]
1486. N. Brambilla, E. Mereghetti, A. Vairo, Hadronic quarkonium decays at order v^7. Phys. Rev. D **79**, 074002 (2009) [Erratum: Phys. Rev. D 83 (2011) 079904]
1487. M. Berwein et al., Poincaré invariance in NRQCD and pNRQCD revisited. Phys. Rev. D **99**, 094008 (2019)

1488. N. Brambilla et al., Inclusive decays of heavy quarkonium to light particles. Phys. Rev. D **67**, 034018 (2003)
1489. A. Pineda, J. Soto, Effective field theory for ultrasoft momenta in NRQCD and NRQED. Nucl. Phys. Proc. Suppl. **64**, 428 (1998)
1490. N. Brambilla et al., Potential NRQCD: an effective theory for heavy quarkonium. Nucl. Phys. B **566**, 275 (2000)
1491. N. Brambilla et al., QCD static energy at next-to-next-to-next-to leading logarithmic accuracy. Phys. Rev. D **80**, 034016 (2009)
1492. N. Brambilla et al., Infrared behavior of the static potential in perturbative QCD. Phys. Rev. D **60**, 091502 (1999)
1493. C. Anzai, Y. Kiyo, Y. Sumino, Static QCD potential at three-loop order. Phys. Rev. Lett. **104**, 112003 (2010)
1494. A.V. Smirnov, V.A. Smirnov, M. Steinhauser, Three-loop static potential. Phys. Rev. Lett. **104**, 112002 (2010)
1495. N. Brambilla et al., The logarithmic contribution to the QCD static energy at N^{4}LO. Phys. Lett. B **647**, 185 (2007)
1496. B.A. Kniehl et al., Non-Abelian $\alpha_S^3/(m_q r^2)$ heavy quark anti-quark potential. Phys. Rev. D **65**, 091503 (2002)
1497. B.A. Kniehl et al., Potential NRQCD and heavy quarkonium spectrum at next-to-next-to-next-to-leading order. Nucl. Phys. B **635**, 357 (2002)
1498. N. Brambilla, A. Vairo, The B_c mass up to order α_s^4. Phys. Rev. D **62**, 094019 (2000)
1499. N. Brambilla, D. Gromes, A. Vairo, Poincaré invariance and the heavy quark potential. Phys. Rev. D **64**, 076010 (2001)
1500. C. Peset, A. Pineda, M. Stahlhofen, Potential NRQCD for unequal masses and the Bc spectrum at N^{3}LO. JHEP **05**, 017 (2016)
1501. D. Gromes, Spin dependent potentials in QCD and the correct long range spin orbit term. Z. Phys. C **26**, 401 (1984)
1502. A. Barchielli, N. Brambilla, G.M. Prosperi, Relativistic corrections to the quark-anti-quark potential and the quarkonium spectrum. Nuovo Cim. A **103**, 59 (1990)
1503. B.A. Kniehl, A.A. Penin, Ultrasoft effects in heavy quarkonium physics. Nucl. Phys. B **563**, 200 (1999)
1504. N. Brambilla et al., The heavy quarkonium spectrum at order $m\alpha_s^5 ln a_s$. Phys. Lett. B **470**, 215 (1999)
1505. A. Pineda, J. Soto, The Renormalization group improvement of the QCD static potentials. Phys. Lett. B **495**, 323 (2000)
1506. A. Pineda, Renormalization group improvement of the NRQCD Lagrangian and heavy quarkonium spectrum. Phys. Rev. D **65**, 074007 (2002)
1507. A. Pineda, Next-to-leading ultrasoft running of the heavy quarkonium potentials and spectrum: spin-independent case. Phys. Rev. D **84**, 014012 (2011)
1508. C. Peset, A. Pineda, J. Segovia, P-wave heavy quarkonium spectrum with next-to-next-to-next-to-leading logarithmic accuracy. Phys. Rev. D **98**, 094003 (2018)
1509. C. Anzai, D. Moreno, A. Pineda, S-wave heavy quarkonium spectrum with next-to-next-to-next-to-leading logarithmic accuracy. Phys. Rev. D **98**, 114034 (2018)
1510. T. Appelquist, M. Dine, I.J. Muzinich, The static limit of quantum chromodynamics. Phys. Rev. D **17**, 2074 (1978)
1511. M. Beneke, A. Signer, V.A. Smirnov, Top quark production near threshold and the top quark mass. Phys. Lett. B **454**, 137–146 (1999)
1512. A.H. Hoang et al., Top -anti-top pair production close to threshold: synopsis of recent NNLO results. Eur. Phys. J. Dir. **2**(1), 3 (2000)
1513. A. Pineda, A. Signer, Heavy quark pair production near threshold with potential non-relativistic QCD. Nucl. Phys. B **762**, 67 (2007)
1514. M. Beneke et al., Hadronic top-quark pair production with NNLL threshold resummation. Nucl. Phys. B **855**, 695–741 (2012)
1515. A.H. Hoang, M. Stahlhofen, The top-antitop threshold at the ILC: NNLL QCD uncertainties. JHEP **05**, 121 (2014)
1516. M. Beneke, J. Piclum, T. Rauh, P-wave contribution to third-order top-quark pair production near threshold. Nucl. Phys. B **880**, 414–434 (2014)
1517. M. Beneke et al., Next-to-next-to-next-to-leading order QCD prediction for the top antitop S-wave pair production cross section near threshold in e^+e^- annihilation. Phys. Rev. Lett. **115**(19), 192001 (2015)
1518. A. Pineda, Review of heavy quarkonium at weak coupling. Prog. Part. Nucl. Phys. **67**, 735 (2012)
1519. N. Brambilla, Y. Sumino, A. Vairo, Quarkonium spectroscopy and perturbative QCD: a new perspective. Phys. Lett. B **513**, 381 (2001)
1520. N. Brambilla, Y. Sumino, A. Vairo, Quarkonium spectroscopy and perturbative QCD: massive quark loop effects. Phys. Rev. D **65**, 034001 (2002)
1521. S. Recksiegel, Y. Sumino, Improved perturbative QCD prediction of the bottomonium spectrum. Phys. Rev. D **67**, 014004 (2003)
1522. C. Ayala, G. Cvetic, A. Pineda, The bottom quark mass from the $\Upsilon(1S)$ system at NNNLO. JHEP **09**, 045 (2014)
1523. M. Beneke et al., The bottom-quark mass from non-relativistic sum rules at NNNLO. Nucl. Phys. B **891**, 42 (2015)
1524. Y. Kiyo, G. Mishima, Y. Sumino, Determination of m_c and m_b from quarkonium $1S$ energy levels in perturbative QCD. Phys. Lett. B **752**, 122 (2016) [Erratum: Phys. Lett. B 772 (2017) 878]
1525. C. Ayala, G. Cvetic, A. Pineda, Mass of the bottom quark from Υ(1S) at NNNLO: an update. J. Phys. Conf. Ser. **762**, 012063 (2016)
1526. V. Mateu, P.G. Ortega, Bottom and charm mass determinations from global fits to $Q\bar{Q}$ bound states at N^{3}LO. JHEP **01**, 122 (2018)
1527. C. Peset, A. Pineda, J. Segovia, The charm/bottom quark mass from heavy quarkonium at N^{3}LO. JHEP **09**, 167 (2018)
1528. S. Recksiegel, Y. Sumino, Fine and hyperfine splittings of charmonium and bottomonium: an improved perturbative QCD approach. Phys. Lett. B **578**, 369 (2004)
1529. N. Brambilla, A. Vairo, The $1P$ quarkonium fine splittings at NLO. Phys. Rev. D **71**, 034020 (2005)
1530. B.A. Kniehl et al., $M(\eta_b)$ and α_s from nonrelativistic renormalization group. Phys. Rev. Lett. **92**, 242001 (2004) [Erratum: Phys. Rev. Lett. 104 (2010) 199901]
1531. A.A. Penin et al., $M(B_c^*) - M(B_c)$ splitting from nonrelativistic renormalization group. Phys. Lett. B **593**, 124 (2004) [Erratum: Phys. Lett. B 677 (2009) 343]
1532. A.A. Penin, M. Steinhauser, Heavy quarkonium spectrum at $O(\alpha_s^5 m_q)$ and bottom/top quark mass determination. Phys. Lett. B **538**, 335 (2002)
1533. A.A. Penin, V.A. Smirnov, M. Steinhauser, Heavy quarkonium spectrum and production/annihilation rates to order $\beta_0^3\alpha_s^3$. Nucl. Phys. B **716**, 303 (2005)
1534. M. Beneke, Y. Kiyo, K. Schuller, Third-order coulomb corrections to the S-wave Green function, energy levels and wave functions at the origin. Nucl. Phys. B **714**, 67 (2005)
1535. M. Beneke, Y. Kiyo, K. Schuller, Third-order non-Coulomb correction to the S-wave quarkonium wave functions at the origin. Phys. Lett. B **658**, 222 (2008)
1536. Y. Kiyo, Y. Sumino, Perturbative heavy quarkonium spectrum at next-to-next-to-next-to-leading order. Phys. Lett. B **730**, 76 (2014)
1537. Y. Kiyo, Y. Sumino, Full formula for heavy quarkonium energy levels at next-to-next-to-next-to-leading order. Nucl. Phys. B **889**, 156 (2014)
1538. A.A. Penin et al., Spin dependence of heavy quarkonium production and annihilation rates: Complete next-to-next-to-leading logarithmic result. INucl. Phys. B **699**, 183 (2004) [Erratum: Nucl. Phys. B 829 (2010) 398]
1539. Y. Kiyo, A. Pineda, A. Signer, New determination of inclusive electromagnetic decay ratios of heavy quarkonium from QCD. Nucl. Phys. B **841**, 231 (2010)

1540. M. Beneke, Y. Kiyo, A.A. Penin, Ultrasoft contribution to quarkonium production and annihilation. Phys. Lett. B **653**, 53 (2007)
1541. M. Beneke et al., Leptonic decay of the $\Upsilon(1S)$ meson at third order in QCD. Phys. Rev. Lett. **112**, 151801 (2014)
1542. A. Pineda, Next-to-leading nonperturbative calculation in heavy quarkonium. Nucl. Phys. B **494**, 213 (1997)
1543. T. Rauh, Higher-order condensate corrections to Υ masses, leptonic decay rates and sum rules. JHEP **05**, 201 (2018)
1544. C.W. Bauer et al., Resumming the color octet contribution to radiative Υ decay. Phys. Rev. D **64**, 114014 (2001)
1545. S. Fleming, A.K. Leibovich, Resummed photon spectrum in radiative Υ decays. Phys. Rev. Lett. **90**, 032001 (2003)
1546. S. Fleming, A.K. Leibovich, The photon spectrum in Υ decays. Phys. Rev. D **67**, 074035 (2003)
1547. X. Garcia i Tormo, J. Soto, Soft, collinear and nonrelativistic modes in radiative decays of very heavy quarkonium. Phys. Rev. D **69**, 114006 (2004)
1548. X. Garcia i Tormo, J. Soto, Semi-inclusive radiative decays of $\Upsilon(1S)$. Phys. Rev. D **72**, 054014 (2005)
1549. X. Garcia i Tormo, J. Soto, Radiative decays and the nature of heavy quarkonia. Phys. Rev. Lett. **96**, 111801 (2006)
1550. N. Brambilla et al., Extraction of alpha(s) from radiative Upsilon(1S) decays. Phys. Rev. D **75**, 074014 (2007)
1551. N. Brambilla, Yu. Jia, A. Vairo, Model-independent study of magnetic dipole transitions in quarkonium. Phys. Rev. D **73**, 054005 (2006)
1552. N. Brambilla, P. Pietrulewicz, A. Vairo, Model-independent study of electric dipole transitions in quarkonium. Phys. Rev. D **85**, 094005 (2012)
1553. J. Antonio Pineda, Segovia, Improved determination of heavy quarkonium magnetic dipole transitions in potential nonrelativistic QCD. Phys. Rev. D **87**, 074024 (2013)
1554. J. Segovia, S. Steinbeißer, A. Vairo, Electric dipole transitions of $1P$ bottomonia. Phys. Rev. D **99**, 074011 (2019)
1555. N. Brambilla, P. Roig, A. Vairo, Precise determination of the η_c mass and width in the radiative $J/\psi \to \eta_c\gamma$ decay. AIP Conf. Proc. **1343**, 418 (2011)
1556. N. Brambilla et al., QCD potential at $O(1/m)$. Phys. Rev. D **63**, 014023 (2001)
1557. A. Pineda, A. Vairo, The QCD potential at $O(1/m^2)$: complete spin dependent and spin independent result. Phys. Rev. D **63**, 054007 (2001) [Erratum: Phys. Rev. D 64 (2001) 039902]
1558. N. Brambilla et al., New predictions for inclusive heavy quarkonium P-wave decays. Phys. Rev. Lett. **88**, 012003 (2002)
1559. N. Brambilla et al., The $\sqrt{m\Lambda_{QCD}}$ scale in heavy quarkonium. Phys. Lett. B **580**, 60 (2004)
1560. G.S. Bali et al., Static potentials and glueball masses from QCD simulations with Wilson sea quarks. Phys. Rev. D **62**, 054503 (2000)
1561. N. Brambilla et al., Long-range properties of $1S$ bottomonium states. Phys. Rev. D **93**, 054002 (2016)
1562. L. Susskind, Coarse grained quantum chromodynamics. In: *Ecole d'Ete de Physique Theorique -Weak and Electromagnetic Interactions at High Energy Les Houches*, France, July 5–August 14 (1976), p. 207
1563. W. Fischler, Quark-antiquark potential in QCD. Nucl. Phys. B **129**, 157 (1977)
1564. L.S. Brown, W.I. Weisberger, Remarks on the static potential in quantum chromodynamics. Phys. Rev. D **20**, 3239 (1979)
1565. C. Peset, A. Pineda, M. Stahlhofen, Relativistic corrections to the static energy in terms of Wilson loops at weak coupling. Eur. Phys. J. C **77**, 681 (2017)
1566. Y. Koma, M. Koma, H. Wittig, Nonperturbative determination of the QCD potential at $O(1/m)$. Phys. Rev. Lett. **97**, 122003 (2006)
1567. Y. Koma, M. Koma, H. Wittig, Relativistic corrections to the static potential at $O(1/m)$ and $O(1/m^2)$. PoS LATTICE **2007**, 111 (2007)
1568. G.S. Bali, QCD forces and heavy quark bound states. Phys. Rep. **343**, 1–136 (2001)
1569. J.B. Kogut, G. Parisi, Long range spin spin forces in gauge theories. Phys. Rev. Lett. **47**, 1089 (1981)
1570. G. Perez-Nadal, J. Soto, Effective string theory constraints on the long distance behavior of the subleading potentials. Phys. Rev. D **79**, 114002 (2009)
1571. N. Brambilla et al., Effective string theory and the long-range relativistic corrections to the quark-antiquark potential. Phys. Rev. D **90**, 114032 (2014)
1572. N. Brambilla et al., Decay and electromagnetic production of strongly coupled quarkonia in pNRQCD. JHEP **04**, 095 (2020)
1573. N. Brambilla, H. Sok Chung, A. Vairo, Inclusive hadroproduction of P-wave heavy quarkonia in potential nonrelativistic QCD. Phys. Rev. Lett. **126**(8), 082003 (2021)
1574. N. Brambilla, H. Sok Chung, A. Vairo, Inclusive production of heavy quarkonia in pNRQCD. JHEP **09**, 032 (2021)
1575. N. Brambilla et al., Production and polarization of S-wave quarkonia in potential nonrelativistic QCD. Phys. Rev. D **105**(11), L111503 (2022)
1576. N. Brambilla et al., Inclusive production of J/ψ, $\psi(2S)$, and Υ states in pNRQCD (2022)
1577. A. Pineda, J. Tarrús Castellà, Novel implementation of the multipole expansion to quarkonium hadronic transitions. Phys. Rev. D **100**(5), 054021 (2019)
1578. N. Brambilla, J. Ghiglieri, A. Vairo, Three-quark static potential in perturbation theory. Phys. Rev. D **81**, 054031 (2010)
1579. N. Brambilla, F. Karbstein, A. Vairo, Symmetries of the three-heavy-quark system and the color-singlet static energy at next-to-next-to-leading logarithmic order. Phys. Rev. D **87**, 074014 (2013)
1580. T.T. Takahashi, H. Suganuma, Gluonic excitation of the three-quark system in SU(3) lattice QCD. Phys. Rev. Lett. **90**, 182001 (2003)
1581. T.T. Takahashi, H. Suganuma, Detailed analysis of the gluonic excitation in the three-quark system in lattice QCD. Phys. Rev. D **70**, 074506 (2004)
1582. Y. Koma, M. Koma, Precise determination of the threequark potential in SU(3) lattice gauge theory. Phys. Rev. D **95**, 094513 (2017)
1583. M.V. Polyakov, P. Schweitzer, Determination of J/ψ chromoelectric polarizability from lattice data. Phys. Rev. D **98**(3), 034030 (2018)
1584. N. Brambilla et al., Effective field theories for van der Waals interactions. Phys. Rev. D **95**, 116004 (2017)
1585. J. Tarrús Castellà, G. Krein, Effective field theory for the nucleon-quarkonium interaction. Phys. Rev. D **98**, 014029 (2018)
1586. E. Braaten, C. Langmack, D. Hudson Smith, Born–Oppenheimer approximation for the XYZ mesons. Phys. Rev. D **90**(1), 014044 (2014)
1587. N. Brambilla et al., Born-Oppenheimer approximation in an effective field theory language. Phys. Rev. D **97**(1), 016016 (2018)
1588. E. Braaten, C. Langmack, D. Hudson Smith, Selection rules for hadronic transitions of XYZ mesons. Phys. Rev. Lett. **112**, 222001 (2014)
1589. M. Berwein et al., Quarkonium hybrids with nonrelativistic effective field theories. Phys. Rev. D **92**, 114019 (2015)
1590. J. Tarrús Castellà, E. Passemar, Exotic to standard bottomonium transitions. Phys. Rev. D **104**(3), 034019 (2021)
1591. J. Tarrús Castellà, Heavy meson thresholds in Born–Oppenheimer effective field theory. Phys. Rev. D **106**(9), 094020 (2022)

1592. N. Brambilla et al., Static quark-antiquark pairs at finite temperature. Phys. Rev. D **78**, 014017 (2008)
1593. M. Angel Escobedo, J. Soto, Non-relativistic bound states at finite temperature (I): the hydrogen atom. Phys. Rev. A **78**, 032520 (2008)
1594. M. Angel Escobedo, J. Soto, Non-relativistic bound states at finite temperature (II): the muonic hydrogen. Phys. Rev. A **82**, 042506 (2010)
1595. N. Brambilla et al., Thermal width and gluo-dissociation of quarkonium in pNRQCD. JHEP **12**, 116 (2011)
1596. N. Brambilla et al., Thermal width and quarkonium dissociation by inelastic parton scattering. JHEP **05**, 130 (2013)
1597. S. Biondini et al., Momentum anisotropy effects for quarkonium in a weakly-coupled quark-gluon plasma below the melting temperature. Phys. Rev. D **95**(7), 074016 (2017)
1598. Y. Akamatsu, Heavy quark master equations in the Lindblad form at high temperatures. Phys. Rev. D **91**(5), 056002 (2015)
1599. N. Brambilla et al., Quarkonium suppression in heavy-ion collisions: an open quantum system approach. Phys. Rev. D **96**(3), 034021 (2017)
1600. N. Brambilla et al., Heavy quarkonium suppression in a fireball. Phys. Rev. D **97**(7), 074009 (2018)
1601. A. Rothkopf, Heavy quarkonium in extreme conditions. Phys. Rep. **858**, 1–117 (2020)
1602. N. Brambilla et al., Heavy quarkonium dynamics at next-to-leading order in the binding energy over temperature. JHEP **08**, 303 (2022)
1603. S. Scherer, M.R. Schindler, A primer for chiral perturbation theory. Lect. Notes Phys. **830**, 1–338 (2012)
1604. M. Gell-Mann, The eightfold way: a theory of strong interaction symmetry (1961)
1605. C. Abel et al., Measurement of the permanent electric dipole moment of the neutron. Phys. Rev. Lett. **124**(8), 081803 (2020)
1606. A. Manohar, H. Georgi, Chiral quarks and the nonrelativistic quark model. Nucl. Phys. B **234**, 189–212 (1984)
1607. H. Leutwyler, Theoretical chiral dynamics. In: *3rd Workshop on Chiral Dynamics—Chiral Dynamics 2000: Theory and Experiment*, pp. 3–17 (2000)
1608. M. Gell-Mann, Y. Ne'eman, *The Eightfold Way* (Benjamin, 1964)
1609. S.L. Adler, R.F. Dashen, *Current Algebras and Applications to Particle Physics* (Benjamin, 1968)
1610. J. Gasser, H. Leutwyler, Chiral perturbation theory to one loop. Ann. Phys. **158**, 142 (1984)
1611. H. Leutwyler, On the foundations of chiral perturbation theory. Ann. Phys. **235**, 165–203 (1994)
1612. S.R. Coleman, J. Wess, B. Zumino, Structure of phenomenological Lagrangians. 1. Phys. Rev. **177**, 2239–2247 (1969)
1613. Y. Aoki et al., FLAG Review 2021 (2021)
1614. M. Gell-Mann, R.J. Oakes, B. Renner, Behavior of current divergences under SU(3) x SU(3). Phys. Rev. **175**, 2195–2199 (1968)
1615. S. Weinberg, Dynamical approach to current algebra. Phys. Rev. Lett. **18**, 188–191 (1967)
1616. J.S. Schwinger, Chiral dynamics. Phys. Lett. B **24**, 473–476 (1967)
1617. S. Weinberg, *The Quantum Theory of Fields. Vol. 1: Foundations* (Cambridge University Press, Cambridge, 2005)
1618. J. Bijnens, G. Ecker, Mesonic low-energy constants. Annu. Rev. Nucl. Part. Sci. **64**, 149–174 (2014)
1619. L.-F. Li, H. Pagels, Perturbation theory about a Goldstone symmetry. Phys. Rev. Lett. **26**, 1204–1206 (1971)
1620. J. Wess, B. Zumino, Consequences of anomalous Ward identities. Phys. Lett. B **37**, 95–97 (1971)
1621. E. Witten, Global aspects of current algebra. Nucl. Phys. B **223**, 422–432 (1983)
1622. J.L. Manes, Differential geometric construction of the gauged Wess-Zumino action. Nucl. Phys. B **250**, 369–384 (1985)
1623. J. Bijnens, Chiral perturbation theory and anomalous processes. Int. J. Mod. Phys. A **8**, 3045–3105 (1993)
1624. T. Ebertshauser, H.W. Fearing, S. Scherer, The Anomalous chiral perturbation theory meson Lagrangian to order p^6 revisited. Phys. Rev. D **65**, 054033 (2002)
1625. J. Bijnens, L. Girlanda, P. Talavera, The anomalous chiral Lagrangian of order p^6. Eur. Phys. J. C **23**, 539–544 (2002)
1626. J. Gasser, M.E. Sainio, A. Svarc, Nucleons with chiral loops. Nucl. Phys. B **307**, 779–853 (1988)
1627. V. Bernard, N. Kaiser, U.-G. Meißner, Chiral dynamics in nucleons and nuclei. Int. J. Mod. Phys. E **4**, 193–346 (1995)
1628. L. Geng, Recent developments in SU(3) covariant baryon chiral perturbation theory. Front. Phys. (Beijing) **8**, 328–348 (2013)
1629. G. Ecker, Chiral perturbation theory. Prog. Part. Nucl. Phys. **35**, 1–80 (1995)
1630. E. Ellen Jenkins, A.V. Manohar, Baryon chiral perturbation theory using a heavy fermion Lagrangian. Phys. Lett. B **255**, 558–562 (1991)
1631. P.J. Ellis, H.-B. Tang, Pion nucleon scattering in a new approach to chiral perturbation theory. Phys. Rev. C **57**, 3356–3375 (1998)
1632. T. Becher, H. Leutwyler, Baryon chiral perturbation theory in manifestly Lorentz invariant form. Eur. Phys. J. C **9**, 643–671 (1999)
1633. J. Gegelia, G. Japaridze, Matching heavy particle approach to relativistic theory. Phys. Rev. D **60**, 114038 (1999)
1634. J. Gegelia, G. Japaridze, X.Q. Wang, Is Heavy baryon approach necessary? J. Phys. G **29**, 2303–2309 (2003)
1635. T. Fuchs et al., Renormalization of relativistic baryon chiral perturbation theory and power counting. Phys. Rev. D **68**, 056005 (2003)
1636. N. Fettes et al., The chiral effective pion nucleon Lagrangian of order p^4. Ann. Phys. **283**, 273–302 (2000) [Erratum: Annals Phys. 288, 249–250 (2001)]
1637. S. Scherer, Introduction to chiral perturbation theory. Adv. Nucl. Phys. **27**, 277 (2003) **(Ed. by John W. Negele and E. W. Vogt)**
1638. V. Bernard, Chiral perturbation theory and baryon properties. Prog. Part. Nucl. Phys. **60**, 82–160 (2008)
1639. M.R. Schindler, J. Gegelia, S. Scherer, Infrared and extended on mass shell renormalization of two loop diagrams. Nucl. Phys. B **682**, 367–376 (2004)
1640. T. Fuchs et al., Power counting in baryon chiral perturbation theory including vector mesons. Phys. Lett. B **575**, 11–17 (2003)
1641. M.R. Schindler, J. Gegelia, S. Scherer, Infrared regularization of baryon chiral perturbation theory reformulated. Phys. Lett. B **586**, 258–266 (2004)
1642. P.C. Bruns, U.-G. Meißner, Infrared regularization for spin-1 fields. Eur. Phys. J. C **40**, 97–119 (2005)
1643. S. Steininger, U.-G. Meißner, N. Fettes, On wave function renormalization and related aspects in heavy fermion effective field theories. JHEP **09**, 008 (1998)
1644. T. Fuchs, J. Gegelia, S. Scherer, Structure of the nucleon in chiral perturbation theory. Eur. Phys. J. A **19**, 35–42 (2004)
1645. J.A. McGovern, M.C. Birse, On the absence of fifth order contributions to the nucleon mass in heavy baryon chiral perturbation theory. Phys. Lett. B **446**, 300–305 (1999)
1646. M.R. Schindler et al., Chiral expansion of the nucleon mass to order (q^6). Phys. Lett. B **649**, 390–393 (2007)
1647. M.R. Schindler, et al., Infrared renormalization of two-loop integrals and the chiral expansion of the nucleon mass. Nucl. Phys. A **803**, 68–114 (2008) [Erratum: Nucl. Phys. A 1010, 122175 (2021)]
1648. M. Golterman, Applications of chiral perturbation theory to lattice QCD. In: *Les Houches Summer School: Session 93: Modern Perspectives in Lattice QCD: Quantum Field Theory and High Performance Computing*, pp. 423–515 (2009)

1649. U.-G. Meißner, Quark mass dependence of baryon properties. In: *PoS LAT2005*, 009 (2006) **(Ed. by Christopher Michael)**
1650. D. Djukanovic, J. Gegelia, S. Scherer, Probing the convergence of perturbative series in baryon chiral perturbation theory. Eur. Phys. J. A **29**, 337–342 (2006)
1651. V. Bernard, T.R. Hemmert, U.-G. Meißner, Infrared regularization with spin 3/2 fields. Phys. Lett. B **565**, 137–145 (2003)
1652. C. Hacker et al., Including the $\Delta(1232)$ resonance in baryon chiral perturbation theory. Phys. Rev. C **72**, 055203 (2005)
1653. W. Rarita, J. Schwinger, On a theory of particles with half integral spin. Phys. Rev. **60**, 61 (1941)
1654. P.A. Moldauer, K.M. Case, Properties of half-integral spin Dirac-Fierz-Pauli particles. Phys. Rev. **102**, 279–285 (1956)
1655. L.M. Nath, B. Etemadi, J.D. Kimel, Uniqueness of the interaction involving spin 3/2 particles. Phys. Rev. D **3**, 2153–2161 (1971)
1656. H.-B. Tang, P.J. Ellis, Redundance of Delta isobar parameters in effective field theories. Phys. Lett. B **387**, 9–13 (1996)
1657. T.R. Hemmert, B.R. Holstein, J. Kambor, Chiral Lagrangians and $\Delta(1232)$ interactions: formalism. J. Phys. G **24**, 1831–1859 (1998)
1658. V. Pascalutsa, Quantization of an interacting spin-3/2 field and the Δ isobar. Phys. Rev. D **58**, 096002 (1998)
1659. N. Wies, J. Gegelia, S. Scherer, Consistency of the $\pi\Delta$ interaction in chiral perturbation theory. Phys. Rev. D **73**, 094012 (2006)
1660. H. Krebs, E. Epelbaum, U.G. Meißner, Redundancy of the off-shell parameters in chiral effective field theory with explicit spin-3/2 degrees of freedom. Phys. Lett. B **683**, 222–228 (2010)
1661. V. Pascalutsa, D.R. Phillips, Effective theory of the $\Delta(1232)$ in Compton scattering off the nucleon. Phys. Rev. C **67**, 055202 (2003)
1662. T. Papenbrock, Effective theory for deformed nuclei. Nucl. Phys. A **852**, 36 (2011)
1663. H.W. Hammer, C. Ji, D.R. Phillips, Effective field theory description of halo nuclei. J. Phys. G **44**(10), 103002 (2017)
1664. E. Braaten, H.W. Hammer, Universality in few-body systems with large scattering length. Phys. Rep. **428**, 259–390 (2006)
1665. H.W. Hammer, S. König, U. van Kolck, Nuclear effective field theory: status and perspectives. Rev. Mod. Phys. **92**(2), 025004 (2020)
1666. S. Weinberg, Nuclear forces from chiral Lagrangians. Phys. Lett. B **251**, 288–292 (1990)
1667. S. Weinberg, Effective chiral Lagrangians for nucleon-pion interactions and nuclear forces. Nucl. Phys. B **363**, 3–18 (1991)
1668. E. Epelbaum, J. Gegelia, U.-G. Meißner, Wilsonian renormalization group versus subtractive renormalization in effective field theories for nucleon-nucleon scattering. Nucl. Phys. B **925**, 161–185 (2017)
1669. E. Epelbaum et al., Effective field theory for shallow P-wave states. Few Body Syst. **62**(3), 51 (2021)
1670. I. Tews et al., Nuclear forces for precision nuclear physics: a collection of perspectives. Few Body Syst. **63**(4), 67 (2022)
1671. M.C. Birse, J.A. McGovern, K.G. Richardson, A renormalization group treatment of two-body scattering. Phys. Lett. B **464**, 169–176 (1999)
1672. D.B. Kaplan, M.J. Savage, M.B. Wise, A New expansion for nucleon-nucleon interactions. Phys. Lett. B **424**, 390–396 (1998)
1673. D.B. Kaplan, M.J. Savage, M.B. Wise, Two nucleon systems from effective field theory. Nucl. Phys. B **534**, 329–355 (1998)
1674. T.D. Cohen, J.M. Hansen, Low-energy theorems for nucleon-nucleon scattering. Phys. Rev. C **59**, 13–20 (1999)
1675. S. Fleming, T. Mehen, I.W. Stewart, NNLO corrections to nucleon-nucleon scattering and perturbative pions. Nucl. Phys. A **677**, 313–366 (2000)
1676. S.R. Beane, D.B. Kaplan, A. Vuorinen, Perturbative nuclear physics. Phys. Rev. C **80**, 011001 (2009)
1677. E. Epelbaum et al., $^1S_0$ nucleon-nucleon scattering in the modified Weinberg approach. Eur. Phys. J. A **51**(6), 71 (2015)
1678. D.B. Kaplan, Convergence of nuclear effective field theory with perturbative pions. Phys. Rev. C **102**(3), 034004 (2020)
1679. G.P. Lepage, How to renormalize the Schrodinger equation. In: *8th Jorge Andre Swieca Summer School on Nuclear Physics*, pp. 135–180 (1997)
1680. E. Epelbaum, H. Krebs, P. Reinert, High-precision nuclear forces from chiral EFT: state-of-the-art, challenges and outlook. Front. Phys. **8**, 98 (2020)
1681. A.M. Gasparyan, E. Epelbaum, Nucleon-nucleon interaction in chiral effective field theory with a finite cutoff: explicit perturbative renormalization at next-to-leading order. Phys. Rev. C **105**(2), 024001 (2022)
1682. C. Ordonez, U. van Kolck, Chiral lagrangians and nuclear forces. Phys. Lett. B **291**, 459–464 (1992)
1683. C. Ordonez, L. Ray, U. van Kolck, The two nucleon potential from chiral Lagrangians. Phys. Rev. C **53**, 2086–2105 (1996)
1684. N. Kaiser, R. Brockmann, W. Weise, Peripheral nucleon-nucleon phase shifts and chiral symmetry. Nucl. Phys. A **625**, 758–788 (1997)
1685. S. Pastore, R. Schiavilla, J.L. Goity, Electromagnetic two-body currents of one- and two-pion range. Phys. Rev. C **78**, 064002 (2008)
1686. S. Pastore et al., Electromagnetic currents and magnetic moments in (chi)EFT. Phys. Rev. C **80**, 034004 (2009)
1687. S. Pastore et al., The two-nucleon electromagnetic charge operator in chiral effective field theory (χ EFT) up to one loop. Phys. Rev. C **84**, 024001 (2011)
1688. A. Baroni et al., Nuclear axial currents in chiral effective field theory. Phys. Rev. C **93**(1), 015501 (2016) [Erratum: Phys. Rev. C 93, 049902 (2016), Erratum: Phys. Rev. C 95, 059901 (2017)]
1689. E. Epelbaum, W. Gloeckle, U.-G. Meißner, Nuclear forces from chiral Lagrangians using the method of unitary transformation. 1. Formalism. Nucl. Phys. A **637**, 107–134 (1998)
1690. E. Epelbaum, Four-nucleon force using the method of unitary transformation. Eur. Phys. J. A **34**, 197–214 (2007)
1691. V. Bernard et al., Subleading contributions to the chiral three-nucleon force. I. Long-range terms. Phys. Rev. C **77**, 064004 (2008)
1692. V. Bernard et al., Subleading contributions to the chiral three-nucleon force II: short-range terms and relativistic corrections. Phys. Rev. C **84**, 054001 (2011)
1693. H. Krebs, A. Gasparyan, E. Epelbaum, Chiral three-nucleon force at N^4LO I: longest-range contributions. Phys. Rev. C **85**, 054006 (2012)
1694. H. Krebs, A. Gasparyan, E. Epelbaum, Chiral three-nucleon force at N^4LO II: intermediate-range contributions. Phys. Rev. C **87**(5), 054007 (2013)
1695. S. Kolling et al., Two-nucleon electromagnetic current in chiral effective field theory: one-pion exchange and short-range contributions. Phys. Rev. C **84**, 054008 (2011)
1696. S. Kolling et al., Two-pion exchange electromagnetic current in chiral effective field theory using the method of unitary transformation. Phys. Rev. C **80**, 045502 (2009)
1697. H. Krebs, E. Epelbaum, U.G. Meißner, Nuclear axial current operators to fourth order in chiral effective field theory. Ann. Phys. **378**, 317–395 (2017)
1698. H. Krebs, E. Epelbaum, U.G. Meißner, Nuclear electromagnetic currents to fourth order in chiral effective field theory. Few Body Syst. **60**(2), 31 (2019)
1699. H. Krebs, E. Epelbaum, U.-G. Meißner, Subleading contributions to the nuclear scalar isoscalar current. Eur. Phys. J. A **56**(9), 240 (2020)
1700. E. Epelbaum, *Nuclear Forces from Chiral Effective Field Theory: A Primer* e-Print: 1001.3228 [nucl-th] (2010)

1701. E. Epelbaum, Four-nucleon force in chiral effective field theory. Phys. Lett. B **639**, 456–461 (2006)
1702. J. Lewis Friar, S.A. Coon, Non-adiabatic contributions to static two-pion-exchange nuclear potentials. Phys. Rev. C **49**, 1272–1280 (1994)
1703. V. Baru et al., The multiple-scattering series in pion-deuteron scattering and the nucleon-nucleon potential: perspectives from effective field theory. Eur. Phys. J. A **48**, 69 (2012)
1704. C. Ditsche et al., Roy-Steiner equations for pion-nucleon scattering. JHEP **06**, 043 (2012)
1705. M. Hoferichter et al., Matching pion-nucleon Roy-Steiner equations to chiral perturbation theory. Phys. Rev. Lett. **115**(19), 192301 (2015)
1706. D. Siemens et al., Reconciling threshold and subthreshold expansions for pion-nucleon scattering. Phys. Lett. B **770**, 27–34 (2017)
1707. V. Bernard, N. Kaiser, U.-G. Meißner, Aspects of chiral pion-nucleon physics. Nucl. Phys. A **615**, 483–500 (1997)
1708. N. Kaiser, Chiral 2π exchange NN potentials: two loop contributions. Phys. Rev. C **64**, 057001 (2001)
1709. N. Kaiser, Chiral 2π exchange NN potentials: relativistic $1/M^2$ corrections. Phys. Rev. C **65**, 017001 (2002)
1710. D.R. Entem et al., Peripheral nucleon-nucleon scattering at fifth order of chiral perturbation theory. Phys. Rev. C **91**(1), 014002 (2015)
1711. D.R. Entem et al., Dominant contributions to the nucleon-nucleon interaction at sixth order of chiral perturbation theory. Phys. Rev. C **92**(6), 064001 (2015)
1712. P. Reinert, H. Krebs, E. Epelbaum, Semilocal momentum-space regularized chiral two-nucleon potentials up to fifth order. Eur. Phys. J. A **54**(5), 86 (2018)
1713. E. Epelbaum, H.-W. Hammer, U.-G. Meißner, Modern theory of nuclear forces. Rev. Mod. Phys. **81**, 1773–1825 (2009)
1714. R. Machleidt, D.R. Entem, Chiral effective field theory and nuclear forces. Phys. Rep. **503**, 1–75 (2011)
1715. U. van Kolck, Few nucleon forces from chiral Lagrangians. Phys. Rev. C **49**, 2932–2941 (1994)
1716. E. Epelbaum et al., Three nucleon forces from chiral effective field theory. Phys. Rev. C **66**, 064001 (2002)
1717. S. Ishikawa, M.R. Robilotta, Two-pion exchange three-nucleon potential: $O(q^4)$ chiral expansion. Phys. Rev. C **76**, 014006 (2007)
1718. L. Girlanda, A. Kievsky, M. Viviani, Subleading contributions to the three-nucleon contact interaction. Phys. Rev. C **84**(1), 014001 (2011) [Erratum: Phys. Rev. C 102, 019903 (2020)]
1719. E. Epelbaum et al., Three-nucleon force at large distances: Insights from chiral effective field theory and the large-N_c expansion. Eur. Phys. J. A **51**(3), 26 (2015)
1720. J. de Vries et al., Parity- and time-reversal-violating nuclear forces. Front. Phys. **8**, 218 (2020)
1721. T.-S. Park, D.-P. Min, M. Rho, Chiral dynamics and heavy fermion formalism in nuclei. 1. Exchange axial currents. Phys. Rep. **233**, 341–395 (1993)
1722. T.-S. Park, D.-P. Min, M. Rho, Chiral Lagrangian approach to exchange vector currents in nuclei. Nucl. Phys. A **596**, 515–552 (1996)
1723. M. Hoferichter, P. Klos, A. Schwenk, Chiral power counting of one- and two-body currents in direct detection of dark matter. Phys. Lett. B **746**, 410–416 (2015)
1724. H. Krebs, Nuclear currents in chiral effective field theory. Eur. Phys. J. A **56**(9), 234 (2020)
1725. N. Kaiser, S. Gerstendorfer, Wopl Weise, Peripheral NN scattering: role of Δ excitation, correlated two pion and vector meson exchange. Nucl. Phys. A **637**, 395–420 (1998)
1726. H. Krebs, E. Epelbaum, U.-G. Meißner, Nuclear forces with Delta-excitations up to next-to-next-to-leading order. I. Peripheral nucleon-nucleon waves. Eur. Phys. J. A **32**, 127–137 (2007)
1727. E. Epelbaum, H. Krebs, U.-G. Meißner, Δ-excitations and the three-nucleon force. Nucl. Phys. A **806**, 65–78 (2008)
1728. H. Krebs, A.M. Gasparyan, E. Epelbaum, Three-nucleon force in chiral EFT with explicit $\Delta(1232)$ degrees of freedom: longest-range contributions at fourth order. Phys. Rev. C **98**(1), 014003 (2018)
1729. H. Polinder, J. Haidenbauer, U.-G. Meißner, Hyperonnucleon interactions: a chiral effective field theory approach. Nucl. Phys. A **779**, 244–266 (2006)
1730. J. Haidenbauer et al., Hyperon-nucleon interaction at next-to-leading order in chiral effective field theory. Nucl. Phys. A **915**, 24–58 (2013)
1731. S. Petschauer et al., Leading three-baryon forces from SU(3) chiral effective field theory. Phys. Rev. C **93**(1), 014001 (2016)
1732. J. Haidenbauer, U.G. Meißner, Status of the hyperon-nucleon interaction in chiral effective field theory. In: *14th International Conference on Hypernuclear and Strange Particle Physics* (2022)
1733. E. Epelbaum, W. Gloeckle, U.-G. Meißner, Nuclear forces from chiral Lagrangians using the method of unitary transformation. 2. The two nucleon system. Nucl. Phys. A **671**, 295–331 (2000)
1734. E. Epelbaum, W. Gloeckle, U.G. Meißner, Improving the convergence of the chiral expansion for nuclear forces. 1. Peripheral phases. Eur. Phys. J. A **19**, 125–137 (2004)
1735. A. Gezerlis et al., Quantum Monte Carlo calculations with chiral effective field theory interactions. Phys. Rev. Lett. **111**(3), 032501 (2013)
1736. E. Epelbaum, H. Krebs, U.G. Meißner, Improved chiral nucleonnucleon potential up to next-to-next-to-next-to-leading order. Eur. Phys. J. A **51**(5), 53 (2015)
1737. M. Piarulli et al., Minimally nonlocal nucleon-nucleon potentials with chiral two-pion exchange including Δ resonances. Phys. Rev. C **91**(2), 024003 (2015)
1738. A. Dyhdalo et al., Regulator artifacts in uniform matter for chiral interactions. Phys. Rev. C **94**(3), 034001 (2016)
1739. D.R. Entem, R. Machleidt, Y. Nosyk, High-quality two-nucleon potentials up to fifth order of the chiral expansion. Phys. Rev. C **96**(2), 024004 (2017)
1740. I. Tews et al., New ideas in constraining nuclear forces. J. Phys. G **47**(10), 103001 (2020)
1741. P. Reinert, H. Krebs, E. Epelbaum, Precision determination of pionnucleon coupling constants using effective field theory. Phys. Rev. Lett. **126**(9), 092501 (2021)
1742. E. Epelbaum, H. Krebs, P. Reinert, Semi-local nuclear forces from chiral EFT: state-of-the-art and challenges (2022). arXiv:2206.07072
1743. R.J. Furnstahl et al., Quantifying truncation errors in effective field theory. Phys. Rev. C **92**(2), 024005 (2015)
1744. E. Epelbaum, High-precision nuclear forces: where do we stand? PoS CD2018, p. 006 (2019)
1745. E. Epelbaum et al., Towards high-order calculations of three-nucleon scattering in chiral effective field theory. Eur. Phys. J. A **56**(3), 92 (2020)
1746. A.A. Filin et al., Extraction of the neutron charge radius from a precision calculation of the deuteron structure radius. Phys. Rev. Lett. **124**(8), 082501 (2020)
1747. A.A. Filin et al., High-accuracy calculation of the deuteron charge and quadrupole form factors in chiral effective field theory. Phys. Rev. C **103**(2), 024313 (2021)
1748. K. Pachucki, V. Patkóš, V.A. Yerokhin, Three-photon exchange nuclear structure correction in hydrogenic systems. Phys. Rev. A **97**(6), 062511 (2018)
1749. M. Puchalski, J. Komasa, K. Pachucki, Hyperfine structure of the first rotational level in H_2, D_2 and HD molecules and the deuteron quadrupole moment. Phys. Rev. Lett. **125**(25), 253001 (2020)

1750. M.C.M. Rentmeester et al., Chiral two pion exchange and proton proton partial wave analysis. Phys. Rev. Lett. **82**, 4992–4995 (1999)
1751. M.C. Birse, J.A. McGovern, On the effectiveness of effective field theory in peripheral nucleon nucleon scattering. Phys. Rev. C **70**, 054002 (2004)
1752. E. Epelbaum, H. Krebs, U.G. Meißner, Precision nucleon-nucleon potential at fifth order in the chiral expansion. Phys. Rev. Lett. **115**(12), 122301 (2015)
1753. M. Piarulli, I. Tews, Local nucleon-nucleon and three-nucleon interactions within chiral effective field theory. Front. Phys. **7**, 245 (2020)
1754. W.G. Jiang et al., Accurate bulk properties of nuclei from $A = 2$ to ∞ from potentials with Δ isobars. Phys. Rev. C **102**(5), 054301 (2020)
1755. P. Maris et al., Light nuclei with semilocal momentum-space regularized chiral interactions up to third order. Phys. Rev. C **103**(5), 054001 (2021)
1756. E. Epelbaum et al., Few- and many-nucleon systems with semilocal coordinatespace regularized chiral two- and three-body forces. Phys. Rev. C **99**(2), 024313 (2019)
1757. P. Maris et al., Nuclear properties with semilocal momentum-space regularized chiral interactions beyond N2LO (2022)
1758. B.R. Barrett, P. Navratil, J.P. Vary, Ab initio no core shell model. Prog. Part. Nucl. Phys. **69**, 131–181 (2013)
1759. G. Hagen, G.R. Jansen, T. Papenbrock, Structure of ^{78}Ni from first principles computations. Phys. Rev. Lett. **117**(17), 172501 (2016)
1760. E. Gebrerufael et al., Ab initio description of open-shell nuclei: merging no-core shell model and in-medium similarity renormalization group. Phys. Rev. Lett. **118**(15), 152503 (2017)
1761. D. Lonardoni et al., Properties of nuclei up to $A = 16$ using local chiral interactions. Phys. Rev. Lett. **120**(12), 122502 (2018)
1762. M. Piarulli et al., Light-nuclei spectra from chiral dynamics. Phys. Rev. Lett. **120**(5), 052503 (2018)
1763. H. Hergert, A guided tour of ab initio nuclear many-body theory. Front. Phys. **8**, 379 (2020)
1764. I. Tews, Quantum Monte Carlo methods for astrophysical applications. Front. Phys. **8**, 153 (2020)
1765. N. Kalantar-Nayestanaki et al., Signatures of three-nucleon interactions in few-nucleon systems. Rep. Prog. Phys. **75**, 016301 (2012)
1766. H.-W. Hammer, A. Nogga, A. Schwenk, Three-body forces: from cold atoms to nuclei. Rev. Mod. Phys. **85**, 197 (2013)
1767. S. Pastore et al., Quantum Monte Carlo calculations of electromagnetic transitions in ^{8}Be with meson-exchange currents derived from chiral effective field theory. Phys. Rev. C **90**(2), 024321 (2014)
1768. S. Bacca, S. Pastore, Electromagnetic reactions on light nuclei. J. Phys. G **41**(12), 123002 (2014)
1769. R. Schiavilla et al., Local chiral interactions and magnetic structure of few-nucleon systems. Phys. Rev. C **99**(3), 034005 (2019)
1770. N. Nevo Dinur et al., Zemach moments and radii of ^{2,3}H and ^{3,4}He. Phys. Rev. C **99**(3), 034004 (2019)
1771. G.B. King et al., Weak transitions in light nuclei. Front. Phys. **8**, 363 (2020)
1772. S. Pastore et al., Quantum Monte Carlo calculations of weak transitions in $A = 6 - 10$ nuclei. Phys. Rev. C **97**(2), 022501 (2018)
1773. L.E. Marcucci et al., Implication of the proton-deuteron radiative capture for Big Bang Nucleosynthesis. Phys. Rev. Lett. **116**(10), 102501 (2016). [Erratum: Phys. Rev. Lett. 117, 049901 (2016)]
1774. L. Ceccarelli et al., Muon capture on deuteron using local chiral potentials. Front. Phys. **10**, 1049919 (2023)
1775. S. Pastore et al., Quantum Monte Carlo calculations of electromagnetic moments and transitions in A $\leq$ 9 nuclei with meson-exchange currents derived from chiral effective field theory. Phys. Rev. C **87**(3), 035503 (2013)
1776. Y. Utsuno, Anomalous magnetic moment of C-9 and shell quenching in exotic nuclei. Phys. Rev. C **70**, 011303 (2004)
1777. G.B. King et al., Chiral effective field theory calculations of weak transitions in light nuclei. Phys. Rev. C **102**(2), 025501 (2020)
1778. W.T. Chou, E.K. Warburton, B. Alex Brown, Gamow–Teller β-decay rates for $A \leq 18$ nuclei. Phys. Rev. C **47**, 163–177 (1993)
1779. P. Gysbers et al., Discrepancy between experimental and theoretical β-decay rates resolved from first principles. Nat. Phys. **15**(5), 428–431 (2019)
1780. Z. Davoudi et al., Nuclear matrix elements from lattice QCD for electroweak and beyond-Standard-Model processes. Phys. Rep. **900**, 1–74 (2021)
1781. E. Epelbaum, U.-G. Meißner, W. Gloeckle, Nuclear forces in the chiral limit. Nucl. Phys. A **714**, 535–574 (2003)
1782. S.R. Beane, M.J. Savage, The quark mass dependence of two nucleon systems. Nucl. Phys. A **717**, 91–103 (2003)
1783. J.-W. Chen et al., On the quark mass dependence of two nucleon observables. Phys. Rev. C **86**, 054001 (2012)
1784. J.C. Berengut et al., Varying the light quark mass: impact on the nuclear force and Big Bang nucleosynthesis. Phys. Rev. D **87**(8), 085018 (2013)
1785. X.L. Ren, E. Epelbaum, J. Gegelia, Λ-nucleon scattering in baryon chiral perturbation theory. Phys. Rev. C **101**(3), 034001 (2020)
1786. Q.-Q. Bai et al., Pion-mass dependence of the nucleon-nucleon interaction. Phys. Lett. B, 135745 (2020)
1787. V. Baru et al., Low-energy theorems for nucleon-nucleon scattering at unphysical pion masses. Phys. Rev. C **92**(1), 014001 (2015)
1788. V. Baru, E. Epelbaum, A.A. Filin, Low-energy theorems for nucleon-nucleon scattering at $M_\pi = 450$ MeV. Phys. Rev. C **94**(1), 014001 (2016)
1789. M. Eliyahu, B. Bazak, N. Barnea, Extrapolating lattice QCD results using effective field theory. Phys. Rev. C **102**(4), 044003 (2020)
1790. W. Detmold, P.E. Shanahan, Few-nucleon matrix elements in pionless effective field theory in a finite volume. Phys. Rev. D **103**(7), 074503 (2021)
1791. X. Sun et al., Finite-volume pionless effective field theory for fewnucleon systems with differentiable programming. Phys. Rev. D **105**(7), 074508 (2022)
1792. L. Meng, E. Epelbaum, Two-particle scattering from finite-volume quantization conditions using the plane wave basis. JHEP **10**, 051 (2021)
1793. N. Barnea et al., Effective field theory for lattice nuclei. Phys. Rev. Lett. **114**(5), 052501 (2015)
1794. T.A. Lähde, U.-G. Meißner, E. Epelbaum, An update on fine-tunings in the triple-alpha process. Eur. Phys. J. A **56**(3), 89 (2020)
1795. E. Epelbaum et al., Ab initio calculation of the Hoyle state. Phys. Rev. Lett. **106**, 192501 (2011)
1796. S. Elhatisari et al., Ab initio alpha-alpha scattering. Nature **528**, 111 (2015)
1797. T.A. Lähde, U.-G. Meißner, *Nuclear Lattice Effective Field Theory: An introduction*, vol. 957 (Springer, Berlin, 2019)
1798. D. Frame et al., Eigenvector continuation with subspace learning. Phys. Rev. Lett. **121**(3), 032501 (2018)
1799. S. König et al., Eigenvector continuation as an efficient and accurate emulator for uncertainty quantification. Phys. Lett. B **810**, 135814 (2020)
1800. R.J. Furnstahl et al., Efficient emulators for scattering using eigenvector continuation. Phys. Lett. B **809**, 135719 (2020)
1801. C.W. Bauer, S. Fleming, M.E. Luke, Summing Sudakov logarithms in $B \to X_s\gamma$ in effective field theory. Phys. Rev. D **63**, 014006 (2000)

1802. C.W. Bauer et al., An effective field theory for collinear and soft gluons: heavy to light decays. Phys. Rev. D **63**, 114020 (2001)
1803. C.W. Bauer, I.W. Stewart, Invariant operators in collinear effective theory. Phys. Lett. B **516**, 134–142 (2001)
1804. C.W. Bauer, D. Pirjol, I.W. Stewart, Soft collinear factorization in effective field theory. Phys. Rev. D **65**, 054022 (2002)
1805. G. Peter Lepage, S.J. Brodsky, Exclusive processes in quantum chromodynamics: evolution equations for hadronic wave functions and the form-factors of mesons. Phys. Lett. B **87**, 359–365 (1979)
1806. J.C. Collins, D.E. Soper, G. Sterman, Soft gluons and factorization. Nucl. Phys. B **308**, 833 (1988)
1807. C.W. Bauer et al., Hard scattering factorization from effective field theory. Phys. Rev. D **66**, 014017 (2002)
1808. M.A. Ebert, A. Gao, I.W. Stewart, Factorization for azimuthal asymmetries in SIDIS at next-to-leading power. JHEP **06**, 007 (2022)
1809. S. Fleming et al., Jets from massive unstable particles: top-mass determination. Phys. Rev. D **77**, 074010 (2008)
1810. M.D. Schwartz, Resummation and NLO matching of event shapes with effective field theory. Phys. Rev. D **77**, 014026 (2008)
1811. C.W. Bauer et al., Factorization of e^+e^- event shape distributions with hadronic final states in soft collinear effective theory. Phys. Rev. D **78**, 034027 (2008)
1812. T. Becher, M.D. Schwartz, A precise determination of as from LEP thrust data using effective field theory. JHEP **07**, 034 (2008)
1813. X. Liu, F. Petriello, Resummation of jet-veto logarithms in hadronic processes containing jets. Phys. Rev. D **87**, 014018 (2013)
1814. T.T. Jouttenus et al., Jet mass spectra in Higgs boson plus one jet at next-to-next-to-leading logarithmic order. Phys. Rev. D **88**(5), 054031 (2013)
1815. R. Kelley, M.D. Schwartz, 1-loop matching and NNLL resummation for all partonic 2 to 2 processes in QCD. Phys. Rev. D **83**, 045022 (2011)
1816. I.W. Stewart, F.J. Tackmann, W.J. Waalewijn, NJettiness: an inclusive event shape to veto jets. Phys. Rev. Lett. **105**, 092002 (2010)
1817. S.D. Ellis et al., Jet shapes and jet algorithms in SCET. JHEP **11**, 101 (2010)
1818. C.W. Bauer et al., Factorization and resummation for dijet invariant mass spectra. Phys. Rev. D **85**, 074006 (2012)
1819. I. Feige et al., Precision jet substructure from boosted event shapes. Phys. Rev. Lett. **109**, 092001 (2012)
1820. W.J. Waalewijn, Calculating the charge of a jet. Phys. Rev. D **86**, 094030 (2012)
1821. A.J. Larkoski, I. Moult, D. Neill, Power counting to better jet observables. JHEP **12**, 009 (2014)
1822. A.J. Larkoski, I. Moult, D. Neill, Analytic boosted boson discrimination. JHEP **05**, 117 (2016)
1823. Y.-T. Chien, A. Hornig, C. Lee, Soft-collinear mode for jet cross sections in soft collinear effective theory. Phys. Rev. D **93**(1), 014033 (2016)
1824. T. Becher et al., Effective field theory for jet processes. Phys. Rev. Lett. **116**(19), 192001 (2016)
1825. A. Hornig, Y. Makris, T. Mehen, Jet shapes in dijet events at the LHC in SCET. JHEP **04**, 097 (2016)
1826. C. Frye et al., Factorization for groomed jet substructure beyond the next-to-leading logarithm. JHEP **07**, 064 (2016)
1827. P. Pietrulewicz, F.J. Tackmann, W.J. Waalewijn, Factorization and resummation for generic hierarchies between jets. JHEP **08**, 002 (2016)
1828. A.J. Larkoski, I. Moult, D. Neill, Analytic boosted boson discrimination at the large hadron collider (2017). arXiv:1708.06760
1829. A.J. Larkoski, I. Moult, B. Nachman, Jet substructure at the large hadron collider: a review of recent advances in theory and machine learning. Phys. Rep. **841**, 1–63 (2020)
1830. A.H. Hoang et al., Nonperturbative corrections to soft drop jet mass. JHEP **12**, 002 (2019)
1831. M. Beneke et al., Soft-collinear effective theory and heavy-to-light currents beyond leading power. Nucl. Phys. B **643**, 431–476 (2002)
1832. C.W. Bauer, D. Pirjol, I.W. Stewart, Factorization and endpoint singularities in heavy to light decays. Phys. Rev. D **67**, 071502 (2003)
1833. M. Beneke, T. Feldmann, Factorization of heavy to light form-factors in soft collinear effective theory. Nucl. Phys. B **685**, 249–296 (2004)
1834. C.W. Bauer, D. Pirjol, I.W. Stewart, A proof of factorization for $B \to D_\pi$. Phys. Rev. Lett. **87**, 201806 (2001)
1835. S. Mantry, D. Pirjol, I.W. Stewart, Strong phases and factorization for color suppressed decays. Phys. Rev. D **68**, 114009 (2003)
1836. C.W. Bauer et al., $B \to M_1 M_2$: factorization, charming penguins, strong phases, and polarization. Phys. Rev. D **70**, 054015 (2004)
1837. K.S.M. Lee, I.W. Stewart, Factorization for power corrections to $B \to X_s\gamma$ and $B \to X_{u\ell\bar{\nu}}$. Nucl. Phys. B **721**, 325–406 (2005)
1838. S.W. Bosch, M. Neubert, G. Paz, Subleading shape functions in inclusive B decays. JHEP **11**, 073 (2004)
1839. M. Beneke et al., Power corrections to $\bar{B} \to X_u\ell\bar{\nu}(X_s\gamma)$ decay spectra in the shape-function region. JHEP **06**, 071 (2005)
1840. Z. Ligeti, I.W. Stewart, F.J. Tackmann, Treating the b quark distribution function with reliable uncertainties. Phys. Rev. D **78**, 114014 (2008)
1841. M. Benzke et al., Factorization at subleading power and irreducible uncertainties in $B \to X_s\gamma$ decay. JHEP **08**, 099 (2010)
1842. S. Fleming, A.K. Leibovich, T. Mehen, Resumming the color-octet contribution to $e^+e^- \to J/\psi + X$. Phys. Rev. D **68**, 094011 (2003)
1843. S. Fleming, A.K. Leibovich, T. Mehen, J/ψ photo-production at large Z in soft collinear effective theory, pp. 239–252 (2005)
1844. S. Fleming, A.K. Leibovich, T. Mehen, Resummation of large endpoint corrections to color-octet J/ψ photoproduction. Phys. Rev. D **74**, 114004 (2006)
1845. A.K. Leibovich, X. Liu, The color-singlet contribution to $e^+e^- \to J/\psi + X$ at the endpoint. Phys. Rev. D **76**, 034005 (2007)
1846. S. Fleming, C. Lee, A.K. Leibovich, Exclusive radiative decays of Upsilon in SCET. Phys. Rev. D **71**, 074002 (2005)
1847. S. Fleming, A.K. Leibovich, Flavor-singlet light-cone amplitudes and radiative Upsilon decays in SCET. Phys. Rev. D **70**, 094016 (2004)
1848. X. Garcia i Tormo, J. Soto, Soft, collinear and nonrelativistic modes in radiative decays of very heavy quarkonium. Phys. Rev. D **69**, 114006 (2004)
1849. X. Garcia i Tormo, J. Soto, Semi-inclusive radiative decays of Upsilon(1S). Phys. Rev. D **72**, 054014 (2005)
1850. I.Z. Rothstein, I.W. Stewart, An effective field theory for forward scattering and factorization violation. JHEP **08**, 025 (2016)
1851. I. Moult et al., Fermionic Glauber operators and quark reggeization. JHEP **02**, 134 (2018)
1852. A. Bhattacharya, A.V. Manohar, M.D. Schwartz, Quark-gluon backscattering in the Regge limit at one-loop. JHEP **02**, 091 (2022)
1853. I. Moult et al., Anomalous dimensions from soft Regge constants (2022)
1854. F. D'Eramo, H. Liu, K. Rajagopal, Transverse momentum broadening and the jet quenching parameter. Redux. Phys. Rev. D **84**, 065015 (2011)

1855. G. Ovanesyan, I. Vitev, An effective theory for jet propagation in dense QCD matter: jet broadening and medium-induced bremsstrahlung. JHEP **1106**, 080 (2011)
1856. G. Ovanesyan, I. Vitev, Medium-induced parton splitting kernels from soft collinear effective theory with Glauber gluons. Phys. Lett. B **706**, 371–378 (2012)
1857. M. Benzke et al., Gauge invariant definition of the jet quenching parameter. JHEP **02**, 129 (2013)
1858. V. Vaidya, X. Yao, Transverse momentum broadening of a jet in quark-gluon plasma: an open quantum system EFT. JHEP **10**, 024 (2020)
1859. V. Vaidya, Effective field theory for jet substructure in heavy ion collisions. JHEP **11**, 064 (2021)
1860. M. Beneke, G. Kirilin, Soft-collinear gravity. JHEP **09**, 066 (2012)
1861. T. Cohen, G. Elor, A.J. Larkoski, Soft-collinear supersymmetry. JHEP **03**, 017 (2017)
1862. T. Okui, A. Yunesi, Soft collinear effective theory for gravity. Phys. Rev. D **97**(6), 066011 (2018)
1863. T. Cohen et al., Navigating collinear superspace. JHEP **02**, 146 (2020)
1864. S. Chakraborty, T. Okui, A. Yunesi, Topics in soft collinear effective theory for gravity: the diffeomorphism invariant Wilson lines and reparametrization invariance. Phys. Rev. D **101**(6), 066019 (2020)
1865. M. Beneke, P. Hager, R. Szafron, Soft-collinear gravity beyond the leading power. JHEP **03**, 080 (2022)
1866. J. Chiu et al., Electroweak Sudakov corrections using effective field theory. Phys. Rev. Lett. **100**, 021802 (2008)
1867. J. Chiu et al., Electroweak corrections in high energy processes using effective field theory. Phys. Rev. D **77**, 053004 (2008)
1868. J. Chiu, R. Kelley, A.V. Manohar, Electroweak corrections using effective field theory: applications to the LHC. Phys. Rev. D **78**, 073006 (2008)
1869. A. Fuhrer et al., Radiative corrections to longitudinal and transverse gauge boson and Higgs production. Phys. Rev. D **81**, 093005 (2010)
1870. T. Becher, X. Garcia i Tormo, Electroweak Sudakov effects in W, Z and γ production at large transverse momentum. Phys. Rev. D **88**(1), 013009 (2013)
1871. A.V. Manohar, W.J. Waalewijn, Electroweak logarithms in inclusive cross sections. JHEP **08**, 137 (2018)
1872. B. Fornal, A.V. Manohar, W.J. Waalewijn, Electroweak gauge boson parton distribution functions. JHEP **05**, 106 (2018)
1873. M. Baumgart, I.Z. Rothstein, V. Vaidya, Calculating the annihilation rate of weakly interacting massive particles. Phys. Rev. Lett. **114**, 211301 (2015)
1874. M. Bauer et al., Soft collinear effective theory for heavy WIMP annihilation. JHEP **01**, 099 (2015) **(Ed. by M. Tecchio and D. Levin)**
1875. G. Ovanesyan, T.R. Slatyer, I.W. Stewart, Heavy dark matter annihilation from effective field theory. Phys. Rev. Lett. **114**(21), 211302 (2015)
1876. M. Baumgart et al., Resummed photon spectra for WIMP annihilation. JHEP **03**, 117 (2018)
1877. M. Beneke, S. Lederer, K. Urban, Sommerfeld enhancement of resonant dark matter annihilation. Phys. Lett. B **839**, 137773 (2023)
1878. O. Tomalak et al., Theory of QED radiative corrections to neutrino scattering at accelerator energies. Phys. Rev. D **106**(9), 093006 (2022)
1879. O. Tomalak et al., QED radiative corrections for accelerator neutrinos. Nat. Commun. **13**(1), 5286 (2022)
1880. A.V. Manohar et al., Reparameterization invariance for collinear operators. Phys. Lett. B **539**, 59–66 (2002)
1881. J. Chay, C. Kim, Collinear effective theory at subleading order and its application to heavy-light currents. Phys. Rev. D **65**, 114016 (2002)
1882. C.W. Bauer, D. Pirjol, I.W. Stewart, Power counting in the soft collinear effective theory. Phys. Rev. D **66**, 054005 (2002)
1883. P.P. Srivastava, S.J. Brodsky, Light front quantized QCD in covariant gauge. Phys. Rev. D **61**, 025013 (2000)
1884. C. Marcantonini, I.W. Stewart, Reparameterization invariant collinear. Operators. Phys. Rev. D **79**, 065028 (2009)
1885. I. Moult et al., Employing helicity amplitudes for resummation. Phys. Rev. D **93**(9), 094003 (2016)
1886. D.W. Kolodrubetz, I. Moult, I.W. Stewart, Building blocks for subleading helicity operators. JHEP **05**, 139 (2016)
1887. I. Moult, I.W. Stewart, G. Vita, A subleading operator basis and matching for $gg \to H$. JHEP **07**, 067 (2017)
1888. I. Feige et al., A complete basis of helicity operators for subleading factorization. JHEP **11**, 142 (2017)
1889. A. Bhattacharya et al., Helicity methods for high multiplicity subleading soft and collinear limits. JHEP **05**, 192 (2019)
1890. A.V. Manohar, I.W. Stewart, The zero-bin and mode factorization in quantum field theory. Phys. Rev. D **76**, 074002 (2007)
1891. C.W. Bauer, B.O. Lange, G. Ovanesyan, On Glauber modes in soft-collinear effective theory. JHEP **07**, 077 (2011)
1892. M.D. Schwartz, K. Yan, H. Xing Zhu, Collinear factorization violation and effective field theory. Phys. Rev. D **96**(5), 056005 (2017)
1893. J.C. Collins, D.E. Soper, G.F. Sterman, Factorization for one loop corrections in the Drell-Yan process. Nucl. Phys. B **223**, 381–421 (1983)
1894. G.T. Bodwin, Factorization of the Drell–Yan cross-section in perturbation theory. Phys. Rev. D **31**, 2616 (1985) [Erratum: Phys. Rev. D 34, 3932 (1986)]
1895. J. Collins, J.-W. Qiu, k_T factorization is violated in production of high-transverse-momentum particles in hadron-hadron collisions. Phys. Rev. D **75**, 114014 (2007)
1896. T.C. Rogers, P.J. Mulders, No generalized TMD-factorization in hadro-production of high transverse momentum hadrons. Phys. Rev. D **81**, 094006 (2010)
1897. S. Catani, D. de Florian, G. Rodrigo, Space-like (versus time-like) collinear limits in QCD: is factorization violated? JHEP **07**, 026 (2012)
1898. M.D. Schwartz, K. Yan, H. Xing Zhu, Factorization violation and scale invariance. Phys. Rev. D **97**(9), 096017 (2018)
1899. M. Baumgart et al., Breakdown of the naive parton model in superweak scale collisions. Phys. Rev. D **100**(9), 096008 (2019)
1900. T. Becher, M. Neubert, D. Yu Shao, Resummation of super-leading logarithms. Phys. Rev. Lett. **127**(21), 212002 (2021)
1901. M. Beneke, T. Feldmann, Multipole-expanded soft-collinear effective theory with non-abelian gauge symmetry. Phys. Lett. B **553**, 267–276 (2003)
1902. C.W. Bauer, D. Pirjol, I.W. Stewart, On power suppressed operators and gauge invariance in SCET. Phys. Rev. D **68**, 034021 (2003)
1903. R.J. Hill, M. Neubert, Spectator interactions in softcollinear effective theory. Nucl. Phys. B **657**, 229–256 (2003)
1904. D. Pirjol, I.W. Stewart, A complete basis for power suppressed collinear ultrasoft operators. Phys. Rev. D **67**, 094005 (2003) [Erratum: Phys. Rev. D 69, 019903 (2004)]
1905. S.W. Bosch et al., Factorization and Sudakov resummation in leptonic radiative B decay. Phys. Rev. D **67**, 094014 (2003)
1906. M. Beneke, Y. Kiyo, D. Yang, Loop corrections to subleading heavy quark currents in SCET. Nucl. Phys. B **692**, 232–248 (2004)
1907. R.J. Hill et al., Sudakov resummation for subleading SCET currents and heavy-to-light form-factors. JHEP **07**, 081 (2004)
1908. A.H. Hoang, I.W. Stewart, Designing gapped soft functions for jet production. Phys. Lett. B **660**, 483–493 (2008)

1909. R. Abbate et al., Precision thrust cumulant moments at N^3LL. Phys. Rev. D **86**, 094002 (2012)
1910. T. Becher, M. Neubert, D. Wilhelm, Electroweak gauge-boson production at small q_T?: infrared safety from the collinear anomaly. JHEP **02**, 124 (2012)
1911. M.G. Echevarria, A. Idilbi, I. Scimemi, Factorization theorem for Drell-Yan at low q_T and transverse momentum distributions on-the-light-cone. JHEP **07**, 002 (2012)
1912. J.-Y. Chiu et al., A formalism for the systematic treatment of rapidity logarithms in quantum field theory. JHEP **05**, 084 (2012)
1913. Y. Li, D. Neill, H. Xing Zhu, An exponential regulator for rapidity divergences. Nucl. Phys. B **960**, 115193 (2020)
1914. J. Chiu et al., The rapidity renormalization group. Phys. Rev. Lett. **108**, 151601 (2012)
1915. A.J. Larkoski et al., Soft drop. JHEP **05**, 146 (2014)
1916. M. Dasgupta et al., Towards an understanding of jet substructure. JHEP **09**, 029 (2013)
1917. Z.-B. Kang, F. Ringer, I. Vitev, The semi-inclusive jet function in SCET and small radius resummation for inclusive jet production. JHEP **10**, 125 (2016)
1918. Z.-B. Kang et al., The groomed and ungroomed jet mass distribution for inclusive jet production at the LHC. JHEP **10**, 137 (2018)
1919. A.H. Hoang et al., Extracting a short distance top mass with light grooming. Phys. Rev. D **100**(7), 074021 (2019)
1920. A.J. Larkoski, I. Moult, D. Neill, Factorization and resummation for groomed multi-prong jet shapes. JHEP **02**, 144 (2018)
1921. Y. Makris, D. Neill, V. Vaidya, Probing transverse-momentum dependent evolution with groomed jets. JHEP **07**, 167 (2018)
1922. J. Baron, S. Marzani, V. Theeuwes, Soft-drop thrust. JHEP **08**, 105 (2018) [Erratum: JHEP 05, 056 (2019)]
1923. Y. Makris, V. Vaidya, Transverse momentum spectra at threshold for groomed heavy quark jets. JHEP **10**, 019 (2018)
1924. Z.-B. Kang et al., Soft drop groomed jet angularities at the LHC. Phys. Lett. B **793**, 41–47 (2019)
1925. C. Lee, P. Shrivastava, V. Vaidya, Predictions for energy correlators probing substructure of groomed heavy quark jets. JHEP **09**, 045 (2019)
1926. D. Gutierrez-Reyes et al., Probing transverse-momentum distributions with groomed jets. JHEP **08**, 161 (2019)
1927. Y.-T. Chien, I.W. Stewart, Collinear drop. JHEP **06**, 064 (2020)
1928. Z.-B. Kang et al., The soft drop groomed jet radius at NLL. JHEP **02**, 054 (2020)
1929. P. Cal et al., Calculating the angle between jet axes. JHEP **04**, 211 (2020)
1930. P. Cal et al., Jet energy drop. JHEP **11**, 012 (2020)
1931. A. Pathak et al., EFT for soft drop double differential cross section. JHEP **04**, 032 (2021)
1932. Y. Makris, Revisiting the role of grooming in DIS. Phys. Rev. D **103**(5), 054005 (2021)
1933. P. Cal et al., The soft drop momentum sharing fraction zg beyond leading-logarithmic accuracy. Phys. Lett. B **833**, 137390 (2022)
1934. P. Pietrulewicz et al., Variable flavor number scheme for final state jets in thrust. Phys. Rev. D **90**(11), 114001 (2014)
1935. Y.-T. Chien, M.D. Schwartz, Resummation of heavy jet mass and comparison to LEP data. JHEP **08**, 058 (2010)
1936. A.H. Hoang et al., C-parameter distribution at N^{3}LL including power corrections. Phys. Rev. D **91**(9), 094017 (2015)
1937. M.A. Ebert, B. Mistlberger, G. Vita, The energy-energy correlation in the back-to-back limit at N^{3}LO and N^{3}LL'. JHEP **08**, 022 (2021)
1938. V. Mateu, G. Rodrigo, Oriented event shapes at N^{3}LL $+ O(\alpha_S^2)$. JHEP **11**, 030 (2013)
1939. A. Kardos, A.J. Larkoski, Z. Trócsányi, Groomed jet mass at high precision. Phys. Lett. B **809**, 135704 (2020)
1940. B. Bachu et al., Boosted top quarks in the peak region with NL3L resummation. Phys. Rev. D **104**(1), 014026 (2021)
1941. Z.-B. Kang, S. Mantry, J.-W. Qiu, N-jettiness as a probe of nuclear dynamics. Phys. Rev. D **86**, 114011 (2012)
1942. D. Kang, C. Lee, I.W. Stewart, 1-Jettiness in DIS: measuring 2 jets in 3 ways. PoS **DIS2013**, 158 (2013)
1943. Z.-B. Kang, X. Liu, S. Mantry, 1-jettiness DIS event shape: NNLL+NLO results. Phys. Rev. D **90**(1), 014041 (2014)
1944. D. Kang, C. Lee, I.W. Stewart, DIS Event Shape at N3LL. PoS **DIS2015**, 142 (2015)
1945. T. Becher, T. Neumann, Fiducial q_T resummation of colorsinglet processes at N^{3}LL+NNLO. JHEP **03**, 199 (2021)
1946. M.A. Ebert et al., Drell-Yan q_T resummation of fiducial power corrections at N3LL. JHEP **04**, 102 (2021)
1947. D. Neill, I.Z. Rothstein, V. Vaidya, The Higgs transverse momentum distribution at NNLL and its theoretical errors. JHEP **12**, 097 (2015)
1948. X. Chen et al., Precise QCD description of the Higgs boson transverse momentum spectrum. Phys. Lett. B **788**, 425–430 (2019)
1949. G. Billis et al., Higgs pT spectrum and total cross section with fiducial cuts at third resummed and fixed order in QCD. Phys. Rev. Lett. **127**(7), 072001 (2021)
1950. M.A. Ebert, J.K.L. Michel, F.J. Tackmann, Resummation improved rapidity spectrum for gluon fusion Higgs production. JHEP **05**, 088 (2017)
1951. C.F. Berger et al., Higgs production with a central jet veto at NNLL+NNLO. JHEP **1104**, 092 (2011)
1952. T. Becher, M. Neubert, Factorization and NNLL resummation for Higgs production with a jet veto. JHEP **07**, 108 (2012)
1953. F.J. Tackmann, J.R. Walsh, S. Zuberi, Resummation properties of jet vetoes at the LHC. Phys. Rev. D **86**, 053011 (2012)
1954. T. Becher, M. Neubert, L. Rothen, Factorization and N^3LL_p+NNLO predictions for the Higgs cross section with a jet veto. JHEP **10**, 125 (2013)
1955. I.W. Stewart et al., Jet p_T resummation in Higgs production at $NNLL' + NNLO$. Phys. Rev. D **89**(5), 054001 (2014)
1956. J.K.L. Michel, P. Pietrulewicz, F.J. Tackmann, Jet veto resummation with jet rapidity cuts. JHEP **04**, 142 (2019)
1957. C. Duhr, B. Mistlberger, G. Vita, Four-loop rapidity anomalous dimension and event shapes to fourth logarithmic order. Phys. Rev. Lett. **129**(16), 162001 (2022)
1958. B. Agarwal et al., Four-loop collinear anomalous dimensions in QCD and N = 4 super Yang-Mills. Phys. Lett. B **820**, 136503 (2021)
1959. R.N. Lee et al., Quark and gluon form factors in four-loop QCD. Phys. Rev. Lett. **128**(21), 212002 (2022)
1960. I. Moult, H. XingZhu, Yu. JiaoZhu, The four loop QCD rapidity anomalous dimension. JHEP **08**, 280 (2022)
1961. J.M. Henn, G.P. Korchemsky, B. Mistlberger, The full four-loop cusp anomalous dimension in $\mathcal{N} = 4$ super Yang-Mills and QCD. JHEP **04**, 018 (2020)
1962. F. Herzog et al., Five-loop contributions to low-N non-singlet anomalous dimensions in QCD. Phys. Lett. B **790**, 436–443 (2019)
1963. M. Luo et al., Quark transverse parton distribution at the next-to-next-to-next-to-leading order. Phys. Rev. Lett. **124**(9), 092001 (2020)
1964. M.A. Ebert, B. Mistlberger, G. Vita, Transverse momentum dependent PDFs at N^{3}LO. JHEP **09**, 146 (2020)
1965. M. Luo et al., Unpolarized quark and gluon TMD PDFs and FFs at N^{3}LO. JHEP **06**, 115 (2021)
1966. M.A. Ebert, B. Mistlberger, G. Vita, TMD fragmentation functions at N^{3}LL. JHEP **07**, 121 (2021)
1967. A.V. Manohar, Deep inelastic scattering as $x \to 1$ using soft collinear effective theory. Phys. Rev. D **68**, 114019 (2003)

1968. A. Idilbi et al., Threshold resummation for Higgs production in effective field theory. Phys. Rev. D **73**, 077501 (2006)
1969. A. Idilbi, X. Ji, F. Yuan, Resummation of threshold logarithms in effective field theory for DIS, Drell-Yan and Higgs production. Nucl. Phys. B **753**, 42–68 (2006)
1970. T. Becher, M. Neubert, B.D. Pecjak, Factorization and momentum-space resummation in deep-inelastic scattering. JHEP **01**, 076 (2007)
1971. T. Becher, C. Lorentzen, M.D. Schwartz, Resummation for W and Z production at large pT. Phys. Rev. Lett. **108**, 012001 (2012)
1972. T. Becher, G. Bell, M. Neubert, Factorization and resummation for jet broadening. Phys. Lett. B **704**, 276–283 (2011)
1973. T. Becher, C. Lorentzen, M.D. Schwartz, Precision direct photon and W-boson spectra at high p_T and comparison to LHC data. Phys. Rev. D **86**, 054026 (2012)
1974. S. Dawson, I.M. Lewis, M. Zeng, Threshold resummed and approximate next-to-next-to-leading order results for W^+W^- pair production at the LHC. Phys. Rev. D **88**(5), 054028 (2013)
1975. V. Ahrens et al., Renormalization-group improved predictions for top-quark pair production at hadron colliders. JHEP **09**, 097 (2010)
1976. H. Xing Zhu et al., Transverse-momentum resummation for top-quark pairs at hadron colliders. Phys. Rev. Lett. **110**(8), 082001 (2013)
1977. Y.-T. Chien et al., Resummation of jet mass at hadron colliders. Phys. Rev. D **87**(1), 014010 (2013)
1978. S. Dawson et al., Resummation effects in vector-boson and Higgs associated production. Phys. Rev. D **86**, 074007 (2012)
1979. S. Fleming, O.Z. Labun, Rapidity divergences and deep inelastic scattering in the endpoint region. Phys. Rev. D **91**(9), 094011 (2015)
1980. T. Becher, G. Bell, NNLL resummation for jet broadening. JHEP **11**, 126 (2012)
1981. Y.-T. Chien, I. Vitev, Jet shape resummation using soft-collinear effective theory. JHEP **12**, 061 (2014)
1982. S. Alioli et al., Drell-Yan production at NNLL+NNLO matched to parton showers. Phys. Rev. D **92**(9), 094020 (2015)
1983. S. Fleming, O.Z. Labun, Rapidity regulators in the semi-inclusive deep inelastic scattering and Drell-Yan processes. Phys. Rev. D **95**(11), 114020 (2017)
1984. Z.-B. Kang, F. Ringer, W.J. Waalewijn, The energy distribution of subjets and the jet shape. JHEP **07**, 064 (2017)
1985. D. Gutierrez-Reyes et al., Transverse momentum dependent distributions with jets. Phys. Rev. Lett. **121**(16), 162001 (2018)
1986. A. Hornig et al., Transverse vetoes with rapidity cutoff in SCET. JHEP **12**, 043 (2017)
1987. E.L. Berger, J. Gao, H. Xing Zhu, Differential distributions for t-channel single top-quark production and decay at next-to- next-to-leading order in QCD. JHEP **11**, 158 (2017)
1988. G. Bell et al., e^+e^- angularity distributions at NNLL' accuracy. JHEP **01**, 147 (2019)
1989. C.W. Bauer, P. Francesco Monni, A numerical formulation of resummation in effective field theory. JHEP **02**, 185 (2019)
1990. G. Lustermans et al., Joint two-dimensional resummation in q_T and 0-jettiness at NNLL. JHEP **03**, 124 (2019)
1991. D. Gutierrez-Reyes et al., Transverse momentum dependent distributions in e^+e^- and semi-inclusive deep-inelastic scattering using jets. JHEP **10**, 031 (2019)
1992. C.W. Bauer, P. Francesco Monni, A formalism for the resummation of non-factorizable observables in SCET. JHEP **05**, 005 (2020)
1993. A. Broggio et al., Top-quark pair hadroproduction in association with a heavy boson at NLO+NNLL including EW corrections. JHEP **08**, 039 (2019)
1994. A. Bris, V. Mateu, M. Preisser, Massive event-shape distributions at N^2LL. JHEP **09**, 132 (2020)
1995. S. Gangal et al., Higgs production at NNLL$'$ + NNLO using rapidity dependent jet vetoes. JHEP **05**, 054 (2020)
1996. Y. Makris, F. Ringer, W.J. Waalewijn, Joint thrust and TMD resummation in electron-positron and electron-proton collisions. JHEP **02**, 070 (2021)
1997. L. Dai, C. Kim, A.K. Leibovich, Heavy quark jet production near threshold. JHEP **09**, 148 (2021)
1998. K. Benkendorfer, A.J. Larkoski, Grooming at the cusp: allorders predictions for the transition region of jet groomers. JHEP **11**, 188 (2021)
1999. Y.-T. Chien et al., Precision boson-jet azimuthal decorrelation at hadron colliders (2022)
2000. M. Beneke et al., Anomalous dimension of subleading-power N-jet operators. JHEP **03**, 001 (2018)
2001. C.-H. Chang, I.W. Stewart, G. Vita, A subleading power operator basis for the scalar quark current. JHEP **04**, 041 (2018)
2002. S.M. Freedman, R. Goerke, Renormalization of subleading dijet operators in soft-collinear effective theory. Phys. Rev. D **90**(11), 114010 (2014)
2003. R. Goerke, M. Inglis-Whalen, Renormalization of dijet operators at order $1/Q^2$ in soft-collinear effective theory. JHEP **05**, 023 (2018)
2004. M. Beneke et al., Anomalous dimension of subleading-power N-jet operators. Part II. JHEP **11**, 112 (2018)
2005. I. Moult et al., First subleading power resummation for event shapes. JHEP **08**, 013 (2018)
2006. M.A. Ebert et al., Subleading power rapidity divergences and power corrections for q_T. JHEP **04**, 123 (2019)
2007. I. Moult, I.W. Stewart, G. Vita, Subleading power factorization with radiative functions. JHEP **11**, 153 (2019)
2008. Z. Long Liu et al., Renormalization and scale evolution of the soft-quark soft function. JHEP **07**, 104 (2020)
2009. A.J. Larkoski, D. Neill, I.W. Stewart, Soft theorems from effective field theory. JHEP **06**, 077 (2015)
2010. Z. Long Liu, M. Neubert, Factorization at subleading power and endpoint-divergent convolutions in $h \to \gamma\gamma$ decay. JHEP **04**, 033 (2020)
2011. Z. Long Liu et al., Factorization at subleading power, Sudakov resummation, and endpoint divergences in soft-collinear effective theory. Phys. Rev. D **104**(1), 014004 (2021)
2012. M. Inglis-Whalen et al., Factorization of power corrections in the Drell-Yan process in EFT. Phys. Rev. D **104**(7), 076018 (2021)
2013. M. Luke, J. Roy, A. Spourdalakis, Factorization at subleading power in deep inelastic scattering in the $x \to 1$ limit (2022)
2014. I. Moult et al., The soft quark Sudakov. JHEP **05**, 089 (2020)
2015. M. Beneke et al., Next-to-leading power endpoint factorization and resummation for off-diagonal gluon thrust. JHEP **07**, 144 (2022)
2016. M. Beneke et al., Leading-logarithmic threshold resummation of the Drell-Yan process at next-to-leading power. JHEP **03**, 043 (2019)
2017. M. Beneke et al., Threshold factorization of the Drell-Yan process at next-to-leading power. JHEP **07**, 078 (2020)
2018. M. Beneke et al., Leading-logarithmic threshold resummation of Higgs production in gluon fusion at next-to-leading power. JHEP **01**, 094 (2020)
2019. I. Moult, G. Vita, K. Yan, Subleading power resummation of rapidity logarithms: the energy-energy correlator in $\mathcal{N} = 4$ SYM. JHEP **07**, 005 (2020)
2020. R. Boughezal et al., W-boson production in association with a jet at next-to-next-to-leading order in perturbative QCD. Phys. Rev. Lett. **115**(6), 062002 (2015)
2021. J. Gaunt et al., N-jettiness subtractions for NNLO QCD calculations. JHEP **09**, 058 (2015)
2022. I. Moult et al., Subleading power corrections for N-jettiness subtractions (2016)

2023. R. Boughezal, X. Liu, F. Petriello, Power corrections in the N-jettiness subtraction scheme. JHEP **03**, 160 (2017)
2024. I. Moult et al., N-jettiness subtractions for $gg \to H$ at subleading power. Phys. Rev. D **97**(1), 014013 (2018)
2025. R. Boughezal, A. Isgrò, F. Petriello, Next-to-leading logarithmic power corrections for N-jettiness subtraction in color-singlet production. Phys. Rev. D **97**(7), 076006 (2018)
2026. M.A. Ebert et al., Power corrections for N-jettiness subtractions at $\mathcal{O}(\alpha_s)$. JHEP **12**, 084 (2018)
2027. G. Billis et al., A toolbox for q_T and 0-jettiness subtractions at N^{3}LO. Eur. Phys. J. Plus **136**(2), 214 (2021)
2028. M.A. Ebert, F.J. Tackmann, Impact of isolation and fiducial cuts on q$_T$ and N-jettiness subtractions. JHEP **03**, 158 (2020)
2029. R. Boughezal, A. Isgrò, F. Petriello, Next-to-leading power corrections to $V + 1$ jet production in N-jettiness subtraction. Phys. Rev. D **101**(1), 016005 (2020)
2030. G. Lustermans, J.K.L. Michel, F.J. Tackmann, Generalized threshold factorization with full collinear dynamics (2019)
2031. M.A. Ebert, B. Mistlberger, G. Vita, Collinear expansion for color singlet cross sections. JHEP **09**, 181 (2020)
2032. R. Kelley et al., The two-loop hemisphere soft function. Phys. Rev. D **84**, 045022 (2011)
2033. A. Hornig et al., Non-global structure of the $\mathcal{O}(\alpha_s^2)$ dijet soft function. JHEP **08**, 054 (2011) [Erratum: JHEP 10, 101 (2017)]
2034. A. Hornig et al., Double non-global logarithms in-n-out of jets. JHEP **01**, 149 (2012)
2035. R. Kelley et al., Jet mass with a jet veto at two loops and the universality of non-global structure. Phys. Rev. D **86**, 054017 (2012)
2036. M.D. Schwartz, H. Xing Zhu, Nonglobal logarithms at three loops, four loops, five loops, and beyond. Phys. Rev. D **90**(6), 065004 (2014)
2037. A.J. Larkoski, I. Moult, D. Neill, Non-global logarithms, factorization, and the soft substructure of jets. JHEP **09**, 143 (2015)
2038. D. Neill, The edge of jets and subleading non-global logs (2015). arXiv:1508.07568
2039. A.J. Larkoski, I. Moult, Nonglobal correlations in collider physics. Phys. Rev. D **93**(1), 014012 (2016)
2040. T. Becher et al., Factorization and resummation for jet processes. JHEP **11**, 019 (2016) [Erratum: JHEP 05, 154 (2017)]
2041. A.J. Larkoski, I. Moult, D. Neill, The analytic structure of non-global logarithms: convergence of the dressed gluon expansion. JHEP **11**, 089 (2016)
2042. D. Neill, The asymptotic form of non-global logarithms, black disc saturation, and gluonic deserts. JHEP **01**, 109 (2017)
2043. D. Neill, Non-global and clustering effects for groomed multi-prong jet shapes. JHEP **02**, 114 (2019)
2044. D. Neill, F. Ringer, Soft fragmentation on the celestial sphere. JHEP **06**, 086 (2020)
2045. D. Neill, F. Ringer, N. Sato, Leading jets and energy loss. JHEP **07**, 041 (2021)
2046. C. Lee, G.F. Sterman, Momentum flow correlations from event shapes: factorized soft gluons and soft-collinear effective theory. Phys. Rev. D **75**, 014022 (2007)
2047. V. Mateu, I.W. Stewart, J. Thaler, Power corrections to event shapes with mass-dependent operators. Phys. Rev. D **87**(1), 014025 (2013)
2048. I.W. Stewart, F.J. Tackmann, W.J. Waalewijn, Dissecting soft radiation with factorization. Phys. Rev. Lett. **114**(9), 092001 (2015)
2049. M. Procura, I.W. Stewart, Quark fragmentation within an identified jet. Phys. Rev. D **81**, 074009 (2010) [Erratum: Phys. Rev. D 83, 039902 (2011)]
2050. A. Jain, M. Procura, W.J. Waalewijn, Parton fragmentation within an identified jet at NNLL. JHEP **05**, 035 (2011)
2051. M. Procura, W.J. Waalewijn, Fragmentation in jets: cone and threshold effects. Phys. Rev. D **85**, 114041 (2012)
2052. A. Jain et al., Fragmentation with a cut on thrust: predictions for B-factories. Phys. Rev. D **87**(7), 074013 (2013)
2053. C.W. Bauer, E. Mereghetti, Heavy quark fragmenting jet functions. JHEP **04**, 051 (2014)
2054. M. Baumgart et al., Probing quarkonium production mechanisms with jet substructure. JHEP **11**, 003 (2014)
2055. M. Ritzmann, W.J. Waalewijn, Fragmentation in jets at NNLO. Phys. Rev. D **90**(5), 054029 (2014)
2056. R. Bain et al., Analytic and Monte Carlo studies of jets with heavy mesons and quarkonia. JHEP **06**, 121 (2016)
2057. R. Bain, Y. Makris, T. Mehen, Transverse momentum dependent fragmenting jet functions with applications to quarkonium production. JHEP **11**, 144 (2016)
2058. L. Dai, C. Kim, A.K. Leibovich, Fragmentation of a jet with small radius. Phys. Rev. D **94**(11), 114023 (2016)
2059. L. Dai, C. Kim, A.K. Leibovich, Fragmentation to a jet in the large z limit. Phys. Rev. D **95**(7), 074003 (2017)
2060. L. Dai, C. Kim, A.K. Leibovich, Heavy quark jet fragmentation. JHEP **09**, 109 (2018)
2061. S. Fleming, Y. Makris, T. Mehen, An effective field theory approach to quarkonium at small transverse momentum. JHEP **04**, 122 (2020)
2062. A.V. Manohar, W.J. Waalewijn, A QCD analysis of double parton scattering: color correlations, interference effects and evolution. Phys. Rev. D **85**, 114009 (2012)
2063. S. Fleming et al., The systematics of quarkonium production at the LHC and double parton fragmentation. Phys. Rev. D **86**, 094012 (2012)
2064. S. Fleming et al., Anomalous dimensions of the double parton fragmentation functions. Phys. Rev. D **87**, 074022 (2013)
2065. M. Procura, W.J. Waalewijn, L. Zeune, Resummation of double-differential cross sections and fully-unintegrated parton distribution functions. JHEP **02**, 117 (2015)
2066. I. Moult, H. Xing Zhu, Simplicity from recoil: the three-loop soft function and factorization for the energy-energy correlation. JHEP **08**, 160 (2018)
2067. L.J. Dixon, I. Moult, H. Xing Zhu, Collinear limit of the energy-energy correlator. Phys. Rev. D **100**(1), 014009 (2019)
2068. H. Chen et al., Three point energy correlators in the collinear limit: symmetries, dualities and analytic results. JHEP **08**(08), 028 (2020)
2069. H. Chen et al., Rethinking jets with energy correlators: tracks, resummation, and analytic continuation. Phys. Rev. D **102**(5), 054012 (2020)
2070. A.J. Gao et al., Precision QCD event shapes at hadron colliders: the transverse energy-energy correlator in the back-to-back limit. Phys. Rev. Lett. **123**(6), 062001 (2019)
2071. K. Lee, B. Meçaj, I. Moult, Conformal colliders meet the LHC (2022). arXiv:2205.03414
2072. I.W. Stewart, F.J. Tackmann, W.J. Waalewijn, Factorization at the LHC: from PDFs to initial state jets. Phys. Rev. D **81**, 094035 (2010)
2073. I.W. Stewart, F.J. Tackmann, W.J. Waalewijn, The beam thrust cross section for Drell-Yan at NNLL order. Phys. Rev. Lett. **106**, 032001 (2011)
2074. J. Thaler, K. Van Tilburg, Identifying boosted objects with N-subjettiness. JHEP **03**, 015 (2011)
2075. R. Bain et al., NRQCD confronts LHCb data on quarkonium production within jets. Phys. Rev. Lett. **119**(3), 032002 (2017)
2076. A.J. Larkoski, I. Moult, D. Neill, Building a better boosted top tagger. Phys. Rev. D **91**(3), 034035 (2015)
2077. I. Moult, L. Necib, J. Thaler, New angles on energy correlation functions. JHEP **12**, 153 (2016)
2078. P. Cal, J. Thaler, W.J. Waalewijn, Power counting energy flow polynomials. JHEP **09**, 021 (2022)

2079. A.J. Larkoski, D. Neill, J. Thaler, Jet shapes with the broadening axis. JHEP **04**, 017 (2014)
2080. D. Neill, I. Scimemi, W.J. Waalewijn, Jet axes and universal transverse-momentum-dependent fragmentation. JHEP **04**, 020 (2017)
2081. D. Neill et al., Phenomenology with a recoil-free jet axis: TMD fragmentation and the jet shape. JHEP **01**, 067 (2019)
2082. H.-M. Chang et al., Calculating track-based observables for the LHC. Phys. Rev. Lett. **111**, 102002 (2013)
2083. H.-M. Chang et al., Calculating track thrust with track functions. Phys. Rev. D **88**, 034030 (2013)
2084. Y. Li et al., Extending precision perturbative QCD with track functions. Phys. Rev. Lett. **128**(18), 182001 (2022)
2085. M. Jaarsma et al., Renormalization group flows for track function moments. JHEP **06**, 139 (2022)
2086. I.W. Stewart et al., XCone: N-jettiness as an exclusive cone jet algorithm. JHEP **11**, 072 (2015)
2087. I.W. Stewart, X. Yao, Pure quark and gluon observables in collinear drop. JHEP **09**, 120 (2022)
2088. J. Holguin et al., New paradigm for precision top physics: weighing the top with energy correlators. Phys. Rev. D **107**(11), 114002 (2023)
2089. X. Liu, H. Xing Zhu, Nucleon energy correlators. Phys. Rev. Lett. **130**(9), 091901 (2023)
2090. J.I. Kapusta, C. Gale, Finite-temperature field theory: principles and applications. Cambridge Monographs on Mathematical Physics. 2nd edn. Cambridge monographs on mathematical physics. Previous edition: 1989 (Cambridge University Press, Cambridge, 2006)
2091. J. Ghiglieri et al., Perturbative thermal QCD: formalism and applications. Phys. Rep. **880**, 1–73 (2020)
2092. M. Strickland, *Relativistic Quantum Field Theory*, vol. 3 (Institute of Physics, Morgan & Claypool, 2019), pp. 2053–2571
2093. A.D. Linde, Infrared problem in thermodynamics of the Yang-Mills gas. Phys. Lett. B **96**, 289–292 (1980)
2094. D.J. Gross, R.D. Pisarski, L.G. Yaffe, QCD and instantons at finite temperature. Rev. Mod. Phys. **53**, 43 (1981)
2095. M. Abraao York, G.D. Moore, Second order hydrodynamic coefficients from kinetic theory. Phys. Rev. D **79**, 054011 (2009)
2096. K. Farakos et al., 3-D physics and the electroweak phase transition: a framework for lattice Monte Carlo analysis. Nucl. Phys. B **442**, 317–363 (1995)
2097. P. Navarrete, Y. Schröder, Tackling the infamous g^6 term of the QCD pressure. In: *16th DESY Workshop on Elementary Particle Physics: Loops and Legs in Quantum Field Theory 2022* (2022)
2098. E. Braaten, R.D. Pisarski, Soft amplitudes in hot gauge theories: a general analysis. Nucl. Phys. B **337**, 569–634 (1990)
2099. E. Braaten, R.D. Pisarski, Resummation and gauge invariance of the gluon damping rate in hot QCD. Phys. Rev. Lett. **64**, 1338 (1990)
2100. E. Braaten, R.D. Pisarski, Calculation of the gluon damping rate in hot QCD. Phys. Rev. D **42**, 2156–2160 (1990)
2101. P. Brockway Arnold, C.-X. Zhai, The three loop free energy for pure gauge QCD. Phys. Rev. D **50**, 7603–7623 (1994)
2102. P. Brockway Arnold, C. Zhai, The three loop free energy for high temperature QED and QCD with fermions. Phys. Rev. D **51**, 1906–1918 (1995)
2103. C. Zhai, B.M. Kastening, The free energy of hot gauge theories with fermions through g^5. Phys. Rev. D **52**, 7232–7246 (1995)
2104. E. Braaten, A. Nieto, Effective field theory approach to high temperature thermodynamics. Phys. Rev. D **51**, 6990–7006 (1995)
2105. E. Braaten, A. Nieto, Free energy of QCD at high temperature. Phys. Rev. D **53**, 3421–3437 (1996)
2106. K. Kajantie et al., 3-D SU(N) + adjoint Higgs theory and finite temperature QCD. Nucl. Phys. B **503**, 357–384 (1997)
2107. J.O. Andersen, E. Braaten, M. Strickland, Hard thermal loop resummation of the free energy of a hot gluon plasma. Phys. Rev. Lett. **83**, 2139–2142 (1999)
2108. J.O. Andersen, E. Braaten, M. Strickland, Hard thermal loop resummation of the thermodynamics of a hot gluon plasma. Phys. Rev. D **61**, 014017 (2000)
2109. J.O. Andersen, E. Braaten, M. Strickland, Hard thermal loop resummation of the free energy of a hot quark-gluon plasma. Phys. Rev. D **61**, 074016 (2000)
2110. J.P. Blaizot, E. Iancu, A. Rebhan, The entropy of the QCD plasma. Phys. Rev. Lett. **83**, 2906–2909 (1999)
2111. J.P. Blaizot, E. Iancu, A. Rebhan, Selfconsistent hard thermal loop thermodynamics for the quark gluon plasma. Phys. Lett. B **470**, 181–188 (1999)
2112. J.P. Blaizot, E. Iancu, A. Rebhan, Approximately selfconsistent resummations for the thermodynamics of the quark gluon plasma. 1. Entropy and density. Phys. Rev. D **63**, 065003 (2001)
2113. J.P. Blaizot, E. Iancu, A. Rebhan, Quark number susceptibilities from HTL resummed thermodynamics. Phys. Lett. B **523**, 143–150 (2001)
2114. J.O. Andersen et al., HTL perturbation theory to two loops. Phys. Rev. D **66**, 085016 (2002)
2115. J.O. Andersen, E. Petitgirard, M. Strickland, Two loop HTL thermodynamics with quarks. Phys. Rev. D **70**, 045001 (2004)
2116. J.O. Andersen, M. Strickland, S. Nan, Three-loop HTL gluon thermodynamics at intermediate coupling. JHEP **08**, 113 (2010)
2117. J.O. Andersen et al., Three-loop HTL QCD thermodynamics. JHEP **08**, 053 (2011)
2118. N. Haque et al., Three-loop pressure and susceptibility at finite temperature and density from hard-thermal-loop perturbation theory. Phys. Rev. D **89**(6), 061701 (2014)
2119. N. Haque et al., Three-loop HTLpt thermodynamics at finite temperature and chemical potential. JHEP **05**, 027 (2014)
2120. E. Braaten, R.D. Pisarski, Simple effective Lagrangian for hard thermal loops. Phys. Rev. D **45**(6), R1827 (1992)
2121. P.H. Ginsparg, First order and second order phase transitions in gauge theories at finite temperature. Nucl. Phys. B **170**, 388–408 (1980)
2122. T. Appelquist, R.D. Pisarski, High-temperature Yang-Mills theories and three-dimensional quantum chromodynamics. Phys. Rev. D **23**, 2305 (1981)
2123. K. Kajantie et al., Generic rules for high temperature dimensional reduction and their application to the standard model. Nucl. Phys. B **458**, 90–136 (1996)
2124. J.O. Andersen et al., N = 4 supersymmetric Yang-Mills thermodynamics from effective field theory. Phys. Rev. D **105**(1), 015006 (2022)
2125. S. Borsanyi et al., The QCD equation of state with dynamical quarks. JHEP **11**, 077 (2010)
2126. S. Borsanyi, Thermodynamics of the QCD transition from lattice. Nucl. Phys. A **904–905**, 270c–277c (2013) **(Ed. by Thomas Ullrich, Bolek Wyslouch, and John W. Harris)**
2127. S. Borsanyi et al., Freeze-out parameters: lattice meets experiment. Phys. Rev. Lett. **111**, 062005 (2013)
2128. A. Bazavov et al., Quark number susceptibilities at high temperatures. Phys. Rev. D **88**(9), 094021 (2013)
2129. P. Cea, L. Cosmai, A. Papa, Critical line of 2+1 flavor QCD: toward the continuum limit. Phys. Rev. D **93**(1), 014507 (2016)
2130. A. Bazavov et al., Chiral crossover in QCD at zero and non-zero chemical potentials. Phys. Lett. B **795**, 15–21 (2019)
2131. N. Haque, M. Strickland, Next-to-next-to leading-order hard-thermal-loop perturbation-theory predictions for the curvature of the QCD phase transition line. Phys. Rev. C **103**(3), 031901 (2021)
2132. J. Berges et al., QCD thermalization: ab initio approaches and interdisciplinary connections. Rev. Mod. Phys. **93**(3), 035003 (2021)

2133. M. Strickland, Pseudothermalization of the quark-gluon plasma. J. Phys. Conf. Ser. **1602**(1), 012018 (2020) **(Ed. by Rene Bellwied et al.)**
2134. J.-Y. Ollitrault, F.G. Gardim, Hydro overview. Nucl. Phys. A **904–905**, 75c–82c (2013) **(Ed. by Thomas Ullrich, Bolek Wyslouch, and John W. Harris)**
2135. P. Romatschke, U. Romatschke, *Relativistic Fluid Dynamics In and Out of Equilibrium* (Cambridge Monographs on Mathematical Physics (Cambridge University Press, Cambridge, 2019)
2136. M. Alqahtani, M. Nopoush, M. Strickland, Relativistic anisotropic hydrodynamics. Prog. Part. Nucl. Phys. **101**, 204–248 (2018)
2137. J. Casalderrey-Solana, C.A. Salgado, Introductory lectures on jet quenching in heavy ion collisions. Acta Phys. Polon. B **38**, 3731–3794 (2007) **(Ed. by Michal Praszalowicz, Marek Kutschera, and Edward Malec)**
2138. J. Casalderrey-Solana, D. Teaney, Heavy quark diffusion in strongly coupled N = 4 Yang-Mills. Phys. Rev. D **74**, 085012 (2006)
2139. M. Le Bellac, *Thermal Field Theory* (Cambridge Monographs on Mathematical Physics (Cambridge University Press, Cambridge, 2011)
2140. M.E. Peskin, D.V. Schroeder, *An Introduction to Quantum Field Theory* (Addison-Wesley, Reading, 1995)
2141. A. Baidya et al., Renormalization in open quantum field theory. Part I. Scalar field theory. JHEP **11**, 204 (2017)
2142. F.M. Haehl, R. Loganayagam, M. Rangamani, Schwinger–Keldysh formalism. Part I: BRST symmetries and superspace. JHEP **06**, 069 (2017)
2143. M. Crossley, P. Glorioso, H. Liu, Effective field theory of dissipative fluids. JHEP **09**, 095 (2017)
2144. K. Jensen, N. Pinzani-Fokeeva, A. Yarom, Dissipative hydrodynamics in superspace. JHEP **09**, 127 (2018)
2145. H.P. Breuer, F. Petruccione, The theory of open quantum systems (2002)
2146. V. Gorini, A. Kossakowski, E.C.G. Sudarshan, Completely positive dynamical semigroups of N level systems. J. Math. Phys. **17**, 821 (1976)
2147. G. Lindblad, On the generators of quantum dynamical semigroups. Commun. Math. Phys. **48**, 119 (1976)
2148. T. Miura et al., Simulation of Lindblad equations for quarkonium in the quark-gluon plasma. Phys. Rev. D **106**(7), 074001 (2022)
2149. N. Brambilla et al., Bottomonium suppression in an open quantum system using the quantum trajectories method. JHEP **05**, 136 (2021)
2150. N. Brambilla et al., Bottomonium production in heavy-ion collisions using quantum trajectories: differential observables and momentum anisotropy. Phys. Rev. D **104**(9), 094049 (2021)
2151. H. Ba Omar et al., QTRAJ 1.0: a Lindblad equation solver for heavy-quarkonium dynamics. Comput. Phys. Commun. **273**, 108266 (2022)
2152. T. Matsui, H. Satz, J/ψ suppression by quark-gluon plasma formation. Phys. Lett. B **178**, 416–422 (1986)
2153. M. Laine et al., Real-time static potential in hot QCD. JHEP **03**, 054 (2007)
2154. M. Angel Escobedo, J. Soto, M. Mannarelli, Non-relativistic bound states in a moving thermal bath. Phys. Rev. D **84**, 016008 (2011)
2155. M. Angel Escobedo et al., Heavy quarkonium moving in a quark-gluon plasma. Phys. Rev. D **87**(11), 114005 (2013)
2156. N. Brambilla et al., The spin-orbit potential and Poincaré invariance in finite temperature pNRQCD. JHEP **07**, 096 (2011)
2157. X. Yao, B. Müller, Approach to equilibrium of quarkonium in quark-gluon plasma. Phys. Rev. C **97**(1), 014908 (2018) [Erratum: Phys. Rev. C 97, 049903 (2018)]
2158. X. Yao, T. Mehen, Quarkonium in-medium transport equation derived from first principles. Phys. Rev. D **99**(9), 096028 (2019)
2159. N. Brambilla et al., Heavy quarkonium in a weakly-coupled quarkgluon plasma below the melting temperature. JHEP **09**, 038 (2010)
2160. G. Bhanot, M.E. Peskin, Short distance analysis for heavy quark systems. 2. Applications. Nucl. Phys. B **156**, 391–416 (1979)
2161. A. Idilbi, A. Majumder, Extending soft-collinear-effective-theory to describe hard jets in dense QCD media. Phys. Rev. D **80**, 054022 (2009)
2162. I. Vitev, Hard probes in heavy ion collisions: current status and prospects for application of QCD evolution techniques. Int. J. Mod. Phys. Conf. Ser. **37**, 1560059 (2015) **(Ed. by Alexei Prokudin, Anatoly Radyushkin, and Leonard Gamberg)**
2163. V. Vaidya, Radiative corrections for factorized jet observables in heavy ion collisions (2021)
2164. G. 't Hooft, M.J.G. Veltman, DIAGRAMMAR. NATO Sci. Ser. B **4**, 177–322 (1974)
2165. C. Gattringer, K. Langfeld, Approaches to the sign problem in lattice field theory. Int. J. Mod. Phys. A **31**(22), 1643007 (2016)
2166. B.V. Jacak, B. Müller, The exploration of hot nuclear matter. Science **337**, 310–314 (2012)
2167. B. Müller, J. Schukraft, B. Wyslouch, First Results from Pb+Pb collisions at the LHC. Annu. Rev. Nucl. Part. Sci. **62**, 361–386 (2012)
2168. P. Braun-Munzinger et al., Properties of hot and dense matter from relativistic heavy ion collisions. Phys. Rep. **621**, 76–126 (2016)
2169. W. Busza, K. Rajagopal, W. van der Schee, Heavy ion collisions: the big picture, and the big questions. Annu. Rev. Nucl. Part. Sci. **68**, 339–376 (2018)
2170. P. Braun-Munzinger et al., Relativistic nuclear collisions: establishing a non-critical baseline for fluctuation measurements. Nucl. Phys. A **1008**, 122141 (2021)
2171. K. Abe et al., Leading particle distributions in 200-GeV/c P + A interactions. Phys. Lett. B **200**, 266–271 (1988)
2172. J. Benecke et al., Hypothesis of limiting fragmentation in high-energy collisions. Phys. Rev. **188**, 2159–2169 (1969)
2173. H. Appelshauser et al., Baryon stopping and charged particle distributions in central Pb + Pb collisions at 158-GeV per nucleon. Phys. Rev. Lett. **82**, 2471–2475 (1999)
2174. I.C. Arsene et al., Nuclear stopping and rapidity loss in Au+Au collisions at $\sqrt{s_N N} = 62.4$GeV. Phys. Lett. B **677**, 267–271 (2009)
2175. J.D. Bjorken, Highly relativistic nucleus-nucleus collisions: the central rapidity region. Phys. Rev. D **27**, 140–151 (1983)
2176. S. Chatrchyan et al., Measurement of the pseudorapidity and centrality dependence of the transverse energy density in PbPb collisions at $\sqrt{s_{NN}} = 2.76$TeV. Phys. Rev. Lett. **109**, 152303 (2012)
2177. J. Barrette et al., Measurement of transverse energy production with Si and Au beams at relativistic energy: towards hot and dense hadronic matter. Phys. Rev. Lett. **70**, 2996–2999 (1993)
2178. M.M. Aggarwal et al., Scaling of particle and transverse energy production in Pb-208 + Pb-208 collisions at 158-A-GeV. Eur. Phys. J. C **18**, 651–663 (2001)
2179. A. Adare et al., Transverse energy production and charged-particle multiplicity at midrapidity in various systems from $\sqrt{s_{NN}} = 7.7$to 200 GeV. Phys. Rev. C **93**(2), 024901 (2016)
2180. A. Bauswein et al., Identifying a first-order phase transition in neutron star mergers through gravitational waves. Phys. Rev. Lett. **122**(6), 061102 (2019)
2181. G. Baym et al., New neutron star equation of state with quark-hadron crossover. Astrophys. J. **885**, 42 (2019)
2182. C. Shen et al., Radial and elliptic flow in Pb+Pb collisions at the large hadron collider from viscous hydrodynamic. Phys. Rev. C **84**, 044903 (2011)

2183. J.E. Parkkila et al., New constraints for QCD matter from improved Bayesian parameter estimation in heavy-ion collisions at LHC. Phys. Lett. B **835**, 137485 (2022)
2184. S.S. Adler et al., Elliptic flow of identified hadrons in Au+Au collisions at $\sqrt{s_{\rm NN}} = 200$GeV. Phys. Rev. Lett. **91**, 182301 (2003)
2185. J. Adams et al., Azimuthal anisotropy in Au+Au collisions at $\sqrt{s_{NN}} = 200$GeV. Phys. Rev. C **72**, 014904 (2005)
2186. K. Aamodt et al., Elliptic flow of charged particles in Pb-Pb collisions at 2.76 TeV. Phys. Rev. Lett. **105**, 252302 (2010)
2187. P. Danielewicz, M. Gyulassy, Dissipative phenomena in quark gluon plasmas. Phys. Rev. D **31**, 53–62 (1985)
2188. P. Kovtun, D.T. Son, A.O. Starinets, Viscosity in strongly interacting quantum field theories from black hole physics. Phys. Rev. Lett. **94**, 111601 (2005)
2189. R. Baier et al., Relativistic viscous hydrodynamics, conformal invariance, and holography. JHEP **04**, 100 (2008)
2190. J.E. Bernhard, J. ScottMoreland, S.A. Bass, Bayesian estimation of the specific shear and bulk viscosity of quark-gluon plasma. Nat. Phys. **15**(11), 1113–1117 (2019)
2191. J.L. Nagle, W.A. Zajc, Small system collectivity in relativistic hadronic and nuclear collisions. Annu. Rev. Nucl. Part. Sci. **68**, 211–235 (2018)
2192. C. Shen et al., Collectivity and electromagnetic radiation in small systems. Phys. Rev. C **95**(1), 014906 (2017)
2193. A. Huss et al., Predicting parton energy loss in small collision systems. Phys. Rev. C **103**(5), 054903 (2021)
2194. R. Baier et al., Radiative energy loss of high-energy quarks and gluons in a finite volume quark-gluon plasma. Nucl. Phys. B **483**, 291–320 (1997)
2195. S. Chatrchyan et al., Study of high $-$ p_T charged particle suppression in PbPb compared to pp collisions at $\sqrt{s_{NN}} = 2.76$ TeV. Eur. Phys. J. C **72**, 1945 (2012)
2196. M. Aaboud et al., Measurement of the nuclear modification factor for inclusive jets in Pb+Pb collisions at $\sqrt{s_{\rm NN}} = 5.02$ TeV with the ATLAS detector. Phys. Lett. B **790**, 108–128 (2019)
2197. A. Beraudo et al., Extraction of heavy-flavor transport coefficients in QCD matter. Nucl. Phys. A **979**, 21–86 (2018) **(Ed. by R. Rapp et al.)**
2198. K. Zapp et al., A Monte Carlo model for 'jet quenching'. Eur. Phys. J. C **60**, 617–632 (2009)
2199. N. Armesto et al., Comparison of jet quenching formalisms for a quark-gluon plasma 'brick'. Phys. Rev. C **86**, 064904 (2012)
2200. S. Cao et al., Determining the jet transport coefficient $\hat{q}$ from inclusive hadron suppression measurements using Bayesian parameter estimation. Phys. Rev. C **104**(2), 024905 (2021)
2201. W. Deng, X.-N. Wang, Multiple parton scattering in nuclei: modified DGLAP evolution for fragmentation functions. Phys. Rev. C **81**, 024902 (2010)
2202. R. Peng et al., Global extraction of the jet transport coefficient in cold nuclear matter. Phys. Rev. D **103**(3), L031901 (2021)
2203. A. Andronic et al., Decoding the phase structure of QCD via particle production at high energy. Nature **561**(7723), 321–330 (2018)
2204. R. Dashen, S.-K. Ma, H.J. Bernstein, S Matrix formulation of statistical mechanics. Phys. Rev. **187**, 345–370 (1969)
2205. P. Man Lo et al., S-matrix analysis of the baryon electric charge correlation. Phys. Lett. B **778**, 454–458 (2018)
2206. A. Andronic et al., The thermal proton yield anomaly in Pb-Pb collisions at the LHC and its resolution. Phys. Lett. B **792**, 304–309 (2019)
2207. L. Adamczyk et al., Bulk properties of the medium produced in relativistic heavy-ion collisions from the beam energy scan program. Phys. Rev. C **96**(4), 044904 (2017)
2208. J. Stroth (HADES Collaboration), Private Communications
2209. P. Braun-Munzinger, J. Stachel, C. Wetterich, Chemical freezeout and the QCD phase transition temperature. Phys. Lett. B **596**, 61–69 (2004)
2210. A. Bzdak, V. Koch, N. Strodthoff, Cumulants and correlation functions versus the QCD phase diagram. Phys. Rev. C **95**(5), 054906 (2017)
2211. A. Bzdak et al., Mapping the phases of quantum chromodynamics with beam energy scan. Phys. Rept. **853**, 1–87 (2020)
2212. P. Braun-Munzinger, A. Rustamov, J. Stachel, Experimental results on fluctuations of conserved charges confronted with predictions from canonical thermodynamics. Nucl. Phys. A **982**, 307–310 (2019) **(Ed. by Federico Antinori et al.)**
2213. P. Braun-Munzinger, A. Rustamov, J. Stachel, The role of the local conservation laws in fluctuations of conserved charges (2019). arXiv:1907.03032 [nucl-th]
2214. V. Vovchenko, R.V. Poberezhnyuk, V. Koch, Cumulants of multiple conserved charges and global conservation laws. JHEP **10**, 089 (2020)
2215. P. Braun-Munzinger, A. Rustamov, J. Stachel, Bridging the gap between event-by-event fluctuation measurements and theory predictions in relativistic nuclear collisions. Nucl. Phys. A **960**, 114–130 (2017)
2216. V. Skokov, B. Friman, K. Redlich, Volume fluctuations and higher order cumulants of the net baryon number. Phys. Rev. C **88**, 034911 (2013)
2217. A. Bazavov et al., Skewness, kurtosis, and the fifth and sixth order cumulants of net baryon-number distributions from lattice QCD confront high-statistics STAR data. Phys. Rev. D **101**(7), 074502 (2020)
2218. A. Rustamov, Net-baryon fluctuations measured with ALICE at the CERN LHC. Nucl. Phys. A **967**, 453–456 (2017) **(Ed. by Ulrich Heinz, Olga Evdokimov, and Peter Jacobs)**
2219. S. Acharya et al., Global baryon number conservation encoded in net-proton fluctuations measured in Pb-Pb collisions at $\sqrt{s_{\rm NN}} = 2.76$ TeV. Phys. Lett. B **807**, 135564 (2020)
2220. A. Rustamov, Overview of fluctuation and correlation measurements. Nucl. Phys. A **1005**, 121858 (2021) **(Ed. by Feng Liu et al.)**
2221. A. Rustamov, Deciphering the phases of QCD matter with fluctuations and correlations of conserved charges. EPJ Web Conf. **276**, 01007 (2023)
2222. M.A. Stephanov, On the sign of kurtosis near the QCD critical point. Phys. Rev. Lett. **107**, 052301 (2011)
2223. J. Adamczewski-Musch et al., Proton-number fluctuations in $\sqrt{s_{NN}} = 2.4$ GeV Au + Au collisions studied with the High-Acceptance DiElectron Spectrometer (HADES). Phys. Rev. C **102**(2), 024914 (2020)
2224. J. Adam et al., Nonmonotonic energy dependence of net-proton number fluctuations. Phys. Rev. Lett. **126**(9), 092301 (2021)
2225. B. Friman et al., Fluctuations as probe of the QCD phase transition and freeze-out in heavy ion collisions at LHC and RHIC. Eur. Phys. J. C **71**, 1694 (2011)
2226. G. Andras Almasi, B. Friman, K. Redlich, Baryon number fluctuations in chiral effective models and their phenomenological implications. Phys. Rev. D **96**(1), 014027 (2017)
2227. S. Borsanyi et al., Higher order fluctuations and correlations of conserved charges from lattice QCD. JHEP **10**, 205 (2018)
2228. M. Abdallah et al., Measurement of the sixth-order cumulant of net-proton multiplicity distributions in Au+Au collisions at $\sqrt{s_{NN}} = 27, 54.4,$ and 200 GeV at RHIC. Phys. Rev. Lett. **127**(26), 262301 (2021)
2229. M. Kitazawa, M. Asakawa, Relation between baryon number fluctuations and experimentally observed proton number fluctuations in relativistic heavy ion collisions. Phys. Rev. C **86**, 024904 (2012) [Erratum: Phys. Rev. C 86, 069902 (2012)]

2230. S. Acharya et al., Prompt D^0, D^+, and D^{*+} production in Pb-Pb collisions at $\sqrt{s_{NN}}$ = 5.02TeV. JHEP **01**, 174 (2022)
2231. A. Andronic et al., The multiple-charm hierarchy in the statistical hadronization model. JHEP **07**, 035 (2021)
2232. A. Andronic et al., Transverse momentum distributions of charmonium states with the statistical hadronization model. Phys. Lett. B **797**, 134836 (2019)
2233. L. Altenkort et al., Heavy quark momentum diffusion from the lattice using gradient flow. Phys. Rev. D **103**(1), 014511 (2021)
2234. E. Abbas et al., J/ψ elliptic flow in Pb–Pb collisions at $\sqrt{s_{NN}}$ = 2.76TeV. Phys. Rev. Lett. **111**, 162301 (2013)
2235. W. Min He, R.R. Biaogang, Collectivity of J/ψ mesons in heavy-ion collisions. Phys. Rev. Lett. **128**(16), 162301 (2022)
2236. S. Cho et al., Charmed hadron production in an improved quark coalescence model. Phys. Rev. C **101**(2), 024909 (2020)
2237. J. Zhao et al., Sequential coalescence with charm conservation in high energy nuclear collisions (2018)
2238. S. Cho et al., Exotic hadrons from heavy ion collisions. Prog. Part. Nucl. Phys. **95**, 279–322 (2017)
2239. K. Zhou et al., Medium effects on charmonium production at ultrarelativistic energies available at the CERN Large Hadron Collider. Phys. Rev. C **89**(5), 054911 (2014)
2240. V. Greco, C.M. Ko, R. Rapp, Quark coalescence for charmed mesons in ultrarelativistic heavy ion collisions. Phys. Lett. B **595**, 202–208 (2004)
2241. G. Aarts et al., Heavy-flavor production and medium properties in highenergy nuclear collisions–what next? Eur. Phys. J. A **53**(5), 93 (2017)
2242. L. Maiani, A. Pilloni, GGI lectures on exotic hadrons (2022). arXiv:2207.05141
2243. T. Song, G. Coci, Prerequisites for heavy quark coalescence in heavy-ion collisions. Nucl. Phys. A **1028**, 122539 (2022)
2244. P. Braun-Munzinger, J. Stachel, (Non)thermal aspects of charmonium production and a new look at J/ψ suppression. Phys. Lett. B **490**, 196–202 (2000)
2245. A. Andronic et al., Statistical hadronization of charm at SPS, RHIC and LHC. Nucl. Phys. A **715**, 529–532 (2003) **(Ed. by H. Gutbrod, J. Aichelin, and K. Werner)**
2246. L. Grandchamp, R. Rapp, G.E. Brown, In medium effects on charmonium production in heavy ion collisions. Phys. Rev. Lett. **92**, 212301 (2004)
2247. F. Becattini, Production of multiply heavy flavored baryons from quark gluon plasma in relativistic heavy ion collisions. Phys. Rev. Lett. **95**, 022301 (2005)
2248. A. Andronic et al., Statistical hadronization of heavy quarks in ultrarelativistic nucleus-nucleus collisions. Nucl. Phys. A **789**, 334–356 (2007)
2249. S. Acharya et al., Measurements of inclusive J/ψ production at midrapidity and forward rapidity in Pb-Pb collisions at $\sqrt{s_{NN}}$ = 5.02 TeV (2023). arXiv:2303.13361 [nucl-ex]
2250. A.M. Sirunyan et al., Suppression of excited. Phys. Rev. Lett. **120**(14), 142301 (2018)
2251. B. Krouppa, A. Rothkopf, M. Strickland, Bottomonium suppression using a lattice QCD vetted potential. Phys. Rev. D **97**(1), 016017 (2018)
2252. R. Rapp, E.V. Shuryak, Resolving the anti-baryon production puzzle in high-energy heavy ion collisions. Phys. Rev. Lett. **86**, 2980–2983 (2001)
2253. A. Andronic et al., Hadron production in ultra-relativistic nuclear collisions: quarkyonic matter and a triple point in the phase diagram of QCD. Nucl. Phys. A **837**, 65–86 (2010)
2254. G. Baym, RHIC: from dreams to beams in two decades. Nucl. Phys. A **698**, XXIII–XXXII (2002) **(Ed. by T. J. Hallman et al.)**
2255. Y. Nambu, G. Jona Lasinio, Dynamical model of elementary particles based on an analogy with superconductivity. II. Phys. Rev. **124**, 246–254 (1961)
2256. Y. Hatta, K. Fukushima, Linking the chiral and deconfinement phase transitions. Phys. Rev. D **69**, 097502 (2004)
2257. S. Borsanyi et al., Is there still any T_c mystery in lattice QCD? Results with physical masses in the continuum limit III. JHEP **09**, 073 (2010)
2258. K. Fukushima, Phase structure and instability problem in color superconductivity. Subnucl. Ser. **43**, 334–344 (2007) **(Ed. by Antonino Zichichi)**
2259. K. Fukushima, T. Hatsuda, The phase diagram of dense QCD. Rep. Prog. Phys. **74**, 014001 (2011)
2260. N. Itoh, Hydrostatic equilibrium of hypothetical quark stars. Prog. Theor. Phys. **44**, 291 (1970)
2261. B.A. Freedman, L.D. McLerran, Fermions and gauge vector mesons at finite temperature and density. 1. Formal techniques. Phys. Rev. D **16**, 1130 (1977)
2262. B.A. Freedman, L.D. McLerran, Fermions and gauge vector mesons at finite temperature and density. 3. The ground state energy of a relativistic quark gas. Phys. Rev. D **16**, 1169 (1977)
2263. A. Kurkela, P. Romatschke, A. Vuorinen, Cold quark matter. Phys. Rev. D **81**, 105021 (2010)
2264. T. Gorda et al., Soft interactions in cold quark matter. Phys. Rev. Lett. **127**(16), 162003 (2021)
2265. T. Gorda et al., Cold quark matter at N3LO: soft contributions. Phys. Rev. D **104**(7), 074015 (2021)
2266. D.H. Rischke, D.T. Son, M.A. Stephanov, Asymptotic deconfinement in high density QCD. Phys. Rev. Lett. **87**, 062001 (2001)
2267. T. Schäfer, F. Wilczek, Continuity of quark and hadron matter. Phys. Rev. Lett. **82**, 3956–3959 (1999)
2268. Y. Fujimoto, K. Fukushima, W. Weise, Continuity from neutron matter to two-flavor quark matter with $^1S_0$ and $^3P_2$ superfluidity. Phys. Rev. D **101**(9), 094009 (2020)
2269. A.P. Balachandran, S. Digal, T. Matsuura, Semi-superfluid strings in high density QCD. Phys. Rev. D **73**, 074009 (2006)
2270. A. Cherman, S. Sen, L.G. Yaffe, Anyonic particlevortex statistics and the nature of dense quark matter. Phys. Rev. D **100**(3), 034015 (2019)
2271. Y. Hirono, Y. Tanizaki, Quark-hadron continuity beyond the Ginzburg-Landau paradigm. Phys. Rev. Lett. **122**(21), 212001 (2019)
2272. L. McLerran, R.D. Pisarski, Phases of cold, dense quarks at large N(c). Nucl. Phys. A **796**, 83–100 (2007)
2273. K. Fukushima, T. Kojo, W. Weise, Hard-core deconfinement and soft-surface delocalization from nuclear to quark matter. Phys. Rev. D **102**(9), 096017 (2020)
2274. Y. Aoki et al., The QCD transition temperature: results with physical masses in the continuum limit. Phys. Lett. B **643**, 46–54 (2006)
2275. M. Asakawa, K. Yazaki, Chiral restoration at finite density and temperature. Nucl. Phys. A **504**, 668–684 (1989)
2276. A. Barducci et al., Chiral symmetry breaking in QCD at finite temperature and density. Phys. Lett. B **231**, 463–470 (1989)
2277. F. Wilczek, Remarks on the phase transition in QCD. In: *1st IFT Workshop: Dark Matter* (1992)
2278. D.T. Son, M.A. Stephanov, Dynamic universality class of the QCD critical point. Phys. Rev. D **70**, 056001 (2004)
2279. K. Fukushima, B. Mohanty, N. Xu, Little-bang and femto-nova in nucleus-nucleus collisions. AAPPS Bull. **31**, 1 (2021)
2280. M. Stephanov, Y. Yin, Hydrodynamics with parametric slowing down and fluctuations near the critical point. Phys. Rev. D **98**(3), 036006 (2018)
2281. D. Nickel, How many phases meet at the chiral critical point? Phys. Rev. Lett. **103**, 072301 (2009)
2282. E. Nakano, T. Tatsumi, Chiral symmetry and density wave in quark matter. Phys. Rev. D **71**, 114006 (2005)
2283. M. Buballa, S. Carignano, Inhomogeneous chiral condensates. Prog. Part. Nucl. Phys. **81**, 39–96 (2015)

2284. Y. Hidaka et al., Phonons, pions and quasi-long-range order in spatially modulated chiral condensates. Phys. Rev. D **92**(3), 034003 (2015)
2285. T.-G. Lee et al., Landau-Peierls instability in a Fulde-Ferrell type inhomogeneous chiral condensed phase. Phys. Rev. D **92**(3), 034024 (2015)
2286. R.D. Pisarski, F. Rennecke, Signatures of moat regimes in heavy-ion collisions. Phys. Rev. Lett. **127**(15), 152302 (2021)
2287. P. Demorest et al., Shapiro delay measurement of a two solar mass neutron star. Nature **467**, 1081–1083 (2010)
2288. J. Antoniadis et al., A massive pulsar in a compact relativistic binary. Science **340**, 6131 (2013)
2289. H.T. Cromartie et al., Relativistic Shapiro delay measurements of an extremely massive millisecond pulsar. Nat. Astron. **4**(1), 72–76 (2019)
2290. M.G. Alford et al., Constraining and applying a generic high-density equation of state. Phys. Rev. D **92**(8), 083002 (2015)
2291. C. Drischler et al., Limiting masses and radii of neutron stars and their implications. Phys. Rev. C **103**(4), 045808 (2021)
2292. M. Al-Mamun et al., Combining electromagnetic and gravitational-wave constraints on neutron-star masses and radii. Phys. Rev. Lett. **126**(6), 061101 (2021)
2293. G. Raaijmakers et al., Constraints on the dense matter equation of state and neutron star properties from NICER's mass-radius estimate of PSR J0740+6620 and multimessenger observations. Astrophys. J. Lett. **918**(2), L29 (2021)
2294. T. Gorda, O. Komoltsev, A. Kurkela, Ab-initio QCD calculations impact the inference of the neutron-star-matter equation of state (2022)
2295. Y. Fujimoto et al., Trace anomaly as signature of conformality in neutron stars. Phys. Rev. Lett. **129**(25), 252702 (2022)
2296. E. Annala et al., Gravitational-wave constraints on the neutron-starmatter equation of state. Phys. Rev. Lett. **120**(17), 172703 (2018)
2297. B.P. Abbott et al., GW170817: measurements of neutron star radii and equation of state. Phys. Rev. Lett. **121**(16), 161101 (2018)
2298. S. Gandolfi, J. Carlson, S. Reddy, The maximum mass and radius of neutron stars and the nuclear symmetry energy. Phys. Rev. C **85**, 032801 (2012)
2299. M. Aguilar-Benitez et al., Review of particle properties. Particle data group. Phys. Lett. B **170**, 1–350 (1986)
2300. F. Giacosa, A. Koenigstein, R.D. Pisarski, How the axial anomaly controls flavor mixing among mesons. Phys. Rev. D **97**(9), 091901 (2018)
2301. D. Parganlija et al., Meson vacuum phenomenology in a three-flavor linear sigma model with (axial)-vector mesons. Phys. Rev. D **87**(1), 014011 (2013)
2302. S. Jafarzade et al., From well-known tensor mesons to yet unknown axial-tensor mesons. Phys. Rev. D **106**(3), 036008 (2022)
2303. A. Koenigstein, F. Giacosa, Phenomenology of pseudotensor mesons and the pseudotensor glueball. Eur. Phys. J. A **52**(12), 356 (2016)
2304. S. Jafarzade, A. Koenigstein, F. Giacosa, Phenomenology of $J^{PC} = 3^-$ tensor mesons. Phys. Rev. D **103**(9), 096027 (2021)
2305. J.E. Augustin et al., Radiative decay of J/ψ into $\eta(1430)$ and nearby states. Phys. Rev. D **42**, 10–19 (1990)
2306. J.E. Augustin et al., Partial wave analysis of DM2 data in the $\eta(1430)$ energy range. Phys. Rev. D **46**, 1951–1958 (1992)
2307. N.R. Stanton et al., Evidence for axial vector and pseudoscalar resonances near 1.275-GeV in $\eta\pi^+\pi^-$. Phys. Rev. Lett. **42**, 346–349 (1979)
2308. S. Fukui et al., Study on the $\eta\pi^+\pi^-$ system in the $\pi^- p$ charge exchange reaction at 8.95-GeV/c. Phys. Lett. B **267**, 293–298 (1991) **(Ed. by K. Nakai and T. Ohshima)**
2309. D. Alde et al., Partial-wave analysis of the $\eta\pi^0\pi^0$ system produced in $\pi^- p$ charge exchange collisions at 100-GeV/c. Phys. Atom. Nucl. **60**, 386–390 (1997)
2310. J.J. Manak et al., Partial-wave analysis of the $\eta\pi^+\pi^-$ system produced in the reaction $\pi^- p \to \eta\pi^+\pi^- n$ at 18-GeV/c. Phys. Rev. D **62**, 012003 (2000)
2311. G.S. Adams et al., Observation of pseudoscalar and axial vector resonances in $\pi^- p \to \eta K^+ K^- n$ at 18-GeV. Phys. Lett. B **516**, 264–272 (2001)
2312. C. Amsler et al., E decay to $\eta\pi\pi$ in $\bar{p}p$ annihilation at rest. Phys. Lett. B **358**, 389–398 (1995)
2313. A. Bertin et al., A search for axial vectors in $\bar{p}p \to K^\pm K^0_{\text{miss}}\pi^\mp\pi^+\pi^-$ annihilations at rest in gaseous hydrogen at NTP. Phys. Lett. B **400**, 226–238 (1997)
2314. P. Eugenio et al., Observation of a new $J(PC) = 1^{+-}$ isoscalar state in the reaction π^- proton $\to \omega\eta$ neutron at 18-GeV/c. Phys. Lett. B **497**, 190–198 (2001)
2315. F. Divotgey, L. Olbrich, F. Giacosa, Phenomenology of axial-vector and pseudovector mesons: decays and mixing in the kaonic sector. Eur. Phys. J. A **49**, 135 (2013)
2316. P. Gavillet et al., Evidence for a new $K^*\bar{K}$ state at a mass of 1530-MeV with $J^{PC} = 1^{++}$ observed in $K - p$ interactions at 4.2-GeV/c. Z. Phys. C **16**, 119 (1982)
2317. D. Aston et al., Evidence for two strangeonium resonances with $J^{PC} = 1^{++}$ and 1^{+-} in $K^- p$ interactions at 11-GeV/c. Phys. Lett. B **201**, 573–578 (1988)
2318. A. Birman et al., Partial wave analysis of the $K^+\bar{K}^0\pi^-$ system. Phys. Rev. Lett. **61**, 1557 (1988) [Erratum: Phys. Rev. Lett. 62, 1577 (1989)]
2319. M. Aghasyan et al., Light isovector resonances in $\pi^- p \to \pi^-\pi^-\pi^+ p$ at 190 GeV/c. Phys. Rev. D **98**(9), 092003 (2018)
2320. P. d'Argent et al., Amplitude analyses of $D^0 \to \pi^+\pi^-\pi^+\pi^-$ and $D^0 \to K^+K^-\pi^+\pi^-$ decays. JHEP **05**, 143 (2017)
2321. V.K. Grigorev et al., Investigation of a resonance structure in the system of two K_s mesons in the mass region around 1775-MeV. Phys. Atom. Nucl. **62**, 470–478 (1999)
2322. M. Lu et al., Exotic meson decay to $\omega\pi^0\pi^-$. Phys. Rev. Lett. **94**, 032002 (2005)
2323. J. Nys et al., Features of $\pi\Delta$ photoproduction at high energies. Phys. Lett. B **779**, 77–81 (2018)
2324. A. Rodas et al., Determination of the pole position of the lightest hybrid meson candidate. Phys. Rev. Lett. **122**(4), 042002 (2019)
2325. A. Abele et al., Observation of resonances in the reaction $\bar{p}p \to \pi^0\eta\eta$ at 1.94-GeV/c. Eur. Phys. J. C **8**, 67–79 (1999)
2326. C. Amsler et al., Proton anti-proton annihilation at 900-MeV/c into $\pi^0\pi^0\pi^0$, $\pi^0\pi^0\eta$ and $\pi^0\eta\eta$ Eur. Phys. J. C **23**, 29–41 (2002)
2327. V.V. Anisovich, A.V. Sarantsev, The combined analysis of $\pi N \to$ two mesons $+N$ reactions within Reggeon exchanges and data for $\bar{p}p$ (at rest) $\to$ three mesons. Int. J. Mod. Phys. A **24**, 2481–2549 (2009)
2328. M. Albrecht et al., Coupled channel analysis of $\bar{p}p \to \pi^0\pi^0\eta$, $\pi^0\eta\eta$ and $K^+K^-\pi^0$ at 900 MeV/c and of $\pi\pi$-scattering data. Eur. Phys. J. C **80**(5), 453 (2020)
2329. M. Acciarri et al., Resonance formation in the $\pi^+\pi^-\pi^0$ final state in two photon collisions. Phys. Lett. B **413**, 147–158 (1997)
2330. M. Acciarri et al., $K^0_S K^0_S$ final state in two photon collisions and implications for glueballs. Phys. Lett. B **501**, 173–182 (2001)
2331. M. Ablikim et al., Amplitude analysis of the $\chi_{c1} \to \eta\pi^+\pi^-$ decays. Phys. Rev. D **95**(3), 032002 (2017)
2332. A. Etkin et al., Increased statistics and observation of the $g(T)$, g'_T, and g''_T 2^{++} resonances in the glueball enhanced channel $\pi^- p \to \phi\phi n$. Phys. Lett. B **201**, 568–572 (1988)
2333. J. Adomeit et al., Evidence for two isospin zero $J^{PC} = 2^{-+}$ mesons at 1645-MeV and 1875-MeV. Z. Phys. C **71**, 227–238 (1996)

2334. A. Hasan, D.V. Bugg, Amplitudes for $\bar{p}p \to \pi\pi$ from 0.36-GeV/c to 2.5-GeV/c. Phys. Lett. B **334**, 215–219 (1994)
2335. A.V. Anisovich et al., Combined analysis of meson channels with I = 1, C = -1 from 1940 to 2410 MeV. Phys. Lett. B **542**, 8–18 (2002)
2336. M. Ablikim et al., Partial wave analysis of $\psi(3686) \to K^+K^-\eta$. Phys. Rev. D **101**(3), 032008 (2020)
2337. J.-K. Chen, Structure of the meson Regge trajectories. Eur. Phys. J. A **57**(7), 238 (2021)
2338. G.F. Chew, S.C. Frautschi, Principle of equivalence for all strongly interacting particles within the S matrix framework. Phys. Rev. Lett. **7**, 394–397 (1961)
2339. M.H. Johnson, E. Teller, Classical field theory of nuclear forces. Phys. Rev. **98**, 783–787 (1955)
2340. M. Gell-Mann, M. Levy, The axial vector current in β decay. Nuovo Cim. **16**, 705 (1960)
2341. R.H. Dalitz, Resonant states and strong interactions. In: *Oxford International Conference on Elementary Particles*, pp. 157–181 (1966)
2342. J.R. Pelaez, From controversy to precision on the sigma meson: a review on the status of the non-ordinary $f_0(500)$ resonance. Phys. Rep. **658**, 1 (2016)
2343. J.R. Peláez, A. Rodas, Dispersive $\pi K \to \pi K$ and $\pi\pi \to K\bar{K}$ amplitudes from scattering data, threshold parameters, and the lightest strange resonance κ or $K_0^*(700)$. Phys. Rep. **969**, 1–126 (2022)
2344. A.V. Anisovich, V.V. Anisovich, A.V. Sarantsev, Systematics of $q\bar{q}$ states in the (n, M^2) and (J, M^2) planes. Phys. Rev. D **62**, 051502 (2000)
2345. J.T. Londergan et al., Identification of non-ordinary mesons from the dispersive connection between their poles and their Regge trajectories. The $f_0(500)$ resonance. Phys. Lett. B **729**, 9–14 (2014)
2346. J.R. Pelaez, A. Rodas, The non-ordinary Regge behavior of the $K_0^*(800)$ or κ -meson versus the ordinary $K_0^*(1430)$. Eur. Phys. J. C **77**(6), 431 (2017)
2347. R.L. Jaffe, Multi-quark hadrons. 1. The phenomenology of $Q^2\bar{Q}^2$ mesons. Phys. Rev. D **15**, 267 (1977)
2348. J.P. Lees et al., Light meson spectroscopy from Dalitz plot analyses of η_c decays to $\eta' K^+K^-$, $\eta'\pi^+\pi^-$, and $\eta\pi^+\pi^-$ produced in two-photon interactions. Phys. Rev. D **104**(7), 072002 (2021)
2349. M. Ablikim et al., Study of the decay $D_s^+ \to K_S^0 K_S^0 \pi^+$ and observation an isovector partner to $f_0(1710)$. Phys. Rev. D **105**(5), L051103 (2022)
2350. M. Ablikim et al., Observation of an a_0-like state with mass of 1.817 GeV in the study of $D_s^+ \to K_S^0 K^+ \pi^0$ decays. Phys. Rev. Lett. **129**(18), 182001 (2022)
2351. R. Aaij et al., Study of charmonium decays to $K_S^0 K\pi$ in the $B \to (K_S^0 K\pi)K$ channels (2023)
2352. J.A. Carrasco et al., Dispersive calculation of complex Regge trajectories for the lightest f_2 resonances and the K*(892). Phys. Lett. B **749**, 399–406 (2015)
2353. S.M. Roy, Exact integral equation for pion pion scattering involving only physical region partial waves. Phys. Lett. **36B**, 353–356 (1971)
2354. J. Baacke, F. Steiner, πN partial wave relations from fixed-t dispersion relations. Fortsch. Phys. **18**, 67–87 (1970)
2355. F. Steiner, Partial wave crossing relations for meson-baryon scattering. Fortsch. Phys. **19**, 115–159 (1971)
2356. R. García-Martín et al., The Pion-pion scattering amplitude. IV: improved analysis with once subtracted Roy-like equations up to 1100 MeV. Phys. Rev. **D83**, 074004 (2011)
2357. B. Ananthanarayan et al., Roy equation analysis of $\pi\pi$ scattering. Phys. Rep. **353**, 207–279 (2001)
2358. G. Colangelo, J. Gasser, H. Leutwyler, $\pi\pi$ scattering. Nucl. Phys. B **603**, 125–179 (2001)
2359. P. Buettiker, S. Descotes-Genon, B. Moussallam, A new analysis of πK scattering from Roy and Steiner type equations. Eur. Phys. J. C **33**, 409–432 (2004)
2360. I. Caprini, G. Colangelo, H. Leutwyler, Mass and width of the lowest resonance in QCD. Phys. Rev. Lett. **96**, 132001 (2006)
2361. S. Descotes-Genon, B. Moussallam, The $K_0^*(800)$ scalar resonance from Roy-Steiner representations of πK scattering. Eur. Phys. J. C **48**, 553 (2006)
2362. R. García-Martín et al., Precise determination of the $f_0(600)$ and $f_0(980)$ pole parameters from a dispersive data analysis. Phys. Rev. Lett. **107**, 072001 (2011)
2363. J.R. Pelaez, A. Rodas, $\pi\pi \to K\bar{K}$ scattering up to 1.47 GeV with hyperbolic dispersion relations. Eur. Phys. J. C **78**(11), 897 (2018)
2364. J.R. Peláez, A. Rodas, Determination of the lightest strange resonance $K_0^*(700)$ or κ, from a dispersive data analysis. Phys. Rev. Lett. **124**(17), 172001 (2020)
2365. H. Leutwyler, Model independent determination of the sigma pole. AIP Conf. Proc. **1030**(1), 46–55 (2008) **(Ed. by George Rupp et al.)**
2366. B. Moussallam, Couplings of light I=0 scalar mesons to simple operators in the complex plane. Eur. Phys. J. C **71**, 1814 (2011)
2367. J.R. Peláez, A. Rodas, J. Ruiz de Elvira, Strange resonance poles from $K\pi$ scattering below 1.8 GeV. Eur. Phys. J. C **77**(2), 91 (2017)
2368. J.R. Pelaez, A. Rodas, J. Ruiz de Elvira, $f_0(1370)$ controversy from dispersive meson-meson scattering data analyses. Phys. Rev. Lett. **130**(5), 051902 (2023)
2369. A. Dobado, J.R. Pelaez, The Inverse amplitude method in chiral perturbation theory. Phys. Rev. D **56**, 3057–3073 (1997)
2370. J. Nieves, M. Pavon Valderrama, E. Ruiz Arriola, The Inverse amplitude method in $\pi\pi$ scattering in chiral perturbation theory to two loops. Phys. Rev. D **65**, 036002 (2002)
2371. A. Dobado, J.R. Pelaez, Chiral perturbation theory and the $f_2(1270)$ resonance. Phys. Rev. D **65**, 077502 (2002)
2372. T.N. Truong, Chiral perturbation theory and final state theorem. Phys. Rev. Lett. **61**, 2526 (1988)
2373. A. Dobado, M.J. Herrero, T.N. Truong, Unitarized chiral perturbation theory for elastic pion-pion scattering. Phys. Lett. B **235**, 134–140 (1990)
2374. A. Dobado, J.R. Pelaez, A Global fit of $\pi\pi$ and πK elastic scattering in ChPT with dispersion relations. Phys. Rev. D **47**, 4883–4888 (1993)
2375. F. Guerrero, J. Antonio Oller, $K\bar{K}$ scattering amplitude to one loop in chiral perturbation theory, its unitarization and pion formfactors. Nucl. Phys. B **537**, 459–476 (1999) [Erratum: Nucl. Phys. B 602, 641–643 (2001)]
2376. A. Gomez Nicola, J.R. Pelaez, Meson meson scattering within one loop chiral perturbation theory and its unitarization. Phys. Rev. D **65**, 054009 (2002)
2377. J.R. Pelaez, Light scalars as tetraquarks or two-meson states from large N_c and unitarized chiral perturbation theory. Mod. Phys. Lett. A **19**, 2879 (2004)
2378. J.A. Oller, E. Oset, Chiral symmetry amplitudes in the S wave isoscalar and isovector channels and the σ, $f_0(980)$, $a_0(980)$ scalar mesons. Nucl. Phys. A **620**, 438–456 (1997) [Erratum: Nucl. Phys. A 652, 407 (1999)]
2379. J.A. Oller, E. Oset, J.R. Pelaez, Nonperturbative approach to effective chiral Lagrangians and meson interactions. Phys. Rev. Lett. **80**, 3452–3455 (1998)
2380. J.A. Oller, Coupled-channel approach in hadron- hadron scattering. Prog. Part. Nucl. Phys. **110**, 103728 (2020)
2381. J.R. Peláez, A. Rodas, J.R. de Elvira, Precision dispersive approaches versus unitarized chiral perturbation theory for the lightest scalar resonances $\sigma/f_0(500)$ and $\kappa/K_0^*(700)$. Eur. Phys. J. ST **230**(6), 1539–1574 (2021)

2382. J.A. Oller, Unitarization technics in hadron physics with historical remarks. Symmetry **12**(7), 1114 (2020)
2383. E. Witten, Large N chiral dynamics. Ann. Phys. **128**, 363 (1980)
2384. S. Weinberg, Tetraquark mesons in large N quantum chromodynamics. Phys. Rev. Lett. **110**, 261601 (2013)
2385. M. Knecht, S. Peris, Narrow tetraquarks at large N. Phys. Rev. D **88**, 036016 (2013)
2386. J. Nebreda, J.R. Pelaez, G. Rios, Enhanced non-quark-antiquark and non-glueball N_c behavior of light scalar mesons. Phys. Rev. D **84**, 074003 (2011)
2387. S. Peris, E. de Rafael, On the large N_c behavior of the L_7 coupling in χPT. Phys. Lett. B **348**, 539–542 (1995)
2388. J.R. Pelaez, On the nature of light scalar mesons from their large N_c behavior. Phys. Rev. Lett. **92**, 102001 (2004)
2389. J.R. Pelaez, G. Rios, Nature of the $f_0(600)$ from its N_c dependence at two loops in unitarized Chiral Perturbation Theory. Phys. Rev. Lett. **97**, 242002 (2006)
2390. J. Ruiz de Elvira et al., Chiral Perturbation Theory, the $1/N_c$ expansion and Regge behaviour determine the structure of the lightest scalar meson. Phys. Rev. D **84**, 096006 (2011)
2391. E. van Beveren et al., A low lying scalar meson nonet in a unitarized meson model. Z. Phys. C **30**, 615–620 (1986)
2392. Z.-H. Guo, J.A. Oller, Resonances from meson-meson scattering in U(3) CHPT. Phys. Rev. D **84**, 034005 (2011)
2393. Z.-H. Guo, J.A. Oller, J. Ruiz de Elvira, Chiral dynamics in form factors, spectral-function sum rules, meson-meson scattering and semilocal duality. Phys. Rev. D **86**, 054006 (2012)
2394. J. Nieves, A. Pich, E. Ruiz Arriola, Large-N_c properties of the ρ and $f_0(600)$ mesons from unitary resonance chiral dynamics. Phys. Rev. D **84**, 096002 (2011)
2395. C. Hanhart, J.R. Pelaez, G. Rios, Quark mass dependence of the ρ and σ from dispersion relations and Chiral Perturbation Theory. Phys. Rev. Lett. **100**, 152001 (2008)
2396. J. Nebreda, J.R. Pelaez, G. Rios, Chiral extrapolation of pion-pion scattering phase shifts within standard and unitarized Chiral Perturbation Theory. Phys. Rev. D **83**, 094011 (2011)
2397. J. Nebreda, J.R. Pelaez, Strange and non-strange quark mass dependence of elastic light resonances from SU(3) Unitarized Chiral Perturbation Theory to one loop. Phys. Rev. D **81**, 054035 (2010)
2398. A. Gomez Nicola, J.R. Pelaez, G. Rios, The inverse amplitude method and Adler zeros. Phys. Rev. D **77**, 056006 (2008)
2399. J.R. Pelaez, G. Rios, Chiral extrapolation of light resonances from one and two-loop unitarized Chiral Perturbation Theory versus lattice results. Phys. Rev. D **82**, 114002 (2010)
2400. J.R. Pelaez et al., Unitarized chiral perturbation theory and the meson spectrum. AIP Conf. Proc. **1257**(1), 141–148 (2010). (**Ed. by V. Crede, P. Eugenio, and A. Ostrovidov**)
2401. C. Hanhart, J.R. Pelaez, G. Rios, Remarks on pole trajectories for resonances. Phys. Lett. B **739**, 375–382 (2014)
2402. T. Kunihiro et al., Scalar mesons in lattice QCD. Phys. Rev. D **70**, 034504 (2004)
2403. M. Wakayama et al., Lattice QCD study of four-quark components of the isosinglet scalar mesons: significance of disconnected diagrams. Phys. Rev. D **91**(9), 094508 (2015)
2404. S. Prelovsek et al., Lattice study of light scalar tetraquarks with I = 0, 2, 1/2, 3/2: are σ and κ tetraquarks? Phys. Rev. D **82**, 094507 (2010)
2405. G. Rendon et al., $I = 1/2$ S-wave and P-wave $K\pi$ scattering and the κ and K^* resonances from lattice QCD. Phys. Rev. D **102**(11), 114520 (2020)
2406. J.A. Oller, The mixing angle of the lightest scalar nonet. Nucl. Phys. A **727**, 353–369 (2003)
2407. R.L. Workman et al. (Particle Data Group), Heavy non-$q\bar{q}$ mesons. Prog. Theor. Exp. Phys. **2022**, 083C01 (2022)
2408. R.L. Workman et al. (Particle Data Group), Spectroscopy of light meson resonances. Prog. Theor. Exp. Phys. **2022**, 083C01 (2022)
2409. F.E. Close, N.A. Tornqvist, Scalar mesons above and below 1 GeV. J. Phys. G **28**, R249–R267 (2002)
2410. C. Amsler, N.A. Tornqvist, Mesons beyond the naive quark model. Phys. Rep. **389**, 61–117 (2004)
2411. D.V. Bugg, Four sorts of meson. Phys. Rep. **397**, 257–358 (2004)
2412. C.A. Meyer, Y. Van Haarlem, The status of exotic-quantum-number mesons. Phys. Rev. C **82**, 025208 (2010)
2413. B. Ketzer, Hybrid mesons. PoS QNP **2012**, 025 (2012)
2414. C.A. Meyer, E.S. Swanson, Hybrid mesons. Prog. Part. Nucl. Phys. **82**, 21–58 (2015)
2415. T. Barnes, Colored Quark and Gluon Constituents in the MIT Bag Model. Nucl. Phys. B **158**, 171–188 (1979)
2416. M. Flensburg, C. Peterson, L. Skold, Applications of an improved bag model. Z. Phys. C **22**, 293 (1984)
2417. N. Isgur, J.E. Paton, A flux tube model for hadrons. Phys. Lett. B **124**, 247–251 (1983)
2418. N. Isgur, J.E. Paton, A flux-tube model for hadrons in QCD. Phys. Rev. D **31**, 2910 (1985)
2419. N. Isgur, R. Kokoski, J. Paton, Gluonic excitations of mesons: why they are missing and where to find them. Phys. Rev. Lett. **54**, 869 (1985)
2420. R. Kokoski, N. Isgur, Meson decays by flux-tube breaking. Phys. Rev. D **35**, 907 (1987)
2421. F.E. Close, P.R. Page, The production and decay of hybrid mesons by flux-tube breaking. Nucl. Phys. B **443**, 233–254 (1995)
2422. E.S. Swanson, A.P. Szczepaniak, Decays of hybrid mesons. Phys. Rev. D **56**, 5692–5695 (1997)
2423. P.R. Page, E.S. Swanson, A.P. Szczepaniak, Hybrid meson decay phenomenology. Phys. Rev. D **59**, 034016 (1999)
2424. D. Horn, J. Mandula, Model of mesons with constituent gluons. Phys. Rev. D **17**, 898 (1978)
2425. M. Tanimoto, Decay patterns of $q\bar{q}g$ hybrid mesons. Phys. Lett. B **116**, 198–202 (1982)
2426. A. Le Yaouanc et al., $q\bar{q}g$ hybrid mesons in $\psi \to \gamma +$ hadrons. Z. Phys. C **28**, 309–315 (1985)
2427. F. Iddir et al., $q\bar{q}g$ hybrid and $qq\bar{q}\bar{q}$ diquonium interpretation of the GAMS 1^{-+} resonance. Phys. Lett. B **205**, 564–568 (1988)
2428. C.S. Fischer, S. Kubrak, R. Williams, Mass spectra and Regge trajectories of light mesons in the Bethe-Salpeter approach. Eur. Phys. J. A **50**, 126 (2014)
2429. Z.-N. Xu et al., Bethe-Salpeter kernel and properties of strange-quark mesons (2022)
2430. R.L. Workman et al. (Particle Data Group), Resonances. Prog. Theor. Exp. Phys. **2022**, 083C01 (2022)
2431. S.U. Chung, T.L. Trueman, Positivity conditions on the spin density matrix: a simple parametrization. Phys. Rev. D **11**, 633 (1975)
2432. B. Ketzer, B. Grube, D. Ryabchikov, Light-meson spectroscopy with COMPASS. Prog. Part. Nucl. Phys. **113**, 103755 (2020)
2433. D. Alde et al., Evidence for a 1^{-+} exotic meson. Phys. Lett. B **205**, 397 (1988)
2434. H. Aoyagi et al., Study of the $\eta\pi^-$ system in the $\pi^- p$ reaction at 6.3 GeV$/c$. Phys. Lett. B **314**, 246–254 (1993)
2435. D.R. Thompson et al., Evidence for exotic meson production in the reaction $\pi^- p \to \eta\pi^- p$ at 18 GeV$/c$. Phys. Rev. Lett. **79**, 1630–1633 (1997)
2436. A. Abele et al., Exotic $\eta\pi$ state in $\bar{p}d$ annihilation at rest into $\pi^-\pi^0\eta p_{\mathrm{spectator}}$. Phys. Lett. B **423**, 175–184 (1998)
2437. A. Abele et al., Evidence for a $\pi\eta$-P-wave in $\bar{p}p$-annihilations at rest into $\pi^0\pi^0\eta$. Phys. Lett. B **446**, 349–355 (1999)
2438. V. Dorofeev et al., The $J^{PC} = 1^{-+}$ hunting season at VES. AIP Conf. Proc. **619**, 143–154 (2002)
2439. G.S. Adams et al., Confirmation of the 1^{-+} meson exotics in the $\eta\pi^0$ system. Phys. Lett. B **657**, 27–31 (2007)

2440. P. Salvini et al., $\bar{p}p$ annihilation into four charged pions at rest and in flight. Eur. Phys. J. C **35**, 21–33 (2004)
2441. W. Dünnweber, F. Meyer-Wildhagen, Exotic states in crystal barrel analyses of annihilation channels. AIP Conf. Proc. **717**, 388–393 (2004)
2442. G.S. Adams et al., Observation of a new $J^{PC} = 1^{-+}$ exotic state in the reaction $\pi^- p \to \pi^+\pi^-\pi^- p$ at 18 GeV/c. Phys. Rev. Lett. **81**, 5760–5763 (1998)
2443. S.U. Chung et al., Exotic and $q\bar{q}$ resonances in the $\pi^+\pi^-\pi^-$ system produced in $\pi^- p$ collisions at 18 GeV/c. Phys. Rev. D **65**, 072001 (2002)
2444. M. Alekseev et al., Observation of a $J^{PC} = 1^{-+}$ exotic resonance in diffractive dissociation of 190 GeV/c π^- into $\pi^-\pi^-\pi^+$. Phys. Rev. Lett. **104**, 241803 (2010)
2445. M.G. Alexeev et al., Exotic meson $\pi_1(1600)$ with $J^{PC} = 1^{-+}$ and its decay into $\rho(770)\pi$. Phys. Rev. D **105**, 012005 (2022)
2446. E.I. Ivanov et al., Observation of exotic meson production in the reaction $\pi^- p \to \eta'\pi^- p$ at 18 GeV/c. Phys. Rev. Lett. **86**, 3977–3980 (2001)
2447. V. Dorofeev, New results from VES. Frascati Phys. Ser. **15**, 3–12 (1999)
2448. Y.A. Khokhlov, Study of $X(1600)$ 1^{-+} hybrid. Nucl. Phys. A **663**, 596–599 (2000)
2449. D.V. Amelin et al., Investigation of hybrid states in the VES experiment at the Institute for High Energy Physics (Protvino). Phys. Atom. Nucl. **68**, 359–371 (2005) **(Ed. by Yu. G. Abov)**
2450. G.S. Adams et al., Amplitude analyses of the decays $\chi_{c1} \to \eta\pi^+\pi^-$ and $\chi_{c1} \to \eta'\pi^+\pi^-$. Phys. Rev. D **84**, 112009 (2011)
2451. J. Kuhn et al., Exotic meson production in the $f_1(1285)\pi^-$ system observed in the reaction $\pi^- p \to \eta\pi^+\pi^-\pi^- p$ at 18 GeV/c. Phys. Lett. B **595**, 109–117 (2004)
2452. C.A. Baker et al., Confirmation of $a_0(1450)$ and $\pi_1(1600)$ in $\bar{p}p \to \omega\pi^+\pi^-\pi^0$ at rest. Phys. Lett. B **563**, 140–149 (2003)
2453. A.R. Dzierba et al., A partial wave analysis of the $\pi^-\pi^-\pi^+$ and $\pi^-\pi^0\pi^0$ systems and the search for a $J^{PC} = 1^{-+}$ meson. Phys. Rev. D **73**, 072001 (2006)
2454. C. Adolph et al., Resonance production and $\pi\pi$ S-wave in $\pi^- + p \to \pi^-\pi^-\pi^+ + p_{\text{recoil}}$ at 190 GeV/c. Phys. Rev. D **95**, 032004 (2017)
2455. A. Zaitsev et al., Study of exotic resonances in diffractive reactions. Nucl. Phys. A **675**, 155C-160C (2000)
2456. B. Grube, Light-meson spectroscopy at lepto- and hadroproduction experiments. In: *18th International Conference on Hadron Spectroscopy and Structure (HADRON 2019)* (2020), pp. 43–49
2457. C. Adolph et al., Odd and even partial waves of $\eta\pi^-$ and $\eta'\pi^-$ in $\pi^- p \to \eta^{(\prime)}\pi^- p$ at 191 GeV/c. Phys. Lett. B **740**, 303–311 (2015) [Erratum: Phys. Lett. B 811 (2020), p. 135913]
2458. B. Kopf et al., Investigation of the lightest hybrid meson candidate with a coupled-channel analysis of $\bar{p}p$, $\pi^- p$ and $\pi\pi$ data. Eur. Phys. J. C **81**, 1056 (2021)
2459. M. Nozar et al., Search for the photoexcitation of exotic mesons in the $\pi^+\pi^+\pi^-$ system. Phys. Rev. Lett. **102**, 102002 (2009)
2460. S. Grabmüller, Cryogenic silicon detectors and analysis of Primakoff contributions to the reaction $\pi^-\text{Pb} \to \pi^-\pi^-\pi^+\text{Pb}$ at COMPASS. CERN-THESIS-2012-170. PhD thesis. Technische Universität München (2012)
2461. M. Ablikim et al., Observation of an isoscalar resonance with exotic $J^{PC} = 1^{-+}$ quantum numbers in $J/\psi \to \gamma\eta\eta'$. Phys. Rev. Lett. **129**(19), 192002 (2022)
2462. M. Ablikim et al., Partial wave analysis of $J/\psi \to \gamma\eta\eta'$. Phys. Rev. D **106**(7), 072012 (2022)
2463. C.A. Heusch, Gluonium: an unfulfilled promise of QCD? In: *Workshop on QCD: 20 Years Later*, pp. 555–574 (1992)
2464. D.L. Scharre et al., Observation of the radiative transition $\psi \to \gamma E(1420)$. Phys. Lett. B **97**, 329–332 (1980)
2465. C. Edwards et al., Observation of a pseudoscalar state at 1440-MeV in J/ψ radiative decays. Phys. Rev. Lett. **49**, 259 (1982) [Erratum: Phys. Rev. Lett. 50, 219 (1983)]
2466. C. Edwards et al., Observation of an $\eta\eta$ resonance in J/ψ radiative decays. Phys. Rev. Lett. **48**, 458 (1982)
2467. W. Dunwoodie, J/ψ radiative decay to two pseudoscalar mesons from MARK III. AIP Conf. Proc. **432**(1), 753–757 (1998). **(Ed. by S. U. Chung and H. J. Willutzki,)**
2468. F.G. Binon et al., G(1590) $G(1590)$: A Scalar Meson Decaying Into Two η Mesons. Nuovo Cim. A **78**, 313 (1983)
2469. A. Etkin et al., The reaction $\pi^- p \to \phi\phi n$ and evidence for glueballs. Phys. Rev. Lett. **49**, 1620 (1982)
2470. E. Klempt, Do $\bar{p}p$ annihilations at rest choose the eightfold way? Phys. Lett. B **308**, 179–185 (1993)
2471. E. Klempt, C. Batty, J.-M. Richard, The antinucleon-nucleon interaction at low energy?: annihilation dynamics. Phys. Rep. **413**, 197–317 (2005)
2472. K. Johnson, The M.I.T. bag model. Acta Phys. Polon. B **6**, 865 (1975)
2473. D. Robson, A basic guide for the glueball spotter. Nucl. Phys. B **130**, 328–348 (1977)
2474. H.J. Rothe, Vol. 82 (World Scientific Publishing Company, 2012), pp. 1–606
2475. Y. Chen et al., Glueball spectrum and matrix elements on anisotropic lattices. Phys. Rev. D **73**, 014516 (2006)
2476. C.J. Morningstar, M.J. Peardon, The glueball spectrum from an anisotropic lattice study. Phys. Rev. D **60**, 034509 (1999)
2477. A. Athenodorou, M. Teper, The glueball spectrum of SU(3) gauge theory in 3 + 1 dimensions. JHEP **11**, 172 (2020)
2478. E. Gregory et al., Towards the glueball spectrum from unquenched lattice QCD. JHEP **10**, 170 (2012)
2479. A.P. Szczepaniak, E.S. Swanson, The low lying glueball spectrum. Phys. Lett. B **577**, 61–66 (2003)
2480. H.-X. Chen, W. Chen, S.-L. Zhu, Two- and three-gluon glueballs of $C = +$. Phys. Rev. D **104**(9), 094050 (2021)
2481. M.Q. Huber, C.S. Fischer, H. Sanchis-Alepuz, Higher spin glueballs from functional methods. Eur. Phys. J. C **81**(12), 1083 (2021) [Erratum: Eur. Phys. J. C 82, 38 (2022)]
2482. M.Q. Huber, C.S. Fischer, H. Sanchis-Alepuz, Spectrum of scalar and pseudoscalar glueballs from functional methods. Eur. Phys. J. C **80**(11), 1077 (2020)
2483. S. Narison, Masses, decays and mixings of gluonia in QCD. Nucl. Phys. B **509**, 312–356 (1998)
2484. J. Sexton, A. Vaccarino, D. Weingarten, Coupling constants for scalar glueball decay. Nucl. Phys. B Proc. Suppl. **47**, 128–135 (1996) **(Ed. by T. D. Kieu, B. H. J. McKellar, and A. J. Guttmann)**
2485. M. Iwasaki et al., A flux tube model for glueballs. Phys. Rev. D **68**, 074007 (2003)
2486. P. Bicudo et al., The BES $f_0(1810)$: a new glueball candidate. Eur. Phys. J. C **52**, 363–374 (2007)
2487. L.-C. Gui et al., Scalar glueball in radiative J/ψ decay on the lattice. Phys. Rev. Lett. **110**(2), 021601 (2013)
2488. Y. Chen et al., Glueballs in charmonia radiative decays. PoS **LATTICE2013**, 435 (2014)
2489. L.-C. Gui et al., Study of the pseudoscalar glueball in J/ψ radiative decays. Phys. Rev. D **100**(5), 054511 (2019)
2490. E. Klempt, A.V. Sarantsev, Singlet-octet-glueball mixing of scalar mesons. Phys. Lett. B **826**, 136906 (2022)
2491. C. Amsler, F.E. Close, Evidence for a scalar glueball. Phys. Lett. B **353**, 385–390 (1995)
2492. C. Amsler, F.E. Close, Is $f_0(1500)$ a scalar glueball? Phys. Rev. D **53**, 295–311 (1996)
2493. A.V. Sarantsev et al., Scalar isoscalar mesons and the scalar glueball from radiative J/ψ decays. Phys. Lett. B **816**, 136227 (2021)

2494. A. Rodas et al., Scalar and tensor resonances in J/ψ radiative decays. Eur. Phys. J. C **82**(1), 80 (2022)
2495. E. Klempt, Scalar mesons and the fragmented glueball. Phys. Lett. B **820**, 136512 (2021)
2496. M. Ablikim et al., Amplitude analysis of the $\pi^0\pi^0$ system produced in radiative J/ψ decays. Phys. Rev. D **92**(5), 052003 (2015) [Erratum: Phys. Rev. D 93, 039906 (2016)]
2497. M. Ablikim et al., Amplitude analysis of the $K_S K_S$ system produced in radiative J/ψ decays. Phys. Rev. D **98**(7), 072003 (2018)
2498. M. Ablikim et al., Partial wave analysis of $J/\psi \to \gamma\eta'\eta'$. Phys. Rev. D **105**(7), 072002 (2022)
2499. E. Klempt et al., Scalar mesons in a relativistic quark model with instanton induced forces. Phys. Lett. B **361**, 160–166 (1995)
2500. R. Aaij et al., Measurement of resonant and CP components in $\bar{B}_s^0 \to J/\psi\pi^+\pi^-$ decays. Phys. Rev. D **89**(9), 092006 (2014)
2501. R. Aaij et al., Resonances and CP violation in B_s^0 and $\overline{B}_s^0 \to J/\psi K^+K^-$ decays in the mass region above the $\phi(1020)$. JHEP **08**, 037 (2017)
2502. A.V. Sarantsev, E. Klempt, Scalar and tensor mesons in $d\bar{d}, s\bar{s}$ and $gg \to f_0, f_2$ (2022). arXiv:2211.08791
2503. S. Ropertz, C. Hanhart, B. Kubis, A new parametrization for the scalar pion form factors. Eur. Phys. J. C **78**(12), 1000 (2018)
2504. P. Minkowski, W. Ochs, Identification of the glueballs and the scalar meson nonet of lowest mass. Eur. Phys. J. C **9**, 283–312 (1999)
2505. W. Ochs, Scalar mesons: in search of the lightest glueball. Nucl. Phys. B Proc. Suppl. **174**, 146–150 (2007) **(Ed. by Stephan Narison)**
2506. D.V. Bugg, A study in depth of $f_0(1370)$. Eur. Phys. J. C **52**, 55–74 (2007)
2507. E. Klempt et al., Search for the tensor glueball. Phys. Lett. B **830**, 137171 (2022)
2508. M. Ablikim et al., Observation of a state X(2600) in the $\pi^+\pi^-\eta'$. System in the process J/$\psi \to \gamma\pi^+\pi^-\eta'$. Phys. Rev. Lett. **129**(4), 042001 (2022)
2509. S. Dobbs et al., Comprehensive study of the radiative decays of J/ψ and ψ(2S) to pseudoscalar meson pairs, and search for glueballs. Phys. Rev. D **91**(5), 052006 (2015)
2510. J.P. Lees et al., Study of Υ(1S) radiative decays to $\pi^+\pi^-\eta'$ and γ K$^+$K$^-$. Phys. Rev. D **97**(11), 112006 (2018)
2511. R. Zhu, Factorization for radiative heavy quarkonium decays into scalar Glueball. JHEP **09**, 166 (2015)
2512. X.G. He, H.Y. Jin, J.P. Ma, Radiative decay of Υ into a scalar glueball. Phys. Rev. D **66**, 074015 (2002)
2513. B. Aubert et al. [BaBar Collaboration], Observation of a narrow meson decaying to $D_s^+\pi^0$ at a mass of 2.32 GeV/c^2. Phys. Rev. Lett. **90**, 242001 (2003)
2514. S.K. Choi et al., [Belle Collaboration], Observation of a narrow charmonium-like state in exclusive $B^\pm \to K^\pm\pi^+\pi^- J/\psi$ decays. Phys. Rev. Lett. **91**, 262001 (2003)
2515. T. Nakano et al., [LEPS Collaboration], Evidence for a narrow S =+1 baryon resonance in photoproduction from the neutron. Phys. Rev. Lett. **91**, 012002 (2003)
2516. K.H. Hicks, On the conundrum of the pentaquark. Eur. Phys. J. H **37**, 1–31 (2012)
2517. F.E. Close, P.R. Page, The D$^{*0}\bar{D}_0$ threshold resonance. Phys. Lett. B **578**, 119–123 (2004)
2518. L. Maiani et al., Diquark-antidiquarks with hidden or open charm and the nature of X(3872). Phys. Rev. D **71**, 014028 (2005)
2519. S. Dubynskiy, M.B. Voloshin, Hadro-charmonium. Phys. Lett. B **666**, 344–346 (2008)
2520. D.V. Bugg, An explanation of Belle states Z$_b$(10610) and Z$_b$(10650). EPL **96**(1), 11002 (2011)
2521. P. Pakhlov, T. Uglov, Charged charmonium-like Z$^+$(4430) from rescattering in conventional B decays. Phys. Lett. B **748**, 183–186 (2015)
2522. LHCb Collaboration, Exotic hadron naming convention (2022). arXiv:2206.15233
2523. D. Acosta et al. [CDF Collaboration], Observation of the narrow state X(3872) $\to J/\psi\pi^+\pi_-$ in $\bar{p}$p collisions at $\sqrt{s}$ = 1.96 TeV. Phys. Rev. Lett. **93**, 072001 (2004)
2524. V.M. Abazov et al. [D0 Collaboration], Observation and properties of the X(3872) decaying to $J/\psi\pi^+\pi_-$ in p$\bar{p}$ collisions at $\sqrt{s}$ = 1.96 TeV. Phys. Rev. Lett. **93**, 162002 (2004)
2525. B. Aubert et al. [BaBar Collaboration], Study of the B$^-$ $\to J/\psi K^-\pi^+\pi^-$ decay and measurement of the B$^-$ $\to$ X(3872)K$^-$ branching fraction. In: Phys. Rev. D **71**, 071103 (2005)
2526. R. Aaij et al., [LHCb Collaboration], Observation of X(3872) production in pp collisions at $\sqrt{s}$ = 7 TeV. Eur. Phys. J. C **72**, 1972 (2012)
2527. S. Chatrchyan et al., [CMS Collaboration], Measurement of the X(3872) production cross section via decays to J/$\psi\pi^+\pi^-$ in pp collisions at $\sqrt{s}$ = 7 TeV. JHEP **04**, 154 (2013)
2528. M. Aaboud et al., [ATLAS Collaboration], Measurements of ψ(2S) and X(3872) $\to J/\psi\pi^+\pi^-$ production in pp collisions at $\sqrt{s}$ = 8 TeV with the ATLAS detector. JHEP **01**, 117 (2017)
2529. M. Ablikim et al., [BESIII Collaboration], Observation of $e^+e^- \to \gamma$ X(3872) at BESIII. Phys. Rev. Lett. **112**(9), 092001 (2014)
2530. LHCb Collaboration, Modification of χ_{c1}(3872) and ψ(2S) production in pPb collisions at $\sqrt{s_{NN}}$= 8.16 TeV. Quark Matter 2022, Krakow, Poland, April 4–10, 2022 (2022)
2531. A.M. Sirunyan et al. [CMS Collaboration], Evidence for X(3872) in Pb-Pb collisions and studies of its prompt production at $\sqrt{s_{NN}}$=5.02 TeV. Phys. Rev. Lett. **128**(3), 032001 (2022)
2532. A.M. Sirunyan et al., [CMS Collaboration], Observation of the B$_s^0$ $\to X(3872)\phi$ decay. Phys. Rev. Lett. **125**(15), 152001 (2020)
2533. R. Aaij et al., [LHCb Collaboration], Observation of the $\Lambda_b^0 \to \chi_{c1}$(3872)pK$^-$ decay. JHEP **09**, 028 (2019)
2534. A. Abulencia et al., [CDF Collaboration], Measurement of the dipion mass spectrum in X(3872) $\to$ J/$\psi\pi^+\pi^-$ decays. Phys. Rev. Lett. **96**, 102002 (2006)
2535. LHCb Collaboration, Observation of sizeable ω. contribution to $\chi_{c1}(3872) \to \pi^+\pi^- J/\psi$ decays (2022). arXiv:2204.12597
2536. P. del Amo Sanchez et al. [BaBar Collaboration], Evidence for the decay X(3872) $\to J/\psi\omega$. Phys. Rev. D **82**, 011101 (2010)
2537. M. Ablikim et al., [BESIII Collaboration], Study of $e^+e^- \to \gamma\omega J/\psi$ and observation of X(3872) $\to J/\psi$. Phys. Rev. Lett. **122**(23), 232002 (2019)
2538. G. Gokhroo et al., [Belle Collaboration], Observation of a nearthreshold D$^0\bar{D}\pi^0$ enhancement in B $\to D^0\bar{D}^0\pi^0 K$ decay. Phys. Rev. Lett. **97**, 162002 (2006)
2539. T. Aushev et al. [Belle Collaboration], Study of the B $\to X(3872)(D^{*0}\bar{D}^0)K$ decay. Phys. Rev. D **81**, 031103 (2010). arXiv:2204.11295
2540. M. Ablikim et al., [BESIII Collaboration], Observation of the decay X(3872) $\to \pi^0\chi_{c1}(1P)$. Phys. Rev. Lett. **122**(20), 202001 (2019)
2541. V. Bhardwaj et al., [Belle Collaboration], Observation of X(3872) $\to J/\psi\gamma$ and search for X(3872) $\to \psi'\gamma$ in B decays. Phys. Rev. Lett. **107**, 091803 (2011)
2542. R. Aaij et al., [LHCb Collaboration], Evidence for the decay X(3872) $\to \psi(2S)\gamma$. Nucl. Phys. B **886**, 665–680 (2014)
2543. B. Aubert et al., [BaBar Collaboration], Evidence for X(3872) $\to \psi(2S)\gamma$ in B$^\pm$ $\to X(3872)K^\pm$ decays, and a study of $B \to c\bar{c}\gamma K$. Phys. Rev. Lett. **102**, 132001 (2009)
2544. M. Ablikim et al., [BESIII Collaboration], Study of open-charm decays and radiative transitions of the X(3872). Phys. Rev. Lett. **124**(24), 242001 (2020)

2545. E.S. Swanson, Diagnostic decays of the X(3872). Phys. Lett. B **598**, 197–202 (2004)
2546. J. Ferretti, G. Galatà, E. Santopinto, Quark structure of the X(3872) and $\chi_b(3P)$ resonances. Phys. Rev. D **90**(5), 054010 (2014)
2547. T. Barnes, S. Godfrey, E.S. Swanson, Higher charmonia. Phys. Rev. D **72**, 054026 (2005)
2548. B.-Q. Li, K.-T. Chao, Higher charmonia and X, Y, Z states with screened potential. Phys. Rev. D **79**, 094004 (2009)
2549. A. Abulencia et al., [CDF Collaboration], Analysis of the quantum numbers JPC of the X(3872). Phys. Rev. Lett. **98**, 132002 (2007)
2550. R. Aaij et al., [LHCb Collaboration], Determination of the X(3872) meson quantum numbers. Phys. Rev. Lett. **110**, 222001 (2013)
2551. R. Aaij et al., [LHCb Collaboration], Quantum numbers of the X(3872) state and orbital angular momentum in its $\rho^0 J\psi$ decay. Phys. Rev. D **92**(1), 011102 (2015)
2552. N.A. Tornqvist, Isospin breaking of the narrow charmonium state of Belle at 3872 MeV as a deuson. Phys. Lett. B **590**, 209–215 (2004)
2553. R. Aaij et al., [LHCb Collaboration], Study of the $\psi_2(3823)$ and $\chi_{c1}(3872)$ states in $B^+ \to \left(J\psi\pi^+\pi^-\right) K^+$ decays. JHEP **08**, 123 (2020)
2554. R. Aaij et al., [LHCb Collaboration], Study of the lineshape of the $\chi_{c1}(3872)$ state. Phys. Rev. D **102**(9), 092005 (2020)
2555. E. Braaten, H.-W. Hammer, T. Mehen, Scattering of an ultrasoft pion and the X(3872). Phys. Rev. D **82**, 034018 (2010)
2556. R. Aaij et al., [LHCb Collaboration], Observation of multiplicity dependent prompt $\chi_{c1}(3872)$ and $\psi(2S)$ production in pp collisions. Phys. Rev. Lett. **126**(9), 092001 (2021)
2557. A. Esposito et al., The nature of X(3872) from high-multiplicity pp collisions. Eur. Phys. J. C **81**(7), 669 (2021)
2558. V.M. Abazov et al. [D0 Collaboration], Studies of $X(3872)$ and $\psi(2S)$ production in $p\bar{p}$ collisions at 1.96 TeV. Phys. Rev. D **102**(7), 072005 (2020)
2559. E. Braaten, L.P. He, K. Ingles, Production of $X(3872)$ accompanied by a soft pion at hadron colliders. Phys. Rev. D **100**(9), 094006 (2019)
2560. R. Aaij et al., [LHCb Collaboration], Measurement of $\chi_{c1}(3872)$ production in proton-proton collisions at $\sqrt{s} = 8$ and 13 TeV. JHEP **01**, 131 (2022)
2561. A. Esposito et al., Observation of light nuclei at ALICE and the X(3872) conundrum. Phys. Rev. D **92**(3), 034028 (2015)
2562. J. Adam et al., [ALICE Collaboration], Production of light nuclei and anti-nuclei in pp and Pb-Pb collisions at energies available at the CERN Large Hadron Collider. Phys. Rev. C **93**(2), 024917 (2016)
2563. C. Hanhart, Y.S. Kalashnikova, A.V. Nefediev, Interplay of quark and meson degrees of freedom in a near-threshold resonance: multi-channel case. Eur. Phys. J. A **47**, 101–110 (2011)
2564. B. Aubert et al., [BaBar Collaboration], Search for a charged partner of the $X(3872)$ in the B meson decay $B \to X^- K$, $X^- \to J/\psi\pi^-\pi^0$. Phys. Rev. D **71**, 031501 (2005)
2565. S.K. et al. [Belle Collaboration], Bounds on the width, mass difference and other properties of $X(3872) \to \pi^+\pi^- J/\psi$ decays. Phys. Rev. D **84**, 052004 (2011)
2566. R. Aaij et al., [LHCb Collaboration], Study of the doubly charmed tetraquark T_{cc}^+. Nat. Commun. **13**(1), 3351 (2022)
2567. L. Maiani, A.D. Polosa, V. Riquer, The new resonances $Z_{cs}(3985)$ and $Z_{cs}(4003)$ (almost) fill two tetraquark nonets of broken $SU(3)_f$. Sci. Bull. **66**, 1616–1619 (2021)
2568. M. Ablikim et al., Observation of a near-threshold structure in the K^+ recoil-mass spectra in $e^+e^- \to K^+(D_s^- D^{*0} + D_s^{*-} D^0)$. Phys. Rev. Lett. **126**(10), 102001 (2021)
2569. R. Aaij et al., [LHCb Collaboration], Observation of new resonances decaying to $J/\psi K^+$ and $J/\psi\phi$. Phys. Rev. Lett. **127**(8), 082001 (2021)
2570. K. Terasaki, $X(3872)$ and its iso-triplet partners. Prog. Theor. Phys. **127**, 577–582 (2012)
2571. B. Aubert et al., [BaBar Collaboration], Observation of the decay $B \to J/\psi\eta K$ and search for $X(3872) \to J/\psi\eta$. Phys. Rev. Lett. **93**, 041801 (2004)
2572. T. Iwashita et al. [Belle Collaboration], Measurement of branching fractions for $B \to J/\psi\eta K$ decays and search for a narrow resonance in the $J/\psi\eta$ final state. PTEP **2014**(4), 043C01 (2014)
2573. R. Aaij et al., [LHCb Collaboration], Study of charmonium and charmonium-like contributions in $B^+ \to J/\psi\eta K^+$ decays. JHEP **22**, 046 (2020)
2574. V. Bhardwaj et al., [Belle Collaboration], Evidence of a new narrow resonance decaying to $\chi_{c1}\gamma$ in $B \to \chi_{c1}\gamma K$ Phys. Rev. Lett. **111**(3), 032001 (2013)
2575. M. Aghasyan et al., [COMPASS Collaboration], Search for muoproduction of $X(3872)$ at COMPASS and indication of a new state $\widetilde{X}(3872)$. Phys. Lett. B **783**, 334–340 (2018)
2576. S. Chatrchyan et al., [CMS Collaboration], Search for a new bottomonium state decaying to $\Upsilon(1S)\pi^+\pi^-$ in pp collisions at $\sqrt{s}$ = 8 TeV. Phys. Lett. B **727**, 57–76 (2013)
2577. G. Aad et al., [ATLAS Collaboration], Search for the X_b and other hidden-beauty states in the $\pi^+\pi^-\Upsilon(1S)$ channel at ATLAS. Phys. Lett. B **740**, 199–217 (2015)
2578. I. Adachi et al. [Belle-II Collaboration], Observation of $e^+e^- \to \omega\chi_{bJ}(1P)$ and search for $X_b \to \omega\Upsilon(1S)$ at $\sqrt{s}$ near 10.75 GeV (2022)
2579. S.K. Choi et al., [Belle Collaboration], Observation of a resonance-like structure in the $\pi^\pm\psi'$ mass distribution in exclusive $B \to K\pi^\pm\psi'$ decays. Phys. Rev. Lett. **100**, 142001 (2008)
2580. B. Aubert et al. [BaBar Collaboration]. Search for the $Z(4430)^-$ at BABAR. Phys. Rev. D **79**, 112001 (2009)
2581. R. Mizuk et al., [Belle Collaboration], Dalitz analysis of $B \to K\pi^+\psi'$ decays and the $Z(4430)^+$. Phys. Rev. D **80**, 031104 (2009)
2582. K. Chilikin et al. [Belle Collaboration].,Experimental constraints on the spin and parity of the $Z(4430)^+$. Phys. Rev. D **88**(7), 074026 (2013)
2583. R. Aaij et al., [LHCb Collaboration], Observation of the resonant character of the $Z(4430)^-$ state. Phys. Rev. Lett. **112**(22), 222002 (2014)
2584. R. Aaij et al., [LHCb Collaboration], Model-independent confirmation of the $Z(4430)^-$ state. Phys. Rev. D **92**(11), 112009 (2015)
2585. K. Chilikin et al., [Belle Collaboration], Observation of a new charged charmoniumlike state in $\bar{B}^0 \to J/\psi K^-\pi^+$ decays. Phys. Rev. D **90**(11), 112009 (2014)
2586. M. Ablikim et al., [BESIII Collaboration], Observation of $e^+e^- \to \pi^0\pi^0 h_c$ and a neutral charmoniumlike structure $Z_c(4020)^0$. Phys. Rev. Lett. **113**(21), 212002 (2014)
2587. M. Ablikim et al., [BESIII Collaboration], Observation of a neutral charmoniumlike state $Z_c(4025)^0$ in $e^+e^- \to (D^*\bar{D}^*)^0\pi^0$. Phys. Rev. Lett. **115**(18), 182002 (2015)
2588. M. Ablikim et al. [BESIII Collaboration], Observation of a charged charmoniumlike structure in $e^+e^- \to \pi^+\pi^- J/\psi$ at $\sqrt{s}$ =4.26 GeV. Phys. Rev. Lett. **110**, 252001 (2013)
2589. Z.Q. Liu et al. [Belle Collaboration], Study of $e^+e^- \to \pi^+\pi^- J/\psi$ and observation of a charged charmoniumlike state at Belle. Phys. Rev. Lett. **110**, 252002 (2013) [Erratum: Phys. Rev. Lett. 111, 019901 (2013)]
2590. M. Ablikim et al., [BESIII Collaboration], Determination of the spin and parity of the $Z_c(3900)$. Phys. Rev. Lett. **119**(7), 072001 (2017)

2591. M. Ablikim et al. [BESIII Collaboration], Observation of a charged $(D\bar{D}^*)^{\pm}$ mass peak in $e^+e^- \rightarrow \pi D\bar{D}^*$ at $\sqrt{s} = 4.26$ GeV. Phys. Rev. Lett. **112**(2), 022001 (2014)
2592. M. Ablikim et al., [BESIII Collaboration], Confirmation of a charged charmoniumlike state $Z_c(3885)^{\mp}$ in $e^+e^- \rightarrow \pi^{\pm}(D\bar{D}^*)^{\mp}$ with double D tag. Phys. Rev. D **92**(9), 092006 (2015)
2593. M. Ablikim et al., [BESIII Collaboration], Observation of a charged charmoniumlike structure $Z_c(4020)$ and search for the $Z_c(3900)$ in $e^+e^- \rightarrow \pi^+\pi^-h_c$. Phys. Rev. Lett. **111**(24), 242001 (2013)
2594. M. Ablikim et al. [BESIII Collaboration], Observation of a charged charmoniumlike structure in $e^+e^- \rightarrow (D^*\bar{D}^*)^{\pm}\pi^{\mp}$ at $\sqrt{s} = 4.26$ GeV. Phys. Rev. Lett. **112**(13), 132001 (2014)
2595. R. Mizuk et al., [Belle Collaboration], Observation of two resonance-like structures in the $\pi^+\chi_{c1}$ mass distribution in exclusive $\bar{B}^0 \rightarrow K^-\pi^+\chi_{c1}$ decays. Phys. Rev. D **78**, 072004 (2008)
2596. X.L. Wang et al., [Belle Collaboration], Measurement of $e^+e^- \rightarrow \pi^+\pi^-\psi(2S)$ via initial state radiation at Belle. Phys. Rev. D **91**, 112007 (2015)
2597. R. Aaij et al., [LHCb Collaboration], Evidence for an $\eta_c(1S)\pi^-$ resonance in $B^0 \rightarrow \eta_c(1S)K^+\pi^-$ decays. Eur. Phys. J. C **78**(12), 1019 (2018)
2598. A. Bondar et al., [Belle Collaboration], Observation of two charged bottomonium-like resonances in $\Upsilon(5S)$ decays. Phys. Rev. Lett. **108**, 122001 (2012)
2599. A. Garmash et al. [Belle Collaboration], Amplitude analysis of $e^+e^- \rightarrow \Upsilon(nS)\pi^+\pi^-$ at $\sqrt{s} = 10.865$ GeV. Phys. Rev. D **91**(7), 072003 (2015)
2600. A. Garmash et al., [Belle Collaboration], Observation of $Z_b(10610)$ and $Z_b(10650)$ decaying to B mesons. Phys. Rev. Lett. **116**(21), 212001 (2016)
2601. F.K. Guo et al., Interplay of quark and meson degrees of freedom in nearthreshold states: a practical parametrization for line shapes. Phys. Rev. D **93**(7), 074031 (2016)
2602. E.J. Eichten, C. Quigg, Mesons with beauty and charm: spectroscopy. Phys. Rev. D **49**, 5845–5856 (1994)
2603. S.S. Gershtein et al., Bc spectroscopy. Phys. Rev. D **51**, 3613–3627 (1995)
2604. F. Abe et al. [CDF Collaboration], Observation of the B_c meson in $p\bar{p}$ collisions at $\sqrt{s} = 1.8$ TeV. Phys. Rev. Lett. **81**, 2432–2437 (1998)
2605. R. Aaij et al., [LHCb Collaboration], Precision measurement of the B_c^+ meson mass. JHEP **07**, 123 (2020)
2606. R. Aaij et al., [LHCb Collaboration], Measurement of the B_c^+ meson lifetime using $B_c^+ \rightarrow J/\psi\mu^+\nu_\mu X$ decays. Eur. Phys. J. C **74**(5), 2839 (2014)
2607. R. Aaij et al., [LHCb Collaboration], Measurement of the lifetime of the B_c^+ meson using the $B_c^+ \rightarrow J/\psi\pi^+$ decay mode. Phys. Lett. B **742**, 29–37 (2015)
2608. A.M. Sirunyan et al. [CMS Collaboration], Measurement of b hadron lifetimes in pp collisions at $\sqrt{s} = 8$ TeV. Eur. Phys. J. C **78**(6), 457 (2018) [Erratum: Eur. Phys. J. C 78, 561 (2018)]
2609. A. Tumasyan et al. [CMS Collaboration], Observation of the B_c^+ meson in PbPb and pp collisions at $\sqrt{s_{NN}}$=5.02 TeV and measurement of its nuclear modification factor. Phys. Rev. Lett. **128**(25), 252301 (2022)
2610. G. Aad et al., [ATLAS Collaboration], Observation of an excited $B_c^{\pm}$ meson state with the ATLAS detector. Phys. Rev. Lett. **113**(21), 212004 (2014)
2611. A. Sirunyan et al., [CMS Collaboration], Observation of two excited B_c^+ States and measurement of the $B_c^+(2S)$ mass in pp collisions at $\sqrt{s} = 13$ TeV. Phys. Rev. Lett. **122**(13), 132001 (2019)
2612. R. Aaij et al., [LHCb Collaboration], Observation of an excited B_c^+ state. Phys. Rev. Lett. **122**(23), 232001 (2019)
2613. P.G. Ortega et al., Spectroscopy of Bc mesons and the possibility of finding exotic B_c-like structures. Eur. Phys. J. C **80**(3), 223 (2020)
2614. Y. Ikeda et al., Charmed tetraquarks T_{cc} and T_{cs} from dynamical lattice QCD simulations. Phys. Lett. B **729**, 85–90 (2014)
2615. R. Aaij et al., [LHCb Collaboration], Observation of the doubly charmed baryon Ξ_{cc}^{++}. Phys. Rev. Lett. **119**(11), 112001 (2017)
2616. R. Aaij et al., [LHCb Collaboration], Observation of the doubly charmed baryon decay $\Xi_{cc}^{++} \rightarrow \Xi_c^{\prime+}\pi^+$. JHEP **05**, 038 (2022)
2617. R. Aaij et al., [LHCb Collaboration], Measurement of the lifetime of the doubly charmed baryon Ξ_{cc}^{++}. Phys. Rev. Lett. **121**(5), 052002 (2018)
2618. R. Aaij et al., [LHCb Collaboration], Precision measurement of the Ξ_{cc}^{++} mass. JHEP **02**, 049 (2020)
2619. R. Aaij et al., [LHCb Collaboration], Observation of structure in the J/ψ-pair mass spectrum. Sci. Bull. **65**(23), 1983–1993 (2020)
2620. CMS Collaboration, Observation of new structures in the $J/\psi J/\psi$ mass spectrum in pp collisions at $\sqrt{s} = 13$ TeV. In: *CMS-PAS-BPH-21-003* (2022)
2621. ATLAS Collaboration, Observation of an excess of di-charmonium events in the four-muon final state with the ATLAS detector. In: *ATLASCONF–2022-040* (2022)
2622. H.A. Bethe, Theory of the effective range in nuclear scattering. Phys. Rev. **76**, 38–50 (1949)
2623. S. Weinberg, Evidence that the deuteron is not an elementary particle. Phys. Rev. **137**, B672–B678 (1965)
2624. J.P. Ader, J.M. Richard, P. Taxil, Do narrow heavy multiquark states exist? Phys. Rev. D **25**, 2370 (1982)
2625. M. Karliner, S. Nussinov, J.L. Rosner, $QQ\bar{Q}\bar{Q}$ states: masses, production, and decays. Phys. Rev. D **95**(3), 034011 (2017)
2626. A. Esposito et al., Hunting for tetraquarks in ultraperipheral heavy ion collisions. Phys. Rev. D **104**(11), 114029 (2021)
2627. M. Mikhasenko, L. An, R. McNulty, The determination of the spin and parity of a vector-vector system (2020). arXiv:2007.05501
2628. R. Aaij et al., [LHCb Collaboration], Search for beautiful tetraquarks in the $\Upsilon(1S)\mu^+\mu^-$ invariant-mass spectrum. JHEP **10**, 086 (2018)
2629. A.M. Sirunyan et al., [CMS Collaboration], Measurement of the Υ(1S) pair production cross section and search for resonances decaying to $\Upsilon(1S)\mu^+\mu^-$ in proton-proton collisions at $\sqrt{s} = 13$ TeV. Phys. Lett. B **808**, 135578 (2020)
2630. N. Brambilla et al., Heavy quarkonium physics (2004). arXiv:hep-ph/0412158
2631. A. Andronic et al., Heavy-flavour and quarkonium production in the LHC era: from proton-proton to heavy-ion collisions. Eur. Phys. J. C **76**(3), 107 (2016)
2632. E. Chapon et al., Prospects for quarkonium studies at the highluminosity LHC. Prog. Part. Nucl. Phys. **122**, 103906 (2022)
2633. R. Aaij et al. [LHCb Collaboration], Physics case for an LHCb Upgrade II—Opportunities in flavour physics, and beyond, in the HL-LHC era (2018). arXiv:1808.08865
2634. M. Ablikim et al., [BESIII Collaboration], Future physics programme of BESIII. Chin. Phys. C **44**(4), 040001 (2020)
2635. G. Barucca et al., PANDA Phase One. Eur. Phys. J. A **57**(6), 184 (2021)
2636. O. Brüning, A. Seryi, S. Verdú-Andrés, Electron-hadron. Colliders, EIC, LHeC and FCC-eh. Front. Phys. **10**, 886473 (2022)
2637. A. Esposito et al., From the line shape of the X(3872) to its structure. Phys. Rev. D **105**(3), L031503 (2022)
2638. N. Brambilla, A. Vairo, Quark confinement and the hadron spectrum. In: *13th Annual HUGS AT CEBAF (HUGS 98)* (1999), pp. 151–220
2639. N. Brambilla, Quark nuclear physics with heavy quarks (2022). arXiv:2204.11295

2640. M. Creutz, Gauge fixing, the transfer matrix, and confinement on a lattice. Phys. Rev. D **15**, 1128 (1977) **(Ed. by J. Julve and M. Ramón-Medrano)**
2641. N. Brambilla et al., Static energy in $(2+1+1)$-flavor lattice QCD: scale setting and charm effects. Phys. Rev. D **107**, 074503 (2023)
2642. E. Eichten et al., Charmonium: comparison with experiment. Phys. Rev. D **21**, 203 (1980)
2643. W. Lucha, F.F. Schoberl, D. Gromes, Bound states of quarks. Phys. Rep. **200**, 127–240 (1991)
2644. M. Campostrini et al., Dynamical quark effects on the hadronic spectrum and $Q\bar{Q}$ potential in lattice QCD. Phys. Lett. B **193**, 78–84 (1987)
2645. A. Barchielli, E. Montaldi, G.M. Prosperi, On a systematic derivation of the quark-anti-quark potential. Nucl. Phys. B **296**, 625 (1988) [Erratum: Nucl. Phys. B 303, 752 (1988)]
2646. N. Brambilla, P. Consoli, G.M. Prosperi, Consistent derivation of the quark-antiquark and three-quark potentials in a Wilson loop context. Phys. Rev. D **50**, 5878 (1994)
2647. P. Bicudo, N. Cardoso, M. Cardoso, Color field densities of the quarkantiquark excited flux tubes in SU(3) lattice QCD. Phys. Rev. D **98**(11), 114507 (2018)
2648. R. Yanagihara, M. Kitazawa, A study of stress-tensor distribution around the flux tube in the Abelian-Higgs model. PTEP **2019**(9), 093B02 (2019) [Erratum: PTEP 2020, 079201 (2020)]
2649. M. Baker et al., The flux tube profile in full QCD. PoS LATTICE2021, 355 (2022)
2650. K. Amemiya, H. Suganuma, Off diagonal gluon mass generation and infrared Abelian dominance in the maximally Abelian gauge in lattice QCD. Phys. Rev. D **60**, 114509 (1999)
2651. S. Sasaki, H. Suganuma, H. Toki, Dual Ginzburg-Landau theory with QCD monopoles for dynamical chiral symmetry breaking. Prog. Theor. Phys. **94**, 373–384 (1995)
2652. M. Baker, J.S. Ball, F. Zachariasen, Dual QCD. Phys. Rep. **209**, 73–127 (1991)
2653. H. Gunter Dosch, Y.A. Simonov, The area law of the Wilson loop and vacuum field correlators. Phys. Lett. B **205**, 339–344 (1988)
2654. M. Baker et al., Confinement: understanding the relation between the Wilson loop and dual theories of long distance Yang–Mills theory. Phys. Rev. D **54**, 2829–2844 (1996) [Erratum: Phys. Rev. D 56, 2475 (1997)]
2655. N. Brambilla, A. Vairo, Heavy quarkonia: Wilson area law, stochastic vacuum model and dual QCD. Phys. Rev. D **55**, 3974–3986 (1997)
2656. M. Baker et al., Field strength correlators and dual effective dynamics in QCD. Phys. Rev. D **58**, 034010 (1998)
2657. G. Perez-Nadal, J. Soto, Effective string theory constraints on the long distance behavior of the subleading potentials. Phys. Rev. D **79**, 114002 (2009)
2658. K. Nawa, H. Suganuma, T. Kojo, Baryons in holographic QCD. Phys. Rev. D **75**, 086003 (2007)
2659. J. Soto, J. Tarrús Castellà, Effective QCD string and doubly heavy baryons. Phys. Rev. D **104**, 074027 (2021)
2660. G.S. Bali, K. Schilling, C. Schlichter, Observing long color flux tubes in SU(2) lattice gauge theory. Phys. Rev. D **51**, 5165–5198 (1995)
2661. K.D. Born et al., Spin dependence of the heavy quark potential: a QCD lattice analysis. Phys. Lett. B **329**, 332–337 (1994)
2662. G.S. Bali, K. Schilling, A. Wachter, Complete $O(v^2)$ corrections to the static interquark potential from SU(3) gauge theory. Phys. Rev. D **56**, 2566–2589 (1997)
2663. A combination of preliminary electroweak measurements and constraints on the standard model (2003). hep-ex/0312023
2664. J. Koponen et al., Properties of low-lying charmonia and bottomonia from lattice QCD + QED. Rev. Mex. Fis. Suppl. **3**(3), 0308018 (2022)
2665. A. Gray et al., The Υ spectrum and m_b from full lattice QCD Phys. Rev. D **72**, 094507 (2005)
2666. J. Bulava et al., Hadron spectroscopy with lattice QCD. In: *2022 Snowmass Summer Study* (2022)
2667. D. Tims et al., Charmonium and charmed meson spectroscopy from lattice QCD. PoS LATTICE **2016**, 137 (2017)
2668. C. O'Hara et al., Towards radiative transitions in charmonium. PoS Lattice **2016**, 120 (2016)
2669. A. Bazavov et al., Determination of the QCD coupling from the static energy and the free energy. Phys. Rev. D **100**(11), 114511 (2019)
2670. A. Bazavov et al., Determination of as from the QCD static energy. Phys. Rev. D **86**, 114031 (2012)
2671. C. Ayala, X. Lobregat, A. Pineda, Determination of $\alpha(M_z)$ from an hyperasymptotic approximation to the energy of a static quark-antiquark pair. JHEP **09**, 016 (2020)
2672. H. Takaura et al., Determination of as from static QCD potential: OPE with renormalon subtraction and lattice QCD. JHEP **04**, 155 (2019)
2673. N. Brambilla et al., Lattice gauge theory computation of the static force. Phys. Rev. D **105**(5), 054514 (2022)
2674. A. Vairo, Strong coupling from the QCD static energy. Mod. Phys. Lett. A **31**(34), 1630039 (2016)
2675. Y.-Q. Ma, K. Wang, K.-T. Chao, A complete NLO calculation of the J/ψ and ψ' production at hadron colliders. Phys. Rev. D **84**, 114001 (2011)
2676. H. Han et al., $\Upsilon(nS)$ and $\chi_b(nP)$ production at hadron colliders in nonrelativistic QCD. Phys. Rev. D **94**(1), 014028 (2016)
2677. M. Butenschoen, B.A. Kniehl, World data of J/ψ production consolidate NRQCD factorization at NLO. Phys. Rev. D **84**, 051501 (2011)
2678. G.T. Bodwin et al., Fragmentation contributions to J/ψ production at the Tevatron and the LHC. Phys. Rev. Lett. **113**(2), 022001 (2014)
2679. B. Gong et al., Complete next-to-leading-order study on the yield and polarization of $\Upsilon(1S, 2S, 3S)$ at the Tevatron and LHC. Phys. Rev. Lett. **112**(3), 032001 (2014)
2680. M. Butenschoen, B.A. Kniehl, Global analysis of $\psi(2S)$ inclusive hadroproduction at next-to-leading order in nonrelativistic-QCD factorization. Phys. Rev. D **107**(3), 034003 (2023)
2681. Y.-Q. Ma, K. Wang, K.-T. Chao, $J/\psi(\psi')$ production at the Tevatron and LHC at $\mathcal{O}(\alpha_s^4 v^4)$ in nonrelativistic QCD. Phys. Rev. Lett. **106**, 042002 (2011)
2682. A. Rothkopf, T. Hatsuda, S. Sasaki, Complex heavy-quark potential at finite temperature from lattice QCD. Phys. Rev. Lett. **108**, 162001 (2012)
2683. D. Bala et al., Static quark-antiquark interactions at nonzero temperature from lattice QCD. Phys. Rev. D **105**(5), 054513 (2022)
2684. X. Yao, Open quantum systems for quarkonia. Int. J. Mod. Phys. A **36**(20), 2130010 (2021)
2685. Y. Akamatsu, Quarkonium in quark-gluon plasma: open quantum system approaches re-examined. Prog. Part. Nucl. Phys. **123**, 103932 (2022)
2686. M. Tanabashi et al., Review of particle physics. Phys. Rev. D **98**(3), 030001 (2018)
2687. N. Brambilla, Effective field theories and lattice QCD for the X Y Z frontier. PoS LATTICE **2021**, 020 (2022)
2688. N. Brambilla et al., Substructure of Multiquark Hadrons (Snowmass 2021 White Paper) (2022). arXiv:2203.16583
2689. heavy pentaquarks and tetraquarks, A. Ali, J. Sören Lange, S. Stone, Exotics. Prog. Part. Nucl. Phys. **97**, 123–198 (2017)
2690. A. Ali, L. Maiani, A.D. Polosa, *Multiquark Hadrons* (Cambridge University Press, Cambridge, 2019)
2691. R.F. Lebed, R.E. Mitchell, E.S. Swanson, Heavy-quark QCD exotica. Prog. Part. Nucl. Phys. **93**, 143–194 (2017)

2692. F.-K. Guo et al., Hadronic molecules. Rev. Mod. Phys. **90**(1), 015004 (2018) [Erratum: Rev. Mod. Phys. 94, 029901 (2022)]
2693. M.T. AlFiky, F. Gabbiani, A.A. Petrov, X(3872): hadronic molecules in effective field theory. Phys. Lett. B **640**, 238–245 (2006)
2694. E. Braaten, L. Meng, Line shapes of the X(3872). Phys. Rev. D **76**, 094028 (2007)
2695. E. Braaten, M. Kusunoki, Low-energy universality and the new charmonium resonance at 3870-MeV. Phys. Rev. D **69**, 074005 (2004)
2696. S. Fleming, T. Mehen, The decay of the $X(3872)$ into χ_{cJ} and the operator product expansion in XEFT. Phys. Rev. D **85**, 014016 (2012)
2697. R. Oncala, J. Soto, Heavy quarkonium hybrids: spectrum, decay and mixing. Phys. Rev. D **96**(1), 014004 (2017)
2698. N. Brambilla et al., QCD spin effects in the heavy hybrid potentials and spectra. Phys. Rev. D **101**(5), 054040 (2020)
2699. N. Brambilla et al., Spin structure of heavy-quark hybrids. Phys. Rev. D **99**(1), 014017 (2019) [Erratum: Phys. Rev. D 101, 099902 (2020)]
2700. C. Schlosser, M. Wagner, Hybrid static potentials in SU(3) lattice gauge theory at small quark-antiquark separations. Phys. Rev. D **105**(5), 054503 (2022)
2701. R. Bruschini, P. González, Is $\chi_{c1}(3872)$ generated from string breaking? Phys. Rev. D **105**(5), 054028 (2022)
2702. R. Bruschini, P. González, Coupled-channel meson-meson scattering in the diabatic framework. Phys. Rev. D **104**, 074025 (2021)
2703. Z. Davoudi et al., Report of the Snowmass 2021 Topical Group on Lattice Gauge Theory. In: *2022 Snowmass Summer Study* (2022)
2704. M. Sadl, S. Prelovsek, Tetraquark systems $\bar{b}b\bar{d}u$ in the static limit and lattice QCD. Phys. Rev. D **104**(11), 114503 (2021)
2705. S. Prelovsek, H. Bahtiyar, J. Petkovic, Zb tetraquark channel from lattice QCD and Born-Oppenheimer approximation. Phys. Lett. B **805**, 135467 (2020)
2706. P. Bicudo et al., Bottomonium resonances with $I = 0$ from lattice QCD correlation functions with static and light quarks. Phys. Rev. D **101**(3), 034503 (2020)
2707. P. Bicudo et al., Doubly heavy tetraquark resonances in lattice QCD. J. Phys. Conf. Ser. **1137**(1), 012039 (2019) **(Ed. by Fernando Barãoet al.)**
2708. M. Padmanath, S. Prelovsek, Signature of a doubly charm tetraquark pole in DD* scattering on the lattice. Phys. Rev. Lett. **129**(3), 032002 (2022)
2709. S. Capstick, W. Roberts, Quark models of baryon masses and decays. Prog. Part. Nucl. Phys. **45**, S241–S331 (2000)
2710. E. Klempt, J.-M. Richard, Baryon spectroscopy. Rev. Mod. Phys. **82**, 1095–1153 (2010)
2711. V. Crede, W. Roberts, Progress towards understanding baryon resonances. Rep. Prog. Phys. **76**, 076301 (2013)
2712. D.G. Ireland, E. Pasyuk, I. Strakovsky, Photoproduction reactions and non-strange baryon spectroscopy. Prog. Part. Nucl. Phys. **111**, 103752 (2020)
2713. A. Thiel, F. Afzal, Y. Wunderlich, Light baryon spectroscopy. Prog. Part. Nucl. Phys. **125**, 103949 (2022)
2714. M. Gell-Mann, Applications of Regge poles. In: *11th International Conference on High-Energy Physics*, pp. 533–542 (1962)
2715. N. Isgur, G. Karl, Ground state baryon magnetic moments. Phys. Rev. D **21**, 3175 (1980)
2716. E. Klempt, A mass formula for baryon resonances. Phys. Rev. C **66**, 058201 (2002)
2717. G. Karl, E. Obryk, On wave functions for three-body systems. Nucl. Phys. B **8**, 609–621 (1968)
2718. N. Isgur, G. Karl, Ground state baryons in a quark model with hyperfine interactions. Phys. Rev. D **20**, 1191–1194 (1979)
2719. N. Isgur, G. Karl, Positive parity excited baryons in a quark model with hyperfine interactions. Phys. Rev. D **19**, 2653 (1979) [Erratum: Phys. Rev. D 23, 817 (1981)]
2720. S. Capstick, A comparison with experimental results and outstanding issues in baryon physics. In: *Nato Advanced Study Institute: Hadron Spectroscopy and the Confinement Problem*, pp. 329–344 (1995)
2721. R. Koniuk, N. Isgur, Baryon decays in a quark model with chromodynamics. Phys. Rev. D **21**, 1868 (1980) [Erratum: Phys. Rev. D 23, 818 (1981)]
2722. J. Carlson, J.B. Kogut, V.R. Pandharipande, Hadron spectroscopy in a flux tube quark model. Phys. Rev. D **28**, 2807 (1983)
2723. S. Capstick, P.R. Page, Hybrid and conventional baryons in the flux tube model. Phys. Rev. C **66**, 065204 (2002)
2724. N. Isgur, G. Karl, R. Koniuk, Violations of SU(6) selection rules from quark hyperfine interactions. Phys. Rev. Lett. **41**, 1269 (1978) [Erratum: Phys. Rev. Lett. 45, 1738 (1980)]
2725. L.Y. Glozman, D.O. Riska, The baryon spectrum and chiral dynamics. PiN Newslett. **10**, 115–120 (1995)
2726. L.Y. Glozman, D.O. Riska, Systematics of the light and strange baryons and the symmetries of QCD (1994)
2727. L.Y. Glozman, Z. Papp, W. Plessas, Light baryons in a constituent quark model with chiral dynamics. Phys. Lett. B **381**, 311–316 (1996)
2728. Z. Dziembowski, M. Fabre de la Ripelle, G.A. Miller, Nonperturbative gluons and pseudoscalar mesons in baryon spectroscopy. Phys. Rev. C **53**, R2038–R2042 (1996)
2729. U. Löring et al., Relativistic quark models of baryons with instantaneous forces: theoretical background. Eur. Phys. J. A **10**, 309–346 (2001)
2730. U. Löring, B.C. Metsch, H.R. Petry, The light baryon spectrum in a relativistic quark model with instanton induced quark forces: the nonstrange baryon spectrum and ground states. Eur. Phys. J. A **10**, 395–446 (2001)
2731. U. Löring, B.C. Metsch, H.R. Petry, The light baryon spectrum in a relativistic quark model with instanton induced quark forces: the strange baryon spectrum. Eur. Phys. J. A **10**, 447–486 (2001)
2732. S. Migura et al., Charmed baryons in a relativistic quark model. Eur. Phys. J. A **28**, 41 (2006)
2733. G. Eichmann, C.S. Fischer, Baryon structure and reactions. Few Body Syst. **60**(1), 2 (2019) **(Ed. by R. Gothe et al.)**
2734. C.D. Roberts, Strong QCD and Dyson-Schwinger equations. IRMA Lect. Math. Theor. Phys. **21**, 355–458 (2015)
2735. D.B. Leinweber, Do quarks really form diquark clusters in the nucleon? Phys. Rev. D **47**, 5096–5103 (1993)
2736. R.G. Edwards et al., Flavor structure of the excited baryon spectra from lattice QCD. Phys. Rev. D **87**(5), 054506 (2013)
2737. D. Faiman, A.W. Hendry, Harmonic oscillator model for baryons. Phys. Rev. **173**, 1720–1729 (1968)
2738. D. Faiman, A.W. Hendry, Harmonic-oscillator model for baryons. Phys. Rev. **180**, 1609–1610 (1969)
2739. R. Bijker, F. Iachello, A. Leviatan, Strong decays of nonstrange q^3 baryons. Phys. Rev. D **55**, 2862–2873 (1997)
2740. R. Sartor, F. Stancu, Strong decay of hadrons in a semirelativistic quark model. Phys. Rev. D **34**, 3405–3413 (1986)
2741. N. Kaiser, P.B. Siegel, W. Weise, Chiral dynamics and the $S_{11}(1535)$ nucleon resonance. Phys. Lett. B **362**, 23–28 (1995)
2742. K. Nakamura et al., Review of Particle Physics. J. Phys. G **37**, 075021 (2010)
2743. V. Sokhoyan et al., High-statistics study of the reaction $\gamma p \to p\, 2\pi^0$. Eur. Phys. J. A **51**(8), 95 (2015) [Erratum: Eur. Phys. J. A 51, 187 (2015)]
2744. L.Y. Glozman, Parity doublets and chiral symmetry restoration in baryon spectrum. Phys. Lett. B **475**, 329–334 (2000)
2745. T.D. Cohen, L.Y. Glozman, Chiral multiplets versus parity doublets in highly excited baryons. Phys. Rev. D **65**, 016006 (2001)

2746. A.V. Anisovich et al., Evidence for $\Delta(2200)7/2^-$ from photoproduction and consequence for chiral-symmetry restoration at high mass. Phys. Lett. B **766**, 357–361 (2017)
2747. T. Barnes, F.E. Close, Where are hermaphrodite baryons. Phys. Lett. B **123**, 89–92 (1983)
2748. C.-K. Chow, D. Pirjol, T.-M. Yan, Hybrid baryons in large N_c QCD. Phys. Rev. D **59**, 056002 (1999)
2749. L.S. Kisslinger, Z.P. Li, Hybrid baryons via QCD sum rules. Phys. Rev. D **51**, R5986–R5989 (1995)
2750. S. Capstick, P.R. Page, Constructing hybrid baryons with flux tubes. Phys. Rev. D **60**, 111501 (1999)
2751. N. Isgur, Why N^*'s are important (2000). nucl-th/0007008
2752. N. Isgur, G. Karl, Hyperfine interactions in negative parity baryons. Phys. Lett. B **72**, 109 (1977)
2753. U.-G. Meißner, Towards a theory of baryon resonances. EPJ Web Conf. **241**, 02003 (2020) **(Ed. by R. Beck et al.)**
2754. G. Höhler et al., *Handbook of Pion Nucleon Scattering*, vol. 12N1 (1979)
2755. R.E. Cutkosky et al., Pion-nucleon partial wave amplitudes. Phys. Rev. D **20**, 2839 (1979)
2756. R.A. Arndt et al., Extended partial-wave analysis of πN scattering data. Phys. Rev. C **74**, 045205 (2006)
2757. L. Tiator et al., Eta and etaprime photoproduction on the nucleon with the isobar model EtaMAID2018. Eur. Phys. J. A **54**(12), 210 (2018)
2758. V.L. Kashevarov et al., Study of η and η' photoproduction at MAMI. Phys. Rev. Lett. **118**(21), 212001 (2017)
2759. F. Afzal et al., Observation of the $p\eta$' Cusp in the New Precise Beam Asymmetry Σ Data for $\gamma p \to p\eta$. Phys. Rev. Lett. **125**(15), 152002 (2020)
2760. J. Müller et al., New data on $\vec{\gamma}\vec{p} \to \eta p$ with polarized photons and protons and their implications for $N^* \to N\eta$ decays. Phys. Lett. B **803**, 135323 (2020)
2761. I. Senderovich et al., First measurement of the helicity asymmetry E in η photoproduction on the proton. Phys. Lett. B **755**, 64–69 (2016)
2762. S. Capstick, W. Roberts, Quasi two-body decays of nonstrange baryons. Phys. Rev. D **49**, 4570–4586 (1994)
2763. A.V. Anisovich et al., $N^* \to N\eta'$ decays from photoproduction of η' mesons off protons. Phys. Lett. B **772**, 247–252 (2017)
2764. A.V. Anisovich et al., Proton-η' interactions at threshold. Phys. Lett. B **785**, 626–630 (2018)
2765. A.V. Anisovich et al., Properties of baryon resonances from a multichannel partial wave analysis. Eur. Phys. J. A **48**, 15 (2012)
2766. M.E. McCracken et al., Differential cross section and recoil polarization measurements for the $\gamma p \to K^+\Lambda$ reaction using CLAS at Jefferson Lab. Phys. Rev. C **81**, 025201 (2010)
2767. B. Dey et al., Differential cross sections and recoil polarizations for the reaction $\gamma p \to K^+\Sigma^0$. Phys. Rev. C **82**, 025202 (2010)
2768. C.A. Paterson et al., Photoproduction of Λ and Σ^0 hyperons using linearly polarized photons. Phys. Rev. C **936**, 065201 (2016)
2769. H. Osmanovic et al., Single-energy partial wave analysis for π^0 photoproduction on the proton with fixed-t analyticity imposed. Phys. Rev. C **100**(5), 055203 (2019)
2770. H. Osmanovic et al., Single-energy partial-wave analysis for pion photoproduction with fixed-t analyticity. Phys. Rev. C **104**(3), 034605 (2021)
2771. A.V. Anisovich et al., Strong evidence for nucleon resonances near 1900 MeV. Phys. Rev. Lett. **119**(6), 062004 (2017)
2772. J. Hartmann et al., The $N(1520)3/2^-$ helicity amplitudes from an energyindependent multipole analysis based on new polarization data on photoproduction of neutral pions. Phys. Rev. Lett. **113**, 062001 (2014)
2773. A. Švarc, Y. Wunderlich, L. Tiator, Application of the single-channel, single-energy amplitude and partial-wave analysis method to $K^+\Lambda$ photoproduction. Phys. Rev. C **105**(2), 024614 (2022)
2774. G. Penner, U. Mosel, Vector meson production and nucleon resonance analysis in a coupled channel approach for energies $m_N < \sqrt{s} < 2 -$ GeV. 2. Photon induced results. Phys. Rev. C **66**, 055212 (2002)
2775. G. Penner, U. Mosel, Vector meson production and nucleon resonance analysis in a coupled channel approach for energies $m_N < \sqrt{s} < 2 -$ GeV. 1. Pion induced results and hadronic parameters. Phys. Rev. C **66**, 055211 (2002)
2776. D. Rönchen, M. Döring, U.G. Meißner, C.W. Shen, Light baryon resonances from a coupled-channel study including $\mathbf{K}\Sigma$ photoproduction. Eur. Phys. J. A **58**, 229 (2022)
2777. V. Shklyar, H. Lenske, U. Mosel, η-meson production in the resonanceenergy region. Phys. Rev. C **87**(1), 015201 (2013)
2778. B.C. Hunt, D.M. Manley, Updated determination of N^* resonance parameters using a unitary, multichannel formalism. Phys. Rev. C **99**(5), 055205 (2019)
2779. A.V. Anisovich et al., The impact of new polarization data from Bonn, Mainz and Jefferson Laboratory on $\gamma p \to \pi N$ multipoles. Eur. Phys. J. A **52**(9), 284 (2016)
2780. X. Cao, V. Shklyar, H. Lenske, Coupled-channel analysis of $K\Sigma$ production on the nucleon up to 2.0 GeV. Phys. Rev. C **88**(5), 055204 (2013)
2781. R.L. Workman et al., Unified Chew-Mandelstam SAID analysis of pion photoproduction data. Phys. Rev. C **86**, 015202 (2012)
2782. B. Julia-Diaz et al., Dynamical coupled-channel model of πN scattering in the $W \leq$ 2-GeV nucleon resonance region. Phys. Rev. C **76**, 065201 (2007)
2783. T. Seifen et al., Polarization observables in double neutral pion photoproduction (2022)
2784. H. Kamano et al., The ANL-Osaka Partial-Wave Amplitudes of πN and γN Reactions (2019)
2785. E. Gutz et al., High statistics study of the reaction $\gamma p \to p\pi^0\eta$. Eur. Phys. J. A **50**, 74 (2014)
2786. A. Thiel et al., Three-body nature of N^* and Δ^* resonances from sequential decay chains. Phys. Rev. Lett. **114**(9), 091803 (2015)
2787. H. Forkel, E. Klempt, Diquark correlations in baryon spectroscopy and holographic QCD. Phys. Lett. B **679**, 77–80 (2009)
2788. E. Klempt, Nucleon excitations. Chin. Phys. C **34**(9), 1241–1246 (2010)
2789. E. Klempt, Delta resonances, quark models, chiral symmetry and AdS/QCD. Eur. Phys. J. A **38**, 187–194 (2008) **(Ed. by Luigi Benussi et al.)**
2790. S. Prakhov et al., Measurement of $\pi^0\Lambda$, $\bar{K}^0n$, and $\pi^0\Sigma^0$ production in K^-p interactions for p_{K-} between 514 and 750-MeV/c. Phys. Rev. C **80**, 025204 (2009)
2791. K. Moriya et al., Measurement of the $\Sigma\pi$ photoproduction line shapes near the $\Lambda(1405)$. Phys. Rev. C **87**(3), 035206 (2013)
2792. H. Zhang et al., Partial-wave analysis of $\bar{K}N$ scattering reactions. Phys. Rev. C **88**(3), 035204 (2013)
2793. H. Zhang et al., Multichannel parametrization of $\bar{K}N$ scattering amplitudes and extraction of resonance parameters. Phys. Rev. C **88**(3), 035205 (2013)
2794. C. Fernandez-Ramirez et al., Coupled-channel model for $\bar{K}N$ scattering in the resonant region. Phys. Rev. D **93**(3), 034029 (2016)
2795. H. Kamano et al., Dynamical coupled-channels model of K^-p reactions: determination of partial-wave amplitudes. Phys. Rev. C **90**(6), 065204 (2014)
2796. H. Kamano et al., Dynamical coupled-channels model of K^-p reactions. II. Extraction of Λ^* and Σ^* hyperon resonances. Phys. Rev. C **92**(2), 025205 (2015) [Erratum: Phys. Rev. C 95, 049903 (2017)]
2797. M. Matveev et al., Hyperon I: partial-wave amplitudes for K$^-$p scattering. Eur. Phys. J. A **55**(10), 179 (2019)

2798. A.V. Sarantsev et al., Hyperon II: properties of excited hyperons. Eur. Phys. J. A **55**(10), 180 (2019)
2799. E. Klempt et al., Λ and Σ excitations and the quark model. Eur. Phys. J. A **56**(10), 261 (2020)
2800. Philipp Mahlberg, In: PhD-thesis Bonn, in preparation
2801. A.J.G. Hey, R.L. Kelly, Baryon spectroscopy. Phys. Rep. **96**, 71 (1983)
2802. L.Y. Glozman, Chiral multiplets of excited mesons. Phys. Lett. B **587**, 69–77 (2004)
2803. P.C. Bruns, M. Mai, U.G. Meißner, Chiral dynamics of the $S_{11}(1535)$ and $S_{11}(1650)$ resonances revisited. Phys. Lett. B **697**, 254–259 (2011)
2804. M. Mai, P.C. Bruns, U.-G. Meißner, Pion photoproduction off the proton in a gauge-invariant chiral unitary framework. Phys. Rev. D **86**, 094033 (2012)
2805. N. Kaiser, T. Waas, W. Weise, SU(3) chiral dynamics with coupled channels: eta and kaon photoproduction. Nucl. Phys. A **612**, 297–320 (1997)
2806. J.A. Oller, U.G. Meißner, Chiral dynamics in the presence of bound states: kaon nucleon interactions revisited. Phys. Lett. B **500**, 263–272 (2001)
2807. D. Jido et al., Chiral dynamics of the two $\Lambda(1405)$ states. Nucl. Phys. A **725**, 181–200 (2003)
2808. A.V. Anisovich et al., Hyperon III: $K^- p - \pi\Sigma$ coupled-channel dynamics in the $\Lambda(1405)$ mass region. Eur. Phys. J. A **56**(5), 139 (2020)
2809. P. Stoler, Baryon form-factors at high Q^2 and the transition to perturbative QCD. Phys. Rep. **226**, 103–171 (1993)
2810. V.D. Burkert, T.S.H. Lee, Electromagnetic meson production in the nucleon resonance region Int. J. Mod. Phys. E **13**, 1035–1112 (2004)
2811. I.G. Aznauryan, V.D. Burkert, Electroexcitation of nucleon resonances. Prog. Part. Nucl. Phys. **67**, 1–54 (2012)
2812. I.G. Aznauryan et al., Studies of nucleon resonance structure in exclusive meson electroproduction. Int. J. Mod. Phys. E **22**, 1330015 (2013)
2813. S.J. Brodsky et al., Strong QCD from hadron structure experiments: Newport News, VA, USA, November 4–8, 2019. Int. J. Mod. Phys. E **29**(08), 2030006 (2020)
2814. V.D. Burkert, N^* Experiments and what they tell us about strong QCD physics. EPJ Web Conf. **241**, 01004 (2020) **(Ed. by R. Beck et al.)**
2815. K.M. Watson, Some general relations between the photoproduction and scattering of pi mesons. Phys. Rev. **95**, 228–236 (1954)
2816. R.L. Walker, Phenomenological analysis of single pion photoproduction. Phys. Rev. **182**, 1729–1748 (1969)
2817. F.A. Berends, A. Donnachie, D.L. Weaver, Photoproduction and electroproduction of pions. 1. Dispersion relation theory. Nucl. Phys. B **4**, 1–53 (1967)
2818. J.J. Kelly et al., Recoil polarization measurements for neutral pion electroproduction at $Q^2 = 1$ (GeV/c)^2 near the Delta resonance. Phys. Rev. C **75**, 025201 (2007)
2819. S.S. Kamalov et al., $\gamma^* N \rightarrow \Delta$ transition form-factors: a new analysis of the JLab data on $p(e, e'p)\pi^0$ at $Q^2 = 2.8$ and 4.0 (GeV/c)^2. Phys. Rev. C **64**, 032201 (2001)
2820. T. Sato, T.S.H. Lee, Dynamical study of the Δ excitation in $N(e, e'\pi)$ reactions. Phys. Rev. C **63**, 055201 (2001)
2821. I.G. Aznauryan et al., Electroexcitation of nucleon resonances from CLAS data on single pion electroproduction. Phys. Rev. C **80**, 055203 (2009)
2822. M. Ungaro et al., Measurement of the $N \rightarrow \Delta^+(1232)$ transition at high momentum transfer by π^0 electroproduction. Phys. Rev. Lett. **97**, 112003 (2006)
2823. K. Joo et al., Q^2 dependence of quadrupole strength in the $\gamma^* p \rightarrow \Delta^+(1232) \rightarrow p\pi^0$ transition. Phys. Rev. Lett. **88**, 122001 (2002)
2824. V.V. Frolov et al., Electroproduction of the $\Delta(1232)$ resonance at high momentum transfer. Phys. Rev. Lett. **82**, 45–48 (1999)
2825. L. Tiator et al., Electromagnetic excitation of nucleon resonances. Eur. Phys. J. ST **198**, 141–170 (2011)
2826. I.G. Aznauryan, V.D. Burkert, Nucleon electromagnetic form factors and electroexcitation of low lying nucleon resonances in a light-front relativistic quark model. Phys. Rev. C **85**, 055202 (2012)
2827. I.G. Aznauryan, V.D. Burkert, Configuration mixings and light-front relativistic quark model predictions for the electroexcitation of the $\Delta(1232)3/2^+$, $N(1440)1/2^+$, and $\Delta(1600)3/2^+$ (2016)
2828. J. Segovia et al., Nucleon and Δ elastic and transition form factors. Few Body Syst. **55**, 1185–1222 (2014)
2829. C. Alexandrou et al., Nucleon to Δ electromagnetic transition form factors in lattice QCD. Phys. Rev. D **77**, 085012 (2008)
2830. K. Behrndt, M. Cvetic, General N = 1 supersymmetric flux vacua of (massive) type IIA string theory. Phys. Rev. Lett. **95**, 021601 (2005)
2831. D. Drechsel et al., A unitary isobar model for pion photoproduction and electroproduction on the proton up to 1-GeV. Nucl. Phys. A **645**, 145–174 (1999)
2832. R.D. Peccei, Chiral lagrangian model of single-pion photoproduction. Phys. Rev. **181**, 1902–1904 (1969)
2833. R.A. Arndt et al., Analysis of pion photoproduction data. Phys. Rev. C **66**, 055213 (2002)
2834. T. Sato, T.-S.H. Lee, Meson exchange model for π_N scattering and $\gamma N \rightarrow \pi N$ reaction. Phys. Rev. C **54**, 2660–2684 (1996)
2835. S.S. Kamalov, S. Nan Yang, Pion cloud and the Q^2 dependence of $\gamma^* N \leftrightarrow \Delta$ transition form-factors. Phys. Rev. Lett. **83**, 4494–4497 (1999)
2836. K. Park et al., Cross sections and beam asymmetries for $\vec{e}p \rightarrow n\pi^+$ in the nucleon resonance region for $1.7 < Q2 \leq 4.5(\mathrm{GeV})^2$. Phys. Rev. C **77**, 015208 (2008)
2837. E. Golovatch et al., First results on nucleon resonance photocouplings from the $\gamma p \rightarrow \pi^+\pi^- p$ reaction. Phys. Lett. B **788**, 371–379 (2019)
2838. V.I. Mokeev et al., Evidence for the $N'(1720)3/2^+$ nucleon resonance from combined studies of CLAS $\pi^+\pi^- p$ photo- and electroproduction data. Phys. Lett. B **805**, 135457 (2020)
2839. H.L. Anderson et al., Total cross-sections of positive pions in hydrogen. Phys. Rev. **85**, 936 (1952)
2840. W.W. Ash et al., Measurement of the $\gamma N N^*$ form factor. Phys. Lett. B **24**, 165–168 (1967)
2841. T. Bauer, S. Scherer, L. Tiator, Electromagnetic transition form factors of the Roper resonance in effective field theory. Phys. Rev. C **90**(1), 015201 (2014)
2842. V.I. Mokeev et al., Experimental study of the $P_{11}(1440)$ and $D_{13}(1520)$ resonances from CLAS data on $ep \rightarrow e'\pi^+\pi^- p'$. Phys. Rev. C **86**, 035203 (2012)
2843. D. Drechsel, S.S. Kamalov, L. Tiator, Unitary Isobar Model–MAID2007. Eur. Phys. J. A **34**, 69–97 (2007)
2844. S. Štajner et al., Beam-recoil polarization measurement of π^0 electroproduction on the proton in the region of the Roper resonance. Phys. Rev. Lett. **119**(2), 022001 (2017)
2845. H.R. Grigoryan, T.S.H. Lee, H.-U. Yee, Electromagnetic nucleon-to-delta transition in holographic QCD. Phys. Rev. D **80**, 055006 (2009)
2846. L. David Roper, Evidence for a P_{11} pion-nucleon resonance at 556 MeV. Phys. Rev. Lett. **12**, 340–342 (1964)
2847. N. Suzuki et al., Disentangling the dynamical origin of P-11 nucleon resonances. Phys. Rev. Lett. **104**, 042302 (2010)
2848. J. Segovia et al., Phys. Rev. Lett. **115**(17), 171801 (2015)
2849. N. Mathur et al., Roper resonance and $S_{11}(1535)$ from lattice QCD. Phys. Lett. B **605**, 137–143 (2005)

2850. H.-W. Lin, S.D. Cohen, Roper properties on the lattice: an update. AIP Conf. Proc. **1432**(1), 305–308 (2012) **(Ed. by Volker Burkert et al.)**
2851. V.D. Burkert, C.D. Roberts, Colloquium?: Roper resonance: toward a solution to the fifty year puzzle. Rev. Mod. Phys. **91**(1), 011003 (2019)
2852. G.F. de Teramond, S.J. Brodsky, Excited baryons in holographic QCD. AIP Conf. Proc. **1432**(1), 168–175 (2012) **(Ed. by Volker Burkert et al.)**
2853. G. Ramalho, D. Melnikov, Valence quark contributions for the $\gamma^* N \to N(1440)$ form factors from light-front holography. Phys. Rev. D **97**(3), 034037 (2018)
2854. M.M. Giannini, E. Santopinto, A. Vassallo, An overview of the hypercentral constituent quark model. Prog. Part. Nucl. Phys. **50**, 263–272 (2003) **(Ed. by A. Faessler)**
2855. K. Bermuth et al., Photoproduction of Δ and Roper resonances in the cloudy bag model. Phys. Rev. D **37**, 89–100 (1988)
2856. I.T. Obukhovsky et al., Electroproduction of the Roper resonance on the proton: the role of the three-quark core and the molecular $N\sigma$ component. Phys. Rev. D **84**, 014004 (2011)
2857. V.I. Mokeev et al., New results from the studies of the $N(1440)\frac{1}{2}^+$, $N(1520)\frac{3}{2}^-$, and $\Delta(1620)\frac{1}{2}^-$ resonances in exclusive $ep \to e'p'\pi^+\pi^-$ electroproduction with the CLAS detector. Phys. Rev. C **93**(2), 025206 (2016)
2858. V.M. Braun et al., Electroproduction of the N*(1535) resonance at large momentum transfer. Phys. Rev. Lett. **103**, 072001 (2009)
2859. I.G. Aznauryan, V. Burkert, Electroexcitation of nucleon resonances of the [70,1$^-$] multiplet in a light-front relativistic quark model. Phys. Rev. C **95**(6), 065207 (2017)
2860. I.G. Aznauryan, V.D. Burkert, Electroexcitation of the $\Delta(1232)\frac{3}{2}^+$ and $\Delta(1600)\frac{3}{2}^+$ in a light-front relativistic quark model. Phys. Rev. C **92**(3), 035211 (2015)
2861. I.V. Anikin, V.M. Braun, N. Offen, Electroproduction of the $N^*(1535)$ nucleon resonance in QCD. Phys. Rev. D **92**(1), 014018 (2015)
2862. D. Jido, M. Doering, E. Oset, Transition form factors of the N*(1535) as a dynamically generated resonance. Phys. Rev. C **77**, 065207 (2008)
2863. I.G. Aznauryan, V.D. Burkert, Extracting meson-baryon contributions to the electroexcitation of the $N(1675)\frac{5}{2}^-$ nucleon resonance. Phys. Rev. C **92**(1), 015203 (2015)
2864. E. Santopinto, M.M. Giannini, Systematic study of longitudinal and transverse helicity amplitudes in the hypercentral constituent quark model. Phys. Rev. C **86**, 065202 (2012)
2865. B. Julia-Diaz et al., Dynamical coupled-channels effects on pion photoproduction. Phys. Rev. C **77**, 045205 (2008)
2866. L. Tiator, M. Vanderhaeghen, Empirical transverse charge densities in the nucleon-to-$P_{11}(1440)$ transition. Phys. Lett. B **672**, 344–348 (2009)
2867. C.E. Carlson, M. Vanderhaeghen, Empirical transverse charge densities in the nucleon and the nucleon-to-delta transition. Phys. Rev. Lett. **100**, 032004 (2008)
2868. V.D. Burkert, N* experiments and their impact on strong QCD physics. Few Body Syst. **59**(4), 57 (2018) **(Ed. by R. Gothe et al.)**
2869. A.J.G. Hey, J. Weyers, Quarks and the helicity structure of photoproduction amplitudes. Phys. Lett. B **48**, 69–72 (1974)
2870. W.N. Cottingham, I.H. Dunbar, Baryon multipole moments in the single quark transition model. Z. Phys. C **2**, 41 (1979)
2871. V.D. Burkert et al., Single quark transition model analysis of electromagnetic nucleon resonance transitions in the [70,1-] supermultiplet. Phys. Rev. C **67**, 035204 (2003)
2872. G. Ramalho, Using the single quark transition model to predict nucleon resonance amplitudes. Phys. Rev. D **90**(3), 033010 (2014)
2873. Z. Li, V. Burkert, Z. Li, Electroproduction of the Roper resonance as a hybrid state. Phys. Rev. D **46**, 70–74 (1992)
2874. L. Lanza, A. D'Angelo, KY electroproduction at CLAS12. Nuovo Cim. C **44**(2–3), 51 (2021)
2875. C.D. Roberts, Hadron properties and Dyson–Schwinger equations. Prog. Part. Nucl. Phys. **61**, 50–65 (2008) **(Ed. by Amand Faessler)**
2876. D.S. Carman, K. Joo, V.I. Mokeev, Strong QCD insights from excited nucleon structure studies with CLAS and CLAS12. Few Body Syst. **61**(3), 29 (2020)
2877. Y. Tian et al., Exclusive π^- Electroproduction off the Neutron in Deuterium in the Resonance Region (2022)
2878. V.D. Burkert, Jefferson Lab at 12 GeV: the science program. Annu. Rev. Nucl. Part. Sci. **68**, 405–428 (2018)
2879. V.D. Burkert, L. Elouadrhiri, F.X. Girod, The pressure distribution inside the proton. Nature **557**(7705), 396–399 (2018)
2880. V.D. Burkert, L. Elouadrhiri, F.X. Girod, Determination of shear forces inside the proton (2021). arXiv:2104.02031
2881. P. Chatagnon et al., First measurement of timelike compton Scattering. Phys. Rev. Lett. **127**(26), 262501 (2021)
2882. M.V. Polyakov, P. Schweitzer, Forces inside hadrons: pressure, surface tension, mechanical radius, and all that. Int. J. Mod. Phys. A **33**(26), 1830025 (2018)
2883. U.Özdem, K. Azizi, Gravitational transition form factors of $N(1535) \to N$. Phys. Rev. D **101**(5), 054031 (2020)
2884. M.V. Polyakov, A. Tandogan, Comment on "Gravitational transition form factors of $N(1535) \to N$." Phys. Rev. D **101**(11), 118501 (2020)
2885. R. Aaij et al., Observation of $J/\psi p$ resonances consistent with pentaquark states in $\Lambda_b^0 \to J/\psi K^- p$ decays. Phys. Rev. Lett. **115**, 072001 (2015)
2886. R. Aaij et al., Observation of a narrow pentaquark state, $P_c(4312)^+$, and of two-peak structure of the $P_c(4450)^+$. Phys. Rev. Lett. **122**(22), 222001 (2019)
2887. M. Mattson et al., First observation of the doubly charmed baryon Ξ_{cc}^+. Phys. Rev. Lett. **89**, 112001 (2002)
2888. A. Ocherashvili et al., Confirmation of the double charm baryon $\Xi^+(cc)(3520)$ via its decay to pD^+K^-. Phys. Lett. B **628**, 18–24 (2005)
2889. R. Aaij et al., Search for the doubly charmed baryon Ξ_{cc}^+ in the $\Xi_c^+\pi^-\pi^+$ final state. JHEP **12**, 107 (2021)
2890. R. Aaij et al., Search for the doubly heavy baryon Ξ_{bc}^+ decaying to $J/\psi\Xi_c^+$. Chin. Phys. C **47**, 093001 (2023)
2891. B. Aubert et al., Observation of an excited charm baryon Ω_c^* decaying to $\Omega_c^0\gamma$. Phys. Rev. Lett. **97**, 232001 (2006) **(Ed. by Alexey Sissakian, Gennady Kozlov, and Elena Kolganova)**
2892. T.J. Moon et al., First determination of the spin and parity of the charmed-strange baryon $\Xi_c(2970)^+$. Phys. Rev. D **103**(11), L111101 (2021)
2893. R. Aaij et al., First observation of excited Ω_b^- states. Phys. Rev. Lett. **124**(8), 082002 (2020)
2894. H.-X. Chen et al., A review of the open charm and open bottom systems. Rep. Prog. Phys. **80**(7), 076201 (2017)
2895. D. Ebert, R.N. Faustov, V.O. Galkin, Spectroscopy and Regge trajectories of heavy baryons in the relativistic quark-diquark picture. Phys. Rev. D **84**, 014025 (2011)
2896. G.-L. Yu et al., Systematic analysis of single heavy baryons Λ_Q, Σ_Q and Ω_Q (2022)
2897. Z.-Y. Li et al., Systematic analysis of strange single heavy baryons and Ξ_c and Ξ_b^*. Chin. Phys. C **47**(7), 073105 (2023)
2898. S. Migura et al., Semileptonic decays of baryons in a relativistic quark model. Eur. Phys. J. A **28**, 55 (2006)
2899. A. Valcarce, H. Garcilazo, J. Vijande, Heavy baryon spectroscopy with relativistic kinematics. Phys. Lett. B **733**, 288–295 (2014)
2900. B. Chen, K.-W. Wei, A. Zhang, Assignments of Λ_Q and Ξ_Q baryons in the heavy quark-light diquark picture. Eur. Phys. J. A **51**, 82 (2015)

2901. R.N. Faustov, V.O. Galkin, Heavy baryon spectroscopy in the relativistic quark model. Particles **3**(1), 234–244 (2020)
2902. R. Aaij et al., Observation of five new narrow Ω_c^0 states decaying to $\Xi_c^+ K^-$. Phys. Rev. Lett. **118**(18), 182001 (2017)
2903. J. Yelton et al., Observation of excited charmed Ω_c baryons in e^+e^- collisions. Phys. Rev. D **97**(5), 051102 (2018)
2904. Y. Kim et al., Heavy baryon spectrum with chiral multiplets of scalar and vector diquarks. Phys. Rev. D **104**(5), 054012 (2021)
2905. H.-M. Yang et al., Decay properties of P-wave bottom baryons within light-cone sum rules. Eur. Phys. J. C **80**(2), 80 (2020)
2906. H. Bahtiyar et al., Charmed baryon spectrum from lattice QCD near the physical point. Phys. Rev. D **102**(5), 054513 (2020)
2907. J. Nieves, R. Pavao, Nature of the lowest-lying odd parity charmed baryon $\Lambda_c(2595)$ and $\Lambda_c(2625)$ resonances. Phys. Rev. D **101**(1), 014018 (2020)
2908. J. Hofmann, M.F.M. Lutz, D-wave baryon resonances with charm from coupled-channel dynamics. Nucl. Phys. A **776**, 17–51 (2006)
2909. W. Jia-Jun et al., Dynamically generated N^* and Λ^* resonances in the hidden charm sector around 43 GeV. Phys. Rev. C **84**, 015202 (2011)
2910. J.-J. Wu, T.S.H. Lee, B.S. Zou, Nucleon resonances with hidden charm in coupled-channel models. Phys. Rev. C **85**, 044002 (2012)
2911. H.-X. Chen et al., The hidden-charm pentaquark and tetraquark states. Phys. Rep. **639**, 1–121 (2016)
2912. S. Lars Olsen, T. Skwarnicki, D. Zieminska, Nonstandard heavy mesons and baryons: experimental evidence. Rev. Mod. Phys. **90**(1), 015003 (2018)
2913. Y.-R. Liu et al., Pentaquark and tetraquark states. Prog. Part. Nucl. Phys. **107**, 237–320 (2019)
2914. T.J. Burns, E.S. Swanson, Production of P_c states in Λ_b decays. Phys. Rev. D **106**(5), 054029 (2022)
2915. M.-L. Du et al., Revisiting the nature of the P_c pentaquarks. JHEP **08**, 157 (2021)
2916. R. Aaij et al., Evidence for a new structure in the $J/\psi p$ and $J/\psi \bar{p}$ systems in $B_s^0 \to J/\psi p \bar{p}$ decays. Phys. Rev. Lett. **128**(6), 062001 (2022)
2917. J.-Z. Wang, X. Liu, T. Matsuki, Evidence supporting the existence of $P_c(4380)^{\pm}$ from the recent measurements of $B_s \to J/\psi p \bar{p}$. Phys. Rev. D **104**(11), 114020 (2021)
2918. R. Aaij et al., Evidence of a $J/\psi \Lambda$ structure and observation of excited Ξ^- states in the $\Xi_b^- \to J/\psi \Lambda K^-$ decay. Sci. Bull. **66**, 1278–1287 (2021)
2919. C. Chen, E.S. Norella, Particle Zoo 2.0: New Tetraand Pentaquarks at LHCb. In: *CERN Seminar*, July, 5 (2022)
2920. A.M. Sirunyan et al., Study of the $\mathrm{B}^+ \to \mathrm{J}/\psi \overline{\Lambda}\mathrm{p}$ decay in proton-proton collisions at $\sqrt{s}$ = 8 TeV. JHEP **12**, 100 (2019)
2921. LHCb Collaboration, Observation of a $J/\psi \Lambda$ resonance consistent with a strange pentaquark candidate in $B^- \to J/\psi \Lambda \bar{p}$ decays. Phys. Rev. Lett. **131**, 031901 (2023)
2922. F.-K. Guo et al., How to reveal the exotic nature of the $\mathrm{P}_c(4450)$. Phys. Rev. D **92**(7), 071502 (2015)
2923. X.-H. Liu, Q. Wang, Q. Zhao, Understanding the newly observed heavy pentaquark candidates. Phys. Lett. B **757**, 231–236 (2016)
2924. M. Bayar et al., A discussion on triangle singularities in the $\Lambda_b \to J/\psi K^- p$ reaction. Phys. Rev. D **94**(7), 074039 (2016)
2925. F.-K. Guo, X.-H. Liu, S. Sakai, Threshold cusps and triangle singularities in hadronic reactions. Prog. Part. Nucl. Phys. **112**, 103757 (2020)
2926. X.-K. Dong, F.-K. Guo, B.-S. Zou, Explaining the many threshold structures in the heavy-quark hadron spectrum. Phys. Rev. Lett. **126**(15), 152001 (2021)
2927. C.-W. Shen et al., Exploring possible triangle singularities in the $\Xi_b^- \to K^- J/\psi \Lambda$ decay. Symmetry **12**(10), 1611 (2020)
2928. S.X. Nakamura, $P_c(4312)^+$, $P_c(4380)^+$, and $P_c(4457)^+$ as double triangle cusps. Phys. Rev. D **103**, 111503 (2021)
2929. M.I. Eides, V.Y. Petrov, M.V. Polyakov, Narrow nucleon-$\psi(2S)$ bound state and LHCb pentaquarks. Phys. Rev. D **93**(5), 054039 (2016)
2930. F.-K. Guo et al., Isospin breaking decays as a diagnosis of the hadronic molecular structure of the $P_c(4457)$. Phys. Rev. D **99**(9), 091501 (2019)
2931. M.-L. Du et al., Interpretation of the LHCb P_c states as hadronic molecules and hints of a narrow $P_c(4380)$. Phys. Rev. Lett. **124**(7), 072001 (2020)
2932. X. Hao et al., Recently observed P_c as molecular states and possible mixture of $P_c(4457)$. Phys. Rev. D **101**(5), 054037 (2020)
2933. R. Chen, Can the newly reported $P_{cs}(4459)$ be a strange hidden-charm $\Xi_c \bar{D}^*$ molecular pentaquark? Phys. Rev. D **103**(5), 054007 (2021)
2934. H.-X. Chen et al., Establishing the first hidden-charm pentaquark with strangeness. Eur. Phys. J. C **81**(5), 409 (2021)
2935. W. Qi, D.-Y. Chen, R. Ji, Production of $P_{cs}(4459)$ from Ξ_b decay. Chin. Phys. Lett. **38**(7), 071301 (2021)
2936. L. Jun-Xu et al., Understanding Pcs(4459) as a hadronic molecule in the $\Xi_b^- \to J/\psi \Lambda K^-$ decay. Phys. Rev. D **104**(3), 034022 (2021)
2937. J.-T. Zhu, L.-Q. Song, J. He, $P_{cs}(4459)$ and other possible molecular states from $\Xi_c^{(*)} \bar{D}^{(*)}$ and $\Xi_c' \bar{D}^{(*)}$ interactions. Phys. Rev. D **103**(7), 074007 (2021)
2938. B.B. Malabarba, K.P. Khemchandani, A. Martinez Torres, N^* states with hidden charm and a three-body nature. Eur. Phys. J. A **58**(2), 33 (2022)
2939. N. Yalikun et al., Coupled-channel effects of the $\Sigma_c^* D^{*-} \Lambda_(2595) D^-$ system and molecular nature of the P_c pentaquark states from one-boson exchange model. Phys. Rev. D **104**(9), 094039 (2021)
2940. R. Zhu, C.-F. Qiao, Pentaquark states in a diquark-triquark model. Phys. Lett. B **756**, 259–264 (2016)
2941. A. Ali, A.Y. Parkhomenko, Interpretation of the narrow $J/\psi p$ Peaks in $\Lambda_b \to J/\psi p K^-$ decay in the compact diquark model. Phys. Lett. B **793**, 365–371 (2019)
2942. P.-P. Shi, F. Huang, W.-L. Wang, Hidden charm pentaquark states in a diquark model. Eur. Phys. J. A **57**(7), 237 (2021)
2943. K. Azizi, Y. Sarac, H. Sundu, Investigation of $P_{cs}(4459)^0$ pentaquark via its strong decay to $\Lambda J/\Psi$. Phys. Rev. D **103**(9), 094033 (2021)
2944. Z.-G. Wang, Analysis of the $P_c(4312)$, $P_c(4440)$, $P_c(4457)$ and related hidden-charm pentaquark states with QCD sum rules. Int. J. Mod. Phys. A **35**(01), 2050003 (2020)
2945. Z.-G. Wang, Analysis of the $P_{cs}(4459)$ as the hidden-charm pentaquark state with QCD sum rules. Int. J. Mod. Phys. A **36**(10), 2150071 (2021)
2946. U. Mosel, Neutrino interactions with nucleons and nuclei: importance for long-baseline experiments. Annu. Rev. Nucl. Part. Sci. **66**, 171–195 (2016)
2947. D.S. Armstrong, R.D. McKeown, Parity-violating electron scattering and the electric and magnetic strange form factors of the nucleon. Annu. Rev. Nucl. Part. Sci. **62**, 337–359 (2012)
2948. J. Erler et al., Weak polarized electron scattering. Annu. Rev. Nucl. Part. Sci. **64**, 269–298 (2014)
2949. R.D. Carlini et al., Determination of the proton's weak charge and its constraints on the standard model. Annu. Rev. Nucl. Part. Sci. **69**, 191–217 (2019)
2950. F.J. Ernst, R.G. Sachs, K.C. Wali, Electromagnetic form factors of the nucleon. Phys. Rev. **119**, 1105–1114 (1960)
2951. M.N. Rosenbluthl, High energy elastic scattering of electrons on protons. Phys. Rev. **79**, 615–619 (1950)
2952. L.N. Hand, D.G. Miller, R. Wilson, Electric and magnetic formfactor of the nucleon. Rev. Mod. Phys. **35**, 335 (1963)

2953. A.I. Akhiezer, M.P. Rekalo, Polarization phenomena in electron scattering by protons in the high energy region. Sov. Phys. Dokl. **13**, 572 (1968)
2954. N. Dombey, Scattering of polarized leptons at high energy. Rev. Mod. Phys. **41**, 236–246 (1969)
2955. R.G. Arnold, C.E. Carlson, F. Gross, Polarization transfer in elastic electron scattering from nucleons and deuterons. Phys. Rev. C **23**, 363 (1981)
2956. T.W. Donnelly, A.S. Raskin, Considerations of polarization in inclusive electron scattering from nuclei. Ann. Phys. **169**, 247–351 (1986)
2957. J.C. Bernauer et al., High-precision determination of the electric and magnetic form factors of the proton. Phys. Rev. Lett. **105**, 242001 (2010)
2958. W. Xiong et al., A small proton charge radius from an electron-proton scattering experiment. Nature **575**(7781), 147–150 (2019)
2959. P.N. Kirk et al., Elastic electron-proton scattering at large four momentum transfer. Phys. Rev. D **8**, 63–91 (1973)
2960. A.F. Sill et al., Measurements of elastic electron-proton scattering at large momentum transfer. Phys. Rev. D **48**, 29–55 (1993)
2961. M.E. Christy et al., Form factors and two-photon exchange in high- energy elastic electron-proton scattering. Phys. Rev. Lett. **128**(10), 102002 (2022)
2962. H. Gao, M. Vanderhaeghen, The proton charge radius. Rev. Mod. Phys. **94**(1), 015002 (2022)
2963. T. Janssens et al., Proton form factors from elastic electron-proton scattering. Phys. Rev. **142**, 922–931 (1966)
2964. W. Bartel et al., Measurement of proton and neutron electromagnetic form-factors at squared four momentum transfers up to 3-GeV/c^2. Nucl. Phys. B **58**, 429–475 (1973)
2965. C. Berger et al., Electromagnetic form-factors of the proton at squared four momentum transfers between 10-fm^{-2} and 50-fm^{-2}. Phys. Lett. B **35**, 87–89 (1971)
2966. L.E. Price et al., Backward-angle electron-proton elastic scattering and proton electromagnetic form-factors. Phys. Rev. D **4**, 45–53 (1971)
2967. F. Borkowski et al., Electromagnetic form-factors of the proton at low four-momentum transfer. Nucl. Phys. B **93**, 461–478 (1975)
2968. R.C. Walker et al., Measurements of the proton elastic form-factors for 1-GeV/c^2 $\leq Q^2 \leq$ 3-GeV/c^2 at SLAC. Phys. Rev. D **49**, 5671–5689 (1994)
2969. L. Andivahis et al., Measurements of the electric and magnetic form-factors of the proton from Q^2 = 1.75-GeV/c^2 to 8.83-GeV/^{2}. Phys. Rev. D **50**, 5491–5517 (1994)
2970. I.A. Qattan et al., Precision Rosenbluth measurement of the proton elastic form-factors. Phys. Rev. Lett. **94**, 142301 (2005)
2971. M.E. Christy et al., Measurements of electron proton elastic cross-sections for 0.4<Q^2<5.5 (GeV/c)^2. Phys. Rev. C **70**, 015206 (2004)
2972. B.D. Milbrath et al., A Comparison of polarization observables in electron scattering from the proton and deuteron. Phys. Rev. Lett. **80**, 452–455 (1998) [Erratum: Phys. Rev. Lett. 82, 2221 (1999)]
2973. M.K. Jones et al., G_{Ep}/G_{Mp} ratio by polarization transfer in $\vec{e}p \to e\vec{p}$. Phys. Rev. Lett. **84**, 1398–1402 (2000)
2974. O. Gayou et al., Measurement of G_{Ep}/G_{Mp} in $\vec{e}p \to e\vec{p}$ to $Q^2 = 5.6$-GeV^2. Phys. Rev. Lett. **88**, 092301 (2002)
2975. V. Punjabi et al., Proton elastic form-factor ratios to Q^2 = 3.5-GeV^2 by polarization transfer. Phys. Rev. C **71**, 055202 (2005) [Erratum: Phys. Rev. C 71, 069902 (2005)]
2976. O. Gayou et al., Measurements of the elastic electromagnetic form-factor ratio $\mu_p G_{Ep}/G_{Mp}$ via polarization transfer. Phys. Rev. C **64**, 038202 (2001)
2977. T. Pospischil et al., Measurement of G_{Ep}/G_{Mp} via polarization transfer at Q^2 = 0.4-GeV/c^2. Eur. Phys. J. A **12**, 125–127 (2001)
2978. G. MacLachlan et al., The ratio of proton electromagnetic form factors via recoil polarimetry at $Q^2 = 1.13$ (GeV/c)^2. Nucl. Phys. A **764**, 261–273 (2006)
2979. A.J.R. Puckett et al., Recoil polarization measurements of the proton electromagnetic form factor ratio to Q^2 = 8.5 GeV^2. Phys. Rev. Lett. **104**, 242301 (2010)
2980. A.J.R. Puckett et al., Final analysis of proton form factor ratio data at Q^2 = 4.0, 4.8 and 5.6 GeV^2. Phys. Rev. C **85**, 045203 (2012)
2981. M. Meziane et al., Search for effects beyond the Born approximation in polarization transfer observables in $\vec{e}p$ elastic scattering. Phys. Rev. Lett. **106**, 132501 (2011)
2982. A.J.R. Puckett et al., Polarization transfer observables in elastic electron proton scattering at Q^2 =2.5, 5.2, 6.8, and 8.5 GeV^2. Phys. Rev. C 96(5), 055203 (2017) [Erratum: Phys. Rev. C 98, 019907 (2018)]
2983. G. Ron et al., Low Q^2 measurements of the proton form factor ratio $mu_p G_E/G_M$. Phys. Rev. C **84**, 055204 (2011)
2984. X. Zhan et al., High-precision measurement of the proton elastic form factor ratio $\mu_p G_E/G_M$ at low Q^2. Phys. Lett. B **705**, 59–64 (2011)
2985. M. Paolone et al., Polarization transfer in the $^4He(\vec{e}, e'\vec{p})^3H$ reaction at Q^2 = 0.8 and 1.3 (GeV/c)^2. Phys. Rev. Lett. **105**, 072001 (2010)
2986. M.K. Jones et al., Proton G_E/G_M from beam-target asymmetry. Phys. Rev. C **74**, 035201 (2006)
2987. C.B. Crawford et al., Measurement of the proton electric to magnetic form factor ratio from $^1\vec{\mathrm{H}}(\vec{e}, e'p)$. Phys. Rev. Lett. **98**, 052301 (2007)
2988. A. Liyanage et al., Proton form factor ratio $\mu_p G_E^p/\ G_M^p$ from double spin asymmetry. Phys. Rev. C **101**(3), 035206 (2020)
2989. G.G. Simon et al., Absolute electron proton cross-sections at low momentum transfer measured with a high pressure gas target system. Nucl. Phys. A **333**, 381–391 (1980)
2990. A.V. Gramolin, D.M. Nikolenko, Reanalysis of Rosenbluth measurements of the proton form factors. Phys. Rev. C **93**(5), 055201 (2016)
2991. C.F. Perdrisat, V. Punjabi, M. Vanderhaeghen, Nucleon electromagnetic form factors. Prog. Part. Nucl. Phys. **59**, 694–764 (2007)
2992. P.A.M. Guichon, M. Vanderhaeghen, How to reconcile the Rosenbluth and the polarization transfer method in the measurement of the proton form-factors. Phys. Rev. Lett. **91**, 142303 (2003)
2993. A. Afanasev et al., Two-photon exchange in elastic electron-proton scattering. Prog. Part. Nucl. Phys. **95**, 245–278 (2017)
2994. Y.-S. Tsai, Radiative corrections to electron-proton scattering. Phys. Rev. **122**, 1898–1907 (1961)
2995. L.W. Mo, Y.-S. Tsai, Radiative corrections to elastic and inelastic e p and mu p scattering. Rev. Mod. Phys. **41**, 205–235 (1969)
2996. L.C. Maximon, J.A. Tjon, Radiative corrections to electron proton scattering. Phys. Rev. C **62**, 054320 (2000)
2997. R.E. Gerasimov, V.S. Fadin, Analysis of approximations used in calculations of radiative corrections to electron-proton scattering cross section. Phys. Atom. Nucl. **78**(1), 69–91 (2015)
2998. D. Besset et al., A set of efficient estimators for polarization measurements. Nucl. Instrum. Meth. **166**, 515–520 (1979)
2999. A. Afanasev, I. Akushevich, N. Merenkov, Model independent radiative corrections in processes of polarized electron nucleon elastic scattering. Phys. Rev. D **64**, 113009 (2001)
3000. A.V. Afanasev et al., QED radiative corrections to asymmetries of elastic e p scattering in hadronic variables. Phys. Lett. B **514**, 269–278 (2001)
3001. I. Akushevich et al., Monte Carlo generator ELRADGEN 2.0 for simulation of radiative events in elastic ep-scattering of polarized particles. Comput. Phys. Commun. **183**, 1448–1467 (2012)
3002. R. Pohl et al., The size of the proton. Nature **466**, 213–216 (2010)

3003. S. Platchkov et al., Deuteron $A(Q^2)$ structure function and the neutron electric form-factor. Nucl. Phys. A **510**, 740–758 (1990)
3004. R. Schiavilla, I. Sick, Neutron charge form-factor at large q^2. Phys. Rev. C **64**, 041002 (2001)
3005. S. Galster et al., Elastic electron-deuteron scattering and the electric neutron form factor at four-momentum transfers 5fm$^{-2}<q^2<$14fm^{-2}. Nucl. Phys. B **32**, 221–237 (1971)
3006. G.G. Simon, C. Schmitt, V.H. Walther, Elastic electric and magnetic eD scattering at low momentum transfer. Nucl. Phys. A **364**, 285–296 (1981)
3007. E. Geis et al., The charge form factor of the neutron at low momentum transfer from the ^{2}H-$(\vec{e}, e'n)p$ reaction. Phys. Rev. Lett. **101**, 042501 (2008)
3008. G. Warren et al., Measurement of the electric form-factor of the neutron at $Q^2=0.5$ and $1.0\ GeV^2/c^2$. Phys. Rev. Lett. **92**, 042301 (2004)
3009. H. Zhu et al., A measurement of the electric form-factor of the neutron through $\vec{d}(\vec{e}, e'n)p$ at Q^2 =0.5 (GeV/c)^2. Phys. Rev. Lett. **87**, 081801 (2001)
3010. I. Passchier et al., The charge form-factor of the neutron from the reaction polarized ^{2}H$\vec{e}, e'n)p$. Phys. Rev. Lett. **82**, 4988–4991 (1999)
3011. S. Riordan et al., Measurements of the electric form factor of the neutron up to $Q^2 = 3.4GeV^2$ using the reaction $^3\vec{\mathrm{He}}(\vec{e}, e'n)pp$. Phys. Rev. Lett. **105**, 262302 (2010)
3012. V. Sulkosky et al., Extraction of the neutron electric form factor from measurements of inclusive double spin asymmetries. Phys. Rev. C **96**(6), 065206 (2017)
3013. B.S. Schlimme et al., Measurement of the neutron electric to magnetic form factor ratio at $Q^2 = 1.58GeV^2$ using the reaction $^3\vec{He}(\vec{e}, e'n)pp$. Phys. Rev. Lett. **111**(13), 132504 (2013)
3014. J. Bermuth et al., The neutron charge form-factor and target analyzing powers from polarized-He-3 (polarized-e, e-prime n) scattering. Phys. Lett. B **564**, 199–204 (2003)
3015. J. Becker et al., Determination of the neutron electric form-factor from the reaction ^{3}He $(e, e'n)$ at medium momentum transfer. Eur. Phys. J. A **6**, 329–344 (1999)
3016. D.I. Glazier et al., Measurement of the electric form-factor of the neutron at Q^2 = 0.3 (GeV/c)^2 to 0.8 (GeV/c)^2. Eur. Phys. J. A **24**, 101–109 (2005)
3017. C. Herberg et al., Determination of the neutron electric form-factor in the $D(e, e'n)p$ reaction and the influence of nuclear binding. Eur. Phys. J. A **5**, 131–135 (1999)
3018. B. Plaster et al., Measurements of the neutron electric to magnetic form-factor ratio G_{En}/G_{Mn} via the ^{2}H$(\vec{e}, e'\vec{n})^1$H reaction to Q^2 = 1.45 (GeV/c)^2. Phys. Rev. C **73**, 025205 (2006)
3019. L. Durand, Inelastic electron-deuteron scattering cross sections at high energies. Phys. Rev. **115**, 1020–1038 (1959)
3020. J. Lachniet et al., A precise measurement of the neutron magnetic form factor G_M^n in the few-GeV^2 region. Phys. Rev. Lett. **102**, 192001 (2009)
3021. H. Anklin et al., Precision measurement of the neutron magnetic form-factor. Phys. Lett. B **336**, 313–318 (1994)
3022. H. Anklin et al., Precise measurements of the neutron magnetic form-factor. Phys. Lett. B **428**, 248–253 (1998)
3023. E.E.W. Bruins et al., Measurement of the neutron magnetic form-factor. Phys. Rev. Lett. **75**, 21–24 (1995)
3024. G. Kubon et al., Precise neutron magnetic form-factors. Phys. Lett. B **524**, 26–32 (2002)
3025. W. Xu et al., The transverse asymmetry $A_{T'}$ from quasielastic polarized ^{3}He $(\vec{e}, e')$ process and the neutron magnetic form-factor. Phys. Rev. Lett. **85**, 2900–2904 (2000)
3026. W. Xu et al., PWIA extraction of the neutron magnetic form-factor from quasielastic $^3\vec{\mathrm{He}}(\vec{e}, e')$ at Q^2 = 0.3-(GeV/c)^2 − 0.6-(GeV/c)^2. Phys. Rev. C **67**, 012201 (2003)
3027. B. Anderson et al., Extraction of the Neutron Magnetic Form Factor from Quasi-elastic $^3\vec{He}(\vec{e}, e')$ at Q^2 = 0.1 - 0.6 (GeV/c)^2. Phys. Rev. C **75**, 034003 (2007)
3028. H. Gao et al., Measurement of the neutron magnetic form-factor from inclusive quasielastic scattering of polarized electrons from polarized ^{3}He. Phys. Rev. C **50**, R546–R549 (1994)
3029. A. Lung et al., Measurements of the electric and magnetic form-factors of the neutron from Q^2 = 1.75-GeV/c^2 to 4-GeV/c^2. Phys. Rev. Lett. **70**, 718–721 (1993)
3030. S. Rock et al., Measurement of elastic electron - neutron scattering and inelastic electron-deuteron scattering cross-sections at high momentum transfer. Phys. Rev. D **46**, 24–44 (1992)
3031. P. Markowitz et al., Measurement of the magnetic form factor of the neutron. Phys. Rev. C **48**(1), R5–R9 (1993)
3032. E.L. Lomon, Effect of recent R(p) and R(n) measurements on extended Gari-Krumpelmann model fits to nucleon electromagnetic form-factors. Phys. Rev. C **66**, 045501 (2002)
3033. M. Diehl et al., Generalized parton distributions from nucleon form-factor data. Eur. Phys. J. C **39**, 1–39 (2005)
3034. F. Gross, G. Ramalho, M.T. Pena, A pure S-wave covariant model for the nucleon. Phys. Rev. C **77**, 015202 (2008)
3035. I.C. Cloet, G.A. Miller, Nucleon form factors and spin content in a quark-diquark model with a pion cloud. Phys. Rev. C **86**, 015208 (2012)
3036. A.J. Chambers et al., Electromagnetic form factors at large momenta from lattice QCD. Phys. Rev. D **96**(11), 114509 (2017)
3037. M. Batelaan et al., Nucleon form factors from the Feynman–Hellmann method in lattice QCD. PoS **LATTICE2021**, 426 (2022)
3038. C.H. Nathan Isgur, L. Smith, The applicability of perturbative QCD to exclusive processes. Nucl. Phys. B **317**, 526–572 (1989)
3039. C.H. Nathan Isgur, L. Smith, Perturbative QCD inexclusive processes. Phys. Lett. B **217**, 535–538 (1989)
3040. A.V. Belitsky, X. Ji, F. Yuan, A perturbative QCD analysis of the nucleon's Pauli form-factor $F_2(Q^2)$. Phys. Rev. Lett. **91**, 092003 (2003)
3041. G.D. Cates et al., Flavor decomposition of the elastic nucleon electromagnetic form factors. Phys. Rev. Lett. **106**, 252003 (2011)
3042. E.L. Lomon, S. Pacetti, Time-like and space-like electromagnetic form factors of nucleons, a unified description. Phys. Rev. D **85**, 113004 (2012) [Erratum: Phys. Rev. D 86, 039901 (2012)]
3043. Y.-H. Lin, H.-W. Hammer, U.-G. Meißner, Dispersion-theoretical analysis of the electromagnetic form factors of the nucleon: past, present and future. Eur. Phys. J. A **57**(8), 255 (2021)
3044. J.J. Kelly, Nucleon charge and magnetization densities from Sachs form-factors. Phys. Rev. C **66**, 065203 (2002)
3045. G.A. Miller, Charge density of the neutron. Phys. Rev. Lett. **99**, 112001 (2007)
3046. G.A. Miller, Transverse charge densities. Annu. Rev. Nucl. Part. Sci. **60**, 1–25 (2010)
3047. S. Venkat et al., Realistic transverse images of the proton charge and magnetic densities. Phys. Rev. C **83**, 015203 (2011)
3048. M. Guidal et al., Nucleon form-factors from generalized parton distributions. Phys. Rev. D **72**, 054013 (2005)
3049. M. Diehl, P. Kroll, Nucleon form factors, generalized parton distributions and quark angular momentum. Eur. Phys. J. C **73**(4), 2397 (2013)
3050. V. Punjabi et al., The structure of the nucleon: elastic electromagnetic form factors. Eur. Phys. J. A **51**, 79 (2015)
3051. A. Accardi et al., An experimental program with high duty-cycle polarized and unpolarized positron beams at Jefferson Lab. Eur. Phys. J. A **57**(8), 261 (2021)
3052. B. Schmookler et al., High Q^2 electron-proton elastic scattering at the future electron-ion collider (2022). arXiv:2207.04378
3053. A. Bogacz et al., 20–24 GeV FFA CEBAF energy upgrade. JACoW IPAC **2021**, 715 (2021)

3054. J. Blumlein, The theory of deeply inelastic scattering. Prog. Part. Nucl. Phys. **69**, 28–84 (2013)
3055. P. Jimenez-Delgado, W. Melnitchouk, J.F. Owens, Parton momentum and helicity distributions in the nucleon. J. Phys. G **40**, 093102 (2013)
3056. S. Forte, G. Watt, Progress in the determination of the partonic structure of the proton. Annu. Rev. Nucl. Part. Sci. **63**, 291–328 (2013)
3057. J. Gao, L. Harland-Lang, J. Rojo, The structure of the proton in the LHC precision era. Phys. Rep. **742**, 1–121 (2018)
3058. J.J. Ethier, E.R. Nocera, Parton distributions in nucleons and nuclei. Annu. Rev. Nucl. Part. Sci. **70**, 43–76 (2020)
3059. H. Abramowicz et al., Combination of measurements of inclusive deep inelastic $e^{\pm}p$ scattering cross sections and QCD analysis of HERA data. Eur. Phys. J. C **75**(12), 580 (2015)
3060. G. Aad et al., Determination of the strange quark density of the proton from ATLAS measurements of the $W \to \ell\nu$ and $Z \to \ell\ell$ cross sections. Phys. Rev. Lett. **109**, 012001 (2012)
3061. M. Aaboud et al., Precision measurement and interpretation of inclusive W^+, W^- and Z/γ^* production cross sections with the ATLAS detector. Eur. Phys. J. C **77**(6), 367 (2017)
3062. N. Sato et al., Strange quark suppression from a simultaneous Monte Carlo analysis of parton distributions and fragmentation functions. Phys. Rev. D **101**(7), 074020 (2020)
3063. D. d'Enterria, J. Rojo, Quantitative constraints on the gluon distribution function in the proton from collider isolated-photon data. Nucl. Phys. B **860**, 311–338 (2012)
3064. D.W. Duke, J.F. Owens, Q^2 dependent parametrizations of parton distribution functions. Phys. Rev. D **30**, 49–54 (1984)
3065. J.G. Morfin, W.-K. Tung, Parton distributions from a global QCD analysis of deep inelastic scattering and lepton pair production. Z. Phys. C **52**, 13–30 (1991)
3066. S. Forte et al., Neural network parametrization of deep inelastic structure functions. JHEP **05**, 062 (2002)
3067. H. Honkanen et al., New avenue to the parton distribution functions: self-organizing maps. Phys. Rev. D **79**, 034022 (2009)
3068. F.E. Close, R.G. Roberts, Consistent analysis of the spin content of the nucleon. Phys. Lett. B **316**, 165–171 (1993)
3069. W. Melnitchouk, R. Ent, C. Keppel, Quark-hadron duality in electron scattering. Phys. Rep. **406**, 127–301 (2005)
3070. H. Howard Georgi, D. Politzer, Freedom at moderate energies: masses in color dynamics. Phys. Rev. D **14**, 1829 (1976)
3071. R. Keith Ellis, W. Furmanski, R. Petronzio, Unraveling higher twists. Nucl. Phys. **B212**, 29 (1983)
3072. M.A.G. Aivazis, F.I. Olness, W.-K. Tung, Leptoproduction of heavy quarks. 1. General formalism and kinematics of charged current and neutral current production processes. Phys. Rev. D **50**, 3085–3101 (1994)
3073. I. Schienbein et al., A review of target mass corrections. J. Phys. G **35**, 053101 (2008)
3074. E. Moffat et al., What does kinematical target mass sensitivity in DIS reveal about hadron structure. Phys. Rev. D **99**(9), 096008 (2019)
3075. J.J. Aubert et al., Measurement of the deuteron structure function $F2$ and a comparison of proton and neutron structure. Phys. Lett. B **123**, 123–126 (1983)
3076. D.F. Geesaman, K. Saito, A. William Thomas, The nuclear EMC effect. Annu. Rev. Nucl. Part. Sci. **45**, 337–390 (1995)
3077. P.R. Norton, The EMC effect. Rep. Prog. Phys. **66**, 1253–1297 (2003)
3078. W. Melnitchouk, A.W. Schreiber, A. William Thomas, Deep inelastic scattering from off-shell nucleons. Phys. Rev. D **49**, 1183–1198 (1994)
3079. S.A. Kulagin, G. Piller, W. Weise, Shadowing, binding and off-shell effects in nuclear deep inelastic scattering. Phys. Rev. C **50**, 1154–1169 (1994)
3080. A. Sergey Kulagin, R. Petti, Global study of nuclear structure functions. Nucl. Phys. A **765**, 126–187 (2006)
3081. W. Melnitchouk, A. William Thomas, Neutron/proton structure function ratio at large x. Phys. Lett. B **377**, 11–17 (1996)
3082. J.F. Owens, A. Accardi, W. Melnitchouk, Global parton distributions with nuclear and finite-Q^2 corrections. Phys. Rev. D **87**(9), 094012 (2013)
3083. A.D. Martin et al., Extended parameterisations for MSTW PDFs and their effect on lepton charge asymmetry from W decays. Eur. Phys. J. C **73**(2), 2318 (2013)
3084. A. Accardi et al., Constraints on large-x parton distributions from new weak boson production and deep-inelastic scattering data. Phys. Rev. D **93**(11), 114017 (2016)
3085. S.I. Alekhin, S.A. Kulagin, R. Petti, Nuclear effects in the deuteron and constraints on the d/u ratio. Phys. Rev. D **96**(5), 054005 (2017)
3086. C. Cocuzza et al., Isovector EMC effect from global QCD analysis with MARATHON data. Phys. Rev. Lett. **127**(24), 242001 (2021)
3087. A.O. Bazarko et al., Determination of the strange quark content of the nucleon from a next-to-leading order QCD analysis of neutrino charm production. Z. Phys. C **65**, 189–198 (1995)
3088. D. Mason et al., Measurement of the nucleon strange-antistrange asymmetry at next-to-leading order in QCD from NuTeV dimuon data. Phys. Rev. Lett. **99**, 192001 (2007)
3089. S.A. Kulagin, R. Petti, Neutrino inelastic scattering off nuclei. Phys. Rev. D **76**, 094023 (2007)
3090. N. Kalantarians, C. Keppel, M. Eric Christy, Comparison of the structure function F2 as measured by charged lepton and neutrino scattering from iron targets. Phys. Rev. C **96**(3), 032201 (2017)
3091. A. Accardi et al., Parton propagation and fragmentation in QCD matter. Riv. Nuovo Cim. **32**(9–10), 439–554 (2009)
3092. J. Pumplin et al., Uncertainties of predictions from parton distribution functions. 2. The Hessian method. Phys. Rev. D **65**, 014013 (2001)
3093. J. Pumplin et al., New generation of parton distributions with uncertainties from global QCD analysis. JHEP **07**, 012 (2002)
3094. N.T. Hunt-Smith et al., On the determination of uncertainties in parton densities (2022)
3095. L. Del Debbio et al., Unbiased determination of the proton structure function F_2^p with faithful uncertainty estimation. JHEP **03**, 080 (2005)
3096. L. Del Debbio et al., Neural network determination of parton distributions: the nonsinglet case. JHEP **03**, 039 (2007)
3097. R.D. Ball et al., A determination of parton distributions with faithful uncertainty estimation. Nucl. Phys. B **809**, 1–63 (2009) [Erratum: Nucl. Phys. B 816, 293 (2009)]
3098. A. Accardi et al., A critical appraisal and evaluation of modern PDFs. Eur. Phys. J. C **76**(8), 471 (2016)
3099. J. Butterworth et al., PDF4LHC recommendations for LHC Run II. J. Phys. G **43**, 023001 (2016)
3100. R.D. Ball et al., The path to proton structure at 1% accuracy. Eur. Phys. J. C **82**(5), 428 (2022)
3101. J. McGowan et al., Approximate N^3LO parton distribution functions with theoretical uncertainties: MSHT20aN^3LO PDFs. Eur. Phys. J. C **83**(3), 185 (2023) [Erratum: Eur. Phys. J. C 83, 302 (2023)]
3102. S. Alekhin et al., Parton distribution functions, α_s, and heavy-quark masses for LHC Run II. Phys. Rev. D **96**(1), 014011 (2017)
3103. P. Jimenez-Delgado, E. Reya, Delineating parton distributions and the strong coupling. Phys. Rev. D **89**(7), 074049 (2014)
3104. C. Cocuzza et al., Bayesian Monte Carlo extraction of the sea asymmetry with SeaQuest and STAR data. Phys. Rev. D **104**(7), 074031 (2021)
3105. F.E. Close, νW_2 at small ω' and resonance form-factors in a quark model with broken su (6). Phys. Lett. B **43**, 422–426 (1973)

3106. R.J. Holt, C.D. Roberts, Distribution functions of the nucleon and pion in the valence region. Rev. Mod. Phys. **82**, 2991–3044 (2010)
3107. L.T. Brady et al., Impact of PDF uncertainties at large x on heavy boson production. JHEP **06**, 019 (2012)
3108. N. Baillie et al., Measurement of the neutron F2 structure function via spectator tagging with CLAS. Phys. Rev. Lett. **108**, 142001 (2012) [Erratum: Phys. Rev. Lett. 108, 199902 (2012)]
3109. S. Tkachenko et al., Measurement of the structure function of the nearly free neutron using spectator tagging in inelastic ^{2}H(e, e'p)X scattering with CLAS. Phys. Rev. C **89**, 045206 (2014) [Addendum: Phys. Rev. C 90, 059901 (2014)]
3110. T. Aaltonen et al., Direct measurement of the W production charge asymmetry in $p\bar{p}$ collisions at $\sqrt{s} = 1.96$ TeV. Phys. Rev. Lett. **102**, 181801 (2009)
3111. V. Mukhamedovich Abazov et al., Measurement of the W boson production charge asymmetry in $p\bar{p} \to W+X \to e\nu+X$ Events at $\sqrt{s} = 1.96$ TeV. Phys. Rev. Lett. **112**(15), 151803 (2014) [Erratum: Phys. Rev. Lett. 114, 049901 (2015)]
3112. T. Antero Aaltonen et al., Measurement of $d\sigma/dy$ of Drell-Yan e^+e^- pairs in the Z mass region from $p\bar{p}$ collisions at $\sqrt{s} = 1.96$ TeV. Phys. Lett. B **692**, 232–239 (2010)
3113. M. Arneodo et al., Measurement of the proton and the deuteron structure functions, F_2^p and F_2^d). Phys. Lett. B **364**, 107–115 (1995)
3114. M. Arneodo et al., Measurement of the proton and deuteron structure functions, F_2^p and F_2^d, and of the ratio σ_L/σ_T. Nucl. Phys. B **483**, 3–43 (1997)
3115. J. Adam et al., Measurements of W and Z/γ^* cross sections and their ratios in p+p collisions at RHIC. Phys. Rev. D **103**(1), 012001 (2021)
3116. R.S. Towell et al., Improved measurement of the $\bar{d}/\bar{u}$ asymmetry in the nucleon sea. Phys. Rev. D **64**, 052002 (2001)
3117. J. Dove et al., The asymmetry of antimatter in the proton. Nature **590**(7847), 561–565 (2021) [Erratum: Nature 604, E26 (2022)]
3118. A. William Thomas, A limit on the pionic component of the nucleon through SU(3) flavor breaking in the sea. Phys. Lett. B **126**, 97–100 (1983)
3119. J. Speth, A. William Thomas, Mesonic contributions to the spin and flavor structure of the nucleon. Adv. Nucl. Phys. **24**, 83–149 (1997) **(Ed. by John W. Negele and E. Vogt)**
3120. Y. Salamu et al., $\bar{d} - \bar{u}$ asymmetry in the proton in chiral effective theory. Phys. Rev. Lett. **114**, 122001 (2015)
3121. E. Leader, A.V. Sidorov, D.B. Stamenov, Determination of polarized PDFs from a QCD analysis of inclusive and semi inclusive deep inelastic scattering data. Phys. Rev. D **82**, 114018 (2010)
3122. E. Leader, A.V. Sidorov, D.B. Stamenov, A Possible Resolution of the Strange Quark Polarization Puzzle? Phys. Rev. D **84**, 014002 (2011)
3123. N. Sato et al., First Monte Carlo analysis of fragmentation functions from single-inclusive e^+e^- annihilation. Phys. Rev. D **94**(11), 114004 (2016)
3124. G. Aad et al., Determination of the parton distribution functions of the proton from ATLAS measurements of differential W and Z boson production in association with jets. JHEP **07**, 223 (2021)
3125. A.I. Signal, A. William Thomas, Possible strength of the nonperturbative strange sea of the nucleon. Phys. Lett. B **191**, 205 (1987)
3126. S. Catani et al., Perturbative generation of a strange-quark asymmetry in the nucleon. Phys. Rev. Lett. **93**, 152003 (2004)
3127. X.G. Wang et al., Strange quark asymmetry in the proton in chiral effective theory. Phys. Rev. D **94**(9), 094035 (2016)
3128. Y. Salamu et al., Parton distributions from nonlocal chiral SU(3) effective theory: flavor asymmetries. Phys. Rev. D **100**(9), 094026 (2019)
3129. X.G. Wang et al., Strange quark helicity in the proton from chiral effective theory. Phys. Rev. D **102**(11), 116020 (2020)
3130. F. He et al., Helicity-dependent distribution of strange quarks in the proton from nonlocal chiral effective theory. Phys. Rev. D **105**(9), 094007 (2022)
3131. E.C. Aschenauer et al., Semi-inclusive deep-inelastic scattering, parton distributions and fragmentation functions at a future electron-ion collider. Phys. Rev. D **99**(9), 094004 (2019)
3132. G. Aad et al., Measurement of the production of a W boson in association with a charm quark in pp collisions at $\sqrt{s} = 7$TeV with the ATLAS detector. JHEP **05**, 068 (2014)
3133. S. Chatrchyan et al., Measurement of associated W + charm production in pp collisions at $\sqrt{s} = 7$ TeV. JHEP **02**, 013 (2014)
3134. S.J. Brodsky et al., The intrinsic charm of the proton. Phys. Lett. B **93**, 451–455 (1980)
3135. F.S. Navarra et al., On the intrinsic charm component of the nucleon. Phys. Rev. D **54**, 842–846 (1996)
3136. W. Melnitchouk, A. William Thomas, HERA anomaly and hard charm in the nucleon. Phys. Lett. B **414**, 134–139 (1997)
3137. J. Pumplin, H.L. Lai, W.K. Tung, The charm parton content of the nucleon. Phys. Rev. D **75**, 054029 (2007)
3138. T.J. Hobbs, J.T. Londergan, W. Melnitchouk, Phenomenology of nonperturbative charm in the nucleon. Phys. Rev. D **89**, 074008 (2014)
3139. P. Jimenez-Delgado et al., "New limits on intrinsic charm in the nucleon from global analysis of parton distributions". Phys. Rev. Lett. **114**(8), 082002 (2015)
3140. P. Jimenez-Delgado et al., Reply to Comment on "New limits on intrinsic charm in the nucleon from global analysis of parton distributions." Phys. Rev. Lett. **116**(1), 019102 (2016)
3141. R.D. Ball et al., A determination of the charm content of the proton. Eur. Phys. J. C **76**(11), 647 (2016)
3142. R.D. Ball et al., Evidence for intrinsic charm quarks in the proton. Nature **608**, 483–487 (2022)
3143. M. Guzzi et al., The persistent nonperturbative charm enigma. Phys. Lett. B **843**, 137975 (2023)
3144. D. de Florian et al., Evidence for polarization of gluons in the proton. Phys. Rev. Lett. **113**(1), 012001 (2014)
3145. D. De Florian et al., Monte Carlo sampling variant of the DSSV14 set of helicity parton densities. Phys. Rev. D **100**(11), 114027 (2019)
3146. R.D. Ball et al., Unbiased determination of polarized parton distributions and their uncertainties. Nucl. Phys. B **874**, 36–84 (2013)
3147. C. Cocuzza et al., Polarized antimatter in the proton from a global QCD analysis. Phys. Rev. D **106**(3), L031502 (2022)
3148. J. Blumlein, H. Bottcher, QCD analysis of polarized deep inelastic scattering data. Nucl. Phys. B **841**, 205–230 (2010)
3149. A.N. Khorramian et al., Polarized deeply inelastic scattering (DIS) structure functions for nucleons and nuclei. Phys. Rev. D **83**, 054017 (2011)
3150. M. Hirai, S. Kumano, N. Saito, Determination of polarized parton distribution functions with recent data on polarization asymmetries. Phys. Rev. D **74**, 014015 (2006)
3151. A. Candido, S. Forte, F. Hekhorn, Can $\overline{\text{MS}}$ parton distributions be negative? JHEP **11**, 129 (2020)
3152. J. Collins, T.C. Rogers, N. Sato, Positivity and renormalization of parton densities. Phys. Rev. D **105**(7), 076010 (2022)
3153. P. Jimenez-Delgado, A. Accardi, W. Melnitchouk, Impact of hadronic and nuclear corrections on global analysis of spin-dependent parton distributions. Phys. Rev. D **89**(3), 034025 (2014)
3154. J. Adam et al., Measurement of the longitudinal spin asymmetries for weak boson production in proton-proton collisions at $\sqrt{s} = 510$ GeV. Phys. Rev. D **99**(5), 051102 (2019)
3155. A. Adare et al., Measurement of parity-violating spin asymmetries in $W^\pm$ production at midrapidity in longitudinally polarized $p + p$ collisions. Phys. Rev. D **93**(5), 051103 (2016)

3156. A. Adare et al., Cross section and longitudinal single-spin asymmetry A_L for forward $W^{\pm} \to \mu^{\pm}\nu$ production in polarized $p+p$ collisions at $\sqrt{s} = 510$ GeV. Phys. Rev. D **98**(3), 032007 (2018)
3157. A.W. Schreiber, A.I. Signal, A. William Thomas, Structure functions in the bag model. Phys. Rev. D **44**, 2653–2662 (1991)
3158. D. Diakonov et al., Unpolarized and polarized quark distributions in the large N_c limit. Phys. Rev. D **56**, 4069–4083 (1997)
3159. M. Wakamatsu, T. Watabe, Do we expect light flavor sea quark asymmetry also for the spin dependent distribution functions of the nucleon? Phys. Rev. D **62**, 017506 (2000)
3160. C. Bourrely, J. Soffer, New developments in the statistical approach of parton distributions: tests and predictions up to LHC energies. Nucl. Phys. A **941**, 307–334 (2015)
3161. R.M. Whitehill et al., Accessing gluon polarization with high-P_T hadrons in SIDIS (2022)
3162. C. Egerer et al., Towards the determination of the gluon helicity distribution in the nucleon from lattice quantum chromodynamics (2022)
3163. R. Abdul Khalek et al., Science Requirements and Detector Concepts for the Electron-Ion Collider: EIC Yellow Report (2021)
3164. P. Jimenez-Delgado, H. Avakian, W. Melnitchouk, Constraints on spin-dependent parton distributions at large x from global QCD analysis. Phys. Lett. B **738**, 263–267 (2014)
3165. Y. Zhou et al., Revisiting quark and gluon polarization in the proton at the EIC. Phys. Rev. D **104**(3), 034028 (2021)
3166. D. Adamiak et al., First analysis of world polarized DIS data with small-x helicity evolution. Phys. Rev. D **104**(3), L031501 (2021)
3167. T. Liu et al., Factorized approach to radiative corrections for inelastic lepton-hadron collisions. Phys. Rev. D **104**(9), 094033 (2021)
3168. T. Liu et al., A new approach to semi-inclusive deep-inelastic scattering with QED and QCD factorization. JHEP **11**, 157 (2021)
3169. J. Bringewatt et al., Confronting lattice parton distributions with global QCD analysis. Phys. Rev. D **103**(1), 016003 (2021)
3170. T.H.R. Skyrme, A unified field theory of mesons and baryons. Nucl. Phys. **31**, 556–569 (1962)
3171. M. Gell-Mann, A schematic model of baryons and mesons. Phys. Lett. **8**, 214–215 (1964)
3172. G. Zweig, An SU(3) model for strong interaction symmetry and its breaking. Version 1 (1964)
3173. R.K. Bhaduri, *Models of the Nucleon: From Quarks to Soliton* (Addison Wesley, ISBN-10: 0201156733, 1988)
3174. A. William Thomas, W. Weise, *The Structure of the Nucleon* (Wiley, Weinheim, 2001)
3175. F.E. Close, *An Introduction to Quarks and Partons* (Academic Press Inc, ISDN: 978-0-12-175152-4, 1979)
3176. V.W. Hughes, J. Kuti, Internal spin structure of the nucleon. Annu. Rev. Nucl. Part. Sci. **33**, 611–644 (1983) **(Ed. by V. W. Hughes and C. Cavata)**
3177. J. Ashman et al., A measurement of the spin asymmetry and determination of the structure function g1 in deep elastic muon-proton scattering. Phys. Lett. B **206**, 364 (1988) **(Ed. by V.W. Hughes and C. Cavata)**
3178. J. Ashman et al., An investigation of the spin structure of the proton in deep inelastic scattering of polarized muons on polarized protons. Nucl. Phys. B **328**, 1 (1989) **(Ed. by V. W. Hughes and C. Cavata)**
3179. B.W. Filippone, X.-D. Ji, The spin structure of the nucleon. Adv. Nucl. Phys. **26**, 1 (2001)
3180. S.D. Bass, The spin structure of the proton. Rev. Mod. Phys. **77**, 1257–1302 (2005)
3181. C.A. Aidala et al., The spin structure of the nucleon. Rev. Mod. Phys. **85**, 655–691 (2013)
3182. E. Leader, C. Lorcé, The angular momentum controversy: what's it all about and does it matter. Phys. Rept. **541**(3), 163–248 (2014)
3183. A. Deur, S.J. Brodsky, G.F. De Téramond, The spin structure of the nucleon. Rep. Prog. Phys. **82**, 076201 (2019)
3184. G. Bunce et al., Prospects for spin physics at RHIC. Annu. Rev. Nucl. Part. Sci. **50**, 525–575 (2000)
3185. J. Dudek et al., Physics opportunities with the 12 GeV upgrade at Jefferson Lab. Eur. Phys. J. A **48**, 187 (2012)
3186. D. Boer et al., Gluons and the quark sea at high energies: distributions, polarization, tomography (2011). arXiv:1108.1713
3187. W.K. Tung, Group Theory in Physics (World Scientific. Singapore (1985). https://doi.org/10.1142/0097
3188. R.L. Jaffe, A. Manohar, The G_1 problem: fact and fantasy on the spin of the proton. Nucl. Phys. B **337**, 509–546 (1990)
3189. X.-D. Ji, Lorentz symmetry and the internal structure of the nucleon. Phys. Rev. D **58**, 056003 (1998)
3190. X. Ji, Y. Xu, Y. Zhao, Gluon spin, canonical momentum, and gauge symmetry. JHEP **08**, 082 (2012)
3191. A.V. Manohar, Polarized parton distribution functions. Phys. Rev. Lett. **66**, 289–292 (1991)
3192. X. Ji, J.-H. Zhang, Y. Zhao, Physics of the gluon-helicity contribution to proton spin. Phys. Rev. Lett. **111**, 112002 (2013)
3193. M. Wakamatsu, On gauge-invariant decomposition of nucleon spin. Phys. Rev. D **81**, 114010 (2010)
3194. M. Burkardt, Parton orbital angular momentum and final state interactions. Phys. Rev. D **88**(1), 014014 (2013)
3195. X. Ji, F. Yuan, Transverse spin sum rule of the proton. Phys. Lett. B **810**, 135786 (2020)
3196. X. Ji, X. Xiong, F. Yuan, Proton spin structure from measurable parton distributions. Phys. Rev. Lett. **109**, 152005 (2012)
3197. X. Ji, X. Xiong, F. Yuan, Transverse polarization of the nucleon in parton picture. Phys. Lett. B **717**, 214–218 (2012)
3198. Y. Guo, X. Ji, K. Shiells, Novel twist-three transverse-spin sum rule for the proton and related generalized parton distributions. Nucl. Phys. B **969**, 115440 (2021)
3199. C. Alexandrou et al., Nucleon spin and momentum decomposition using lattice QCD simulations. Phys. Rev. Lett. **119**(14), 142002 (2017)
3200. J. Liang et al., Quark spins and anomalous ward identity. Phys. Rev. D **98**(7), 074505 (2018)
3201. H.-W. Lin et al., Quark contribution to the proton spin from 2+1+1-flavor lattice QCD. Phys. Rev. D **98**(9), 094512 (2018)
3202. C. Adolph et al., The spin structure function g_1^{rmp} of the proton and a test of the Bjorken sum rule. Phys. Lett. B **753**, 18–28 (2016)
3203. K.-F. Liu, Status on lattice calculations of the proton spin decomposition. AAPPS Bull. **32**(1), 8 (2022)
3204. C. Alexandrou et al., Complete flavor decomposition of the spin and momentum fraction of the proton using lattice QCD simulations at physical pion mass. Phys. Rev. D **101**(9), 094513 (2020)
3205. H.-W. Lin et al., Parton distributions and lattice QCD calculations: a community white paper. Prog. Part. Nucl. Phys. **100**, 107–160 (2018)
3206. M. Deka et al., Lattice study of quark and glue momenta and angular momenta in the nucleon. Phys. Rev. D **91**(1), 014505 (2015)
3207. M. Gong et al., Strange and charm quark spins from the anomalous Ward identity. Phys. Rev. D **95**(11), 114509 (2017)
3208. N. Mathur et al., Quark orbital angular momentum from lattice QCD. Phys. Rev. D **62**, 114504 (2000)
3209. P. Hagler et al., Moments of nucleon generalized parton distributions in lattice QCD. Phys. Rev. D **68**, 034505 (2003)
3210. M. Gockeler et al., Generalized parton distributions from lattice QCD. Phys. Rev. Lett. **92**, 042002 (2004)
3211. D. Brommel et al., Moments of generalized parton distributions and quark angular momentum of the nucleon. PoS LATTICE2007, 158 (2007) **(Ed. by Gunnar Bali et al.)**

3212. J.D. Bratt et al., Nucleon structure from mixed action calculations using 2+1 flavors of asqtad sea and domain wall valence fermions. Phys. Rev. D **82**, 094502 (2010)
3213. S.N. Syritsyn et al., Quark contributions to nucleon momentum and spin from domain wall fermion calculations. PoS LATTICE **2011**, 178 (2011) **(Ed. by Pavlos Vranas)**
3214. C. Alexandrou et al., Moments of nucleon generalized parton distributions from lattice QCD. Phys. Rev. D **83**, 114513 (2011)
3215. C. Alexandrou et al., Nucleon form factors and moments of generalized parton distributions using $N_f = 2 + 1 + 1$ twisted mass fermions. Phys. Rev. D **88**(1), 014509 (2013)
3216. G. Wang et al., Proton momentum and angular momentum decompositions with overlap fermions. Phys. Rev. D **106**(1), 014512 (2022)
3217. M. Engelhardt, Quark orbital dynamics in the proton from Lattice QCD–from Ji to Jaffe-Manohar orbital angular momentum. Phys. Rev. D **95**(9), 094505 (2017)
3218. M. Engelhardt et al., From Ji to Jaffe-Manohar orbital angular momentum in lattice QCD using a direct derivative method. Phys. Rev. D **102**(7), 074505 (2020)
3219. X. Ji, J.-H. Zhang, Y. Zhao, Justifying the naive partonic sum rule for proton spin. Phys. Lett. B **743**, 180–183 (2015)
3220. Y. Guo, X. Ji, K. Shiells, Generalized parton distributions through universal moment parameterization: zero skewness case. JHEP **09**, 215 (2022)
3221. M. Mazouz et al., Deeply virtual compton scattering off the neutron. Phys. Rev. Lett. **99**, 242501 (2007)
3222. L. Adamczyk et al., Precision measurement of the longitudinal double-spin asymmetry for inclusive jet production in polarized proton collisions at $\sqrt{s} = 200$ GeV. Phys. Rev. Lett. **115**(9), 092002 (2015)
3223. J. Adam et al., Longitudinal double-spin asymmetry for inclusive jet and dijet production in pp collisions at $\sqrt{s} = 510$ GeV. Phys. Rev. D **100**(5), 052005 (2019)
3224. J. Adam et al., Measurement of the longitudinal spin asymmetries for weak boson production in proton-proton collisions at $\sqrt{s} = 510$ GeV. Phys. Rev. D **99**(5), 051102 (2019)
3225. A. Airapetian et al., Measurement of azimuthal asymmetries with respect to both beam charge and transverse target polarization in exclusive electroproduction of real photons. JHEP **06**, 066 (2008)
3226. K. Kumericki, D. Mueller, A. Schäfer, Neural network generated parametrizations of deeply virtual Compton form factors. JHEP **07**, 073 (2011)
3227. S.V. Goloskokov, P. Kroll, The target asymmetry in hard vector-meson electroproduction and parton angular momenta. Eur. Phys. J. C **59**, 809–819 (2009)
3228. G.R. Goldstein, J. OsvaldoGonzalez Hernandez, S. Liuti, Flexible parametrization of generalized parton distributions from deeply virtual Compton scattering observables. Phys. Rev. D **84**, 034007 (2011)
3229. D. Mueller, A. Schäfer, Complex conformal spin partial wave expansion of generalized parton distributions and distribution amplitudes. Nucl. Phys. B **739**, 1–59 (2006)
3230. K. Kumericki, D. Mueller, Deeply virtual Compton scattering at small x_B and the access to the GPD H. Nucl. Phys. B **841**, 1–58 (2010)
3231. Y.V. Kovchegov, D. Pitonyak, M.D. Sievert, Helicity evolution at small-x. JHEP **01**, 072 (2016) [Erratum: JHEP 10, 148 (2016)]
3232. Y.V. Kovchegov, D. Pitonyak, M.D. Sievert, Small-x asymptotics of the quark helicity distribution. Phys. Rev. Lett. **118**(5), 052001 (2017)
3233. Y.V. Kovchegov, M.D. Sievert, Small-x helicity evolution: an operator treatment. Phys. Rev. D **99**(5), 054032 (2019)
3234. R. Boussarie, Y. Hatta, F. Yuan, Proton spin structure at small-x. Phys. Lett. B **797**, 134817 (2019)
3235. Y.V. Kovchegov, A. Tarasov, Y. Tawabutr, Helicity evolution at small x: the single-logarithmic contribution. JHEP **03**, 184 (2022)
3236. A. Tarasov, R. Venugopalan, Role of the chiral anomaly in polarized deeply inelastic scattering. II. Topological screening and transitions from emergent axionlike dynamics. Phys. Rev. D **105**(1), 014020 (2022)
3237. A. Tarasov, R. Venugopalan, Role of the chiral anomaly in polarized deeply inelastic scattering: Finding the triangle graph inside the box diagram in Bjorken and Regge asymptotics. Phys. Rev. D **102**(11), 114022 (2020)
3238. F. Cougoulic et al., Quark and gluon helicity evolution at small x: revised and updated. JHEP **07**, 095 (2022)
3239. Y. Hatta, J. Zhou, Small-x evolution of the gluon GPD E_g. Phys. Rev. Lett. **129**(25), 252002 (2022)
3240. E. Rutherford, The scattering of alpha and beta particles by matter and the structure of the atom. Philos. Mag. Ser. **6**(21), 669–688 (1911)
3241. D. Müller et al., Wave functions, evolution equations and evolution kernels from light ray operators of QCD. Fortsch. Phys. **42**, 101–141 (1994)
3242. A.V. Radyushkin, Nonforward parton distributions. Phys. Rev. D **56**, 5524–5557 (1997)
3243. K. Goeke, M.V. Polyakov, M. Vanderhaeghen, Hard exclusive reactions and the structure of hadrons. Prog. Part. Nucl. Phys. **47**, 401–515 (2001)
3244. M. Diehl, Generalized parton distributions. Phys. Rep. **388**, 41–277 (2003)
3245. A.V. Belitsky, A.V. Radyushkin, Unraveling hadron structure with generalized parton distributions. Phys. Rep. **418**, 1–387 (2005)
3246. S. Boffi, B. Pasquini, Generalized parton distributions and the structure of the nucleon. Riv. Nuovo Cim. **30**(9), 387–448 (2007)
3247. P.J. Mulders, R.D. Tangerman, The complete tree level result up to order 1/Q for polarized deep inelastic leptoproduction. Nucl. Phys. B **461**, 197–237 (1996) [Erratum: Nucl. Phys. B 484, 538–540 (1997)]
3248. D. Boer, P.J. Mulders, Time reversal odd distribution functions in leptoproduction. Phys. Rev. D **57**, 5780–5786 (1998)
3249. M. Burkardt, Impact parameter space interpretation for generalized parton distributions. Int. J. Mod. Phys. A **18**, 173–208 (2003)
3250. X. Ji, Viewing the proton through 'color' filters. Phys. Rev. Lett. **91**, 062001 (2003)
3251. A.V. Belitsky, X. Ji, F. Yuan, Quark imaging in the proton via quantum phase space distributions. Phys. Rev. D **69**, 074014 (2004)
3252. S. Meißner, A. Metz, K. Goeke, Relations between generalized and transverse momentum dependent parton distributions. Phys. Rev. D **76**, 034002 (2007)
3253. C. Lorce, B. Pasquini, Quark Wigner distributions and orbital angular momentum. Phys. Rev. D **84**, 014015 (2011)
3254. C. Lorce et al., The quark orbital angular momentum from Wigner distributions and light-cone wave functions. Phys. Rev. D **85**, 114006 (2012)
3255. X. Ji, X. Xiong, F. Yuan, Probing parton orbital angular momentum in longitudinally polarized nucleon. Phys. Rev. D **88**(1), 014041 (2013)
3256. Y. Hatta, Notes on the orbital angular momentum of quarks in the nucleon. Phys. Lett. B **708**, 186–190 (2012)
3257. X. Ji, F. Yuan, Y. Zhao, Hunting the gluon orbital angular momentum at the electron-ion collider. Phys. Rev. Lett. **118**(19), 192004 (2017)
3258. Y. Hatta et al., Gluon orbital angular momentum at small-x. Phys. Rev. D **95**(11), 114032 (2017)
3259. A. Courtoy et al., On the observability of the quark orbital angular momentum distribution. Phys. Lett. B **731**, 141–147 (2014)

3260. A. Courtoy et al., Identification of observables for quark and gluon orbital angular momentum (2014). arXiv:1412.0647
3261. S. Bhattacharya, R. Boussarie, Y. Hatta, Signature of the gluon orbital angular momentum. Phys. Rev. Lett. **128**(18), 182002 (2022)
3262. F. Yuan, Generalized parton distributions at x → 1. Phys. Rev. D **69**, 051501 (2004)
3263. M. Göckeler et al., Transverse spin structure of the nucleon from lattice QCD simulations. Phys. Rev. Lett. **98**, 222001 (2007)
3264. A.V. Belitsky, D. Mueller, Predictions from conformal algebra for the deeply virtual Compton scattering. Phys. Lett. B **417**, 129–140 (1998)
3265. X.-D. Ji, J. Osborne, One loop QCD corrections to deeply virtual Compton scattering: the parton helicity independent case. Phys. Rev. D **57**, 1337–1340 (1998)
3266. L. Mankiewicz et al., NLO corrections to deeply virtual Compton scattering. Phys. Lett. B 425, 186-192 (1998) [Erratum: Phys. Lett. B 461, 423–423 (1999)]
3267. D. Mueller, Next-to-next-to leading order corrections to deeply virtual Compton scattering: the non-singlet case. Phys. Lett. B **634**, 227–234 (2006)
3268. K. Kumericki et al., Deeply virtual Compton scattering beyond next-to-leading order: the flavor singlet case. Phys. Lett. B **648**, 186–194 (2007)
3269. K. Kumericki, D. Mueller, K. Passek-Kumericki, Towards a fitting procedure for deeply virtual Compton scattering at next-to-leading order and beyond. Nucl. Phys. B **794**, 244–323 (2008)
3270. B. Pire, L. Szymanowski, J. Wagner, NLO corrections to timelike, spacelike and double deeply virtual Compton scattering. Phys. Rev. D **83**, 034009 (2011)
3271. V.M. Braun et al., Three-loop evolution equation for flavor-nonsinglet operators in off-forward kinematics. JHEP **06**, 037 (2017)
3272. V.M. Braun et al., Two-loop coefficient function for DVCS: vector contributions. JHEP **09**, 117 (2020)
3273. V.M. Braun, Y. Ji, J. Schoenleber, Deeply virtual Compton scattering at next-to-next-to-leading order. Phys. Rev. Lett. **129**(17), 172001 (2022)
3274. A.V. Belitsky, D. Mueller, A. Kirchner, Theory of deeply virtual Compton scattering on the nucleon. Nucl. Phys. B **629**, 323–392 (2002)
3275. A.V. Belitsky, D. Mueller, Exclusive electroproduction revisited: treating kinematical effects. Phys. Rev. D **82**, 074010 (2010)
3276. B. Kriesten et al., Extraction of generalized parton distribution observables from deeply virtual electron proton scattering experiments. Phys. Rev. D **101**(5), 054021 (2020)
3277. B. Kriesten, S. Liuti, Theory of deeply virtual Compton scattering off the unpolarized proton. Phys. Rev. D **105**(1), 016015 (2022)
3278. J. Grigsby et al., Deep learning analysis of deeply virtual exclusive photoproduction. Phys. Rev. D **104**(1), 016001 (2021)
3279. B. Kriesten et al., Parametrization of quark and gluon generalized parton distributions in a dynamical framework. Phys. Rev. D **105**(5), 056022 (2022)
3280. Y. Guo, X. Ji, K. Shiells, Higher-order kinematical effects in deeply virtual Compton scattering. JHEP **12**, 103 (2021)
3281. K. Shiells, Y. Guo, X. Ji, On extraction of twist-two Compton form factors from DVCS observables through harmonic analysis. JHEP **08**, 048 (2022)
3282. Y. Guo et al., Twist-three cross-sections in deeply virtual Compton scattering. JHEP **06**, 096 (2022)
3283. C. Alexandrou et al., Unpolarized and helicity generalized parton distributions of the proton within lattice QCD. Phys. Rev. Lett. **125**(26), 262001 (2020)
3284. A. Prokudin, P. Sun, F. Yuan, Scheme dependence and transverse momentum distribution interpretation of Collins-Soper-Sterman resummation. Phys. Lett. B **750**, 533–538 (2015)
3285. A. Bermudez Martinez, A. Vladimirov, Determination of the Collins-Soper kernel from cross-sections ratios. Phys. Rev. D **106**(9), L091501 (2022)
3286. M. Bury, A. Prokudin, A. Vladimirov, Extraction of the Sivers function from SIDIS, Drell-Yan, and $W^{\pm}/Z$ boson production data with TMD evolution. JHEP **05**, 151 (2021)
3287. S.J. Brodsky, D. Sung Hwang, I. Schmidt, Initial state interactions and single spin asymmetries in Drell-Yan processes. Nucl. Phys. B **642**, 344–356 (2002)
3288. D. Boer, P.J. Mulders, F. Pijlman, Universality of T odd effects in single spin and azimuthal asymmetries. Nucl. Phys. B **667**, 201–241 (2003)
3289. X. Ji et al., Single transverse-spin asymmetry in Drell-Yan production at large and moderate transverse momentum. Phys. Rev. D **73**, 094017 (2006)
3290. X. Ji et al., Single-transverse spin asymmetry in semi-inclusive deep inelastic scattering. Phys. Lett. B **638**, 178–186 (2006)
3291. Y. Koike, W. Vogelsang, F. Yuan, On the relation between mechanisms for single-transverse-spin asymmetries. Phys. Lett. B **659**, 878–884 (2008)
3292. A. Airapetian et al., Observation of the Naive-T-odd Sivers effect in deep-inelastic scattering. Phys. Rev. Lett. **103**, 152002 (2009)
3293. A. Airapetian et al., Azimuthal single- and double-spin asymmetries in semi-inclusive deep-inelastic lepton scattering by transversely polarized protons. JHEP **12**, 010 (2020)
3294. M. Alekseev et al., Collins and Sivers asymmetries for pions and kaons in muon-deuteron DIS. Phys. Lett. B **673**, 127–135 (2009)
3295. C. Adolph et al., Collins and Sivers asymmetries in muonproduction of pions and kaons off transversely polarised protons. Phys. Lett. B **744**, 250–259 (2015)
3296. C. Adolph et al., II-Experimental investigation of transverse spin asymmetries in μ -p SIDIS processes: Sivers asymmetries. Phys. Lett. B **717**, 383–389 (2012)
3297. C. Adolph et al., Sivers asymmetry extracted in SIDIS at the hard scales of the Drell-Yan process at COMPASS. Phys. Lett. B **770**, 138–145 (2017)
3298. X. Qian et al., Single spin asymmetries in charged pion production from semi-inclusive deep inelastic scattering on a transversely polarized 3He target. Phys. Rev. Lett. **107**, 072003 (2011)
3299. Y.X. Zhao et al., Single spin asymmetries in charged kaon production from semi-inclusive deepinelastic scattering on a transversely polarized ^{3}He target. Phys. Rev. C **90**(5), 055201 (2014)
3300. M. Aghasyan et al., First measurement of transverse-spin-dependent azimuthal asymmetries in the Drell-Yan process. Phys. Rev. Lett. **119**(11), 112002 (2017)
3301. L. Adamczyk et al., Measurement of the transverse single-spin asymmetry in $p^{\uparrow} + p \rightarrow W^{\pm}/Z^0$ at RHIC. Phys. Rev. Lett. **116**(13), 132301 (2016)
3302. M. Bury, A. Prokudin, A. Vladimirov, Extraction of the Sivers function from SIDIS, Drell-Yan, and $W^{\pm}/Z$ data at next-to-next-to-next-to leading order. Phys. Rev. Lett. **126**(11), 112002 (2021)
3303. A. Bacchetta et al., Extraction of partonic transverse momentum distributions from semi-inclusive deep-inelastic scattering, Drell-Yan and Z-boson production. JHEP **06**, 081 (2017) [Erratum: JHEP 06, 051 (2019)]
3304. I. Scimemi, A. Vladimirov, Analysis of vector boson production within TMD factorization. Eur. Phys. J. C **78**(2), 89 (2018)
3305. I. Scimemi, A. Vladimirov, Non-perturbative structure of semi-inclusive deep-inelastic and Drell-Yan scattering at small transverse momentum. JHEP **06**, 137 (2020)
3306. A. Bacchetta et al., Unpolarized transverse momentum distributions from a global fit of Drell-Yan and semi-inclusive deep-inelastic scattering data. JHEP **10**, 127 (2022)
3307. P. Sun et al., Nonperturbative functions for SIDIS and Drell-Yan processes. Int. J. Mod. Phys. A **33**(11), 1841006 (2018)

3308. A. Bacchetta et al., Difficulties in the description of Drell-Yan processes at moderate invariant mass and high transverse momentum. Phys. Rev. D **100**(1), 014018 (2019)
3309. J.O. Gonzalez-Hernandez et al., Challenges with large transverse momentum in semi-inclusive deeply inelastic scattering. Phys. Rev. D **98**(11), 114005 (2018)
3310. W. Vogelsang, F. Yuan, Next-to-leading order calculation of the single transverse spin asymmetry in the Drell-Yan process. Phys. Rev. D **79**, 094010 (2009)
3311. J. Zhou, F. Yuan, Z.-T. Liang, QCD evolution of the transverse momentum dependent correlations. Phys. Rev. D **79**, 114022 (2009)
3312. A. Schafer, J. Zhou, A note on the scale evolution of the ETQS function $T_F(x, x)$. Phys. Rev. D **85**, 117501 (2012)
3313. Z.-B. Kang, J.-W. Qiu, QCD evolution of naive-time-reversal odd parton distribution functions. Phys. Lett. B **713**, 273–276 (2012)
3314. I. Scimemi, A. Tarasov, A. Vladimirov, Collinear matching for Sivers function at next-to-leading order. JHEP **05**, 125 (2019)
3315. A. Idilbi et al., Collins-Soper equation for the energy evolution of transverse-momentum and spin dependent parton distributions. Phys. Rev. D **70**, 074021 (2004)
3316. Z.-B. Kang, B.-W. Xiao, F. Yuan, QCD resummation for single spin asymmetries. Phys. Rev. Lett. **107**, 152002 (2011)
3317. S. Mert Aybat et al., The QCD evolution of the Sivers function. Phys. Rev. D **85**, 034043 (2012)
3318. P. Sun, F. Yuan, Transverse momentum dependent evolution: matching semi-inclusive deep inelastic scattering processes to Drell-Yan and W/Z boson production. Phys. Rev. D **88**(11), 114012 (2013)
3319. X. Ji et al., Soft factor subtraction and transverse momentum dependent parton distributions on the lattice. Phys. Rev. D **91**, 074009 (2015)
3320. X. Ji et al., Transverse momentum dependent parton quasidistributions. Phys. Rev. D **99**(11), 114006 (2019)
3321. X. Ji, Y. Liu, Y.-S. Liu, TMD soft function from large-momentum effective theory. Nucl. Phys. B **955**, 115054 (2020)
3322. X. Ji, Y. Liu, Y.-S. Liu, Transverse-momentum-dependent parton distribution functions from large-momentum effective theory. Phys. Lett. B **811**, 135946 (2020)
3323. X. Ji et al., Single transverse-spin asymmetry and Sivers function in large momentum effective theory. Phys. Rev. D **103**(7), 074005 (2021)
3324. M.A. Ebert, I.W. Stewart, Y. Zhao, Towards quasi-transverse momentum dependent PDFs computable on the lattice. JHEP **09**, 037 (2019)
3325. M.A. Ebert, I.W. Stewart, Y. Zhao, Renormalization and matching for the Collins-Soper kernel from lattice QCD. JHEP **03**, 099 (2020)
3326. M.A. Ebert et al., One-loop matching for spin-dependent quasi-TMDs. JHEP **09**, 099 (2020)
3327. P. Shanahan, M.L. Wagman, Y. Zhao, Non-perturbative renormalization of staple-shaped Wilson line operators in lattice QCD. Phys. Rev. D **101**(7), 074505 (2020)
3328. M.-H. Chu et al., Nonperturbative Determination of Collins-Soper Kernel from Quasi Transverse-Momentum Dependent Wave Functions (2022)
3329. M.A. Ebert et al., Factorization connecting continuum and lattice TMDs. JHEP **04**, 178 (2022)
3330. S.T. Schindler, I.W. Stewart, Y. Zhao, One-loop matching for gluon lattice TMDs. JHEP **08**, 084 (2022)
3331. A.A. Vladimirov, A. Schäfer, Transverse momentum dependent factorization for lattice observables. Phys. Rev. D **101**(7), 074517 (2020)
3332. A.H. Mueller, Soft gluons in the infinite momentum wave function and the BFKL pomeron. Nucl. Phys. B **415**, 373–385 (1994)
3333. A.H. Mueller, Parton saturation at small x and in large nuclei. Nucl. Phys. B **558**, 285–303 (1999)
3334. L.D. McLerran, R. Venugopalan, Computing quark and gluon distribution functions for very large nuclei. Phys. Rev. D **49**, 2233–2241 (1994)
3335. L.D. McLerran, R. Venugopalan, Gluon distribution functions for very large nuclei at small transverse momentum. Phys. Rev. D **49**, 3352–3355 (1994)
3336. L.D. McLerran, R. Venugopalan, Green's functions in the color field of a large nucleus. Phys. Rev. D **50**, 2225–2233 (1994)
3337. C. Marquet, B.-W. Xiao, F. Yuan, Semi-inclusive deep inelastic scattering at small x. Phys. Lett. B **682**, 207–211 (2009)
3338. F. Dominguez, B.-W. Xiao, F. Yuan, k_t-factorization for hard processes in nuclei. Phys. Rev. Lett. **106**, 022301 (2011)
3339. F. Dominguez et al., Universality of unintegrated gluon distributions at small x. Phys. Rev. D **83**, 105005 (2011)
3340. A. Metz, J. Zhou, Distribution of linearly polarized gluons inside a large nucleus. Phys. Rev. D **84**, 051503 (2011)
3341. I. Balitsky, A. Tarasov, Gluon TMD in particle production from low to moderate x. JHEP **06**, 164 (2016)
3342. T. Altinoluk, R. Boussarie, P. Kotko, Interplay of the CGC and TMD frameworks to all orders in kinematic twist. JHEP **05**, 156 (2019)
3343. T. Altinoluk, R. Boussarie, Low x physics as an infinite twist (G)TMD framework: unravelling the origins of saturation. JHEP **10**, 208 (2019)
3344. A.H. Mueller, B.-W. Xiao, F. Yuan, Sudakov resummation in small-x saturation formalism. Phys. Rev. Lett. **110**(8), 082301 (2013)
3345. A.H. Mueller, B.-W. Xiao, F. Yuan, Sudakov double logarithms resummation in hard processes in the small-x saturation formalism. Phys. Rev. D **88**(11), 114010 (2013)
3346. I. Balitsky, A. Tarasov, Rapidity evolution of gluon TMD from low to moderate x. JHEP **10**, 017 (2015)
3347. B.-W. Xiao, F. Yuan, J. Zhou, Transverse momentum dependent parton distributions at small-x. Nucl. Phys. B **921**, 104–126 (2017)
3348. I. Balitsky, Gauge-invariant TMD factorization for Drell-Yan hadronic tensor at small x. JHEP **05**, 046 (2021)
3349. P. Taels et al., Dijet photoproduction at low x at next-to-leading order and its back-to-back limit. JHEP **10**, 184 (2022)
3350. Y. Hatta, B.-W. Xiao, F. Yuan, Probing the small- x gluon tomography in correlated hard diffractive dijet production in deep inelastic scattering. Phys. Rev. Lett. **116**(20), 202301 (2016)
3351. S. Bhattacharya, A. Metz, J. Zhou, Generalized TMDs and the exclusive double Drell-Yan process. Phys. Lett. B **771**, 396–400 (2017)
3352. S. Bhattacharya et al., Exclusive double quarkonium production and generalized TMDs of gluons. Phys. Lett. B **833**, 137383 (2022)
3353. T. Altinoluk et al., Diffractive dijet production in deep inelastic scattering and photon-hadron collisions in the color glass condensate. Phys. Lett. B **758**, 373–383 (2016)
3354. J. Zhou, Elliptic gluon generalized transverse-momentum-dependent distribution inside a large nucleus. Phys. Rev. D **94**(11), 114017 (2016)
3355. Y. Hagiwara et al., Accessing the gluon Wigner distribution in ultraperipheral pA collisions. Phys. Rev. D **96**(3), 034009 (2017)
3356. H. Mäntysaari, N. Mueller, B. Schenke, Diffractive dijet production and Wigner distributions from the color glass condensate. Phys. Rev. D **99**(7), 074004 (2019)
3357. H. Mäntysaari et al., Multigluon correlations and evidence of saturation from dijet measurements at an electron-ion collider. Phys. Rev. Lett. **124**(11), 112301 (2020)
3358. E. Iancu, A.H. Mueller, D.N. Triantafyllopoulos, Probing parton saturation and the gluon dipole via diffractive jet production at the electron-ion collider. Phys. Rev. Lett. **128**(20), 202001 (2022)

3359. E. Iancu et al., Gluon dipole factorisation for diffractive dijets. JHEP **10**, 103 (2022)
3360. R. Keith Ellis, D.A. Ross, A.E. Terrano, The perturbative calculation of jet structure in e^+e^- annihilation. Nucl. Phys. B **178**, 421–456 (1981)
3361. Z. Kunszt, Comment on the $O(\alpha_s^2)$ corrections to jet production in e^+e^- annihilation. Phys. Lett. B **99**, 429–432 (1981)
3362. K. Fabricius et al., Higher order perturbative QCD calculation of jet cross-sections in e^+e^- annihilation. Z. Phys. C **11**, 315 (1981)
3363. G. Passarino, M.J.G. Veltman, One loop corrections for e^+e^- annihilation into $\mu^+\mu^-$ in the Weinberg model. Nucl. Phys. B **160**, 151–207 (1979)
3364. G. 't Hooft, M.J.G. Veltman, Scalar one loop integrals. Nucl. Phys. B **153**, 365–401 (1979)
3365. G.J. van Oldenborgh, J.A.M. Vermaseren, New algorithms for one loop integrals. Z. Phys. C **46**, 425–438 (1990)
3366. Z. Bern, L.J. Dixon, D.A. Kosower, Dimensionally regulated pentagon integrals. Nucl. Phys. B **412**, 751–816 (1994)
3367. S. Frixione, Z. Kunszt, A. Signer, Three jet cross-sections to next-to-leading order. Nucl. Phys. B **467**, 399–442 (1996)
3368. F. Aversa et al., Jet production in hadronic collisions to O (α_s^3). Z. Phys. C **46**, 253 (1990)
3369. S.D. Ellis, Z. Kunszt, D.E. Soper, Two jet production in hadron collisions at order α_s^3 in QCD. Phys. Rev. Lett. **69**, 1496–1499 (1992)
3370. W.T. Giele, E.W. Nigel Glover, D.A. Kosower, Higher order corrections to jet cross-sections in hadron colliders. Nucl. Phys. B **403**, 633–670 (1993)
3371. Z. Nagy, Next-to-leading order calculation of three jet observables in hadron hadron collision. Phys. Rev. D **68**, 094002 (2003)
3372. Z. Bern et al., One loop n point gauge theory amplitudes, unitarity and collinear limits. Nucl. Phys. B **425**, 217–260 (1994)
3373. R. Britto, F. Cachazo, B. Feng, Generalized unitarity and one-loop amplitudes in N=4 super-Yang-Mills. Nucl. Phys. B **725**, 275–305 (2005)
3374. C. Anastasiou et al., D-dimensional unitarity cut method. Phys. Lett. B **645**, 213–216 (2007)
3375. G. Ossola, C.G. Papadopoulos, R. Pittau, Reducing full one-loop amplitudes to scalar integrals at the integrand level. Nucl. Phys. B **763**, 147–169 (2007)
3376. C.F. Berger et al., An automated implementation of on-shell methods for one-loop amplitudes. Phys. Rev. D **78**, 036003 (2008)
3377. R. Keith Ellis et al., Masses, fermions and generalized D-dimensional unitarity. Nucl. Phys. B **822**, 270–282 (2009)
3378. S. Badger et al., Next-to-leading order QCD corrections to five jet production at the LHC. Phys. Rev. D **89**(3), 034019 (2014)
3379. S. Höche et al., Next-to-leading order QCD predictions for top-quark pair production with up to three jets. Eur. Phys. J. C **77**(3), 145 (2017)
3380. F.R. Anger et al., NLO QCD predictions for $Wb\bar{b}$ production in association with up to three light jets at the LHC. Phys. Rev. D **97**(3), 036018 (2018)
3381. A. Denner, G. Pelliccioli, Combined NLO EW and QCD corrections to off-shell $t\bar{t}W$ production at the LHC. Eur. Phys. J. C **81**(4), 354 (2021)
3382. G. Bevilacqua et al., HELAC-NLO. Comput. Phys. Commun. **184**, 986–997 (2013)
3383. G. Cullen et al., Automated one-loop calculations with GoSam. Eur. Phys. J. C **72**, 1889 (2012)
3384. F. Cascioli, P. Maierhofer, S. Pozzorini, Scattering amplitudes with open loops. Phys. Rev. Lett. **108**, 111601 (2012)
3385. J. Alwall et al., The automated computation of tree-level and next-to-leading order differential cross sections, and their matching to parton shower simulations. JHEP **07**, 079 (2014)
3386. S. Actis et al., RECOLA: REcursive Computation of One-Loop Amplitudes. Comput. Phys. Commun. **214**, 140–173 (2017)
3387. R. Frederix et al., The automation of next-to-leading order electro weak calculations. JHEP **07**, 185 (2018)
3388. S. Honeywell et al., NLOX, a one-loop provider for Standard Model processes. Comput. Phys. Commun. **257**, 107284 (2020)
3389. V.A. Smirnov, Analytical result for dimensionally regularized massless on shell double box. Phys. Lett. B **460**, 397–404 (1999)
3390. J.B. Tausk, Nonplanar massless two loop Feynman diagrams with four on-shell legs. Phys. Lett. B **469**, 225–234 (1999)
3391. T. Binoth, G. Heinrich, An automatized algorithm to compute infrared divergent multiloop integrals. Nucl. Phys. B **585**, 741–759 (2000)
3392. L.W. Garland et al., The two loop QCD matrix element for $e^+e^- \to 3$ jets. Nucl. Phys. B **627**, 107–188 (2002)
3393. S. Moch, P. Uwer, S. Weinzierl, Two loop amplitudes with nested sums: fermionic contributions to $e^+e^- \to q\bar{q}g$. Phys. Rev. D **66**, 114001 (2002)
3394. M. Czakon, A. Mitov, S. Moch, Heavy-quark production in massless quark scattering at two loops in QCD. Phys. Lett. B **651**, 147–159 (2007)
3395. M. Czakon, A. Mitov, S. Moch, Heavy-quark production in gluon fusion at two loops in QCD. Nucl. Phys. B **798**, 210–250 (2008)
3396. M. Czakon, P. Fiedler, A. Mitov, Total top-quark pair-production cross section at hadron colliders through $O(\frac{4}{S})$. Phys. Rev. Lett. **110**, 252004 (2013)
3397. T. Gehrmann et al., W^+W^- production at hadron colliders in next to next to leading order QCD. Phys. Rev. Lett. **113**(21), 212001 (2014)
3398. F. Cascioli et al., ZZ production at hadron colliders in NNLO QCD. Phys. Lett. B **735**, 311–313 (2014)
3399. F. Caola et al., QCD corrections to W^+W^- production through gluon fusion. Phys. Lett. B **754**, 275–280 (2016)
3400. F. Caola et al., QCD corrections to ZZ production in gluon fusion at the LHC. Phys. Rev. D **92**(9), 094028 (2015)
3401. T. Gehrmann, A. von Manteuffel, L. Tancredi, The two-loop helicity amplitudes for $q\overline{q}' \to V_1V_2 \to 4$ leptons. JHEP **09**, 128 (2015)
3402. A. von Manteuffel, L. Tancredi, The two-loop helicity amplitudes for $gg \to V_1V_2 \to 4$ 4 leptons. JHEP **06**, 197 (2015)
3403. S. Borowka et al., Higgs boson pair production in gluon fusion at next-to-leading order with full top-quark mass dependence. Phys. Rev. Lett. **117**(1), 012001 (2016) [Erratum: Phys. Rev. Lett. 117(7), 079901 (2016)]
3404. J. Baglio et al., Gluon fusion into Higgs pairs at NLO QCD and the top mass scheme. Eur. Phys. J. C **79**(6), 459 (2019)
3405. S.P. Jones, M. Kerner, G. Luisoni, Next-to-leading-order QCD corrections to Higgs boson plus jet production with full top-quark mass dependence. Phys. Rev. Lett. **120**(16), 162001 (2018)
3406. J. Davies, G. Mishima, M. Steinhauser, Virtual corrections to $gg \to ZH$ in the high-energy and large-m_t limits. JHEP **03**, 034 (2021)
3407. L. Chen et al., ZH production in gluon fusion: two-loop amplitudes with full top quark mass dependence. JHEP **03**, 125 (2021)
3408. L. Alasfar et al., Virtual corrections to $gg \to ZH$ via a transverse momentum expansion. JHEP **05**, 168 (2021)
3409. C. Brønum-Hansen, C.-Y. Wang, Contribution of third generation quarks to two-loop helicity amplitudes for W boson pair production in gluon fusion. JHEP **01**, 170 (2021)
3410. B. Agarwal, S.P. Jones, A. von Manteuffel, Two-loop helicity amplitudes for $gg \to ZZ$ with full top-quark mass effects. JHEP **05**, 256 (2021)
3411. C. Brønnum-Hansen, C.-Y. Wang, Top quark contribution to two-loop helicity amplitudes for Z boson pair production in gluon fusion. JHEP **05**, 244 (2021)
3412. G. Heinrich, Collider physics at the precision Frontier. Phys. Rep. **922**, 1–69 (2021)

3413. A. Huss et al., Les Houches 2021: physics at TeV colliders: report on the standard model precision wishlist (2022). arXiv:2207.02122
3414. F. Caola et al., The path forward to N^3LO. In: *2021 Snowmass Summer Study*. J. Phys. G **50**, 043001 (2023)
3415. A. Gehrmann-De Ridder et al., Infrared structure of $e^+e^- \to 3$ jets at NNLO. JHEP **11**, 058 (2007)
3416. S. Weinzierl, NNLO corrections to 3-jet observables in electron-positron annihilation. Phys. Rev. Lett. **101**, 162001 (2008)
3417. A. Gehrmann-De Ridder, T. Gehrmann, E.W. Nigel Glover, Antenna subtraction at NNLO. JHEP **09**, 056 (2005)
3418. J. Currie, E.W.N. Glover, Steven wells, infrared structure at NNLO using antenna subtraction. JHEP **04**, 066 (2013)
3419. J. Currie, E.W.N. Glover, J. Pires, Next-to-next-to leading order QCD predictions for single jet inclusive production at the LHC. Phys. Rev. Lett. **118**(7), 072002 (2017)
3420. X. Chen et al., NNLO QCD corrections in full colour for jet production observables at the LHC. JHEP **09**, 025 (2022)
3421. R. Gauld et al., Precise predictions for WH+jet production at the LHC. Phys. Lett. B **817**, 136335 (2021)
3422. M. Czakon, A novel subtraction scheme for double-real radiation at NNLO. Phys. Lett. B **693**, 259–268 (2010)
3423. R. Boughezal, K. Melnikov, F. Petriello, A subtraction scheme for NNLO computations. Phys. Rev. D **85**, 034025 (2012)
3424. M. Czakon, D. Heymes, Four-dimensional formulation of the sector-improved residue subtraction scheme. Nucl. Phys. B **890**, 152–227 (2014)
3425. M. Czakon et al., NNLO QCD predictions for W+c-jet production at the LHC (2020)
3426. M. Czakon, A. Mitov, R. Poncelet, Tour de force in quantum chromodynamics: a first next-to-next-to-leading order study of three-jet production at the LHC (2021)
3427. F. Caola et al., NNLO QCD corrections to associated WH production and $H \to b\bar{b}$ decay. Phys. Rev. D **97**(7), 074022 (2018)
3428. W. Bizon et al., Anomalous couplings in associated VH production with Higgs boson decay to massive b quarks at NNLO in QCD. Phys. Rev. D **105**(1), 014023 (2022)
3429. F. Caola, K. Melnikov, R. Röntsch, Nested soft-collinear subtractions in NNLO QCD computations. Eur. Phys. J. C **77**(4), 248 (2017)
3430. M. Delto, K. Melnikov, Integrated triple-collinear counter-terms for the nested soft-collinear subtraction scheme. JHEP **05**, 148 (2019)
3431. W. Bizon, M. Delto, Analytic double-soft integrated subtraction terms for two massive emitters in a back-to-back kinematics. JHEP **07**, 011 (2020)
3432. K. Asteriadis et al., NNLO QCD corrections to weak boson fusion Higgs boson production in the $H \to b\bar{b}$ and $H \to WW^* \to 4l$ decay channels. JHEP **02**, 046 (2022)
3433. M. Delto et al., Mixed QCD⊗QED corrections to on-shell Z boson production at the LHC. JHEP **01**, 043 (2020)
3434. A. Behring et al., Mixed QCD-electroweak corrections to W-boson production in hadron collisions. Phys. Rev. D **103**(1), 013008 (2021)
3435. F. Buccioni et al., Mixed QCD-electroweak corrections to dilepton production at the LHC in the high invariant mass region. JHEP **06**, 022 (2022)
3436. G. Somogyi, Z. Trocsanyi, V. Del Duca, Matching of singly- and doubly-unresolved limits of tree-level QCD squared matrix elements. JHEP **06**, 024 (2005)
3437. G. Somogyi, A subtraction scheme for computing QCD jet cross sections at NNLO: integrating the doubly unresolved subtraction terms. JHEP **04**, 010 (2013)
3438. V. Del Duca et al., Three-jet production in electron-positron collisions at next-to-next-to-leading order accuracy. Phys. Rev. Lett. **117**(15), 152004 (2016)
3439. V. Del Duca et al., Higgs boson decay into b-quarks at NNLO accuracy. JHEP **04**, 036 (2015)
3440. M. Cacciari et al., Fully differential vector-boson-fusion Higgs production at next-to-next-to-leading order. Phys. Rev. Lett. **115**(8), 082002 (2015) [Erratum: Phys. Rev. Lett. 120(13), 139901 (2018)]
3441. F.A. Dreyer, A. Karlberg, Fully differential vector-boson fusion Higgs pair production at next-to-next-to-leading order. Phys. Rev. D **99**(7), 074028 (2019)
3442. F.A. Dreyer, A. Karlberg, Vector-boson fusion higgs production at three loops in QCD. Phys. Rev. Lett. **117**(7), 072001 (2016)
3443. E.L. Berger et al., NNLO QCD corrections to t-channel single top-quark production and decay. Phys. Rev. D **94**(7), 071501 (2016)
3444. J. Campbell, T. Neumann, Z. Sullivan, Single-top-quark production in the t-channel at NNLO. JHEP **02**, 040 (2021)
3445. L. Magnea et al., Local analytic sector subtraction at NNLO. JHEP **12**, 107 (2018) [Erratum: JHEP 06, 013 (2019)]
3446. L. Magnea et al., Factorisation and subtraction beyond NLO. JHEP **12**, 062 (2018)
3447. L. Magnea et al., Analytic integration of soft and collinear radiation in factorised QCD cross sections at NNLO. JHEP **02**, 037 (2021)
3448. Z. Capatti, V. Hirschi, B. Ruijl, Local unitarity: cutting raised propagators and localising renormalisation. JHEP **10**, 120 (2022)
3449. Z. Capatti et al., Local unitarity: a representation of differential cross-sections that is locally free of infrared singularities at any order. JHEP **04**, 104 (2021)
3450. S. Catani, M. Grazzini, An NNLO subtraction formalism in hadron collisions and its application to Higgs boson production at the LHC. Phys. Rev. Lett. **98**, 222002 (2007)
3451. S. Catani et al., Vector boson production at hadron colliders: a fully exclusive QCD calculation at NNLO. Phys. Rev. Lett. **103**, 082001 (2009)
3452. M. Grazzini, S. Kallweit, M. Wiesemann, Fully differential NNLO computations with MATRIX. Eur. Phys. J. C **78**(7), 537 (2018)
3453. S. Catani et al., Top-quark pair production at the LHC: fully differential QCD predictions at NNLO. JHEP **07**, 100 (2019)
3454. R. Bonciani et al., Mixed strong-electroweak corrections to the Drell-Yan process (2021)
3455. T. Armadillo et al., Two-loop mixed QCD-EW corrections to neutral current Drell-Yan. JHEP **05**, 072 (2022)
3456. J.M. Campbell, R. Keith Ellis, C. Williams, Direct photon production at next-to2013next-to-leading order. Phys. Rev. Lett. **118**(22), 222001 (2017)
3457. R. Boughezal et al., Higgs boson production in association with a jet at NNLO using jettiness subtraction. Phys. Lett. B **748**, 5–8 (2015)
3458. J.M. Campbell, R. Keith Ellis, S. Seth, H + 1 jet production revisited. JHEP **10**, 136 (2019)
3459. J. Campbell, T. Neumann, Precision phenomenology with MCFM. JHEP **12**, 034 (2019)
3460. C. Duhr, F. Dulat, B. Mistlberger, Drell-Yan crosssection to third order in the strong coupling constant. Phys. Rev. Lett. **125**(17), 172001 (2020)
3461. C. Duhr, F. Dulat, B. Mistlberger, Charged current Drell-Yan production at N^3LO. JHEP **11**, 143 (2020)
3462. C. Duhr, B. Mistlberger, Lepton-pair production at hadron colliders at N^3LO in QCD. JHEP **03**, 116 (2022)
3463. X. Chen et al., Transverse Mass Distribution and Charge Asymmetry in W Boson Production to Third Order in QCD (2022)
3464. T. Neumann, J. Campbell, Fiducial Drell-Yan production at the LHC improved by transverse-momentum resummation at N4LLp+N3LO. Phys. Rev. D **107**(1), L011506 (2023)
3465. C. Anastasiou et al., Higgs boson gluon-fusion production in QCD at three loops. Phys. Rev. Lett. **114**, 212001 (2015)

3466. F. Dulat, B. Mistlberger, A. Pelloni, Precision predictions at N^3LO for the Higgs boson rapidity distribution at the LHC. Phys. Rev. D **99**(3), 034004 (2019)
3467. L. Cieri et al., Higgs boson production at the LHC using the q_T subtraction formalism at N^3LO QCD. JHEP **02**, 096 (2019)
3468. X. Chen et al., Fully Differential Higgs Boson Production to Third Order in QCD (2021)
3469. J. Baglio et al., Inclusive production cross sections at N^3LO. JHEP **12**, 066 (2022)
3470. F.A. Dreyer, A. Karlberg, Vector-boson fusion Higgs pair production at N^3LO. Phys. Rev. D **98**(11), 114016 (2018)
3471. L.-B. Chen et al., Higgs boson pair production via gluon fusion at N^3LO in QCD. Phys. Lett. B **803**, 135292 (2020)
3472. C. Duhr, F. Dulat, B. Mistlberger, Higgs boson production in bottom-quark fusion to third order in the strong coupling. Phys. Rev. Lett. **125**(5), 051804 (2020)
3473. A.H. Ajjath et al., Resummed prediction for Higgs boson production through $b\bar{b}$ annihilation at N^3LL. JHEP **11**, 006 (2019)
3474. M.A. Ebert, B. Mistlberger, G. Vita, N-jettiness beam functions at N^3LO. JHEP **09**, 143 (2020)
3475. C. Duhr, B. Mistlberger, G. Vita, Soft integrals and soft anomalous dimensions at N^3LO and beyond. JHEP **09**, 155 (2022)
3476. A. Behring, Zero-jettiness beam functions at N^3LO. In: *16th DESY Workshop on Elementary Particle Physics: Loops and Legs in Quantum Field Theory 2022* (2022)
3477. D. Baranowski et al., Same-hemisphere three-gluon-emission contribution to the zero-jettiness soft function at N3LO QCD. Phys. Rev. D **106**(1), 014004 (2022)
3478. W. Chen et al., Double-real-virtual and double-virtual-real corrections to the three-loop thrust soft function. JHEP **22**, 094 (2020)
3479. O. Braun-White, N. Glover, Decomposition of triple collinear splitting functions. JHEP **09**, 059 (2022)
3480. V. Del Duca et al., Tree-level soft emission of a quark pair in association with a gluon. JHEP **01**, 040 (2023)
3481. J. Henn et al., Massive three-loop form factor in the planar limit. JHEP **01**, 074 (2017)
3482. A.G. Grozin, Heavy-quark form factors in the large β_0 limit. Eur. Phys. J. C **77**(7), 453 (2017)
3483. R.N. Lee et al., Three-loop massive form factors: complete light-fermion and large-N_c corrections for vector, axial-vector, scalar and pseudoscalar currents. JHEP **05**, 187 (2018)
3484. J. Ablinger et al., Heavy quark form factors at three loops in the planar limit. Phys. Lett. B **782**, 528–532 (2018)
3485. J. Blümlein et al., The heavy fermion contributions to the massive three loop form factors. Nucl. Phys. B **949**, 114751 (2019)
3486. M. Fael et al., Massive vector form factors to three loops. Phys. Rev. Lett. **128**(17), 172003 (2022)
3487. M. Fael et al., Singlet and nonsinglet three-loop massive form factors. Phys. Rev. D **106**(3), 034029 (2022)
3488. F. Caola, A. Von Manteuffel, L. Tancredi, Diphoton amplitudes in three-loop quantum chromo-dynamics. Phys. Rev. Lett. **126**(11), 112004 (2021)
3489. P. Bargiela et al., Three-loop helicity amplitudes for diphoton production in gluon fusion. JHEP **02**, 153 (2022)
3490. F. Caola et al., Three-loop helicity amplitudes for four-quark scattering in massless QCD. JHEP **10**, 206 (2021)
3491. F. Caola et al., Three-loop helicity amplitudes for quark-gluon scattering in QCD. JHEP **12**, 082 (2022)
3492. F. Caola et al., Three-loop gluon scattering in QCD and the gluon Regge trajectory. Phys. Rev. Lett. **128**(21), 212001 (2022)
3493. D.D. Canko, N. Syrrakos, Planar three-loop master integrals for $2 \rightarrow 2$ processes with one external massive particle. JHEP **04**, 134 (2022)
3494. M. Czakon et al., Exact top-quark mass dependence in hadronic Higgs production (2021)
3495. H.A. Chawdhry et al., NNLO QCD corrections to three-photon production at the LHC. JHEP **02**, 057 (2020)
3496. S. Kallweit, V. Sotnikov, M. Wiesemann, Triphoton production at hadron colliders in NNLO QCD. Phys. Lett. B **812**, 136013 (2021)
3497. S. Badger et al., Next-to-leading order QCD corrections to diphoton-plus-jet production through gluon fusion at the LHC. Phys. Lett. B **824**, 136802 (2022)
3498. S. Badger et al., Virtual QCD corrections to gluon-initiated diphoton plus jet production at hadron colliders. JHEP **11**, 083 (2021)
3499. B. Agarwal et al., Two-loop helicity amplitudes for diphoton plus jet production in full color. Phys. Rev. Lett. **127**(26), 262001 (2021)
3500. H.A. Chawdhry et al., NNLO QCD corrections to diphoton production with an additional jet at the LHC. JHEP **09**, 093 (2021)
3501. S. Badger, H. Bayu Hartanto, S. Zoia, Two-loop QCD corrections to $Wb\bar{b}$ production at hadron colliders. Phys. Rev. Lett. **127**(1), 012001 (2021)
3502. H. Bayu Hartanto et al., Next-to-next-to-leading order QCD corrections to Wbb^- production at the LHC. Phys. Rev. D **106**(7), 074016 (2022)
3503. A. von Manteuffel, E. Panzer, R.M. Schabinger, Cuspand collinear anomalous dimensions in four-loop QCD from form factors. Phys. Rev. Lett. **124**(16), 162001 (2020)
3504. G. Das, S. Moch, A. Vogt, Approximate four-loop QCD corrections to the Higgs-boson production cross section. Phys. Lett. B **807**, 135546 (2020)
3505. G. Das, S.-O. Moch, A. Vogt, Soft corrections to inclusive deep-inelastic scattering at four loops and beyond. JHEP **03**, 116 (2020)
3506. P.A. Baikov, K.G. Chetyrkin, J.H. Kühn, Five-loop running of the QCD coupling constant. Phys. Rev. Lett. **118**(8), 082002 (2017)
3507. F. Herzog et al., The five-loop beta function of Yang-Mills theory with fermions. JHEP **02**, 090 (2017)
3508. T. Luthe et al., The five-loop Beta function for a general gauge group and anomalous dimensions beyond Feynman gauge. JHEP **10**, 166 (2017)
3509. K.G. Chetyrkin et al., Five-loop renormalisation of QCD in covariant gauges. JHEP **10**, 179 (2017) [Addendum: JHEP 12, 006 (2017)]
3510. M. Borinsky et al., Five-loop renormalization of ϕ^3 theory with applications to the Lee-Yang edge singularity and percolation theory. Phys. Rev. D **103**(11), 116024 (2021)
3511. T. Aoyama et al., Tenth-order QED contribution to the electron g-2 and an improved value of the fine structure constant. Phys. Rev. Lett. **109**, 111807 (2012)
3512. T. Aoyama et al., Tenth-order electron anomalous magnetic moment—contribution of diagrams without closed lepton loops. Phys. Rev. D **91**(3), 033006 (2015) [Erratum: Phys. Rev. D 96, 019901 (2017)]
3513. T. Aoyama, T. Kinoshita, M. Nio, Revised and improved value of the QED tenth-order electron anomalous magnetic moment. Phys. Rev. D **97**(3), 036001 (2018)
3514. S. Volkov, Calculating the five-loop QED contribution to the electron anomalous magnetic moment: graphs without lepton loops. Phys. Rev. D **100**(9), 096004 (2019)
3515. M.V. Kompaniets, E. Panzer, Minimally subtracted six loop renormalization of $O(n)$-symmetric ϕ^4 theory and critical exponents. Phys. Rev. D **96**(3), 036016 (2017)
3516. A. Bednyakov, A. Pikelner, Six-loop anomalous dimension of the ϕ^Q operator in the $O(N)$ symmetric model. Phys. Rev. D **106**(7), 076015 (2022)
3517. D.J. Broadhurst, D. Kreimer, Knots and numbers in ϕ^4 theory to 7 loops and beyond. Int. J. Mod. Phys. C **6**, 519–524 (1995). (**Ed. by Bruce H. Denby and D. Perret-Gallix**)
3518. O. Schnetz, Numbers and functions in quantum field theory. Phys. Rev. D **97**(8), 085018 (2018)

3519. J. Currie et al., Infrared sensitivity of single jet inclusive production at hadron colliders. JHEP **10**, 155 (2018)
3520. D. Britzger et al., NNLO interpolation grids for jet production at the LHC. Eur. Phys. J. C **82**(10), 930 (2022)
3521. F. Bloch, A. Nordsieck, Note on the radiation field of the electron. Phys. Rev. **52**, 54 (1937)
3522. T. Kinoshita, Mass singularities of Feynman amplitudes. J. Math. Phys. **3**, 650 (1962)
3523. T.D. Lee, M. Nauenberg, Degenerate systems and mass singularities. Phys. Rev. B **133**, 1549 (1964)
3524. S. Catani, L. Trentadue, Resummation of the QCD perturbative series for hard processes. Nucl. Phys. B **327**, 323–352 (1989)
3525. S. Catani et al., Resummation of large logarithms in e^+e^- event shape distributions. Nucl. Phys. B **407**, 3–42 (1993)
3526. N. Kidonakis, G.F. Sterman, Resummation for QCD hard scattering. Nucl. Phys. B **505**, 321–348 (1997)
3527. T. Becher, A. Broggio, A. Ferroglia, Introduction to soft-collinear effective theory. Lect. Notes Phys. **896**, 1–206 (2015)
3528. G. Sterman, M. Zeng, Quantifying comparisons of threshold resummations. JHEP **05**, 132 (2014)
3529. L.G. Almeida et al., Comparing and counting logs in direct and effective methods of QCD resummation. JHEP **04**, 174 (2014)
3530. M. Bonvini et al., Resummation prescriptions and ambiguities in SCET vs. direct QCD: Higgs production as a case study. JHEP **01**, 046 (2015)
3531. M. Bonvini et al., The scale of soft resummation in SCET vs perturbative QCD. Nucl. Phys. B Proc. Suppl. 241–242, 121–126 (2013) **(Ed. by G. Ricciardi et al.)**
3532. an analytic comparison, M. Bonvini et al., Threshold resummation in SCET vs. perturbative QCD. Nucl. Phys. B **861**, 337–360 (2012)
3533. M. Bonvini, L. Rottoli, Three loop soft function for N^{3}LL$'$ gluon fusion Higgs production in soft-collinear effective theory. Phys. Rev. D **91**(5), 051301 (2015)
3534. G. Altarelli, G. Parisi, R. Petronzio, Transverse momentum in Drell-Yan processes. Phys. Lett. B **76**, 351–355 (1978)
3535. G. Bozzi et al., The q(T) spectrum of the Higgs boson at the LHC in QCD perturbation theory. Phys. Lett. B **564**, 65–72 (2003)
3536. G. Bozzi et al., Transverse-momentum resummation and the spectrum of the Higgs boson at the LHC. Nucl. Phys. B **737**, 73–120 (2006)
3537. G. Bozzi et al., Production of Drell-Yan lepton pairs in hadron collisions: transverse-momentum resummation at next-to-next-to-leading logarithmic accuracy. Phys. Lett. B **696**, 207–213 (2011)
3538. S. Catani, M. Grazzini, QCD transverse-momentum resummation in gluon fusion processes. Nucl. Phys. B **845**, 297–323 (2011)
3539. T. Becher, M. Neubert, Drell-Yan production at small q_T, transverse parton distributions and the collinear anomaly. Eur. Phys. J. C **71**, 1665 (2011)
3540. T. Becher, M. Neubert, D. Wilhelm, Higgs-boson production at small transverse momentum. JHEP **05**, 110 (2013)
3541. S. Catani et al., Universality of transverse-momentum resummation and hard factors at the NNLO. Nucl. Phys. B **881**, 414–443 (2014)
3542. T. Gehrmann, T. Luebbert, L. Lin Yang, Calculation of the transverse parton distribution functions at next-to-next-to-leading order. JHEP **06**, 155 (2014)
3543. G.A. Ladinsky, C.P. Yuan, The non-perturbative regime in QCD resummation for gauge boson production at hadron colliders. Phys. Rev. D **50**, R4239 (1994)
3544. F. Landry et al., Tevatron Run-1 Z boson data and Collins-Soper-Sterman resummation formalism. Phys. Rev. D **67**, 073016 (2003)
3545. A. Banfi et al., Predictions for Drell-Yan ϕ^* and Q_T observables at the LHC. Phys. Lett. B **715**, 152–156 (2012)
3546. D. de Florian et al., Transverse-momentum resummation: Higgs boson production at the T-evatron and the LHC. JHEP **11**, 064 (2011)
3547. D. de Florian et al., Higgs boson production at the LHC: transverse momentum resummation effects in the H $\rightarrow$ $\gamma\gamma$, H$\rightarrow$ WW$\rightarrow$ lνlν and H$\rightarrow$ ZZ$\rightarrow$ 4l decay modes. JHEP **06**, 132 (2012)
3548. S. Camarda et al., DYTurbo: fast predictions for Drell-Yan processes. Eur. Phys. J. C **80**(3), 251 (2020) [Erratum: Eur. Phys. J. C 80, 440 (2020)]
3549. W. Bizon et al., Momentum-space resummation for transverse observables and the Higgs p$_\perp$ at N^{3}LL+NNLO. JHEP **02**, 108 (2018)
3550. W. Bizon et al., Fiducial distributions in Higgs and Drell-Yan production at N^{3}LL+NNLO. JHEP **12**, 132 (2018)
3551. W. Bizon et al., The transverse momentum spectrum of weak gauge bosons at N ^{3} LL + NNLO. Eur. Phys. J. C **79**(10), 868 (2019)
3552. X. Chen et al., Third-order fiducial predictions for Drell-Yan production at the LHC. Phys. Rev. Lett. **128**(25), 252001 (2022)
3553. M. Vesterinen, T.R. Wyatt, A novel technique for studying the Z boson transverse momentum distribution at hadron colliders. Nucl. Instrum. Meth. A **602**, 432–437 (2009)
3554. A. Banfi et al., Optimisation of variables for studying dilepton transverse momentum distributions at hadron colliders. Eur. Phys. J. C **71**, 1600 (2011)
3555. A. Banfi, M. Dasgupta, R.M.D. Delgado, The a_T distribution of the Z boson at hadron colliders. JHEP **12**, 022 (2009)
3556. A. Banfi et al., Probing the low transverse momentum domain of Z production with novel variables. JHEP **01**, 044 (2012)
3557. A. Banfi, M. Dasgupta, S. Marzani, QCD predictions for new variables to study dilepton transverse momenta at hadron colliders. Phys. Lett. B **701**, 75–81 (2011)
3558. M. Guzzi, P.M. Nadolsky, B. Wang, Non-perturbative contributions to a resummed leptonic angular distribution in inclusive neutral vector boson production. Phys. Rev. D **90**(1), 014030 (2014)
3559. A. Banfi, G.P. Salam, G. Zanderighi, Principles of general final-state resummation and automated implementation. JHEP **03**, 073 (2005)
3560. S. Catani et al., Soft gluon resummation for Higgs boson production at hadron colliders. JHEP **07**, 028 (2003)
3561. G. Aad et al., Measurement of the transverse momentum distribution of Drell-Yan lepton pairs in proton-proton collisions at $\sqrt{s}$ = 13 TeV with the ATLAS detector. Eur. Phys. J. C **80**(7), 616 (2020)
3562. S.D. Ellis, D.E. Soper, Successive combination jet algorithm for hadron collisions. Phys. Rev. D **48**, 3160–3166 (1993)
3563. S. Marzani, G. Soyez, M. Spannowsky, Looking inside jets: an introduction to jet substructure and boosted-object phenomenology. Lect. Notes Phys. 958 (2019)
3564. E. Farhi, A QCD test for jets. Phys. Rev. Lett. **39**, 1587–1588 (1977)
3565. S. Catani et al., Thrust distribution in e^+e^- annihilation. Phys. Lett. B **263**, 491–497 (1991)
3566. M. Dasgupta, G.P. Salam, Resummation of nonglobal QCD observables. Phys. Lett. B **512**, 323–330 (2001)
3567. A. Banfi et al., Non-global logarithms and jet algorithms in high-pT jet shapes. JHEP **08**, 064 (2010)
3568. A. Banfi, G. Marchesini, G. Smye, Away from jet energy flow. JHEP **08**, 006 (2002)
3569. J.R. Forshaw, A. Kyrieleis, M.H. Seymour, Super-leading logarithms in non-global observables in QCD. JHEP **08**, 059 (2006)
3570. J.R. Forshaw, A. Kyrieleis, M.H. Seymour, Super-leading logarithms in non-global observables in QCD: colour basis independent calculation. JHEP **09**, 128 (2008)
3571. H. Weigert, Nonglobal jet evolution at finite N(c). Nucl. Phys. B **685**, 321–350 (2004)

3572. Y. Hatta, T. Ueda, Resummation of non-global logarithms at finite N_c. Nucl. Phys. B **874**, 808–820 (2013)
3573. S. Caron-Huot, Resummation of non-global logarithms and the BFKL equation. JHEP **03**, 036 (2018)
3574. A. Banfi, F.A. Dreyer, P. Francesco Monni, Next-to leading non-global logarithms in QCD. JHEP **10**, 006 (2021)
3575. A.J. Larkoski, J. Thaler, W.J. Waalewijn, Gaining (mutual) information about quark/gluon discrimination. JHEP **11**, 129 (2014)
3576. A. Tumasyan et al., Study of quark and gluon jet substructure in Z+ jet and dijet events from pp collisions. JHEP **01**, 188 (2022)
3577. S. Caletti et al., Jet angularities in Z+ jet production at the LHC. JHEP **07**, 076 (2021)
3578. D. Reichelt et al., Phenomenology of jet angularities at the LHC. JHEP **03**, 131 (2022)
3579. E. Bothmann et al., Event generation with Sherpa 2.2. SciPost Phys. **7**(3), 034 (2019)
3580. M. Dasgupta et al., Jet substructure with analytical methods. Eur. Phys. J. C **73**(11), 2623 (2013)
3581. J.R. Forshaw, M.H. Seymour, A. Siodmok, On the breaking of collinear factorization in QCD. JHEP **11**, 066 (2012)
3582. J. Bellm et al., Herwig 7.2 release note. Eur. Phys. J. C **80**(5), 452 (2020)
3583. C. Bierlich et al., A comprehensive guide to the physics and usage of PYTHIA 8.3. Sci Post Phys. 8 (2022)
3584. T. Kinoshita, Mass singularities of Feynman amplitudes. J. Math. Phys. **3**, 650–677 (1962)
3585. T.D. Lee, M. Nauenberg, Degenerate systems and mass singularities. Phys. Rev. **133**, B1549–B1562 (1964) **(Ed. by G. Feinberg)**
3586. T. Sjostrand, A model for initial state parton showers. Phys. Lett. B **157**, 321–325 (1985)
3587. G.C. Fox, S. Wolfram, A model for parton showers in QCD. Nucl. Phys. B **168**, 285–295 (1980)
3588. M. Bengtsson, T. Sjostr, Coherent parton showers versus matrix. Elements, implications of PETRA-PEP data. Phys. Lett. B **185**, 435 (1987)
3589. G. Marchesini, B.R. Webber, Simulation of QCD jets including soft gluon interference. Nucl. Phys. B **238**, 1–29 (1984)
3590. B.R. Webber, A QCD model for jet fragmentation including soft gluon interference. Nucl. Phys. B **238**, 492–528 (1984)
3591. G. Gustafson, U. Pettersson, Dipole formulation of QCD cascades. Nucl. Phys. B **306**, 746–758 (1988)
3592. L. Lonnblad, ARIADNE version 4: a program for simulation of QCD cascades implementing the color dipole model. Comput. Phys. Commun. **71**, 15–31 (1992)
3593. B. Andersson, *The Lund Model*, vol. 7 (Cambridge University Press, Cambridge, 2005)
3594. G. Gustafson, Dual description of a confined color field. Phys. Lett. B **175**, 453 (1986) **(Ed. by J. Tran Thanh Van)**
3595. N. Fischer et al., Vincia for hadron colliders. Eur. Phys. J. C **76**(11), 589 (2016)
3596. Z. Nagy, D.E. Soper, Matching parton showers to NLO computations. JHEP **10**, 024 (2005)
3597. S. Schumann, F. Krauss, A Parton shower algorithm based on Catani-Seymour dipole factorisation. JHEP **03**, 038 (2008)
3598. S. Platzer, S. Gieseke, Coherent parton showers with local recoils. JHEP **01**, 024 (2011)
3599. S. Höche, S. Prestel, The midpoint between dipole and parton showers. Eur. Phys. J. C **75**(9), 461 (2015)
3600. S. Frixione, B.R. Webber, Matching NLO QCD computations and parton shower simulations. JHEP **06**, 029 (2002)
3601. P. Nason, A new method for combining NLO QCD with shower Monte Carlo algorithms. JHEP **11**, 040 (2004)
3602. S. Frixione, P. Nason, C. Oleari, Matching NLO QCD computations with parton shower simulations: the POWHEG method. JHEP **11**, 070 (2007)
3603. K. Hamilton et al., Merging H/W/Z + 0 and 1 jet at NLO with no merging scale: a path to parton shower + NNLO matching. JHEP **05**, 082 (2013)
3604. S. Höche, Y. Li, S. Prestel, Drell-Yan lepton pair production at NNLO QCD with parton showers. Phys. Rev. D **91**(7), 074015 (2015)
3605. S. Catani et al., QCD matrix elements + parton showers. JHEP **11**, 063 (2001)
3606. L. Lonnblad, Correcting the color dipole cascade model with fixed order matrix elements. JHEP **05**, 046 (2002)
3607. J. Alwall et al., Comparative study of various algorithms for the merging of parton showers and matrix elements in hadronic collisions. Eur. Phys. J. C **53**, 473–500 (2008)
3608. S. Hoeche et al., QCD matrix elements + parton showers: the NLO case. JHEP **04**, 027 (2013)
3609. R. Frederix, S. Frixione, Merging meets matching in MC@NLO. JHEP **12**, 061 (2012)
3610. S. Höche, D. Reichelt, F. Siegert, Momentum conservation and unitarity in parton showers and NLL resummation. JHEP **01**, 118 (2018)
3611. M. Dasgupta et al., Logarithmic accuracy of parton showers: a fixed order study. JHEP **09**, 033 (2018) [Erratum: JHEP 03, 083 (2020)]
3612. H. Tao Li, P. Skands, A framework for second-order parton showers. Phys. Lett. B **771**, 59–66 (2017)
3613. S. Höche, F. Krauss, S. Prestel, Implementing NLO DGLAP evolution in parton showers. JHEP **10**, 093 (2017)
3614. F. Dulat, S. Höche, S. Prestel, Leading-color fully differential two-loop soft corrections to QCD dipole showers. Phys. Rev. D **98**(7), 074013 (2018)
3615. S. Platzer, M. Sjodahl, Subleading Nc improved parton showers. JHEP **07**, 042 (2012)
3616. Z. Nagy, D.E. Soper, Effects of subleading color in a parton shower. JHEP **07**, 119 (2015)
3617. R. Ángeles Martínez et al., Soft gluon evolution and non-global logarithms. JHEP **05**, 044 (2018)
3618. A. Buckley et al., General-purpose event generators for LHC physics. Phys. Rep. **504**, 145–233 (2011)
3619. J.M. Campbell et al., Event generators for high-energy physics experiments. In: *2022 Snowmass Summer Study* (2022)
3620. X. Artru, G. Mennessier, String model and multiproduction. Nucl. Phys. B **70**, 93–115 (1974)
3621. R.D. Field, R.P. Feynman, A Parametrization of the Properties of Quark Jets. Nucl. Phys. B **136**, 1 (1978) **(Ed. by L. M. Brown)**
3622. P. Hoyer et al., Quantum chromodynamics and jets in e^+e^-. Nucl. Phys. B **161**, 349–372 (1979)
3623. A. Ali et al., QCD predictions for four jet final states in e^+e^- annihilation. Nucl. Phys. B **167**, 454–478 (1980)
3624. B. Andersson, G. Gustafson, T. Sjöstrand, How to find the gluon jets in e^+e^- annihilation. Phys. Lett. B **94**, 211–215 (1980)
3625. W. Bartel et al., Experimental study of jets in electron-positron annihilation. Phys. Lett. B **101**, 129–134 (1981)
3626. F.E. Paige, S.D. Protopopescu, Isajet: A Monte Carlo Event Generator for Isabelle, Version 2. BNL-Report 29777 (1981)
3627. K. Konishi, A. Ukawa, G. Veneziano, Jet calculus: a simple algorithm for resolving QCD jets. Nucl. Phys. B **157**, 45–107 (1979)
3628. S. Alioli et al., A general framework for implementing NLO calculations in shower Monte Carlo programs: the POWHEG BOX. JHEP **06**, 043 (2010)
3629. G. Ingelman, P.E. Schlein, Jet structure in high mass diffractive scattering. Phys. Lett. B **152**, 256–260 (1985)
3630. V.A. Abramovsky, V.N. Gribov, O.V. Kancheli, Character of inclusive spectra and fluctuations produced in inelastic processes by multi-Pomeron exchange. Yad. Fiz. **18**, 595–616 (1973) [Sov. J. Nucl. Phys. 18, 308 (1974)]

3631. P. Bartalini, J. Richard Gaunt (eds.) *Multiple Parton Interactions at the LHC*, Vol. 29 (WSP, 2019)
3632. J. Bellm, S. Gieseke, P. Kirchgaesser, Improving the description of multiple interactions in Herwig. Eur. Phys. J. C **80**(5), 469 (2020)
3633. G. Aad et al., Charged-particle distributions in $\sqrt{s} = 13$ TeV pp interactions measured with the ATLAS detector at the LHC. Phys. Lett. B **758**, 67–88 (2016)
3634. J.R. Christiansen, P.Z. Skands, String formation beyond leading colour. JHEP **08**, 003 (2015)
3635. J. Alcaraz et al., A combination of preliminary electroweak measurements and constraints on the standard model (2006). arXiv:hep-ex/0612034
3636. T. Sjöstrand, Status and developments of event generators. In: PoS LHCP2016, 007 (2016) **(Ed. by J. Bijnens, A. Hoecker, J. Olsen)**
3637. C. Bierlich et al., Effects of overlapping strings in pp collisions. JHEP **03**, 148 (2015)
3638. C. Bierlich, G. Gustafson, L. Lönnblad, A shoving model for collectivity in hadronic collisions (2016). arXiv:1612.05132
3639. D. Amati, G. Veneziano, Preconfinement as a property of perturbative QCD. Phys. Lett. B **83**, 87–92 (1979)
3640. T. Pierog et al., EPOS LHC: test of collective hadronization with data measured at the CERN Large Hadron Collider. Phys. Rev. C **92**(3), 034906 (2015)
3641. J. Alwall et al., A standard format for Les Houches event files. Comput. Phys. Commun. **176**, 300–304 (2007)
3642. A. Buckley et al., The HepMC3 event record library for Monte Carlo event generators. Comput. Phys. Commun. **260**, 107310 (2021)
3643. A. Buckley et al., LHAPDF6: parton density access in the LHC precision era. Eur. Phys. J. C **75**, 132 (2015)
3644. C. Bierlich et al., Robust independent validation of experiment and theory: Rivet version 3. SciPost Phys. **8**, 026 (2020)
3645. J.E. Huth et al., Toward a standardization of jet definitions. In: *1990 DPF Summer Study on High-energy Physics: Research Directions for the Decade (Snowmass 90)*, pp. 134–136 (1990)
3646. G.C. Blazey et al., Run II jet physics. In: *Physics at Run II: QCD and Weak Boson Physics Workshop: Final General Meeting*, pp. 47–77 (2000)
3647. S.D. Ellis, J. Huston, M. Tonnesmann, On building better cone jet algorithms. eConf **C010630**, 513 (2001) **(Ed. by Norman Graf)**
3648. V. Khachatryan et al., Jet energy scale and resolution in the CMS experiment in pp collisions at 8 TeV. JINST **12**(02), P02014 (2017)
3649. J.M. Butterworth et al., Jet substructure as a new Higgs search channel at the LHC. Phys. Rev. Lett. **100**, 242001 (2008)
3650. M. Cacciari, G.P. Salam, G. Soyez, The catchment area of jets. JHEP **04**, 005 (2008)
3651. S.D. Ellis, C.K. Vermilion, J.R. Walsh, Techniques for improved heavy particle searches with jet substructure. Phys. Rev. D **80**, 051501 (2009)
3652. D. Krohn, J. Thaler, L.-T. Wang, Jet trimming. JHEP **02**, 084 (2010)
3653. G. Aad et al., Topological cell clustering in the ATLAS calorimeters and its performance in LHC Run 1. Eur. Phys. J. C **77**, 490 (2017)
3654. M. Aaboud et al., Jet reconstruction and performance using particle flow with the ATLAS detector. Eur. Phys. J. C **77**(7), 466 (2017)
3655. A.M. Sirunyan et al., Particle-flow reconstruction and global event description with the CMS detector. JINST **12**(10), P10003 (2017)
3656. D. Bertolini et al., Pileup per particle identification. JHEP **10**, 059 (2014)
3657. A.M. Sirunyan et al., Pileup mitigation at CMS in 13 TeV data. JINST **15**(09), P09018 (2020)
3658. G. Aad et al., Performance of pile-up mitigation techniques for jets in pp collisions at $\sqrt{s} = 8$ TeV using the ATLAS detector. Eur. Phys. J. C **76**(11), 581 (2016)
3659. P. Berta et al., Particle-level pileup subtraction for jets and jet shapes. JHEP **06**, 092 (2014)
3660. M. Cacciari, G.P. Salam, G. Soyez, SoftKiller, a particle level pileup removal method. Eur. Phys. J. C **75**(2), 59 (2015)
3661. G. Aad et al., Optimisation of large-radius jet reconstruction for the ATLAS detector in 13 TeV proton-proton collisions. Eur. Phys. J. C **81**(4), 334 (2021)
3662. M. Aaboud et al., Determination of jet calibration and energy resolution in proton-proton collisions at $\sqrt{s} = 8$ TeV using the ATLAS detector. Eur. Phys. J. C **80**(12), 1104 (2020)
3663. G. Aad et al., Jet energy scale and resolution measured in proton-proton collisions at $\sqrt{s} = 13$ TeV with the ATLAS detector. Eur. Phys. J. C **81**(8), 689 (2021)
3664. M. Aaboud et al., In situ calibration of large-radius jet energy and mass in 13 TeV proton-proton collisions with the ATLAS detector. Eur. Phys. J. C **79**(2), 135 (2019)
3665. G. Aad et al., Jet energy measurement and its systematic uncertainty in proton-proton collisions at $\sqrt{s} = 7$ TeV with the ATLAS detector. Eur. Phys. J. C **75**, 17 (2015)
3666. D. Bertolini, T. Chan, J. Thaler, Jet observables without jet algorithms. JHEP **04**, 013 (2014)
3667. M. Aaboud et al., Performance of top-quark and W-boson tagging with ATLAS in Run 2 of the LHC. Eur. Phys. J. C **79**(5), 375 (2019)
3668. A.M. Sirunyan et al., Identification of heavy, energetic, hadronically decaying particles using machine-learning techniques. JINST **15**(06), P06005 (2020)
3669. R. Assmann, M. Lamont, S. Myers. A brief history of the LEP collider. Nucl. Phys. B Proc. Suppl. **109**, 17–31 (2002) **(F.L. Navarria, M. Paganoni, and P.G. Pelfer)**
3670. S. Schael et al., Precision electroweak measurements on the Z resonance. Phys. Rept. **427**, 257–454 (2006)
3671. B. Naroska, e^+e^- physics with the JADE detector at PETRA. Phys. Rep. **148**, 67 (1987)
3672. R.J. Barlow, Jets in high-energy interactions. Rep. Prog. Phys. **56**, 1067–1144 (1993)
3673. G. Altarelli, Experimental tests of perturbative QCD. Annu. Rev. Nucl. Part. Sci. **39**, 357–406 (1989)
3674. S. Bethke, Experimental overview of jet physics and tests of QCD. J. Phys. G **17**, 1455–1480 (1991)
3675. G. Alexander et al., Measurement of three jet distributions sensitive to the gluon spin in e^+e^- annihilations at $s^{1/2}$ = 91-GeV. Z. Phys. C **52**, 543–550 (1991)
3676. S. Schael et al., Electroweak measurements in electron-positron collisions at W-boson-pair energies at LEP. Phys. Rep. **532**, 119–244 (2013)
3677. J. Abdallah et al., Measurement of the energy dependence of hadronic jet rates and the strong coupling α_s from the four-jet rate with the DELPHI detector at LEP. Eur. Phys. J. C **38**, 413–426 (2005)
3678. K. Koller, H. Krasemann, Excluding scalar gluons. Phys. Lett. B **88**, 119–122 (1979)
3679. R. Keith Ellis, W. James Stirling, B.R. Webber, *QCD and Collider Physics*, vol. 8 (Cambridge University Press, Cambridge, 2011)
3680. S. Bethke, A. Ricker, P.M. Zerwas, Four jet decays of the Z0: prospects of testing the triple gluon coupling. Z. Phys. C **49**, 59–72 (1991)
3681. Z. Nagy, Z. Trocsanyi, Four jet angular distributions and color charge measurements: leading order versus next-to-leading order. Phys. Rev. D **57**, 5793–5802 (1998)
3682. G. Abbiendi et al., A simultaneous measurement of the QCD color factors and the strong coupling. Eur. Phys. J. C **20**, 601–615 (2001)

3683. A. Heister et al., Measurements of the strong coupling constant and the QCD color factors using four jet observables from hadronic Z decays. Eur. Phys. J. C **27**, 1–17 (2003)
3684. S. Kluth et al., A measurement of the QCD color factors using event shape distributions at $s^{1/2}$ = 14-GeV to 189-GeV. Eur. Phys. J. C **21**, 199–210 (2001)
3685. S. Kluth, Tests of quantum chromo dynamics at e^+e^- colliders. Rep. Prog. Phys. **69**, 1771–1846 (2006)
3686. G. Abbiendi et al., Measurement of the longitudinal cross-section using the direction of the thrust axis in hadronic events at LEP. Phys. Lett. B **440**, 393–402 (1998)
3687. P.D. Acton et al., A study of the electric charge distributions of quark and gluon jets in hadronic Z0 decays. Phys. Lett. B **302**, 523–532 (1993)
3688. W. Bartel et al., Experimental studies on multi-jet production in e^+e^- annihilation at PETRA energies. Z. Phys. C **33**, 23 (1986) **(Ed. by J. Tran Thanh Van)**
3689. S. Komamiya et al., Determination of a-s from a differential jet multiplicity distribution at SLC and PEP. Phys. Rev. Lett. **64**, 987 (1990)
3690. A. Heister et al., Studies of QCD at e^+e^- centre-of-mass energies between 91-GeV and 209-GeV. Eur. Phys. J. C **35**, 457–486 (2004)
3691. G. Abbiendi et al., Measurement of event shape distributions and moments in $e^+e^- \to$ hadrons at 91-GeV-209-GeV and a determination of α_s. Eur. Phys. J. C **40**, 287–316 (2005)
3692. G. Abbiendi et al., Determination of $alpha_s$ using OPAL hadronic event shapes at $\sqrt{s}$ = 91 - 209 GeV and resummed NNLO calculations. Eur. Phys. J. C **71**, 1733 (2011)
3693. G. Dissertori et al., Determination of the strong coupling constant using matched NNLO+NLLA predictions for hadronic event shapes in e+eannihilations. JHEP **08**, 036 (2009)
3694. G. Dissertori et al., Precise determination of the strong coupling constant at NNLO in QCD from the three-jet rate in electron-positron annihilation at LEP. Phys. Rev. Lett. **104**, 072002 (2010)
3695. S. Bethke et al., Determination of the strong coupling as from hadronic event shapes with $O(\alpha_s^3)$ and resummed QCD predictions using JADE data. Eur. Phys. J. C **64**, 351–360 (2009)
3696. A. Verbytskyi et al., High precision determination of as from a global fit of jet rates. JHEP **08**, 129 (2019)
3697. A. Kardos, G. Somogyi, A. Verbytskyi, Determination of α_s as beyond NNLO using event shape averages. Eur. Phys. J. C **81**(4), 292 (2021)
3698. F. Caola et al., Linear power corrections to e^+e^- shape variables in the three-jet region. JHEP **12**, 062 (2022)
3699. Z. Nagy, Z. Trocsanyi, Next-to-leading order calculation of four jet shape variables. Phys. Rev. Lett. **79**, 3604–3607 (1997)
3700. G. Abbiendi et al., Measurement of the strong coupling α_s from four-jet observables in e^+e^- annihilation. Eur. Phys. J. C **47**, 295–307 (2006)
3701. J. Schieck et al., Measurement of the strong coupling as from the fourjet rate in e^+e^- annihilation using JADE data. Eur. Phys. J. C **48**, 3–13 (2006) [Erratum: Eur. Phys. J. C 50, 769 (2007)]
3702. R. Frederix et al., NLO QCD corrections to five-jet production at LEP and the extraction of α_s (MZ). JHEP **11**, 050 (2010)
3703. J. Abdallah et al., A study of the energy evolution of event shape distributions and their means with the DELPHI detector at LEP. Eur. Phys. J. C **29**, 285–312 (2003)
3704. S. Bethke et al., Experimental investigation of the energy dependence of the strong coupling strength. Phys. Lett. B **213**, 235–241 (1988)
3705. D. Buskulic et al., Measurement of as from scaling violations in fragmentation functions in e^+e^- annihilation. Phys. Lett. B **357**, 487–499 (1995) [Erratum: Phys. Lett. B 364, 247–248 (1995)]
3706. D.P. Anderle, F. Ringer, M. Stratmann, Fragmentation functions at next-to-next-to-leading order accuracy. Phys. Rev. D **92**(11), 114017 (2015)
3707. G. Abbiendi et al., Charged particle momentum spectra in e^+e^--annihilation at $s^{1/2} = 192 - $GeVto209 $-$ GeV. Eur. Phys. J. C **27**, 467–481 (2003)
3708. C.P. Fong, B.R. Webber, One and two particle distributions at small x in QCD jets. Nucl. Phys. B **355**, 54–81 (1991)
3709. R. Perez-Ramos, D. d'Enterria, Energy evolution of the moments of the hadron distribution in QCD jets including NNLL resummation and NLO running-coupling corrections. JHEP **08**, 068 (2014)
3710. E.R. Boudinov, P.V. Chliapnikov, V.A. Uvarov, Is there experimental evidence for coherence of soft gluons from the momentum spectra of hadrons in e^+e^- data? Phys. Lett. B **309**, 210–221 (1993)
3711. V.A. Khoze, W. Ochs, Perturbative QCD approach to multiparticle production. Int. J. Mod. Phys. A **12**, 2949–3120 (1997)
3712. A. Banfi, G. Corcella, M. Dasgupta, Angular ordering and parton showers for non-global QCD observables. JHEP **03**, 050 (2007)
3713. P. Skands, S. Carrazza, J. Rojo, Tuning PYTHIA 8.1: the Monash 2013 Tune. Eur. Phys. J. C **74**(8), 3024 (2014)
3714. S. Argyropoulos, T. Sjöstrand, Effects of color reconnection on $t = \bar{t}$ final states at the LHC. JHEP **11**, 043 (2014)
3715. A.M. Sirunyan et al., Measurement of the top quark mass with lepton+ jets final states using p p collisions at $\sqrt{s}$ = 13 TeV. Eur. Phys. J. C **78**(11), 891 (2018) [Erratum: Eur. Phys. J. C 82, 323 (2022)]
3716. F. Wilczek, Asymptotic freedom: from paradox to paradigm. Proc. Natl. Acad. Sci. **102**, 8403–8413 (2005)
3717. K.G. Chetyrkin, J.H. Kuhn, A. Kwiatkowski, QCD corrections to the e^+e^- cross-section and the Z boson decay rate. Phys. Rep. **277**, 189–281 (1996)
3718. Y.L. Dokshitzer, V.A. Khoze, S.I. Troian, On specific QCD properties of heavy quark fragmentation ('dead cone'). J. Phys. G **17**, 1602–1604 (1991)
3719. M.S. Bilenky, G. Rodrigo, A. Santamaria, Three jet production at LEP and the bottom quark mass. Nucl. Phys. B **439**, 505–535 (1995)
3720. R. Barate et al., A measurement of the b quark mass from hadronic Z decays. Eur. Phys. J. C **18**, 1–13 (2000)
3721. J. Aparisi et al., $m_b$atm_H: the running bottom quark mass and the Higgs boson. Phys. Rev. Lett. **128**(12), 122001 (2022)
3722. R. Akers et al., QCD studies using a cone based jet finding algorithm for e^+e^- collisions at LEP. Z. Phys. C **63**, 197–212 (1994)
3723. Y.L. Dokshitzer, V.A. Khoze, S.I. Troian, Particle spectra in light and heavy quark jets. J. Phys. G **17**, 1481–1492 (1991)
3724. Y.L. Dokshitzer et al., Multiplicity difference between heavy and light quark jets revisited. Eur. Phys. J. C **45**, 387–400 (2006)
3725. J. Abdallah et al., A study of the b-quark fragmentation function with the DELPHI detector at LEP I and an averaged distribution obtained at the Z Pole. Eur. Phys. J. C **71**, 1557 (2011)
3726. J. Haller et al., Update of the global electroweak fit and constraints on two-Higgs-doublet models. Eur. Phys. J. C **78**(8), 675 (2018)
3727. M.A. Benitez-Rathgeb et al., Reconciling the contour-improved and fixed-order approaches for t hadronic spectral moments. Part II. Renormalon norm and application in α_s determinations. JHEP **09**, 223 (2022)
3728. S. Brandt et al., The principal axis of jets. An attempt to analyze high energy collisions as two-body processes. Phys. Lett. **12**, 57–61 (1964)
3729. J.D. Bjorken, S.J. Brodsky, Statistical model for electron-positron annihilation into hadrons. Phys. Rev. D **1**, 1416 (1970)
3730. C. Berger et al., Topology of the Υ decay. Z. Phys. C **8**, 101 (1981)
3731. M. Banner et al., Observation of very large transverse momentum jets at the CERN anti-p p collider. Phys. Lett. B **118**, 203–210 (1982)
3732. R. Horgan, M. Jacob, Jet production at collider energy. Nucl. Phys. B **179**, 441 (1981)

3733. G. Arnison et al., Observation of jets in high transverse energy events at the CERN proton-anti-proton collider. Phys. Lett. B **123**, 115–122 (1983)
3734. T. Akesson et al., Direct evidence for the emergence of jets in events triggered on large transverse energy in pp collisions at $\sqrt{s} = 63$ GeV. Phys. Lett. B **118**, 185–192 (1982)
3735. B. Flaugher, K. Meier, a compilation of jet finding algorithms. In: *Proceedings, 5th DPF Summer Study on High-energy Physics: Research Directions for the Decade (Snowmass 90)*, Snowmass, Jun 25–Jul 13, p. 128 (1990)
3736. N. Brown, W. James Stirling, Finding jets and summing soft gluons: a new algorithm. Z. Phys. C **53**, 629 (1992)
3737. T. Hebbeker, Tests of quantum chromodynamics in hadronic decays of Z0 bosons produced in e^+e^- annihilation. Phys. Rep. **217**, 69 (1992)
3738. D. Graudenz, N. Magnussen, Jet cross-sections in deeply inelastic scattering at HERA. In: *Workshop on Physics at HERA* (1991)
3739. G.P. Salam, G. Soyez, A practical seedless infrared-safe cone jet algorithm. JHEP **05**, 086 (2007)
3740. F. Aversa et al., Jet inclusive production to O(α_s^3): comparison with data. Phys. Rev. Lett. **65**, 401–403 (1990)
3741. S.D. Ellis, Z. Kunszt, D.E. Soper, One-jet inclusive cross section at order α_s^3: quarks and gluons. Phys. Rev. Lett. **64**, 2121 (1990)
3742. E. Eichten et al., Super collider physics. Rev. Mod. Phys. **56**, 579 (1984) [Erratum: Rev. Mod. Phys. 56, 579 (1984)]
3743. M. Diemoz et al., Parton densities from deep inelastic scattering to hadronic processes at super collider energies. Z. Phys. C **39**, 21 (1988)
3744. A.D. Martin, R.G. Roberts, W. James Stirling, Structure function analysis and psi, Jet, W, Z production: pinning down the gluon. Phys. Rev. D **D37**, 1161 (1988)
3745. A.D. Martin, W. James Stirling, R.G. Roberts, Benchmark cross sections for $p\bar{p}$ collisions at 1.8 TeV. Z. Phys. C **42**, 277 (1989)
3746. F. Abe et al., Inclusive jet cross section in $\bar{p}p$ collisions at $\sqrt{s} =$ 1.8 TeV. Phys. Rev. Lett. **77**, 438 (1996)
3747. E. Eichten, K.D. Lane, M.E. Peskin, New tests for quark and lepton substructure. Phys. Rev. Lett. **50**, 811–814 (1983)
3748. D.E. Soper, Summary of the XXX Rencontres de Moriond QCD session. In: *30th Rencontres de Moriond: QCD and High-energy Hadronic Interactions*, pp. 615–628 (1995)
3749. W.T. Giele, S. Keller, Implications of hadron collider observables on parton distribution function uncertainties. Phys. Rev. D **58**, 094023 (1998)
3750. S. Alekhin, Extraction of parton distributions and as from DIS data within the Bayesian treatment of systematic errors. Eur. Phys. J. C **10**, 395–403 (1999)
3751. G.E. Wolf, First results from HERA. In *Proceedings, QCD: 20 Years Later?: Aachen, June 9–13, 1992*. ed. by P.M. Zerwas, H.A. Kastrup (World Scientific, 1993), pp. 335–384
3752. S. Bethke, Jets in Z0 decays, in *Proceedings, QCD?: 20 Years Later?: Aachen, June 9–13, 1992*. ed. by P.M. Zerwas, H.A. Kastrup (World Scientific, 1993), pp. 43–72
3753. G. Altarelli, QCD and experiment: status of aS, in *Proceedings, QCD?: 20 Years Later?: Aachen, June 9–13, 1992*. ed. by P.M. Zerwas, H.A. Kastrup (World Scientific, 1993), pp.172–202
3754. I. Abt et al., The tracking, calorimeter and muon detectors of the H1 experiment at HERA. Nucl. Instrum. Meth. A **386**, 348–396 (1997)
3755. I. Abt et al., The H1 detector at HERA. Nucl. Instrum. Meth. A **386**, 310–347 (1997)
3756. U. Holm et al., The ZEUS detector: status report 1993. Tech. rep. ZEUSSTATUS-REPT, p. 597 (1993)
3757. H. Abramowicz et al., Inclusive dijet cross sections in neutral current deep inelastic scattering at HERA. Eur. Phys. J. C **70**, 965–982 (2010)
3758. V. Andreev et al., Measurement of multijet production in *ep* collisions at high Q^2 and determination of the strong coupling as. Eur. Phys. J. C **75**(2), 65 (2015)
3759. M. Derrick et al., Measurement of the proton structure function F_2 in $e^- p$ scattering at HERA. Phys. Lett. B **316**, 412–426 (1993)
3760. I. Abt et al., Measurement of the proton structure function $F_2(x, Q^2)$ in the low x region at HERA. Nucl. Phys. B **407**, 515–538 (1993)
3761. T. Ahmed et al., Hard scattering in γp interactions. Phys. Lett. B **297**, 205–213 (1992)
3762. M. Derrick et al., Observation of hard scattering in photoproduction at HERA. Phys. Lett. B **297**, 404–416 (1992)
3763. M. Kuhlen, QCD at HERA: the hadronic final state in deep inelastic scattering. Springer Tracts Mod. Phys. **150**, 1–172 (1999)
3764. H. Abramowicz, A. Caldwell, HERA collider physics. Rev. Mod. Phys. **71**, 1275–1410 (1999)
3765. M. Klein, R. Yoshida, Collider physics at HERA. Prog. Part. Nucl. Phys. **61**, 343–393 (2008)
3766. P. Newman, M. Wing, The hadronic final state at HERA. Rev. Mod. Phys. **86**(3), 1037 (2014)
3767. O. Behnke, A. Geiser, M. Lisovyi, Charm, beauty and top at HERA. Prog. Part. Nucl. Phys. **84**, 1–72 (2015)
3768. I. Abt et al., A measurement of multi-jet rates in deep inelastic scattering at HERA. Z. Phys. C **61**, 59–66 (1994)
3769. M. Derrick et al., Observation of two jet production in deep inelastic scattering at HERA. Phys. Lett. B **306**, 158–172 (1993)
3770. T. Carli, Hadronic final state in deep inelastic scattering at HERA. In: *16th International Conference on Physics in Collision (PIC 96)*, pp. 415–438 (1996)
3771. D. Graudenz, Three jet production in deep inelastic electron-proton scattering to order α_s^2. Phys. Lett. B **256**, 518–522 (1991)
3772. T. Ahmed et al., Determination of the strong coupling constant from jet rates in deep inelastic scattering. Phys. Lett. B **346**, 415–425 (1995)
3773. M. Derrick et al., Measurement of as from jet rates in deep inelastic scattering at HERA. Phys. Lett. B **363**, 201–216 (1995)
3774. R. Michael Barnett et al., Review of Particle Physics. Particle Data Group. Phys. Rev. D **54**, 1–720 (1996)
3775. E. Mirkes, D. Zeppenfeld, Dijet production at HERA in nexttoleading order. Phys. Lett. B **380**, 205–212 (1996)
3776. S. Catani, Y.L. Dokshitzer, B.R. Webber, The K^- perpendicular clustering algorithm for jets in deep inelastic scattering and hadron collisions. Phys. Lett. B **285**, 291–299 (1992)
3777. B.R. Webber, Factorization and jet clustering algorithms for deep inelastic scattering. J. Phys. G **19**, 1567–1575 (1993)
3778. C. Adloff et al., Measurement and QCD analysis of jet cross-sections in deep inelastic positron-proton collisions at $s^{1/2}$ of 300-GeV. Eur. Phys. J. C **19**, 289–311 (2001)
3779. C. Adloff et al., Measurement of inclusive jet cross-sections in deep inelastic ep scattering at HERA. Phys. Lett. B **542**, 193–206 (2002)
3780. S. Chekanov et al., Inclusive jet cross-sections in the Breit frame in neutral current deep inelastic scattering at HERA and determination of α_s. Phys. Lett. B **547**, 164–180 (2002)
3781. S. Bethke, Determination of the QCD coupling α_s. J. Phys. **G26**, R27 (2000)
3782. S. Chekanov et al., An NLO QCD analysis of inclusive cross-section and jet-production data from the Zeus experiment. Eur. Phys. J. C **42**, 1–16 (2005)
3783. V. Andreev et al., Measurement of jet production cross sections in deep inelastic ep scattering at HERA. Eur. Phys. J. C **77**(4), 215 (2017) [Erratum: Eur. Phys. J. C 81, 739 (2021)]
3784. J. Currie, T. Gehrmann, J. Niehues, Precise QCD predictions for the production of dijet final states in deep inelastic scattering. Phys. Rev. Lett. **117**(4), 042001 (2016)

3785. J. Niehues et al., Precise QCD predictions for the production of dijet final states in deep inelastic scattering. In: *52nd Rencontres de Moriond on QCD and High Energy Interactions* (SISSA, 2017), pp. 199–202
3786. V. Andreev et al., Determination of the strong coupling constant $\alpha_s(m_Z)$ in next-to-next-to-leading order QCD using H1 jet cross section measurements. Eur. Phys. J. C **77**(11), 791 (2017) [Erratum: Eur. Phys. J. C 81, 738 (2021)]
3787. D. Britzger et al., Calculations for deep inelastic scattering using fast interpolation grid techniques at NNLO in QCD and the extraction of α_s from HERA data. Eur. Phys. J. C **79**(10), 845 (2019) [Erratum: arXiv:1906.05303v3]
3788. I. Abt et al., Impact of jet-production data on the next-to-next-to-leading order determination of HERAPDF2.0 parton distributions. Eur. Phys. J. C **82**(3), 243 (2022)
3789. V. Khachatryan et al., Measurement and QCD analysis of double differential inclusive jet cross-sections in pp collisions at $\sqrt{s}$ = 8 TeV and ratios to 2.76 and 7 TeV. JHEP **03**, 156 (2017)
3790. G. Dissertori et al., First determination of the strong coupling constant using NNLO predictions for hadronic event shapes in e^+e^- annihilations. JHEP **02**, 040 (2008)
3791. J. Schieck et al., Measurement of the strong coupling α_s from the three-jet rate in e^+e^- annihilation using JADE data. Eur. Phys. J. C **73**(3), 2332 (2013)
3792. M. Jacob, ed. *Proceedings of the ECFA-CERN Workshop: Large Hadron Collider in the LEP Tunnel*, Lausanne and Geneva, Switzerland 21–27 Mar 1984 (CERN, Geneva, 1984)
3793. F. Aversa et al., QCD corrections to parton-parton scattering processes. Nucl. Phys. B **327**, 105 (1989)
3794. F. Abe et al., Comparison of jet production in $\bar{p}p$ collisions at $\sqrt{s}$ = 546 GeV and 1800 GeV. Phys. Rev. Lett. **70**, 1376–1380 (1993)
3795. B. Abbott et al., High-pT jets in $\bar{p}p$ collisions at $\sqrt{s}$= 630 GeV and 1800 GeV. Phys. Rev. D **64**, 032003 (2001)
3796. B. Abbott et al., Inclusive jet production in $p\bar{p}$ collisions. Phys. Rev. Lett. **86**, 1707–1712 (2001)
3797. T. Affolder et al., Measurement of the inclusive jet cross section in $\bar{p}p$ collisions at $\sqrt{s}$ = 1.8 TeV. Phys. Rev. D **64**, 032001 (2001) [Erratum: Phys. Rev. D 65, 039903 (2002)]
3798. B.I. Abelev et al., Longitudinal double-spin asymmetry and cross section for inclusive jet production in polarized proton collisions at $s^{1/2}$ = 200-GeV. Phys. Rev. Lett. **97**, 252001 (2006)
3799. S. Chekanov et al., Inclusive-jet and dijet cross-sections in deep inelastic scattering at HERA. Nucl. Phys. B **765**, 1 (2007)
3800. A. Abulencia et al., Measurement of the inclusive jet cross section using the k_T algorithm in $p\bar{p}$ collisions at $\sqrt{s}$ = 1.96 TeV with the CDF II detector. Phys. Rev. D **75**, 092006 (2007) [Erratum: Phys. Rev. D 75, 119901 (2007)]
3801. T. Aaltonen et al., Measurement of the inclusive jet cross section at the Fermilab Tevatron $p\bar{p}$ collider using a cone-based jet algorithm. Phys. Rev. D **78**, 052006 (2008) [Erratum: Phys. Rev. D 79, 119902 (2009)]
3802. V.M. Abazov et al., Measurement of the inclusive jet cross-section in $p\bar{p}$ collisions at $s^{(1/2)}$ =1.96-TeV. Phys. Rev. Lett. **101**, 062001 (2008)
3803. S. Chatrchyan et al., Measurements of differential jet cross sections in proton-proton collisions at $\sqrt{s}$ = 7 TeV with the CMS detector. Phys. Rev. D **87**(11), 112002 (2013) [Erratum: Phys. Rev. D 87, 119902 (2013)]
3804. G. Aad et al., Measurement of the inclusive jet cross section in pp collisions at $\sqrt{s}$ = 2.76 TeV and comparison to the inclusive jet cross section at $\sqrt{s}$ = 7 TeV using the ATLAS detector. Eur Phys. J. C **73**(8), 2509 (2013)
3805. G. Aad et al., Measurement of the inclusive jet cross-section in proton-proton collisions at $\sqrt{s}$ = 7 TeV using 4.5 fb^{-1} of data with the ATLAS detector. JHEP **02**, 153 (2015) [Erratum: JHEP 09, 141 (2015)]
3806. V. Khachatryan et al., Measurement of the inclusive jet cross section in pp collisions at $\sqrt{s}$ = 2.76TeV. Eur. Phys. J. C **76**(5), 265 (2016)
3807. M. Aaboud et al., Measurement of inclusive jet and dijet cross-sections in proton-proton collisions at $\sqrt{s}$ = 13 TeV with the ATLAS detector. JHEP **05**, 195 (2018)
3808. M. Aaboud et al., Measurement of the inclusive jet cross-sections in proton-proton collisions at $\sqrt{s}$ = 8 TeV with the ATLAS detector. JHEP **09**, 020 (2017)
3809. A. Tumasyan et al., Measurement and QCD analysis of double-differential inclusive jet cross sections in proton-proton collisions at $\sqrt{s}$ = 13TeV. JHEP **02**, 142 (Nov.2022)
3810. R.D. Ball et al., The PDF4LHC21 combination of global PDF fits for the LHC Run III. J. Phys. G **49**(8), 080501 (2022)
3811. T. Carli et al., A posteriori inclusion of parton density functions in NLO QCD final-state calculations at hadron colliders: the APPLGRID Project. Eur. Phys. J. C **66**, 503–524 (2010)
3812. D. Britzger et al., New features in version 2 of the fastNLO project. In: *Proceedings, XX. International Workshop on Deep-Inelastic Scattering and Related Subjects (DIS 2012)*, Bonn, March 26–30, (2012), p. 217
3813. T. Gehrmann et al., Jet cross sections and transverse momentum distributions with NNLOJET. PoS RADCOR2017, 074 (2018) **(Ed. by A. Hoang and C. Schneider)**
3814. N. Kidonakis, J.F. Owens, Effects of higher order threshold corrections in high E_T jet production. Phys. Rev. D **63**, 054019 (2001)
3815. Z. Nagy, Three jet cross-sections in hadron hadron collisions at next-to-leading order. Phys. Rev. Lett. **88**, 122003 (2002)
3816. M. Wobisch et al., Theory-Data Comparisons for Jet Measurements in Hadron-Induced Processes (2011)
3817. M. Cacciari, N. Houdeau, Meaningful characterisation of perturbative theoretical uncertainties. JHEP **09**, 039 (2011)
3818. E. Bagnaschi et al., An extensive survey of the estimation of uncertainties from missing higher orders in perturbative calculations. JHEP **02**, 133 (2015)
3819. M. Bonvini, Probabilistic definition of the perturbative theoretical uncertainty from missing higher orders. Eur. Phys. J. C **80**(10), 989 (2020)
3820. C. Duhr et al., An analysis of Bayesian estimates for missing higher orders in perturbative calculations (2021)
3821. A. David, G. Passarino, How well can we guess theoretical uncertainties? Phys. Lett. B **726**, 266–272 (2013)
3822. F.I. Olness, D.E. Soper, Correlated theoretical uncertainties for the one-jet inclusive cross section. Phys. Rev. D **81**, 035018 (2010)
3823. R. Abdul Khalek et al., A first determination of parton distributions with theoretical uncertainties. Eur. Phys. J. C **79**, 838 (2019)
3824. V. Khachatryan et al., Search for quark contact interactions and extra spatial dimensions using dijet angular distributions in proton-proton collisions at $\sqrt{s}$ = 8 TeV. Phys. Lett. B **746**, 79 (2015)
3825. ATLAS Collaboration. Determination of the parton distribution functions of the proton using diverse ATLAS data from pp collisions at $\sqrt{s}$ = 7, 8 and 13 TeV. Eur. Phys. J. C 82(5), 438 (2022)
3826. J. Campbell, J. Huston, F. Krauss, *The Black Book of Quantum Chromodynamics: A Primer for the LHC Era* (Oxford University Press, Oxford, 2017)
3827. R.K. Ellis, W.J. Stirling, B.R. Webber, *QCD and Collider Physics* (Nuclear Physics and Cosmology (Cambridge University Press, Cambridge, Cambridge Monographs on Particle Physics, 1996)
3828. A. Denner, S. Dittmaier, Electroweak radiative corrections for collider physics. Phys. Rep. **864**, 1–163 (2020)
3829. UA1 Collaboration, Studies of intermediate vector boson production and decay in UA1 at the CERN proton-antiproton collider. Z. Phys. C Part. Fields **44**(1) (1989)
3830. TASSO Collaboration, Evidence for a spin one gluon in three jet events. Phys. Lett. B **97**, 453 (1980)

3831. UA1 Collaboration, Angular distributions and structure functions from two jet events at the CERN SPS $p\bar{p}$ collider. Phys. Lett. B **136**, 294 (1984)
3832. UA2 Collaboration, A determination of the strong coupling constant α_s from W production at the CERN $p\bar{p}$ collider. Phys. Lett. B **263**, 563–572 (1991)
3833. P.D. Acton et al., A global determination of $\alpha_s(M_{Z^0})$ at LEP. Z. Phys. C **55**, 1–24 (1992)
3834. M. Schott, M. Dunford, Review of single vector boson production in pp collisions at $\sqrt{s} = 7$ TeV. Eur. Phys. J. C **74**, 2916 (2014)
3835. CDF Collaboration, Measurement of the cross section for W^- boson production in association with jets in $p\bar{p}$ collisions at $\sqrt{s}$ = 1.96-TeV. Phys. Rev. D **77**, 011108 (2008)
3836. DO Collaboration, Studies of W boson plus jets production in $p\bar{p}$ collisions at $\sqrt{s} = 1.96$ TeV. Phys. Rev. D **88**(9), 092001 (2013)
3837. Z. Bern et al., Missing energy and jets for supersymmetry searches. Phys. Rev. D **87**(3), 034026 (2013)
3838. C.M.S. Collaboration, Measurement of differential cross sections for the production of a Z boson in association with jets in proton-proton collisions at $\sqrt{s}$ = 13. TeV. Phys. Rev. D **108**, 252004 (2023)
3839. C.M.S. Collaboration, Measurement of the differential cross sections for the associated production of a W boson and jets in proton-proton collisions at $\sqrt{s} = 13$ TeV. Phys. Rev. D **96**(7), 072005 (2017)
3840. ATLAS Collaboration, Measurements of the production cross section of a Z boson in association with jets in pp collisions at $\sqrt{s} = 13$ TeV with the ATLAS detector. Eur. Phys. J. C **77**(6), 361 (2017)
3841. ATLAS Collaboration, Measurement of differential cross sections and W^+/W^- cross-section ratios for W boson production in association with jets at $\sqrt{s} = 8$ TeV with the ATLAS detector. JHEP **05**, 077 (2018) [Erratum: JHEP 10, 048 (2020)]
3842. C.M.S. Collaboration, Measurement of differential cross sections for Z boson production in association with jets in proton-proton collisions at $\sqrt{s} = 13$ TeV. Eur. Phys. J. C **78**(11), 965 (2018)
3843. Y.L. Dokshitzer, D. Diakonov, S.I. Troian, On the transverse momentum distribution of massive lepton pairs. Phys. Lett. B **79**, 269–272 (1978)
3844. ATLAS Collaboration, Cross-section measurements for the production of a Z boson in association with high-transverse-momentum jets in pp collisions at $\sqrt{s}$ = 13 TeV with the ATLAS detector. JHEP **06**, 080 (2023)
3845. C.M.S. Collaboration, Measurements of the differential cross sections of the production of Z + jets and γ + jets and of Z boson emission collinear with a jet in pp collisions at $\sqrt{s}$ = 13 TeV. JHEP **05**, 285 (2021)
3846. ATLAS Collaboration, Measurement of W boson angular distributions in events with high transverse momentum jets at $\sqrt{s} =$ 8 TeV using the ATLAS detector. Phys. Lett. B **765**, 132–153 (2017)
3847. C.M.S. Collaboration, Measurements of angular distance and momentum ratio distributions in three-jet and Z + two-jet final states in pp collisions. Eur. Phys. J. C **81**(9), 852 (2021)
3848. ATLAS Collaboration, Measurement of the electroweak production of dijets in association with a Z-boson and distributions sensitive to vector boson fusion in proton-proton collisions at $\sqrt{s} =$ 8 TeV using the ATLAS detector. JHEP **04**, 031 (2014)
3849. ATLAS Collaboration, Measurements of electro-weak Wjj production and constraints on anomalous gauge couplings with the ATLAS detector. Eur. Phys. J. C **77**(7), 474 (2017)
3850. C.M.S. Collaboration, Measurement of the hadronic activity in events with a Z and two jets and extraction of the cross section for the electroweak production of a Z with two jets in pp collisions at $\sqrt{s}$ = 7 TeV. JHEP **10**, 062 (2013)
3851. C.M.S. Collaboration, Measurement of electroweak production of a W boson and two forward jets in proton-proton collisions at $\sqrt{s} = 8$ TeV. JHEP **11**, 147 (2016)
3852. C.M.S. Collaboration, Electroweak production of two jets in association with a Z boson in proton-proton collisions at $\sqrt{s} = 13$ TeV. Eur. Phys. J. C **78**(7), 589 (2018)
3853. C.M.S. Collaboration, Measurement of electroweak production of a W boson in association with two jets in proton-proton collisions at $\sqrt{s} = 13$ TeV. Eur. Phys. J. C **80**(1), 43 (2020)
3854. LHCb Collaboration, Measurement of forward W and Z boson production in association with jets in proton-proton collisions at $\sqrt{s} = 8$ TeV. JHEP **05**, 131 (2016)
3855. LHCb Collaboration, Study of forward Z + jet production in pp collisions at $\sqrt{s} = 7$ TeV. JHEP **01**, 033 (2014)
3856. ATLAS Collaboration, Measurement of detector-corrected observables sensitive to the anomalous production of events with jets and large missing transverse momentum in pp collisions at $\sqrt{s} = \mathbf{13}$ TeV using the ATLAS detector. Eur. Phys. J. C **77**(11), 765 (2017)
3857. ATLAS Collaboration, A measurement of the ratio of the production cross sections for W and Z bosons in association with jets with the ATLAS detector. Eur. Phys. J. C **74**(12), 3168 (2014)
3858. E. Gerwick et al., Scaling patterns for QCD jets. JHEP **1210**, 162 (2012)
3859. G. Aad et al., Measurement of the production cross section of jets in association with a Z boson in pp collisions at $\sqrt{s}$ = 7 TeV with the ATLAS detector. JHEP **07**, 032 (2013)
3860. J.M. Campbell et al., Associated production of a W boson and one b Jet. Phys. Rev. D **79**, 034023 (2009)
3861. S. Badger, J.M. Campbell, R.K. Ellis, QCD corrections to the hadronic production of a heavy quark pair and a W-boson including decay correlations. JHEP **03**, 027 (2011)
3862. F. Febres Cordero, L. Reina, D. Wackeroth, Associated production of a W or Z boson with bottom quarks at the Tevatron and the LHC. PoS RADCOR **2009**, 055 (2010)
3863. J.M. Campbell et al., NLO QCD predictions for $W + 1$ jet and $W + 2$ jet production with at least one b jet at the 7 TeV LHC. Phys. Rev. D **86**, 034021 (2012)
3864. C.M.S. Collaboration, Measurement of the production cross section for Z+b jets in proton-proton collisions at $\sqrt{s}$ = 13 TeV. Phys. Rev. D **105**(9), 092014 (2022)
3865. CMS Collaboration, Measurements of the associated production of a W boson and a charm quark in proton-proton collisions at $\sqrt{s}$ = 8 TeV (2021)
3866. ATLAS Collaboration, Measurements of the production cross-section for a Z boson in association with b-jets in proton-proton collisions at $\sqrt{s} = 13$ TeV with the ATLAS detector. JHEP **07**, 044 (2020)
3867. C.M.S. Collaboration, Measurement of differential cross sections for Z bosons produced in association with charm jets in pp collisions at $\sqrt{s} = 13$ TeV. JHEP **04**, 109 (2021)
3868. C.M.S. Collaboration, Measurements of the associated production of a Z boson and b jets in pp collisions at $\sqrt{s} = 8$ TeV. Eur. Phys. J. C **77**(11), 751 (2017)
3869. ATLAS Collaboration, Measurement of differential production cross-sections for a Z boson in association with b-jets in 7 TeV proton-proton collisions with the ATLAS detector. JHEP **10**, 141 (2014)
3870. ATLAS Collaboration, Measurement of cross-sections for production of a Z boson in association with a flavor-inclusive or doubly b-tagged large-radius jet in proton-proton collisions at $\sqrt{s} =$ 13TeV with the ATLAS experiment. Phys. Rev. D **108**, 012022 (2023)
3871. LHCb Collaboration, Study of Z bosons produced in association with charm in the forward region. Phys. Rev. Lett. **128**(8), 082001 (2022)

3872. LHCb Collaboration, Study of W boson production in association with beauty and charm. Phys. Rev. D **92**(5), 052001 (2015)
3873. LHCb Collaboration, Measurement of the Z+b-jet cross-section in pp collisions at $\sqrt{s}$ = 7 TeV in the forward region. JHEP **01**, 064 (2015)
3874. R. Gauld et al., Predictions for Z-boson production in association with a b-jet at $\mathcal{O}(\alpha_s^3)$. Phys. Rev. Lett. **125**(22), 222002 (2020)
3875. S. Alam Malik, G. Watt, Ratios of W and Z cross sections at large boson p_T as a constraint on PDFs and background to new physics. JHEP **02**, 025 (2014)
3876. S. Farry, R. Gauld, Leptonic $W^{\pm}$ boson asymmetry in association with jets at LHCb and parton distribution function constraints at large x. Phys. Rev. D **93**(1), 014008 (2016)
3877. S.J. Brodsky et al., A review of the intrinsic heavy quark content of the nucleon. Adv. High Energy Phys. **2015**, 231547 (2015)
3878. T.-J. Hou et al., CT14 intrinsic charm parton distribution functions from CTEQ-TEA global analysis. JHEP **02**, 059 (2018)
3879. LHC Higgs Cross Section Working Group, Handbook of LHC Higgs Cross Sections: 4. Deciphering the nature of the Higgs sector. In: *CERN Yellow Rep. Monogr.* 2 (2017)
3880. S. Chatrchyan et al., Observation of a new boson with mass near 125 GeV in pp collisions at $\sqrt{s}$ = 7 and 8 TeV. JHEP **06**, 081 (2013)
3881. P.W. Higgs, Broken symmetries and the masses of gauge bosons. Phys. Rev. Lett. **13**, 508 (1964) **(Ed. by J.C. Taylor)**
3882. R. Barate et al., Search for the standard model Higgs boson at LEP. Phys. Lett. B **565**, 61 (2003)
3883. T. Aaltonen et al., Evidence for a particle produced in association with weak bosons and decaying to a bottom-antibottom quark pair in Higgs boson searches at the Tevatron. Phys. Rev. Lett. **109**, 071804 (2012)
3884. LHC Higgs Cross Section Working Group, Handbook of LHC Higgs cross sections: 1. Inclusive observables. In: *CERN Yellow Rep. Monogr.* 2 (2011)
3885. LHC Higgs Cross Section Working Group, Handbook of LHC Higgs cross sections: 2. Differential distributions. In: *CERN Yellow Rep. Monogr.* 2 (2012)
3886. LHC Higgs Cross Section Working Group. Handbook of LHC Higgs cross sections: 3. Higgs properties. In *CERN Yellow Rep. Monogr.* 4 (2013) **(Ed. by S. Heinemeyer et al.)**
3887. ATLAS Collaboration, A detailed map of Higgs boson interactions by the ATLAS experiment ten years after the discovery. Nature **607**(7917), 52–59 (2022)
3888. C.M.S. Collaboration, A portrait of the Higgs boson by the CMS experiment ten years after the discovery. Nature **607**(7917), 60–68 (2022)
3889. G. Aad et al., Measurement of the Higgs boson mass in the $H \to ZZ^* \to 4\ell$ decay channel using 139 fb^{-1} of $\sqrt{s} = 13$ TeV pp collisions recorded by the ATLAS detector at the LHC. Phys. Lett. B **843**, 137880 (2023)
3890. A.M. Sirunyan et al., A measurement of the Higgs boson mass in the diphoton decay channel. Phys. Lett. B **805**, 135425 (2020)
3891. G. Aad et al., Measurement of the properties of Higgs boson production at $\sqrt{s} = 13$ TeV in the $H \to \gamma\gamma$ channel using 139 fb^{-1} of pp collision data with the ATLAS experiment. JHEP **07**, 088 (2023)
3892. V. Khachatryan et al., Constraints on the spin-parity and anomalous HVV couplings of the Higgs boson in proton collisions at 7 and 8 TeV. Phys. Rev. D **92**, 012004 (2015)
3893. G. Aad et al., Study of the spin and parity of the Higgs boson in diboson decays with the ATLAS detector. Eur. Phys. J. C **75**(10), 476 (2015) [Erratum: Eur. Phys. J. C 76, 152 (2016)]
3894. A. Tumasyan et al., Measurement of the Higgs boson width and evidence of its off-shell contributions to ZZ production. Nat. Phys. **18**(11), 1329–1334 (2022)
3895. G. Aad et al., A search for the $Z\gamma$ decay mode of the Higgs boson in pp collisions at $\sqrt{s}$ = 13 TeV with the ATLAS detector. Phys. Lett. B **809**, 135754 (2020)
3896. A. Tumasyan et al., Search for Higgs boson decays to a Z boson and a photon in proton-proton collisions at $\sqrt{s}$ = 13 TeV. JHEP **05**, 233 (2023)
3897. G. Aad et al., Measurement of the total and differential Higgs boson production cross-sections at $\sqrt{s}$ = 13 TeV with the ATLAS detector by combining the $H \to ZZ^* \to 4\ell$ and $H \to \gamma\gamma$ decay channels. JHEP **05**, 028 (2023)
3898. CMS Collaboration, Measurement of the Higgs boson inclusive and differential fiducial production cross sections in the diphoton decay channel with pp collisions at $\sqrt{s} = 13$ TeV with the CMS detector. In: *CMS-PAS-HIG-19-016* (2022)
3899. G. Aad et al., Measurements of WH and ZH production in the $H \to b\bar{b}$ decay channel in pp collisions at 13 TeV with the ATLAS detector. Eur. Phys. J. C **81**(2), 178 (2021)
3900. Tumasyan, A. et al., Search for Higgs Boson and Observation of Z Boson through their Decay into a Charm Quark-Antiquark Pair in Boosted Topologies in Proton-Proton Collisions at s=13 TeV. Phys. Rev. Lett. **131**(4), 041801 (2023)
3901. A.M. Sirunyan et al., Observation of Higgs boson decay to bottom quarks. Phys. Rev. Lett. **121**(12), 121801 (2018)
3902. G. Aad et al., Constraints on Higgs boson production with large transverse momentum using $H \to b\bar{b}$ decays in the ATLAS detector. Phys. Rev. D **105**, 092003 (2022)
3903. A.M. Sirunyan et al., Inclusive search for highly boosted Higgs bosons decaying to bottom quark-antiquark pairs in proton-proton collisions at $\sqrt{s}$ = 13 TeV. JHEP **12**, 085 (2020)
3904. G. Aad et al., Direct constraint on the Higgs-charm coupling from a search for Higgs boson decays into charm quarks with the ATLAS detector. Eur. Phys. J. C **82**, 717 (2022)
3905. M. Aaboud et al., Observation of Higgs boson production in association with a top quark pair at the LHC with the ATLAS detector. Phys. Lett. B **784**, 173–191 (2018)
3906. A.M. Sirunyan et al., Measurement of the Higgs boson production rate in association with top quarks in final states with electrons, muons, and hadronically decaying tau leptons at $\sqrt{s} = 13$ TeV. Eur. Phys. J. C **81**(4), 378 (2021)
3907. S.W. Herb et al., Observation of a dimuon resonance at 9.5-GeV in 400-GeV proton-nucleus collisions. Phys. Rev. Lett. **39**, 252–255 (1977)
3908. K. Hagiwara, M. Tanaka, T. Stelzer, Single top production at LEP-200. Phys. Lett. B **325**, 521–525 (1994)
3909. D. Haidt, Top mass from electroweak data. Nucl. Phys. B Proc. Suppl. **16**, 294–295 (1990) **(Ed. by F. Barreiro et al.)**
3910. W.J. Marciano, Heavy quark mass predictions. Phys. Rev. Lett. **62**, 2793–2796 (1989)
3911. K. Hagiwara et al., A novel approach to confront electroweak data and theory. Z. Phys. C **64**, 559–620 (1994) [Erratum: Z. Phys. C 68, 352 (1995)]
3912. D. Schaile, Tests of the electroweak theory at LEP. Fortsch. Phys. **42**, 429–484 (1994)
3913. B. Jacobsen, Top mass from electroweak measurements. In: *29th Rencontres de Moriond: QCD and High-energy Hadronic Interactions*, pp. 531–538 (1994)
3914. S. Abachi et al., Observation of the top quark. Phys. Rev. Lett. **74**, 2632–2637 (1995)
3915. T. Aaltonen et al., First observation of electroweak single top quark production. Phys. Rev. Lett. **103**, 092002 (2009)
3916. V.M. Abazov et al., Observation of single top quark production. Phys. Rev. Lett. **103**, 092001 (2009)
3917. T. Antero Aaltonen et al., Observation of s-channel production of single top quarks at the Tevatron. Phys. Rev. Lett. **112**, 231803 (2014)

3918. J.A. Aguilar-Saavedra et al., Asymmetries in top quark pair production at hadron colliders. Rev. Mod. Phys. **87**, 421–455 (2015)
3919. T. Aaltonen et al., Combination of CDF and D0 measurements of the W boson helicity in top quark decays. Phys. Rev. D **85**, 071106 (2012)
3920. CDF and D0 Collaborations, Combination of CDF and D0 results on the mass of the top quark using up to 9.7 fb^{-1} at the Tevatron (2014). arXiv:1407.2682
3921. LHC Machine, JINST **3**, S08001 (2008) **(Ed. by L. Evans and P. Bryant)**
3922. J.H. Kuhn, G. Rodrigo, Charge asymmetry in hadroproduction of heavy quarks. Phys. Rev. Lett. **81**, 49–52 (1998)
3923. G.L. Kane, G.A. Ladinsky, C.P. Yuan, Using the top quark for testing standard model polarization and CP predictions. Phys. Rev. D **45**, 124–141 (1992)
3924. V.D. Barger, J. Ohnemus, R.J.N. Phillips, Spin correlation effects in the hadroproduction and decay of very heavy top quark pairs. Int. J. Mod. Phys. A **4**, 617 (1989)
3925. G. Mahlon, S.J. Parke, Spin Correlation Effects in Top Quark Pair Production at the LHC. Phys. Rev. D **81**, 074024 (2010)
3926. Y. Afik, J.R.M. de Nova, Entanglement and quantum tomography with top quarks at the LHC. Eur. Phys. J. Plus **136**(9), 907 (2021)
3927. M. Czakon, D. Heymes, A. Mitov, High-precision differential predictions for top-quark pairs at the LHC. Phys. Rev. Lett. **116**(8), 082003 (2016)
3928. M. Czakon et al., Top-pair production at the LHC through NNLO QCD and NLO EW. JHEP **10**, 186 (2017)
3929. M. Czakon, D. Heymes, A. Mitov, Dynamical scales for multi-TeV top-pair production at the LHC. JHEP **04**, 071 (2017)
3930. ATLAS Collaboration, Measurements of top-quark pair differential and double-differential cross-sections in the ℓ+jets channel with pp collisions at $\sqrt{s} = 13$ TeV using the ATLAS detector. Eur. Phys. J. C **79**, 1028 (2019)
3931. ATLAS Collaboration, Measurement of the $t\bar{t}$ production cross-section and lepton differential distributions in $e\mu$ dilepton events from pp collisions at $\sqrt{s} = 13$ TeV with the ATLAS detector. Eur. Phys. J. C **80**, 528 (2020)
3932. ATLAS Collaboration, Measurements of top-quark pair differential cross-sections in the lepton+jets channel in pp collisions at $\sqrt{s} = 8$ TeV using the ATLAS detector. Eur. Phys. J. C **76**, 538 (2016)
3933. C.M.S. Collaboration, Measurement of differential $t\bar{t}$ production cross sections in the full kinematic range using lepton+jets events from proton-proton collisions at $\sqrt{s} = 13$ TeV. Phys. Rev. D **104**, 092013 (2021)
3934. C.M.S. Collaboration, Measurement of differential $t\bar{t}$ production cross sections using top quarks at large transverse momenta in pp collisions at $\sqrt{s} = 13$ TeV. Phys. Rev. D **103**, 052008 (2021)
3935. C.M.S. Collaboration, Measurements of $t\bar{t}$ differential cross sections in proton-proton collisions at $\sqrt{s} = 13$ TeV using events containing two leptons. JHEP **02**, 149 (2019)
3936. C.M.S. Collaboration, Measurement of the differential cross section for top quark pair production in pp collisions at $\sqrt{s} = 8$ TeV. Eur. Phys. J. C **75**, 542 (2015)
3937. V. Miralles et al., The top quark electroweak couplings after LHC Run 2. JHEP **02**, 032 (2022)
3938. A. Kulesza et al., Associated top quark pair production with a heavy boson: differential cross sections at NLO+NNLL accuracy. Eur. Phys. J. C **80**(5), 428 (2020)
3939. S. Catani et al., $t\bar{t}H$ production at NNLO: the flavour off-diagonal channels. Eur. Phys. J. C **81**(6), 491 (2021)
3940. P. Azzi et al., Report from Working Group 1: Standard Model Physics at the HL-LHC and HE-LHC. CERN Yellow Rep. Monogr. **7**, 1–220 (2019) **(Ed. by Andrea Dainese et al.)**
3941. G. Bevilacqua et al., Complete off-shell effects in top quark pair hadroproduction with leptonic decay at next-to-leading order. JHEP **02**, 083 (2011)
3942. T. Sjostrand et al., An introduction to PYTHIA 8.2. Comput. Phys. Commun. **191**, 159–177 (2015)
3943. J. Bellm et al., Herwig 7.0/Herwig++ 3.0 release note. Eur. Phys. J. C **76**(4), 196 (2016)
3944. T. Ježo, P. Nason, On the treatment of resonances in next-to-leading order calculations matched to a parton shower. JHEP **12**, 065 (2015)
3945. J. Mazzitelli et al., Top-pair production at the LHC with MINNLO$_{PS}$. JHEP **04**, 079 (2022)
3946. J. Mazzitelli et al., Next-to-next-to-leading order event generation for top-quark pair production (2020)
3947. ATLAS and CMS Collaborations, Combinations of single-top-quark production cross-section measurements and $|f_{LV}V_{tb}|$ determinations at $\sqrt{s}$ = 7 and 8 TeV with the ATLAS and CMS experiments. JHEP **05**, 088 (2019)
3948. R. Kogler et al., Jet substructure at the large hadron collider: experimental review. Rev. Mod. Phys. **91**(4), 045003 (2019)
3949. ATLAS Collaboration, Jet mass and substructure of inclusive jets in $\sqrt{s} = 7$ TeV pp collisions with the ATLAS experiment. JHEP **05**, 128 (2012)
3950. C.M.S. Collaboration, Measurement of jet substructure observables in $\mathrm{t\bar{t}}$ events from proton-proton collisions at $\sqrt{s} = 13$ TeV. Phys. Rev. D **98**(9), 092014 (2018)
3951. C.M.S. Collaboration, Measurement of differential $t\bar{t}$ production cross sections in the full kinematic range using lepton+jets events from proton-proton collisions at $\sqrt{s} = 13$ TeV. Phys. Rev. D **104**(9), 092013 (2021)
3952. G. Aad et al., Measurements of differential cross-sections in top-quark pair events with a high transverse momentum top quark and limits on beyond the Standard Model contributions to top-quark pair production with the ATLAS detector at $\sqrt{s}$ = 13 TeV. JHEP **06**, 063 (2022)
3953. J. Ellis et al., Top, Higgs, diboson and electroweak fit to the standard model effective field theory. JHEP **04**, 279 (2021)
3954. J.J. Ethier et al., Combined SMEFT interpretation of Higgs, diboson, and top quark data from the LHC. JHEP **11**, 089 (2021)
3955. K. Lopi, Measurements of inclusive and differential cross-sections of combined $t\bar{t}\gamma$ and $tW\gamma$ production in the eμ channel at 13 TeV with the ATLAS detector. JHEP **09**, 049 (2020)
3956. A. Tumasyan et al., Measurement of the inclusive and differential $t\bar{t}\gamma$ cross sections in the dilepton channel and effective field theory interpretation in proton-proton collisions at $\sqrt{s}$ =13 TeV. JHEP **05**, 091 (2022)
3957. C.M.S. Collaboration, Measurement of top quark pair production in association with a Z boson in proton-proton collisions at $\sqrt{s} =$ 13 TeV. JHEP **03**, 056 (2020)
3958. G. Aad et al., Measurements of the inclusive and differential production cross sections of a top-quark-antiquark pair in association with a Z boson at $\sqrt{s} = 13$ TeV with the ATLAS detector. Eur. Phys. J. C **81**(8), 737 (2021)
3959. ATLAS Collaboration, Observation of the associated production of a top quark and a Z boson in pp collisions at $\sqrt{s} = 13$ TeV with the ATLAS detector. JHEP **07**, 124 (2020)
3960. C.M.S. Collaboration, Inclusive and differential cross section measurements of single top quark production in association with a Z boson in proton-proton collisions at $\sqrt{s}$ = 13 TeV. JHEP **02**, 107 (2022)
3961. ATLAS Collaboration, Observation of single-top-quark production in association with a photon at the ATLAS detector. Tech. rep. All figures including auxiliary figures are available at arXiv:2302.01283 (CERN, Geneva 2022)
3962. C.M.S. Collaboration, Observation of $\mathrm{t\bar{t}}$H production. Phys. Rev. Lett. **120**(23), 231801 (2018)

3963. ATLAS Collaboration, Observation of four-top-quark production in the multilepton final state with the ATLAS detector. Eur. Phys. J. C **83**(6), 496 (2023)
3964. CMS Collaboration, Observation of four top quark production in proton-proton collisions at $\sqrt{s}$ = 13 TeV (2023)
3965. B. Lillie, L. Randall, L.-T. Wang, The Bulk RS KK-gluon at the LHC. JHEP **09**, 074 (2007)
3966. C.M.S. Collaboration, Search for resonant $t\bar{t}$ production in proton-proton collisions at $\sqrt{s} = 13$ TeV. JHEP **04**, 031 (2019)
3967. K. Agashe et al., Working Group Report: Top Quark. In: *Community Summer Study 2013: Snowmass on the Mississippi* (2013)
3968. G.C. Branco et al., Theory and phenomenology of two-Higgs-doublet models. Phys. Rep. **516**, 1–102 (2012)
3969. F.J. Botella et al., Flavour changing Higgs couplings in a class of two Higgs doublet models. Eur. Phys. J. C **76**(3), 161 (2016)
3970. U. Langenfeld, S. Moch, P. Uwer, Measuring the running top-quark mass. Phys. Rev. D **80**, 054009 (2009)
3971. S. Alioli et al., A new observable to measure the top-quark mass at hadron colliders. Eur. Phys. J. C **73**, 2438 (2013)
3972. ATLAS Collaboration, Measurement of the top-quark mass in $t\bar{t}+1$-jet events collected with the ATLAS detector in pp collisions at $\sqrt{s} = 8$ TeV. JHEP **11**, 150 (2019)
3973. Y. Kiyo et al., Top-quark pair production near threshold at LHC. Eur. Phys. J. C **60**, 375–386 (2009)
3974. First combination of Tevatron and LHC measurements of the top-quark mass (2014)
3975. A.H. Hoang, S. Plätzer, D. Samitz, On the cutoff dependence of the quark mass parameter in angular ordered parton showers. JHEP **10**, 200 (2018)
3976. M. Butenschoen et al., Top quark mass calibration for Monte Carlo event generators. Phys. Rev. Lett. **117**(23), 232001 (2016)
3977. ATLAS Collaboration, A precise interpretation for the top quark mass parameter in ATLAS Monte Carlo simulation. Tech. rep. All figures including auxiliary figures are available at https://atlas.web.cern.ch/Atlas/GROUPS/PHYSICS/PUBNOTES/ATL-PHYS-PUB-2021-034 (CERN, Geneva, 2021)
3978. A.H. Hoang, What is the top quark mass? Annu. Rev. Nucl. Part. Sci. **70**, 225–255 (2020)
3979. T. Ježo et al., An NLO+PS generator for $t\bar{t}$ and Wt production and decay including non-resonant and interference effects. Eur. Phys. J. C **76**(12), 691 (2016)
3980. S. Ferrario Ravasio et al., A theoretical study of top-mass measurements at the LHC using NLO+PS generators of increasing accuracy. Eur. Phys. J. C **78**(6), 458 (2018) [Addendum: Eur. Phys. J. C 79, 859 (2019)]
3981. A profile likelihood approach to measure the top quark mass in the lepton+jets channel at $\sqrt{s} = 13$TeV. Tech. rep. (CERN, Geneva, 2022)
3982. R. Schwienhorst, D. Wackeroth, et al., Top quark physics and heavy flavor production. In: *Summary of the EF03 Topical Group at Snowmass 2021* (2022)
3983. A.M. Sirunyan et al., Measurement of $t\bar{t}$ normalised multi-differential cross sections in pp collisions at $\sqrt{s} = 13$ TeV, and simultaneous determination of the strong coupling strength, top quark pole mass, and parton distribution functions. Eur. Phys. J. C **80**(7), 658 (2020)
3984. J. de Blas et al., Global analysis of electroweak data in the Standard Model. Phys. Rev. D **106**(3), 033003 (2022)
3985. T. Aaltonen et al., High-precision measurement of the W boson mass with the CDF II detector. Science **376**(6589), 170–176 (2022)
3986. L. Chih-Ting et al., Electroweak precision fit and new physics in light of the W boson mass. Phys. Rev. D **106**(3), 035034 (2022)
3987. J. de Blas et al., Impact of the recent measurements of the top-quark and W-boson masses on electroweak precision fits. Phys. Rev. Lett. **129**(27), 271801 (2022)
3988. N.P. Hartland et al., A Monte Carlo global analysis of the standard model effective field theory: the top quark sector. JHEP **04**, 100 (2019)
3989. I. Brivio et al., O new physics, where art thou? A global search in the top sector. JHEP **02**, 131 (2020)
3990. H. Abramowicz et al., Top-quark physics at the CLIC electron-positron linear collider. JHEP **11**, 003 (2019)
3991. G. Durieux et al., The electro-weak couplings of the top and bottom quarks—global fit and future prospects. JHEP **12**, 98 (2019) [Erratum: JHEP 01, 195 (2021)]
3992. G. Durieux et al., Snowmass White Paper: prospects for the measurement of top-quark couplings. In: *2021 Snowmass Summer Study* (2022)
3993. J. de Blas et al., The CLIC potential for new physics. In: *CERN Yellow Rep. Monogr.* 3 (2018)
3994. U. Amaldi et al., The real part of the forward proton proton scattering amplitude measured at the CERN intersecting storage rings. Phys. Lett. B **66**, 390–394 (1977)
3995. C. Augier et al., Predictions on the total cross-section and real part at LHC and SSC. Phys. Lett. B **315**, 503–506 (1993)
3996. M. Froissart, Asymptotic behavior and subtractions in the Mandelstam representation. Phys. Rev. **123**, 1053–1057 (1961)
3997. A. Martin, Extension of the axiomatic analyticity domain of scattering amplitudes by unitarity-I. Il Nuovo Cimento A (1965–1970) **42**(4), 930–953 (1966)
3998. P.D.B. Collins, *An Introduction to Regge Theory and High-Energy Physics* (Cambridge Monographs on Mathematical Physics (Cambridge University Press, Cambridge, 2009)
3999. S. Donnachie et al., *Pomeron Physics and QCD*, vol. 19 (Cambridge University Press, Cambridge, 2004)
4000. C. Patrignani et al., Review of particle physics. Chin. Phys. C **40**(10), 100001 (2016)
4001. O. Nachtmann, Pomeron physics and QCD. In: *Ringberg Workshop on New Trends in HERA Physics 2003*, pp. 253–267 (2004)
4002. L. Lukaszuk, B. Nicolescu, A possible interpretation of p p rising total cross-sections. Lett. Nuovo Cim. **8**, 405–413 (1973)
4003. G. Antchev et al., First determination of the ρ parameter at $\sqrt{s} = 13$ TeV: probing the existence of a colourless C-odd three-gluon compound state. Eur. Phys. J. C **79**(9), 785 (2019)
4004. W. Heisenberg, Mesonenerzeugung als Stosswellenproblem. Z. Phys. **133**, 65 (1952)
4005. J.R. Cudell et al., Benchmarks for the forward observables at RHIC, the Tevatron Run II and the LHC. Phys. Rev. Lett. **89**, 201801 (2002)
4006. M. Giordano, E. Meggiolaro, N. Moretti, Asymptotic energy dependence of hadronic total cross sections from lattice QCD. JHEP **09**, 031 (2012)
4007. E. Ferreiro et al., Froissart bound from gluon saturation. Nucl. Phys. A **710**, 373–414 (2002)
4008. G. Anelli et al., The TOTEM experiment at the CERN Large Hadron Collider. JINST **3**, S08007 (2008)
4009. J. Kaspar, Slides Presented at the LHC Working Group of Forward Physics and Diffraction **16–17**, 2019 (Decemberd 2019)
4010. G. Antchev et al., First measurement of elastic, inelastic and total cross-section at $\sqrt{s} = 13$ TeV by TOTEM and overview of cross-section data at LHC energies. Eur. Phys. J. C **79**(2), 103 (2019)
4011. V.A. Schegelsky, M.G. Ryskin, The diffraction cone shrinkage speed up with the collision energy. Phys. Rev. D **85**, 094024 (2012)
4012. A. Donnachie, P.V. Landshoff, The interest of large-t elastic scattering. Phys. Lett. B **387**, 637–641 (1996)
4013. A. Donnachie, P.V. Landshoff, Small t elastic scattering and the ρ parameter. Phys. Lett. B **798**, 135008 (2019)
4014. V.M. Abazov et al., Odderon exchange from elastic scattering differences between pp and $p\bar{p}$ data at 1.96 TeV and from pp forward scattering measurements. Phys. Rev. Lett. **127**(6), 062003 (2021)

4015. E. Martynov, B. Nicolescu, Did TOTEM experiment discover the Odderon? Phys. Lett. B **778**, 414–418 (2018)
4016. B. Abelev et al., Measurement of inelastic, single- and double-diffraction cross sections in proton-proton collisions at the LHC with ALICE. Eur. Phys. J. C **73**(6), 2456 (2013)
4017. G. Aad et al., Rapidity gap cross sections measured with the ATLAS detector in pp collisions at $\sqrt{s} = 7$ TeV. Eur. Phys. J. C **72**, 1926 (2012)
4018. J. Bartels, M.G. Ryskin, G.P. Vacca, On the triple pomeron vertex in perturbative QCD. Eur. Phys. J. C **27**, 101–113 (2003)
4019. S. Chekanov et al., Exclusive electroproduction of J/psi mesons at HERA. Nucl. Phys. B **695**, 3–37 (2004)
4020. A. Aktas et al., Elastic J/ψ production at HERA. Eur. Phys. J. C **46**, 585–603 (2006)
4021. L. Frankfurt, M. McDermott, M. Strikman, A fresh look at diffractive J/ψ photoproduction at HERA, with predictions for THERA. JHEP **03**, 045 (2001)
4022. J.C. Collins, Proof of factorization for diffractive hard scattering. Phys. Rev. D **57**, 3051–3056 (1998)
4023. T. Affolder et al., Diffractive dijets with a leading antiproton in $\bar{p}p$ collisions at $\sqrt{s} = 1800$ GeV. Phys. Rev. Lett. **84**, 5043–5048 (2000)
4024. M. Aaboud et al., Measurement of charged-particle distributions sensitive to the underlying event in $\sqrt{s} = 13$ TeV proton-proton collisions with the ATLAS detector at the LHC. JHEP **03**, 157 (2017)
4025. G. Antchev et al., Measurement of the forward charged particle pseudorapidity density in pp collisions at $\sqrt{s} = 8$ TeV using a displaced interaction point. Eur. Phys. J. C **75**(3), 26 (2015)
4026. S. Chatrchyan et al., Measurement of pseudorapidity distributions of charged particles in proton-proton collisions at $\sqrt{s} = 8$ TeV by the CMS and TOTEM experiments. Eur. Phys. J. C **74**(10), 3053 (2014)
4027. M.K. Gaillard, B.W. Lee, Rare decay modes of the K-mesons in gauge theories. Phys. Rev. D **10**, 897 (1974)
4028. N. Cabibbo, Unitary symmetry and leptonic decays. Phys. Rev. Lett. **10**, 531–533 (1963)
4029. W. Zimmermann, Normal products and the short distance expansion in the perturbation theory of renormalizable interactions. Ann. Phys. **77**, 570–601 (1973) [Lect. Notes Phys. 558, 278 (2000)]
4030. W.A. Bardeen, A.J. Buras, J.-M. Gérard, A consistent analysis of the $\Delta I = 1/2$ rule for K decays. Phys. Lett. B **192**, 138 (1987)
4031. A.J. Buras, J.-M. Gérard, W.A. Bardeen, Large N approach to kaon decays and mixing 28 years later: $\Delta I = 1/2$ Rule, $\hat{B}_K$ and ΔM_K. Eur. Phys. J. C **74**(5), 2871 (2014)
4032. A.J. Buras, Weak Hamiltonian, CP violation and rare decays. In: *Probing the Standard Model of Particle Interactions. Proceedings, Summer School in Theoretical Physics*, NATO Advanced Study Institute, 68th session, Les Houches, France, July 28–September 5, 1997. Pt. 1, 2, pp. 281–539 (1998)
4033. A.J. Buras, P.H. Weisz, QCD nonleading corrections to weak decays in dimensional regularization and 't Hooft-Veltman schemes. Nucl. Phys. B **333**, 66–99 (1990)
4034. A.J. Buras, *Gauge Theory of Weak Decays* (Cambridge University Press, Cambridge, 2020)
4035. G. Buchalla, A.J. Buras, M.E. Lautenbacher, Weak decays beyond leading logarithms. Rev. Mod. Phys. **68**, 1125–1144 (1996)
4036. A.J. Buras et al., Charm quark contribution to $K^+ \to \pi^+ \nu\bar{\nu}$ at next-to-next-to-leading order. JHEP **11**, 002 (2006)
4037. M.A. Shifman, A.I. Vainshtein, V.I. Zakharov, Nonleptonic decays of K mesons and hyperons. Sov. Phys. JETP **45**, 670 (1977) [Zh. Eksp. Teor. Fiz. 72, 1275 (1977)]
4038. F.J. Gilman, M.B. Wise, Effective Hamiltonian for $\Delta s = 1$ weak nonleptonic decays in the six quark model. Phys. Rev. D **20**, 2392 (1979)
4039. F.J. Gilman, M.B. Wise, $K^0 - \bar{K}^0$ mixing in the six quark model. Phys. Rev. D **27**, 1128 (1983)
4040. C. Dib, I. Dunietz, F.J. Gilman, Strong interaction corrections to the decay $K \to \pi$ neutrino anti-neutrino for large M(t). Mod. Phys. Lett. A **6**, 3573–3582 (1991)
4041. A.J. Buras, Climbing NLO and NNLO summits of weak decays (2011). arXiv:1102.5650
4042. M. Ciuchini et al., Next-to-leading order QCD corrections to $\Delta F = 2$ effective Hamiltonians. Nucl. Phys. B **523**, 501–525 (1998)
4043. A.J. Buras, M. Misiak, J. Urban, Two loop QCD anomalous dimensions of flavor changing four quark operators within and beyond the standard model. Nucl. Phys. B **586**, 397–426 (2000)
4044. J. Aebischer et al., General non-leptonic $\Delta F = 1$ WET at the NLO in QCD. JHEP **11**, 227 (2021)
4045. J. Aebischer et al., SMEFT ATLAS of ΔF = 2 transitions. JHEP **12**, 187 (2020)
4046. J. Aebischer, A.J. Buras, J. Kumar, NLO QCD renormalization group evolution for nonleptonic ΔF = 2 transitions in the SMEFT. Phys. Rev. D **106**(3), 035003 (2022)
4047. A. Bazavov et al., $B^0_{(s)}$-mixing matrix elements from lattice QCD for the Standard Model and beyond. Phys. Rev. D **93**(11), 113016 (2016)
4048. F. Mescia, C. Smith, Improved estimates of rare K decay matrix-elements from $K_{\ell 3}$ decays. Phys. Rev. D **76**, 034017 (2007)
4049. R.-X. Shi et al., Revisiting the new-physics interpretation of the $b \to c\tau\nu$ data. JHEP **12**, 065 (2019)
4050. P. Colangelo, F. De Fazio, F. Loparco, Probing New Physics with $\bar{B} \to \rho(770)\,\ell^- \bar{\nu}_\ell$ and $\bar{B} \to a_1(1260)\,\ell^- \bar{\nu}_\ell$. Phys. Rev. D **100**(7), 075037 (2019)
4051. P. Ball, R. Zwicky, New results on $B \to \pi, K, \eta$ decay formfactors from light-cone sum rules. Phys. Rev. D **71**, 014015 (2005)
4052. C. Bouchard et al., Rare decay $B \to Kll$ form factors from lattice QCD. Phys. Rev. D **88**(054509), 054509 (2013)
4053. R.R. Horgan et al., Rare B decays using lattice QCD form factors. PoS LATTICE2014, 372 (2015)
4054. A. Bharucha, D.M. Straub, R. Zwicky, $B \to V\ell^+\ell^-$ in the Standard Model from light-cone sum rules. JHEP **08**, 098 (2016)
4055. N. Gubernari, A. Kokulu, D. van Dyk, $B \to P$ and $B \to V$ form factors from B-meson light-cone sum rules beyond leading twist. JHEP **01**, 150 (2019)
4056. W.G. Parrott, C. Bouchard, C.T.H. Davies, Standard Model predictions for $\to K\ell^+\ell^-$, $B \to K\nu\bar{\nu}$ using form factors from Nf = 2+1+1 lattice QCD. Phys. Rev. D **107**(1), 014511 (2023) [Erratum: Phys. Rev. D 107, 119903 (2023)]
4057. N. Isgur, M.B. Wise, Heavy quark symmetry. Adv. Ser. Dir. High Energy Phys. **10**, 234–285 (1992)
4058. T. Mannel, W. Roberts, Z. Ryzak, A derivation of the heavy quark effective Lagrangian from QCD. Nucl. Phys. B **368**, 204–217 (1992)
4059. I.I.Y. Bigi et al., The question of CP noninvariance–as seen through the eyes of neutral beauty. Adv. Ser. Dir. High Energy Phys. **3**, 175–248 (1989)
4060. M. Artuso, G. Borissov, A. Lenz, CP violation in the B^0_s system. Rev. Mod. Phys. **88**(4), 045002 (2016)
4061. B.J. Choi et al., Kaon BSM B-parameters using improved staggered fermions from $N_f = 2 + 1$ unquenched QCD. Phys. Rev. D **93**(1), 014511 (2016)
4062. P.A. Boyle et al., Neutral kaon mixing beyond the Standard Model with $n_f = 2 + 1$ chiral fermions. Part 2: non perturbative renormalisation of the $\Delta F = 2$ four-quark operators. JHEP **10**, 054 (2017)

4063. A.J. Buras, J.-M. Gérard, Dual QCD insight into BSM hadronic matrix elements for $K^0 - \bar{K}^0$ mixing from lattice QCD. Acta Phys. Polon. B **50**, 121 (2019)
4064. J. Aebischer, A.J. Buras, J.-M. Gérard, BSM hadronic matrix elements for ϵ'/ϵ and $K \to \pi\pi$ decays in the Dual QCD approach. JHEP **02**, 021 (2019)
4065. M. Beneke et al., QCD factorization for $B \to K\pi, \pi\pi$ decays: strong phases and CP violation in the heavy quark limit. Phys. Rev. Lett. **83**, 1914–1917 (1999)
4066. M. Beneke et al., QCD factorization for exclusive, nonleptonic B meson decays: general arguments and the case of heavy light final states. Nucl. Phys. B **591**, 313–418 (2000)
4067. M. Beneke, Soft-collinear factorization in B decays. Nucl. Part. Phys. Proc. **261–262**, 311–337 (2015)
4068. Robert Fleischer et al., Exploring $B \to \pi\pi, \pi K$ Decays at the High- Precision Frontier. (2018)
4069. L. Wolfenstein, Parametrization of the Kobayashi-Maskawa matrix. Phys. Rev. Lett. **51**, 1945 (1983)
4070. M. Bona et al., Unitarity triangle global fits testing the Standard Model: UTfit 2021 SM update. PoS EPS-HEP2021, 512 (2022)
4071. C.-Y. Seng et al., Reduced hadronic uncertainty in the determination of V_{ud}. Phys. Rev. Lett. **121**(24), 241804 (2018)
4072. A. Czarnecki, W.J. Marciano, A. Sirlin, Radiative corrections to neutron and nuclear beta decays revisited. Phys. Rev. D **100**(7), 073008 (2019)
4073. M. Gorchtein, γW box inside out: nuclear polarizabilities distort the beta decay spectrum. Phys. Rev. Lett. **123**(4), 042503 (2019)
4074. J.C. Hardy, I.S. Towner, Superallowed $0^+ \to 0^+$ nuclear β decays: 2020 critical survey, with implications for V_{ud} and CKM unitarity. Phys. Rev. C **102**(4), 045501 (2020)
4075. V. Cirigliano et al., Scrutinizing CKM unitarity with a new measurement of the Kμ3/Kμ2 branching fraction. Phys. Lett. B **838**, 137748 (2023)
4076. D. Pocanic et al., Precise measurement of the $\pi^+ \to \pi^0 e^+ \nu$ branching ratio. Phys. Rev. Lett. **93**, 181803 (2004)
4077. W. Altmannshofer et al., PIONEER: studies of rare pion decays (2022). arXiv:2203.01981
4078. E. Gamiz et al., V_{us} and m_s from hadronic τ decays. Phys. Rev. Lett. **94**, 011803 (2005)
4079. R.J. Hudspith et al., A resolution of the inclusive flavor-breaking $\tau|V_{us}|$ puzzle. Phys. Lett. B **781**, 206–212 (2018)
4080. P. Boyle et al., Novel $|V_{us}|$ determination using inclusive strange τ decay and lattice hadronic vacuum polarization functions. Phys. Rev. Lett. **121**(20), 202003 (2018)
4081. Y. Sara Amhis et al., Averages of b-hadron, c-hadron, and τ-lepton properties as of 2021. Phys. Rev. D **107**(5), 052008 (2023)
4082. C. Andrea Manzari, A.M. Coutinho, A. Crivellin, Modified lepton couplings and the Cabibbo-angle anomaly. PoS LHCP **2020**, 242 (2021) (**Ed. by Bruno Mansoulie et al.**)
4083. B. Capdevila et al., Explaining $b \to s\ell^+\ell^-$ and the Cabibbo angle anomaly with a vector triplet. Phys. Rev. D **103**(1), 015032 (2021)
4084. P. Gambino et al., Challenges in semileptonic B decays. Eur. Phys. J. C **80**(10), 966 (2020)
4085. G. Ricciardi, M. Rotondo, Determination of the Cabibbo-Kobayashi-Maskawa matrix element $|V_{cb}|$. J. Phys. G **47**, 113001 (2020)
4086. M. Jung, D.M. Straub, Constraining new physics in $b \to c\ell\nu$ transitions (2018)
4087. A. Crivellin, S. Pokorski, Can the differences in the determinations of V_{ub} and V_{cb} be explained by New Physics? Phys. Rev. Lett. **114**(1), 011802 (2015)
4088. B. Blok et al., Differential distributions in semileptonic decays of the heavy flavors in QCD. Phys. Rev. D **49**, 3356 (1994)
4089. A.V. Manohar, M.B. Wise, Inclusive semileptonic B and polarized Λ_b decays from QCD. Phys. Rev. D **49**, 1310–1329 (1994)
4090. I. Bigi et al., The two roads to 'intrinsic charm' in B decays. JHEP **1004**, 073 (2010)
4091. T. Mannel, A.A. Pivovarov, QCD corrections to inclusive heavy hadron weak decays at $\Lambda^3_{\rm QCD}/m^3_Q$. Phys. Rev. D **100**(9), 093001 (2019)
4092. K. Melnikov, $O(\alpha_s{}^2)$ corrections to semileptonic decay $b \to c\ell\bar{\nu}$. Phys. Lett. B **666**, 336–339 (2008)
4093. A. Pak, A. Czarnecki, Mass effects in muon and semileptonic $b \to c$ decays. Phys. Rev. Lett. **100**, 241807 (2008)
4094. P. Gambino, B semileptonic moments at NNLO. JHEP **1109**, 055 (2011)
4095. A. Alberti, P. Gambino, S. Nandi, Perturbative corrections to power suppressed effects in semileptonic B decays. JHEP **1401**, 1–16 (2014)
4096. I.I.Y. Bigi et al., High power n of m_b in beauty widths. Phys. Rev. D **56**, 4017–4030 (1997)
4097. M. Fael, K. Schönwald, M. Steinhauser, Kinetic heavy quark mass to three loops. Phys. Rev. Lett. **125**(5), 052003 (2020)
4098. T. Mannel, S. Turczyk, N. Uraltsev, Higher order power corrections in inclusive B decays. JHEP **1011**, 109 (2010)
4099. P. Gambino, K.J. Healey, S. Turczyk, Taming the higher power corrections in semileptonic B decays. Phys. Lett. B **763**, 60–65 (2016)
4100. M. Fael, T. Mannel, K. Keri Vos, V_{cb} determination from inclusive $b \to c$ decays: an alternative method. JHEP **02**, 177 (2019)
4101. M. Bordone, B. Capdevila, P. Gambino, Three loop calculations and inclusive Vcb. Phys. Lett. B **822**, 136679 (2021)
4102. F. Bernlochner et al., First extraction of inclusive V_{cb} from q^2 moments. JHEP **10**, 068 (2022)
4103. P. Gambino, S. Hashimoto, Inclusive semileptonic decays from lattice QCD. Phys. Rev. Lett. **125**(3), 032001 (2020)
4104. B.O. Lange, M. Neubert, G. Paz, Theory of charmless inclusive B decays and the extraction of V_{ub}. Phys. Rev. D **72**, 073006 (2005)
4105. P. Gambino et al., Inclusive semileptonic B decays and the determination of $|V_{ub}|$. JHEP **0710**, 058 (2007)
4106. J.R. Andersen, E. Gardi, Inclusive spectra in charmless semileptonic B decays by dressed gluon exponentiation. JHEP **01**, 097 (2006)
4107. I.I.Y. Bigi, N.G. Uraltsev, Weak annihilation and the endpoint spectrum in semileptonic B decays. Nucl. Phys. B **423**, 33–55 (1994)
4108. Z. Ligeti, M. Luke, A.V. Manohar, Constraining weak annihilation using semileptonic D decays. Phys. Rev. D **82**, 033003 (2010)
4109. P. Gambino, J.F. Kamenik, Lepton energy moments in semileptonic charm decays. Nucl. Phys. B **840**, 424–437 (2010)
4110. J.P. Lees et al., Measurement of the inclusive electron spectrum from B meson decays and determination of $|V_{ub}|$. Phys. Rev. D **95**(7), 072001 (2017)
4111. L. Cao et al., Measurements of partial branching fractions of inclusive $B \to X_u \ell^+ \nu_\ell$ decays with hadronic tagging. Phys. Rev. D **104**(1), 012008 (2021)
4112. B. Capdevila, P. Gambino, S. Nandi, Perturbative corrections to power suppressed effects in $\bar{B} \to X_u \ell\nu$. JHEP **04**, 137 (2021)
4113. M. Brucherseifer, F. Caola, K. Melnikov, On the $O(\alpha_s^2)$ corrections to $b \to X_u e\bar{\nu}$ inclusive decays. Phys. Lett. B **721**, 107–110 (2013)
4114. L. Cao et al., Measurement of differential branching fractions of inclusive $B \to X_u \ell^+ \nu_\ell$ decays. Phys. Rev. Lett. **127**(26), 261801 (2021)
4115. P. Gambino, K.J. Healey, C. Mondino, Neural network approach to $B \to X_u \ell\nu$. Phys. Rev. D **94**(1), 014031 (2016)
4116. C. Glenn Boyd, B. Grinstein, R.F. Lebed, Precision corrections to dispersive bounds on form-factors. Phys. Rev. D **56**, 6895–6911 (1997)

4117. C. Bourrely, I. Caprini, L. Lellouch, Model-independent description of $B \to \pi \ell \nu$ decays and a determination of $|V_{ub}|$. Phys. Rev. D **79**, 013008 (2009) [Erratum: Phys. Rev. D 82, 099902 (2010)]
4118. I. Caprini, L. Lellouch, M. Neubert, Dispersive bounds on the shape of $\bar{B} \to D^* \ell \bar{\nu}$ form-factors. Nucl. Phys. B **530**, 153–181 (1998)
4119. F.U. Bernlochner et al., Combined analysis of semileptonic B decays to D and D^* : $R(D^{(*)})$, $|V_{cb}|$, and new physics. Phys. Rev. D **95**(11), 115008 (2017)
4120. D. Bigi, P. Gambino, S. Schacht, $R(D^*)$, $|V_{cb}|$, and the Heavy Quark Symmetry relations between form factors. JHEP **11**, 061 (2017)
4121. S. Jaiswal, S. Nandi, S. Kumar Patra, Extraction of $|V_{cb}|$ from $B \to D^{(*)} \ell \nu_\ell$ and the Standard Model predictions of $R(D^{(*)})$. JHEP **12**, 060 (2017)
4122. M. Bordone, M. Jung, D. van Dyk, Theory determination of $\bar{B} \to D^{(*)} \ell^- \bar{\nu}$ form factors at $O(1/m_c^2)$. Eur. Phys. J. C **80**(2), 74 (2020)
4123. R. Glattauer et al., Measurement of the decay $B \to D \ell \nu_\ell$ in fully reconstructed events and determination of the Cabibbo-Kobayashi-Maskawa matrix element $|V_{cb}|$ (2015)
4124. A. Abdesselam et al., Precise determination of the CKM matrix element $|V_{cb}|$ with $\bar{B}^0 \to D^{*+} \ell^- \bar{\nu}_\ell$ decays with hadronic tagging at Belle (2017). arXiv:1702.01521
4125. E. Waheed et al., Measurement of the CKM matrix element $|V_{cb}|$ from $B^0 \to D^{*-} \ell^+ \nu_\ell$ at Belle. Phys. Rev. D **100**(5), 052007 (2019) [Erratum: Phys. Rev. D 103, 079901 (2021)]
4126. J.A. Bailey et al., $B \to D \ell \nu$ form factors at nonzero recoil and $|V_{cb}|$ from 2+1-flavor lattice QCD. Phys. Rev. D **92**(3), 034506 (2015)
4127. H. Na et al., $B \to D \ell \nu$ form factors at nonzero recoil and extraction of $|V_{cb}|$. Phys. Rev. D **92**(5), 054510 (2015) [Erratum: Phys. Rev. D 93(11), 119906 (2016)]
4128. D. Bigi, P. Gambino, Revisiting $B \to D \ell \nu$. Phys. Rev. D **94**(9), 094008 (2016)
4129. J.A. Bailey et al., $B \to D \ell \nu$ form factors at nonzero recoil and $|V_{cb}|$ from 2+1-flavor lattice QCD. Phys. Rev. D **92**(3), 034506 (2015)
4130. B. Aubert et al., Measurement of $-V_{cb}-$ and the form-factor slope in $\bar{B} \to D l^- \bar{\nu}$ decays in events tagged by a fully reconstructed B meson. Phys. Rev. Lett. **104**, 011802 (2010)
4131. T. Kaneko et al., $B \to D^{(*)} \ell \nu$ semileptonic decays in lattice QCD with domain-wall heavy quarks. PoS LATTICE2021, 561 (2022)
4132. D. Bigi, P. Gambino, S. Schacht, A fresh look at the determination of $|V_{cb}|$ from $B \to D^* \ell \nu$. Phys. Lett. B **769**, 441–445 (2017)
4133. B. Grinstein, A. Kobach, Model-independent extraction of $|V_{cb}|$ from $\bar{B} \to D^* \ell \bar{\nu}$. Phys. Lett. B **771**, 359–364 (2017)
4134. M.T. Prim et al., Measurement of Differential Distributions of $B \to D^* \ell \bar{\nu}_\ell$ and Implications on $|V_{cb}|$ (2023)
4135. C. Bobeth et al., Lepton-flavour non-universality of $\bar{B} \to D^* \ell \bar{\nu}$ angular distributions in and beyond the Standard Model. Eur. Phys. J. C **81**(11), 984 (2021)
4136. P. Gambino, M. Jung, S. Schacht, The V_{cb} puzzle: an update. Phys. Lett. B **795**, 386–390 (2019)
4137. G. D'Agostini, On the use of the covariance matrix to fit correlated data. Nucl. Instrum. Meth. A **346**, 306–311 (1994)
4138. T. Kaneko, Private communication (2022)
4139. G. Martinelli, S. Simula, L. Vittorio, Exclusive determinations of $|V_{cb}|$ and $R(D^*)$ through unitarity (2021)
4140. R. Aaij et al., Measurement of $|V_{cb}|$ with $B_s^0 \to D_s^{(*)-} \mu^+ \nu_\mu$ decays. Phys. Rev. D **101**(7), 072004 (2020)
4141. E. McLean et al., Lattice QCD form factor for $B_s \to D_s^* \ell \nu$ at zero recoil with non-perturbative current renormalisation. Phys. Rev. D **99**(11), 114512 (2019)
4142. J.P. Lees et al., Extraction of form factors from a four-dimensional angular analysis of $\bar{B} \to D^* \ell^- \bar{\nu}_\ell$. Phys. Rev. Lett. **123**(9), 091801 (2019)
4143. J.A. Bailey et al., $|V_{ub}|$ from $B \to \pi \ell \nu$ decays and (2+1)-flavor lattice QCD. Phys. Rev. D **92**(1), 014024 (2015)
4144. A. Bharucha, Two-loop corrections to the $Bto\pi$ form factor from QCD sum rules on the light-cone and $|V_{ub}|$. JHEP **05**, 092 (2012)
4145. D. Leljak, B. Melic, D. van Dyk, The $\bar{B} \to \pi$ form factors from QCD and their impact on $|V_{ub}|$. JHEP **07**, 036 (2021)
4146. A. Biswas et al., A closer look at the extraction of $|V_{ub}|$ from $B \to \pi \ell \nu$. JHEP **07**, 082 (2021)
4147. R. Aaij et al., First observation of the decay $B_s^0 \to K^- \mu^+ \nu_\mu$ and measurement of $|V_{ub}|/|V_{cb}|$. Phys. Rev. Lett. **126**(8), 081804 (2021)
4148. A. Bazavov et al., $B_s \to K \ell \nu$ decay from lattice QCD. Phys. Rev. D **100**(3), 034501 (2019)
4149. A. Khodjamirian, A.V. Rusov, $B_s \to K \ell \nu_\ell$ and $B_{(s)} \to \pi(K) \ell^+ \ell^-$ decays at large recoil and CKM matrix elements. JHEP **08**, 112 (2017)
4150. D. King et al., $|V_{cb}|$ and γ from B-mixing—addendum to B_s mixing observables and $|V_{td}/V_{ts}|$ from sum rules (2019) [Addendum: JHEP 03, 112 (2020)]
4151. W. Altmannshofer, N. Lewis, Loop-induced determinations of V_{ub} and V_{cb}. Phys. Rev. D **105**(3), 033004 (2022)
4152. A.J. Buras, E. Venturini, The Exclusive Vision of Rare K and B Decays and of the Quark Mixing in the Standard Model. Eur. Phys. J. C **82**, 615 (2022)
4153. A.J. Buras, On the superiority of the $|V_{cb}| - \gamma$ plots over the unitarity triangle plots in the 2020s. Eur. Phys. J. C **82**(7), 612 (2022)
4154. J. Charles et al., CP violation and the CKM matrix: assessing the impact of the asymmetric B factories. Eur. Phys. J. C **41**, 1–131 (2005). http://www.ckmfitter.in2p3.fr
4155. Y. Nir, Flavour physics, CP violation. CERN Yellow Rep. School Proc. **5**, 79–128 (2020) **(Ed. by M. Mulders and J. Trân Thanh Vân)**
4156. L. Silvestrini, Effective Theories for Quark Flavour Physics (2019). Les Houches Lect. Notes 108 (2020) **(Ed. by S. Davidson et al.)**
4157. J. Zupan, Introduction to flavour physics. CERN Yellow Rep. School Proc. **6**, 181–212 (2019) **(Ed. by M. Mulders and C. Duhr)**
4158. W. Altmannshofer et al., The Belle II Physics Book. PTEP **2019**(12), 123C01 (2019) [Erratum: PTEP 2020, 029201 (2020)] **(Ed. by E. Kou and P. Urquijo)**
4159. M. Ciuchini, M. Pierini, L. Silvestrini, The effect of penguins in the $B_d \to J/\psi K^0$ CP asymmetry. Phys. Rev. Lett. **95**, 221804 (2005)
4160. S. Faller et al., The golden modes $B^0 \to J/\psi K_{S,L}$ in the era of precision flavour physics. Phys. Rev. D **79**, 014030 (2009)
4161. M. Jung, Determining weak phases from $B \to J/\psi P$ decays. Phys. Rev. D **86**, 053008 (2012)
4162. M. Gronau, D. London, Isospin analysis of CP asymmetries in B decays. Phys. Rev. Lett. **65**, 3381–3384 (1990)
4163. G. Isidori, Flavour physics and implication for new phenomena. Adv. Ser. Dir. High Energy Phys. **26**, 339–355 (2016)
4164. R. Ammar et al., Evidence for penguins: first observation of $B \to K^*(892)\gamma$. Phys. Rev. Lett. **71**, 674–678 (1993)
4165. M.S. Alam et al., First measurement of the rate for the inclusive radiative penguin decay $b \to s\gamma$. Phys. Rev. Lett. **74**, 2885–2889 (1995)
4166. M. Misiak et al., Estimate of $\mathcal{B}(\bar{B} \to X(s)\gamma)$ at $\mathcal{O}(\alpha_s^2)$. Phys. Rev. Lett. **98**, 022002 (2007)
4167. M. Misiak et al., Updated NNLO QCD predictions for the weak radiative B-meson decays. Phys. Rev. Lett. **114**(22), 221801 (2015)

4168. Y. Amhis et al., Averages of b-hadron, c-hadron, and τ-lepton properties as of summer 2016 (2016)
4169. S. Bertolini, F. Borzumati, A. Masiero, QCD enhancement of radiative b decays. Phys. Rev. Lett. **59**, 180 (1987)
4170. N.G. Deshpande et al., $B \to K^*\gamma$ and the top quark mass. Phys. Rev. Lett. **59**, 183–185 (1987)
4171. M. Misiak, QCD corrected effective Hamiltonian for the $b \to s\gamma$ decay. Phys. Lett. B **269**, 161–168 (1991)
4172. M. Misiak, The $b \to se^+e^-$ and $b \to s\gamma$ decays with next-to-leading logarithmic QCD corrections. Nucl. Phys. B **393**, 23–45 (1993) [Erratum: Nucl. Phys. B 439, 461(1995)]
4173. M. Ciuchini et al., Scheme independence of the effective Hamiltonian for $b \to s\gamma$ and $b \to sg$ decays. Phys. Lett. B **316**, 127–136 (1993)
4174. M. Ciuchini et al., Leading order QCD corrections to $b \to s\gamma$ and $b \to sg$ decays in three regularization schemes. Nucl. Phys. B **421**, 41–64 (1994)
4175. A.J. Buras et al., Theoretical uncertainties and phenomenological aspects of $B \to X_{s\gamma}$ decay. Nucl. Phys. B **424**, 374–398 (1994)
4176. A. Ali, C. Greub, T. Mannel, Rare B decays in the Standard Model (1993)
4177. A.J. Buras, M. Misiak, $\bar{B} \to X_{s\gamma}$ after completion of the NLO QCD calculations. Acta Phys. Polon. B **33**, 2597–2612 (2002)
4178. P. Gambino, M. Misiak, Quark mass effects in $\bar{B} \to X_{s\gamma}$. Nucl. Phys. B **611**, 338–366 (2001)
4179. A.J. Buras, ε'/ε in the Standard Model and Beyond: 2021. In: *11th International Workshop on the CKM Unitarity Triangle* (2022). arXiv:2203.12632
4180. M. Tanabashi et al., Review of particle physics. Phys. Rev. D **98**(3), 030001 (2018)
4181. M. Gell-Mann, A. Pais, Behavior of neutral particles under charge conjugation. Phys. Rev. **97**, 1387–1389 (1955)
4182. M. Gell-Mann, A.H. Rosenfeld, Hyperons and heavy mesons (systematics and decay). Annu. Rev. Nucl. Part. Sci. **7**, 407–478 (1957)
4183. E. Fermi, An attempt of a theory of beta radiation. 1. Z. Phys. **88**, 161–177 (1934)
4184. R.P. Feynman, M. Gell-Mann, Theory of Fermi interaction. Phys. Rev. **109**, 193–198 (1958)
4185. E.C.G. Sudarshan, R. Marshak, Chirality invariance and the universal Fermi interaction. Phys. Rev. **109**, 1860–1860 (1958)
4186. G.E. Brown et al., Final state interactions in K meson decays. Phys. Lett. B **238**, 20–24 (1990)
4187. E. Pallante, A. Pich, Final state interactions in kaon decays. Nucl. Phys. B **592**, 294–320 (2001)
4188. P.A. Boyle et al., Emerging understanding of the $\Delta I = 1/2$ rule from lattice QCD (2012)
4189. R. Abbott et al., Direct CP violation and the $\Delta I = 1/2$ rule in $K \to \pi\pi$ decay from the Standard Model (2020)
4190. G. Altarelli et al., QCD nonleading corrections to weak decays as an application of regularization by dimensional reduction. Nucl. Phys. B **187**, 461–513 (1981)
4191. A.J. Buras, F. De Fazio, J. Girrbach, $\Delta I = 1/2$ rule, ε'/ε and $K \to \pi\nu\bar{\nu}$ in $Z'(Z)$ and G' models with FCNC quark couplings. Eur. Phys. J. C **74**, 2950 (2014)
4192. A.J. Buras, The ϵ'/ϵ-Story: 1976–2021. Acta Phys. Polon. B **52**(1), 7–41 (2021)
4193. J.R. Batley et al., A precision measurement of direct CP violation in the decay of neutral kaons into two pions. Phys. Lett. B **544**, 97–112 (2002)
4194. A. Alavi-Harati et al., Measurements of direct CP violation, CPT symmetry, and other parameters in the neutral kaon system. Phys. Rev. D **67**, 012005 (2003)
4195. E. Abouzaid et al., Precise measurements of direct CP violation, CPT symmetry, and other parameters in the neutral kaon system. Phys. Rev. D **83**, 092001 (2011)
4196. F.J. Gilman, M.B. Wise, The $\Delta I = 1/2$ rule and violation of CP in the six quark model. Phys. Lett. B **83**, 83–86 (1979)
4197. W.A. Bardeen, A.J. Buras, J.-M. Gérard, The $\Delta I = 1/2$ rule in the large N limit. Phys. Lett. B **180**, 133 (1986)
4198. W.A. Bardeen, A.J. Buras, J.-M. Gérard, The $K \to \pi\pi$ decays in the large N limit: quark evolution. Nucl. Phys. B **293**, 787 (1987)
4199. J.F. Donoghue et al., Electromagnetic and isospin breaking effects decrease ϵ'/ϵ. Phys. Lett. B **179**, 361 (1986) [Erratum: Phys. Lett. B 188, 511 (1987)]
4200. A.J. Buras, J.M. Gérard, Isospin breaking contributions to ε'/ε. Phys. Lett. B **192**, 156 (1987)
4201. J.M. Flynn, L. Randall, The electromagnetic penguin contribution to ε'/ε for large top quark mass. Phys. Lett. B **224**, 221 (1989)
4202. G. Buchalla, A.J. Buras, M.K. Harlander, The anatomy of ε'/ε in the standard model. Nucl. Phys. B **337**, 313–362 (1990)
4203. A.J. Buras et al., Effective Hamiltonians for $\Delta S = 1$ and $\Delta B = 1$ nonleptonic decays beyond the leading logarithmic approximation. Nucl. Phys. B **370**, 69–104 (1992) [Addendum: Nucl. Phys. B 375, 501 (1992)]
4204. A.J. Buras et al., Two loop anomalous dimension matrix for $\Delta S = 1$ weak nonleptonic decays. 1. $\mathcal{O}(\alpha_s^2)$. Nucl. Phys. B **400**, 37–74 (1993)
4205. A.J. Buras, M. Jamin, M.E. Lautenbacher, Two loop anomalous dimension matrix for $\Delta S = 1$ weak nonleptonic decays. 2. $\mathcal{O}(\alpha\alpha_s)$. Nucl. Phys. B **400**, 75–102 (1993)
4206. A.J. Buras, M. Jamin, M.E. Lautenbacher, The anatomy of ε'/ε beyond leading logarithms with improved hadronic matrix elements. Nucl. Phys. B **408**, 209–285 (1993)
4207. M. Ciuchini et al., ε'/ε at the next-to-leading order in QCD and QED. Phys. Lett. B **301**, 263–271 (1993)
4208. M. Ciuchini et al., The $\Delta S = 1$ effective Hamiltonian including next-to-leading order QCD and QED corrections. Nucl. Phys. B **415**, 403–462 (1994)
4209. A.J. Buras, P. Gambino, U.A. Haisch, Electroweak penguin contributions to non-leptonic $\Delta F = 1$ decays at NNLO. Nucl. Phys. B **570**, 117–154 (2000)
4210. A.J. Buras et al., Improved anatomy of ε'/ε in the Standard Model. JHEP **11**, 202 (2015)
4211. V. Cirigliano et al., Isospin violation in ϵ'. Phys. Rev. Lett. **91**, 162001 (2003)
4212. V. Cirigliano et al., Isospin breaking in $K \to \pi\pi$ decays. Eur. Phys. J. C **33**, 369–396 (2004)
4213. J. Bijnens, F. Borg, Isospin breaking in $K \to 3\pi$ decays III: Bremsstrahlung and fit to experiment. Eur. Phys. J. C **40**, 383–394 (2005)
4214. A.J. Buras, J.-M. Gerard, Isospin-breaking in ε'/ε: impact of η_0 at the Dawn of the 2020s (2020)
4215. V. Cirigliano et al., Theoretical status of ε'/ε. J. Phys. Conf. Ser. **1526**, 012011 (2020) **(Ed. by Patrizia Cenci and Mauro Piccini)**
4216. J. Aebischer, C. Bobeth, A.J. Buras, ε'/ε in the Standard Model at the Dawn of the 2020s. Eur. Phys. J. C **80**(8), 705 (2020)
4217. V. Antonelli et al., The $\Delta I = 1/2$ selection rule. Nucl. Phys. B **469**, 181–201 (1996)
4218. S. Bertolini, J.O. Eeg, M. Fabbrichesi, A new estimate of ε'/ε. Nucl. Phys. B **476**, 225–254 (1996)
4219. E. Pallante, A. Pich, Strong enhancement of ε'/ε through final state interactions. Phys. Rev. Lett. **84**, 2568–2571 (2000)
4220. E. Pallante, A. Pich, I. Scimemi, The standard model prediction for ε'/ε. Nucl. Phys. B **617**, 441–474 (2001)
4221. A.J. Buras, J.-M. Gérard, Upper bounds on ε'/ε parameters $B_6^{(1/2)}$ and $B_8^{(3/2)}$ from large N QCD and other news. JHEP **12**, 008 (2015)
4222. A.J. Buras, J.-M. Gérard, Final state interactions in $K \to \pi\pi$ decays: $\Delta I = 1/2$ rule vs ε'/ε. Eur. Phys. J. C **77**(1), 10 (2017)

4223. R. Aaij et al., Measurement of form-factor-independent observables in the decay $B^0 \to K^{*0}\mu^+\mu^-$. Phys. Rev. Lett. **111**, 191801 (2013)
4224. C. Bobeth, M. Misiak, J. Urban, Photonic penguins at two loops and m_t-dependence of $BR(B \to X_s\ell^+\ell^-)$. Nucl. Phys. B **574**, 291–330 (2000)
4225. M. Gorbahn, U. Haisch, Effective Hamiltonian for non-leptonic $|\Delta F| = 1$ decays at NNLO in QCD. Nucl. Phys. B **713**, 291–332 (2005)
4226. T. Huber et al., Electromagnetic logarithms in $\bar{B} \to X(s)l^+l^-$ Nucl. Phys. B **740**, 105–137 (2006)
4227. M. Beneke, C. Bobeth, R. Szafron, Enhanced electromagnetic correction to the rare B-meson decay $B_{s,d} \to \mu^+\mu^-$. Phys. Rev. Lett. **120**(1), 011801 (2018)
4228. N. Carrasco et al., A $N_f = 2 + 1 + 1$ "twisted" determination of the b-quark mass, f_B and f_{B_s}. PoS LATTICE **2013**, 313 (2014)
4229. Combination of the ATLAS, CMS and LHCb results on the $B^0_{(s)} \to \mu^+\mu^-$ decays (2020)
4230. J. Albrecht, D. van Dyk, C. Langenbruch, Flavour anomalies in heavy quark decays. Prog. Part. Nucl. Phys. **120**, 103885 (2021)
4231. C. Bobeth, G. Hiller, D. van Dyk, General analysis of $\bar{B} \to \bar{K}^{(*)}\ell^+\ell^-$ decays at low recoil. Phys. Rev. D **87**, 034016 (2013)
4232. S. Jäger, J. Martin Camalich, On $B \to V\ell\ell$ at small dilepton invariant mass, power corrections, and new physics. JHEP **1305**, 043 (2013)
4233. F. Kruger, J. Matias, Probing new physics via the transverse amplitudes of $B^0 \to K^{*0}(K^-\pi^+)l^+l^-$ at large recoil. Phys. Rev. D **71**, 094009 (2005)
4234. C. Bobeth, G. Hiller, G. Piranishvili, CP asymmetries in bar $B \to \bar{K}^*(\to \bar{K}\pi)\bar{\ell}\ell$ and untagged $\bar{B}_s, B_s \to \phi(\to K^+K^-)\bar{\ell}\ell$ Decays at NLO. JHEP **0807**, 106 (2008)
4235. W. Altmannshofer et al., Symmetries and asymmetries of $B \to K^*\mu^+\mu^-$ decays in the standard model and beyond. JHEP **0901**, 019 (2009)
4236. C. Bobeth, G. Hiller, G. Piranishvili, Angular distributions of $\bar{B} \to K\ell^+\ell^-$ decays. JHEP **12**, 040 (2007)
4237. J. Matias, On the S-wave pollution of $B \to K*l^+l^-$ observables. Phys. Rev. D **86**, 094024 (2012)
4238. S. Descotes-Genon, A. Khodjamirian, J. Virto, Light-cone sum rules for $B \to K\pi$ form factors and applications to rare decays. JHEP **12**, 083 (2019)
4239. J. Charles et al., Heavy to light form-factors in the heavy mass to large energy limit of QCD. Phys. Rev. D **60**, 014001 (1999)
4240. M. Beneke, T. Feldmann, Symmetry breaking corrections to heavy to light B meson form-factors at large recoil. Nucl. Phys. B **592**, 3–34 (2001)
4241. U. Egede et al., New observables in the decay mode $\bar{B}_d \to \bar{K}^{*0}l^+l^-$. JHEP **0811**, 032 (2008)
4242. C. Bobeth, G. Hiller, D. van Dyk, The benefits of $\bar{B} \to \bar{K}^*l^+l^-$ decays at low recoil. JHEP **1007**, 098 (2010)
4243. S. Descotes-Genon et al., Optimizing the basis of $B \to K^*\ell^+\ell^-$ observables in the full kinematic range. JHEP **1305**, 137 (2013)
4244. S. Descotes-Genon et al., Implications from clean observables for the binned analysis of $B \to K*\mu^+\mu^-$ at large recoil. JHEP **01**, 048 (2013)
4245. A. Bharucha, D.M. Straub, R. Zwicky, $B \to V\ell^+\ell^-$ in the Standard Model from light-cone sum rules. JHEP **08**, 098 (2016)
4246. R.R. Horgan et al., Lattice QCD calculation of form factors describing the rare decays $B \to K^*\ell^+\ell^-$ and $B_s \to \phi\ell^+\ell^-$. Phys. Rev. D **89**, 094501 (2014)
4247. J.A. Bailey et al., $B \to Kl^+l^-$ decay form factors from three-flavor lattice QCD. Phys. Rev. D **93**(2), 025026 (2016)
4248. N. Gubernari et al., Improved Theory Predictions and Global Analysis of Exclusive $\boldsymbol{b \to s\mu^+\mu^-}$ Processes (2022)
4249. I. Caprini, *Functional Analysis and Optimization Methods in Hadron Physics. Springer Briefs in Physics* (Springer, 2019)
4250. S. Cheng, A. Khodjamirian, J. Virto, $B \to \pi\pi$ form factors from light-cone sum rules with B-meson distribution amplitudes. JHEP **05**, 157 (2017)
4251. S. Cheng, A. Khodjamirian, J. Virto, Timelike-helicity $B \to \pi\pi$ form factor from light-cone sum rules with dipion distribution amplitudes. Phys. Rev. D **96**(5), 051901 (2017)
4252. M. Beneke, T. Feldmann, D. Seidel, Systematic approach to exclusive $B \to Vl^+l^-$, $V\gamma$ decays. Nucl. Phys. B **612**, 25–58 (2001)
4253. A. Khodjamirian et al., Charm-loop effect in $B \to K^{(*)}\ell^+\ell^-$ and $B \to K^*\gamma$. JHEP **1009**, 089 (2010)
4254. B. Grinstein, D. Pirjol, Exclusive rare $B \to K^*\ell^+\ell^-$ decays at low recoil: Controlling the long-distance effects. Phys. Rev. D **70**, 114005 (2004)
4255. M. Beylich, G. Buchalla, T. Feldmann, Theory of $B \to K^{(*)}l^+l^-$ decays at high q^2: OPE and quark-hadron duality. Eur. Phys. J. C **71**, 1635 (2011)
4256. M. Beneke, T. Feldmann, D. Seidel, Exclusive radiative and electroweak $b \to d$ and $b \to s$ penguin decays at NLO. Eur. Phys. J. C **41**, 173–188 (2005)
4257. N. Gubernari, D. van Dyk, J. Virto, Non-local matrix elements in $B_{(s)} \to \{K^{(*)}, \phi\}\ \ell^+\ell^-$. JHEP **02**, 088 (2021)
4258. C. Bobeth, G. Hiller, D. van Dyk, More benefits of semileptonic rare B decays at low recoil: CP violation. JHEP **1107**, 067 (2011)
4259. C. Bobeth et al., The decay $B \to K\ell^+\ell^-$ at low hadronic recoil and model-independent $\Delta B = 1$ constraints. JHEP **01**, 107 (2012)
4260. J. Lyon, R. Zwicky, Resonances gone topsy turvy—the charm of QCD or new physics in $b \to s\ell^+\ell^-$? arXiv:1406.0566 (2014)
4261. S. Braß, G. Hiller, I. Nisandzic, Zooming in on $B \to K^*\ell\ell$ decays at low recoil. Eur. Phys. J. C **77**(1), 16 (2017)
4262. C. Bobeth et al., Long-distance effects in $B \to K^*\ell\ell$ from analyticity (2017)
4263. M. Algueró et al., $b \to s\ell^+\ell^-$ global fits after R_{K_S} and $R_{K^{*+}}$. Eur. Phys. J. C **82**(4), 326 (2022)
4264. W. Altmannshofer, P. Stangl, New physics in rare B decays after Moriond 2021. Eur. Phys. J. C **81**(10), 952 (2021)
4265. M. Ciuchini et al., Lessons from the $B^{0,+} \to K^{*0,+}\mu^+\mu^-$ angular analyses. Phys. Rev. D **103**(1), 015030 (2021)
4266. T. Hurth et al., More indications for lepton nonuniversality in $b \to s\ell^+\ell^-$. Phys. Lett. B **824**, 136838 (2022)
4267. D. Du et al., Phenomenology of semileptonic B-meson decays with form factors from lattice QCD. Phys. Rev D **93**, 035005 (2015)
4268. M. Chrzaszcz et al., Prospects for disentangling long- and short-distance effects in the decays $B \to K^*\mu^+\mu^-$. JHEP **10**, 236 (2019)
4269. S. Descotes-Genon et al., Global analysis of $b \to s\ell\ell$ anomalies. JHEP **06**, 092 (2016)
4270. M. Ciuchini et al., $B \to K^*\ell^+\ell^-$ decays at large recoil in the Standard Model: a theoretical reappraisal. JHEP **06**, 116 (2016)
4271. U. Egede, M. Patel, K.A. Petridis, Method for an unbinned measurement of the q^2 dependent decay amplitudes of $\overline{B}^0 \to K^{*0}\mu^+\mu^-$ decays. JHEP **06**, 084 (2015)
4272. T. Hurth, F. Mahmoudi, S. Neshatpour, On the anomalies in the latest LHCb data. Nucl. Phys. B **909**, 737–777 (2016)
4273. F. Kruger, L.M. Sehgal, Lepton polarization in the decays $b \to X_s\mu^+\mu^-$ and $B \to X_s\tau^+\tau^-$. Phys. Lett. B **380**, 199–204 (1996)
4274. T. Blake et al., An empirical model to determine the hadronic resonance contributions to $\overline{B}^0 \to \overline{K}^{*0}\mu^+\mu^-$ transitions. Eur. Phys. J. C **78**(6), 453 (2018)
4275. F. Jegerlehner, The anomalous magnetic moment of the muon. Springer Tracts Mod. Phys. **274**, 1–693 (2017)
4276. J.S. Schwinger, On quantum electrodynamics and the magnetic moment of the electron. Phys. Rev. **73**, 416–417 (1948)

4277. V.B. Berestetskii, O.N. Krokhin, A.K. Khlebnikov, Concerning the radiative correction to the μ-meson magnetic moment. JETP **3**(5), 761 (1956) [Zh. Eksp. Teor. Fiz. 30, 788 (1956)]
4278. W.S. Cowland, On Schwinger's theory of the muon. Nucl. Phys. **8**, 397–401 (1958)
4279. R.L. Garwin et al., Accurate determination of the μ^+ magnetic moment. Phys. Rev. **118**, 271–283 (1960)
4280. B. Lee Roberts, The history of the muon $(g-2)$ experiments. SciPost Phys. Proc. **1**, 032 (2019)
4281. V. Bargmann, L. Michel, V.L. Telegdi, Precession of the polarization of particles moving in a homogeneous electromagnetic field. Phys. Rev. Lett. **2**, 435–436 (1959)
4282. J. Bailey et al., Final report on the CERN muon storage ring including the anomalous magnetic moment and the electric dipole moment of the muon, and a direct test of relativistic time dilation. Nucl. Phys. B **150**, 1–75 (1979)
4283. G.W. Bennett et al., Final report of the muon E821 anomalous magnetic moment measurement at BNL. Phys. Rev. D **73**, 072003 (2006)
4284. F. Jegerlehner, A. Nyffeler, The muon $g-2$. Phys. Rep. **477**, 1–110 (2009)
4285. G. Venanzoni, The new muon $g-2$ experiment at Fermilab. Nucl. Part. Phys. Proc. 273–275, 584–588 (2016) **(Ed. by M Aguilar-Benítez et al.)**
4286. T. Aoyama et al., The anomalous magnetic moment of the muon in the Standard Model. Phys. Rep. **887**, 1–166 (2020)
4287. B. Abi et al., Measurement of the positive muon anomalous magnetic moment to 0.46 ppm. Phys. Rev. Lett. **126**(14), 141801 (2021)
4288. S. Borsanyi et al., Leading hadronic contribution to the muon magnetic moment from lattice QCD. Nature **593**(7857), 51–55 (2021)
4289. T. Mibe, Measurement of muon $g-2$ and EDM with an ultra-cold muon beam at J-PARC. Nucl. Phys. Proc. Suppl. **218**, 242–246 (2011)
4290. R.R. Akhmetshin et al., Reanalysis of hadronic cross-section measurements at CMD-2. Phys. Lett. B **578**, 285–289 (2004)
4291. V.M. Aul'chenko et al., Measurement of the pion form-factor in the range 1.04-GeV to 1.38-GeV with the CMD-2 detector. JETP Lett. **82**, 743–747 (2005)
4292. V.M. Aul'chenko et al., Measurement of the $e^+e^- \to \pi^+\pi^-$ cross section with the CMD-2 detector in the 370–520-MeV c.m. energy range. JETP Lett. **84**, 413–417 (2006)
4293. R.R. Akhmetshin et al., High-statistics measurement of the pion form factor in the rho-meson energy range with the CMD-2 detector. Phys. Lett. B **648**, 28–38 (2007)
4294. M.N. Achasov et al., Study of the process $e^+e^- \to \pi^+\pi^-$ in the energy region $400 <\sqrt{s}<$ 1000-MeV. J. Exp. Theor. Phys. **101**(6), 1053–1070 (2005)
4295. A. Anastasi et al., Combination of KLOE $\sigma\big(e^+e^- \to \pi^+\pi^-\gamma(\gamma)\big)$ measurements and determination of $a_\mu^{\pi^+\pi^-}$ in the energy range $0.10<s<0.95$ GeV^2. JHEP **03**, 173 (2018)
4296. B. Aubert et al., Precise measurement of the $e^+e^- \to \pi^+\pi^-\gamma$ cross section with the Initial State Radiation method at BABAR. Phys. Rev. Lett. **103**, 231801 (2009)
4297. J.P. Lees et al., Precise measurement of the $e^+e^- \to \pi^+\pi^-(\gamma)$ cross section with the initial-state radiation method at BABAR. Phys. Rev. D **86**, 032013 (2012)
4298. M. Ablikim et al., Measurement of the $e^+e^- \to \pi^+\pi^-$ cross section between 600 and 900 MeV using initial state radiation. Phys. Lett. B **753**, 629–638 (2016) [Erratum: Phys. Lett. B 812, 135982 (2021)]
4299. V.P. Druzhinin et al., Hadron production via e^+e^- collisions with initial state radiation. Rev. Mod. Phys. **83**, 1545 (2011)
4300. R. Alemany, M. Davier, A. Höcker, Improved determination of the hadronic contribution to the muon (g-2) and to $\alpha(M_Z)$ using new data from hadronic τ decays. Eur. Phys. J. C **2**, 123–135 (1998)
4301. M.N. Achasov et al., Measurement of the $e^+e^- \to \pi^+\pi^-$ process cross section with the SND detector at the VEPP-2000 collider in the energy region $0.525<\sqrt{s}<0.883$ GeV. JHEP **01**, 113 (2021)
4302. T. Xiao et al., Precision measurement of the hadronic contribution to the muon anomalous magnetic moment. Phys. Rev. D **97**(3), 032012 (2018)
4303. A. Keshavarzi, D. Nomura, T. Teubner, The muon $g-2$ and $\alpha(M_Z^2)$: a new data-based analysis. Phys. Rev. D **97**(11), 114025 (2018)
4304. M. Davier et al., A new evaluation of the hadronic vacuum polarisation contributions to the muon anomalous magnetic moment and to $\alpha(m_Z^2)$. Eur. Phys. J. C **80**(3), 241 (2020) [Erratum: Eur. Phys. J. C 80, 410 (2020)]
4305. M. Davier et al., Reevaluation of the hadronic vacuum polarisation contributions to the Standard Model predictions of the muon $g-2$ and $\alpha(m_Z^2)$ using newest hadronic cross-section data. Eur. Phys. J. C **77**(12), 827 (2017)
4306. G. Colangelo, M. Hoferichter, P. Stoffer, Two-pion contribution to hadronic vacuum polarization. JHEP **02**, 006 (2019)
4307. M. Hoferichter, B.-L. Hoid, B. Kubis, Three-pion contribution to hadronic vacuum polarization. JHEP **08**, 137 (2019)
4308. A. Keshavarzi, D. Nomura, T. Teubner, The $g-2$ of charged leptons, $\alpha(M_Z^2)$ and the hyperfine splitting of muonium. Phys. Rev. D **101**, 014029 (2020)
4309. F. Ambrosino et al., Measurement of $\sigma(e^+e^- \to \pi^+\pi^-\gamma(\gamma)$ and the dipion contribution to the muon anomaly with the KLOE detector. Phys. Lett. B **670**, 285–291 (2009)
4310. F. Ambrosino et al., Measurement of $\sigma(e^+e^- \to \pi^+\pi^-)$ from threshold to 0.85 GeV^2 using Initial State Radiation with the KLOE detector. Phys. Lett. **700**, 102–110 (2011)
4311. D. Babusci et al., Precision measurement of $\sigma(e^+e^- \to \pi^+\pi^-\gamma)/\sigma(e^+e^- \to \mu^+\mu^-\gamma)$ and determination of the $\pi^+\pi^-$ contribution to the muon anomaly with the KLOE detector. Phys. Lett. **720**, 336–343 (2013)
4312. T. Blum, Lattice calculation of the lowest order hadronic contribution to the muon anomalous magnetic moment. Phys. Rev. Lett. **91**, 052001 (2003)
4313. D. Bernecker, H.B. Meyer, Vector correlators in lattice QCD: methods and applications. Eur. Phys. J. A **47**, 148 (2011)
4314. M. DellaMorte et al., The hadronic vacuum polarization contribution to the muon $g-2$ from lattice QCD. JHEP **10**, 020 (2017)
4315. B. Chakraborty et al., Strong-isospin-breaking correction to the muon anomalous magnetic moment from lattice QCD at the physical point. Phys. Rev. Lett. **120**(15), 152001 (2018)
4316. S. Borsanyi et al., Hadronic vacuum polarization contribution to the anomalous magnetic moments of leptons from first principles. Phys. Rev. Lett. **121**, 022002 (2018)
4317. T. Blum et al., Calculation of the hadronic vacuum polarization contribution to the muon anomalous magnetic moment. Phys. Rev. Lett. **121**, 022003 (2018)
4318. D. Giusti et al., Electromagnetic and strong isospin-breaking corrections to the muon $g-2$ from Lattice QCD+QED. Phys. Rev. D **99**(11), 114502 (2019)
4319. E. Shintani, Y. Kuramashi, Hadronic vacuum polarization contribution to the muon $g-2$ with 2+1 flavor lattice QCD on a larger than (10 fm)^4 lattice at the physical point. Phys. Rev. D **100**(3), 034517 (2019)
4320. C.T.H. Davies et al., Hadronic-vacuum-polarization contribution to the muon's anomalous magnetic moment from four-flavor lattice QCD. Phys. Rev. D **101**(3), 034512 (2020)

4321. A. Gérardin et al., The leading hadronic contribution to $(g-2)_\mu$ from lattice QCD with $N_\mathrm{f} = 2+1$ flavours of O(a) improved Wilson quarks. Phys. Rev. D **100**(1), 014510 (2019)
4322. C. Aubin et al., Light quark vacuum polarization at the physical point and contribution to the muon $g-2$. Phys. Rev. D **101**(1), 014503 (2020)
4323. D. Giusti, S. Simula, Lepton anomalous magnetic moments in Lattice QCD+QED. PoS LATTICE **2019**, 104 (2019)
4324. M. Cè et al., Window observable for the hadronic vacuum polarization contribution to the muon $g-2$ from lattice QCD. Phys. Rev. D **106**, 114502 (2022)
4325. C. Lehner, The hadronic vacuum polarization (RBC/UKQCD). Talk at the Fifth Plenary Workshop of the Muon g−2 Theory Initiative, Edinburgh (2022). https://indico.ph.ed.ac.uk/event/112/contributions/1660/
4326. C. Alexandrou et al., Ratio of kaon and pion leptonic decay constants with $N_f = 2+1+1$ Wilson-clover twisted-mass fermions. Phys. Rev. D **104**(7), 074520 (2021)
4327. G. Colangelo et al., Data-driven evaluations of Euclidean windows to scrutinize hadronic vacuum polarization. Phys. Lett. B **833**, 137313 (2022)
4328. G. Wang et al., Muon g-2 with overlap valence fermions. Phys. Rev. D **107**(3), 034513 (2023)
4329. C. Aubin et al., Muon anomalous magnetic moment with staggered fermions: is the lattice spacing small enough? Phys. Rev. D **106**(5), 054503 (2022)
4330. C.T.H. Davies et al., Windows on the hadronic vacuum polarization contribution to the muon anomalous magnetic moment. Phys. Rev. D **106**(7), 074509 (2022)
4331. M. Bruno et al., On isospin breaking in τ decays for $(g-2)_\mu$ from Lattice QCD. PoS LATTICE **2018**, 135 (2018)
4332. M. Hayakawa, T. Kinoshita, A.I. Sanda, Hadronic light by light scattering contribution to muon g-2. Phys. Rev. D **54**, 3137–3153 (1996)
4333. M. Hayakawa, T. Kinoshita, Comment on the sign of the pseudoscalar pole contribution to the muon g-2 (2001). arXiv:hep-ph/0112102
4334. J. Bijnens, E. Pallante, J. Prades, Analysis of the hadronic light by light contributions to the muon g-2. Nucl. Phys. B **474**, 379–420 (1996)
4335. J. Bijnens, E. Pallante, J. Prades, Comment on the pion pole part of the light by light contribution to the muon g-2. Nucl. Phys. B **626**, 410–411 (2002)
4336. J. Prades, E. de Rafael, A. Vainshtein, The hadronic light-by-light scattering contribution to the muon and electron anomalous magnetic moments. Adv. Ser. Dir. High Energy Phys. **20**, 303–317 (2009)
4337. F. Jegerlehner, The role of mesons in muon g-2. EPJ Web Conf. **199**, 01010 (2019)
4338. G. Colangelo et al., Dispersion relation for hadronic light-by-light scattering: theoretical foundations. JHEP **09**, 074 (2015)
4339. G. Colangelo et al., Dispersive approach to hadronic light-by-light scattering. JHEP **09**, 091 (2014)
4340. V. Pauk, M. Vanderhaeghen, Anomalous magnetic moment of the muon in a dispersive approach. Phys. Rev. D **90**(11), 113012 (2014)
4341. A. Nyffeler, Precision of a data-driven estimate of hadronic light-by- light scattering in the muon $g-2$: pseudoscalar-pole contribution. Phys. Rev. D **94**(5), 053006 (2016)
4342. I. Danilkin, C. Florian Redmer, M. Vanderhaeghen, The hadronic light-by-light contribution to the muon's anomalous magnetic moment. Prog. Part. Nucl. Phys. **107**, 20–68 (2019)
4343. J. Gronberg et al., Measurements of the meson-photon transition form-factors of light pseudoscalar mesons at large momentum transfer. Phys. Rev. D **57**, 33–54 (1998)
4344. H.J. Behrend et al., A measurement of the π^0, η and η' electromagnetic form-factors. Z. Phys. C **49**, 401–410 (1991)
4345. A. Gérardin, H.B. Meyer, A. Nyffeler, Lattice calculation of the pion transition form factor with $N_f = 2+1$ Wilson quarks. Phys. Rev. D **100**(3), 034520 (2019)
4346. P. Masjuan, P. Sanchez-Puertas, Pseudoscalar-pole contribution to the $(g_\mu - 2)$: a rational approach. Phys. Rev. D **95**(5), 054026 (2017)
4347. M. Hoferichter et al., Dispersion relation for hadronic light-by-light scattering: pion pole. JHEP **10**, 141 (2018)
4348. M. Hoferichter et al., Pion-pole contribution to hadronic light-by-light scattering in the anomalous magnetic moment of the muon. Phys. Rev. Lett. **121**(11), 112002 (2018)
4349. K. Melnikov, A. Vainshtein, Hadronic light-by-light scattering contribution to the muon anomalous magnetic moment revisited. Phys. Rev. D **70**, 113006 (2004)
4350. G. Colangelo et al., Dispersion relation for hadronic light-by-light scattering: two-pion contributions. JHEP **04**, 161 (2017)
4351. J. Bijnens, N. Hermansson-Truedsson, A. Rodríguez-Sánchez, Short-distance constraints for the HLbL contribution to the muon anomalous magnetic moment. Phys. Lett. B **798**, 134994 (2019)
4352. G. Colangelo et al., Longitudinal short-distance constraints for the hadronic light-by-light contribution to $(g-2)_\mu$ with large-N_c Regge models. JHEP **03**, 101 (2020)
4353. V. Pauk, M. Vanderhaeghen, Single meson contributions to the muon's anomalous magnetic moment. Eur. Phys. J. C **74**(8), 3008 (2014)
4354. I. Danilkin, M. Vanderhaeghen, Light-by-light scattering sum rules in light of new data. Phys. Rev. D **95**(1), 014019 (2017)
4355. M. Knecht et al., Scalar meson contributions to a μ from hadronic light-by-light scattering. Phys. Lett. B **787**, 111–123 (2018)
4356. G. Eichmann, C.S. Fischer, R. Williams, Kaon-box contribution to the anomalous magnetic moment of the muon. Phys. Rev. D **101**(5), 054015 (2020)
4357. P. Roig, P. Sanchez-Puertas, Axial-vector exchange contribution to the hadronic light-by-light piece of the muon anomalous magnetic moment. Phys. Rev. D **101**(7), 074019 (2020)
4358. M. Hayakawa et al., Hadronic light-by-light scattering contribution to the muon $g-2$ from lattice QCD: methodology. PoS LAT2005, 353 (2006)
4359. T. Blum, M. Hayakawa, T. Izubuchi, Hadronic corrections to the muon anomalous magnetic moment from lattice QCD. PoS LATTICE **2012**, 022 (2012) **(Ed. by Derek Leinweber et al.)**
4360. T. Blum et al., Hadronic light-by-light scattering contribution to the muon anomalous magnetic moment from lattice QCD. Phys. Rev. Lett. **114**(1), 012001 (2015)
4361. T. Blum et al., Lattice calculation of hadronic light-by-light contribution to the muon anomalous magnetic moment. Phys. Rev. D **93**(1), 014503 (2016)
4362. T. Blum et al., Connected and leading disconnected hadronic light-by-light contribution to the muon anomalous magnetic moment with a physical pion mass. Phys. Rev. Lett. **118**(2), 022005 (2017)
4363. T. Blum et al., The hadronic light-by-light scattering contribution to the muon anomalous magnetic moment from lattice QCD. Phys. Rev. Lett. **124**(13), 132002 (2020)
4364. J. Green et al., Direct calculation of hadronic light-by-light scattering. PoS LATTICE **2015**, 109 (2016)
4365. N. Asmussen et al., Position-space approach to hadronic light-by-light scattering in the muon $g-2$ on the lattice. PoS LATTICE **2016**, 164 (2016)
4366. N. Asmussen et al., Exploratory studies for the position-space approach to hadronic light-by-light scattering in the muon $g-2$. EPJ Web Conf. **175**, 06023 (2018)

4367. T. Blum et al., Using infinite volume, continuum QED and lattice QCD for the hadronic light-by-light contribution to the muon anomalous magnetic moment. Phys. Rev. D **96**(3), 034515 (2017)
4368. E.-H. Chao et al., Hadronic light-by-light contribution to $(g-2)_\mu$ from lattice QCD with SU(3) flavor symmetry. Eur. Phys. J. C **80**(9), 869 (2020)
4369. E.-H. Chao et al., Hadronic light-by-light contribution to $(g-2)_\mu$ from lattice QCD: a complete calculation. Eur. Phys. J. C **81**(7), 651 (2021)
4370. E.-H. Chao et al., The charm-quark contribution to light-by-light scattering in the muon $(g-2)$ from lattice QCD. Eur. Phys. J. C **82**(8), 664 (2022)
4371. A. Nyffeler, Hadronic light-by-light scattering in the muon g-2: A New short-distance constraint on pion-exchange. Phys. Rev. D **79**, 073012 (2009)
4372. F.V. Ignatov et al., Measurement of the $e^+e^- \to \pi^+\pi^-$ cross section from threshold to 1.2 GeV with the CMD-3 detector (2023). arXiv:2302.08834
4373. S. Actis et al., Quest for precision in hadronic cross sections at low energy: Monte Carlo tools vs. experimental data. Eur. Phys. J. C **66**, 585–686 (2010)
4374. S. Binner, J.H. Kuhn, K. Melnikov, Measuring $\sigma(e^+e^- \to$ hadrons) using tagged photon. Phys. Lett. B **459**, 279–287 (1999)
4375. G. Rodrigo et al., Radiative return at NLO and the measurement of the hadronic cross-section in electron positron annihilation. Eur. Phys. J. C **24**, 71–82 (2002)
4376. J.H. Kuhn, G. Rodrigo, The Radiative return at small angles: virtual corrections. Eur. Phys. J. C **25**, 215–222 (2002)
4377. H. Czyz et al., The radiative return at phi and B factories: small angle photon emission at next-to-leading order. Eur. Phys. J. C **27**, 563–575 (2003)
4378. H. Czyz et al., The radiative return at Phi and B factories: FSR at next-to-leading order. Eur. Phys. J. C **33**, 333–347 (2004)
4379. H. Czyz et al., Nucleon form-factors, B meson factories and the radiative return. Eur. Phys. J. C **35**, 527–536 (2004)
4380. H. Czyz et al., The radiative return at phi and B factories: FSR for muon pair production at next-to-leading order. Eur. Phys. J. C **39**, 411–420 (2005)
4381. H. Czyz, A. Grzelinska, J.H. Kuhn, Charge asymmetry and radiative phi decays. Phys. Lett. B **611**, 116–122 (2005)
4382. H. Czyz et al., Electron-positron annihilation into three pions and the radiative return. Eur. Phys. J. C **47**, 617–624 (2006)
4383. H. Czyz, A. Grzelinska, J.H. Kuhn, Spin asymmetries and correlations in lambda-pair production through the radiative return method. Phys. Rev. D **75**, 074026 (2007)
4384. H. Czyz, J.H. Kuhn, Strong and electromagnetic J/ψ and $\psi(2S)$ decays into pion and kaon pairs. Phys. Rev. D **80**, 034035 (2009)
4385. H. Czyz, A. Grzelinska, J.H. Kuhn, Narrow resonances studies with the radiative return method. Phys. Rev. D **81**, 094014 (2010)
4386. H. Czyz, J.H. Kuhn, A. Wapienik, Four-pion production in τ decays and e^+e^- annihilation: an update. Phys. Rev. D **77**, 114005 (2008)
4387. H. Czyz, M. Gunia, J.H. Kühn, Simulation of electron-positron annihilation into hadrons with the event generator PHOKHARA. JHEP **08**, 110 (2013)
4388. F. Campanario et al., Complete QED NLO contributions to the reaction $e^+e^- \to \mu^+\mu^-\gamma$ and their implementation in the event generator PHOKHARA. JHEP **02**, 114 (2014)
4389. H. Czyz, J.H. Kühn, S. Tracz, Nucleon form factors and final state radiative corrections to $e^+e^- \to p\bar{p}$?. Phys. Rev. D **90**(11), 114021 (2014)
4390. H. Czyz, P. Kisza, S. Tracz, Modeling interactions of photons with pseudoscalar and vector mesons. Phys. Rev. D **97**(1), 016006 (2018)
4391. F. Campanario et al., Standard model radiative corrections in the pion form factor measurements do not explain the a_μ anomaly. Phys. Rev. D **100**(7), 076004 (2019)
4392. G. Balossini et al., Matching perturbative and parton shower corrections to Bhabha process at flavour factories. Nucl. Phys. B **758**, 227–253 (2006)
4393. H. Czyz, P. Kisza, EKHARA 3.0: an update of the EKHARA Monte Carlo event generator. Comput. Phys. Commun. **234**, 245–255 (2019)
4394. A.B. Arbuzov et al., Monte-Carlo generator for e^+e^- annihilation into lepton and hadron pairs with precise radiative corrections. Eur. Phys. J. C **46**, 689–703 (2006)
4395. V.P. Druzhinin, L.V. Kardapoltsev, V.A. Tayursky, GGRESRC: a Monte Carlo generator for the two-photon process $e^+e^- \to e^+e^- R(J^{PC} = 0^{-+})$ in the single-tag mode. Comput. Phys. Commun. **185**, 236–243 (2014)
4396. E. Barberio, Z. Was, PHOTOS: a universal Monte Carlo for QED radiative corrections. Version 2.0. Comput. Phys. Commun. **79**, 291–308 (1994)
4397. S. Jadach, B.F.L. Ward, Z. Was, The precision Monte Carlo event generator K K for two fermion final states in e^+e^- collisions. Comput. Phys. Commun. **130**, 260–325 (2000)
4398. C.M. Carloni Calame et al., A new approach to evaluate the leading hadronic corrections to the muon g-2. Phys. Lett. B **746**, 325–329 (2015)
4399. G. Abbiendi et al., Measuring the leading hadronic contribution to the muon g-2 via μe scattering. Eur. Phys. J. C **77**(3), 139 (2017)
4400. F. Jegerlehner, $\alpha_{QED,eff}(s)$ for precision physics at the FCC-ee/ILC. CERN Yellow Rep. Monogr. **3**, 9–37 (2020) **(Ed. by A. Blondel et al.)**
4401. V.D. Burkert et al., The CLAS12 spectrometer at Jefferson Laboratory. Nucl. Instrum. Meth. A **959**, 163419 (2020)
4402. J. Arrington et al., Physics with CEBAF at 12 GeV and future opportunities. Prog. Part. Nucl. Phys. **127**, 103985 (2022)
4403. I.A. Qattan, Precision Rosenbluth Measurement of the Proton Elastic Electromagnetic Form Factors and Their Ratio at Q^2 = 2.64-GeV^2, 3.20-GeV^2 and 4.10-GeV^2. Ph.D. Thesis, Northwestern University (2005)
4404. E. Cisbani et al., Large acceptance proton form factor ratio measurements at 13 and 15 $(\mathrm{GeV}/c)^2$ using recoil polarization method. Jefferson Lab Experiment E12-07-109 (2007)
4405. T. Averett et al., Measurement of the neutron electromagnetic form factor ratio G^n_E/G^n_M at high Q^2. Jefferson Lab Experiment E12-09-016 (2009)
4406. D. Hamilton, B. Quinn, B. Wojtsekhowski, Precision measurement of the neutron magnetic form factor up to $Q^2 = 18.0$ (GeV/c)^2 by the ratio method. Jefferson Lab Experiment E12-09-019. (2009)
4407. B.D. Anderson et al., The neutron electric form factor at Q^2 up to 7 (GeV/c)^2 from the reaction $d(e, e'n)p$ via recoil polarimetry. Jefferson Lab Experiment E12-11-009 (2011)
4408. V. Bellini et al., Measurement of the ratio G^n_E/G^n_M by the double-polarized $^2H(\vec{e}, e'\vec{n})$ reaction. Jefferson Lab Experiment E12-17-004 (2017)
4409. S. Alsalmi, E. Fuchey, B. Wojtsekhowski, Measurement of the argon and titanium spectral functions through the Ar - Ti $(e, e'p)$ reactions. Jefferson Lab Experiment E12-20-012 (2020)
4410. G. Gilfoyle et al., Measurement of the neutron magnetic form factor at high Q^2 using the ratio method on deuterium. Jefferson Lab Experiment E12-07-104 (2007)
4411. S. Kuhn et al., The longitudinal spin structure of the nucleon. Jefferson Lab Experiment E12-06-109 (2006)
4412. A. Gasparian et al., PRad-II: a new upgraded high precision measurement of the proton charge radius (2020). arXiv:2009.10510

4413. D. Abrams et al., Measurement of the nucleon F_2^n/F_2^p structure function ratio by the Jefferson Lab MARATHON tritium/helium-3 deep inelastic scattering experiment. Phys. Rev. Lett. **128**(13), 132003 (2022)
4414. S. Bultmann et al., The structure of the free neutron at large x-Bjorken. Jefferson Lab Experiment E12-06-113 (BoNUS) (2006)
4415. I.M. Niculescu, S.P. Malace, C. Keppel, Precision measurements of the F_2 structure function at large x in the resonance region and beyond. Jefferson Lab Experiment E12-10-002 (2010)
4416. A. Bodek et al., Experimental studies of the neutron and proton electromagnetic structure functions. Phys. Rev. D **20**, 1471–1552 (1979)
4417. P. Souder et al., Precision measurement of parity-violation in deep inelastic scattering over a broad kinematic range. Jefferson Lab Experiment E12-10-007 (2010)
4418. J. Anlett et al., SoLID Updated Preliminary Conceptual Design Report. BNL-77977-2006-V1-V2 Formal Report (2019)
4419. A. Deur, Nucleon spin structure measurements at Jefferson Lab. In: *13th Conference on the Intersections of Particle and Nuclear Physics* (2018). arXiv:1810.08073
4420. X. Zheng et al., Measurement of neutron spin asymmetry A_1^n in the valence quark region using an 11 GeV beam and a polarized ^{3}He target in Hall C. Jefferson Lab Experiment E12-06-110 (2006)
4421. J.H. Chen, JLab polarized ^{3}He collaboration. Upgraded Polarized Helium-3 Target and Its Performance in Experiments at Jefferson Lab. APS meeting (2021)
4422. P. Rossi, M. Anselmino, M. Guidal, Topical issue on the 3-D structure of the nucleon. Eur. Phys. J. A **52**, 150 (2016)
4423. H. Avakian, B. Parsamyan, A. Prokudin, Spin orbit correlations and the structure of the nucleon. Riv. Nuovo Cim. **42**(1), 1–48 (2019)
4424. H. Avakian et al., Measurement of single and double spin asymmetries in deep inelastic pion electroproduction with a longitudinally polarized target. Phys. Rev. Lett. **105**, 262002 (2010)
4425. J. Huang et al., Beam-target double spin asymmetry A_{LT} in charged pion production from deep inelastic scattering on a transversely polarized ^{3}He target at $1.4<Q^2<2.7$ GeV^2. Phys. Rev. Lett. **108**, 052001 (2012)
4426. Y. Zhang et al., Measurement of pretzelosity asymmetry of charged pion production in semi-inclusive deep inelastic scattering on a polarized ^{3}He target. Phys. Rev. C **90**(5), 055209 (2014)
4427. H. Avakian et al., Measurement of beam-spin asymmetries for π^+ electroproduction above the baryon resonance region. Phys. Rev. D **69**, 112004 (2004)
4428. Y.X. Zhao et al., Double spin asymmetries of inclusive hadron electroproductions from a transversely polarized ^{3}He target. Phys. Rev. C **92**(1), 015207 (2015)
4429. G. Gates et al., Measurement of the semi-inclusive π and K electro-production in DIS regime from transversely polarized 3He target with the SBS and BB spectrometers in Hall A. Jefferson Lab Experiment E12-09-018 (2009)
4430. H. Gao et al., Target single spin asymmetry in semi-inclusive deep-inelastic $(e, e\pi^{\pm})$ reaction on a transversely polarized proton target. Jefferson Lab Experiment E12-11-108 (2011)
4431. H. Gao et al., Target single spin asymmetry in semi-inclusive deep-inelastic electro pion production on a trasversely polarized ^{3}He target at 8.8 and 11 GeV. Jefferson Lab Experiment E12-10-006 (2010)
4432. J.P. Chen et al., Asymmetries in semi-inclusive deep-inelastic $(e, e'\pi^{\pm})$ reactions on a longitudinally polarized ^{3}He target at 8.8 and 11 GeV. Jefferson Lab Experiment E12-11-007 (2011)
4433. H. Avakian et al., Probing the Proton's Quark Dynamics in Semi-Inclusive Pion Production at 11 GeV. Jefferson Lab Experiment E12-06-112. (2006)
4434. H. Avakian et al., Studies of spin-orbit correlations with longitudinally polarized target. Jefferson Lab Experiment E12-07-107 (2007)
4435. H. Avakian et al., Boer-Mulders asymmetry in K SIDIS w/H and D targets. Jefferson Lab Experiment E12-09-008 (2009)
4436. H. Avakian et al., Spin–orbit correlations in K production w/pol. targets. Jefferson Lab Experiment E12-09-009 (2009)
4437. H. Avakian et al., A program of spin-dependent electron scattering from a polarized ^3He target in CLAS12. Jefferson Lab Experiment C12-20-002 (2020)
4438. R. Ent, H. Mkrtchyan, Measurement of the ratio $R = \sigma_L/\sigma_T$ in semi-inclusive deep-inelastic scattering. Jefferson Lab Experiment E12-06-104 (2006)
4439. R. Ent, P. Bosted, H. Mkrtchyan, Transverse momentum dependence of semi-inclusive pion production. Jefferson Lab Experiment E12-09-017 (2009)
4440. R. Ent et al., Measurement of semi-inclusive π^0 production as validation of factorization. Jefferson Lab Experiment E12-13-007 (2014)
4441. S. Diehl et al., Multidimensional, high precision measurements of beam single spin asymmetries in semi-inclusive π^+ electroproduction off protons in the valence region. Phys. Rev. Lett. **128**(6), 062005 (2022)
4442. T.B. Hayward et al., Observation of beam spin asymmetries in the process $ep \rightarrow e'\pi^+\pi^-X$ with CLAS12. Phys. Rev. Lett. **126**, 152501 (2021)
4443. H. Avakian et al., Observation of correlations between spin and transverse momenta in back-to-back dihadron production at CLAS12. Phys. Rev. Lett. **130**(2), 022501 (2023)
4444. M. Mirazita et al., Beam spin asymmetry in semi-inclusive electroproduction of hadron pairs. Phys. Rev. Lett. **126**(6), 062002 (2021)
4445. M. Anselmino, V. Barone, A. Kotzinian, Double hadron leptoproduction in the current and target fragmentation regions. Phys. Lett. B **706**, 46–52 (2011)
4446. M.V. Polyakov, Generalized parton distributions and strong forces inside nucleons and nuclei. Phys. Lett. B **555**, 57–62 (2003)
4447. K. Kumericki, Measurability of pressure inside the proton. Nature **570**(7759), E1–E2 (2019)
4448. H. Dutrieux et al., Phenomenological assessment of proton mechanical properties from deeply virtual Compton scattering. Eur. Phys. J. C **81**(4), 300 (2021)
4449. S. Stepanyan et al., Observation of exclusive deeply virtual Compton scattering in polarized electron beam asymmetry measurements. Phys. Rev. Lett. **87**, 182002 (2001)
4450. N. d'Hose, S. Niccolai, A. Rostomyan, Experimental overview of deeply virtual compton scattering. Eur. Phys. J. A **52**(6), 151 (2016)
4451. C. Muñoz Camacho et al., Scaling tests of the cross-section for deeply virtual compton scattering. Phys. Rev. Lett. **97**, 262002 (2006)
4452. M. Defurne et al., E00–110 experiment at Jefferson Lab Hall A: deeply virtual Compton scattering off the proton at 6 GeV. Phys. Rev. C **92**(5), 055202 (2015)
4453. F. Georges et al., deeply virtual Compton scattering cross section at high Bjorken xB. Phys. Rev. Lett. **128**(25), 252002 (2022)
4454. C. Munoz Camacho et al., Exclusive deeply virtual Compton and neutral pion cross-section measurements in Hall C. Jefferson Lab Experiment PR12-13-010 (2013)
4455. L. Elouadrhiri et al., Deeply virtual Compton scattering with CLAS12 at 11 GeV. Jefferson Lab E12-06-119 (2006)
4456. L. Elouadrhiri, F.-X. Girod, Deeply virtual Compton scattering with CLAS12 at 6.6 GeV and 8.8 GeV. Jefferson Lab E12-16-010B (2016)

4457. L. Elouadrhiri et al., Deeply virtual Compton scattering at 11 GeV with transversely polarized target using the CLAS12 detector. Jefferson Lab Experiment E12-12-010 (2012)
4458. M. Dlamini et al., Deep exclusive electroproduction of π^0 at high Q^2 in the quark valence regime. Phys. Rev. Lett. **127**(15), 152301 (2021)
4459. P. Stoler et al., Hard exclusive electroproduction of π^0 and η with CLAS12. Jefferson Lab Experiment E12-06-108 (2006)
4460. P. Stoler et al., Exclusive phi meson electroproduction with CLAS12. Jefferson Lab Experiment E12-12-007 (2012)
4461. T. Horn, G.M. Huber, P. Markowitz, Studies of the L-T separated kaon electroproduction cross section from 5–11 GeV. Jefferson Lab Experiment E12-09-011 (2009)
4462. T. Horn et al., Scaling study of the L-T separated pion electroproduction cross section at 11 GeV. Jefferson Lab Experiment E12-07-105 (2007)
4463. Z. Meziani et al., Partonic structure of light nuclei. Jefferson Lab Experiment E12-17-012 (2017)
4464. M. Vanderhaeghen, P.A.M. Guichon, M. Guidal, Hard electroproduction of photons and mesons on the nucleon. Phys. Rev. Lett. **80**, 5064–5067 (1998)
4465. S.V. Goloskokov, P. Kroll, Vector meson electroproduction at small Bjorken-x and generalized parton distributions. Eur. Phys. J. C **42**, 281–301 (2005)
4466. A. Rodas et al., Determination of the pole position of the lightest hybrid meson candidate. Phys. Rev. Lett. **122**(4), 042002 (2019)
4467. C. Meyer et al., Mapping the spectrum of light quark mesons and gluonic excitations with linearly polarized photons. Jefferson Lab Experiment E12-06-102 (2006)
4468. S. Adhikari et al., The GLUEX beamline and detector. Nucl. Instrum. Meth. A **987**, 164807 (2021)
4469. M. Battaglieri et al., Meson spectroscopy with low Q^2 electron scattering in CLAS12 . Jefferson Lab Experiment E12-11-005 (2011)
4470. S. Adhikari et al., Measurement of beam asymmetry for $\pi^-\Delta^{++}$ photoproduction on the proton at E_γ=8.5 GeV. Phys. Rev. C **103**(2), L022201 (2021)
4471. S. Adhikari et al., Beam asymmetry Σ for the photoproduction of η and η' mesons at $E_\gamma = 8.8$ GeV. Phys. Rev. C **100**(5), 052201 (2019)
4472. H. Al Ghoul et al., Measurement of the beam asymmetry Σ for π^0 and η photoproduction on the proton at $E_\gamma = 9$ GeV. Phys. Rev. C **95**(4), 042201 (2017)
4473. S. Adhikari et al., Measurement of the photon beam asymmetry in $\vec{\gamma} p \to K^+\Sigma^0$ at $E_\gamma = 8.5$ GeV. Phys. Rev. C **101**(6), 065206 (2020)
4474. S. Adhikari et al., Measurement of spin density matrix elements in $\Lambda(1520)$ photoproduction at 8.2–8.8 GeV. Phys. Rev. C **105**(3), 035201 (2022)
4475. A. Austregesilo, Spin-density matrix elements for vector meson photoproduction at GlueX. AIP Conf. Proc. **2249**(1), 030005 (2020) **(Ed. by Curtis Meyer and Reinhard A. Schumacher)**
4476. S. Daniel, Carman, Excited nucleon spectrum and structure studies with CLAS and CLAS12. AIP Conf. Proc. **2249**(1), 030004 (2020) **(Ed. by Curtis Meyer and Reinhard A. Schumacher)**
4477. R.W. Gothe et al., Nucleon resonance studies with CLAS12. Jefferson Lab Experiment E12-09-003 (2009)
4478. D.S. Carman, R.W. Gothe, V.I. Mokeev, Exclusive $N^* \to KY$ studies with CLAS12. Jefferson Lab Experiment E12-06-108A (2006)
4479. M. Dugger et al., A study of decays to strange final states with GlueX in Hall D using components of the BaBar DIRC (2014). arXiv:1408.0215
4480. L. Guo et al., Photoproduction of the very strangest baryons on a proton target in CLAS12. Jefferson Lab Experiment E12-12-008 (2012)
4481. M. Amaryan et al., Strange hadron spectroscopy with secondary K_L beam in hall D (2020). arXiv:2008.08215 (2020)
4482. Q. Wang, X.-H. Liu, Q. Zhao, Photoproduction of hidden charm pentaquark states $P_c^+(4380)$ and $P_c^+(4450)$. Phys. Rev. D **92**, 034022 (2015)
4483. V. Kubarovsky, M.B. Voloshin, Formation of hidden-charm pentaquarks in photon-nucleon collisions. Phys. Rev. D **92**(3), 031502 (2015)
4484. M. Karliner, J.L. Rosner, Photoproduction of exotic baryon resonances. Phys. Lett. B **752**, 329–332 (2016)
4485. A.N. Hiller Blin et al., Studying the $P_c(4450)$ resonance in J/ψ photoproduction off protons. Phys. Rev. D **94**(3), 034002 (2016)
4486. A. Ali et al., First measurement of near-threshold J/ψ exclusive photoproduction off the proton. Phys. Rev. Lett. **123**(7), 072001 (2019)
4487. S. Joosten, Quarkonium production near threshold at JLab and EIC. In: *9th Workshop of the APS Topical Group on Hadronic Physics* (2021)
4488. Mattaglieri et al., Near threshold J/ψ photoproduction and study of LHCb pentaquarks with CLAS12. Jefferson Lab Experiment E12-12-001A (2017)
4489. Z.-E. Meziani et al., Near threshold electroproduction of J/ψ at 11 GeV. Jefferson Lab Experiment E12-12-006 (2012)
4490. O. Hen et al., Nucleon-nucleon correlations, short-lived excitations, and the quarks within. Rev. Mod. Phys. **89**(4), 045002 (2017)
4491. L. Frankfurt, M. Sargsian, M. Strikman, Recent observation of short range nucleon correlations in nuclei and their implications for the structure of nuclei and neutron stars. Int. J. Mod. Phys. A **23**, 2991–3055 (2008)
4492. L.L. Frankfurt et al., Evidence for short range correlations from high $Q^2(e, e')$ reactions. Phys. Rev. C **48**, 2451–2461 (1993)
4493. K.S. Egiyan et al., Observation of nuclear scaling in the $A(e, e')$ reaction at $x_B>1$. Phys. Rev. C **68**, 014313 (2003)
4494. K.S. Egiyan et al., Measurement of 2- and 3-nucleon short range correlation probabilities in nuclei. Phys. Rev. Lett. **96**, 082501 (2006)
4495. J. Arrington et al., x- and ξ-scaling of the nuclear structure function at large x. Phys. Rev. C **64**, 014602 (2001)
4496. J. Seely et al., New measurements of the EMC effect in very light nuclei. Phys. Rev. Lett. **103**, 202301 (2009)
4497. J. Arrington et al., Measurement of the EMC effect in light and heavy nuclei. Phys. Rev. C **104**(6), 065203 (2021)
4498. J. Gomez et al., Measurement of the A-dependence of deep inelastic electron scattering. Phys. Rev. D **49**, 4348–4372 (1994)
4499. I. Korover et al., Probing the repulsive core of the nucleon-nucleon interaction via the ^{4}He(e, e′pN) triple-coincidence reaction. Phys. Rev. Lett. **113**(2), 022501 (2014)
4500. M. Duer et al., Direct observation of proton-neutron short-range correlation dominance in heavy nuclei. Phys. Rev. Lett. **122**(17), 172502 (2019)
4501. M. Duer et al., Probing high-momentum protons and neutrons in neutron-rich nuclei. Nature **560**(7720), 617–621 (2018)
4502. D. Nguyen et al., Novel observation of isospin structure of short-range correlations in calcium isotopes. Phys. Rev. C **102**(6), 064004 (2020)
4503. S. Li et al., Revealing the short-range structure of the mirror nuclei ^{3}H and ^{3}He. Nature **609**(7925), 41–45 (2022)
4504. Z. Ye et al., Search for three-nucleon short-range correlations in light nuclei. Phys. Rev. C **97**(6), 065204 (2018)
4505. J. Arrington et al., Inclusive scattering from nuclei at $x>1$ in the quasielastic and deeply inelastic regimes. Jefferson Lab Experiment E12-06-105 (2006)
4506. I.C. Cloët, W. Bentz, A. William Thomas, EMC and polarized EMC effects in nuclei. Phys. Lett. B **642**, 210–217 (2006)

4507. S. Tronchin, H.H. Matevosyan, A.W. Thomas, Polarized EMC effect in the QMC model. Phys. Lett. B **783**, 247–252 (2018)
4508. W. Brooks, S. Kuhn, The EMC effect in spin structure functions. Jefferson Lab Experiment E12-14-001 (2012)
4509. R. Dupre et al., PR12-16-011: nuclear exclusive and semi-inclusive measurements with a new CLAS12 low energy recoil tracker (2016)
4510. S. Moran et al., Measurement of charged-pion production in deep-inelastic scattering off nuclei with the CLAS detector. Phys. Rev. C **105**(1), 015201 (2022)
4511. X. Qian et al., Experimental study of the $A(e, e'\pi^+)$ Reaction on ^{1}H, ^{2}H, ^{12}C, ^{27}Al, ^{63}Cu and ^{197}Au. Phys. Rev. C **81**, 055209 (2010)
4512. L. El Fassi et al., Evidence for the onset of color transparency in ρ^0 electroproduction off nuclei. Phys. Lett. B **712**, 326–330 (2012)
4513. L. Gu et al., Measurement of the Ar(e, e′p) and Ti(e, e′p) cross sections in Jefferson Lab Hall A. Phys. Rev. C **103**(3), 034604 (2021)
4514. M. Khachatryan et al., Electron-beam energy reconstruction for neutrino oscillation measurements. Nature **599**, 565–570 (2021)
4515. O. Hen et al., Electrons for neutrinos: addressing critical neutrino-nucleus issues. Jefferson Lab Experiment E12-17-006 (2017)
4516. D. Adhikari et al., Accurate determination of the neutron skin thickness of ^{208}Pb through parity-violation in electron scattering. Phys. Rev. Lett. **126**(17), 172502 (2021)
4517. D. Adhikari et al., Precision determination of the neutral weak form factor of Ca48. Phys. Rev. Lett. **129**(4), 042501 (2022)
4518. G. Hagen et al., Neutron and weak-charge distributions of the ^{48}Ca nucleus. Nature Phys. **12**(2), 186–190 (2015)
4519. N. Alemanos et al., Topical issue on an experimental program with positron beams at Jefferson Lab. Eur. Phys. J. A **58** (2022)
4520. F. Willeke, J. Beebe-Wang, Electron ion collider conceptual design. Report. https://doi.org/10.2172/1765663 (2021)
4521. A. Aprahamian et al., Reaching for the horizon: the 2015 long range plan for nuclear science. DOE/NSF Nuclear Science Advisory Panel Report (2015)
4522. National Academies of Sciences, Engineering, and Medicine. *An Assessment of U.S.-Based Electron-Ion Collider Science* (The National Academies Press, Washington, DC, 2018). https://doi.org/10.17226/25171
4523. F. Hekhorn, M. Stratmann, Next-to-leading order QCD corrections to inclusive heavy-flavor production in polarized deep-inelastic scattering. Phys. Rev. D **98**(1), 014018 (2018)
4524. K. Kumericki, S. Liuti, H. Moutarde, GPD phenomenology and DVCS fitting: entering the high-precision era. Eur. Phys. J. A **52**(6), 157 (2016)
4525. C. Lorcé, H. Moutarde, A.P. Trawinski, Revisiting the mechanical properties of the nucleon. Eur. Phys. J. C **79**(1), 89 (2019)
4526. C. Lorcé, On the hadron mass decomposition. Eur. Phys. J. C **78**(2), 120 (2018)
4527. Y. Hatta, A. Rajan, K. Tanaka, Quark and gluon contributions to the QCD trace anomaly. JHEP **12**, 008 (2018)
4528. A. Metz, B. Pasquini, S. Rodini, Revisiting the proton mass decomposition. Phys. Rev. D **102**(11), 114042 (2021)
4529. D. Kharzeev, Quarkonium interactions in QCD. Proc. Int. Sch. Phys. Fermi **130**, 105–131 (1996) **(Ed. by A. Di Giacomo and Dmitri Diakonov)**
4530. Y. Hatta, D.-L. Yang, Holographic J/ψ production near threshold and the proton mass problem. Phys. Rev. D **98**(7), 074003 (2018)
4531. R. Boussarie, Y. Hatta, QCD analysis of near-threshold quarkonium leptoproduction at large photon virtualities. Phys. Rev. D **101**(11), 114004 (2020)
4532. D. Kharzeev et al., J/ψ photoproduction and the gluon structure of the nucleon. Eur. Phys. J. C **9**, 459–462 (1999)
4533. O. Gryniuk, M. Vanderhaeghen, Accessing the real part of the forward J/ψ-p scattering amplitude from J/ψ photoproduction on protons around threshold. Phys. Rev. D **94**(7), 074001 (2016)
4534. D. Meng-Lin et al., Deciphering the mechanism of near-threshold J/ψ photoproduction. Eur. Phys. J. C **80**(11), 1053 (2020)
4535. K.A. Mamo, I. Zahed, Diffractive photoproduction of J/ψ and Υ using holographic QCD: gravitational form factors and GPD of gluons in the proton. Phys. Rev. D **101**(8), 086003 (2020)
4536. O. Gryniuk et al., Υ photoproduction on the proton at the electron-ion collider. Phys. Rev. D **102**(1), 014016 (2020)
4537. S. Joosten, Z.E. Meziani, Heavy quarkonium production at threshold: from JLab to EIC. PoS QCDEV2017, 017 (2018)
4538. J. Arrington et al., Revealing the structure of light pseudoscalar mesons at the electron-ion collider. J. Phys. G **48**(7), 075106 (2021)
4539. E.-C. Aschenauer et al., Deeply virtual compton scattering at a proposed high-luminosity electron-ion collider. JHEP **09**, 093 (2013)
4540. E.R. Berger et al., Generalized parton distributions in the deuteron. Phys. Rev. Lett. **87**, 142302 (2001)
4541. V. Guzey, M. Strikman, DVCS on spinless nuclear targets in impulse approximation. Phys. Rev. C **68**, 015204 (2003)
4542. A. Kirchner, D. Mueller, Deeply virtual Compton scattering off nuclei. Eur. Phys. J. C **32**, 347–375 (2003)
4543. S. Liuti, S.K. Taneja, Microscopic description of deeply virtual Compton scattering off spin-0 nuclei. Phys. Rev. C **72**, 032201 (2005)
4544. M. Rinaldi, S. Scopetta, Neutron orbital structure from generalized parton distributions of 3He. Phys. Rev. C **85**, 062201 (2012)
4545. S. Fucini, M. Rinaldi, S. Scopetta, Generalized parton distributions of light nuclei. Few Body Syst. **62**(1), 3 (2021)
4546. S. Fucini, S. Scopetta, M. Viviani, Coherent deeply virtual Compton scattering off ^{4}He. Phys. Rev. C **98**(1), 015203 (2018)
4547. V. Guzey et al., Coherent J/ψ electroproduction on He4 and He3 at the electron-ion collider: probing nuclear shadowing one nucleon at a time. Phys. Rev. Lett. **129**(24), 242503 (2022)
4548. B. Gamage et al., Design concept for the second interaction region for electron-ion collider. JACoW IPAC2021, TUPAB040 (2021)
4549. K.J. Eskola et al., EPPS16: nuclear parton distributions with LHC data. Eur. Phys. J. C **77**(3), 163 (2017)
4550. D. de Florian et al., Global analysis of nuclear parton distributions. Phys. Rev. D **85**, 074028 (2012)
4551. K. Kovarik et al., nCTEQ15–global analysis of nuclear parton distributions with uncertainties in the CTEQ framework. Phys. Rev. D **93**(8), 085037 (2016)
4552. S. Hamzeh Khanpour, A. Tehrani, Global analysis of nuclear parton distribution functions and their uncertainties at next-to-nextto-leading order. Phys. Rev. D **93**(1), 014026 (2016)
4553. E.C. Aschenauer et al., Nuclear structure functions at a future electron-ion collider. Phys. Rev. D **96**(11), 114005 (2017)
4554. T. Toll, T. Ullrich, Exclusive diffractive processes in electron-ion collisions. Phys. Rev. C **87**(2), 024913 (2013)
4555. W. Chang et al., Investigation of the background in coherent J/ψ production at the EIC. Phys. Rev. D **104**(11), 114030 (2021)
4556. L. Frankfurt, V. Guzey, M. Strikman, Leading twist nuclear shadowing phenomena in hard processes with nuclei. Phys. Rep. **512**, 255–393 (2012)
4557. I. Balitsky, Operator expansion for high-energy scattering. Nucl. Phys. B **463**, 99–160 (1996)
4558. Y.V. Kovchegov, Small x F(2) structure function of a nucleus including multiple pomeron exchanges. Phys. Rev. D **60**, 034008 (1999)
4559. J. Jalilian-Marian et al., The BFKL equation from the Wilson renormalization group. Nucl. Phys. B **504**, 415–431 (1997)

4560. J. Jalilian-Marian, A. Kovner, H. Weigert, The Wilson renormalization group for low x physics: gluon evolution at finite parton density. Phys. Rev. D **59**, 014015 (1998)
4561. E. Iancu, A. Leonidov, L.D. McLerran, Nonlinear gluon evolution in the color glass condensate. 1. Nucl. Phys. A **692**, 583–645 (2001)
4562. E. Ferreiro et al., Nonlinear gluon evolution in the color glass condensate. 2. Nucl. Phys. A **703**, 489–538 (2002)
4563. J. Jalilian-Marian, Y.V. Kovchegov, Saturation physics and deuteron-Gold collisions at RHIC. Prog. Part. Nucl. Phys. **56**, 104–231 (2006)
4564. F. Gelis et al., The color glass condensate. Annu. Rev. Nucl. Part. Sci. **60**, 463–489 (2010)
4565. J.L. Albacete, C. Marquet, Gluon saturation and initial conditions for relativistic heavy ion collisions. Prog. Part. Nucl. Phys. **76**, 1–42 (2014)
4566. D. Kharzeev, E. Levin, L. McLerran, Jet azimuthal correlations and parton saturation in the color glass condensate. Nucl. Phys. A **748**, 627–640 (2005)
4567. L. Zheng et al., Probing gluon saturation through dihadron correlations at an electron-ion collider. Phys. Rev. D **89**(7), 074037 (2014)
4568. N. Armesto et al., Inclusive diffraction in future electron-proton and electron-ion colliders. Phys. Rev. D **100**(7), 074022 (2019)
4569. A. Jentsch, T. Zhoudunming, C. Weiss, Deep-inelastic electron-deuteron scattering with spectator nucleon tagging at the future electron ion collider: extracting free nucleon structure. Phys. Rev. C **104**(6), 065205 (2021)
4570. L.L. Frankfurt, M.I. Strikman, High-energy phenomena, short range nuclear structure and QCD. Phys. Rep. **76**, 215–347 (1981)
4571. M. Sargsian, M. Strikman, Model independent method for determination of the DIS structure of free neutron. Phys. Lett. B **639**, 223–231 (2006)
4572. W. Cosyn, C. Weiss, Polarized electron-deuteron deep-inelastic scattering with spectator nucleon tagging. Phys. Rev. C **102**, 065204 (2020)
4573. W. Melnitchouk, M. Sargsian, M.I. Strikman, Probing the origin of the EMC effect via tagged structure functions of the deuteron. Z. Phys. A **359**, 99–109 (1997)
4574. T. Zhoudunming et al., Probing short-range correlations in the deuteron via incoherent diffractive J/ψ production with spectator tagging at the EIC. Phys. Lett. B **811**, 135877 (2020)
4575. A. Metz, A. Vossen, Parton fragmentation functions. Prog. Part. Nucl. Phys. **91**, 136–202 (2016)
4576. V. Bertone et al., A determination of the fragmentation functions of pions, kaons, and protons with faithful uncertainties. Eur. Phys. J. C **77**(8), 516 (2017)
4577. R.J. Hernández-Pinto et al., Global extraction of the parton-to-pion fragmentation functions at NLO accuracy in QCD. J. Phys. Conf. Ser. **761**(1), 012037 (2016) **(Ed. by Eduard de la Cruz Burelo, Arturo Fernandez Tellez, and Pablo Roig)**
4578. R.J. Hernández-Pinto et al., Global extraction of the parton-to-kaon fragmentation functions at NLO in QCD. J. Phys. Conf. Ser. **912**(1), 012043 (2017) **(Ed. by I. Bautista et al.)**
4579. Z.-B. Kang et al., Transverse lambda production at the future electron-ion collider. Phys. Rev. D **105**(9), 094033 (2022)
4580. A. Bacchetta, M. Radici, Partial wave analysis of two hadron fragmentation functions. Phys. Rev. D **67**, 094002 (2003)
4581. S. Gliske, A. Bacchetta, Ma. Radici, Production of two hadrons in semi-inclusive deep inelastic scattering. Phys. Rev. D **90**(11), 114027 (2014) [Erratum: Phys. Rev. D 91, 019902 (2015)]
4582. H.H. Matevosyan, A. Kotzinian, A.W. Thomas, Accessing quark helicity through dihadron studies. Phys. Rev. Lett. **120**(25), 252001 (2018)
4583. E.-C. Aschenauer et al., Jet angularities in photoproduction at the electron-ion collider. Phys. Rev. D **101**(5), 054028 (2020)
4584. M. Dasgupta et al., Small-radius jets to all orders in QCD. JHEP **04**, 039 (2015)
4585. D.J. Scott, W.J. Waalewijn, The leading jet transverse momentum in inclusive jet production and with a loose jet veto. JHEP **03**, 159 (2020)
4586. D. Neill, F. Ringer, N. Sato, Calculating the energy loss of leading jets (2020)
4587. P. Schweitzer, M. Strikman, C. Weiss, Intrinsic transverse momentum and parton correlations from dynamical chiral symmetry breaking. JHEP **01**, 163 (2013)
4588. L. Trentadue, G. Veneziano, Fracture functions: an improved description of inclusive hard processes in QCD. Phys. Lett. B **323**, 201–211 (1994)
4589. F. Alberto Ceccopieri, D. Mancusi, QCD analysis of lambda hyperon production in DIS target-fragmentation region. Eur. Phys. J. C **73**, 2435 (2013)
4590. H. Tao Li, Z. Long Liu, I. Vitev, Heavy meson tomography of cold nuclear matter at the electron-ion collider. Phys. Lett. B **816**, 136261 (2021)
4591. X. Li, Heavy flavor and jet studies for the future electron-ion collider. PoS HardProbes **2020**, 175 (2021)
4592. S.R. Klein, Y.-P. Xie, Photoproduction of charged final states in ultraperipheral collisions and electroproduction at an electron-ion collider. Phys. Rev. C **100**(2), 024620 (2019)
4593. M. Albaladejo et al., XYZ spectroscopy at electron-hadron facilities: exclusive processes. Phys. Rev. D **102**, 114010 (2020)
4594. EIC User Group Webpages. https://www.eicug.org
4595. J-PARC Center, J-PARC web page: https://j-parc.jp/researcher/index-e.html; Program Advisory Committee for Nuclear and Particle Physics Experiments: https://j-parc.jp/researcher/Hadron/en/PAC_for_NuclPart_e.html
4596. H. Ohnishi, F. Sakuma, T. Takahashi, Hadron physics at J-PARC. Prog. Part. Nucl. Phys. **113**, 103773 (2020)
4597. K. Aoki et al., Extension of the J-PARC hadron experimental facility: third white paper (2021)
4598. J.K. Ahn et al., Studying generalized parton distributions with exclusive Drell-Yan process at J-PARC. Letter of Intent (2018), 7th J-PARC PAC meeting, January 16–18, 2019
4599. K. Aoki et al. (J-PARC-HI Collaboration), Proposal for dielectron measurements in heavy-ion collisions at J-PARC with E16 upgrades, June 14, 2021. J-PARC PAC: https://j-parc.jp/researcher/Hadron/en/Proposal_e.html#2107
4600. S. Kumano, *Nuclear Physics (in Japanese). KEK Physics Series*, vol. 2 (Kyoritsu Shuppan Co., Ltd., 2015)
4601. S.N. Nakamura, Future prospects of spectroscopic study of Lambda hypernuclei at JLab and J-PARC HIHR. EPJ Web Conf. **271**, 11003 (2022)
4602. T.O. Yamamoto et al., Observation of spin-dependent charge symmetry breaking in ΛN interaction: gamma-ray spectroscopy of ${}^{4}_{\Lambda}$He. Phys. Rev. Lett. **115**(22), 222501 (2015)
4603. H. Ekawa et al., Observation of a Be double-Lambda hypernucleus in the J-PARC E07 experiment. PTEP **2019**(2), 021D02 (2019)
4604. S.H. Hayakawa et al., Observation of Coulomb-assisted nuclear bound state of Ξ-N14 system. Phys. Rev. Lett. **126**(6), 062501 (2021)
4605. M. Yoshimoto et al., First observation of a nuclear s-state of a Ξ hypernucleus, ${}^{15}_{\Xi}$C. PTEP **2021**(7), 073D02 (2021)
4606. T. Yamaga et al., Observation of a $\bar{K}NN$ bound state in the ${}^{3}\mathrm{He}(K^-, \Lambda p)n$ reaction. Phys. Rev. C **102**(4), 044002 (2020)
4607. T. Hashimoto et al., Measurements of strong-interaction effects in kaonic-helium isotopes at sub-eV precision with X-ray microcalorimeters. Phys. Rev. Lett. **128**(11), 112503 (2022)

4608. Y. Ichikawa et al., An event excess observed in the deeply bound region of the ^{12}C (K^-, p) missing-mass spectrum. PTEP **2020**(12), 123D01 (2020)
4609. K. Miwa et al., Measurement of the differential cross sections of the $\Sigma^- p$ elastic scattering in momentum range 470 to 850 MeV/c. Phys. Rev. C **104**(4), 045204 (2021)
4610. K. Miwa et al., Precise measurement of differential cross sections of the $\Sigma^- p \to \Lambda n$ reaction in momentum range 470–650 MeV$/c$. Phys. Rev. Lett. **128**(7), 072501 (2022)
4611. T. Nanamura et al., Measurement of differential cross sections for Σ+p elastic scattering in the momentum range 0.44–0.80 GeV/c. PTEP **2022**(9), 093D01 (2022)
4612. S. Yokkaichi et al., Proposal, electron pair spectrometer at the J-PARC 50-GeV PS to explore the chiral symmetry in QCD. http://j-parc.jp/researcher/Hadron/en/pac_0606/pdf/p16-Yokkaichi_2.pdf, http://j-parc.jp/researcher/Hadron/en/pac_1707/pdf/E16_2017-10.pdf, see E16 home page: https://ribf.riken.jp/~yokkaich/E16/E16-index.html
4613. X.-D. Ji, A QCD analysis of the mass structure of the nucleon. Phys. Rev. Lett. **74**, 1071–1074 (1995)
4614. D.P. Anderle et al., Electron-ion collider in China. Front. Phys. (Beijing) **16**(6), 64701 (2021)
4615. S. Kumano, Q.-T. Song, O.V. Teryaev, Hadron tomography by generalized distribution amplitudes in pion-pair production process $\gamma^*\gamma \to \pi^0\pi^0$ and gravitational form factors for pion. Phys. Rev. D **97**(1), 014020 (2018)
4616. R.S. Hayano, T. Hatsuda, Hadron properties in the nuclear medium. Rev. Mod. Phys. **82**, 2949 (2010)
4617. P. Gubler, D. Satow, Recent progress in QCD condensate evaluations and sum rules. Prog. Part. Nucl. Phys. **106**, 1–67 (2019)
4618. M. Naruki et al., Experimental signature of the medium modification for ρ and ω mesons in 12-GeV p + A reactions. Phys. Rev. Lett. **96**, 092301 (2006)
4619. R. Muto et al., Evidence for in-medium modification of the ϕ meson at normal nuclear density. Phys. Rev. Lett. **98**, 042501 (2007)
4620. S. Ashikaga et al., Measurement of vector meson mass in nuclear matter at J-PARC. JPS Conf. Proc. **26**, 024005 (2019) **(Ed. by Akinobu Dote et al.)**
4621. Y. Nara et al., Relativistic nuclear collisions at 10A GeV energies from $p +$ Be to Au+Au with the hadronic cascade model. Phys. Rev. C **61**, 024901 (2000)
4622. P. Gubler, The ϕ meson in nuclear matter in a transport approach. PoS PANIC **2021**, 215 (2022)
4623. K. Shirotori et al., Charmed baryon spectroscopy experiment at J-PARC. JPS Conf. Proc. **8**, 022012 (2015)
4624. L. Heller et al., Pion-nucleon Bremsstrahlung and Δ electromagnetic moments. Phys. Rev. C **35**, 718 (1987)
4625. T. Sawada et al., Accessing proton generalized parton distributions and pion distribution amplitudes with the exclusive pion-induced Drell- Yan process at J-PARC. Phys. Rev. D **93**(11), 114034 (2016)
4626. Y. Morino et al., Charmed baryon spectroscopy via the (π, D^{*-}) reaction. P50 proposal (2013), 16th J-PARC PAC meeting, January 9–11, 2013. http://www.j-parc.jp/researcher/Hadron/en/Proposal_e.html, see also https://www.rcnp.osaka-u.ac.jp/~noumi/puki/E50
4627. B. Pire, K. Semenov-Tian-Shansky, L. Szymanowski, Backward charmonium production in πN collisions. Phys. Rev. D **95**(3), 034021 (2017)
4628. S. Kumano, M. Strikman, K. Sudoh, Novel two-to-three hard hadronic processes and possible studies of generalized parton distributions at hadron facilities. Phys. Rev. D **80**, 074003 (2009)
4629. H. Kawamura, S. Kumano, T. Sekihara, Determination of exotic hadron structure by constituent-counting rule for hard exclusive processes. Phys. Rev. D **88**, 034010 (2013)
4630. H. Sako et al. (J-PARC-HI Collaboration), Letter of Intent for J-PARC Heavy-Ion Program (J-PARC-HI), July 25, 2016. J-PARC PAC: https://j-parc.jp/researcher/Hadron/en/Proposal_e.html#1607
4631. J-PARC-HI Collaboration, J-PARC Heavy Ion Project. https://asrc.jaea.go.jp/soshiki/gr/hadron/jparc-hi/
4632. K. Ozawa for the J-PARC-HI Collaboration, J-PARC Heavy Ion Project. Presentation given at the 14th International Conference on Hypernuclear and Strange Particle Physics (HYP2022), June 27, 2022– July 1, 2022, Prague. https://indico.cern.ch/event/896088/contributions/4866677/
4633. T. Galatyuk, https://github.com/tgalatyuk/interaction_rate_facilities/blob/main/hist_rates_detectors_2022_jun.pdf (2022)
4634. T. Galatyuk, Future facilities for high μ_B physics. Nucl. Phys. A **982**, 163–169 (2019) **(Ed. by Federico Antinori et al.)**
4635. V.D. Kekelidze et al., Three stages of the NICA accelerator complex. Eur. Phys. J. A **52**(8), 211 (2016)
4636. V.D. Kekelidze, NICA project at JINR: status and prospects. JINST **12**(06), C06012 (2017) **(Ed. by Lev Shekhtman)**
4637. E. Syresin et al., NICA Ion Collider at JINR. 27th Russian Particle Accelerator Conference (2021)
4638. E.M. Syresin et al., Formation of polarized proton beams in the NICA collider-accelerator complex. Phys. Part. Nucl. **52**(5), 997–1017 (2021)
4639. Y. Aoki et al., The order of the quantum chromodynamics transition predicted by the standard model of particle physics. Nature **443**, 675–678 (2006)
4640. P. Senger et al., Upgrading the baryonic matter at the nuclotron experiment at NICA for studies of dense nuclear matter. Particles **2**(4), 481–490 (2019)
4641. M. Kapishin, The fixed target experiment for studies of baryonic matter at the Nuclotron (BM@N). EPJ Web Conf. **182**, 02061 (2018) **(Ed. by Y. Aharonov, L. Bravina, and S. Kabana)**
4642. J. Steinheimer et al., Strangeness at the international facility for antiproton and ion research. Prog. Part. Nucl. Phys. **62**, 313–317 (2009) **(Ed. by Amand Faessler)**
4643. J. Steinheimer et al., Hypernuclei, dibaryon and antinuclei production in high energy heavy ion collisions: thermal production versus Coalescence. Phys. Lett. B **714**, 85–91 (2012)
4644. A. Andronic et al., Production of light nuclei, hypernuclei and their antiparticles in relativistic nuclear collisions. Phys. Lett. B **697**, 203–207 (2011)
4645. M. Patsyuk et al., Unperturbed inverse kinematics nucleon knockout measurements with a 48 GeV/c carbon beam. Nat. Phys. **17**, 693 (2021)
4646. C. Blume, Energy dependence of hadronic observables. J. Phys. G **31**, S57–S68 (2005) **(Ed. by F. Antinori et al.)**
4647. V. Golovatyuk et al., The multi-purpose detector (MPD) of the collider experiment. Eur. Phys. J. A **52**(8), 212 (2016)
4648. Kh. Abraamyan et al., The multipurpose detector—MPD to study heavy ion collisions at NICA (Conceptual Design Report) (2014)
4649. J. Adamczewski-Musch et al., Identical pion intensity interferometry in central Au + Au collisions at 1.23 A GeV. Phys. Lett. B **795**, 446–451 (2019)
4650. C. Gale et al., Event-by-event anisotropic flow in heavy-ion collisions from combined Yang-Mills and viscous fluid dynamics. Phys. Rev. Lett. **110**(1), 012302 (2013)
4651. U. Heinz, R. Snellings, Collective flow and viscosity in relativistic heavy-ion collisions. Annu. Rev. Nucl. Part. Sci. **63**, 123–151 (2013)
4652. P. Parfenov et al., The comparison of methods for anisotropic flow measurements with the MPD Experiment at NICA (2020). arXiv:2012.06763
4653. V. Abgaryan et al., Status and initial physics performance studies of the MPD experiment at NICA. Eur. Phys. J. A **58**(7), 140 (2022)

4654. V.M. Abazov et al., Conceptual design of the spin physics detector (2021). arXiv:2102.00442
4655. A. Arbuzov et al., On the physics potential to study the gluon content of proton and deuteron at NICA SPD. Prog. Part. Nucl. Phys. **119**, 103858 (2021)
4656. A. Kotzinian, New quark distributions and semiinclusive electroproduction on the polarized nucleons. Nucl. Phys. B **441**, 234–248 (1995)
4657. K. Goeke, A. Metz, M. Schlegel, Parameterization of the quark-quark correlator of a spin-1/2 hadron. Phys. Lett. B **618**, 90–96 (2005)
4658. R. Angeles-Martinez et al., Transverse momentum dependent (TMD) parton distribution functions: status and prospects. Acta Phys. Polon. B **46**(12), 2501–2534 (2015)
4659. V.V. Abramov et al., Possible studies at the first stage of the NICA collider operation with polarized and unpolarized proton and deuteron beams. Phys. Part. Nucl. **52**(6), 1044–1119 (2021)
4660. P. Spiller, G. Franchetti, The FAIR accelerator project at GSI. Nucl. Instrum. Meth. A **561**, 305–309 (2006)
4661. H. Geissel et al., The super-FRS project at GSI. Nucl. Instrum. Meth. B **204**, 71–85 (2003)
4662. P. Spiller et al., Acceleration of intermediate charge state heavy ions in SIS18. Conf. Proc. C **100523**, MOPD002 (2010) **(Ed. by A. Noda et al.)**
4663. F. Kaether et al., Superconducting dipole magnets for the SIS100 synchrotron. In: *12th International Particle Accelerator Conference* (2021)
4664. I.C. Arsene et al., Dynamical phase trajectories for relativistic nuclear collisions. Phys. Rev. C **75**, 034902 (2007)
4665. R. Rapp, J. Wambach, Chiral symmetry restoration and dileptons in relativistic heavy ion collisions. Adv. Nucl. Phys. **25**, 1 (2000)
4666. L.D. McLerran, T. Toimela, Photon and dilepton emission from the quark-gluon plasma: some general considerations. Phys. Rev. D **31**, 545 (1985)
4667. F. Seck et al., Dilepton signature of a first-order phase transition. Phys. Rev. C **106**(1), 014904 (2022)
4668. R. Rapp, H. van Hees, Thermal dileptons as fireball thermometer and chronometer. Phys. Lett. B **753**, 586–590 (2016)
4669. R. Arnaldi et al., Evidence for the production of thermal-like muon pairs with masses above 1-GeV/c^2 in 158-A-GeV Indium-Indium Collisions. Eur. Phys. J. C **59**, 607–623 (2009)
4670. J. Adamczewski-Musch et al., Probing dense baryon-rich matter with virtual photons. Nat. Phys. **15**(10), 1040–1045 (2019)
4671. P. Salabura, J. Stroth, Dilepton radiation from strongly interacting systems. Prog. Part. Nucl. Phys. **120**, 103869 (2021)
4672. G. Barucca et al., Precision resonance energy scans with the PANDA experiment at FAIR: sensitivity study for width and line-shape measurements of the X(3872). Eur. Phys. J. A **55**(3), 42 (2019)
4673. F. Nerling, Charm(-onium) physics at PANDA. PoS CHARM2020, 004 (2021)
4674. A. Jackura et al., New analysis of $\eta\pi$ tensor resonances measured at the COMPASS experiment. Phys. Lett. B **779**, 464–472 (2018)
4675. C. Adolph et al., Observation of a new narrow axial-vector meson $a_1(1420)$. Phys. Rev. Lett. **115**(8), 082001 (2015)
4676. N. Brambilla et al., Spin structure of heavy-quark hybrids. Phys. Rev. D **99**, 014017 (2019)
4677. C. Amsler, Nucleon-antinucleon annihilation at LEAR (2019). arXiv:1908.08455
4678. M. Christian Mertens, Determination of the $D^*_{s0}(2317)$ width with the PANDA detector. Hyperfine Interact. **209**(1–3), 111–115 (2012)
4679. BESIII Collaboration, Probing CP symmetry and weak phases with entangled double-strange baryons. Nature **606**, 64–69 (2022)
4680. V. Abazov et al., Prospects for spin-parity determination of excited baryons via the $\overline{\Xi}^+ \Lambda K^-$ final state with PANDA (2022). arXiv:2201.03852
4681. B.P. Singh et al., Experimental access to transition distribution amplitudes with the $\bar{P}$ANDA experiment at FAIR. Eur. Phys. J. A **51**(8), 107 (2015)
4682. B. Singh et al., Feasibility study for the measurement of πN transition distribution amplitudes at $\overline{P}$ANDA in $\bar{p}p \to J/\psi\pi^0$. Phys. Rev. D **95**(3), 032003 (2017)
4683. A. Freund et al., Exclusive annihilation $p\bar{p} \to \gamma\gamma$ in a generalized parton picture. Phys. Rev. Lett. **90**, 092001 (2003)
4684. P. Kroll, A. Schäfer, The process $p\bar{p} \to \gamma\pi^0$ within the handbag approach. Eur. Phys. J. A **26**, 89 (2005)
4685. P. Kroll, A. Schäfer, Probing moments of baryon-antibaryon generalized parton distributions at BELLE and FAIR. Eur. Phys. J. A **50**, 1 (2014)
4686. G. Bardin et al., Determination of the electric and magnetic form factors of the proton in the time-like region. Nucl. Phys. B **411**(1), 3–32 (1994)
4687. J.P. Lees et al., Study of $e^+e^- \to p\bar{p}$ via initial-state radiation at BABAR. Phys. Rev. D **87**(9), 092005 (2013)
4688. J.P. Lees et al., Measurement of the $e^+e^- \to p\bar{p}$ cross section in the energy range from 3(0) to 6.5 GeV. Phys. Rev. D **88**(7), 072009 (2013)
4689. M. Ablikim et al., Measurement of the proton form factor by studying $e^+e^- \to p\bar{p}$. Phys. Rev. D **91**(11), 112004 (2015)
4690. M. Ablikim et al., Measurement of proton electromagnetic form factors in $e^+e^- \to p\bar{p}$ in the energy region 2.00–3.08 GeV. Phys. Rev. Lett. **124**(4), 042001 (2020)
4691. M. Ablikim et al., Study of the process $e^+e^- \to p\bar{p}$ via initial state radiation at BESIII. Phys. Rev. D **99**(9), 092002 (2019)
4692. M. Ablikim et al., Measurement of proton electromagnetic form factors in the time-like region using initial state radiation at BESIII. Phys. Lett. B **817**, 136328 (2021)
4693. R.R. Akhmetshin et al., Study of the process $e^+e^- \to p\bar{p}$ in the c.m. energy range from threshold to 2 GeV with the CMD-3 detector. Phys. Lett. B **759**, 634–640 (2016)
4694. H.B. Li et al., Physics in the τ-charm region at BESIII. Snowmass 2021 (2022)
4695. M. Ablikim et al., Measurement of the cross section for $e^+e^- \to$hadrons at energies from 2.2324 to 3.6710 GeV. Phys. Rev. Lett. **128**(6), 062004 (2022)
4696. M. Ablikim et al., Measurement of azimuthal asymmetries in inclusive charged dipion production in e^+e^- annihilations at $\sqrt{s}$ = 3.65 GeV. Phys. Rev. Lett. **116**(4), 042001 (2016)
4697. M. Ablikim et al., Oscillating features in the electromagnetic structure of the neutron. Nat. Phys. **17**(11), 1200–1204 (2021)
4698. G. Huang, R. Baldini Ferroli, Probing the internal structure of baryons. Natl. Sci. Rev. **8**(11), nwab187 (2021)
4699. M. Ablikim et al., Complete measurement of the Λ electromagnetic form factors. Phys. Rev. Lett. **123**(12), 122003 (2019)
4700. M. Ablikim et al., Measurements of weak decay asymmetries of $\Lambda_c^+ \to pK_S^0$, $\Lambda\pi^+$, $\Sigma^+\pi^0$, and $\Sigma^0\pi^+$. Phys. Rev. D **100**(7), 072004 (2019)
4701. E.V. Abakumova et al., The beam energy measurement system for the Beijing electron-positron collider. Nucl. Instrum. Meth. A **659**, 21–29 (2011)
4702. S. Jin, X. Shen, Highlights of light meson spectroscopy at the BESIII experiment. Natl. Sci. Rev. 8(11), nwab198 (2021)
4703. F. Brünner, A. Rebhan, Constraints on the $\eta\eta'$ decay rate of a scalar glueball from gauge/gravity duality. Phys. Rev. D **92**(12), 121902 (2015)
4704. M. Ablikim et al., Observation of a state $X(2600)$ in the $\pi^+\pi^-\eta'$ system in the process $J/\psi \to \gamma\pi^+\pi^-\eta'$. Phys. Rev. Lett. **129**(4), 042001 (2022)

4705. M. Ablikim et al., Observation of the $Y(4220)$ and $Y(4360)$ in the process $e^+e^- \to \eta J/\psi$. Phys. Rev. D **102**(3), 031101 (2020)
4706. M. Ablikim et al., Observation of $e^+e^- \to \pi^+\pi^- \psi(3770)$ and $D_1(2420)^0\bar{D}^0 + c.c.$. Phys. Rev. D **100**(3), 032005 (2019)
4707. M. Ablikim et al., Observation of resonance structures in $e^+e^- \to \pi^+\pi^-\psi_2(3823)$ and mass measurement of $\psi_2(3823)$. Phys. Rev. Lett. **129**(10), 102003 (2022)
4708. M. Ablikim et al., Measurement of $e^+e^- \to \gamma\chi_{c0,c1,c2}$ cross sections at center-of-mass energies between 3.77 and 4.60 GeV. Phys. Rev. D **104**(9), 092001 (2021)
4709. M. Ablikim et al., Search for new decay modes of the $\psi_2(3823)$ and the process $e^+e^- \to \pi^0\pi^0\ \psi_2(3823)$. Phys. Rev. D **103**(9), L091102 (2021)
4710. M. Ablikim et al., First observation of the direct production of the x_{c1} in e^+e^- annihilation. Phys. Rev. Lett. **129**(12), 122001 (2022)
4711. C.-Z. Yuan, Charmonium and charmoniumlike states at the BESIII experiment. Natl. Sci. Rev. 8(11), nwab182 (2021)
4712. M. Ablikim et al., Cross section measurement of $e^+e^- \to \pi^+\pi^-(3686)$ from $\sqrt{s} = 4.0076$ to 4.6984 GeV. Phys. Rev. D **104**(5), 052012 (2021)
4713. M. Ablikim et al., Evidence for a neutral near-threshold structure in the K^0_S recoil-mass spectra in $e^+e^- \to K^0_S D^+_s D^{*-}$ and $e^+e^- \to K^0_S D^{*+}_s D^-$. Phys. Rev. Lett. **129**(11), 112003 (2022)
4714. M. Ablikim et al., Measurement of $e^+e^- \to \pi^+\pi^-\ \psi(3686)$ from 4.008 to 4.600 GeV and observation of a charged structure in the $\pi^\pm\psi(3686)$ mass spectrum. Phys. Rev. D **96**(3), 032004 (2017) [Erratum: Phys. Rev. D 99, 019903 (2019)]
4715. K. Zhu, Triangle relations for XY Z states. Int. J. Mod. Phys. A **36**(14), 2150126 (2021)
4716. C.-P. Shen, C.-Z. Yuan, Observation of pentaquark states and perspectives of further studies. Sci. Bull. **60**(17), 1549–1550 (2015)
4717. J.Z. Bai et al., Search for the pentaquark state in $\psi(2S)$ and J/ψ decays to $K^0_S pK^-\bar{n}$ and $K^0_S \bar{p}K^+n$. Phys. Rev. D **70**, 012004 (2004)
4718. S.D. Bass, P. Moskal, η' and η mesons with connection to anomalous glue. Rev. Mod. Phys. **91**(1), 015003 (2019)
4719. S.-S. Fang, Light meson physics at BESIII. Natl. Sci. Rev. **8**(11), nwab052 (2021)
4720. R. Escribano, S. Gonzàlez-Solís, A data-driven approach to π^0, η and η' single and double Dalitz decays. Chin. Phys. C **42**(2), 023109 (2018)
4721. T. Petri, Anomalous decays of pseudoscalar mesons (2010). arXiv:1010.2378. PhD thesis
4722. B. Kubis, S.P. Schneider, The Cusp effect in $\eta' \to \eta\pi\pi$ decays. Eur. Phys. J. C **62**, 511–523 (2009)
4723. M. Ablikim et al., Polarization and entanglement in baryon-antibaryon pair production in electron-positron annihilation. Nat. Phys. **15**, 631–634 (2019)
4724. M. Ablikim et al., Precise measurements of decay parameters and CP asymmetry with entangled $\Lambda - \bar{\Lambda}$ pairs pairs. Phys. Rev. Lett. **129**(13), 131801 (2022)
4725. H.-B. Li, X.-R. Lyu, Study of the standard model with weak decays of charmed hadrons at BESIII. Natl. Sci. Rev. **8**(11), nwab181 (2021)
4726. H. Ping Peng, Y. Heng Zheng, X. Rong Zhou, Super Tau-Charm Facility of China. Physics **49**(8), 513–524 (2020)
4727. T. Keck et al., The full event interpretation: an exclusive tagging algorithm for the Belle II experiment. Comput. Softw. Big Sci. **3**(1), 6 (2019)
4728. F. Abudinén et al., B-flavor tagging at Belle II. Eur. Phys. J. C **82**(4), 283 (2022)
4729. Y. Amhis et al., Averages of b-hadron, c-hadron, and τ-lepton properties as of 2018. Eur. Phys. J. C **81**(3), 226 (2021)
4730. J. Charles et al., Isospin analysis of charmless B-meson decays. Eur. Phys. J. C **77**(8), 574 (2017)
4731. J. Brod, J. Zupan, The ultimate theoretical error on γ from $B \to DK$ decays. JHEP **1401**, 051 (2014)
4732. M. Gronau, D. London, How to determine all the angles of the unitarity triangle from $B^0_d \to DK_S$ and $B^0_s \to D^0$. Phys. Lett. B **253**, 483–488 (1991)
4733. M. Gronau, D. Wyler, On determining a weak phase from CP asymmetries in charged B decays. Phys. Lett. B **265**, 172–176 (1991)
4734. D. Atwood, I. Dunietz, A. Soni, Improved methods for observing CP violation in $B^\pm \to KD$ and measuring the CKM phase γ. Phys. Rev. D **63**, 036005 (2001)
4735. A. Giri et al., Determining gamma using B+-→ D K+- with multi-body D decays. Phys. Rev. D **68**, 054018 (2003)
4736. A. Bondar, BINP special analysis meeting on Dalitz analysis, unpublished (2002)
4737. A. Poluektov et al., Measurement of ϕ_3 with Dalitz plot analysis of $B^{+-} \to D^{(*)}K^{+-}$ decay. Phys. Rev. D **70**, 072003 (2004)
4738. Y. Grossman, Z. Ligeti, A. Soffer, Measuring γ in $B^\pm \to K^\pm(KK*)_D$ decays. Phys. Rev. D **67**, 071301 (2003)
4739. P.K. Resmi et al., First measurement of the CKM angle ϕ_3 with $B^\pm \to D(K^0_S\pi^+\pi^-\pi^0)K^\pm$ decays. J. High Energy Phys. **10**, 178 (2019)
4740. A. Sibidanov et al., Study of exclusive $B \to X_u\ell\nu$ decays and extraction of $\|V_{ub}\|$ using full reconstruction tagging at the Belle experiment. Phys. Rev. D **88**(3), 032005 (2013)
4741. F.U. Bernlochner et al., Precision global determination of the $B \to X_s\gamma$ decay rate. Phys. Rev. Lett. **127**(10), 102001 (2021)
4742. M. Beneke, Corrections to $\sin(2\beta)$ from CP asymmetries in $B^0 \to (\pi^0, \rho^0, \eta, \eta', \omega, \phi)K_S$ decays. Phys. Lett. B **620**, 143–150 (2005)
4743. G. Caria et al., Measurement of $\mathcal{R}(D)$ and $\mathcal{R}(D^*)$ with a semileptonic tagging method. Phys. Rev. Lett. **124**(16), 161803 (2020)
4744. J.P. Lees et al., Measurement of an excess of $\bar{B} \to D^{(*)}\tau^-\bar{\nu}_\tau$ decays and implications for charged Higgs bosons. Phys. Rev. D **88**(7), 072012 (2013)
4745. R. Aaij et al., Measurement of the ratio of branching fractions $\mathcal{B}(\bar{B}^0 \to D^{*+}\tau^-\bar{\nu}_\tau)\mathcal{B}(\bar{B}^0 \to D^{*+}\ \mu^-\bar{\nu}_\mu)$. Phys. Rev. Lett. **115**(11), 111803 (2015) [Erratum: Phys. Rev. Lett. 115, 159901 (2015)]
4746. R. Aaij et al., Test of Lepton Flavor Universality by the measurement of the $B^0 \to D^{*-}\tau^+\nu_\tau$ branching fraction using three-prong τ decays. Phys. Rev. D **97**(7), 072013 (2018)
4747. M. Huschle et al., Measurement of the branching ratio of $\bar{B} \to D^{(*)}\tau^-\bar{\nu}_\tau$ relative to $\bar{B} \to D^{(*)}\ell^-\bar{\nu}_\ell$ decays with hadronic tagging at Belle. Phys. Rev. D **92**(7), 072014 (2015)
4748. S. Hirose et al., Measurement of the τ lepton polarization and $R(D^*)$ in the decay $\bar{B} \to D^*\tau^-\bar{\nu}_\tau$ with one-prong hadronic τ decays at Belle. Phys. Rev. D **97**(1), 012004 (2018)
4749. R. Aaij et al., Search for lepton-universality violation in $B^+ \to K^+\ell^+\ell^-$ decays. Phys. Rev. Lett. **122**(19), 191801 (2019)
4750. R. Aaij et al., Test of lepton universality with $B^0 \to K^{*0}\ell^+\ell^-$ decays. JHEP **08**, 055 (2017)
4751. R. Aaij et al., Differential branching fractions and isospin asymmetries of $B \to K^{(*)}\mu^+\mu^-$ decays. JHEP **06**, 133 (2014)
4752. R. Aaij et al., Angular analysis of the $B^0 \to K^{*0}\mu^+\mu^-$ decay using 3 fb^{-1} of integrated luminosity. JHEP **02**, 104 (2016)
4753. R. Aaij et al., Measurement of CP-averaged observables in the $B^0 \to K^{*0}\mu^+\mu^-$ decay. Phys. Rev. Lett. **125**(1), 011802 (2020)
4754. E. Manoni (Belle II Collaboration), Electroweak penguins and radiative decays at Belle II. 12–19 March 2022. https://moriond.in2p3.fr/2022/EW/slides/5/2/3_EManoni-v2.pdf
4755. J.P. Lees et al., Search for $B^+ \to K^+\tau^+\tau^-$ at the BaBar experiment. Phys. Rev. Lett. **118**(3), 031802 (2017)

4756. R. Alonso, B. Grinstein, J. Martin Camalich, Lepton universality violation and lepton flavor conservation in B-meson decays. JHEP **10**, 184 (2015)
4757. J.A.L. Hewett, Tau polarization asymmetry in $B \to X_s\tau^+\tau^-$. Phys. Rev. D **53**, 4964–4969 (1996)
4758. T.V. Dong et al., Search for the decay $B^0 \to K^{*0}\tau^+\tau^-$ at the experiment. Phys. Rev. D **108**, L01112 (2023)
4759. M. Benzke et al., Long-distance dominance of the CP asymmetry in $B \to X_{s,d}\gamma$ decays. Phys. Rev. Lett. **106**, 141801 (2011)
4760. J. Lyon, R. Zwicky, Isospin asymmetries in $B \to (K^*, \rho)\gamma/l^+l^-$ and $B \to Kl^+l^-$ in and beyond the Standard Model. Phys. Rev. D **88**, 094004 (2013)
4761. B. Aubert et al., Observation of a broad structure in the $\pi^+\pi^-J/\psi$ mass spectrum around 4.26-GeV/c^2. Phys. Rev. Lett. **95**, 142001 (2005)
4762. A. Abdesselam et al., Energy scan of the $e^+e^- \to h_b(nP)\pi^+\pi^-$ ($n = 1, 2$) cross sections and evidence for $\Upsilon(11020)$ decays into charged bottomonium-like states. Phys. Rev. Lett. **117**(14), 142001 (2016)
4763. R. Mizuk et al., Observation of a new structure near 10.75 GeV in the energy dependence of the $e^+e^- \to \Upsilon(nS)\pi^+\pi^-$ (n = 1, 2, 3) cross sections. JHEP **10**, 220 (2019)
4764. B. McElrath, Invisible quarkonium decays as a sensitive probe of dark matter. Phys. Rev. D **72**, 103508 (2005)
4765. D.E. Hazard, A.A. Petrov, Lepton flavor violating quarkonium decays. Phys. Rev. D **94**(7), 074023 (2016)
4766. M. Abe et al., A new approach for measuring the muon anomalous magnetic moment and electric dipole moment. PTEP **2019**(5), 053C02 (2019)
4767. R. Aaij et al., Measurement of the b-quark production cross-section in 7 and 13 TeV pp collisions. Phys. Rev. Lett. **118**(5), 052002 (2017) [Erratum: Phys. Rev. Lett. 119, 169901 (2017)]
4768. R. Aaij et al., Measurements of prompt charm production cross-sections in pp collisions at $\sqrt{s} = 13$ TeV. JHEP **03**, 159 (2016) [Erratum: JHEP 09, 013 (2016), Erratum: JHEP 05, 074 (2017)]
4769. LHCb Collaboration. Framework TDR for the LHCb Upgrade II—opportunities in flavour physics, and beyond, in the HL-LHC era. http://cds.cern.ch/record/2776420.2021
4770. A. Cerri et al., Opportunities in Flavour Physics at the HL-LHC and HE-LHC (2018)
4771. K. De Bruyn, R. Fleischer, P. Koppenburg, Extracting gamma and penguin topologies through CP violation in $B_s^0 \to J/\psi K_S$. Eur. Phys. J. C **70**, 1025–1035 (2010)
4772. K. De Bruyn, R. Fleischer, A roadmap to control penguin effects in $B_d^0 \to J/\psi K_S^0$ and $B_s^0 \to J/\psi\phi$. JHEP **03**, 145 (2015)
4773. M. Ciuchini, M. Pierini, L. Silvestrini, $B_s \to K^{*0}\bar{K}^{*0}$ decays: the golden channels for new physics searches. Phys. Rev. Lett. **100**, 031802 (2008)
4774. S. Descotes-Genon, J. Matias, J. Virto, An analysis of $B_{d,s}$ mixing angles in presence of New Physics and an update of $B_s \to \bar{K}^{0*}K^{0*}$. Phys. Rev. D **85**, 034010 (2012)
4775. B. Bhattacharya et al., Measuring β_s with $B_s \to K^{0(*)}\bar{K}^{0(*)}$–a reappraisal. Phys. Lett. B **717**, 403–408 (2012)
4776. R. Fleischer, Exploring CP violation and penguin effects through $B_d^0 \to D^+D^-$ and $B_s^0 \to D_s^+D_s^-$. Eur. Phys. J. C **51**, 849–858 (2007)
4777. M. Jung, S. Schacht, Standard model predictions and new physics sensitivity in $B \to DD$ decays. Phys. Rev. D **91**(3), 034027 (2015)
4778. L. Bel et al., Anatomy of $B \to D\overline{D}$ decays. JHEP **07**, 108 (2015)
4779. X.-G. He, SU(3) analysis of annihilation contributions and CP violating relations in $B \to PP$ decays. Eur. Phys. J. C **9**, 443–448 (1999)
4780. M. Gronau, J.L. Rosner, The role of $B_s \to K\pi$ in determining the weak phase γ. Phys. Lett. B **482**, 71–76 (2000)
4781. H.J. Lipkin, Is observed direct CP violation in $B_d \to K^+\pi^-$ due to new physics? Check standard model prediction of equal violation in $B_s \to K^-\pi^+$. Phys. Lett. B **621**, 126–132 (2005)
4782. H.-Y. Cheng, C.-W. Chiang, SU(3) symmetry breaking and CP violation in $D \to PP$ decays. Phys. Rev. D **86**, 014014 (2012)
4783. M. Gronau, High order U-spin breaking: A precise amplitude relation in D^0 decays. Phys. Lett. B **730**, 221–225 (2014) [Addendum: Phys. Lett. B 735, 282 (2014)]
4784. S. Müller, U. Nierste, S. Schacht, Sum rules of charm CP asymmetries beyond the SU(3)$_F$ limit. Phys. Rev. Lett. **115**(25), 251802 (2015)
4785. M. Gavrilova, Y. Grossman, S. Schacht, The mathematical structure of U-spin amplitude sum rules. JHEP **08**, 278 (2022)
4786. R. Aaij et al., Updated measurement of time-dependent CP-violating observables in $B_s^0 \to J/\psi K^+K^-$ decays. Eur. Phys. J. C **79**(8), 706 (2019) [Erratum: Eur. Phys. J. C 80, 601 (2020)]
4787. G. Aad et al., Measurement of the CP-violating phase ϕ_s in $B_s^0 \to J/\psi\phi$ decays in ATLAS at 13 TeV. Eur. Phys. J. C **81**(4), 342 (2021)
4788. A.M. Sirunyan et al., Measurement of the CP-violating phase ϕ_s in the $B_s^0 \to J/\psi\,\phi(1020) \to \mu^+\mu^-K^+K^-$ channel in proton-proton collisions at $\sqrt{s} = 13$ TeV. Phys. Lett. B **816**, 136188 (2021)
4789. R. Aaij et al., Observation of the mass difference between neutral charm-meson eigenstates. Phys. Rev. Lett. **127**(11), 111801 (2021)
4790. R. Aaij et al., Measurement of the charm mixing parameter $y_{CP} - y_{CP}^{K\pi}$ using two-body D^0 meson decays. Phys. Rev. D **105**(9), 092013 (2022)
4791. A. Lenz, G. Wilkinson, Mixing and CP violation in the charm system (2020)
4792. R. Aaij et al., Measurements of CP violation in the three-body phase space of charmless $B^\pm$ decays. Phys. Rev. D **90**(11), 112004 (2014)
4793. R. Aaij et al., Amplitude analysis of $B^\pm \to \pi^\pm K^+K^-$ decays. Phys. Rev. Lett. **123**(23), 231802 (2019)
4794. R. Aaij et al., Observation of several sources of CP violation in $B^+ \to \pi^+\pi^+\pi^-$ decays. Phys. Rev. Lett. **124**(3), 031801 (2020)
4795. R. Aaij et al., Amplitude analysis of the $B^+ \to \pi^+\pi^+\pi^-$ decay. Phys. Rev. D **101**(1), 012006 (2020)
4796. LHCb Collaboration, Search for direct CP violation in charged charmless $B \to PV$ decays (2022)
4797. J.T. Daub, C. Hanhart, B. Kubis, A model-independent analysis of final-state interactions in $\overline{B}_{d/s}^0 \to J/\psi\pi\pi$. JHEP **02**, 009 (2016)
4798. R. Aaij et al., Simultaneous determination of CKM angle γ and charm mixing parameters (2021)
4799. LHCb Collaboration, Simultaneous determination of the CKM angle γ and parameters related to mixing and CP violation in the charm sector. In: *LHCb-CONF-2022-003* (2022)
4800. T. Gershon, A. Poluektov, Double Dalitz plot analysis of the decay $B^0 \to DK^+\pi^-$, $D \to K_S^0\pi^+\pi^-$. Phys. Rev. D **81**, 014025 (2010)
4801. D. Craik, T. Gershon, A. Poluektov, Optimising sensitivity to γ with $B^0 \to DK^+\pi^-$, $D \to K_S^0\pi^+\pi^-$ double Dalitz plot analysis. Phys. Rev. D **97**, 056002 (2018)
4802. A.M. Sirunyan et al., Measurement of properties of $B_s^0 \to \mu^+\mu^-$ decays and search for $B^0 \to \mu^+\mu^-$ with the CMS experiment. JHEP **04**, 188 (2020)
4803. M. Aaboud et al., Study of the rare decays of B_s^0 and B^0 mesons into muon pairs using data collected during 2015 and 2016 with the ATLAS detector. JHEP **04**, 098 (2019)
4804. R. Aaij et al., Analysis of neutral B-meson decays into two muons. Phys. Rev. Lett. **128**(4), 041801 (2022)
4805. R. Aaij et al., Search for the rare decays $B_s^0 \to e^+e^-$ and $B^0 \to e^+e^-$. Phys. Rev. Lett. **124**(21), 211802 (2020)

4806. R. Aaij et al., Search for the decays $B_s^0 \to \tau^+\tau^-$ and $B^0 \to \tau^+\tau^-$. Phys. Rev. Lett. **118**(25), 251802 (2017)
4807. CMS Collaboration, Measurement of rare $B \to \mu^+\mu^-$ decays with the Phase-2 upgraded CMS detector at the HL-LHC (2018). http://cds.cern.ch/record/2650545
4808. ATLAS Collaboration, Prospects for the $\mathcal{B}(B^0_{(s)} \to \mu^+\mu^-)$ measurements with the ATLAS detector in the Run 2 and HL-LHC data campaigns. In: https://cds.cern.ch/record/2317211. All figures including auxiliary figures are available at https://atlas.web.cern.ch/Atlas/GROUPS/PHYSICS/PUBNOTES/ATL-PHYS-PUB-2018-005.Geneva (2018)
4809. K. De Bruyn et al., Probing new physics via the $B_s^0 \to \mu^+\mu^-$ effective lifetime. Phys. Rev. Lett. **109**, 041801 (2012)
4810. R. Aaij et al., Angular analysis of the rare decay $B_s^0 \to \phi\mu^+\mu^-$. JHEP **11**, 043 (2021)
4811. R. Aaij et al., Branching fraction measurements of the rare $B_s^0 \to \phi\mu^+\mu^-$ and $B_s^0 \to f_2'(1525)\mu^+\mu^-$-decays. Phys. Rev. Lett. **127**(15), 151801 (2021)
4812. M. Aaboud et al., Angular analysis of $B_d^0 \to K^*\mu^+\mu^-$ decays in pp collisions at $\sqrt{s} = 8$ TeV with the ATLAS detector. JHEP **10**, 047 (2018)
4813. A.M. Sirunyan et al., Measurement of angular parameters from the decay $\mathrm{B}^0 \to \mathrm{K}^{*0}\mu^+\mu^-$ in proton-proton collisions at $\sqrt{s} =$ 8 TeV. Phys. Lett. B **781**, 517–541 (2018)
4814. T. Hurth, C. Langenbruch, F. Mahmoudi, Direct determination of Wilson coefficients using $B^0 \to K^{*0}\mu^+\mu^-$ decays (2017)
4815. R. Aaij et al., Test of lepton universality in beauty-quark decays. Nat. Phys. **18**(3), 277–282 (2022)
4816. B. Aubert et al., Measurement of time-dependent CP asymmetry in $B^0 \to K_S^0\pi^0\gamma$ decays. Phys. Rev. D **78**, 071102 (2008)
4817. Y. Ushiroda et al., Time-dependent CP asymmetries in $B^0 \to K_S^0\pi^0\gamma$ transitions. Phys. Rev. D **74**, 111104 (2006). (**Ed. by Alexey Sissakian, Gennady Kozlov, and Elena Kolganova**)
4818. R. Aaij et al., Measurement of CP-violating and mixing-induced observables in $B_s^0 \to \phi\gamma$ decays. Phys. Rev. Lett. **123**(8), 081802 (2019)
4819. R. Aaij et al., Measurement of the photon polarization in $\Lambda_b^0 \to \Lambda\,\gamma$ decays. Phys. Rev. D **105**(5), L051104 (2022)
4820. R. Aaij et al., Strong constraints on the $b \to s\gamma$ photon polarisation from $B^0 \to K^{*0}e^+e^-$ decays. JHEP **12**, 081 (2020)
4821. R. Aaij et al., Observation of Photon Polarization in the $b \to s\gamma$ Transition. Phys. Rev. Lett. **112**(16), 161801 (2014)
4822. M. Gronau et al., Measuring the photon helicity in radiative B decays. Phys. Rev. Lett. **88**, 051802 (2002)
4823. E. Kou, A. Le Yaouanc, A. Tayduganov, Determining the photon polarization of the $b \to s\gamma$ using the $B \to K_1(1270)\gamma \to (K\pi\pi)\gamma$ decay. Phys. Rev. D **83**, 094007 (2011)
4824. M. Gronau, D. Pirjol, Reexamining the photon polarization in $B \to \pi\pi\gamma$. Phys. Rev. D **96**(1), 013002 (2017)
4825. S. Akar et al., The time-dependent CP asymmetry in $B^0 \to K_{\mathrm{res}}\gamma \to \pi^+\pi^-K_S^0\gamma$ decays. JHEP **09**, 034 (2019)
4826. P. Koppenburg, List of hadrons observed at the LHC. In: *LHCb-FIGURE-2021-001*. See 2022 update online (2021)
4827. R. Aaij et al., Amplitude analysis of the $B^+ \to D^+D^-K^+$ decay. Phys. Rev. D **102**, 112003 (2020)
4828. R. Aaij et al., A model-independent study of resonant structure in $B^+ \to D^+D^-K^+$ decays. Phys. Rev. Lett. **125**, 242001 (2020)
4829. ATLAS Collaboration, Observation of an excess of di-charmonium events in the four-muon final state with the ATLAS detector (2022). All figures including auxiliary figures are available at https://atlas.web.cern.ch/Atlas/GROUPS/PHYSICS/CONFNOTES/ATLASCONF-2022-040
4830. CMS Collaboration, Observation of new structures in the $\mathrm{J}/\psi\mathrm{J}/\psi$ mass spectrum in pp collisions at $\sqrt{s} = 13$ TeV (2022). http://cds.cern.ch/record/2815336
4831. R. Aaij et al., Search for the doubly charmed baryon Ξ_{cc}^+. Sci. China Phys. Mech. Astron. **63**(2), 221062 (2020)
4832. R. Aaij et al., Search for the doubly charmed baryon Ω_{cc}^+. Sci. China Phys. Mech. Astron. **64**(10), 101062 (2021)
4833. T. Gershon, A. Poluektov, Displaced B_c^- mesons as an inclusive signature of weakly decaying double beauty hadrons. JHEP **01**, 019 (2019)
4834. A. David et al., LHC HXSWG interim recommendations to explore the coupling structure of a Higgs-like particle (2012). arXiv:1209.0040
4835. M. Cepeda et al., Report from Working Group 2: Higgs physics at the HL-LHC and HE-LHC. CERN Yellow Rep. Monogr. **7**, 221–584 (2019) **(Ed. by Andrea Dainese et al.)**
4836. F. Caola, K. Melnikov, Constraining the Higgs boson width with ZZ production at the LHC. Phys. Rev. D **88**, 054024 (2013)
4837. R. Covarelli, M. Pellen, M. Zaro, Vector-boson scattering at the LHC: unraveling the electroweak sector. Int. J. Mod. Phys. A **36**(16), 2130009 (2021)
4838. C. Anastasiou et al., High precision determination of the gluon fusion Higgs boson cross-section at the LHC. JHEP **05**, 058 (2016)
4839. S. Catani et al., Higgs Boson Production in Association with a $t\bar{t}$ Quark Pair in Next-to-Next-to-Leading Order QCD. Phys. Rev. Lett. **130**(11), 111902 (2023)
4840. R. Bonciani et al., Next-to-leading-order QCD corrections to Higgs production in association with a jet. Phys. Lett. B **843**, 137995 (2023)
4841. R. Boughezal et al., Higgs boson production in association with a jet at next-to-next-to-leading order. Phys. Rev. Lett. **115**(8), 082003 (2015)
4842. X. Chen et al., NNLO QCD corrections to Higgs boson production at large transverse momentum. JHEP **10**, 066 (2016)
4843. X. Chen et al., Top-quark mass effects in H+jet and H+2 jets production. JHEP **03**, 096 (2022)
4844. P. Bambade et al., The international linear collider: a global project (2019). arXiv:1903.01629
4845. J. Gao, CEPC and SppC status-from the completion of CDR towards TDR. Int. J. Mod. Phys. A **36**(22), 2142005 (2021)
4846. A. Abada et al., FCC-ee: The Lepton Collider: Future Circular Collider Conceptual Design Report Volume 2. Eur. Phys. J. ST **228**(2), 261–623 (2019)
4847. O. Brunner et al., The CLIC project. In: *Proceedings of the US Community Study on the Future of Particle Physics (Snowmass 2021)* (2022). arXiv:2203.09186
4848. A. Abada et al., FCC-hh: The Hadron Collider: Future Circular Collider Conceptual Design Report Volume 3. Eur. Phys. J. ST **228**(4), 755–1107 (2019)
4849. M.L. Mangano, G. Ortona, M. Selvaggi, Measuring the Higgs self-coupling via Higgs-pair production at a 100 TeV p-p collider. Eur. Phys. J. C **80**(11), 1030 (2020)
4850. J. de Blas et al., Higgs boson studies at future particle colliders. JHEP **01**, 139 (2020)